EMERGING
INFECTIOUS DISEASES®

Zoonoses

September 2017

EMERGING INFECTIOUS DISEASES

EDITOR-IN-CHIEF
D. Peter Drotman

EMERGING INFECTIOUS DISEASES®

On the Cover: Peter Paul Rubens (1577–1640), *Hippopotamus and Crocodile Hunt* (detail) (ca. 1615–1616). Oil on canvas, 97.6 in x 126.4 in/248 cm x 321 cm. Alte Pinakothek, Kunstareal, Munich, Germany; digital image from Art Resource, New York, New York, USA

About the Cover, p. 1613

1473

Dispatches

EMERGING INFECTIOUS DISEASES®

September 2017

1557

EMERGING INFECTIOUS DISEASES®

September 2017

1565

EID SPOTLIGHT TOPIC

Rabies

Rabies is a deadly disease that can kill anyone who gets it. Every year, an estimated 40,000 people in the United States receive a series of shots due to potential exposure to rabies. Each year around the world, rabies results in more than 59,000 deaths—approximately 1 death every 9 minutes, or about 150 per day.

EMERGING INFECTIOUS DISEASES®

http://go.usa.gov/xqWUJ

World Rabies Day is September 28

Every nine minutes, someone dies from this deadly, yet preventable disease.

Join the fight to end human deaths from canine rabies by 2030.

Vaccinate your dog against rabies.

The Rabies Crisis by the Numbers

40%
40% of the people bitten by dogs globally are children.

150
Rabies occurs in more than 150 countries.

70%
Vaccinating just 70% of dogs will protect people in at-risk areas.

Globally, more than 95% of human rabies deaths occur after bites from rabid dogs. Most of these cases are in sub-Saharan Africa and Asia. CDC, in collaboration with the Global Alliance for Rabies Control and Mission Rabies, is helping countries around the world tackle rabies through education and mass dog rabies vaccination campaigns. To learn more, go to www.cdc.gov/rabies.

Bioinformatic Analyses of Whole-Genome Sequence Data in a Public Health Laboratory

Kelly F. Oakeson, Jennifer Marie Wagner, Michelle Mendenhall,
Andreas Rohrwasser, Robyn Atkinson-Dunn

The ability to generate high-quality sequence data in a public health laboratory enables the identification of pathogenic strains, the determination of relatedness among outbreak strains, and the analysis of genetic information regarding virulence and antimicrobial-resistance genes. However, the analysis of whole-genome sequence data depends on bioinformatic analysis tools and processes. Many public health laboratories do not have the bioinformatic capabilities to analyze the data generated from sequencing and therefore are unable to take full advantage of the power of whole-genome sequencing. The goal of this perspective is to provide a guide for laboratories to understand the bioinformatic analyses that are needed to interpret whole-genome sequence data and how these in silico analyses can be implemented in a public health laboratory setting easily, affordably, and, in some cases, without the need for intensive computing resources and infrastructure.

Next-generation sequencing (NGS), also known as high-throughput sequencing, has affected many fields in the study of biology but has dramatically changed the field of genomics by enabling researchers to quickly sequence whole microbial genomes, profile gene expression by sequencing RNA, examine host–pathogen interactions, and study the vast microbial diversity in humans and the environment (1). Despite the benefits of NGS over traditional Sanger sequencing methods, public health laboratories (PHLs) have been slow to implement this revolutionary technology. According to the Association of Public Health Laboratories, no PHLs had NGS capabilities before 2010 (2). The Centers for Disease Control and Prevention (CDC), through its Advanced Molecular Detection program, has supported the adoption of NGS and whole-genome sequencing (WGS) by providing funding and training to PHLs. By the end of 2015, CDC's support had enabled 37 PHLs to acquire NGS instrumentation, with another 9 PHLs gaining NGS technology by the end of 2016 (2).

Author affiliation: Utah Department of Health, Utah Public Health Laboratory, Taylorsville, Utah, USA

For laboratory surveillance of foodborne diseases, pulse-field gel electrophoresis (PFGE) is currently the preferred method for typing bacterial isolates and is widely used in outbreak investigations and source tracking. PFGE has been the backbone of the success of CDC's PulseNet program since 1997 (3,4). However, the PulseNet program is aiming to replace PFGE with WGS by 2018. This trajectory resembles the path taken in the study of human genetics, in which genetic mapping based on restriction fragment length polymorphism was replaced by quasi-complete information obtained by high-throughput genomic sequencing. Although restriction fragment length polymorphism markers initially enabled the measurement of genetic distance and laid the foundation for linkage mapping, its success depended on pronounced phenotypic effects of the underlying trait and regularly dispersed markers. Once linkage to a region was identified, causality could be pinpointed through fine mapping. WGS provided not only a complete marker-map with maximum resolution at the nucleotide level but also enabled the deduction of causality and direct testing of genetic relatedness and genetic origination. The promise of this approach also extended to the study of pathogens, given that WGS ultimately enables testing of specific hypotheses regarding genotype-phenotype relationships (e.g., antimicrobial drug resistance). However, although more PHLs are adopting NGS and WGS, only a small number of these laboratories have the ability to perform the bioinformatic analyses needed to take full advantage of the data they are generating. CDC aids PHLs in conducting foodborne disease surveillance on a national scale but is unable to assist with data analysis for local foodborne disease surveillance.

Some of the obstacles preventing PHLs from implementing the bioinformatic-dependent analysis are the requirements for large-scale computational capabilities, complex molecular evolutionary analyses, and dedicated bioinformatics staff to perform these analyses. However, all that is really needed is a computer with a browser and a connection to the Internet. Web-based tools are available for PHLs that are looking to participate in WGS data analysis but are not ready to perform analyses in-house. Several of these tools are open-source (i.e., free of charge) and can

be used to perform a range of bioinformatics analyses. Two of these tools are Illumina's BaseSpace Sequence Hub (Illumina, Inc., San Diego, CA, USA) and the Galaxy web-based platform (5).

Because many PHLs are already using Illumina's MiSeq sequencing platform, BaseSpace is a convenient solution that enables users to monitor the progress of sequencing runs, share data easily with others, and use 1 terabyte (TB) of data storage free of charge. Illumina provides new users with a 30-day free trial of BaseSpace, enabling users to use all of the wide-ranging bioinformatic tools available.

The Galaxy platform enables users to perform analyses ranging from sequence quality control and timing to whole-genome assemblies (5). Galaxy also enables users to track the details of each step of an analysis, making it easier to reproduce and publish the results. Galaxy enables non-experts to perform advanced and computationally intensive analyses without having training in bioinformatics.

However, neither BaseSpace nor Galaxy is without drawbacks. Uploading or downloading the large files generated by NGS can be slow and might fail before finishing, requiring the entire upload or download process to be restarted. Web-based tools can also be "black boxes" where users may not know exactly what each step of the analysis is, why that step is being performed, or why results might be difficult to understand or interpret. These web-based tools might seem quick and easy to use but often do not perform as expected.

Bioinformatic analyses are often performed in a stepwise manner, with the output of 1 analysis being used as the input for the next. These multistep, multisoftware analyses are frequently referred to as pipelines and are often set up to run automatically from 1 step to the next without input from the user. In this perspective, we describe the bioinformatic pipeline implemented at the Utah Public Health Laboratory (UPHL) to analyze the WGS data. Sharing our experiences with this pipeline will enable PHLs to implement their own pipelines by following each step in our pipeline or by using our pipeline as a template to construct their own unique processes. All the software used in our bioinformatics pipeline are open-source and are available free of charge (online Technical Appendix Table 1, https://wwwnc.cdc.gov/EID/article/23/9/17-0416-Techapp1.xlsx). We present these

analyses as a function of the level of technology required, spanning everything from basic quality control performed on typical desktop or laptop computer to complex molecular evolutionary analyses that require powerful high-end Linux servers or workstations.

Bioinformatic Pipeline

The bioinformatic pipeline developed and implemented at UPHL consists of 8 steps (Figure): 1) read quality control, 2) reference strain determination, 3) read mapping to the reference strain, 4) single-nucleotide polymorphism (SNP) and small insertion or deletion (indel) detection, 5) de novo genome assembly, 6) genome annotation, 7) phylogenetic tree construction, and 8) phylogenetic analysis. Although such processes are standard, several software solutions are available for the respective steps.

The first step in almost all WGS bioinformatics analyses is quality control of the raw sequencing data. It is important to remove poor-quality sequence data and technical sequences (i.e., adapter sequences). Highly accurate sequences are required for SNP detection, enabling the detection of actual SNPs and distinguishing from sequencing artifacts. Quality control in our pipeline is performed by using Trimmomatic (6), a multithreaded command line tool that removes adapter sequences, trims low-quality sequence from the beginning or end of a sequence, removes reads that fall below a user-defined threshold for length, and validates paired-end sequence reads.

The second step in the pipeline is reference sequence determination. To determine SNPs, a reference sequence is needed against which to compare sequencing reads. The choice of reference sequence might have a substantial effect on the number and type of SNPs that are detected, making this step important. We use Mash for reference sequence determination (7). Mash enables us to quickly compare the large set of sequencing reads generated against the reference set of 54,118 National Center for Biotechnology Information RefSeq genomes (https://www.ncbi.nlm.nih.gov/refseq) to determine nucleotide distance and relatedness (8).

Once a reference sequence is determined, the next step in the analysis pipeline is mapping the quality-controlled sequencing reads to the reference genome. We perform
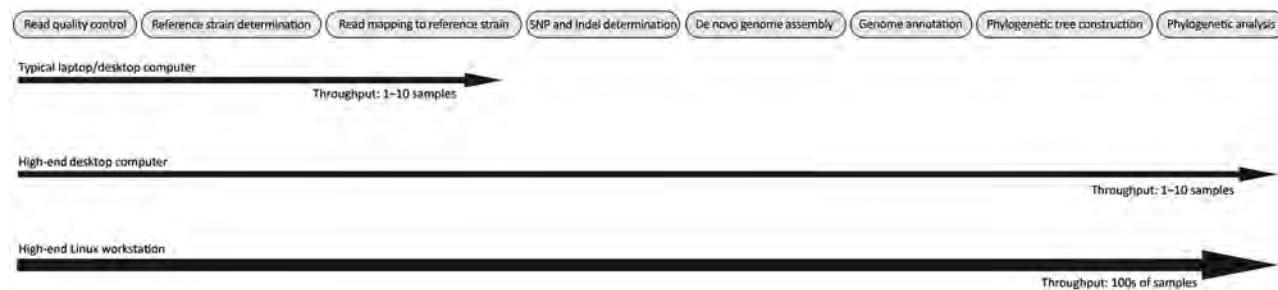
Figure. Steps in the bioinformatics pipeline implemented at Utah Public Health Laboratory.

read mapping by using the Burrows-Wheeler Aligner (BWA) software package with the bwa-mem option (*9*). BWA uses a Burrow-Wheeler Transform to efficiently align sequencing reads to reference genomes allowing for gaps and mismatches. The output of BWA is the standard sequence alignment map format known as SAM, which facilitates the next step in the pipeline.

The fourth step in the pipeline uses mapping of the sequencing reads to the reference sequence to identify SNPs and indels. We perform SNP and indel determination by using SAMtools and VarScan2, which also calculate SNP frequency in the sequence data (*10,11*). The output of VarScan2 can be easily viewed in the Integrative Genomics Viewer, which enables the interactive viewing of large genomic datasets (*12*). The output file of VarScan2 can also be used in more complex downstream analyses (i.e., to build SNP matrixes and phylogenetic trees).

The quality-controlled sequencing reads are then used for de novo genome assembly in the sixth step of the pipeline. We perform de novo genome assembly on individual isolates by using the St. Petersburg genome assembler, also known as SPAdes (*13,14*). The SPAdes assembler has 3 modules: sequencing read error correction; SPAdes assembly; and a mismatch corrector module. The first module error corrects the quality-controlled sequencing reads by using advanced algorithms based on Hamming graphs and Bayesian subclustering. Sequencing error correction in this manner has shown to dramatically improve genome assemblies of NGS data (*15*). The SPAdes assembly module uses the error-corrected reads and performs the actual assembly in an iterative manner making use of de Bruijn graphs. The resulting genome assembly is then used as input for the third module, which greatly reduces the number of mismatches and small indels by using BWA and results in highly accurate contigs (contiguous sequence data made up of overlapping sequencing reads) and scaffolds (ordered and oriented contigs based on paired-end read data).

We then annotate the resulting genome assembly to identify protein-coding genes, tRNAs, and rRNAs. We use Prokka for annotation of protein-coding genes, tRNA, and rRNA on the contigs and scaffolds generated by SPAdes (*16*). Prokka can fully annotate a bacterial genome in approximately 10 minutes on a high-end quad-core desktop computer by making use of a suite of existing software, tools, and sequence databases, such as UniProt (*17*) and NCBI RefSeq (*8*).

We then use shared orthologous genes to construct phylogenetic trees that provide insight into the relatedness of isolates. Once multiple genomes have been annotated, we calculate the pan genome of the combined genomes by using Roary (*18*). The pan genome consists of the union of genes shared by genomes of interest, and Roary can compute the pan genome of 1,000 bacterial genomes on a single CPU computer in 4.5 hours (*19*). In addition to determining the pan genome of the genomes of interest, Roary also generates a concatenated nucleotide alignment of the pan genome, which can be used to build a phylogenetic tree of these sequences. This pan genome alignment is used as the input to RAxML for phylogenetic tree construction (*20*). RAxML is a program that has been designed and optimized for conducting phylogenetic analyses on large datasets by using maximum-likelihood techniques to estimate evolutionary trees from nucleic acid sequence data (*21*).

The last step in the pipeline is phylogenetic analyses. These analyses can detect a signature of selection on individual genes and provide knowledge about the evolutionary forces acting on the genes of the sequenced isolates. The pan genome alignment can also be used to detect signatures of selection by calculating the ratio of the number of nonsynonymous substitutions per nonsynonymous site to the number of synonymous substitutions per synonymous site. The value of this ratio is used to infer the direction and magnitude of natural selection, with values >1 implying positive selection (i.e., driving change), values <1 implying purifying selection (i.e., acting against change), and values of exactly 1 indicating neutral selection (i.e., no selection). To determine the ratios for detecting signatures of selection, we use the YN00 model (*22*) implemented in the PAML software package (*23*). The PAML results are a plain text file that can be viewed in any word processor or imported into statistical analysis software, such as R, for further analysis or plotting.

Laptop or Desktop Hardware

The bioinformatic pipeline we describe can be partitioned as a function of computer resources (i.e., the number of CPUs, the amount of RAM, and the amount of storage space). Typical laptop or desktop computers might only have enough power to perform the first steps in the pipeline, whereas a high-end workstation would have enough power to perform all the steps for hundreds of samples at once. In many cases, the limiting factor is how much RAM a computer has. Many of the more complex steps in the pipeline require large amounts of RAM, often more than what many laptops and desktops can hold. All the software described can easily be installed and run on a typical desktop or laptop computer (Figure). At UPHL, we performed steps 1–4 of the described analyses on bacterial isolates by using an Apple MacBook Pro laptop (Apple, Inc., Cupertino, CA, USA) with a single 3.2-GHz Intel Core i5 processor, 16 gigabytes (GB) of RAM, and 500 GB of storage space (online Technical Appendix Table 2). Many PHLs might already have the computational resources needed to perform these bioinformatic analyses on a small number of samples in a reasonable amount of time. However, some basic command-line instructions would be needed to execute software. Numerous online resources, many of them free, will help novices learn the basics of the command-line interface.

One such resource is the Biostar Handbook (https://www. biostarhandbook.com). This online document and e-book is an excellent resource that introduces bioinformatics and covers all of the major areas of focus in bioinformatics, including a crash course in the command-line interface.

High-end Desktop Hardware

Computers with an increased number of processing cores, more RAM, and more storage space than the typical desktop or laptop computer will allow PHLs to perform all the analyses described here as well as more advanced and computationally intensive analyses (Figure). High-end desktops are relatively inexpensive to purchase, and it might be possible to upgrade desktops a PHL already has. All the analyses we describe here were performed at UPHL on an Apple iMac equipped with a single 3.2-GHz Intel Core i5 processor, 32 GB of RAM, and 2 TB of storage space (online Technical Appendix Table 2). For 10 isolates, the analyses took ≈5 days to complete. Theoretically, the number of isolates that could be analyzed can be increased to up to hundreds of isolates on a similar high-end desktop computer; however, the amount of time to perform these analyses would also increase substantially.

Beyond High-end Desktop Hardware

With a high-end Linux-based workstation (http://www. linux.org) and a network-attached storage array, several hundred genomes can be analyzed in a reasonable timeframe (Figure). At UPHL, we invested in a high-end Hewlett-Packard workstation (HP, Inc., Palo Alto, CA, USA) with four 3.0-GHz Intel Xeon processors (Intel Corp., Santa Clara, CA, USA), each 3.0 GHz with 12 processing cores; 256 GB of RAM; and a Synology network-attached storage array (Synology, Inc., Taipei, Taiwan) with 24 TB of storage (online Technical Appendix Table 2). With such a system and bioinformatics personnel in place, hundreds of genomes can be generated and analyzed in 2–3 days, providing near real-time results for disease outbreak surveillance and monitoring. In addition to high-end computer hardware, experienced personnel are needed to deploy, maintain, curate, and automate bioinformatics pipelines (i.e., bioinformaticians). To take full advantage of computational resources, programs should be automated and linked together so that as data are generated by the sequencer, they are automatically added to the bioinformatics pipelines.

Discussion

With NGS becoming more and more important for public health laboratories, the need for bioinformatic analyses in greatly increasing. Unfortunately, the pace of WGS implementation is far outpacing the number of bioinformaticians being hired to work in PHLs and, understandably, not all PHLs will have the need, desire, or financial capacity to hire a full-time bioinformatician. The objective of this perspective is to show that bioinformatic analyses can be performed on everything from a simple laptop to a high-end Linux workstation and the user can have little to no experience in bioinformatics or can be a full-fledged bioinformatician. As the volume of sequencing data increases, the ability to connect phenotype to genotype becomes a reality. Knowing a priori that a microorganism is likely to be resistant to antimicrobial drugs or could be a highly virulent strain would greatly improve patient outcomes, improve outbreak surveillance, and help prioritize resources to combat outbreaks. By using molecular evolutionary analyses, PHLs can investigate the evolution of antimicrobial-resistance genes to track in near real-time mutations that are linked to newly acquired resistance genes or novel mutations that result in resistance.

NGS has the potential to revolutionize public health. NGS is not only replacing PFGE, but has the potential to replace traditional culture-based testing as well. Culture-independent diagnostic testing though metagenomic sequencing and analysis has the ability to quickly identify pathogens without applying any type of selection.

References

1. Koboldt DC, Steinberg KM, Larson DE, Wilson RK, Mardis ER. The next-generation sequencing revolution and its impact on genomics. Cell. 2013;155:27–38. http://dx.doi.org/10.1016/j.cell.2013.09.006
2. Bahassi M, Stambrook PJ. Next-generation sequencing technologies: breaking the sound barrier of human genetics. Mutagenesis. 2014;29:303–10. http://dx.doi.org/10.1093/mutage/geu031
3. Scharff RL, Besser J, Sharp DJ, Jones TF, Peter G-S, Hedberg CW. An economic evaluation of PulseNet: a network for foodborne disease surveillance. Am J Prev Med. 2016;50(Suppl 1):S66–73. http://dx.doi.org/10.1016/j.amepre.2015.09.018
4. Swaminathan B, Barrett TJ, Hunter SB, Tauxe RV; CDC PulseNet Task Force. PulseNet: the molecular subtyping network for foodborne bacterial disease surveillance, United States. Emerg Infect Dis. 2001;7:382–9. http://dx.doi.org/10.3201/eid0703.017303
5. Afgan E, Baker D, van den Beek M, Blankenberg D, Bouvier D, Čech M, et al. The Galaxy platform for accessible, reproducible and collaborative biomedical analyses: 2016 update. Nucleic Acids Res. 2016;44(W1):W3–10. http://dx.doi.org/10.1093/nar/gkw343
6. Bolger AM, Lohse M, Usadel B. Trimmomatic: a flexible trimmer for Illumina sequence data. Bioinformatics. 2014;30:2114–20. http://dx.doi.org/10.1093/bioinformatics/btu170

7. Ondov BD, Treangen TJ, Melsted P, Mallonee AB, Bergman NH, Koren S, et al. Mash: fast genome and metagenome distance estimation using MinHash. Genome Biol. 2016;17:132. http://dx.doi.org/10.1186/s13059-016-0997-x

8. O'Leary NA, Wright MW, Brister JR, Ciufo S, Haddad D, McVeigh R, et al. Reference sequence (RefSeq) database at NCBI: current status, taxonomic expansion, and functional annotation. Nucleic Acids Res. 2016;44(D1):D733–45. http://dx.doi.org/10.1093/nar/gkv1189

9. Li H, Durbin R. Fast and accurate short read alignment with Burrows-Wheeler transform. Bioinformatics. 2009;25:1754–60. http://dx.doi.org/10.1093/bioinformatics/btp324

10. Li H, Handsaker B, Wysoker A, Fennell T, Ruan J, Homer N, et al.; 1000 Genome Project Data Processing Subgroup. The Sequence Alignment/Map format and SAMtools. Bioinformatics. 2009;25:2078–9. http://dx.doi.org/10.1093/bioinformatics/btp352

11. Koboldt DC, Zhang Q, Larson DE, Shen D, McLellan MD, Lin L, et al. VarScan 2: somatic mutation and copy number alteration discovery in cancer by exome sequencing. Genome Res. 2012;22:568–76. http://dx.doi.org/10.1101/gr.129684.111

12. Thorvaldsdóttir H, Robinson JT, Mesirov JP. Integrative Genomics Viewer (IGV): high-performance genomics data visualization and exploration. Brief Bioinform. 2013;14:178–92. http://dx.doi.org/10.1093/bib/bbs017

13. Bankevich A, Nurk S, Antipov D, Gurevich AA, Dvorkin M, Kulikov AS, et al. SPAdes: a new genome assembly algorithm and its applications to single-cell sequencing. J Comput Biol. 2012;19:455–77. http://dx.doi.org/10.1089/cmb.2012.0021

14. Nurk S, Bankevich A, Antipov D, Gurevich AA, Korobeynikov A, Lapidus A, et al. Assembling single-cell genomes and mini-metagenomes from chimeric MDA products. J Comput Biol. 2013;20:714–37. http://dx.doi.org/10.1089/cmb.2013.0084

15. Nikolenko SI, Korobeynikov AI, Alekseyev MA. BayesHammer: Bayesian clustering for error correction in single-cell sequencing. BMC Genomics. 2013;14(Suppl 1):S7. http://dx.doi.org/ 10.1186/1471-2164-14-S1-S7

16. Seemann T. Prokka: rapid prokaryotic genome annotation. Bioinformatics. 2014;30:2068–9. http://dx.doi.org/10.1093/bioinformatics/btu153

17. The UniProt Consortium. UniProt: the universal protein knowledgebase. Nucleic Acids Res. 2017;45(D1):D158–69. http://dx.doi.org/10.1093/nar/gkw1099

18. Page AJ, Cummins CA, Hunt M, Wong VK, Reuter S, Holden MTG, et al. Roary: rapid large-scale prokaryote pan genome analysis. Bioinformatics. 2015;31:3691–3. http://dx.doi.org/10.1093/bioinformatics/btv421

19. Vernikos G, Medini D, Riley DR, Tettelin H. Ten years of pan-genome analyses. Curr Opin Microbiol. 2015;23:148–54. http://dx.doi.org/10.1016/j.mib.2014.11.016

20. Stamatakis A. RAxML version 8: a tool for phylogenetic analysis and post-analysis of large phylogenies. Bioinformatics. 2014;30:1312–3. http://dx.doi.org/10.1093/bioinformatics/btu033

21. Felsenstein J. Evolutionary trees from DNA sequences: a maximum likelihood approach. J Mol Evol. 1981;17:368–76. http://dx.doi.org/10.1007/BF01734359

22. Yang Z, Nielsen R. Estimating synonymous and nonsynonymous substitution rates under realistic evolutionary models. Mol Biol Evol. 2000;17:32–43. http://dx.doi.org/10.1093/oxfordjournals.molbev.a026236

23. Yang Z. PAML 4: phylogenetic analysis by maximum likelihood. Mol Biol Evol. 2007;24:1586–91. http://dx.doi.org/10.1093/molbev/msm088

Address for correspondence: Kelly F. Oakeson, Utah Department of Health–Utah Public Health Laboratory, 4431 S Constitution Blvd, Taylorsville, Utah 84192, USA; email: koakeson@utah.gov

December 2016: Zoonotic Infections

- Investigation of and Response to 2 Plague Cases, Yosemite National Park, California, USA, 2015

- Anomalous High Rainfall and Soil Saturation as Combined Risk Indicator of Rift Valley Fever Outbreaks, South Africa, 2008–2011

- Cutaneous Granulomas in Dolphins Caused by Novel Uncultivated *Paracoccidioides brasiliensis*
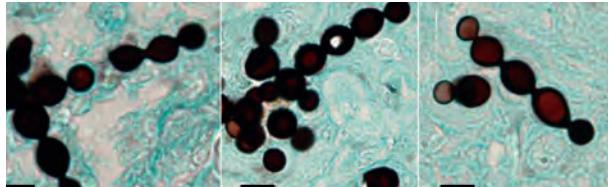
- Vertebrate Host Susceptibility to Heartland Virus

- African Horse Sickness Caused by Genome Reassortment and Reversion to Virulence of Live, Attenuated Vaccine Viruses, South Africa, 2004–2014

- *Streptococcus agalactiae* Serotype IV in Humans and Cattle, Northern Europe

- Effect of Live-Poultry Market Interventions on Influenza A(H7N9) Virus, Guangdong, China

- Baylisascaris procyonis Roundworm Seroprevalence among Wildlife Rehabilitators, United States and Canada, 2012–2015

- Genetically Different Highly Pathogenic Avian Influenza A(H5N1) Viruses in West Africa, 2015

- Highly Divergent Dengue Virus Type 2 in Traveler Returning from Borneo to Australia

- Highly Pathogenic Reassortant Avian Influenza A(H5N1) Virus Clade 2.3.2.1a in Poultry, Bhutan

- Horizontal Transmission of Chronic Wasting Disease in Reindeer

- Human Infection with Novel Spotted Fever Group Rickettsia Genotype, China, 2015

- Detection of Vaccinia Virus in Dairy Cattle Serum Samples from 2009, Uruguay

- Tick-Borne Relapsing Fever, Southern Spain, 2004–2015

- Tuberculosis-Associated Death among Adult Wild Boars, Spain, 2009–2014

EMERGING INFECTIOUS DISEASES

Convergence of Humans, Bats, Trees, and Culture in Nipah Virus Transmission, Bangladesh

Emily S. Gurley,[1] Sonia T. Hegde,[2] Kamal Hossain, Hossain M.S. Sazzad, M. Jahangir Hossain,[3] Mahmudur Rahman, M.A. Yushuf Sharker,[4] Henrik Salje, M. Saiful Islam, Jonathan H. Epstein, Salah U. Khan, A. Marm Kilpatrick, Peter Daszak, Stephen P. Luby

Preventing emergence of new zoonotic viruses depends on understanding determinants for human risk. Nipah virus (NiV) is a lethal zoonotic pathogen that has spilled over from bats into human populations, with limited person-to-person transmission. We examined ecologic and human behavioral drivers of geographic variation for risk of NiV infection in Bangladesh. We visited 60 villages during 2011–2013 where cases of infection with NiV were identified and 147 control villages. We compared case villages with control villages for most likely drivers for risk of infection, including number of bats, persons, and date palm sap trees, and human date palm sap consumption behavior. Case villages were similar to control villages in many ways, including number of bats, persons, and date palm sap trees, but had a higher proportion of households in which someone drank sap. Reducing human consumption of sap could reduce virus transmission and risk for emergence of a more highly transmissible NiV strain.

Emerging zoonoses pose a substantial threat to human health and well-being (*1*). Some of the most devastating human disease pandemics have been caused by diseases originating in livestock or wildlife, including HIV infection, influenza, bubonic plague, and a large Ebola outbreak in West Africa (*1,2*). For this reason, there is considerable scientific and public health interest in predicting which emerging pathogens have the potential to cause pandemics so that these pandemics can be prevented. Emerging lethal zoonotic pathogens that have crossed the species barrier and can be transmitted from 1 person to another, albeit without sustained person-to-person transmission, are particularly concerning because they could evolve to become more highly transmissible and cause large outbreaks or pandemics (*3*). It is therefore critical to focus resources on limiting the opportunity of these pathogens to spillover from wildlife and livestock to infect persons and to better adapt to human hosts.

Effectively preventing cross-species transmission of zoonotic pathogens depends on our ability to determine how transmission occurs, including transmission pathways and determinants of human risk. Efforts to identify and predict risky geographic areas for emerging zoonoses have focused primarily on publicly available data, remote sensing of species habitat, and other large-scale population measures (*4,5*). A major limitation of these risk mapping approaches is that they typically rely on crude measures of spatial risk, including presence or absence of species or population densities. Human behavior patterns are rarely taken into account, although the risk for transmission probably involves complex, time-varying interactions between humans and their environment that are often driven by culture, climate, and economic development (*1,6,7*).

Infection with Nipah virus (NiV), an emerging zoonotic pathogen, can cause encephalitis in humans; the virus can also be transmitted between humans, although somewhat inefficiently (*8*). NiV was first identified as the etiologic agent causing outbreaks in pigs and encephalitis in humans in Malaysia and Singapore during 1998–1999 (*9*). Shortly thereafter, this virus was identified as the cause of outbreaks of human encephalitis in Bangladesh and India

Author affiliations: icddr,b, Dhaka, Bangladesh (E.S. Gurley, S.T. Hegde, K. Hossain, H.M.S. Sazzad, M.J. Hossain, M.A. Yushuf Sharker, M.S. Islam, S.U. Khan, S.P. Luby); Centers for Disease Control and Prevention, Atlanta, Georgia, USA (S.T. Hegde, S.P. Luby); Ministry of Health and Family Welfare, Bangladesh, Dhaka (M. Rahman); Johns Hopkins Bloomberg School of Public Health, Baltimore, Maryland, USA (H. Salje); Institut Pasteur, Paris, France (H. Salje); EcoHealth Alliance, New York, New York, USA (J.H. Epstein, P. Daszak); University of Florida, Gainesville, Florida, USA (S.U. Khan); University of California, Santa Cruz, California, USA (A.M. Kilpatrick); Stanford University, Stanford, California, USA (S.P. Luby)

[1]Current affiliation: Johns Hopkins Bloomberg School of Public Health, Baltimore, Maryland, USA.

[2]Current affiliation: University of Michigan School of Public Health, Ann Arbor, Michigan, USA.

[3]Current affiliation: Medical Research Council, Banjul, The Gambia.

during 2001 (*10,11*). Nearly every year since 2001, NiV has caused outbreaks among humans in Bangladesh; cases are also reported in bordering areas of India (*12*). Initial spillovers during these outbreaks have been amplified by person-to-person transmission; the largest of these outbreaks involved 66 persons, primarily patients and healthcare workers, in Siliguri, India, in 2001 (*10*). In addition, an outbreak in Faridpur, Bangladesh, in 2004 involved 5 generations of transmission (*13*). Although the case-fatality rate for patients in Malaysia and Singapore was ≈40%, it exceeds 70% in Bangladesh and India (*12*).

The natural reservoir for NiV is Old World fruit bats of the genus *Pteropus*, which are found in eastern Africa and throughout Asia, Australia, and the Pacific islands (*14,15*). Antibodies against NiV or NiV-like viruses have been found in pteropid bats throughout Asia, including Malaysia, Thailand, Cambodia, India, and Bangladesh (*16–20*). *Pteropus medius* (formerly *P. giganteus*) is the only pteropid bat species present in India and Bangladesh and is the putative reservoir for NiV in this region (*21*). The widespread evidence of henipavirus infection in *Pteropus* bats suggests that this virus may have co-evolved with bats and has probably been present in these areas for as long as the bats have been there. Infected bats shed NiV in their saliva and urine (*22,23*), and spillover might occur between humans and bats throughout this region. Types of contact that could result in NiV transmission include hunting bats for human consumption; living nearby and under bat roosts; and sharing food resources, including bats drinking date palm sap and humans consuming fruit partially eaten by bats (*8,16,24*). Despite this information, the geographic scope and scale of reported cases of infection with NiV remains limited: only Bangladesh regularly reports cases (*25*). Furthermore, even within Bangladesh, there is unexplained substantial spatial heterogeneity in case occurrence; virtually all cases are detected in the central and northwestern parts of the country (Figure 1) (*25*).

The purpose of our study was to identify differences in endogenous risk and risky human behavior across these areas that drive these human disease patterns. Outbreak investigations in Bangladesh showed that a major risk factor for NiV infection was consumption of raw date palm sap, a national delicacy (*12*). Date palm trees (*Phoenix sylvestris*) are tapped overnight to collect the sap in clay pots, and the sweet sap is retrieved from the tree first thing in the morning and drunk raw (*26*). Wildlife studies have shown that date palm sap is commonly consumed by *Pteropus* bats, particularly during winter months when other fruits are not available (*27*). We sought to understand causes of geographic variation in NiV transmission from bats to humans across Bangladesh. We performed a large-scale, case–control study that used villages as study units and quantified the distribution of bats, humans, date palm sap trees, and human behavior that might influence interactions with bats, such as date palm sap harvesting and consumption.

Methods

Data Collection

We conducted a village-level case–control study to identify characteristics associated with NiV transmission from bats to humans in Bangladesh. Case villages were those in which human infections were identified during 2001–2012 with no evidence that the source of infection was another
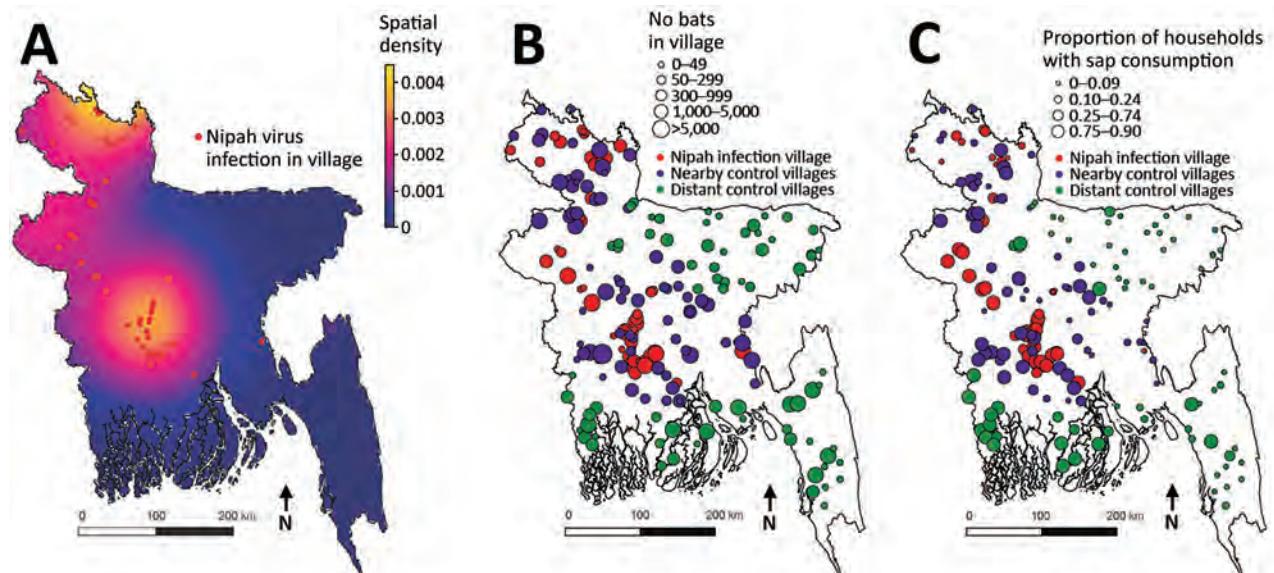
Figure 1. A) Locations of identified bat-to-human transmission of Nipah virus and spatial intensity of transmission events, Bangladesh, 2001–2012. B) Relative sizes of the *Pteropus medius* bat populations in case and control villages (including within 5 km of each village). C) Proportion of households in case and control villages with persons who regularly consume fresh date palm sap.

human case of infection with NiV and thus was probably caused by spillover from bats. We mapped these case villages and drew 50-km buffers around them to define the area of Bangladesh to which NiV was endemic (Figure 1, panel B). This distance chosen was arbitrary but reasonably represents the distance that a person could travel within a day, even without access to good roads, and is within the typical nightly foraging radius of *Pteropus* bats, which has been observed as 20–50 km (*28–30*). We then selected control villages by randomly generating 2 sets of geographic points on a map. The first set was chosen from within the area to which NiV was endemic (nearby controls) but >5 km from a case village. The second set was chosen from points >50 km from case villages (distant controls). We chose control villages near and distant from villages with cases of infection with NiV to determine if characteristics driving transmission were different at varying spatial scales. We sought to enroll 75 controls from nearby villages and 75 controls from distant villages.

Our approach for identifying control villages could have misclassified some villages where cases of infection with NiV have occurred but gone undetected. However, all outbreaks due to NiV have been observed exclusively in the part of the country that includes our case and nearby control villages, despite the fact that surveillance for outbreaks frequently identifies outbreaks of other diseases throughout the country (*31*).

We collected data for study villages at 2 time points: during December 2011–February 2012 and during December 2012–February 2013. These times were chosen to align our surveys with the season that has a high incidence NiV infection in Bangladesh (*12*). Trained data collection teams used hand-held devices to identify the latitude and longitude of the randomly selected points and enrolled the village with that coordinate or the village located closest to that point as a control village. Teams visited case and control villages and identified a group of key village informants who assisted with mapping the village boundary and estimating the number of households located in each village. The teams then asked local residents to identify all of the bat roosts they knew of in their village and within 5 km of the village boundary. Trained data collectors located all of the roosts and counted the number of *Pteropus* bats roosting. In addition, they counted all date palm sap trees in the village and within 500 m of the village boundary.

We then requested that 25 randomly selected households from each village participate in a structured survey. After identifying the village boundary, the field team used a random number table to choose a cardinal direction: north, east, south, or west. The household on the edge of the village in that direction was approached for participation. The team then divided the estimated number of households in the village by the desired sample size (25) and skipped that

number of households to choose the next for participation. This process continued until 25 households were enrolled. For villages with <25 households, all households were enrolled. Data collectors administered the structured survey to an adult household member to obtain data for household demographics, date palm sap consumption practices, experience with observing and hunting bats, number of fruiting trees on their household premises, and behavior regarding eating fruit with animal bite marks off the ground.

Data Analysis

To estimate the number of persons in each village, we multiplied the number of estimated households in each village by the mean number of household residents in households sampled for the study from that particular village. We measured data for each village by direct observation, such as the number of bats roosting, or through the surveys at sampled households. We compared case villages to both sets of controls in terms of human and bat population size, as well as human behavior patterns regarding date palm sap and fruit consumption.

We estimated means and proportions with 95% CIs and compared case and control villages by using generalized linear models with binomial distributions and a logit link, which used robust variance estimates to account for model misspecification. For exposures measured at the household level, we accounted for clustering within the village in the model. Analyses were conducted by using the generalized linear model package in Stata version 13.0 (StataCorp LLC, College Station, TX, USA). Variables that were highly skewed were log-transformed to equalize leverage.

We used multivariable logistic regression models to estimate independent associations (odds ratios with 95% CIs) between village characteristics and being a village with a case of NiV infection. For multivariable regression, each village had 1 value for each exposure, and household-level data from each village was aggregated to estimate the proportion of all village households reporting each exposure or behavior. Therefore, we did not need to account for clustering of observations, but we did calculate the 95% CIs for the odds ratios by using robust variance to account for imprecision in exposures estimated from a sample of households. We first built an inclusive model comparing each set of controls to the case villages on the basis of our a priori hypothesis that NiV spillover risk is determined by human population, number of bats present, number of date palm trees, and proportion of persons in the village who commonly consumed raw date palm sap. In addition, any other behavior patterns that were associated with an increased risk for NiV spillover by univariable analysis were also included in the model. Associations were considered statistically significant if p values were <0.05.

Ethical Considerations

All study participants provided informed consent before participation. The study protocol was reviewed and approved by the institutional review board of the icddr,b.

Results

Data collection teams visited all 60 case villages and 73 nearby control villages and 74 distant control villages where they surveyed 5,024 persons (Figure 1, panel B). Three selected control villages could not be visited because of local security concerns or logistical constraints.

Villages that had cases of infection with NiV were similar to nearby and distant control villages for most characteristics, including human population, bat population, and number of date palm sap trees (Table 1; Figure 2). However, both groups of control villages had a lower proportion of households who reported that ≥1 person commonly drank fresh date palm sap than households in case villages (61% in case villages vs. 49% in nearby control villages and 31% in distant control villages) (Table 1; Figure 1, panel C; Figure 2).

In addition, the average number of household residents who drank ≥1 glass of raw sap when it was in season

Table 1. Characteristics of villages with cases of Nipah virus infection and control villages, Bangladesh 2011–2013*

Characteristic	Villages with cases, n = 60	Nearby control villages, n = 73	p value†	Distant control villages, n = 74	p value‡
Human population					
No. persons in village	1,476 (1,202–1,749)	1,389 (1,102–1,676)	0.20	1,392 (1,010–1,774)	0.10
No. persons/km²	1,168 (1,167–2,169)	1,173 (592–1,754)	0.78	1,335 (456–2,213)	0.95
Pteropus bat population					
Proportion of villages where *P. medius* bats were observed roosting in village or within 5 km of village boundary	0.85 (0.76–0.94)	0.86 (0.78–0.94)	0.86	0.76 (0.66–0.86)	0.19
No. bats roosting in village or within 5 km of village boundary	554 (319–789)	620 (364–875)	0.60	407 (226–587)	0.37
Proportion of respondents reporting large fruit bats					
Roosted nearby during the day in past month	0.25 (0.17–0.34)	0.37 (0.29–0.45)	0.060	0.40 (0.31–0.49)	0.024
Fly overhead at dusk	0.51 (0.43–059)	0.64 (0.56–0.70)	0.019	0.77 (0.71–0.83)	<0.001
Visit fruit trees at night	0.43 (0.35–0.51)	0.52 (0.45–0.60)	0.10	0.53 (0.45–0.61)	0.090
Date palm sap and fruiting trees					
No. trees in village or within 500-m radius of village boundary	120 (88–152)	95 (78–111)	0.91	101 (65–138)	0.14
Proportion of households with fruiting trees on premises	0.97 (0.94–0.99)	0.97 (0.94–0.98)	0.81	0.94 (0.92–0.96)	0.14
No. fruiting trees on each household premise	56 (46–68)	52 (43–61)	0.81	108 (45–170)	0.47
Human behavior					
Proportion of villages with ≥1 date palm sap collector	0.60 (0.47–0.63)	0.40 (0.29–0.52)	0.026	0.51 (0.40–0.63)	0.32
No. sap collectors in villages	4.5 (1.8–7.3)	2.3 (1.0–3.6)	0.41	3.7 (1.9–5.6)	0.54
Proportion of villages with ≥1 fresh date palm sap seller	0.38 (0.28–0.51)	0.32 (0.21–0.43)	0.45	0.39 (0.26–0.51)	0.92
No. (%) fresh sap sellers in villages	1.9 (0.6)	0.9 (0.2)	0.16	2.4 (0.6)	0.47
Proportion of households where ≥1 person drank raw sap	0.61 (0.54–0.68)	0.49 (0.42–0.56)	0.014	0.31 (0.24–0.39)	<0.001
Proportion of households where someone drank raw sap >1×/wk during the past harvest season	0.35 (0.27–0.43)	0.29 (0.23–0.35)	0.26	0.21 (0.16–0.27)	0.005
No. household residents who drank ≥1 glass of raw date palm sap when in season	3.3 (2.7–3.9)	2.1 (1.8–2.5)	0.001	1.5 (1.1–1.9)	<0.001
Proportion of villages where >1 household fed raw date palm sap to livestock	0.16 (0.10–0.21)	0.12 (0.06–0.18)	0.66	0.14 (0.08–0.21)	0.78
Proportion of villages where ≥1 person hunted bats	0.53 (0.40–0.66)	0.64 (0.53–0.75)	0.22	0.27 (0.17–0.38)	0.002
Proportion of households that reported residents ate bitten fruits dropped on the ground	0.42 (0.37–0.48)	0.58 (0.53–0.62)	<0.001	0.66 (0.61–0.71)	<0.001

*Values are mean (95% CI) except as indicated.
†Comparison of villages with cases of Nipah virus infections with nearby control villages by using generalized linear models that account for correlations within villages for characteristics measured in household surveys.
‡Comparison of villages with cases of Nipah virus infections with distant control villages by using generalized linear models that account for correlations within villages for characteristics measured in household surveys.
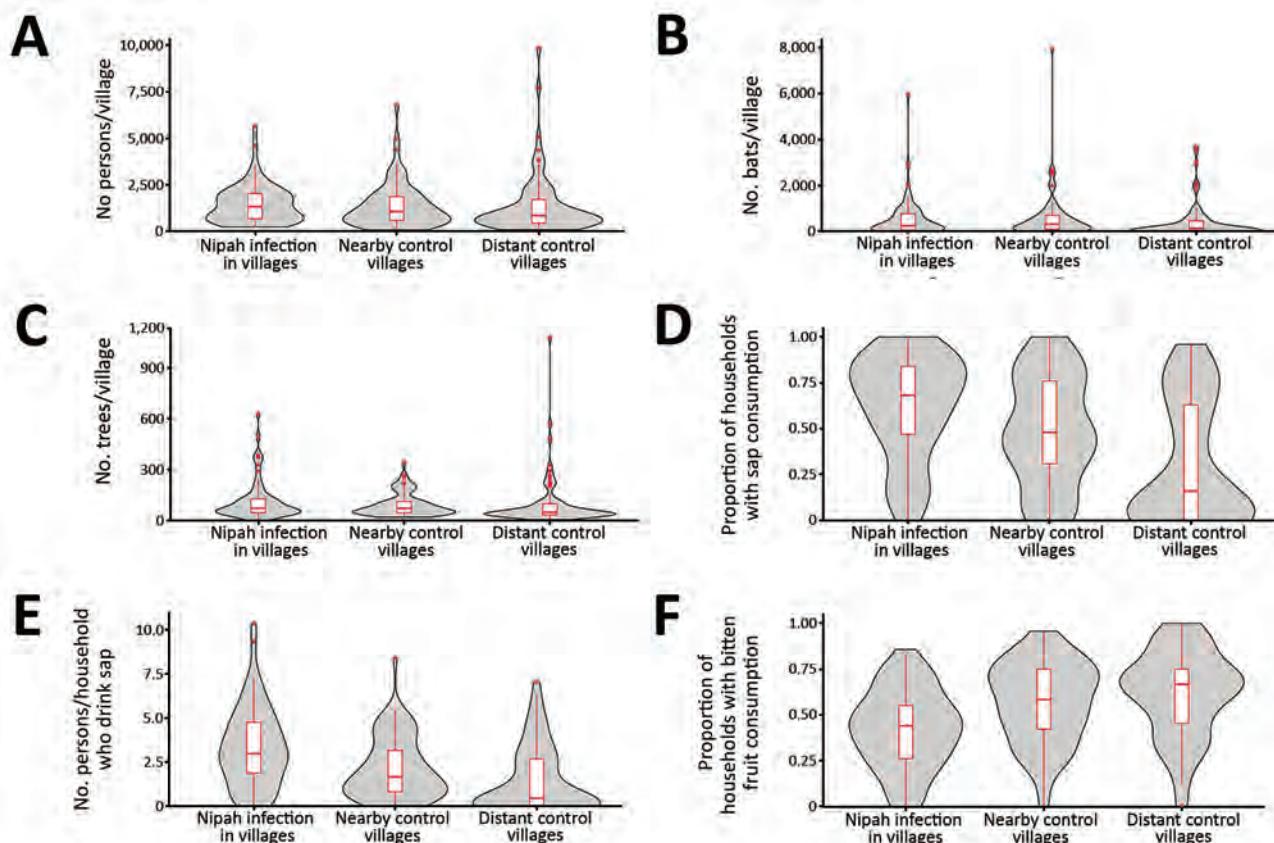
Figure 2. Comparisons of villages with Nipah virus infections with nearby and distant control villages, Bangladesh, 2011–2013. A) Human population size, B) *Pteropus medius* bat population size, C) no. date palm trees, D) proportion of households with members who consume fresh date palm sap, E) average no. of persons per household who consume fresh date palm sap, and F) proportion of households that reported their residents eat bitten fruits dropped on the ground. Gray shading in violin plots indicates distribution of values for each variable. Box plots indicate 25th and 75th percentiles (bottom and top lines), medians (horizontal lines within boxes), and 95 CIs (whiskers). Red dots indicate maximum (outlier) values.

was higher in case villages (3.3 glasses) than in nearby control villages (2.1 glasses) and distant control villages (1.5 glasses) (Table 1; Figure 2, panel E). A larger proportion of villages that had cases of infection with NiV had ≥1 bat hunter than distant control villages (53% vs. 27%; p = 0.002) (Table 1). Households in nearby and distant control villages were more likely to report that someone in the house ate fruits bitten by animals off the ground and saw bats roosting nearby during the day and flying overhead at dusk than were households in villages with cases of infection with NiV (Table 1).

Multivariable analyses showed that, compared with nearby control villages, each additional 10% increase in the proportion of households reporting that someone regularly consumed raw sap was associated with a 6.39 (95% CI 1.61–25.40) increase in odds of being a village with cases of NiV infection (Table 2). Compared with distant control villages, the odds of being a village with cases of NiV infection were 1.18 (95% CI 1.02–1.37) times higher for each order of magnitude increase in bat populations and

26.97 (95% CI 5.98–121.67) times higher for each 10% increase in households that reported someone who regularly consumed sap.

Discussion

NiV is a highly fatal pathogen and poses a risk for pandemic spread because it can be transmitted from person-to-person. To reduce opportunities for a more transmissible strain to emerge, which could lead to regional outbreaks or a pandemic, we must prevent spillover from bats to humans. Bangladesh is the only place where spillover events are predictably identified each year. Therefore, preventing bat-to-human transmission of NiV in rural Bangladesh should be a global public health priority.

Our study reported 2 key findings to achieve this priority. First, our data suggest that human infection, and as a result, selective pressure to adapt to humans (*3*), is determined by the joint probability of a human consuming raw sap in rural Bangladesh and of sap being contaminated by the urine or saliva of a bat that is shedding the virus

Table 2. Odds ratios from logistic regression models estimating associations between village characteristics and Nipah virus spillovers, Bangladesh, 2011–2013*

Characteristic	OR (95% CI) for villages with NiV infections vs. nearby control villages	p value	OR (95% CI) for villages with NiV infections vs. distant control villages	p value
Per each order of magnitude increase in no. persons in village	1.36 (0.90–2.07)	0.14	1.57 (0.90–2.6)	0.12
Per each order of magnitude increase in no. bats ≤5 km from village	1.00 (0.86–1.16)	0.97	1.18 (1.02–1.37)	0.029
Per each order of magnitude increase in no. date palm sap trees ≤5 km from village	0.75 (0.49–1.12)	0.16	.69 (0.45–1.04)	0.078
Per each 10% increase in households reporting that someone consumed raw date palm sap during the harvest season	6.39 (1.61–25.40)	0.008	26.97 (5.98–121.67)	<0.001
Per each 1% increase in villages reporting that someone hunts bats	NA	NA	1.80 (0.80–4.06)	0.16
*CIs were calculated by using robust variance. NA, not applicable; NiV, Nipah virus; OR, odds ratio.				

(*22,32*). Bangladesh has a population of 160 million persons, and according to a United Nations report (http://esa.un.org/unpd/wup/Country-Profiles/), 70% of Bangladeshi residents in 2015 lived in rural areas where date palm sap is collected. We found that ≥30% of rural households have ≥l regular date palm sap drinker, which implies that there are millions of persons drinking fresh sap each year. The reservoir for NiV (the *P. medius* bats) is nearly ubiquitous across the landscape (Figure 1, panel B), and previous studies show that bat visits to date palm sap trees are common (*27*), which suggests that much of the fresh date palm sap consumed is probably contaminated with bat saliva or excreta. Despite this finding, human infections with NiV are rare, which suggests that shedding of transmissible virus by bats is also rare during the date palm sap harvesting season or occurs too infrequently to cause human infection.

Date palm sap consumption was common in control villages, although less common than in case villages. These findings suggest that we need not eliminate date palm sap consumption to reduce NiV spillovers. Date palm sap is deeply rooted in Bengali culture (*32*), and because the risk associated with consumption at the individual level is low, eliminating this practice could be difficult. However, even if we are unable to eliminate sap consumption, modest reductions in consumption of contaminated date palm sap could meaningfully reduce incidence rates for infection with NiV. Case villages were also more likely to have more bats roosting nearby than distant control villages but not nearby control villages. This finding suggests that although large increases in bat population sizes could increase risk for spillover, odds ratios indicate that human behavior patterns are a greater risk for driving NiV transmission than bat population size. Extermination of bats would not be an appropriate approach to mitigating the risk for NiV infection because of the major ecologic role of *P. medius* bats in tree pollination and seed dispersal. Public health messages during outbreaks stress the need for bats in the local ecology, but greater efforts to preserve bat habitat during outbreaks should be considered.

Second, our data suggest that we should target interventions to communities that consume large amounts of raw sap. We identified that consumption of date palm sap was common in many areas across Bangladesh, even in areas where no cases of infection with NiV have been detected. The ability to target resources is key when funding for public health prevention is limited. Our data suggest that areas with high consumption of raw sap should be targeted for enhanced surveillance to track changes in NiV epidemiology and quickly respond to outbreaks and for interventions to interrupt transmission through consumption of contaminated sap. Interventions to reduce human consumption of contaminated sap have been developed and include efforts to reduce fresh sap consumption in general and using physical barriers to keep bats from accessing and contaminating sap (*32–36*). However, sustained changes in behavior patterns regarding consumption of date palm sap will probably require long-term efforts to promote these interventions because this consumption is ingrained in local culture, and there is evidence that knowledge per se about risk for infection with NiV is not associated with behavior patterns regarding date palm sap consumption in areas to which NiV is endemic (*32,36*).

Residents of nearby and distant control villages were more likely to report seeing bats roosting nearby during the day. One possible explanation for this finding could be an association between experiencing an outbreak of infection with NiV and destruction of bat habitat. Local investigation teams have observed that residents in villages in which outbreaks have occurred often cut down trees in which bats roost within the village after the outbreak. Residents of nearby and distant control villages were also more likely than residents of case villages to report eating animal-bitten fruits off the ground. Investigations of the first outbreak of infections with NiV in Malaysia suggested that the most probable pathway of transmission from bats to pigs was through consumption of bat-bitten fruits (*37*). However, there is no evidence that this transmission route plays a major role in human infections in Bangladesh, despite more than a decade of investigation

(*38*), and this study provides further evidence that this factor is not a major contributor to human infection in this setting, given the strong association between human date palm sap consumption and being a village with cases of NiV infection. No outbreaks of infection with NiV have been linked with bat hunting, but Old World fruit bats are hypothesized to be reservoir hosts for several major zoonotic pathogens, including Marburg virus and Ebola virus (*39,40*). In addition to NiV, our group reported evidence of 55 novel viruses in *P. medius* bats (*41*), and evidence for human exposure to these or other batborne pathogens through this type of bat contact should be explored. Efforts to reduce bat hunting would be beneficial for conservation of these species and reduction of disease risk.

Our study objective was to identify the major drivers of spatial patterns of NiV spillovers across Bangladesh by drawing upon evidence we have about individual risk factors for NiV infection. There might be other rare drivers of risk that were not detected because of limited statistical power. However, these drivers would have a smaller role in explaining disease risk than those identified in this study. *P. medius* bats are found throughout Bangladesh (*42*) but spillover of NiV to humans could be driven by spatial or temporal variation in NiV incidence in bats. More evidence about this possible contributor to spatial heterogeneity would improve our understanding of risk.

Our study provides an example of how epidemiologic studies can be used to describe the ecologic drivers of zoonotic disease emergence. The risk for cross-species transmission is complex and depends on the presence of reservoir hosts and permissive contact patterns with humans, as well as the frequency of these interactions. Future studies to explain spatial risk for similar emerging zoonotic infections should incorporate data on all aspects of the transmission, including human behavior patterns.

At the time of this study, Dr. Gurley was an epidemiologist at the icddr,b, Dhaka, Bangladesh. She is currently an associate scientist in the Department of Epidemiology, John Hopkins University School of Public Health, Baltimore, MD. Her primary research interests are Nipah virus, infectious diseases, and disease transmission.

References

1. Wolfe ND, Dunavan CP, Diamond J. Origins of major human infectious diseases. Nature. 2007;447:279–83. http://dx.doi.org/10.1038/nature05775

2. Agua-Agum J, Ariyarajah A, Aylward B, Blake IM, Brennan R, Cori A, et al.; WHO Ebola Response Team. West African Ebola epidemic after one year—slowing but not yet under control. N Engl J Med. 2015;372:584–7. http://dx.doi.org/10.1056/NEJMc1414992

3. Antia R, Regoes RR, Koella JC, Bergstrom CT. The role of evolution in the emergence of infectious diseases. Nature. 2003;426:658–61. http://dx.doi.org/10.1038/nature02104

4. Brownstein JS, Skelly DK, Holford TR, Fish D. Forest fragmentation predicts local scale heterogeneity of Lyme disease risk. Oecologia. 2005;146:469–75. http://dx.doi.org/10.1007/s00442-005-0251-9

5. Fuller T, Thomassen HA, Mulembakani PM, Johnston SC, Lloyd-Smith JO, Kisalu NK, et al. Using remote sensing to map the risk of human monkeypox virus in the Congo Basin. EcoHealth. 2011;8:14–25. http://dx.doi.org/10.1007/s10393-010-0355-5

6. Daszak P, Zambrana-Torrelio C, Bogich TL, Fernandez M, Epstein JH, Murray KA, et al. Interdisciplinary approaches to understanding disease emergence: the past, present, and future drivers of Nipah virus emergence. Proc Natl Acad Sci U S A. 2013;110(Suppl 1):3681–8. http://dx.doi.org/10.1073/pnas.1201243109

7. Horobik V, Keesing F, Ostfeld R. Abundance and *Borrelia burgdorferi* infection prevalence of nymphal *Ixodes scapularis* ticks along forest–field edges. Ecohealth. 2006;3:262–8. http://dx.doi.org/10.1007/s10393-006-0065-1

8. Luby SP, Gurley ES, Hossain MJ. Transmission of human infection with Nipah virus. Clin Infect Dis. 2009;49:1743–8. http://dx.doi.org/10.1086/647951

9. Lam SK, Chua KB. Nipah virus encephalitis outbreak in Malaysia. Clin Infect Dis. 2002;34(Suppl 2):S48–51. http://dx.doi.org/10.1086/338818

10. Chadha MS, Comer JA, Lowe L, Rota PA, Rollin PE, Bellini WJ, et al. Nipah virus-associated encephalitis outbreak, Siliguri, India. Emerg Infect Dis. 2006;12:235–40. http://dx.doi.org/10.3201/eid1202.051247

11. Hsu VP, Hossain MJ, Parashar UD, Ali MM, Ksiazek TG, Kuzmin I, et al. Nipah virus encephalitis reemergence, Bangladesh. Emerg Infect Dis. 2004;10:2082–7. http://dx.doi.org/10.3201/eid1012.040701

12. Luby SP, Gurley ES. Epidemiology of henipaviruses. In: Shapshak P, Sinnott JP, Somboonwit C, Kuhn J, editors. Global virology. Vol. 1. Identifying and investigating viral diseases. New York: Springer Science + Business Media; 2015. p. 55–71.

13. Gurley ES, Montgomery JM, Hossain MJ, Bell M, Azad AK, Islam MR, et al. Person-to-person transmission of Nipah virus in a Bangladeshi community. Emerg Infect Dis. 2007;13:1031–7. http://dx.doi.org/10.3201/eid1307.061128

14. Halpin K, Hyatt AD, Fogarty R, Middleton D, Bingham J, Epstein JH, et al.; Henipavirus Ecology Research Group. Pteropid bats are confirmed as the reservoir hosts of henipaviruses: a comprehensive experimental study of virus transmission. Am J Trop Med Hyg. 2011;85:946–51. http://dx.doi.org/10.4269/ajtmh.2011.10-0567

15. Nowak RM. Old World fruit bats: Pteropodidae (flying foxes). In: Nowak RM, editor. Walker's bats of the world. 5th ed. Baltimore: The Johns Hopkins University Press; 1994. p. 55–8.

16. Epstein JH, Prakash V, Smith CS, Daszak P, McLaughlin AB, Meehan G, et al. Henipavirus infection in fruit bats (*Pteropus giganteus*), India. Emerg Infect Dis. 2008;14:1309–11. http://dx.doi.org/10.3201/eid1408.071492

17. Homaira N, Rahman M, Hossain MJ, Epstein JH, Sultana R, Khan MS, et al. Nipah virus outbreak with person-to-person transmission in a district of Bangladesh, 2007. Epidemiol Infect. 2010;138:1630–6. http://dx.doi.org/10.1017/S0950268810000695

18. Rahman SA, Hassan L, Epstein JH, Mamat ZC, Yatim AM, Hassan SS, et al.; Henipavirus Ecology Research Group. Risk factors for Nipah virus infection among pteropid bats, Peninsular Malaysia. Emerg Infect Dis. 2013;19:51–60. http://dx.doi.org/10.3201/eid1901.120221

19. Reynes JM, Counor D, Ong S, Faure C, Seng V, Molia S, et al. Nipah virus in Lyle's flying foxes, Cambodia. Emerg Infect Dis. 2005;11:1042–7. http://dx.doi.org/10.3201/eid1107.041350

20. Wacharapluesadee S, Lumlertdacha B, Boongird K, Wanghongsa S, Chanhome L, Rollin P, et al. Bat Nipah virus, Thailand. Emerg Infect Dis. 2005;11:1949–51. http://dx.doi.org/10.3201/eid1112.050613

21. Mlikovsky J. Correct name for the Indian flying fox (Pteropodidae). Vespertilio. 2012;16:203–4.

22. Chua KB, Koh CL, Hooi PS, Wee KF, Khong JH, Chua BH, et al. Isolation of Nipah virus from Malaysian island flying-foxes. Microbes Infect. 2002;4:145–51. http://dx.doi.org/10.1016/S1286-4579(01)01522-2

23. Rahman SA, Hassan SS, Olival KJ, Mohamed M, Chang LY, Hassan L, et al.; Henipavirus Ecology Research Group. Characterization of Nipah virus from naturally infected *Pteropus vampyrus* bats, Malaysia. Emerg Infect Dis. 2010;16:1990–3. http://dx.doi.org/10.3201/eid1612.091790

24. Openshaw JJ, Hegde S, Sazzad HM, Khan SU, Hossain MJ, Epstein JH, et al. Increased morbidity and mortality in domestic animals eating dropped and bitten fruit in Bangladeshi villages: implications for zoonotic disease transmission. EcoHealth. 2016;13:39–48. http://dx.doi.org/10.1007/s10393-015-1080-x

25. Luby SP, Hossain MJ, Gurley ES, Ahmed BN, Banu S, Khan SU, et al. Recurrent zoonotic transmission of Nipah virus into humans, Bangladesh, 2001–2007. Emerg Infect Dis. 2009;15:1229–35. http://dx.doi.org/10.3201/eid1508.081237

26. Nahar N, Sultana R, Gurley ES, Hossain MJ, Luby SP. Date palm sap collection: exploring opportunities to prevent Nipah transmission. EcoHealth. 2010;7:196–203. http://dx.doi.org/10.1007/s10393-010-0320-3

27. Khan MS, Hossain J, Gurley ES, Nahar N, Sultana R, Luby SP. Use of infrared camera to understand bats' access to date palm sap: implications for preventing Nipah virus transmission. EcoHealth. 2010;7:517–25. http://dx.doi.org/10.1007/s10393-010-0366-2

28. Eby P. Seasonal movements of gray-headed flying-foxes, *Pteropus poliocephalus* (Chiroptera, Pteropodidae), from 2 maternity camps in northern New South Wales. Wildlife Research. 1991;18:547–59. http://dx.doi.org/10.1071/WR9910547

29. Tidemann CR. Biology and management of the grey-headed flying-fox, *Pteropus poliocephalus*. Acta Chiroptera. 1999;1:151–64.

30. Kunz T, Jones D. *Pteropus vampyrus*. Mammalian Species. 2000; 642:1–6. http://dx.doi.org/10.1644/1545-1410(2000)642<0001: PV>2.0.CO;2

31. Ao TT, Rahman M, Haque F, Chakraborty A, Hossain MJ, Haider S, et al. Low-cost national media-based surveillance system for public health events, Bangladesh. Emerg Infect Dis. 2016;22:720–2. http://dx.doi.org/10.3201/eid2204.150330

32. Nahar N, Sultana R, Gurley ES, Hossain MJ, Luby SP. Date palm sap collection: exploring opportunities to prevent Nipah transmission. EcoHealth. 2010;7:196–203. http://dx.doi.org/10.1007/s10393-010-0320-3

33. Khan SU, Gurley ES, Hossain MJ, Nahar N, Sharker MA, Luby SP. A randomized controlled trial of interventions to impede date palm sap contamination by bats to prevent Nipah virus transmission in Bangladesh. PLoS One. 2012;7:e42689. http://dx.doi.org/10.1371/journal.pone.0042689

34. Nahar N, Mondal UK, Hossain MJ, Khan MS, Sultana R, Gurley ES, et al. Piloting the promotion of bamboo skirt barriers to prevent Nipah virus transmission through date palm sap in Bangladesh. Glob Health Promot Educ. 2014;21:7–15. http://dx.doi.org/10.1177/1757975914528249

35. Nahar N, Mondal UK, Sultana R, Hossain MJ, Khan MS, Gurley ES, et al. Piloting the use of indigenous methods to prevent Nipah virus infection by interrupting bats' access to date palm sap in Bangladesh. Health Promot Int. 2013;28:378–86. http://dx.doi.org/10.1093/heapro/das020

36. Nahar N, Paul RC, Sultana R, Gurley ES, Garcia F, Abedin J, et al. Raw sap consumption habits and its association with knowledge of Nipah virus in two endemic districts in Bangladesh. PLoS One. 2015;10:e0142292. http://dx.doi.org/10.1371/journal.pone.0142292

37. Pulliam JR, Epstein JH, Dushoff J, Rahman SA, Bunning M, Jamaluddin AA, et al.; Henipavirus Ecology Research Group (HERG). Agricultural intensification, priming for persistence and the emergence of Nipah virus: a lethal bat-borne zoonosis. J R Soc Interface. 2012;9:89–101. http://dx.doi.org/10.1098/rsif.2011.0223

38. Hegde ST, Sazzad HM, Hossain MJ, Alam MU, Kenah E, Daszak P, et al. Investigating rare risk factors for Nipah virus in Bangladesh: 2001–2012. Ecohealth. 2016;13:720–8. http://dx.doi.org/10.1007/s10393-016-1166-0

39. Leroy EM, Kumulungui B, Pourrut X, Rouquet P, Hassanin A, Yaba P, et al. Fruit bats as reservoirs of Ebola virus. Nature. 2005;438:575–6. http://dx.doi.org/10.1038/438575a

40. Towner JS, Amman BR, Sealy TK, Carroll SA, Comer JA, Kemp A, et al. Isolation of genetically diverse Marburg viruses from Egyptian fruit bats. PLoS Pathog. 2009;5:e1000536. http://dx.doi.org/10.1371/journal.ppat.1000536

41. Anthony SJ, Epstein JH, Murray KA, Navarrete-Macias I, Zambrana-Torrelio CM, Solovyov A, et al. A strategy to estimate unknown viral diversity in mammals. MBio. 2013;4:e00598–13. http://dx.doi.org/10.1128/mBio.00598-13

42. Hahn MB, Gurley ES, Epstein JH, Islam MS, Patz JA, Daszak P, et al. The role of landscape composition and configuration on *Pteropus giganteus* roosting ecology and Nipah virus spillover risk in Bangladesh. Am J Trop Med Hyg. 2014;90:247–55. http://dx.doi.org/10.4269/ajtmh.13-0256

Address for correspondence: Emily S. Gurley, Department of Epidemiology, John Hopkins University School of Public Health, 615 N Wolfe St, Baltimore, MD 21205, USA; email: egurley1@jhu.edu.

Processes Underlying Rabies Virus Incursions across US–Canada Border as Revealed by Whole-Genome Phylogeography

Hannah Trewby, Susan A. Nadin-Davis, Leslie A. Real, Roman Biek

Disease control programs aim to constrain and reduce the spread of infection. Human disease interventions such as wildlife vaccination play a major role in determining the limits of a pathogen's spatial distribution. Over the past few decades, a raccoon-specific variant of rabies virus (RRV) has invaded large areas of eastern North America. Although expansion into Canada has been largely prevented through vaccination along the US border, several outbreaks have occurred in Canada. Applying phylogeographic approaches to 289 RRV whole-genome sequences derived from isolates collected in Canada and adjacent US states, we examined the processes underlying these outbreaks. RRV incursions were attributable predominantly to systematic virus leakage of local strains across areas along the border where vaccination has been conducted but also to single stochastic events such as long-distance translocations. These results demonstrate the utility of phylogeographic analysis of pathogen genomes for understanding transboundary outbreaks.

Control measures are often used at the edges of a pathogen's range to limit geographic spread and prevent incursions of infection into areas free from disease. Although geopolitical boundaries generally do not directly affect spread of infectious diseases, human-imposed control measures are often structured around national or international borders. Where such control measures fail, the resulting outbreaks can prove extremely costly in terms of public health and economic and political consequences. It is therefore vital to understand the events involved in such transboundary outbreaks of infection and particularly how these events relate to the control measures applied at the boundary.

Rabies virus is a major zoonotic pathogen worldwide. In the United States, the geographic range of the raccoon variant of rabies virus (RRV) has expanded in recent decades and is now endemic throughout the eastern seaboard

Author affiliations: Emory University, Atlanta, Georgia, USA (H. Trewby, L.A. Real); University of Glasgow, Glasgow, Scotland, UK (H. Trewby, R. Biek); Canadian Food Inspection Agency, Ottawa, Ontario, Canada (S.A. Nadin-Davis)

area (1). Further spread of RRV has been largely contained through oral vaccination of raccoons along the edge of its range (2). However, multiple incursions across the vaccination corridor have occurred at the northern edge of the RRV range, corresponding to the US–Canada border; the resulting outbreaks in the Canadian provinces of Ontario, Quebec, and New Brunswick have necessitated large-scale control operations to prevent the establishment of RRV in Canada. By focusing specifically on these outbreaks of RRV in Canada, we are by default highlighting points at which transboundary controls have failed. However, our doing so does not imply that the control measures at the Canada border have been unsuccessful. Despite the epidemic expansion of RRV covering 40–60 km/year in the absence of controls (3–6), spatial spread of RRV has been static in most areas of the Canada border for >15 years (7).

RRV was first reported in the US state of New York in 1990. By 1994, it had spread to reach the Canada border at Niagara in western New York, and by 1996, it had reached the New York–Ontario border at the St. Lawrence River. Implementation of rabies vaccination started along the Niagara River in 1994 and at potential crossing points along the St. Lawrence River from 1995 on, later replaced by larger scale oral vaccination (8). The first RRV outbreak in Ontario occurred in the southeastern part of the province during 1999–2005; 126 cases were confined to an area of the mainland adjacent to the St. Lawrence River, and 6 cases occurred on Wolfe Island between Ontario and New York at the mouth of Lake Ontario (8,9). More recently, in 2015, an outbreak was identified west of the Niagara area and is ongoing (7).

At the US–Canada border between Quebec and Vermont, oral rabies vaccination was implemented in the late 1990s in response to the northward spread of RRV through Vermont. The first outbreak of RRV in Quebec occurred during 2006–2009, near the Vermont border (10). Another isolated case of raccoon rabies was reported in 2015 at the border with New York in southwestern Quebec (7).

In New Brunswick, RRV outbreaks occurred during 2000–2002 and 2014–2016, both in the southwestern part

of the province near the border with Maine (*7*). RRV vaccination was conducted at the New Brunswick–Maine border from 2001 through 2008 and is currently in place after the 2015 outbreak.

In this study, we used RRV whole-genome sequences to investigate the processes giving rise to these outbreaks in Canada, particularly with respect to the effectiveness of the vaccine area at the US–Canada border, and to determine whether these processes were comparable across different outbreaks. We generated 289 RRV whole-genome sequences: 140 sequences from RRV cases covering each of the Canada outbreaks and 149 sequences from cases in the neighboring US states of New York, Vermont, and Maine. Using Bayesian phylogeographic approaches, we addressed the following 3 questions: 1) Did the Canada outbreaks result from multiple simultaneous incursions of RRV or from single introductions? 2) Is there evidence of backflow of RRV from Canada into the United States? 3) Did the Canada outbreaks originate from RRV lineages circulating locally, or are they attributable to long-distance movement?

Materials and Methods

Samples and Sequencing
In eastern Canada, brain samples from animals suspected to be infected with rabies virus are submitted to the Centre of Expertise for Rabies of the Canadian Food Inspection Agency in Ottawa for diagnosis. In addition, any rabies-positive wildlife cases diagnosed by provincial authorities during enhanced surveillance activities are confirmed by the laboratory in Ottawa. We selected a temporally and spatially representative subset of RRV samples for sequencing from the Canada outbreaks in Ontario (n = 57), Quebec (n = 51), and New Brunswick (n = 32). For comparison, we obtained another set of confirmed rabies virus samples, in most cases collected over the same period as the Canada outbreaks, for sequencing from the relevant state rabies laboratories of New York, Vermont, and Maine. The high-density sampling in New York and Vermont enabled us to focus sampling on cases within 75 km of the Canada border in these 2 states (54 sequenced samples in New York and 62 in Vermont), with the aim of capturing representatives of most RRV lineages circulating near the border. A lower density of samples was available from Maine, collected in 2013 and 2014 only, and therefore we sequenced RRV from throughout this state (33 sequences). Details of sequenced samples are shown in online Technical Appendix Table 1 (https://wwwnc.cdc.gov/EID/article/23/9/17-0325-Techapp1.pdf).

We performed RRV genome extraction and sequencing as described in detail by Nadin-Davis et al. (*11*). Viral RNA was extracted from brain tissue of animals with confirmed infection by using Trizol (Life Technologies Inc., Carlsbad, CA, USA) and further purified by using a MagMax instrument (Applied Biosystems, Foster City, CA, USA). RNA was amplified as 3 overlapping amplicons covering the whole RRV genome. Purified amplicons from a single sample were pooled and used to generate indexed libraries with Nextera XT kits (Illumina, Inc., San Diego, CA, USA); libraries were sequenced as 200- or 250-bp paired end reads on an Illumina MiSeq machine. Genomes were sequenced with high depth of coverage (average >1,000×), and reference-based assembly was conducted by use of the NGen program in the DNASTAR Lasergene software package, version 11 (*12*), with either the RRV reference genome (GenBank accession no. EU311738) or more genetically related sequences generated during this study that better facilitated complete assembly, to generate consensus sequences.

Phylogeographic Analyses
To estimate RRV transitions between geographic regions, we conducted discrete trait phylogeographic analysis (*13*). Sequences were grouped into 8 groups according to location: western Ontario, eastern Ontario, western New York, northwestern New York, New Brunswick, Maine, Quebec, and Vermont (this latter group includes 2 New York sequences, New York.1995.3745 and New York.2011.5590 [online Technical Appendix Table 1], which clustered geographically and genetically with Vermont sequences). Independent incursions into Canada were identified as lineages of the maximum clade credibility phylogeny stemming from a most recent common ancestor with a >90% posterior probability of occurring in Ontario, Quebec, or New Brunswick, according to discrete trait ancestral state reconstruction.

We conducted analyses in BEAST version 1.8.2 (*14*) with the BEAGLE library (*15*) by using the generalized time-reversible model with gamma distributed rate variation among sites and separate partitions for coding and noncoding regions and a relaxed molecular clock (*12*) with branch rates drawn from an exponential distribution (identified by model selection as the best fitting models for these data; online Technical Appendix text and Table 2). Asymmetric transition rates were allowed between regions. Significant transitions were identified by using Bayesian stochastic search variable selection to calculate Bayes factors in the program SPREAD version 1.0.6 (*16*), and the number of transitions between regions was estimated by using Markov Jump counts (*17*).

Identifying Long-Distance Movement
If an outbreak in Canada were the result of local spread of infection, we would expect the responsible viruses to be genetically similar to US RRV lineages circulating near the

Canada border. However, even where dense sampling and sequencing was conducted near the Canada border (i.e., in New York and Vermont), sampling was not exhaustive. Therefore, the absence of a virus closely related to that causing the Canada outbreak in neighboring US regions may indicate an outbreak initiated by long-distance virus movement but could also be the result of incomplete sampling of RRV transmission chains circulating in the local area. We extracted the coalescent time between the most recent common ancestor of a Canada outbreak and the most genetically similar US sequence as a measure of the length of time the outbreak lineage had been circulating unsampled. To generate an expectation for the length of time lineages would circulate undetected under our sampling regimen, we took the distribution of coalescent times for US sequences within each of the 3 major clades. Coalescent times falling outside the 95th percentile interval of US times indicate an outbreak that was probably initiated by long-distance movement. Depending on the (unknown) level of long-distance movement underlying the US samples, this 95th percentile might be overly conservative in identifying long-distance movements.

Results

The sequenced samples fell into 3 well-supported major clades (Figure 1) that are largely structured by region. Clade I consists predominantly of sequences from Quebec and Vermont, although it also includes 5 sequences from northwestern New York and from the 1 case in western Ontario (Ontario-15); clade II is restricted to samples from New Brunswick and Maine; and clade III contains samples from Ontario and New York, with the addition of the 1 isolate from western Quebec in 2015 (Quebec-15). Clades I and III correspond to lineages identified in a previous study of RRV in New York (18); clade I corresponds to lineage 3A (found in southeastern New York in the previous study) and clade III to 3B (found in western and northern New York). Because our sampling scheme focuses on RRV infections near the Canada border in western and northern New York, only 5 of the samples from New York sequenced here fall into clade I.

BEAST analysis revealed a molecular clock rate of 3.28×10^{-4} nucleotide substitutions/site across the genome for these sequences (95% highest posterior density [HPD] 2.83×10^{-4} to 3.76×10^{-4}). The time to most recent common ancestor was estimated as 1990 for clade I (95% HPD 1983–1994), 1994 for clade II (95% HPD 1988–1998), and 1987 for clade III (95% HPD 1979–1991). These estimates suggest that the 3 clades were probably already diverged before RRV entered the region, as indicated by Szanto et al. (18).

We identified 10 independent incursions of RRV, giving rise to the 6 Canada outbreaks, from the maximum clade credibility tree (Figure 1). We analyzed each of these outbreaks to determine the number of recorded cases and whether evidence exists for multiple virus introductions, backflow to the United States, or long-distance movement (Table).

Ontario

Ontario was subject to a persistent outbreak of RRV from 1999 through 2005, resulting in reported cases on Wolfe Island and the Leeds/Grenville area in mainland Ontario. Discrete traits reconstruction (Figure 1, eastern Ontario outbreak shown in dark blue) suggested that the Wolfe Island viruses (Ontario-99b) are part of a separate incursion to the mainland (Ontario-99a), confirming previous suggestions from partial genome data (19). Our results give no indication that the mainland Ontario incursion was caused by multiple invading lineages, and we found no evidence for backflow of infection from Ontario to the United States (online Technical Appendix Figure 1). Sequences from the eastern Ontario outbreak were genetically closely related to sequences circulating locally on the US side of the border with eastern Ontario (Figure 2), suggesting that local spread of infection is responsible for initiating this outbreak. The spatial-genetic spread of this Ontario outbreak is described in more detail by Nadin-Davis et al. (11).

By contrast, the outbreak in western Ontario (represented here by 1 sequence, Ontario-15) falls into a completely separate clade (clade I) than other viruses circulating in the neighboring area of New York (clade III; light orange branches in Figure 1). Even in comparison with other sequences in clade I, the Ontario-15 sequence is considerably divergent; coalescent time is >20 years, and it falls distinctly outside the 95th percentile of coalescent times for US sequences in this clade (Figure 2). These findings provide evidence that the variant represented by isolate Ontario-15 was the result of long-distance movement from outside the study area, rather than local spread across the border. Although our results provide some statistical support for the Ontario-15 incursion originating in Vermont (online Technical Appendix Figure 1), a more full exploration of the origins of the Ontario-15 incursion would require a more comprehensive study in which sampling is not restricted to RRV samples within 75 km of the Canada border. An additional isolate from this ongoing outbreak, sequenced subsequent to preparation of this article, differs from the Ontario-15 isolate at 13 of 11,924 sites. This finding represents a genetic similarity of 99.9%, which would place these 2 samples in the same phylogenetic group (data not shown).

Quebec

With the exception of the 1 case in eastern Quebec in 2015 (Quebec-15), all cases of RRV infection from Quebec were

reported from 2006 through 2009 and were again focused on a relatively small area (Figure 3). The combination of the high level of discrimination provided by whole-genome sequencing plus high-density sequencing of samples from close to the Canada border in this study have made it possible to attribute this single temporal outbreak to several separate incursions of RRV into Quebec (lineages Quebec-06, Quebec-07a, Quebec-07b, and Quebec-07c; Figure 1). The last 2 reported cases of RRV in this outbreak, although located near the border, are shown here to be part of an ongoing circulation of lineage Quebec-07b within Quebec, rather than a separate introduction, as might have been assumed in the absence of sequencing.

Incursions of lineages Quebec-07a, Quebec-07b, and Quebec-07c involved viruses closely genetically related to others circulating locally near the Quebec border (Figure 2), indicating that these were probably the result of local spread from RRV circulating near the border. Although the Quebec-06 lineage seems more genetically distinct from other sequences circulating near the border (and also from

the other Quebec lineages; Figure 1), it does fall within the 95th percentile interval for coalescent times in this clade (Figure 2, panel A); therefore, there is no evidence to rule out the possibility that local spread from Vermont initiated this incursion. Phylogenetic analysis using discrete traits provides strong statistical support (online Technical Appendix Figure 1) for backflow of RRV infection from the Quebec outbreak back into the United States. These instances of backflow (Vermont-07 and Vermont-08; Figure 1) were each identified within 30 km of the Quebec border, again consistent with local transmission of disease.

The 1 case reported in 2015, Quebec-15, was located at the western edge of the Quebec border with the United States. Contrary to the previous Quebec outbreak, the sequence for this case falls into clade III (Figure 1), indicating that it is linked to the lineage that has spread north through New York, as opposed to the predominantly Vermont-associated clade I implicated in the 2006–2009 outbreak. This finding is not surprising because Quebec-15 was found in an area directly adjacent to New York (Figure
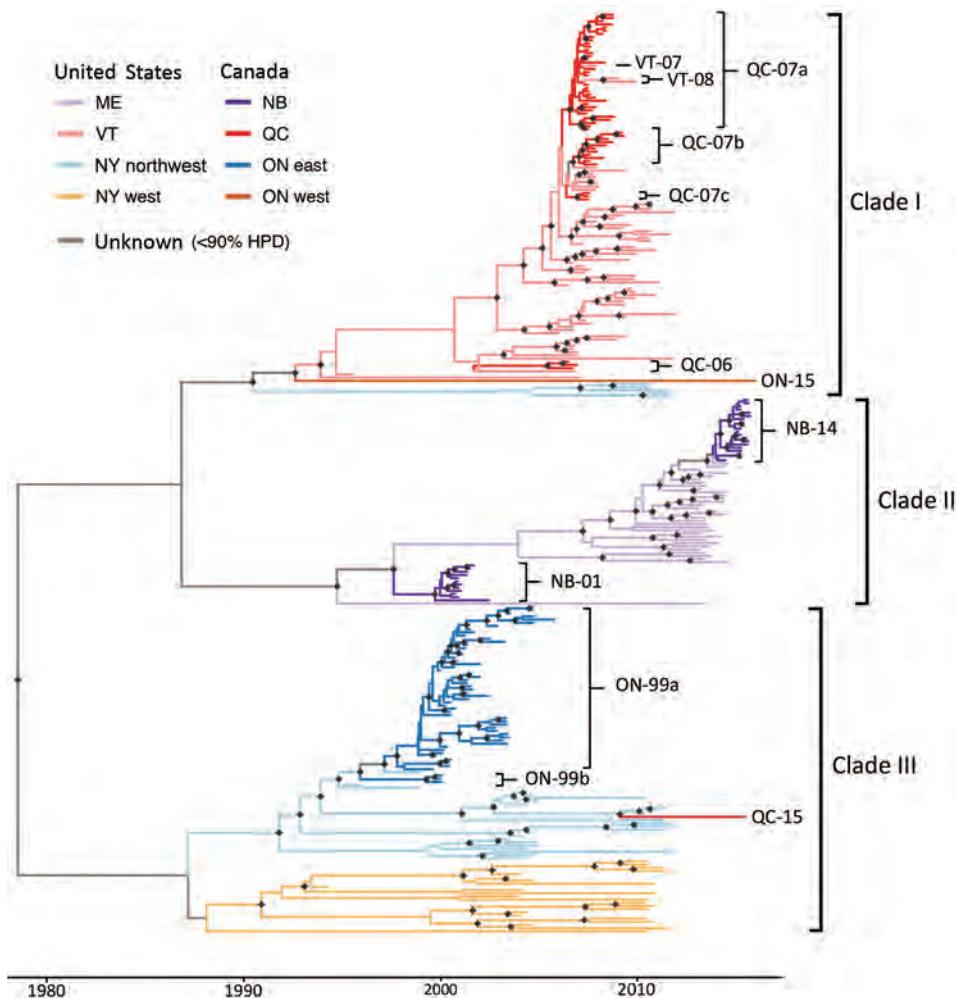
Figure 1. Time-scaled maximum clade credibility phylogeny of sequenced genomes of raccoon-specific variant of rabies virus, US–Canada border. Branches are colored by inferred geographic region. Samples belonging to Canada lineages are labeled by province and year of first sample, as is backflow of infection from Canada into Vermont. Black diamonds indicate nodes with >90% posterior support. HPD, highest posterior density; NB, New Brunswick; ON, Ontario; QC, Quebec.

Table. Summary of Canada outbreaks and evidence of multiple introductions of raccoon-specific variant of rabies virus, backflow from Canada to the United States, and long-distance movement initiating an outbreak

Location	Time	No. recorded cases	Evidence of multiple introductions	Evidence of backflow to the United States	Evidence of long-distance movement
Ontario (east)	1999–2005	132	Yes	No	No
Ontario (west)	2015–ongoing	307*	No	No	Yes
Quebec	2006–2009	104	Yes	Yes (strong)	No
Quebec	2015–2015	1	No	No	No
New Brunswick	2000–2002	64	No	No	No
New Brunswick	2014–ongoing	30*	No	Yes (weak)	No
*Number correct as of April 30, 2017.					

3) and was reported soon after cases of RRV reached Franklin County, New York, adjacent to the Quebec border. The Quebec-15 case was located in an area where vaccination had previously not been conducted and has not been followed by any further reports of RRV in Quebec. Although on first examination the Quebec-15 sequence does exhibit some divergence from other sequences in the clade, it is again within the 95th percentile of coalescent times for this clade (Figure 2, panel B), further confirming that this case is probably the result of local spread of viruses from the New York side of the Quebec border.

Figure 2. Distribution of coalescent times for raccoon-specific variant of rabies virus near the US–Canada border, clade I (A) and clade III (B). Gray histograms give the distribution of coalescent times for each US sample in the clade, and colored bars and labels indicate the coalescent times for the most recent common ancestor of each Canada lineage in the specified clade. Gray dashed lines indicate the 95th percentiles of the coalescent times for virus from the United States. ON, Ontario; QC, Quebec.

New Brunswick

Our results provide no evidence that either of the outbreaks in New Brunswick (2000–2002 and 2014–2015) was initiated by multiple incursions into New Brunswick; however, discrete trait phylogeographic analysis gives some limited statistical support for backflow of RRV from New Brunswick into Maine (online Technical Appendix Figure 1; note that this backflow is not represented in the maximum clade credibility tree in Figure 1). Sequences from the second New Brunswick outbreak seem closely genetically related to sequences circulating in Maine; however, to examine further the suggestion of backflow from New Brunswick into Maine, and to assess whether the 2000–2002 outbreak is the result of local spread or of long-distance translocation of infection as was suggested at the time (21), more extensive sampling and sequencing of RRV from cases near the New Brunswick border would be necessary.

Discussion

The use of high-throughput RRV sequencing enabled us to investigate events giving rise to a series of transboundary RRV outbreaks in eastern provinces of Canada that border the United States. By generating high-resolution whole-genome sequences and comparing results across multiple Canada outbreaks, we were able to discriminate between different epidemiologic scenarios and gain generalizable insights that would not be possible to gain from single-outbreak data.

In most instances, results were consistent with the outbreaks being initiated by 1 lineage, possibly representing 1 infected individual. A major exception was the outbreak in Quebec in 2006–2009, which involved at least 4 cross-border incursions. The Quebec 2006–2009 outbreak also showed strong evidence of backflow of infection from Quebec across the border into the United States. The combination of multiple introductions and backflow of infection indicates that the Quebec–Vermont border and adjacent areas of vaccination were relatively permeable to the spread of RRV during 2006–2008. These results suggest that this particular outbreak was related to systematic challenges in maintaining an effective vaccine corridor at this location and time, as opposed to rare stochastic events. A likely contributing factor for the

Figure 3. Locations of sequenced samples from Canada outbreaks of raccoon-specific variant of rabies virus infection in western Ontario (n = 1), eastern Ontario (n = 56), Quebec (n = 51), and New Brunswick (n = 32); and from the United States within 75 km of the border in western New York (n = 23), northwestern New York (n = 29, including 5 samples into clade I, indicated by squares), and Vermont (n = 64, including 2 samples from New York that grouped within this clade, indicated by squares); and from throughout Maine (n = 33). Map generated by using ggmap package (*20*). NB, New Brunswick; ON, Ontario; QC, Quebec.
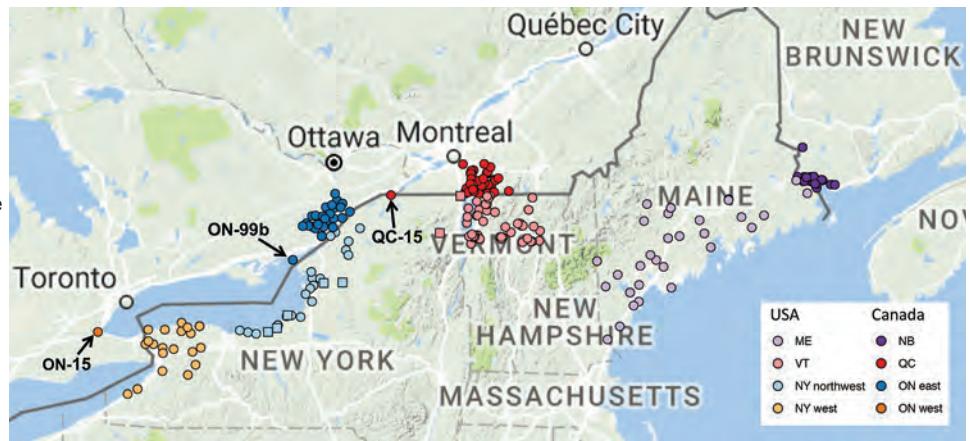
higher transboundary transmission in Quebec is the lack of natural barriers along this border, compared with the major rivers or lakes that reinforce the border between Ontario and the United States. A similar argument can be made for the 1999–2005 Ontario outbreak, given the evidence for 2 separate introductions into Wolfe Island and the mainland, although no indications of backflow or further introductions were found. Weak evidence for backflow of RRV into the United States was also found for New Brunswick, although more in-depth sampling from Maine would be necessary to confirm this; other outbreaks showed no indication of backflow of infection into the United States. Transmission of infection in both directions across the US–Canada border highlights the need for coordination of surveillance programs. For future detection of such backflow events, however, surveillance strategies will probably need detailed genomic data and dense geographic sampling, as described here for New York and Vermont.

Introductions of RRV into Canada were predominantly attributable to viruses closely genetically related to lineages circulating near the US–Canada border. This finding indicates that for many outbreaks, whether multiple introductions or backflow of RRV were evident in the data, the largest risk for introduction stems from local pressure of infection resulting in RRV spreading through the areas of vaccination across the international boundary. This finding is consistent with previous findings of an observed breach of the vaccine corridor within the United States into the state of Ohio, which also implicated local spread of virus lineages through the vaccinated area (*22*). However, we demonstrate that at least 1 introduction into Canada (Ontario-15) was attributable to movement of infection across an exceptionally large distance. The index case was found 64 km from the Ontario–US border, and our results indicate that it is highly unlikely to have originated from US territory within the scale of our

sampling (75 km from the border). Most raccoon movements are <5 km (*23–27*); however, long-distance dispersal of raccoons covering ≥100 km has been reported and is generally attributed to human-mediated translocation, whether deliberate or inadvertent (*4,28,29*). The Ontario-15 introduction was adjacent to the Niagara region, an area where vaccination has been conducted on both sides of the border for over a decade and where the border is further strengthened by the large Niagara River. It is also the area on the US–Canada border that was first reached by the northward expansion of RRV in 1994, resulting in the longest potential for transboundary incursions. The absence of any local spread of infection suggests that the local barrier to transboundary incursion of RRV here is particularly strong. However, our results highlight that such areas are still vulnerable to long-distance translocation events, effectively allowing RRV infection to bypass areas of vaccination completely.

Long-distance translocations are likely to be stochastic events and therefore difficult to predict and prevent; however, on the basis of our evidence, these events seem to be relatively rare compared with breaches of the vaccination corridor by locally circulating viruses. Although such breaches could occur anywhere along the US–Canada border, it is apparent that some areas experience multiple incursions, either in short succession (Ontario, Quebec) or separated by several years (New Brunswick), suggesting deterministic factors. Identification of these factors, which are probably related to temporal and spatial variation in raccoon demography or vaccination coverage affecting local pressure of infection, is an area for future work.

Irrespective of the underlying mechanisms, these results demonstrate the utility of whole-genome data and bioinformatics approaches for resolving transmission processes in sensitive areas such as international borders for infectious diseases of high public concern. Increased

efforts are needed to make these tools available to government agencies dealing with transboundary diseases and to facilitate international collaboration toward controlling and ultimately eliminating the spread of infection.

Dr. Trewby is a research assistant working with the Institute for Biodiversity, Animal Health, and Comparative Medicine at the University of Glasgow, and the Department of Biology at Emory University. Her research interests focus on the use of pathogen genetics and spatial data to understand the spread of infectious disease.

References

1. Wandeler AI, Rosatte RC, Williams D, Lee TK, Gensheimer KF, Montero JT, et al.; Centers for Disease Control and Prevention. Update: raccoon rabies epizootic—United States and Canada, 1999. MMWR Morb Mortal Wkly Rep. 2000;49:31–5.
2. Sterner RT, Meltzer MI, Shwiff SA, Slate D. Tactics and economics of wildlife oral rabies vaccination, Canada and the United States. Emerg Infect Dis. 2009;15:1176–84. http://dx.doi.org/10.3201/eid1508.081061
3. Moore DA. Spatial diffusion of raccoon rabies in Pennsylvania, USA. Prev Vet Med. 1999;40:19–32. http://dx.doi.org/10.1016/S0167-5877(99)00005-7
4. Wilson ML, Bretsky PM, Cooper GH Jr, Egbertson SH, Van Kruiningen HJ, Cartter ML. Emergence of raccoon rabies in Connecticut, 1991–1994: spatial and temporal characteristics of animal infection and human contact. Am J Trop Med Hyg. 1997;57:457–63. http://dx.doi.org/10.4269/ajtmh.1997.57.457
5. Lucey BT, Russell CA, Smith D, Wilson ML, Long A, Waller LA, et al. Spatiotemporal analysis of epizootic raccoon rabies propagation in Connecticut, 1991–1995. Vector Borne Zoonotic Dis. 2002;2:77–86. http://dx.doi.org/10.1089/153036602321131878
6. Biek R, Henderson JC, Waller LA, Rupprecht CE, Real LA. A high-resolution genetic signature of demographic and spatial expansion in epizootic rabies virus. Proc Natl Acad Sci U S A. 2007;104:7993–8. http://dx.doi.org/10.1073/pnas.0700741104
7. Stevenson B, Goltz J, Massé A. Preparing for and responding to recent incursions of raccoon rabies variant into Canada. Can Commun Dis Rep. 2016;42:125–9 [cited 2017 Jun 22]. http://www.phac-aspc.gc.ca/publicat/ccdr-rmtc/16vol42/dr-rm42-6/assets/pdf/16vol42_6-ar-03-eng.pdf
8. Rosatte RC, Donovan D, Allan M, Bruce L, Buchanan T, Sobey K, et al. The control of raccoon rabies in Ontario Canada: proactive and reactive tactics, 1994–2007. J Wildl Dis. 2009;45:772–84. http://dx.doi.org/10.7589/0090-3558-45.3.772
9. Rosatte R, MacDonald E, Sobey K, Donovan D, Bruce L, Allan M, et al. The elimination of raccoon rabies from Wolfe Island, Ontario: animal density and movements. J Wildl Dis. 2007;43:242–50. http://dx.doi.org/10.7589/0090-3558-43.2.242
10. Shwiff S, Aenishaenslin C, Ludwig A, Berthiaume P, Bigras-Poulin M, Kirkpatrick K, et al. Bioeconomic modelling of raccoon rabies spread management impacts in Quebec, Canada. Transbound Emerg Dis. 2013;60:330–7. http://dx.doi.org/10.1111/j.1865-1682.2012.01351.x
11. Nadin-Davis SA, Colville A, Trewby H, Biek R, Real L. Application of high-throughput sequencing to whole rabies viral genome characterisation and its use for phylogenetic re-evaluation of a raccoon strain incursion into the province of Ontario. Virus Res. 2017;232:123–33. http://dx.doi.org/10.1016/j.virusres.2017.02.007
12. Drummond AJ, Ho SYW, Phillips MJ, Rambaut A. Relaxed phylogenetics and dating with confidence. PLoS Biol. 2006;4:e88. http://dx.doi.org/10.1371/journal.pbio.0040088
13. Lemey P, Rambaut A, Drummond AJ, Suchard MA. Bayesian phylogeography finds its roots. PLOS Comput Biol. 2009;5:e1000520. http://dx.doi.org/10.1371/journal.pcbi.1000520
14. Drummond AJ, Suchard MA, Xie D, Rambaut A. Bayesian phylogenetics with BEAUti and the BEAST 1.7. Mol Biol Evol 2012; 29:1969–73. http://dx.doi.org/10.1093/molbev/mss075
15. Ayres DL, Darling A, Zwickl DJ, Beerli P, Holder MT, Lewis PO, et al. BEAGLE: an application programming interface and high-performance computing library for statistical phylogenetics. Syst Biol. 2012;61:170–3. http://dx.doi.org/10.1093/sysbio/syr100
16. Bielejec F, Rambaut A, Suchard MA, Lemey P. SPREAD: spatial phylogenetic reconstruction of evolutionary dynamics. Bioinformatics. 2011;27:2910–2. http://dx.doi.org/10.1093/bioinformatics/btr481
17. Minin VN, Suchard MA. Fast, accurate and simulation-free stochastic mapping. Philos Trans R Soc B 2008;363:3985–95. http://dx.doi.org/: 10.1098/rstb.2008.0176
18. Szanto AG, Nadin-Davis SA, Rosatte RC, White BN. Genetic tracking of the raccoon variant of rabies virus in eastern North America. Epidemics. 2011;3:76–87. http://dx.doi.org/ 10.1016/j.epidem.2011.02.002
19. Nadin-Davis SA, Muldoon F, Wandeler AI. A molecular epidemiological analysis of the incursion of the raccoon strain of rabies virus into Canada. Epidemiol Infect. 2006;134:534–47. http://dx.doi.org/10.1017/S0950268805005108
20. Kahle D, Wickham H. ggmap: spatial visualization with ggplot2. The R Journal. 2013;5:144–61 [cited 2017 June 22]. http://journal.r-project.org/archive/2013-1/kahle-wickham.pdf
21. MacInnes C. Raccoon rabies in New Brunswick. Rabies report. Peterborough (Ontario, Canada); Ontario Ministry of Natural Resources; 2000; vol. 11. p. 10.
22. Henderson JC, Biek R, Hanlon CA, O'Dee S, Real LA. Rabies virus in raccoons, Ohio, 2004. Emerg Infect Dis. 2008;14:650–2. http://dx.doi.org/10.3201/eid1404.070972
23. Cullingham CI, Pond BA, Kyle CJ, Rees EE, Rosatte RC, White BN. Combining direct and indirect genetic methods to estimate dispersal for informing wildlife disease management decisions. Mol Ecol. 2008;17:4874–86. http://dx.doi.org/10.1111/j.1365-294X.2008.03956.x
24. Dharmarajan G, Beasley JC, Fike JA, Rhodes OE. Population genetic structure of raccoons (*Procyon lotor*) inhabiting a highly fragmented landscape. Can J Zool. 2009;87:814–24. http://dx.doi.org/10.1139/Z09-072
25. Rosatte R, Ryckman M, Ing K, Proceviat S, Allan M, Bruce L, et al. Density, movements, and survival of raccoons in Ontario, Canada: implications for disease spread and management. J Mammal. 2010;91:122–35. http://dx.doi.org/10.1644/08-MAMM-A-201R2.1
26. Rosatte R, Sobey K, Donovan D, Bruce L, Allan M, Silver A, et al. Behavior, movements, and demographics of rabid raccoons

in Ontario, Canada: management implications. J Wildl Dis. 2006;42:589–605. http://dx.doi.org/10.7589/0090-3558-42.3.589

27. Rosatte R, Sobey K, Donovan D, Allan M, Bruce L, Buchanan T, et al. Raccoon density and movements after population reduction to control rabies. J Wildl Manage. 2007; 71:2373–8. http://dx.doi.org/10.2193/2006-549

28. Rosatte R, Donovan D, Allan M, Howes LA, Silver A, Bennett K, et al. Emergency response to raccoon rabies introduction into Ontario. J Wildl Dis. 2001;37:265–79. http://dx.doi.org/10.7589/0090-3558-37.2.265

29. Nettles VF, Shaddock JH, Sikes RK, Reyes CR. Rabies in translocated raccoons. Am J Public Health. 1979;69:601–2. http://dx.doi.org/10.2105/AJPH.69.6.601

Address for correspondence: Roman Biek, Boyd Orr Centre for Population and Ecosystem Health, Institute for Biodiversity, Animal Health and Comparative Medicine, Rm 401, Graham Kerr Bldg, University of Glasgow, Glasgow, Scotland G12 8QQ, UK; email: roman.biek@glasgow.ac.uk

etymologia

Negri [neg′rē] Bodies

Ronnie Henry, Frederick A. Murphy

Negri bodies are cytoplasmic inclusions in neurons that are composed of rabies virus proteins and RNA. Adelchi Negri, an assistant pathologist working in the laboratory of Camillo Golgi, observed these inclusions in rabbits and dogs with rabies. These findings were presented in 1903 at a meeting of the Società Medico-Chirurgica of Pavia. Negri was convinced the inclusions were a parasitic protozoon and the etiologic agent of rabies. Later that same year, however, Paul Remlinger and Rifat-Bey Frasheri in Constantinople and, separately, Alfonso di Vestea in Naples showed that the etiologic agent of rabies is a filterable virus. Negri continued until 1909 to try to prove that the intraneuronal neurons named after him corresponded to steps in the developmental cycle of a protozoan. In spite of his incorrect etiologic hypothesis, Negri's discovery represented a breakthrough in the rapid diagnosis of rabies, and the detection of Negri bodies was used for many years until the development of modern diagnostic methods.

Left, Adelchi Negri 1876–1912, right: Neuron showing a cytoplasmic inclusion body (Negri body, arrow). Courtesy Frederick A. Murphy.

Sources

1. Centers for Disease Control and Prevention. Histologic examination. Apr 22, 2011 [cited 2017 Jun 21]. https://www.cdc.gov/rabies/diagnosis/histologic.html
2. Di Vestea A. On the finding of the filtration of the virus of anger [in Italian]. Annali di Igiene Sperimentale. 1905;15:147.
3. Jackson AC. Rabies and other rhabdovirus infections. In: Longo DL, Fauci AS, Kasper DL, Hauser SL, Jameson JL, Loscalzo J, editors. Harrison's principles of internal medicine. 18th ed. New York: McGraw Hill; 2012. p. 1611–7.
4. Remlinger PA, Frasheri RB. Rabies virus crosses the Berkefeld filter [in French]. Comptes Rendus de la Société de Biologie. 1903;55:730–1.

Address for correspondence: Ronnie Henry, Centers for Disease Control and Prevention, 1600 Clifton Rd NE, Mailstop E03, Atlanta, GA 30329-4027, USA; email: boq3@cdc.gov

Real-Time Whole-Genome Sequencing for Surveillance of *Listeria monocytogenes*, France

Alexandra Moura,[1] Mathieu Tourdjman,[1] Alexandre Leclercq,[1] Estelle Hamelin, Edith Laurent, Nathalie Fredriksen, Dieter Van Cauteren, Hélène Bracq-Dieye, Pierre Thouvenot, Guillaume Vales, Nathalie Tessaud-Rita, Mylène M. Maury, Andreea Alexandru, Alexis Criscuolo, Emmanuel Quevillon, Marie-Pierre Donguy, Vincent Enouf, Henriette de Valk, Sylvain Brisse,[2] Marc Lecuit[2]

During 2015–2016, we evaluated the performance of whole-genome sequencing (WGS) as a routine typing tool. Its added value for microbiological and epidemiologic surveillance of listeriosis was compared with that for pulsed-field gel electrophoresis (PFGE), the current standard method. A total of 2,743 *Listeria monocytogenes* isolates collected as part of routine surveillance were characterized in parallel by PFGE and core genome multilocus sequence typing (cgMLST) extracted from WGS. We investigated PFGE and cgMLST clusters containing human isolates. Discrimination of isolates was significantly higher by cgMLST than by PFGE (p<0.001). cgMLST discriminated unrelated isolates that shared identical PFGE profiles and phylogenetically closely related isolates with distinct PFGE profiles. This procedure also refined epidemiologic investigations to include only phylogenetically closely related isolates, improved source identification, and facilitated epidemiologic investigations, enabling identification of more outbreaks at earlier stages. WGS-based typing should replace PFGE as the primary typing method for *L. monocytogenes.*

*L*isteria monocytogenes is a foodborne bacterial pathogen that causes severe illnesses and conditions (*1*) such as septicemia, encephalitis and meningitis, abortion, still-births, and neonatal infections (*2*). Although ingestion of *L. monocytogenes* occurs frequently, incidence of listeriosis is generally low (≈6 cases/1 million persons in France) and primarily affects at-risk groups of persons (elderly, those with impaired immunity, pregnant women and their newborns) (*2,3*). However, the case-fatality rate for listeriosis is one of the highest among foodborne infections (*2,4,5*).

On the basis of *L. monocytogenes* typing studies, most listeriosis cases are believed to be sporadic, although numerous listeriosis outbreaks have been reported over the past few decades in Europe and North America (*6–10*). In addition to its public health burden (*11*), *L. monocytogenes* can lead to major economic losses in the food industry because of its capacity to replicate at low temperatures and persist on food-processing surfaces despite disinfection (*12,13*). Costs associated with recalls of contaminated products (*14*) are high, and international food safety legislations based on microbiological criteria have been established to control *L. monocytogenes* (*15,16*). Surveillance programs, including systematic isolate collection and typing, have been established to detect clusters of microbiologically related cases, identify common sources of infection, and take appropriate control measures to reduce human illness and economic losses.

In France, human listeriosis has been a mandatory reportable disease since 1999 (*3*). The French listeriosis surveillance system relies on the National Public Health Agency, which collects epidemiologic data and food consumption histories from all patients with laboratory-confirmed *L. monocytogenes* infection by using a specific hypothesis-generating questionnaire, and the National Reference Centre for *Listeria* (NRCL), which characterizes all human and food isolates received to detect clusters of genetically related strains. Food and environmental investigations are systematically conducted in refrigerators of patients with neurolisteriosis, in hospital kitchens if hospital-acquired *L. monocytogenes* infection is suspected, and among producers of suspected or incriminated products under the authority of the Ministry of Agriculture.

Author affiliations: Institut Pasteur, Paris, France (A. Moura, A. Leclercq, H. Bracq-Dieye, P. Thouvenot, G. Vales, N. Tessaud-Rita, M. Maury, A. Alexandru, A. Criscuolo, E. Quevillon, V. Enouf, S. Brisse, M. Lecuit); Institut National de la Santé et de la Recherche Médicale Unité 1117, Paris (A. Moura, M.M. Maury, M. Lecuit); Santé Publique France, Saint-Maurice, France (M. Tourdjman, E. Laurent, D. Van Cauteren, H. de Valk); Ministry of Agriculture, Agrifood, and Forestry, Paris (E. Hamelin, N. Fredriksen, M.-P. Donguy); Paris Descartes University, Paris (M. Lecuit); Necker-Enfants Malades University Hospital, Paris (M. Lecuit)

[1]These authors contributed equally to this article.

[2]These authors were co-senior authors.

Microbial typing attempts to characterize bacteria at the strain level to detect and investigate clusters of related isolates and identify sources of infection. The standard method for *L. monocytogenes* typing relies on pulsed-field gel electrophoresis (PFGE) and the restriction enzymes *Asc*I and *Apa*I (*17,18*). However, the discriminatory power of PFGE is limited compared with whole-genome sequencing (WGS) (*19–22*). Core genome multilocus sequence typing (cgMLST) (*23,24*) is a highly reproducible method that enables strain comparison across laboratories by using standardized nomenclatures of alleles and types (*20,23–26*). The power of cgMLST in identifying national or international outbreaks has been demonstrated in several studies and for multiple bacterial species (*10,20,26–30*).

With the advances in sequencing technologies, WGS has become a promising method for routine surveillance to maximize discrimination of isolates. In 2015, the NRCL implemented cgMLST as a typing method for *L. monocytogenes* and has since used it in parallel with PFGE typing. We report the performance of cgMLST as a routine typing tool and its added value for microbiological and epidemiologic surveillance by comparing it with PFGE, the current standard method.

Materials and Methods

Bacterial Isolation
The study included 2,743 *L. monocytogenes* isolates prospectively collected during January 1, 2015–December 31, 2016, in the framework of listeriosis surveillance in France. These isolates consisted of 770 from humans, 1,688 from food, and 285 from food production environments. Food and food environmental isolates were obtained from refrigerators or hospital investigations conducted in connection with confirmed human cases, samples from alerts of food companies, and investigations of the Ministry of Agriculture. Pure cultures were obtained by streaking isolated colonies onto Columbia agar plates (bioMérieux, Marcy l'Etoile, France) and incubating overnight at 35°C.

PFGE Molecular Typing
PFGE profiles were obtained by using restriction enzymes *Asc*I and *Apa*I according to the PulseNet standardized operating procedures (*31*). PFGE runs were performed twice per week, and banding patterns were compared by using the complete linkage clustering algorithm based on number of different bands in BioNumerics version 6.6 (Applied Maths, Sint-Martens-Latem, Belgium); pattern-matching optimization was set at 1%, and band position tolerance was set at 1% (*18*). *Asc*I and *Apa*I profiles were defined for each enzyme separately as differing from other profiles by ≥2 bands (i.e., a difference of only 1 band per enzyme was tolerated). Combined *Asc*I-*Apa*I PFGE

profiles were defined as being of a distinct type for ≥1 of the 2 enzymes.

DNA Extraction and WGS
DNA extraction was performed by using the DNeasy Blood and Tissue Extraction Kit (QIAGEN, København Ø, Denmark), from 5 mL of liquid cultures grown overnight at 35°C in brain heart infusion medium under aerobic conditions, following the manufacturer's protocol for gram-positive bacteria. DNA quantity and purity was assessed by using Qubit fluorimetric quantitation (Thermo Fisher Scientific, Waltham, MA, USA).

Library preparation was conducted by using the Nextera XT DNA Sample Kit (Illumina, San Diego, CA, USA). WGS was performed twice a week on a NextSeq 500 platform (Illumina) by using 2 × 150-bp runs. FqCleaner version 3.0 was used to eliminate adaptor sequences (*32*), reduce redundant or overrepresented reads (*33*), correct sequencing errors (*34*), merge overlapping paired reads (*35*), and discard reads with Phred scores (measure of the quality of identification of nucleobases generated by automated DNA sequencing) ≤20. Sequences with <40 times average coverage after trimming were resequenced to avoid artifacts in allele calling (*20*). Assemblies were obtained by using CLC Assembly Cell version 4.3.0 (QIAGEN) with estimated library insert sizes ranging from 50 bp to 850 bp and a minimum contig size of 500 bases.

Sequence-Based Genotyping
cgMLST profiles were extracted from genome assemblies by using the BLASTN algorithm (*36*) implemented in the BIGSdb-*Lm* platform (*20,37*), with minimum nucleotide identity of 70%, alignment length coverage of 70%, and word size of 10. Phylogenetic classification based on cgMLST profiles was inferred by using the single linkage algorithm implemented in Bionumerics version 6.6. cgMLST types (CTs) were defined by using international nomenclature (http://bigsdb.pasteur.fr/listeria) based on a cgMLST profile similarity cutoff of 99.600% (i.e., isolates belonging to the same type shared a maximum of 7 allelic differences of 1,748 allele calls) (*20*). cgMLST and PFGE typing results were compared by using the Simpson index of diversity (*38*) and the adjusted Wallace index of concordance (*39*). Rarefaction analyses of richness of a type were conducted by using RStudio version 0.98.485 (RStudio, Inc., Boston, MA, USA).

Cluster Definition and Epidemiologic Investigations
Before the WGS era, the listeriosis surveillance system in France categorized *L. monocytogenes* strains according to their *Asc*I-*Apa*I PFGE profile frequency in humans. An operational definition of PFGE clusters has been historically set up to identify food sources likely to still be available on

the market and thus accessible to appropriate control measures to prevent further cases. A PFGE cluster triggering further epidemiologic investigations (hereby referred to as a PFGE cluster-alert) was defined as ≥6 human cases during 6 consecutive weeks for endemic PFGE profiles (profiles associated with >12 human cases each year), or as ≥3 human cases during 6 consecutive weeks for PFGE profiles associated with ≤12 human cases each year. These different definitions were established to limit time- and resource-consuming investigations, after it was shown that the yield for investigations of PFGE cluster-alerts for endemic profiles did not differ when the ≥3 human cases threshold was used compared with the ≥6 human cases threshold during 6 consecutive weeks.

With the implementation of genomic-based surveillance, a pilot definition of cgMLST clusters was set up. We defined a cgMLST cluster triggering further investigations (hereafter referred to as a cgMLST cluster-alert) as a minimum of 2 isolates with the same cgMLST type (CT) identified during 2015–2016, including ≥1 human isolate.

During the pilot period of 2015–2016, all PFGE and cgMLST cluster-alerts were systematically investigated in parallel. To identify sources of PFGE and cgMLST cluster-alerts, case–case studies were conducted by the National Public Health Agency by using food consumption histories and by comparing food exposures of cluster-related cases with food exposures of sporadic listeriosis cases. Trace-back and trace-forward investigations of suspected or incriminated products were conducted by the Ministry of Agriculture. A food source of infection was considered confirmed if a matching food isolate was recovered from the incriminated food as part of the investigation.

Results

Increased Strain Discrimination by cgMLST

Among the 2,743 *L. monocytogenes* isolates prospectively typed during 2015–2016, PFGE identified 268 distinct *Asc*I-*Apa*I combined profiles (Simpson index 0.964, 95% CI 0.962–0.967), whereas cgMLST identified 1,112 CTs (Simpson index 0.992, 95% CI 0.991–0.993) (Figure 1, panel A). Within single PFGE types, 1–280 CTs were identified (Figure 1, panel B). Conversely, 2–7 PFGE types caused by phage insertions and deletions were found in 58 CTs. These results demonstrate that cgMLST significantly increases discrimination of *L. monocytogenes* compared with PFGE (p<0.001 by jack-knife pseudovalues resampling method).

Increased Number of Cluster-Alerts

Although the PFGE cluster definition led to identification of 31 PFGE cluster-alerts (Table 1) (245 human isolates), cgMLST cluster definition triggered investigation of 119 cgMLST cluster-alerts (311 human isolates) (Figure 2,

panel A). Of these cgMLST cluster-alerts, 37 (31%) involved only 1 human isolate, and 82 (69%) involved ≥2 human isolates (median 2) (274 human isolates) (Figure 2, panel B) (Table 2, https://wwwnc.cdc.gov/EID/article/23/9/17-0336-T1.htm). Compared with use of the PFGE cluster definition, we found that use of the cgMLST-based cluster definition resulted in a 3.8-fold increase in cluster-alerts (Figure 2, panel A). The remaining 459 (60%) of 770 human isolates did not match any CTs associated with any other human, food, or environmental isolate identified in 2015–2016 and were considered to be sporadic cases.

Inherent to the different criteria used to define cgMLST and PFGE cluster-alerts, cgMLST cluster-alerts contained lower numbers of human isolates compared with PFGE cluster-alerts (median 2 isolates in cgMLST vs. median 6 in PFGE cluster-alerts) (Figure 2, panel B). Median time from isolate reception to typing results was 7 working days for PFGE and 9 working days for WGS (Figure 2, panel D).

Facilitation of Detection of Food Sources

Epidemiologic investigations identified a confirmed food source in 3 (10%) of 31 PFGE cluster-alerts (Table 1). A confirmed food source was identified in 22 (18%) of 119 cgMLST cluster-alerts (Figure 2, panel C; Table 3).

Among the 37 cgMLST cluster-alerts involving only 1 human isolate, a cgMLST-matching food source of infection was identified in 10 (27%) (Table 3). All of these sources were identified during investigations of refrigerators of patients with neurolisteriosis and after confirmed exposure to the incriminated product. In 9 of 10 of these investigations, the food source was also identified by PFGE, and food strains matched corresponding profiles of human isolates. In 3 (30%) of these 10 conclusive investigations, a product withdrawal and recall was issued as a direct consequence of the investigation (Table 3) and probably contributed to preventing further infections. Among the remaining 27 cgMLST cluster-alerts involving only 1 human isolate and ≥1 food/environmental isolate (Table 3), although these isolate(s) provided an immediate hypothesis, no exposure to the food item from which the matching strain was isolated could be confirmed.

Among the 82 cgMLST cluster-alerts involving ≥2 human isolates (Table 3), a confirmed source of infection was identified for 12 (15%): in 3 (6%) of 53 cgMLST cluster-alerts that contained only human isolates, and in 9 (31%) of 29 cgMLST cluster-alerts containing ≥1 food/environmental isolate. For cgMLST cluster-alerts containing ≥1 food/environmental isolate, matching food/environmental isolate(s) immediately provided a strong hypothesis and facilitated identification of the food source. In 5 (42%) of these 12 conclusive investigations, a product withdrawal and recall was issued as a direct consequence of the investigation and probably contributed to preventing additional

human infections (Table 3). No product withdrawal or recall was issued as a direct consequence of investigations of the 31 PFGE clusters-alerts.

Among 70 (85%) of 82 cgMLST cluster-alerts involving ≥2 human isolates with no source of infection identified, a 6-month follow-up period after identification of the cluster-alert was available for 59 (84%). After identification of these 59 unsolved cgMLST clusters-alerts with 6-month follow-up, no additional cgMLST-matching human case was identified in 43 (73%) of 59, making identification of a source of infection unlikely to have prevented a major number of cases. These clusters without further development might have resulted from point-source contamination

of short shelf-life food products, rather than long-term infection of the food-production environment. In 5 (8%) of these 59 unsolved cgMLST clusters-alerts, additional cgMLST-matching human cases occurred within 3 months of cluster identification and none was identified afterwards, suggesting that early identification of a food source would have likely prevented further listeriosis cases. Finally, in 11 (19%) of the 59 unidentified cgMLST clusters-alerts involving ≥2 human isolates, additional cgMLST-matching human cases occurred >6 months after cluster identification. These clusters could potentially be linked to persistent *L. monocytogenes* contamination of food production environments. Strengthening capacities to identify sources of
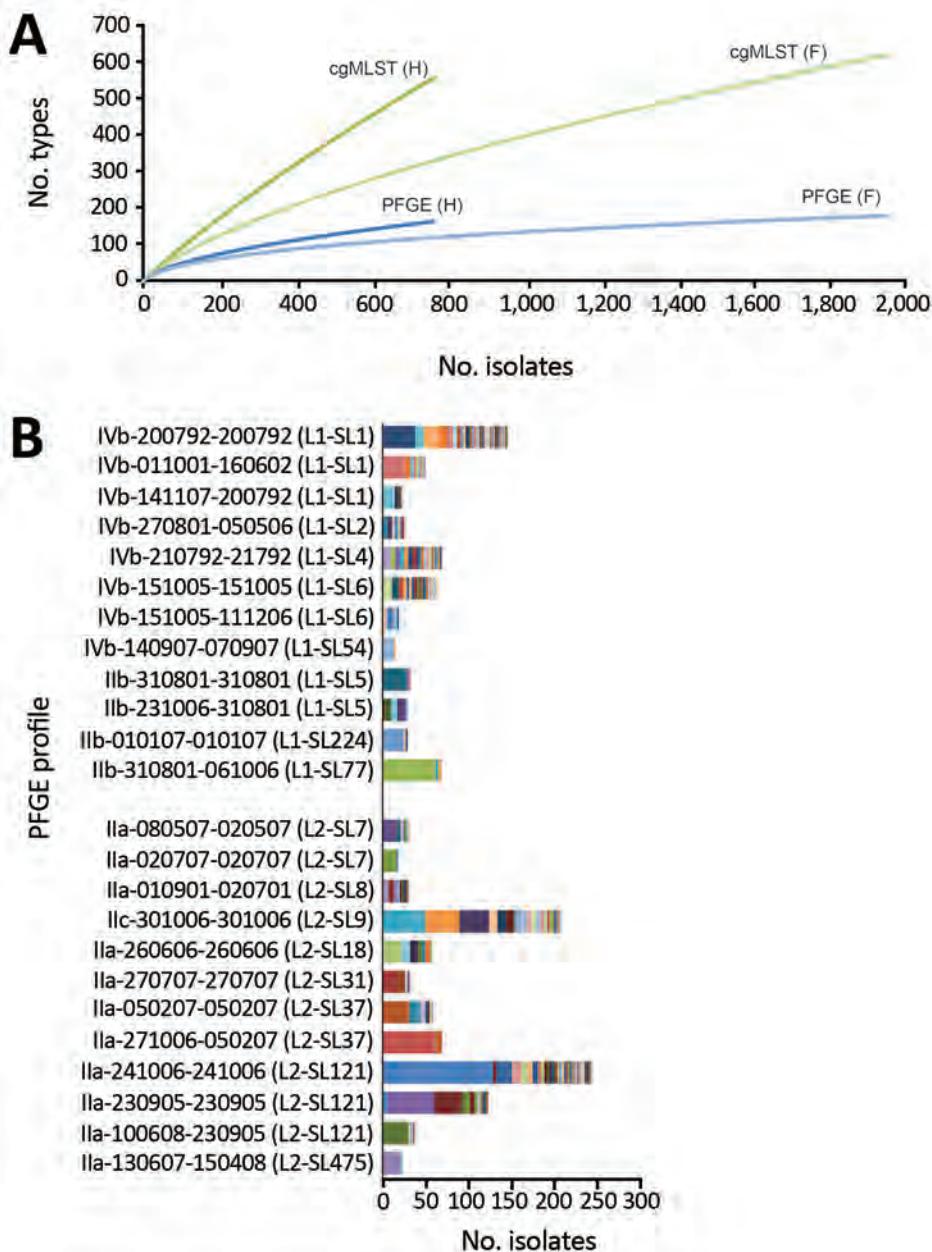
Figure 1. Discriminatory power of pulsed-field gel electrophoresis (PFGE) and core genome multilocus sequence typing (cgMLST) for surveillance of *Listeria monocytogenes*, France. A) Rarefaction analysis of type richness within human (H) and food-associated (F) isolates based on PFGE and cgMLST typing. B) Distribution of number of isolates per PFGE type and cgMLST subtyping. Only the most prevalent PFGE profiles (≥20 isolates) are shown. Within each PFGE type, different cgMLST types (CTs) are represented by different arbitrary colors. PFGE types are coded by using the National Reference Centre for *Listeria* internal nomenclature of *Asc*I-*Apa*I combined profiles. Information on lineage (L) and sublineage (SL) defined by cgMLST is provided for each PFGE type in parentheses.

Table 1. Clusters of PFGE types that triggered epidemiologic investigations for surveillance of *Listeria monocytogenes*, France*

PFGE alert	PFGE type	No. human cases	No. cgMLST types within PFGE alert	Confirmed food source according to PFGE-based investigation
L15/01, L15/06	IIa-260606–260606	7	5	No common source identified, except a specific cheese for 2 cases
L15/02	IVb-210792–210792	8	7	No common source identified, except a specific cheese for 1 case
L15/03	IIa-020707–151007	3	1	NI
L15/04	IIa-010901–020701	3	3	NI
L15/05	IVb-011001–160602	8	8	NI
L15/07	IIb-010107–010107	4	2	Dairy (cheese)
L15/08	IVb-151005–151005	22	18	NI
L15/09	IVb-210792–210792	18	12	No common source identified, except a specific cheese for 4 cases
L15/10	IIb-310801–061006	13	4	Meat (sausage)
L15/11	IVb-011001–160602	17	14	No common source identified, except a specific sausage for 1 case
L15/12	IVb-200792–200792	18	14	NI
L15/13	IVb-270801–050506	6	6	NI
L15/14	IIb-231006–310801	8	5	NI
L15/15	IIa-080507–020507	5	3	NI
L15/16	IIa-010901–020701	6	6	NI
L16/01	IIa-191107–200807	4	1	NI
L16/02	IVb-151005–151005	6	6	NI
L16/03	IVb-151005–111206	4	4	NI
L16/04	IVb-210792–210792	6	5	NI
L16/05	IIa-050207–050207	6	6	NI
L16/06	IVb-270801–050506	3	3	NI
L16/07	IVb-011001–160602	30	11	Dairy (cheese)
L16/08	IIa-260606–260606	3	1	NI
L16/09	IVb-151005–151005	8	8	NI
L16/10	IVb-210792–210792	6	6	NI
L16/11	IIa-271106–271106	4	3	NI
L16/12	IIa-010901–020701	4	4	NI
L16/13	IIa-271106–271106	3	3	NI
L16/14	IVb-210792–210792	7	7	NI
L16/15	IVb-270801–050506	5	5	NI

*cgMLST, core genome multilocus sequence typing; NI, not identified; PFGE, pulsed-field gel electrophoresis.

such clusters is likely to prevent further illnesses by identifying safety gaps in food production plants.

False PFGE Cluster-Alerts
Despite the usefulness of PFGE in identifying clusters of listeriosis cases over the past few decades, the limited discriminatory power of PFGE can indicate that unrelated isolates are indistinguishable, thus leading to identifying and investigating false PFGE cluster-alerts. The increased discriminatory power of cgMLST enabled identification of such false cluster-alerts. In 2015, PFGE cluster-alert L15/08 (Table 1) consisted of 22 human isolates with indistinguishable *Asc*I-*Apa*I combined PFGE profiles (IVb-151005–151005) among nationally distributed cases with onsets spanning >5 months. Despite intensive and time-consuming investigations, including iterative case–case studies as new cases were reported, no common source was identified. cgMLST showed that this PFGE cluster-alert did not consist of highly related isolates: 18/22 isolates had distinct CTs, and 3 cgMLST cluster-alerts (FR022, FR023, and FR025) (Table 2) could be distinguished within this PFGE cluster-alert. Investigations of these cgMLST cluster-alerts were inconclusive,

but using cgMLST clustering rather than PFGE clustering would have saved public health resources at national and local levels.

Detection of Clusters Not Detected by PFGE
For 12 (15%) of 82 cgMLST cluster-alerts involving ≥2 human cases, human isolates exhibited >1 PFGE profile (i.e., corresponded to clusters of highly related isolates that were undetected by PFGE). In cgMLST cluster-alert FR013 (L1-SL1-ST1-CT300) (Table 2), 11 nationally distributed human cases with onsets spanning >12 months were identified and only 4 of them were part of a detected PFGE cluster-alert. Investigation of this cgMLST cluster-alert resulted in several potential sources of infection, none of which could be confirmed because of incomplete trace-back information.

Better Identification of Outbreak-Associated Cases
In 2015, cgMLST cluster-alert FR028 (L1-SL4-ST4-CT1351) (Table 2) identified 2 human isolates matching 1 food isolate recovered from producer A, which was sampled as part of a food alert of the Ministry of Agriculture. None of the case-patients reported having consumed
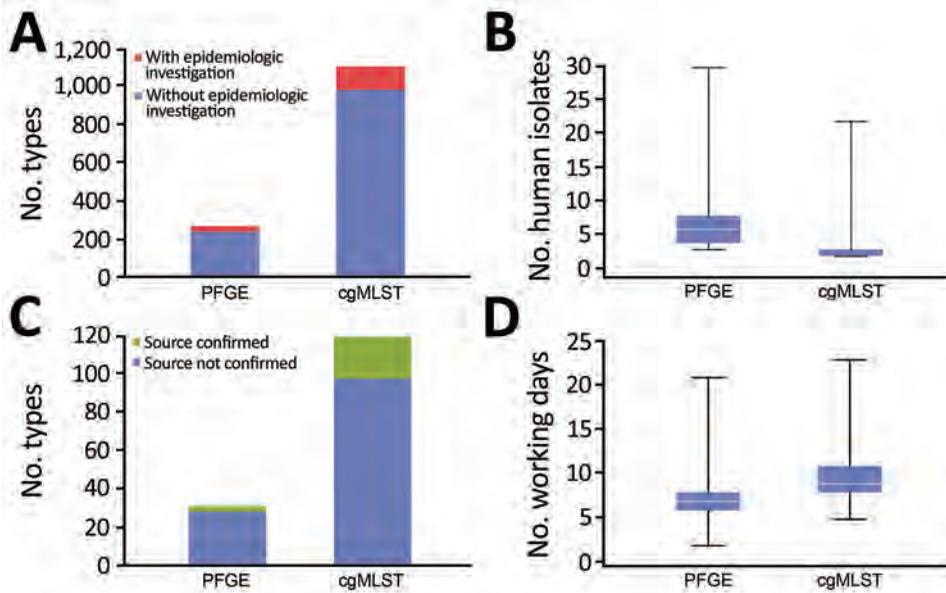
Figure 2. Comparison of pulsed-field gel electrophoresis (PFGE) and core genome multilocus sequence typing (cgMLST) for surveillance of *Listeria monocytogenes*, France. A) Number of total types and number of types triggering epidemiologic alerts. B) Number of human isolates per epidemiologic alert. C) Number of types within epidemiologic alerts with identified source. D) Time delay (days) between obtaining isolate and typing results. Horizontal lines in panels B and D indicate medians, and boxes indicate 25th and 75th percentiles. Error bars indicate maximum and minimum values.

that specific food. Concomitantly, cgMLST cluster-alert FR030 (L1-SL54-ST54-CT1530) (Table 2) identified 6 human isolates in the same geographic area that matched several deli meat items, including a sausage type, from producer A. Food and environmental investigations showed polyclonal contamination of the food production environment of this producer, and a case–case study conducted for all cases implicated in these 2 clusters showed an association with consumption of sausage. Products from producer A were withdrawn and recalled, and no further human cases were identified afterward. Because onsets of the 6 human cases involved in cgMLST cluster-alert FR030 were outside the 6-week period required to define a PFGE cluster-alert, this outbreak was not identified by PFGE.

Detection of Long-Term Persistent
***L. monocytogenes* Strains**
In June 2015, an investigation conducted at a local producer patronized by a patient in whom neurolisteriosis subsequently developed showed food and environmental infections with a distinct CT as the clinical strain. Intensive cleaning and disinfection was implemented at this production facility. In September 2016, investigation of another human case of neurolisteriosis in the same geographic area showed that the case-patient patronized a farmers' market where food from the previously implicated producer was sold. Investigations at the producer's facility identified persistent contamination with the same CT as the 2015 isolates (FR043, L2-SL121-ST121-CT914). Because of the 15-month interval, this persistent contamination would have been missed by the PFGE-based cluster definition.

Identification of Outbreaks after Regulatory Food Testing
In May 2016, an investigation was conducted on a specific cheese type from a major cheese producer in France and identified low-level (<10 CFU/g) *L. monocytogenes* contamination of the final product. The firm issued a nationwide withdrawal of 30 tons of cheese, but no recall was issued according to national regulatory criteria. Food isolates were sequenced at the NRCL and did not have the same CT as any human isolate at that time. In the following 3 months, consistent with the 3-month shelf-life of the implicated product, 22 human isolates had the same CT (L1-SL1-ST1-CT2056; FR083 cluster-alert) (Table 2) and were identified nationwide. Case–case analysis confirmed a significant association between illness and consumption of the implicated product (p = 0.00001). Subsequent food testing confirmed that the implicated cheese was the source for this outbreak. During the same period, PFGE identified 30 human isolates that matched food strains (IVb-011001–160602). However, with cgMLST typing, the analysis was restricted to isolates that were closely related genetically, not just to those that were of the same PFGE profile. This analysis enabled the statistical association to be defined more precisely. This retrospective outbreak was the largest identified in France since 2000.

Discussion
Because listeriosis is a rare infection and primarily affects at-risk populations, listeriosis outbreaks tend to be small and difficult to control. As in most countries, PFGE-based *L. monocytogenes* molecular subtyping has been used for molecular surveillance of this bacterium in France. Since 1999, PFGE identified multiple outbreaks, which led to major improvements in food safety. However, WGS has shown

Table 3. Source identification of cgMLST cluster-alerts for surveillance of *Listeria monocytogenes*, France*

cgMLST cluster-alert size, no. human isolates	No. (%)				
	Clusters, n = 119	Human isolates, n = 770	Food/environment isolates, n = 1,973	Clusters with confirmed source	Cluster-alerts with identified source resulting in withdrawal or recall
Small, 1	37 (31)	37 (5)	145 (7)	10 (27)	3 (30)
Medium, 2–5	73 (61)	185 (24)	123 (6)	9 (12)	5 (55)
Large, >5	9 (8)	89 (12)	83 (4)	3 (38)	0
*cgMLST, core genome multilocus sequence typing.					

the limited discrimination and occasional lack of accuracy of PFGE (*19,20,40*). PFGE does not reflect phylogeny, and it lacks the resolution to distinguish bands of nearly identical sizes. For certain profiles that are highly prevalent, these limitations can result in insufficient discrimination and can hinder appropriate detection of clusters.

We showed the usefulness and feasibility of WGS for prospective *L. monocytogenes* surveillance by using cgMLST and demonstrated its added value over PFGE. cgMLST detected clusters not detected by PGFE, which enabled elimination of several pseudoclusters defined by PFGE and detection of closely related isolates with different PFGE profiles caused by phage insertions or deletions. It also identified clusters of cases associated with persistent food production environmental contamination that were previously unrecognized.

cgMLST results were obtained within 9 working days, compared with 7 working days for PFGE. This difference showed that use of cgMLST for real-time surveillance is feasible because these intervals can be shortened by improved laboratory processing and technological advances.

The unprecedented discriminatory power of cgMLST has provided an opportunity to revisit the criteria used in France since 1999 to define clusters of isolates triggering further investigations. Instead of 3–6 PFGE-matching human isolates identified within a defined period, clusters triggering investigation are now defined by a minimum of 2 genetically related isolates, including ≥1 human isolate regardless of the time interval. However, this procedure has created novel challenges for public health and regulatory agencies to formally prove an outbreak food source through epidemiologic investigations. With more clusters of smaller size being identified by cgMLST, traditional analytic epidemiology is challenged because of the lack of statistical power, and identification of a food source for these small clusters tends to more extensively rely on trace-back or trace-forward investigations, rather than on case–case studies. Increasing demands of product trace-back or trace-forward investigations should be expected as a consequence of increasing identification of small-size clusters by cgMLST. Timely results from these investigations will be fundamental to initiate control measures in instances where a lower level of epidemiologic evidence is available and will likely contribute to an increased number of reported outbreaks (i.e., investigated cluster-alerts with an identified source of infection).

Implementation of WGS-based surveillance has shown that most clusters involving ≥2 human isolates with no source of infection identified did not progress over time. This finding is consistent with the observation that most listeriosis case clusters in France are linked to local products that have limited production and distribution.

With the increasing identification of small size clusters by cgMLST, we envision that centralized collection of human, food, and environmental bacterial genomes, including those from regulatory food testing, into dedicated genomic databases (e.g., BIGSdb-*Lm* and GenomeTrackr) will enable detection of unusual sources of infection and identify atypical vehicles for contamination. The ability to promptly document cases' food consumption histories and to constantly adapt hypothesis-generating questionnaires to newly identified vehicles will be crucial to improve investigations and identify more outbreaks, enabling better control and preventive measures to be implemented.

In conclusion, implementation of WGS for routine *L. monocytogenes* surveillance increases discrimination of isolates, leading to detection of more clusters of related isolates at an earlier stage than PFGE. Optimization of costs and delays is a challenge, which is strongly balanced by gains in genotypic precision. Public health and regulatory agencies will need to adapt their investigation methods to novel challenges raised by WGS-based surveillance. These challenges might lead to better strategies to control *L. monocytogenes* in food-processing plants, and ultimately help reduce the risk for infection. On the basis of results of this prospective study, PFGE typing has been discontinued, and *L. monocytogenes* surveillance in France has relied on cgMLST since January 2017.

Dr. Moura is a microbiologist at the Institut Pasteur, Paris, France. Her primary research interests are the evolution and genomic epidemiology of *L. monocytogenes*.

References

1. Lecuit M. Understanding how *Listeria monocytogenes* targets and crosses host barriers. Clin Microbiol Infect. 2005;11:430–6. http://dx.doi.org/10.1111/j.1469-0691.2005.01146.x
2. Charlier C, Perrodeau É, Leclercq A, Cazenave B, Pilmis B, Henry B, et al.; MONALISA study group. Clinical features and prognostic factors of listeriosis: the MONALISA national prospective cohort study. Lancet Infect Dis. 2017;17:510–9. http://dx.doi.org/10.1016/S1473-3099(16)30521-7
3. Goulet V, Hedberg C, Le Monnier A, de Valk H. Increasing incidence of listeriosis in France and other European countries. Emerg Infect Dis. 2008;14:734–40. http://dx.doi.org/10.3201/eid1405.071395
4. European Centre for Disease Prevention and Control. Surveillance of seven priority food- and waterborne diseases in the EU/EEA. Stockholm; 2015 [cited 2017 May 22]. http://ecdc.europa.eu/en/publications/Publications/food-and-waterborne-diseases-surveillance-report-2015.pdf
5. Scallan E, Hoekstra RM, Angulo FJ, Tauxe RV, Widdowson MA, Roy SL, et al. Foodborne illness acquired in the United States—major pathogens. Emerg Infect Dis. 2011;17:7–15. http://dx.doi.org/10.3201/eid1701.P11101
6. de Valk H, Vaillant V, Jacquet C, Rocourt J, Le Querrec F, Stainer F, et al. Two consecutive nationwide outbreaks of listeriosis in France, October 1999–February 2000. Am J Epidemiol. 2001;154:944–50. http://dx.doi.org/10.1093/aje/154.10.944
7. Cartwright EJ, Jackson KA, Johnson SD, Graves LM, Silk BJ, Mahon BE. Listeriosis outbreaks and associated food vehicles, United States, 1998-2008. Emerg Infect Dis. 2013;19:1–9, quiz 184. http://dx.doi.org/10.3201/eid1901.120393
8. Heiman KE, Garalde VB, Gronostaj M, Jackson K, Beam S, Joseph L, et al. Multistate outbreak of listeriosis caused by imported cheese and evidence of cross-contamination of other cheeses, USA, 2012. Epidemiol Infect. 2015;144:1–11.
9. Kvistholm Jensen A, Nielsen EM, Björkman JT, Jensen T, Müller L, Persson S, et al. Whole-genome sequencing used to investigate a nationwide outbreak of listeriosis caused by ready-to-eat delicatessen meat, Denmark, 2014. Clin Infect Dis. 2016;63:64–70. http://dx.doi.org/10.1093/cid/ciw192
10. Fretz R, Sagel U, Ruppitsch W, Pietzka A, Stöger A, Huhulescu S, et al. Listeriosis outbreak caused by acid curd cheese Quargel, Austria and Germany 2009. Euro Surveill. 2010;15:2009–10.
11. Leclercq A, Charlier C, Lecuit M. Global burden of listeriosis: the tip of the iceberg. Lancet Infect Dis. 2014;14:1027–8. http://dx.doi.org/10.1016/S1473-3099(14)70903-X
12. Ferreira V, Wiedmann M, Teixeira P, Stasiewicz MJ. *Listeria monocytogenes* persistence in food-associated environments: epidemiology, strain characteristics, and implications for public health. J Food Prot. 2014;77:150–70. http://dx.doi.org/10.4315/0362-028X.JFP-13-150
13. Holch A, Webb K, Lukjancenko O, Ussery D, Rosenthal BM, Gram L. Genome sequencing identifies two nearly unchanged strains of persistent *Listeria monocytogenes* isolated at two different fish processing plants sampled 6 years apart. Appl Environ Microbiol. 2013;79:2944–51. http://dx.doi.org/10.1128/AEM.03715-12
14. Thomas MK, Vriezen R, Farber JM, Currie A, Schlech W, Fazil A. Economic cost of a *Listeria monocytogenes* outbreak in Canada, 2008. Foodborne Pathog Dis. 2015;12:966–71. http://dx.doi.org/10.1089/fpd.2015.1965
15. EUR-Lex. Access to European Union law [cited 2017 May 22]. http://eur-lex.europa.eu/legal-content/en/ALL/?uri=CELEX:32005R2073
16. United States Department of Agriculture. Food Safety and Inspection Service. Compliance guides index [cited May 22]. https://www.fsis.usda.gov/wps/portal/fsis/topics/regulatory-compliance/compliance-guides-index#Listeria
17. Graves LM, Swaminathan B. PulseNet standardized protocol for subtyping *Listeria monocytogenes* by macrorestriction and pulsed-field gel electrophoresis. Int J Food Microbiol. 2001;65:55–62. http://dx.doi.org/10.1016/S0168-1605(00)00501-8
18. Martin P, Jacquet C, Goulet V, Vaillant V, De Valk H; Participants in the PulseNet Europe Feasibility Study. Pulsed-field gel electrophoresis of *Listeria monocytogenes* strains: the PulseNet Europe Feasibility Study. Foodborne Pathog Dis. 2006;3:303–8. http://dx.doi.org/10.1089/fpd.2006.3.303
19. Jackson BR, Tarr C, Strain E, Jackson KA, Conrad A, Carleton H, et al. Implementation of nationwide real-time whole-genome sequencing to enhance listeriosis outbreak detection and investigation. Clin Infect Dis. 2016;63:380–6. http://dx.doi.org/10.1093/cid/ciw242
20. Moura A, Criscuolo A, Pouseele H, Maury MM, Leclercq A, Tarr C, et al. Whole genome-based population biology and epidemiological surveillance of *Listeria monocytogenes*. Nat Microbiol. 2016; 2:16185. http://dx.doi.org/10.1038/nmicrobiol.2016.185
21. Sabat AJ, Budimir A, Nashev D, Sá-Leão R, van Dijl J, Laurent F, et al.; ESCMID Study Group of Epidemiological Markers (ESGEM). Overview of molecular typing methods for outbreak detection and epidemiological surveillance. Euro Surveill. 2013;18:20380.
22. den Bakker HC, Allard MW, Bopp D, Brown EW, Fontana J, Iqbal Z, et al. Rapid whole-genome sequencing for surveillance of *Salmonella enterica* serovar enteritidis. Emerg Infect Dis. 2014;20:1306–14. http://dx.doi.org/10.3201/eid2008.131399
23. Sheppard SK, Jolley KA, Maiden MCJ. A gene-by-gene approach to bacterial population genomics: whole genome MLST of *Campylobacter*. Genes (Basel). 2012;3:261–77. http://dx.doi.org/10.3390/genes3020261
24. Maiden MCJ, Jansen van Rensburg MJ, Bray JE, Earle SG, Ford SA, Jolley KA, et al. MLST revisited: the gene-by-gene approach to bacterial genomics. Nat Rev Microbiol. 2013;11:728–36. http://dx.doi.org/10.1038/nrmicro3093
25. Bratcher HB, Corton C, Jolley KA, Parkhill J, Maiden MC. A gene-by-gene population genomics platform: de novo assembly, annotation and genealogical analysis of 108 representative

Neisseria meningitidis genomes. BMC Genomics. 2014;15:1138. http://dx.doi.org/10.1186/1471-2164-15-1138

26. Kohl TA, Diel R, Harmsen D, Rothgänger J, Walter KM, Merker M, et al. Whole-genome-based *Mycobacterium tuberculosis* surveillance: a standardized, portable, and expandable approach. J Clin Microbiol. 2014;52:2479–86. http://dx.doi.org/10.1128/JCM.00567-14

27. Jolley KA, Hill DMC, Bratcher HB, Harrison OB, Feavers IM, Parkhill J, et al. Resolution of a meningococcal disease outbreak from whole-genome sequence data with rapid web-based analysis methods. J Clin Microbiol. 2012;50:3046–53. http://dx.doi.org/10.1128/JCM.01312-12

28. de Been M, Pinholt M, Top J, Bletz S, Mellmann A, van Schaik W, et al. Core genome multilocus sequence typing scheme for high-resolution typing of *Enterococcus faecium*. J Clin Microbiol. 2015;53:3788–97. http://dx.doi.org/10.1128/JCM.01946-15

29. Moran-Gilad J, Prior K, Yakunin E, Harrison TG, Underwood A, Lazarovitch T, et al. Design and application of a core genome multilocus sequence typing scheme for investigation of Legionnaires' disease incidents. Euro Surveill. 2015;20:1–9. http://dx.doi.org/10.2807/1560-7917.ES2015.20.28.21186

30. Cody AJ, McCarthy ND, Jansen van Rensburg M, Isinkaye T, Bentley SD, Parkhill J, et al. Real-time genomic epidemiological evaluation of human *Campylobacter* isolates by use of whole-genome multilocus sequence typing. J Clin Microbiol. 2013;51:2526–34. http://dx.doi.org/10.1128/JCM.00066-13

31. Centers for Disease Control and Prevention. Standard operating procedure for PulseNet PFGE of *Listeria monocytogenes*, 2013 [cited 2017 May 21]. http://www.cdc.gov/pulsenet/PDF/listeria-pfge-protocol-508c.pdf

32. Criscuolo A, Brisse S. AlienTrimmer: a tool to quickly and accurately trim off multiple short contaminant sequences from high-throughput sequencing reads. Genomics. 2013;102:500–6. http://dx.doi.org/10.1016/j.ygeno.2013.07.011

33. Crusoe MR, Alameldin HF, Awad S, Boucher E, Caldwell A, Cartwright R, et al. The khmer software package: enabling efficient nucleotide sequence analysis. F1000Res. 2015;4:900.

34. Liu Y, Schröder J, Schmidt B. Musket: a multistage k-mer spectrum-based error corrector for Illumina sequence data. Bioinformatics. 2013;29:308–15. http://dx.doi.org/10.1093/bioinformatics/bts690

35. Magoč T, Salzberg SL. FLASH: fast length adjustment of short reads to improve genome assemblies. Bioinformatics. 2011;27:2957–63. http://dx.doi.org/10.1093/bioinformatics/btr507

36. Altschul SF, Gish W, Miller W, Myers EW, Lipman DJ. Basic local alignment search tool. J Mol Biol. 1990;215:403–10. http://dx.doi.org/10.1016/S0022-2836(05)80360-2

37. Jolley KA, Maiden MC. BIGSdb: scalable analysis of bacterial genome variation at the population level. BMC Bioinformatics. 2010;11:595. http://dx.doi.org/10.1186/1471-2105-11-595

38. Simpson EH. Measurement of diversity. Nature. 1949;163:688. http://dx.doi.org/10.1038/163688a0

39. Severiano A, Pinto FR, Ramirez M, Carriço JA. Adjusted Wallace coefficient as a measure of congruence between typing methods. J Clin Microbiol. 2011;49:3997–4000. http://dx.doi.org/10.1128/JCM.00624-11

40. Moore G, Cookson B, Gordon NC, Jackson R, Kearns A, Singleton J, et al. Whole-genome sequencing in hierarchy with pulsed-field gel electrophoresis: the utility of this approach to establish possible sources of MRSA cross-transmission. J Hosp Infect. 2015;90:38–45. http://dx.doi.org/10.1016/j.jhin.2014.12.014

Address for correspondence: Marc Lecuit, Biology of Infection Unit, Institut Pasteur, 28 Rue du Dr Roux, 75724 Paris CEDEX 15, France; email: marc.lecuit@pasteur.fr

Role of Food Insecurity in Outbreak of Anthrax Infections among Humans and Hippopotamuses Living in a Game Reserve Area, Rural Zambia

Mark W. Lehman,[1] Allen S. Craig,[2] Constantine Malama, Muzala Kapina-Kany'anga, Philip Malenga, Fanny Munsaka, Sergio Muwowo, Sean Shadomy, Melissa A. Marx[3]

In September 2011, a total of 511 human cases of anthrax (*Bacillus anthracis*) infection and 5 deaths were reported in a game management area in the district of Chama, Zambia, near where 85 hippopotamuses (*Hippopotamus amphibius*) had recently died of suspected anthrax. The human infections generally responded to antibiotics. To clarify transmission, we conducted a cross-sectional, interviewer-administered household survey in villages where human anthrax cases and hippopotamus deaths were reported. Among 284 respondents, 84% ate hippopotamus meat before the outbreak. Eating, carrying, and preparing meat were associated with anthrax infection. Despite the risk, 23% of respondents reported they would eat meat from hippopotamuses found dead again because of food shortage (73%), lack of meat (12%), hunger (7%), and protein shortage (5%). Chronic food insecurity can lead to consumption of unsafe foods, leaving communities susceptible to zoonotic infection. Interagency cooperation is necessary to prevent outbreaks by addressing the root cause of exposure, such as food insecurity.

During August–September 2011, a total of 85 hippopotamuses (*Hippopotamus amphibius*) died of suspected anthrax (*Bacillus anthracis*) infection in a game management area along the South Luangwa River near the district of Chama in northeastern Zambia (Figure 1) (*1*). At least 521 suspected human anthrax cases and 5 deaths were reported near this area during this period. Residents of the area near the river had reportedly found dead hippopotamuses and subsequently butchered, cooked, and consumed meat from the dead animals, which was thought to be the cause of the human outbreak. As previously reported, most human cases of anthrax infection were cutaneous infections, with most patients initially having papular lesions (95%) and the rest having lymphadenopathy and gastrointestinal symptoms (*1*). Most cases resolved after the patient received a course of oral ciprofloxacin. Some additional animal species were reported by local wildlife staff to have been affected, but no empiric data were found to corroborate those reports.

Anthrax outbreaks associated with animals are common and reported worldwide. Herbivores are thought to have onset of disease after ingesting spores in soil, water, or on vegetation. Reports of anthrax outbreaks occurring in wild and domestic animals in Africa have usually been associated with the dry season and have stopped with the onset of the rainy season (*2,3*). Outbreaks can begin with wildlife, expand into domestic livestock, and ultimately affect humans (*4,5*). When anthrax outbreaks occur in national parks in Africa and are limited to the wildlife, the outbreak is usually allowed to run its natural course without any human intervention. Multiple challenges make it impractical to vaccinate free-ranging wildlife populations; sometimes vaccine programs are initiated but usually only to protect endangered species or populations at high risk (*6–8*).

Anthrax outbreaks associated with hippopotamuses have been reported previously in Zambia, Uganda, Zimbabwe, and South Africa (*3,9–11*). Human cases associated with wildlife outbreaks in Africa are generally not well-documented but are known to occur (*5*).

[1]Current affiliation: US Air Force School of Aerospace Medicine, Wright-Patterson AFB, Ohio, USA.

[2]Current affiliation: Centers for Disease Control and Prevention, Atlanta, Georgia, USA.

[3]Current affiliation: Johns Hopkins Bloomberg School of Public Health, Baltimore, Maryland, USA.
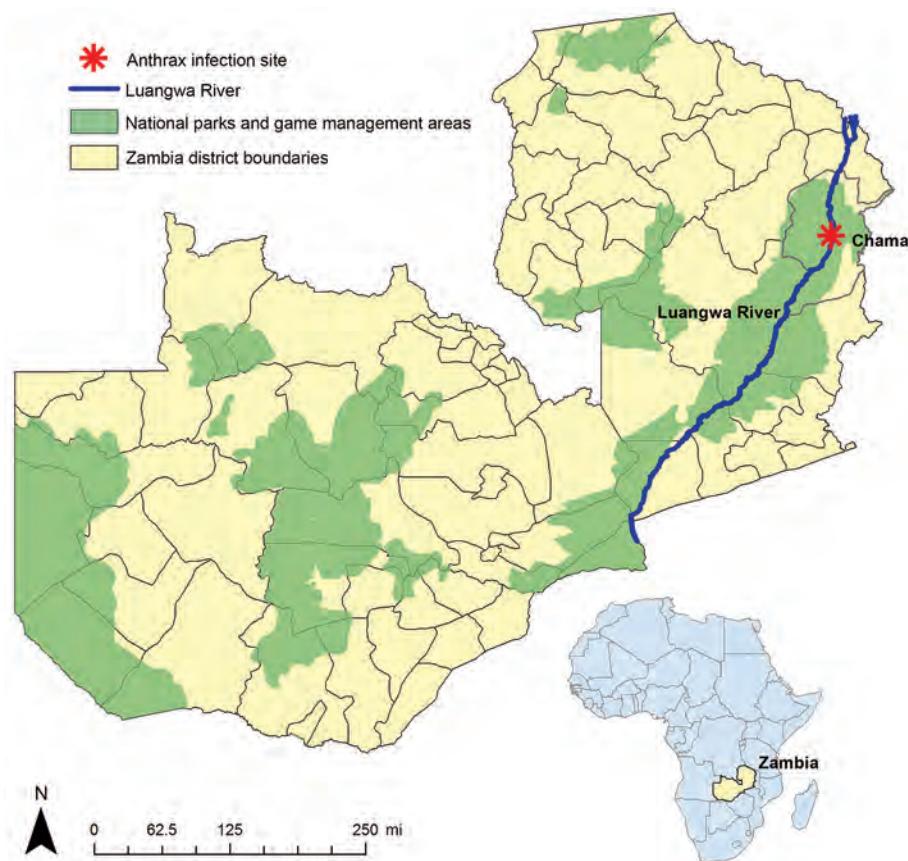
Figure 1. Location of an anthrax outbreak that originated in a game management area along the South Luangwa River in the Chama District of northeastern Zambia, 2011. Inset map shows location of Zambia in Africa.

Zambia's Chama District (population 103,894) borders Malawi, in what is currently known as Muchinga Province (Figure 1) (*12*). Nearly 93% of the district's residents live in rural areas, and overall population density is 5.9 persons/km² (*12*). The rural population resides in small villages largely accessible only by all-terrain vehicles. Communication in many parts of the district is only possible through 2-way radios. Chama is within a game management area that includes the South Luangwa River and contains rich flora and fauna, including hippopotamuses but also other foragers and predators. Because of Chama's status as a game management area, residents are not permitted to protect crops from foragers or hunt on area grounds, which are overseen by the Zambia Wildlife Authority (ZAWA). Food and water are scarce for animals and humans during Zambia's dry season, generally May–November. A delay in the annual rainy season, usually December–March, can put farmers at risk for low crop production, as was the case in 2011 (*13*). During this period, animals forage deep into riverbeds in search of water and food, digging up and activating dormant anthrax spores. Residents, for whom food can also be scarce under these conditions, have been known to consume animals they find dead in their area (Figure 2).

In September 2011, a few months after the first human anthrax cases were reported in the district, a team of

epidemiologists, health officers, and environmental health technicians from the Zambia Central Ministry of Health, the Eastern Provincial Health Office, and Chama District Health Office conducted a preliminary investigation of the possible outbreak under their jurisdiction. Shortly thereafter, upon formal request, epidemiologists from the US Centers for Disease Control and Prevention joined the Zambia team to conduct this outbreak investigation in an effort to further inform prevention activities.

Specifically, we aimed to shorten the outbreak by identifying and eliminating any remaining exposures and by recommending mitigation and prevention strategies for this and future outbreaks. We also wanted to determine the riskiest exposures so that educational messages could be properly tailored. Here we report the results of a household survey used to identify the most common exposures associated with human anthrax and to determine how food insecurity contributed to consumption of the anthrax-contaminated meat and anthrax infection among residents of this game management area.

Methods

We conducted a cross-sectional, interviewer-administered household survey in 3 villages with access to riverbeds where hippopotamuses died: Chikwa, Chigoma, and Chimpamaba.

Figure 2. A family searching for water by digging deep into a dried riverbed during the dry season in northeastern Zambia.

Figure 3. Hippopotamus bones and hides left behind after butchering of animals that were found dead on a river bank and later identified as the source of anthrax causing an outbreak among humans in northeastern Zambia, 2011.

These villages' estimated combined population of adults ≥15 years of age is 6,553 (*12*). A questionnaire (online Technical Appendix, https://wwwnc.cdc.gov/EID/article/23/9/16-1597-Techapp1.pdf) was developed in English and translated into Senga, the local language spoken in these areas. The questionnaire was designed to complement and expand on the data initially collected in the district by local public health officials. It captured age, sex, and occupation and yes/no responses to several questions about symptoms, exposure to hippopotamuses, food sources, and whether respondents would eat meat from an animal they found dead. Those who responded that they would eat animals they found dead were asked an open-ended question to elucidate their reasons for doing so. Interviewers and supervisors were trained on procedures for conducting the survey before fieldwork commenced. Interviewers and supervisors tested questions on each other, which resulted in improvements to question wording. They also practiced administering the survey on one another before interviewing community participants.

Three teams administered the questionnaire, each team made up of a trained District Health Office staff supervisor and 6 trained volunteer interviewers. Each team was assigned to 1 of the 3 communities. Interviewers selected every fifth household they encountered in each village for inclusion and interviewed all adults ≥15 years of age living in selected households. No incentives were offered for participation. Interviewers read each prospective participant a description of the survey, highlighting that it was voluntary and could be stopped at any time by request. The Zambia Ministry of Health deemed this outbreak investigation to be exempt from Research Ethics Committee review. The investigation protocol was reviewed by the CDC-Zambia office and CDC's National Center for Emerging and Zoonotic Infectious Diseases, in accordance with institutional review policies. The protocol was determined to be nonresearch under 45 CFR 46 §102(d) and therefore did not require Institutional Review Board review.

Data from completed questionnaires were entered into an Access database (Microsoft, Redmond, WA, USA) and analyzed by using Epi Info version 3.5.1 (CDC, Atlanta, GA, USA). We defined a case as illness in a respondent who reported having had anthrax infection diagnosed by a healthcare worker since July 2011 and compared demographic characteristics and risk factors by case status by using χ^2 and *t* tests. Associations were quantified with simple and multivariable logistic regression.

The second part of the investigation involved going into the field to view 3 of the areas where most of the infected hippopotamuses were found. The site visits occurred within about a month after the outbreak and were conducted to better understand the topography and the range of the animals and to identify any additional animal species affected by anthrax. All sites were areas frequented by the exposed human populations and were <1 km from residents' homes. The site surveys were not exhaustive; they focused on areas with known human-animal interaction (Figure 3) and recently discovered dead hippopotamuses (Figure 4). N95 masks, Tyvek suits, and rubber boots were worn

Figure 4. A dead hippopotamus floating down the South Luangwa River in northeastern Zambia during an anthrax outbreak in 2011.

during site visits when members exited vehicles. We used these observations and the results of the household-level surveys to develop recommendations to mitigate and control future spread of the infection to humans, animals, and the environment.

Results

All 284 household members (≈4% of the population of the villages) in the 87 households selected agreed to be interviewed (mean 3 participants per household). In total, 31 (11%) of participants reported having anthrax infection diagnosed by a healthcare worker since July 2011; another 137 (48%) reported not having anthrax infection diagnosed, and 116 (41%) did not know whether they had anthrax infection diagnosed. We assumed that those who did not know did not have anthrax infection diagnosed. Male respondents accounted for 48% (n = 136) of total participants but 68% (n = 21) of those reporting having anthrax infection diagnosed, compared with 36% of cases occurring among female respondents (p<0.001) (Table 1). Of the 96 persons who answered the occupation-related question, 91 (95%) listed their occupation as farmer. This finding was not surprising given the rural setting of the outbreak. Because the responses for occupation were so homogenous, occupation was not evaluated as a risk factor. The median age of persons having received an anthrax diagnosis since July 2011 was 33 years, similar to the median age of all participants (32 years) (Table 1). The most common signs and symptoms reported by those reporting having been diagnosed with anthrax included myalgia, skin lesions, fatigue, diarrhea, and fever (Table 2).

Most participants (238 [84%]) reported having eaten hippopotamus meat at the time of the outbreak. Participants who ate the meat were 9 times (95% CI 1.3–369.3 times) more likely to report having had anthrax than those who did not eat the meat. Carrying hippopotamus meat (odds ratio 5.3, 95% CI 2.0–15.4) and preparing it for cooking (odds ratio 3.3, 95% CI 1.1–13.7) were also significantly associated with anthrax infection. After controlling for having eaten the hippopotamus meat, 3 activities (skinning, carrying, and cutting the meat) were all still significantly associated with reported anthrax infection (Table 3).

Most people surveyed (216 [76%]) reported they would not eat meat from a dead hippopotamus knowing now that it can cause anthrax infection, but 65 (23%) of all respondents and 5 (16%) of the 31 respondents in whom cases were reported said that they would eat meat from a dead hippopotamus despite this knowledge. Of the 65 participants saying they would eat the meat if given the chance again, reasons given were because they lacked other options for a side dish ("relish") to Nshima, the maize-based staple food (44 [73%]); lacked meat (14 [22%]); suffered from hunger (4 [7%]); or lacked protein (3 [5%]), in addition to other less commonly reported reasons (Table 4).

The investigation team also visited several field sites. At 1 of the sites, previous human interaction with dead hippopotamuses was evident. Bones and hides were strewn across a large area. Evidence of multiple campfires were found in the vicinity of the hippopotamus remains (Figure 3). According to a Zambia Ministry of Health official and others on the investigation team who had visited the site earlier, the strewn animal parts appeared to have been from the initial human contact with the dead hippopotamuses. Residents appeared to stop handling dead hippopotamuses after human anthrax cases were detected and linked to contact with hippopotamus carcasses.

Discussion

A large outbreak of cutaneous anthrax among humans in the Chama District of Zambia was associated with physical contact with meat from hippopotamuses that had died of anthrax, specifically skinning, carrying, or cutting the meat. Food insecurity was thought to have been the major factor driving the local population to consume meat from dead animals.

Large outbreaks affecting hippopotamus herds occurred within the Luangwa River Valley during 1987–1988 (7). Although no human infections were reported in relation to these outbreaks, positive results with low antibody titers against *B. anthracis* were obtained during a 1989 follow-up study from half of the subjects in a small sample of unvaccinated healthy volunteers from Luangwa River Valley villages, suggesting previous exposures in those persons through handling or consumption of meat from anthrax-infected animal carcasses (7).

Our findings are subject to a few limitations. In the household surveys, we used self-report of anthrax diagnosis to define a case; however, 41% of participants indicated

Table 1. Demographic characteristics of respondents to a survey conducted after an outbreak of anthrax infections among humans and hippopotamuses living in a game reserve area, by case status, Chama District, Zambia, September 2011*

Characteristic	Persons with anthrax diagnosed since July 2011, n = 31	Persons without anthrax diagnosed since July 2011, n = 137
Median age (range), y	33 (15–72)	34 (15–83)
Sex, %		
M	68	36
F	32	64

*116 (41%) of survey participants reported that they did not know whether they had had anthrax diagnosed since July 2011; of these, median age was 30 (range 15–77) years, and 52% were male.

Table 2. Signs and symptoms of respondents reporting having had anthrax in survey conducted after outbreak of anthrax infections among humans and hippopotamuses living in a game reserve area, Chama District, Zambia, September 2011*

Signs/symptoms	No. (%) respondents
Myalgia	21 (67)
Skin lesion	18 (58)
Fatigue	18 (58)
Diarrhea	17 (54)
Fever	16 (52)
*Anthrax infection diagnosed since July 2011.	

they did not know whether they had received an anthrax diagnosis. We assumed that these respondents might not have understood the question and had probably not had anthrax diagnosed. Although this assumption is a limitation, it would probably bias our associations toward the null. We also had to use self-report of diagnosis rather than laboratory confirmation. However, separately some hippopotamus and human samples were confirmed in the laboratory as positive for *B. anthracis*, which does strengthen the epidemiologic linkage (*14*). Finally, slight discrepancies can be noted in the number of cases and hippopotamus deaths in this and the 2 other reports describing other aspects of the outbreak and response that have been published; specifically, the numbers of human cases vary from 511 to 521, and the numbers of hippopotamus deaths vary from 81 to 85 (*14,15*). This discrepancy likely illustrates the difficulty in describing events in very remote areas.

From this investigation we found that the greatest risk for having anthrax diagnosed came from carrying, skinning, or butchering hippopotamuses. This finding is consistent with other anthrax outbreaks associated with contaminated meat (*11,16*).

Recommendations from this investigation built on the initial response of the Zambia Ministry of Health and included community education, enhanced surveillance in human and animal populations, and resolution of food insecurities by working with governmental and nongovernmental agencies. The message to not eat meat from animals found dead was communicated at the time of the initial investigation. On the basis of survey responses indicating persons were no longer touching the meat and that carcasses were

no longer being butchered, we think the messages were received and understood by the communities affected. Because the handling of the carcasses proved to be the most important risk factor for anthrax infection, future education campaigns should also focus on avoiding handling animals that have died of unknown causes. In rural Zimbabwe communities where anthrax awareness was high (71.5%) in a 2013 survey, 41% of persons surveyed reported "forgetting about anthrax," a major reason for consuming meat from anthrax-infected animals (*17*). Residents should be reminded by community-based awareness campaigns or other means of the hazards of consuming meat from animals that have died of unknown causes (*15*).

To inform planning, wildlife authorities should identify high-risk periods and locations for naturally occurring animal outbreaks through ecologic studies that identify conditions favoring anthrax infection among animal populations (*18–20*). Wildlife and public health authorities should work together to ensure that community-based campaigns proactively prepare communities for possible outbreaks according to their risk profile (*20*). Community-based interventions should involve residents in addressing communitywide food insecurity and in educating neighbors on the hazards of consuming meat from animals that die of unknown causes (*16*). These interventions should begin before the dry season in outbreak-prone areas.

Questionnaire responses showed that food insecurities appear to be the primary reason for handling and consuming meat from animals found dead. Other countries in Africa have undertaken successful programs to distribute meat from trophy animals to feed communities with limited access to protein while also reducing poaching by local communities (*21*). Such an approach might be considered as a component of a multisectoral solution to address food insecurity and consumption of unsafe foods in Zambia.

Overall, food insecurity throughout sub-Saharan Africa has improved throughout recent years; however, hunger and malnutrition continue to be concerns in many sub-Saharan countries including Zambia. Zambia maintains a

Table 3. Association of anthrax diagnosis with specific activities involving hippopotamus carcasses based on responses to a survey conducted after an outbreak of anthrax infections among humans and hippopotamuses living in a game reserve area, Chama District, Zambia, September 2011*

Activity	No. (%) persons		OR (95% CI)	aOR (95% CI)
	With anthrax diagnosed since July 2011, n = 31	Without anthrax diagnosed, n = 137		
Skinning	14 (45)	8 (6)	13.3 (4.4–41.5)	12.0 (4.3–36.5)
Cutting	28 (90)	70 (51)	8.9 (2.5–47.5)	8.1 (2.2–29.2)
Eating	30 (97)	106 (77)	8.8 (1.3–369.3)	–
Carrying	24 (77)	54 (39)	5.3 (2.0–15.4)	4.4 (1.7–11.8)
Preparing	27 (87)	92 (67)	3.3 (1.1–13.7)	2.1 (0.5–11.8)
Cooking	27(87)	93(68)	3.2 (1.0–13.2)	2.0 (0.5–1.1)
Drying	21(68)	64(47)	2.4 (1.0–6.1)	1.7 (0.6–4.5)
*aOR, adjusted odds ratio (adjusted for eating hippopotamus meat); OR, odds ratio.				

Table 4. Reasons for intending to eat meat again from hippopotamuses suspected to have died from anthrax among 65 persons who reported consuming dead hippopotamus meat in a survey conducted after an outbreak of anthrax infections among humans and hippopotamuses living in a game reserve area, Chama District, Zambia, September 2011

Reason	No. (%) respondents*
Lack of side dish	44 (73)
Lack of meat	14 (22)
Hunger	4 (7)
Lack of protein	3 (5)
*Respondents could provide >1 response.	

food reserve of maize, and it was suggested throughout the investigation that officials should provide additional corn meal as a possible solution for the food shortage. However, populations at risk for food insecurity need better access to balanced diets rather than more carbohydrates (*22*). Our survey respondents highlighted the desire for more fresh fruits and vegetables, which suggests more balanced diets would be welcomed.

Most of the crops grown in this region were cotton and other nonedible, exportable crops. Assistance is needed to help the population better balance subsistence farming with cash crops on small family farms to improve the overall diversity of crops and ultimately mitigate the risk for food insecurity (*22*).

Our household survey aimed to determine the main risk factors for anthrax transmission and the underlying factors driving those infected to risk exposure. Our results suggest the need to address long-standing political and economic issues related to food insecurity in protected areas, as well as an urgent need for better coordination between wildlife management and public health authorities. A more proactive approach could help prevent future outbreaks.

Acknowledgments

References

1. Hang'ombe MB, Mwansa JC, Muwowo S, Mulenga P, Kapina M, Musenga E, et al. Human-animal anthrax outbreak in the Luangwa valley of Zambia in 2011. Trop Doct. 2012;42:136–9. http://dx.doi.org/10.1258/td.2012.110454
2. Munang'andu HM, Banda F, Siamudaala VM, Munyeme M, Kasanga CJ, Hamududu B. The effect of seasonal variation on anthrax epidemiology in the upper Zambezi floodplain of western Zambia. J Vet Sci. 2012;13:293–8. http://dx.doi.org/10.4142/jvs.2012.13.3.293
3. Clegg SB, Turnbull PC, Foggin CM, Lindeque PM. Massive outbreak of anthrax in wildlife in the Malilangwe Wildlife Reserve, Zimbabwe. Vet Rec. 2007;160:113–8. http://dx.doi.org/10.1136/vr.160.4.113
4. Siamudaala VM, Bwalya JM, Munang'andu HM, Sinyangwe PG, Banda F, Mweene AS, et al. Ecology and epidemiology of anthrax in cattle and humans in Zambia. Jpn J Vet Res. 2006;54:15–23.
5. Tuchili LM, Pandey GS, Sinyangwe PG, Kaji T. Anthrax in cattle, wildlife and humans in Zambia. Vet Rec. 1993;132:487. http://dx.doi.org/10.1136/vr.132.19.487-a
6. Hugh-Jones ME, de Vos V. Anthrax and wildlife. Rev Sci Tech. 2002;21:359–83. http://dx.doi.org/10.20506/rst.21.2.1336
7. Turnbull PC, Bell RH, Saigawa K, Munyenyembe FE, Mulenga CK, Makala LH. Anthrax in wildlife in the Luangwa Valley, Zambia. Vet Rec. 1991;128:399–403. http://dx.doi.org/10.1136/vr.128.17.399
8. World Health Organization. Anthrax in humans and animals, 4th edition. Geneva: World Health Organization; 2008.
9. Wafula MM, Patrick A, Charles T. Managing the 2004/05 anthrax outbreak in Queen Elizabeth and Lake Mburo National Parks, Uganda. Afr J Ecol. 2008;46:24–31. http://dx.doi.org/10.1111/j.1365-2028.2007.00796.x
10. Pienaar UD. Epidemiology of anthrax in wild animals and the control of anthrax epizootics in the Kruger National Park, South Africa. Fed Proc. 1967;26:1496–502.
11. Ndyabahinduka DG, Chu IH, Abdou AH, Gaifuba JK. An outbreak of human gastrointestinal anthrax. Ann Ist Super Sanita. 1984;20:205–8.
12. Central Statistics Office. Zambia census [cited 2017 Apr 18]. http://www.zamstats.gov.zm/index.php/publications/category/11-2010-census
13. Food and Agriculture Organization of the United Nations. FAO in emergencies, Zambia, 2011–2012 [cited 2017 Apr 18]. http://www.fao.org/emergencies/countries/detail/en/c/161518
14. Hang'ombe MB, Mwansa JC, Muwowo S, Mulenga P, Kapina M, Musenga E, et al. Human-animal anthrax outbreak in the Luangwa valley of Zambia in 2011. Trop Doct. 2012;42:136–9. http://dx.doi.org/10.1258/td.2012.110454
15. Kasolo F, Yoti Z, Bakyaita N, Gaturuku P, Katz R, Fischer JE, et al. IDSR as a platform for implementing IHR in African countries. Biosecur Bioterror. 2013;11:163–9. http://dx.doi.org/10.1089/bsp.2013.0032
16. Chirundu D, Chihanga S, Chimusoro A, Chirenda J, Apollo T, Tshimanga M. Behavioural factors associated with cutaneous anthrax in Musadzi area of Gokwe North, Zimbabwe. Cent Afr J Med. 2009;55:50–4.
17. Chikerema SM, Matope G, Pfukenyi DM. Awareness and attitude toward zoonoses with particular reference to anthrax among cattle owners in selected rural communities of Zimbabwe. Vector Borne Zoonotic Dis. 2013;13:243–9. http://dx.doi.org/10.1089/vbz.2011.0916
18. Blackburn JK, McNyset KM, Curtis A, Hugh-Jones ME. Modeling the geographic distribution of *Bacillus anthracis*, the causative agent of anthrax disease, for the contiguous United States using predictive ecological niche modeling. Am J Trop Med Hyg. 2007;77:1103–10.

19. Blackburn JK, Odugbo MO, Van Ert M, O'Shea B, Mullins J, Perreten V, et al. *Bacillus anthracis* diversity and geographic potential across Nigeria, Cameroon and Chad: further support of a novel West African lineage. PLoS Negl Trop Dis. 2015; 9:e0003931. http://dx.doi.org/10.1371/journal.pntd.0003931

20. Gombe NT, Nkomo BM, Chadambuka A, Shambira G, Tshimanga M. Risk factors for contracting anthrax in Kuwirirana ward, Gokwe North, Zimbabwe. Afr Health Sci. 2010;10:159–64.

21. Weaver LC, Petersen T. Namibia communal area conservancies. In: Baldus RD, Damm GR, Wollscheid K-U, editors. Best practices in sustainable hunting: a guide to best practices from around the world. Budakeszi (Hungary): CIC–International Council for Game and Wildlife Conservation; 2008. p. 48–52.

22. McGuire S; Food and Agriculture Organization of the United Nations; International Fund for Agricultural Development; World Food Programme. The state of food insecurity in the world 2015: meeting the 2015 International Hunger Targets: taking stock of uneven progress. Adv Nutr. 2015;6:623–4. http://dx.doi.org/ 10.3945/an.115.009936

Address for correspondence: Melissa A. Marx, Johns Hopkins University Bloomberg School of Public Health, International Health, 615 N Wolf St, Rm E5541, Baltimore, MD 21205-2103, USA; email: mmarx@jhu.edu

Molecular Antimicrobial Resistance Surveillance for *Neisseria gonorrhoeae*, Northern Territory, Australia

David M. Whiley, Ella Trembizki, Cameron Buckley, Kevin Freeman, Robert W. Baird, Miles Beaman, Marcus Chen, Basil Donovan, Ratan L. Kundu, Christopher K. Fairley, Rebecca Guy, Tiffany Hogan, John M. Kaldor, Mahdad Karimi, Athena Limnios, David G. Regan, Nathan Ryder, Jiunn-Yih Su, James Ward, Monica M. Lahra

Neisseria gonorrhoeae antimicrobial resistance (AMR) is a globally recognized health threat; new strategies are needed to enhance AMR surveillance. The Northern Territory of Australia is unique in that 2 different first-line therapies, based primarily on geographic location, are used for gonorrhea treatment. We tested 1,629 *N. gonorrhoeae* nucleic acid amplification test–positive clinical samples, collected from regions where ceftriaxone plus azithromycin or amoxicillin plus azithromycin are recommended first-line treatments, by using 8 *N. gonorrhoeae* AMR PCR assays. We compared results with those from routine culture-based surveillance data. PCR data confirmed an absence of ceftriaxone resistance and a low level of azithromycin resistance (0.2%), and that penicillin resistance was <5% in amoxicillin plus azithromycin regions. Rates of ciprofloxacin resistance and penicillinase-producing *N. gonorrhoeae* were lower when molecular methods were used. Molecular methods to detect *N. gonorrhoeae* AMR can increase the evidence base for treatment guidelines, particularly in settings where culture-based surveillance is limited.

Author affiliations: Pathology Queensland Central Laboratory, Brisbane, Queensland, Australia (D. Whiley); The University of Queensland, Brisbane (D. Whiley, E. Trembizki, C. Buckley); Royal Darwin Hospital, Darwin, Northern Territory, Australia (K. Freeman, R.W. Baird); University of Western Australia, Nedlands, Western Australia, Australia (M. Beaman); University of Notre Dame Australia, Fremantle, Western Australia, Australia (M. Beaman); Western Diagnostic Pathology, Perth, Western Australia, Australia (M. Beaman, M. Karimi); Alfred Health, Carlton, Victoria, Australia (M. Chen, C.K. Fairley); Central Clinical School, Monash University, Melbourne, Victoria, Australia (M. Chen, C.K. Fairley); Sydney Hospital, Sydney, New South Wales, Australia (B. Donovan); University of New South Wales, Sydney (B. Donovan, R. Guy, J.M. Kaldor, D.G. Regan, N. Ryder, M.M. Lahra); Prince of Wales Hospital, Sydney (R.L. Kundu, T. Hogan, A. Limnios, M.M. Lahra); School of Medical Sciences, Hunter New England Local Health District, Sydney (N. Ryder); Menzies School of Health Research and Charles Darwin University, Darwin (J.-Y. Su); South Australian Health and Medical Research Institute, Adelaide, South Australia, Australia (J. Ward); Flinders University, Adelaide (J. Ward)

Resistance to antimicrobial drugs (termed antimicrobial resistance [AMR]) in *Neisseria gonorrhoeae* is recognized as a public health problem of global importance (*1,2*). The overall magnitude of AMR in *N. gonorrhoeae* is largely unknown in many regions because of substantial gaps in global AMR surveillance (*3*). Ceftriaxone, a third-generation extended-spectrum cephalosporin used widely for treatment, is considered to be the last fully effective option currently recommended. However, its durability is not assured; the proportion of gonococcal strains with elevated ceftriaxone MIC values is increasing steadily, and 4 documented cases of resistance to ceftriaxone have been noted, in Japan, France, Spain, and Australia (*4–6*). A dual therapy treatment regimen of ceftriaxone plus azithromycin is now the recommended standard of care in many countries and was implemented in an effort to stem further development of ceftriaxone resistance (*7*); however, failure of this dual therapy has also been reported (*8*).

Surveillance of *N. gonorrhoeae* antimicrobial drug sensitivity is a key component of all strategies to manage the emergence of resistance; gonorrhea treatment guidelines are currently formulated under the principle that an antimicrobial drug should be rejected for clinical use in a particular population once a threshold of 5% resistant isolates is breached (*1*). However, although gonorrhea diagnosis is now widely based on nucleic acid methods, antimicrobial drug sensitivity remains dependent on culture-based methods, which are highly specific but difficult to implement in many settings where gonorrhea is prevalent. The World

Health Organization (WHO) and Centers for Disease Control and Prevention (CDC), in their action plans to control the spread of drug-resistant *N. gonorrhoeae*, have called for the development of molecular assays (*1,2*). We have previously reviewed the potential for real-time PCR assays to achieve these goals (*3*) and, through the Gonorrhoea Resistance Assessment by Nucleic Acid Detection (GRAND) study, developed and validated a range of PCR methods to detect resistance mutations for azithromycin, ciprofloxacin, and penicillin. We have also developed a high-throughput single-nucleotide polymorphism–based typing method for multilocus sequence type (MLST) investigations (*9*).

In Australia, gonorrhea is concentrated primarily in men who have sex with men living predominantly in urban and regional areas and in Aboriginal heterosexual persons living in remote areas of central and northern Australia. Dual therapy comprising ceftriaxone (500 mg intramuscular injection) and oral azithromycin (1 g) (known as CAZ) is used as the standard first-line treatment in urban areas. However, in remote areas of the Northern Territory (Figure 1) and Western Australia, where rates of infection among Aboriginal populations are high and AMR is low, first-line treatment is oral amoxicillin 3 g, probenecid 1 g, and azithromycin 1 g (locally known as a ZAP pack), a treatment strategy that has the benefits of oral administration and avoidance of the unnecessary use of ceftriaxone.

In remote parts of Australia, including much of the ZAP pack region, transport distances and climate pose limits on the viability of samples for culture. Also, even though all clinicians diagnosing or suspecting gonorrhea in Australia are encouraged to send a suitable swab specimen for AMR testing by culture, changes to test reimbursement schemes have tended to favor use of nucleic acid amplification test (NAAT) over culture for gonorrhea diagnosis. For these combined reasons, relatively few isolates are available for AMR testing from these areas (*10*). Our PCR-based method (*11,12*) for direct detection of penicillinase-producing *N. gonorrhoeae* (PPNG) is now routinely used to help inform treatment guidelines in Western Australia (*13*) and the Northern Territory. We report on a study that we have undertaken in the Northern Territory to comprehensively examine the utility of nucleic acid methods to assess AMR against a broad range of antimicrobial drugs, and the potential role of these methods in setting treatment guidelines. The study was approved by the Human Research Ethics Committee (HREC) of Northern Territory Department of Health and Menzies School of Health, the Central Australian HREC, the South Eastern Sydney Local Health District HREC, the Queensland Children's Health Services District HREC, and the University of Queensland HREC.
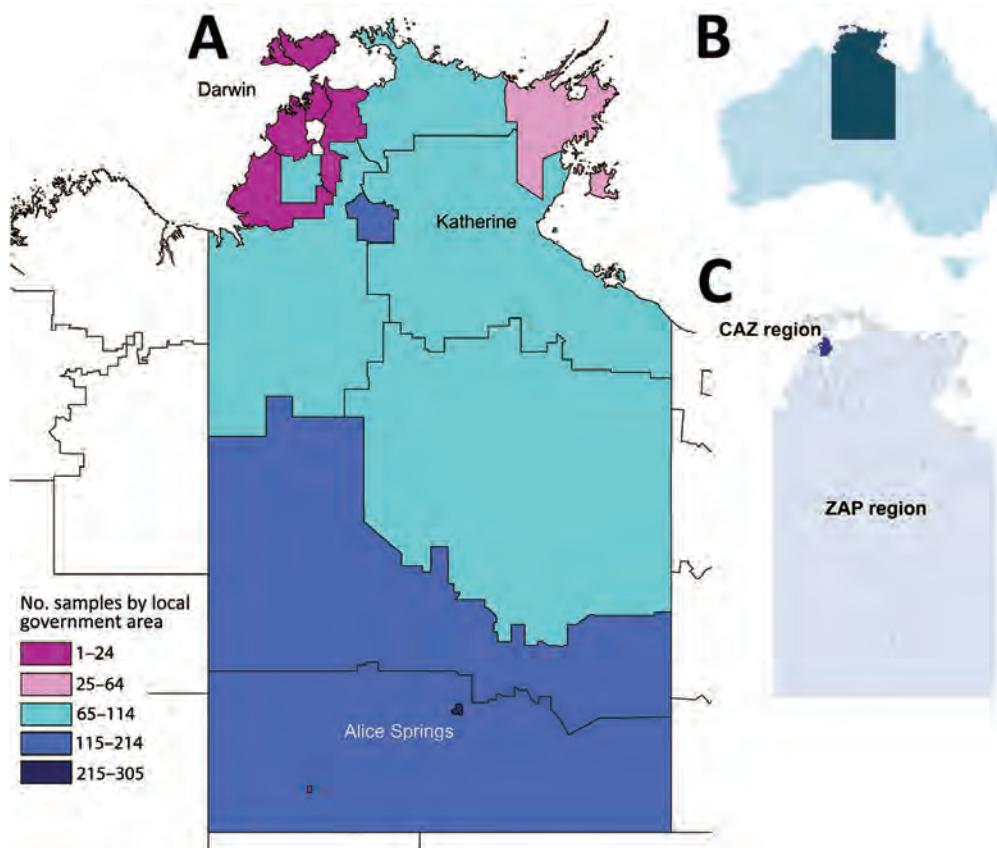
Figure 1. Collection areas for *Neisseria gonorrhoeae* samples within the Northern Territory of Australia, 2014. A) Heat map showing the local government areas from which the 1,629 nucleic acid amplification test–positive clinical samples were collected. B) Location of the Northern Territory within Australia. C) Location of the CAZ and ZAP regions within the Northern Territory. CAZ, ceftriaxone via intramuscular injection and oral azithromycin; ZAP, azithromycin, amoxicillin, probenecid.

Material and Methods

N. gonorrhoeae NAAT-Positive Clinical Samples

For this study, we examined 1,629 *N. gonorrhoeae* NAAT-positive clinical samples collected from patients in the Northern Territory (441 from CAZ regions and 1,188 from ZAP regions; Figure 1) during 2014; these samples represented 93.6% of the total 1,740 notifications of gonorrhea in this region for this year. The samples comprised 21 rectal, 45 pharyngeal, 413 vaginal/cervical, 97 male urethral, and 1 ocular specimen, as well as 1,012 urine samples (590 from men, 418 from women, and 4 from persons whose sex was not specified), 21 joint fluid samples, and 19 samples for which the site was not recorded on the request form. Samples were taken from 756 (46.4%) men, 861 (52.9%) women, and 12 (0.7%) persons for whom sex was not specified; median age was 24 years. The specimens were provided by the 2 laboratories in the Northern Territory that diagnose gonorrhea: Royal Darwin Hospital Pathology, which used Siemens Versant *Chlamydia trachomatis*/*N. gonorrhoeae* (CT/NG) assays (Siemens, Bayswater, Victoria, Australia), and Western Diagnostic Pathology, which used the Aptima Combo 2 test for CT/NG (Hologic, Bedford, MA, USA) (additional information in online Technical Appendix Table, https://wwwnc.cdc.gov/EID/article/23/9/17-0427-Techapp1.pdf).

PCR Methods

We used 8 PCR methods for AMR testing (Table 1): assays to detect PPNG (PPNG-PCR) (*11*); the mosaic penicillin binding protein 2 (PBP2) associated with resistance to the extended-spectrum cephalosporins (mosaicPBP2-PCR); the A8806 strain of ceftriaxone-resistant gonorrhea previously detected in Australia (A8806-PCR assay) (*6*); the GyrA S91F alteration that is highly predictive of resistance to ciprofloxacin (GyrA91-PCR) (*14,15*); 2 mutations on the 23S rRNA genes conferring resistance to azithromycin (2611-PCR and 2059-PCR) (*16*); wild-type PorB sequences (G101/A102 and PorB1a) that we have shown are predictive of penicillin susceptibility, and mutant PorB sequences (G101K/A102D, G101K/A102N and G101K/A102G) that are associated with but not predictive of penicillin resistance (PorB-PCR) (*17*); and a wild-type *mtrR* efflux pump promoter (i.e., lacking the A-deletion) shown to be associated with susceptibility to β lactam antimicrobial drugs (*mtrR* A-deletion-PCR) (online Technical Appendix; *18*). We considered samples uncharacterized by a method if they did not provide a result (e.g., of mutant or wild type) in the respective PCR. For mosaicPBP2-PCR and A8806-PCR, we pooled samples (10 samples/pool) for testing; we then tested samples from any pools returning positive results individually. For all other PCR methods, we tested samples individually (online Technical Appendix).

MLST

We genotyped the first 717 samples (collected during January–May 2014) using a previously described iPLEX14SNP method (*9*). The iPLEX14SNP targets 14 informative single-nucleotide polymorphisms on gonococcal housekeeping genes and provides a high-throughput means of conducting *N. gonorrhoeae* MLST. We further used these data to clarify the potential movement of strains between the CAZ and ZAP zones, irrespective of their AMR profiles.

Multiantigen Sequence Typing

We further investigated samples testing positive for mosaicPBP2 by using *N. gonorrhoeae* multiantigen sequence typing (NG-MAST) (*19*) as described previously (*20*). NG-MAST involves DNA sequencing of 2 variable gonococcal genes and therefore provides greater discrimination than MLST.

Australian Gonococcal Surveillance Program Data

The Australian Gonococcal Surveillance Program receives and tests clinical isolates of gonococci for the purposes of AMR phenotypic surveillance from throughout Australia. In 2014, the program received 222 isolates from the Northern Territory for antimicrobial drug susceptibility testing (Table 2). We compared the phenotypic rates of resistance with the results of PCR testing for the Northern Territory as a whole and individually by CAZ and ZAP regions.

Results

Of the 1,629 samples, 18.8% to 31.2% could not be characterized by the PCR methods (Table 1). However, these values excluded the mosaicPBP2-PCR and A8806-PCR methods; we considered all negative results for the mosaicPBP2-PCR and A8806-PCR characterized because pooled samples were used for screening, and it was therefore not possible to ascertain characterization for individual samples. Compared with culture, which provided 81 isolates from CAZ areas and 141 from ZAP regions in this year (Table 2), the PCR assays (based on the average number of characterized samples by each PCR) provided 4.2 times more data (mean 338.6 samples) from CAZ regions and 9.4 times more data (mean 1,331.6 samples) from ZAP regions.

We compared characterization rates based on anatomic site and originating laboratory (online Technical Appendix Table); only the GyrA91-PCR results were used for this comparison. We observed a significantly lower (p<0.001) characterization rate for pharyngeal samples (26.7%) compared with the combined rate (76.7%, range 56.7%–100%) for all other sample types.

N. gonorrhoeae Resistance

We compared PCR (Table 1) and culture (Table 2) data for resistance to azithromycin, ceftriaxone, ciprofloxacin,

Table 1. PCR results for the 1,629 NAAT-positive *Neisseria gonorrhoeae* clinical samples taken from patients in the Northern Territory of Australia, 2014*

	Results					
	CAZ region, n = 441		ZAP region, n = 1,188		Total for both regions, n = 1,629	
Assay and targets	No. samples/ no. tested	% Samples (95% CI)	No. samples/ no. tested	% Samples (95% CI)	No. samples/ no. tested	% Samples (95% CI)
GyrA91-PCR (*gyrA*)						
Wild type (S91)	235/297	79.1 (74.1–83.4)	922/931	99.0 (98.2–99.5)	1,157/1,228	94.2 (92.8–95.4)
S91F	62/297	20.9 (16.6–25.9)	9/931	1.0 (0.5–1.8)	71/1,228	5.8 (4.6–7.2)
Uncharacterized†	144	32.6	257	21.6	401/1,629	24.6
PPNG-PCR						
Negative	252/286	88.1 (83.8–91.4)	879/888	99 (98.1–99.5)	1,131/1,174	96.3 (95.1–97.3)
PPNG	34/286	11.9 (8.6–16.2)	9/888	1 (0.5–1.9)	43/1,174	3.7 (2.7–4.9)
Uncharacterized†	155	35.1	300	25.3	455/1,629	27.9
2611-PCR (23S rRNA)						
Wild type	321/321	100 (98.8–100)	958/960	99.8 (99.2–99.9)	1,279/1,281	99.8 (99.4–100)
C2611T	0/321	0 (0–1.2)	2/960	0.2 (0.1–0.8)	2/1,281	0.2 (0–0.6)
Uncharacterized†	120	27.2	228	19.2	348/1,629	21.4
2059-PCR (23S rRNA)						
Wild type	319/319	100 (98.8–100)	1,004/1,004	100 (99.6–100)	1,323/1,323	100 (99.7–100)
A2059G	0/319	0 (0–1.2)	0/1,004	0 (0–0.4)	0/1,323	0 (0–0.3)
Uncharacterized†	122	27.7	184	15.5	306/1,629	18.8
PorB-PCR (*porB*)						
G101/A102	98/286	34.3 (29–39.9)	125/835	15.0 (12.7–17.6)	223/1,121	19.9 (17.7–22.3)
[G101/A102, non-PPNG]‡	[80/280]	[28.6 (23.4–34.1)]	[116/823]	[14.1 (11.9–16.6)]	[196/1,103]	[17.8 (15.6–20.1)]
PorB1a	152/286	53.1 (47.4–58.9)	699/835	83.7 (81.1–86.1)	851/1,121	75.9 (73.3–78.3)
[PorB1a, non-PPNG]‡	[120/267]	[44.9 (39.1–50.9)]	[627/770]	[81.3 (78.4–83.9)]	[747/1,037]	[72.0 (69.2–74.7)]
Mutant§	32/286	11.2 (8–15.4)	3/835	0.4 (0.1–1.1)	35/1,121	3.1 (2.3–4.3)
PorB1a and G101/A102	4/286	1.4 (0.5–3.5)	6/835	0.7 (0.3–1.6)	10/1,121	0.9 (0.5–1.6)
PorB1a and mutant§	0/286	0 (0–1.3)	2/835	0.2 (0.1–0.9)	2/1,121	0.2 (0–0.6)
Uncharacterized†	155	35.1	353	29.8	508/1,629	31.2
A-deletion-PCR (*MtrR*)						
Wild type	280/318	88.1 (84–91.2)	944/950	99.4 (98.6–99.7)	1,224/1,268	96.5 (95.4–97.4)
[Wild type, non-PPNG]‡	[226/284]	[79.6 (74.5–84.1)]	[861/873]	[98.6 (97.6–99.2)]	[1,087/1,157]	[93.9 (92.4–95.2)]
A-deletion	38/318	11.9 (8.8–16)	6/950	0.6 (0.3–1.4)	44/1268	3.5 (2.6–4.6)
Uncharacterized†	123	27.9	238	20	361/1629	22.2
mosaicPBP2-PCR (*penA*)						
Negative	431/441	97.7 (95.9–98.8)	1,188/1,188	100 (99.7–100)	1,619/1,629	99.4 (98.9–99.7)
Positive	10/441	2.3 (1.2–4.1)	0/1188	0 (0–0.3)	10/1,629	0.6 (0.3–1.1)
Uncharacterized†¶	NA	NA	NA	NA	NA	NA
A8806-PCR (*penA*)						
Negative	441/441	100 (99.1–100)	1,188/1,188	100 (99.7–100)	1,629/1,629	100 (99.8–100)
Positive	0/441	0 (0–0.9)	0/1,188	0 (0–0.3)	0/1,629	0 (0–0.2)
Uncharacterized†¶	NA	NA	NA	NA	NA	NA

*NA, not applicable; NAAT, nucleic acid amplification test; PPNG, penicillinase-producing *N. gonorrhoeae*.
†These samples could not be characterized by the respective PCR assay.
‡These PorB-PCR and A-deletion-PCR results were combined with the PPNG-PCR results to exclude those that were PPNG. Uncharacterized PPNG-PCR results were omitted from total numbers.
§Mutant = G101K/A102D, G101K/A102N or G101K/A102G.
¶All negative results for the mosaicPBP2-PCR and A8806-PCR were considered valid (i.e., characterized) given that pooled samples were used for screening, and it was therefore not possible to ascertain characterization for individual samples.

and penicillin. The combined results of the 2611-PCR and 2059-PCR assays showed that *N. gonorrhoeae* azithromycin resistance was low (0.2%) across the Northern Territory in 2014, consistent with the 2014 culture-based data that showed no azithromycin-resistant isolates. We found 10 (0.6%) samples positive by the mosaicPBP2-PCR, all in CAZ regions; these data were consistent with 3 (1.4%) isolates exhibiting decreased susceptibility to ceftriaxone in CAZ regions detected by culture. We observed no A8806-PCR

positive samples, consistent with culture data showing no *N. gonorrhoeae* with MICs for ceftriaxone >0.125 mg/L isolated in the Northern Territory or elsewhere in Australia since the A8806 strain was observed in late 2013.

Total ciprofloxacin resistance in the Northern Territory was significantly lower by PCR (5.8%) than by bacterial culture (12.6%; p<0.001). Consistent with the culture data, the GyrA91-PCR indicated that levels of ciprofloxacin resistance were higher in the CAZ region compared with the

Table 2. Summary of the Australian Gonococcal Surveillance Program culture-based *Neisseria gonorrhoeae* antimicrobial drug resistance data for the Northern Territory of Australia, 2014*

Antimicrobial drug	CAZ region, n = 81		ZAP region, n = 141		Total, n = 222	
	No. isolates	% Isolates (95% CI)	No. isolates	% Isolates (95% CI)	No. isolates	% Isolates (95% CI)
Azithromycin R	0	0.0 (0.0–4.5)	0	0.0 (0.0–2.7)	0	0.0 (0.0–1.7)
Ceftriaxone DS	3	3.7 (1.3–10.3)	0	0.0 (0.0–2.7)	3	1.4 (0.5–3.9)
Ciprofloxacin R	25	30.9 (21.9–41.6)	3	2.1 (0.7–6.1)	28	12.6 (8.9–17.6)
Penicillin R	21	25.9 (17.6–36.4)	3	2.1 (0.7–6.1)	24	10.8 (7.4–15.6)
PPNG	15	18.5 (11.6–28.3)	3	2.1 (0.7–6.1)	18	8.1 (5.2–12.5)

*Adapted from the Australian Gonococcal Surveillance Program annual report) (*10*). DS, decreased susceptibility; PPNG, penicillinase-producing *N. gonorrhoeae*; R, resistant.

ZAP region. Similarly, total levels of PPNG in the Northern Territory as determined by PCR (3.7%) were significantly lower than the levels determined by culture (8.1%); p<0.01). For ZAP regions, PPNG-PCR testing showed that 1.0% of samples were PPNG positive, comparable to the 2.1% observed with bacterial culture.

Using bacterial culture, we detected no isolates with chromosomally mediated resistance to penicillin (CMRP) in ZAP regions. Although the porB-PCR is not a definitive marker of CMRP (*17*), it was still able to provide insight into CMRP, given that the G101/A102 and PorB1a markers are highly predictive of penicillin susceptibility (in which PPNG strains are simultaneously detected and excluded). In the ZAP regions, 14.1% of samples were both non-PPNG and G101/A102 and 81.3% were both non-PPNG and PorB1a, providing 95.4% of samples predicted to be susceptible to penicillin. Thus, based on the combined porB-PCR and PPNG-PCR results, we predicted by PCR that 95.4%–99% of samples were susceptible to penicillin. These data are further supported by the combined A-deletion-PCR and PPNG-PCR data; 98.6% of samples from ZAP regions possessed a wild-type *mtrR* promoter and were non-PPNG.

MLST

Of the 717 samples that we subjected to iPLEX14SNP genotyping, 456 (63.6%) were successfully genotyped and 261 (36.4%) were not characterized. We excluded the uncharacterized samples from further analysis. We observed 27 different iPLEX14SNP genotypes for the 456 characterized samples and summarized the 14 most common (NG01 to NG14, consisting of those with 5 or more isolates; total, 437 isolates), indicating whether they were from the CAZ or ZAP regions (Figure 2). A total of 10 iPLEX14SNP genotypes were shared across both CAZ and ZAP regions, including 8 of the 14 most common. Examination of available PCR data associated with these 10 genotypes shared between CAZ and ZAP regions revealed that 3 possessed resistance markers, including NG07 (GyrA S91F, *mtrR* A-deletion, and PorB mutant sequences), NG13 (GyrA S91F and PPNG), and a third genotype (GyrA S91F *mtrR* A-deletion and PPNG), listed among "all others" in Figure 2.

NG-MAST Investigation of mosaicPBP2-PCR Positive Samples

The NG-MAST analyses for the 10 samples positive by the mosaicPBP2-PCR (Table 3) revealed 4 different types, including 3 types (2212, 5622, and 1407) that have previously been associated with the gonococcal mosaic PBP2 in Europe and elsewhere (*21*). Additional demographic data were obtained; the 10 samples were from 7 men and 2 women, including 3 Aboriginal (1 man and 2 women) and 6 non-Aboriginal persons. All of these persons were identified in the metropolitan area of Darwin in the Northern Territory.

Discussion

The results of this study show conclusively that molecular methods can be used to enhance *N. gonorrhoeae* AMR surveillance for a range of antimicrobial drugs in an isolated region where bacterial culture is impractical or not possible. For the Northern Territory of Australia, these new data substantially increase the evidence base for the current treatment guidelines, characterizing approximately two thirds of all notified cases, compared with only 13% (222/1740) that were available for characterization
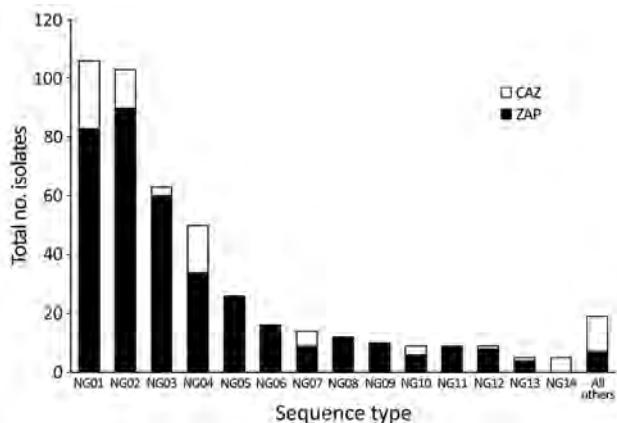
Figure 2. Genotype frequency of the 456 *Neisseria gonorrhoeae* clinical samples taken from patients in the Northern Territory of Australia, 2014, that were successfully genotyped by using the iPLEX14SNP method (*9*). Presence of each genotype in the CAZ or ZAP regions is indicated. CAZ, ceftriaxone via intramuscular injection and oral azithromycin; ZAP, azithromycin, amoxicillin, probenecid.

Table 3. Summary of mosaicPBP2-PCR–positive *Neisseria gonorrhoeae* samples from the Northern Territory of Australia*

Patient no.	Sex	Age group, y	Aborigine	Sample source	Date of collection	NG-MAST genotype
1	M	51–55	No	Urine	January 2014	10038
2	M	21–25	No	Urine	March 2014	2212
3	F	26–30	Yes	Urine	April 2014	2212
				Pharyngeal swab	May 2014	2212
4	M	26–30	Yes	Urine	April 2014	2212
5	F	≤20	Yes	Urine	May 2014	2212
6	M	21–25	No	Urine	February 2014	5622
7	M	56–60	No	Urine	December 2014	5622
8	M	21–25	No	Anal swab	November 2014	1407
9	M	21–25	No	Anal swab	November 2014	1407

*NG-MAST, *N. gonorrhoeae* multiantigen sequence typing.

by culture. Furthermore, the data indicate no ceftriaxone resistance and little azithromycin resistance (0.2%) in this region and provide an estimate that penicillin resistance is <5% in the ZAP regions.

This case study also highlights the potential for molecular assays to inform alternative treatment strategies in areas where culture-based testing may be limited. The high ciprofloxacin susceptibility levels indicate that ciprofloxacin would be suitable as an alternative oral therapy in the ZAP regions; the GyrA91-PCR showed that 99.0% of infections in the ZAP regions were ciprofloxacin susceptible. Thus, ciprofloxacin could be used empirically or could otherwise be of value where use of the ZAP pack is contraindicated (e.g., penicillin allergy) or to facilitate patient-delivered partner therapy (PDPT). Although PDPT for chlamydia is supported in the Northern Territory, it is not recommended for gonorrhea given the risk of anaphylaxis with penicillin and the injection requirement for ceftriaxone. Based on our data, ciprofloxacin could appropriately be used for PDPT for gonorrhea in the ZAP regions, ideally in combination with azithromycin to simultaneously treat both chlamydia and gonorrhea given the high coinfection rates in these areas (*22*).

A further benefit of using ciprofloxacin in ZAP regions is that rates of susceptibility/resistance could be monitored accurately by molecular methods, such as the GyrA91-PCR. This assay could also facilitate use of oral ciprofloxacin in the CAZ regions through individualized treatment, which, based on the prevalence of wild-type (susceptible) strains, could be used for 79.1% of patients, substantially sparing the use of ceftriaxone. Similarly, based on the combined results of the PorB-PCR and PPNG-PCR methods, individualized ZAP pack treatment could potentially be used for 73.5% of infections in the CAZ regions.

The data also provide some evidence of new threats to current treatments. Although there was no further evidence of the A8806 ceftriaxone-resistant strain, the detection of mosaic PBP2 strains in the Northern Territory, particularly among Aboriginal patients, is alarming. These mosaicPBP2 strains typically exhibit CMRP and therefore pose a direct risk to the use of ZAP packs. This risk is heightened by the

ability of these mosaicPBP2 strains to spread rapidly. First reported in Japan in 2001, mosaicPBP2 strains have since become an internationally successful clone. Accordingly, our nationwide study of gonococcal isolates from Australia in 2012 showed that mosaic strains composed 8.9% of all isolates and had spread to every state in Australia except the Northern Territory (*23*). The NG-MAST data from this study (Table 3) indicated that different incursions of the mosaicPBP2 strains into the Northern Territory population occurred in 2014. It is likely that 3 of these involved men who have sex with men, residing in the metropolitan area of Darwin. The presence of the same NG-MAST type (2212; Table 3) in 1 Aboriginal man and 2 Aboriginal women strongly suggests transmission within heterosexual Aboriginal networks in the Darwin region.

It was previously assumed that penicillin resistance has remained low in ZAP regions because of limited bridging of sexual networks in metropolitan areas. This hypothesis was not supported by our MLST data, however, which showed that 10 of the 27 observed gonococcal strain types (including 8 of the 14 most common strain types; Figure 2) were present in both CAZ and ZAP regions. These strains included 3 strain types predicted to be resistant to ciprofloxacin, penicillin, or both, suggesting common sexual networks. Thus, it is theoretically possible that mosaicPBP2 strains or other resistant strains could exploit this bridging and spread into ZAP regions.

The addition of molecular strategies in the remote regions provided a notable increase in the scope of AMR surveillance. With the increased surveillance capture, the rates of both ciprofloxacin resistance and PPNG predicted by PCR were much lower (less than half) than rates detected by bacterial culture. In total, 9 times more samples from the ZAP regions were ascertained by PCR than by bacterial culture, compared with 4 times more samples from CAZ regions ascertained by PCR than by culture. Previous Australia data have shown that the GyrA91-PCR assay is an accurate predictor of ciprofloxacin resistance and the PPNG-PCR assay is an accurate predictor of PPNG (*11,14,15*). Therefore, it is unlikely that the observed differences between PCR and culture-based data were attributable

to problems with accuracy of the PCR target sequences. Rather, we suspect that the observed differences in resistance rates were influenced primarily by the higher proportion of infections that were able to be characterized in the ZAP region with these PCR assays. Our findings strongly support the CDC's and WHO's positions on the utility of molecular strategies to enhance surveillance (1,2). Rates of drug resistance are rising, and refining and rationalizing antimicrobial drug use at the individual patient level is a desirable stewardship strategy.

Our study has several limitations. The predictive value of the molecular markers used in this study are based on Australia sample banks, so they may not be representative of other regions, where different gonococcal strains may be circulating. This limitation is particularly relevant for the PorB-PCR PIA target, which, as previously described, does not specifically target a mechanism of resistance, yet is highly associated with penicillin susceptibility in local Australia gonococci (17). These issues highlight the importance of maintaining culture-based AMR testing for definitive AMR surveillance, as well as for providing ongoing validation material for the molecular methods. In addition, we observed that approximately one third of *N. gonorrhoeae* NAAT-positive clinical samples could not be characterized by 1 or more of the resistance assays; this finding is likely due to low DNA loads, as previously documented (16). The lack of characterization was particularly evident for pharyngeal samples, which likely reflects *N. gonorrhoeae* DNA loads being generally lower in the pharynx compared with other sites.

Overall, this study highlights the potential for molecular methods to enhance culture-based AMR surveillance programs by increasing sample size. These methods have provided, and continue to provide, new representative data to inform local treatment guidelines, identifying alternative treatment options and pinpointing new resistance threats. Molecular methods, such as those described here, offer new opportunities to improve *N. gonorrhoeae* AMR surveillance globally, particularly in remote regions.

Dr. Whiley is a principal research fellow based at the UQ Centre for Clinical Research, The University of Queensland, and Pathology Queensland, Brisbane, Queensland, Australia. His research is focused principally on the development of novel molecular diagnostic and typing tools for infectious diseases. A key focus of his work is to improve *N. gonorrhoeae* resistance surveillance in areas where current surveillance activities by bacterial culture are limited.

References
1. World Health Organization. Global action plan to control the spread and impact of antimicrobial resistance in *Neisseria gonorrhoeae*, 2012 [cited 2016 May 25]. http://www.who.int/reproductivehealth/publications/rtis/9789241503501/en/
2. Centers for Disease Control and Prevention. Cephalosporin-resistant *Neisseria gonorrhoeae* public health response plan 2012 [cited 2016 Nov 11]. https://www.cdc.gov/std/treatment/ceph-r-responseplanjuly30-2012.pdf
3. Goire N, Lahra MM, Chen M, Donovan B, Fairley CK, Guy R, et al. Molecular approaches to enhance surveillance of gonococcal antimicrobial resistance. Nat Rev Microbiol. 2014;12:223–9. http://dx.doi.org/10.1038/nrmicro3217
4. Ohnishi M, Saika T, Hoshina S, Iwasaku K, Nakayama S, Watanabe H, et al. Ceftriaxone-resistant *Neisseria gonorrhoeae*, Japan. Emerg Infect Dis. 2011;17:148–9. http://dx.doi.org/10.3201/eid1701.100397
5. Unemo M, Golparian D, Nicholas R, Ohnishi M, Gallay A, Sednaoui P. High-level cefixime- and ceftriaxone-resistant *Neisseria gonorrhoeae* in France: novel *penA* mosaic allele in a successful international clone causes treatment failure. Antimicrob Agents Chemother. 2012;56:1273–80. http://dx.doi.org/10.1128/AAC.05760-11
6. Lahra MM, Ryder N, Whiley DM. A new multidrug-resistant strain of *Neisseria gonorrhoeae* in Australia. N Engl J Med. 2014;371:1850–1. http://dx.doi.org/10.1056/NEJMc1408109
7. Centers for Disease Control and Prevention. Update to CDC's Sexually Transmitted Diseases Treatment Guidelines, 2010: oral cephalosporins no longer a recommended treatment for gonococcal infections. MMWR Morb Mortal Wkly Rep. 2012;61:590–4.
8. Fifer H, Natarajan U, Jones L, Alexander S, Hughes G, Golparian D, et al. Failure of dual antimicrobial therapy in treatment of gonorrhea. N Engl J Med. 2016;374:2504–6. http://dx.doi.org/10.1056/NEJMc1512757
9. Trembizki E, Smith H, Lahra MM, Chen M, Donovan B, Fairley CK, et al. High-throughput informative single nucleotide polymorphism-based typing of *Neisseria gonorrhoeae* using the Sequenom MassARRAY iPLEX platform. J Antimicrob Chemother. 2014;69:1526–32. http://dx.doi.org/10.1093/jac/dkt544
10. Lahra MM; Australian Gonococcal Surveillance Programme. Australian Gonococcal Surveillance Programme annual report, 2014. Commun Dis Intell Q Rep. 2015;39:E347–54.
11. Buckley C, Trembizki E, Baird RW, Chen M, Donovan B, Freeman K, et al. Multitarget PCR assay for direct detection of penicillinase-producing *Neisseria gonorrhoeae* for enhanced surveillance of gonococcal antimicrobial resistance. J Clin Microbiol. 2015;53:2706–8. http://dx.doi.org/10.1128/JCM.00540-15
12. Goire N, Freeman K, Tapsall JW, Lambert SB, Nissen MD, Sloots TP, et al. Enhancing gonococcal antimicrobial resistance

surveillance: a real-time PCR assay for detection of penicillinase-producing *Neisseria gonorrhoeae* by use of noncultured clinical samples. J Clin Microbiol. 2011;49:513–8. http://dx.doi.org/10.1128/JCM.02024-10

13. Speers DJ, Fisk RE, Goire N, Mak DB. Non-culture *Neisseria gonorrhoeae* molecular penicillinase production surveillance demonstrates the long-term success of empirical dual therapy and informs gonorrhoea management guidelines in a highly endemic setting. J Antimicrob Chemother. 2014;69:1243–7. http://dx.doi.org/10.1093/jac/dkt501

14. Buckley C, Trembizki E, Donovan B, Chen M, Freeman K, Guy R, et al.; GRAND Study Investigators. A real-time PCR assay for direct characterization of the *Neisseria gonorrhoeae* GyrA 91 locus associated with ciprofloxacin susceptibility. J Antimicrob Chemother. 2016;71:353–6. http://dx.doi.org/10.1093/jac/dkv366

15. Trembizki E, Guy R, Donovan B, Kaldor JM, Lahra MM, Whiley DM; GRAND study investigators. Further evidence to support the individualised treatment of gonorrhoea with ciprofloxacin. Lancet Infect Dis. 2016;16:1005–6. http://dx.doi.org/10.1016/S1473-3099(16)30271-7

16. Trembizki E, Buckley C, Donovan B, Chen M, Guy R, Kaldor J, et al. Direct real-time PCR-based detection of *Neisseria gonorrhoeae* 23S rRNA mutations associated with azithromycin resistance. J Antimicrob Chemother. 2015;70:3244–9.

17. Buckley C, Trembizki E, Donovan B, Chen M, Freeman K, Guy R, et al.; Gonorrhoea Resistance Assessment by Nucleic Acid Detection (GRAND) Study Investigators. Real-time PCR detection of *Neisseria gonorrhoeae* susceptibility to penicillin. J Antimicrob Chemother. 2016;71:3090–5. http://dx.doi.org/10.1093/jac/dkw291

18. Kugelman G, Tapsall JW, Goire N, Syrmis MW, Limnios A, Lambert SB, et al. Simple, rapid, and inexpensive detection of *Neisseria gonorrhoeae* resistance mechanisms using heat-denatured isolates and SYBR green-based real-time PCR. Antimicrob Agents Chemother. 2009;53:4211–6. http://dx.doi.org/10.1128/AAC.00385-09

19. Palmer HM, Young H, Graham C, Dave J. Prediction of antibiotic resistance using *Neisseria gonorrhoeae* multi-antigen sequence typing. Sex Transm Infect. 2008;84:280–4. http://dx.doi.org/10.1136/sti.2008.029694

20. Whiley DM, Goire N, Ray ES, Limnios A, Lambert SB, Nissen MD, et al. *Neisseria gonorrhoeae* multi-antigen sequence typing using non-cultured clinical specimens. Sex Transm Infect. 2010;86:51–5. http://dx.doi.org/10.1136/sti.2009.037689

21. Chisholm SA, Unemo M, Quaye N, Johansson E, Cole MJ, Ison CA, et al. Molecular epidemiological typing within the European Gonococcal Antimicrobial Resistance Surveillance Programme reveals predominance of a multidrug-resistant clone. Euro Surveill. 2013;18:18.

22. Guy R, Ward J, Wand H, Rumbold A, Garton L, Hengel B, et al.; STRIVE Investigator Group. Coinfection with *Chlamydia trachomatis*, *Neisseria gonorrhoeae* and *Trichomonas vaginalis*: a cross-sectional analysis of positivity and risk factors in remote Australian Aboriginal communities. Sex Transm Infect. 2015;91:201–6. http://dx.doi.org/10.1136/sextrans-2014-051535

23. Trembizki E, Wand H, Donovan B, Chen M, Fairley CK, Freeman K, et al. The molecular epidemiology and antimicrobial resistance of *Neisseria gonorrhoeae* in Australia: a nationwide cross-sectional study, 2012. Clin Infect Dis. 2016;63:1591–8. http://dx.doi.org/10.1093/cid/ciw648

Address for correspondence: David M. Whiley, UQ Centre for Clinical Research, The University of Queensland, Brisbane, Queensland 4029, Australia; email: d.whiley@uq.edu.au

Estimated Annual Numbers of Foodborne Pathogen–Associated Illnesses, Hospitalizations, and Deaths, France, 2008–2013

Dieter Van Cauteren, Yann Le Strat, Cécile Sommen, Mathias Bruyand, Mathieu Tourdjman, Nathalie Jourdan-Da Silva, Elisabeth Couturier, Nelly Fournet, Henriette de Valk, Jean-Claude Desenclos

Estimates of the annual numbers of foodborne illnesses and associated hospitalizations and deaths are needed to set priorities for surveillance, prevention, and control strategies. The objective of this study was to determine such estimates for 2008–2013 in France. We considered 15 major foodborne pathogens (10 bacteria, 3 viruses, and 2 parasites) and estimated that each year, the pathogens accounted for 1.28–2.23 million illnesses, 16,500–20,800 hospitalizations, and 250 deaths. *Campylobacter* spp., nontyphoidal *Salmonella* spp. and norovirus accounted for >70% of all foodborne pathogen–associated illnesses and hospitalizations; nontyphoidal *Salmonella* spp. and *Listeria monocytogenes* were the main causes of foodborne pathogen–associated deaths; and hepatitis E virus appeared to be a previously unrecognized foodborne pathogen causing ≈68,000 illnesses in France every year. The substantial annual numbers of foodborne illnesses and associated hospitalizations and deaths in France highlight the need for food-safety policymakers to prioritize foodborne disease prevention and control strategies.

Foodborne pathogens are of public health concern worldwide (*1*). Estimates of the total number of foodborne illnesses and associated hospitalizations and deaths are needed to assess their effect on health and to set priorities for surveillance, prevention, and control strategies. In 2000, the number of foodborne illnesses and associated deaths in France was estimated by using data from 1990–2000. However, for most pathogens, data were lacking to derive estimates at the population level (*2*).

Since that study, specific surveillance systems have been implemented in France for *Campylobacter* spp. (2002) (*3*), hepatitis A virus (2005), and hepatitis E virus (2002) (*4*). Additional surveys have been conducted to provide information on healthcare-seeking behavior and the incidence of acute gastroenteritis in the general population (2009–2010) (*5*) and on physician practices in requesting

fecal samples for patients with acute gastroenteritis (2013–2014) (*6*). Furthermore, the quality and availability of other nonspecific data sources (e.g., hospital discharge registers and health insurance reimbursement data) have improved and are increasingly used for epidemiologic studies in France (*7–9*). Thus, recent and valid data are available to estimate the population-level health effects of several foodborne pathogens. Such estimates have recently been generated for *Campylobacter* spp. and nontyphoidal *Salmonella* spp. (hereafter referred to as *Salmonella* spp.), the 2 main causes of foodborne bacterial infections in France (*10*). Taking into account this improved knowledge and data availability, we conducted a study to estimate the annual number of illnesses, hospitalizations, and deaths associated with 15 foodborne pathogens in France.

Methods

Using data sources from 2008–2013, we estimated the number of illnesses, hospitalizations, and deaths in France resulting from 15 foodborne pathogens: 10 bacteria (*Bacillus cereus*, *Campylobacter* spp., *Clostridium botulinum*, *Clostridium perfringens*, Shiga-toxin–producing *Escherichia coli* [STEC], *Listeria monocytogenes*, *Salmonella* spp., *Shigella* spp., *Staphylococcus aureus*, *Yersinia* spp.); 3 viruses (hepatitis A virus, hepatitis E virus, norovirus); and 2 parasites (*Taenia saginata*, *Toxoplasma gondii*). We used France's 2010 census population (62,765,235 persons) for the estimates.

We used different statistical models, depending on the most suitable data available for each pathogen, with many inputs to estimate the number of illnesses, hospitalizations, and deaths (online Technical Appendix Table 1, https://wwwnc.cdc.gov/EID/article/23/9/17-0081-Techapp1.pdf). For most proportions we defined a lower and upper bound and a beta distribution with 2 parameters derived from a method of moments, assuming a mean $m = $ (lower + upper bound)/2 and an SD = (upper bound − m)/2 (*11*). We used lognormal probability distributions for model inputs derived from a national survey on acute gastroenteritis in

France (5) and for the annual numbers of reported illnesses, hospitalizations, and deaths. For final estimates, we multiplied the distributions by using Monte Carlo simulation (10,000 iterations) with R version 3.3.2 (12). We report median values and use ranges between the 5th and 95th percentiles of the output distribution to define a 90% credible interval ($CrI_{90\%}$).

Illnesses

To estimate the numbers of illnesses, we obtained surveillance data from the mandatory notification system (*C. botulinum*, *L. monocytogenes*, hepatitis A virus, and foodborne disease outbreaks) and from national reference laboratories and their laboratory surveillance networks (*C. botulinum, Campylobacter* spp., STEC, *L. monocytogenes*, *Salmonella* spp., *Shigella* spp., *Yersinia* spp., hepatitis A virus, hepatitis E virus, and *T. gondii*). Inclusion in these surveillance systems implies that the ill person sought medical care, had laboratory testing prescribed, and had a specimen submitted for laboratory testing and that the laboratory identified the pathogen and reported the positive result to the surveillance system. These steps can be summarized into 2 multiplication factors: an underreporting factor defined as the match between the total number of laboratory-confirmed illnesses and the number of laboratory-confirmed illnesses reported to the surveillance system; and an underdiagnosis factor taking into account the proportion of cases that were not laboratory-confirmed because the patient did not seek medical advice or was misdiagnosed. We took both multiplication factors into account to estimate the number of illnesses from mandatory notification data and national reference laboratory data.

Previously published parameters for estimating the number of *Campylobacter* spp.– and *Salmonella* spp.–associated illnesses (10) were used as a proxy to estimate the level of underdiagnosis for *Yersinia* spp. (using *Campylobacter* spp. data) and *Shigella* spp. (using *Salmonella* spp. data). For *C. botulinum* and *L. monocytogenes,* we assumed that 80%–100% of the cases were in persons who sought medical care and had laboratory-confirmed diagnoses. To account for underreporting, we conducted ad hoc laboratory surveys for *Campylobacter* spp., *Salmonella* spp., *Shigella* spp., and *Yersinia* spp., and we conducted a capture–recapture study for *L. monocytogenes*.

In France, cases of *B. cereus*, *S. aureus,* and *C. perfringens* infection are notified only through mandatory notification of point-source foodborne disease outbreaks. For these pathogens, we assumed that the multiplier between the number of confirmed outbreak cases and the number of community cases of foodborne origin would be similar to that estimated for *Salmonella* spp. We estimated the number of illness caused by *T. gondii* and hepatitis A and E viruses from seroprevalence data and the number of illnesses

caused by *T. saginata* from health insurance reimbursement data for niclosamide (a drug used to treat tapeworm infestation). We used data from the literature to estimate the number of illnesses caused by STEC. To estimate the number of norovirus cases, we applied a proportion (14%–22%) of norovirus-associated acute gastroenteritis cases to the annual number of acute gastroenteritis illnesses in France (Table 1). This proportion was based on findings from a 2008–2009 community study in the United Kingdom (13) and a meta-analysis of 175 studies published during 1990–2014 (14). Model inputs used for each pathogen are presented in online Technical Appendix Table 1.

Hospitalizations

We used the French Hospital Information System (FHIS) as the main data source for estimating the number of hospitalizations. The system is a national database of hospital records that contains sociodemographic information (age, sex, and residence area) and medical information (main cause for admission, concurrent medical conditions, modes of admission, and discharge) (10). Diseases are coded according to the International Classification of Diseases, 10th revision (ICD-10; http://www.who.int/classifications/icd/en/). We extracted all hospital records with a patient discharge date during January 2008–December 2013 and containing an ICD-10 code of interest as the main cause for admission or as a concurrent medical condition.

We used the number of hospital records with pathogen-specific ICD-10 codes to estimate the annual number of hospitalizations for 8 pathogens, 4 of which cause acute gastroenteritis (Table 2). We did not redistribute records with only unspecified gastroenteritis codes to the 8 pathogens, but we did correct for undercapture, taking into account the proportion of fecal samples tested for each pathogen and the sensitivity of fecal culture. When data were available, we compared trends over time and patient age

Table 1. Data sources used to estimate the number of pathogen-specific illnesses, France, 2008–2013

Pathogen	Data source
Bacillus cereus	Surveillance
Campylobacter spp.	Surveillance
Clostridium botulinum	Surveillance
Clostridium perfringens	Surveillance
Hepatitis A virus	Seroprevalence
Hepatitis E virus	Seroprevalence
Listeria monocytogenes	Surveillance
Norovirus	Literature and national telephone survey
Salmonella spp., nontyphoidal	Surveillance
Shiga toxin–producing *Escherichia coli*	Literature
Shigella spp.	Surveillance
Staphylococcus aureus	Surveillance
Taenia saginata	Health insurance reimbursement data
Toxoplasma gondii	Seroprevalence
Yersinia spp.	Surveillance

Table 2. Methods used to estimate the number of pathogen-specific hospitalizations, France, 2008–2013*

Pathogen	Method
Bacillus cereus	Proportion of hospitalizations for AG applied to annual no. of illnesses for the pathogen
Campylobacter spp.	Annual no. persons hospitalized with a specific ICD-10 code in FHIS
Clostridium botulinum	Mandatory notification data
Clostridium perfringens	Proportion of hospitalizations for AG applied to annual no. of illnesses for the pathogen
Hepatitis A virus	Annual no. persons hospitalized with a specific ICD-10 code in FHIS
Hepatitis E virus	Annual no. persons hospitalized with a specific ICD-10 code in FHIS
Listeria monocytogenes	Mandatory notification data
Norovirus	Proportion of hospitalizations for AG applied to annual no. of illnesses for the pathogen
Salmonella spp., nontyphoidal	Annual no. persons hospitalized with a specific ICD-10 code in FHIS
Shiga toxin–producing *Escherichia coli*	*Salmonella* spp. and *Campylobacter* spp. data used as a proxy
Shigella spp.	Annual no. persons hospitalized with a specific ICD-10 code in FHIS
Staphylococcus aureus	Proportion of hospitalizations for AG applied to annual no. of illnesses for the pathogen
Taenia saginata	Annual no. persons hospitalized with a specific ICD-10 code in FHIS
Toxoplasma gondii	Annual no. persons hospitalized with a specific ICD-10 code in FHIS
Yersinia spp.	Annual no. persons hospitalized with a specific ICD-10 code in FHIS

*AG, acute gastroenteritis; FHIS, French Hospital Information System; ICD-10, International Classification of Diseases, 10th Revision (http://www.who.int/classifications/icd/en/).

and sex distributions of the hospital data with surveillance data from the national reference laboratories (*Campylobacter* spp., *Salmonella* spp., *Shigella* spp., *Yersinia* spp., and hepatitis E virus) and with mandatory notification data (hepatitis A virus).

We used the number of hospital records with acute gastroenteritis–associated ICD-10 codes (A00–A06.2 and A06.9–A09.9) to estimate the annual number of persons hospitalized for acute gastroenteritis. We then divided that number by the total number of persons with acute gastroenteritis to estimate the percentage of those persons who were hospitalized (0.58%–0.75%) (online Technical Appendix Table 1). For norovirus, *B. cereus*, *C. perfringens*, and *S. aureus,* we applied the proportion of hospitalizations for acute gastroenteritis to the annual number of illnesses for each pathogen to estimate the annual number of hospitalizations. For STEC, we used the proportion of hospitalizations estimated for *Salmonella* spp. and *Campylobacter* spp. as a proxy. For *C. botulinum* and *L. monocytogenes*, we used surveillance data from the mandatory notification system (Table 2).

Deaths
We explored death certificate data from the French national mortality database (*Institut National de la Santé et de la Recherche Médicale*, CépiDc [Epidemiology Center on Medical Causes of Death]) and data from FHIS to estimate the number of foodborne illness–associated deaths. For both data sources, we extracted all records for 2008–2013 with an ICD-10 code of interest as the main cause of death or hospitalization or as a concurrent medical condition. Compared with data from FHIS, death certificates contained fewer pathogen-specific ICD-10 codes; therefore, we used the hospital information system data as the main data source for estimating the number of deaths.

To estimate the number of deaths from *Campylobacter* spp., *Salmonella* spp., *Shigella* spp., *Yersinia* spp., hepatitis A and E viruses, *T. saginata*, and *T. gondii* infections, we used the number of hospital records with a pathogen-specific ICD-10 code and death shown as the mode of discharge. To estimate the number of norovirus-associated deaths, we applied the proportion of deaths among hospitalized case-patients with an ICD-10 code associated with viral gastroenteritis (ICD-10 codes A08.0–A08.4) to the annual number of hospitalizations for norovirus (0.18%–0.30%; online Technical Appendix Table 1). This proportion was also used as a proxy to estimate the number of deaths from *B. cereus*–, *C. perfringens*–, and *S. aureus*–associated hospitalizations. For *C. botulinum* and *L. monocytogenes*, we used mandatory notification data to estimate the number of deaths (Table 3).

Foodborne Transmission
To estimate the number of foodborne illnesses and associated hospitalizations and deaths, we applied a pathogen-specific proportion of foodborne transmission (online Technical Appendix Table 2). For 11 of the 15 pathogens, we used estimates published in the United States in 2011 (*15*). For norovirus and hepatitis A virus, data from more recent studies were used (*16,17*). For hepatitis E virus and *T. saginata*, the proportions of foodborne transmission were estimated on the basis of discussions with experts from the French Public Health Agency.

Results
Overall, the pathogens included in our study accounted for 4.9 million cases of illness (CrI$_{90\%}$ 4.2–6.2 million), 42,500 hospitalizations (CrI$_{90\%}$ 37,242–50,526), and 368 deaths (CrI$_{90\%}$ 335–486) each year in France. Of those 4.9 million cases, 1.5 million were caused by foodborne pathogens (CrI$_{90\%}$ 1.28–2.23 million), of which 880,500 (59%) were caused by bacteria; 579,500 (38%) by viruses; and 45,000 (3%) by parasites. These foodborne illnesses led to 17,281 hospitalizations (CrI$_{90\%}$ 15,520–20,785) and 248 deaths (CrI$_{90\%}$ 223–350).

Table 3. Methods used to estimate the number of pathogen-specific deaths, France, 2008–2013*

Pathogen	Method
Bacillus cereus	Hospital discharge data with viral gastroenteritis–associated ICD-10 codes
Campylobacter spp.	Hospital discharge data with pathogen-specific ICD-10 codes
Clostridium botulinum	Mandatory notification data
Clostridium perfringens	Hospital discharge data with viral gastroenteritis–associated ICD-10 codes
Hepatitis A virus	Hospital discharge data with pathogen-specific ICD-10 codes
Hepatitis E virus	Hospital discharge data with pathogen-specific ICD-10 codes
Listeria monocytogenes	Mandatory notification data
Norovirus	Hospital discharge data with viral gastroenteritis–associated ICD-10 codes
Salmonella spp., nontyphoidal	Hospital discharge data with pathogen-specific ICD-10 codes
Shiga toxin–producing *Escherichia coli*	*Salmonella* spp. and *Campylobacter* spp. data used as a proxy
Shigella spp.	Hospital discharge data with pathogen-specific ICD-10 codes
Staphylococcus aureus	Hospital discharge data with viral gastroenteritis–associated ICD-10 codes
Taenia saginata	Hospital discharge data with pathogen-specific ICD-10 codes
Toxoplasma gondii	Hospital discharge data with pathogen-specific ICD-10 codes
Yersinia spp.	Hospital discharge data with pathogen-specific ICD-10 codes

*ICD-10, International Classification of Diseases, 10th Revision (http://www.who.int/classifications/icd/en/).

Norovirus ranked first as the cause of foodborne illnesses (34%), third as a cause for foodborne illness–associated hospitalizations (20%), and seventh as a cause of foodborne illness–associated deaths (3%). *Salmonella* spp. ranked third as the cause of foodborne illnesses (12%), second as a cause for hospitalization (24%), and first as a cause of death (27%). *L monocytogenes* ranked second (26%), before *Campylobacter* spp. (17%), as a cause of foodborne illness–associated deaths (online Technical Appendix Table 2).

Discussion

We estimated the population-level number of illnesses, hospitalizations, and deaths in France caused by 15 pathogens with the potential for foodborne transmission. *Campylobacter* spp., *Salmonella* spp., and norovirus were responsible for 73% of all foodborne illnesses and 76% of all associated hospitalizations. The pathogens that cause most foodborne illnesses or hospitalizations are not necessarily those that cause the most deaths: *L. monocytogenes* caused <0.1% of all foodborne illnesses but ranked second as a cause of foodborne illness–associated deaths, just behind S*almonella* spp.

We used different approaches, depending on the most suitable data that were available, to generate estimates. We could not easily compare our results with previous estimates from France (2) and other countries because of different data sources, assumptions, and methods. Nevertheless, recent estimates of the burden of foodborne illnesses in the European region also indicated that the 3 most frequent causes of foodborne illness were norovirus (ranked first), *Campylobacter* spp. (second), and *Salmonella* spp. (third) (1). These pathogens were also among the leading causes of foodborne illnesses and hospitalizations in North America (15,18) and Oceania (19,20). *Salmonella* spp. and *L. monocytogenes* accounted for ≈50% of all foodborne illness–associated deaths in France, and were also responsible for most foodborne illness–associated deaths in other high-income countries (1,15,18–20).

We estimated the number of most pathogen-specific illnesses by using laboratory-based surveillance data corrected for underreporting and underdiagnosis, and we used well-documented estimates for *Campylobacter* spp. and *Salmonella* spp. (10). We assumed that the parameters regarding healthcare-seeking behavior and laboratory practice for *Yersinia* spp. and *Shigella* spp. were similar to those for *Campylobacter* spp. and *Salmonella* spp., respectively. The validity of these assumptions is difficult to explore; further studies would be needed to produce more robust estimates of the true level of underdiagnosis for these 2 pathogens in France.

For *B. cereus*, *C. perfringens*, and *S. aureus*, we assumed that the multiplier between the number of outbreak cases and the number of foodborne illnesses would be similar to that for *Salmonella* spp. An alternative approach for *C. perfringens* would have been to apply a proportion of acute gastroenteritis cases by this pathogen estimated in the United Kingdom (0.3–1.7%) (13) to the annual number of acute gastroenteritis illnesses in France. This approach would result in an estimate (CrI$_{90\%}$ 84,450–278,964) within the range of the estimate in our study. The estimates for *B. cereus*, *C. perfringens*, and *S. aureus* indicate that the effect of these pathogens in terms of foodborne illnesses appears to be high in France. However, only foodborne illness outbreak data were available to estimate the number of illnesses for these pathogens, and more data are needed to confirm our estimates.

We included hepatitis E virus in our study because, in France, indigenous cases of hepatitis E have been shown to be associated with foodborne transmission, particularly through consumption of products containing undercooked or raw pork liver (21,22). We estimated the number of hepatitis E cases in France from a seroprevalence study conducted in 2013, and the proportion of cases caused by foodborne transmission was assumed to be between 75% and 100%. Further studies, in particular on the proportion of foodborne transmission of hepatitis E in France, are needed to confirm these estimates.

Our use of seroprevalence and health insurance drug reimbursement data to estimate the numbers of *T. gondii*– and *T. saginata*–associated foodborne illnesses was similar to methods previously used in France (*2*). Our results indicated a decrease in the number of foodborne illnesses over the past decade (from 51,600 to 12,000 cases for *T. gondii* and from 64,500 to 33,000 cases for *T. saginata*). These decreases may be explained by fewer exposures to the parasites (*23*), by changes in food habits, and by improved hygiene practices in meat production. For *T. saginata*, the number of illnesses may be underestimated because the decrease might also be explained by a shift of treatment from niclosamide to praziquantel for this infection over the past decade in France.

We estimated the number of illnesses caused by norovirus by applying a proportion of acute gastroenteritis cases caused by this pathogen to the annual number of acute gastroenteritis illnesses in France. The final estimate for France is lower than that for other countries that used a similar method (*15,18*), primarily because of a lower estimated incidence of acute gastroenteritis in France (*5*) but also because we used a lower proportion of foodborne norovirus transmission (12%–16%) on the basis of an extensive study published in 2015 (*16*). Despite these differences and their effect on the final estimate, norovirus ranked first in terms of foodborne illnesses in France and appears to be a key foodborne cause of acute gastroenteritis.

The FHIS was our main data source for estimating numbers of hospitalizations and deaths associated with the 15 pathogens in our study. The relevance of this data source may be questioned because of limitations in diagnosis accuracy and in consistency of disease coding. For most of the pathogens, we estimated the number of hospitalizations by using the number of hospital records with specific ICD-10 codes. We compared trends over time and age and sex distributions of the hospital data with surveillance data from the national reference laboratories and with mandatory notification data. Trends and distributions were similar between the different data sources, supporting the use of FHIS data to estimate the number of hospitalizations. For *Campylobacter* spp., *Salmonella* spp., *Yersinia* spp., and *Shigella* spp., we corrected the number of hospitalizations and deaths for underdiagnosis, taking into account a proportion of fecal samples tested for each pathogen and the sensitivity of fecal culture. However, for the other pathogens, no specific underdiagnosis multiplier could be estimated and, therefore, the estimates presented in this study are probably conservative. An overestimation is also possible if the pathogen of interest did not cause the illness that led to the hospitalization but was, nevertheless, coded as a concurrent medical condition.

A high number of hospitalizations due to acute gastroenteritis were reported in the FHIS without a specific ICD-10 code because not all hospitalized patients were systematically tested for all pathogens that cause acute gastroenteritis. We used the proportion of hospitalizations for acute gastroenteritis as a proxy to estimate the number of hospitalizations for norovirus, *B. cereus*, *C. perfringens*, and *S. aureus* because testing for these pathogens is infrequently performed in France and because these pathogens cause illnesses with similar symptoms and severity. This proportion (0.58%–0.75%) is lower than that estimated for *Campylobacter* spp. (0.9%–1.9%) and for *Salmonella* spp. (1.2%–3.6%), which is plausible considering that illness caused by *B. cereus*, *C. perfringens*, and *S. aureus* is less severe than that caused by *Campylobacter* spp. and *Salmonella* spp. Data sources described in the literature to estimate the number of hospitalizations for norovirus, *B. cereus*, *C. perfringens*, and *S. aureus* infections include hospital discharge data and data from foodborne disease outbreaks (*15,18,19,24,25*). Estimating the number of hospitalizations for these pathogens is challenging, and these different methodologic approaches have a major effect on the final estimate. For norovirus, despite differences in methodology and healthcare systems, our estimate (all modes of transmission) of the number of hospitalizations was in the same range as those estimated in North America (*24,25*) and in the Netherlands (*26*).

Data to estimate the number of deaths associated with foodborne illnesses are scarce and difficult to obtain. We explored death certificate data but decided not to use that source because few records contained pathogen-specific ICD-10 codes. Hospital discharge data were the only or the most reliable data source available to estimate the number of deaths for most pathogens included in this study. However, deaths may occur after hospitalization discharge or without hospitalization at all. Therefore, our estimates are uncertain and are probably underestimated, even though we did not take into account the possibility that underlying concurrent conditions, not foodborne pathogens, may have caused or contributed to death.

As pointed out in the literature, difficulties in accurately determining the proportion of foodborne pathogen transmission is a key factor contributing to the uncertainty of foodborne illness estimates (*15,27*). Different methodologic approaches, such as epidemiologic and microbiologic approaches, intervention studies, and expert elicitation, have been used to estimate the proportion of foodborne transmission (*15,28–32*). Overall, in high-income countries, foodborne transmission has been considered a major transmission route for several bacterial pathogens (*B. cereus*, *Campylobacter* spp., *C. perfringens*, *L. monocytogenes*, *Salmonella* spp., *S. aureus*) and a minor transmission route for norovirus and hepatitis A virus. Nevertheless, comparison of the estimates by using expert elicitation shows greater variability and higher uncertainties, depending on

how the experts were recruited, the expert panel size, or the elicitation method used (*27,33*). We decided to use the proportion of foodborne transmission published in the United States in 2011 (*15*) as these proportions were based on epidemiologic and microbiologic data rather than expert elicitation. It is possible that food consumption patterns and frequency and type of microbiologic contamination differ between the United States and France and may influence pathogen exposure, resulting in a different proportion of foodborne pathogen transmission in the 2 countries. Further research is needed to obtain specific source attribution estimates for France.

The 15 foodborne pathogens in our study were selected on the basis of their perceived public health significance, their occurrence in France, and the availability of a minimum of data. Other known pathogens with potential foodborne transmission exist (e.g., other non-STEC pathogenic *E.coli*, rotavirus, and *Cryptosporidium* spp.), and the total numbers of foodborne illnesses and associated hospitalizations and deaths presented in this study are likely conservative.

We took into account new data sources that allowed for accurate estimates of foodborne illnesses and associated hospitalizations and deaths at the community level in France. Our estimates entail several assumptions, and a high degree of uncertainty remains for some of them. Our estimates indicate that substantial numbers of foodborne pathogen–associated illnesses, hospitalizations, and deaths occur each year in France, necessitating the prioritization of prevention and control strategies by food safety policymakers. We did not specifically consider the effect of sequelae linked to these illnesses when generating our estimates. Thus, our findings capture only part of the overall effect of foodborne infections, and they clear the way for further research on the public health burden of foodborne pathogens in France, taking into account complications and sequelae.

Dr. Van Cauteren is epidemiologist at the Department of Infectious Diseases at Santé Publique France, the French National Public Health Agency. His research focuses on surveillance and the burden of foodborne infections.

References

1. Kirk MD, Pires SM, Black RE, Caipo M, Crump JA, Devleesschauwer B, et al. World Health Organization estimates of the global and regional disease burden of 22 foodborne bacterial, protozoal, and viral diseases, 2010: a data synthesis. PLoS Med. 2015;12:e1001921. http://dx.doi.org/10.1371/journal.pmed.1001921
2. Vaillant V, de Valk H, Baron E, Ancelle T, Colin P, Delmas MC, et al. Foodborne infections in France. Foodborne Pathog Dis. 2005;2:221–32. http://dx.doi.org/10.1089/fpd.2005.2.221
3. Gallay A, Simon F, Mégraud F. Surveillance of human *Campylobacter* infections in France—part 2—implementation of national surveillance. Euro Surveill. 2003;8:218.
4. Couturier E. Hepatitis E: synthesis in human epidemiology [in French]. Bulletin épidémiologique hebdomadaire, 2010; Special issue:18–9
5. Van Cauteren D, De Valk H, Vaux S, Le Strat Y, Vaillant V. Burden of acute gastroenteritis and healthcare-seeking behaviour in France: a population-based study. Epidemiol Infect. 2012;140:697–705. http://dx.doi.org/10.1017/S0950268811000999
6. Van Cauteren D, Turbelin C, Fonteneau L, Hanslik T, De Valk H, Blanchon T. Physician practices in requesting stool samples for patients with acute gastroenteritis, France, August 2013–July 2014. Epidemiol Infect. 2015;143:2532–8. http://dx.doi.org/10.1017/S0950268814003884
7. Gabet A, Juillière Y, Lamarche-Vadel A, Vernay M, Olié V. National trends in rate of patients hospitalized for heart failure and heart failure mortality in France, 2000–2012. Eur J Heart Fail. 2015;17:583–90. http://dx.doi.org/10.1002/ejhf.284
8. Tuppin P, Rivière S, Rigault A, Tala S, Drouin J, Pestel L, et al. Prevalence and economic burden of cardiovascular diseases in France in 2013 according to the national health insurance scheme database. Arch Cardiovasc Dis. 2016;109:399–411. http://dx.doi.org/10.1016/j.acvd.2016.01.011
9. van Cauteren D, Millon L, de Valk H, Grenouillet F. Retrospective study of human cystic echinococcosis over the past decade in France, using a nationwide hospital medical information database. Parasitol Res. 2016;115:4261–5. http://dx.doi.org/10.1007/s00436-016-5204-1
10. Van Cauteren D, De Valk H, Sommen C, King LA, Jourdan-Da Silva N, Weill FX, et al. Community incidence of campylobacteriosis and nontyphoidal salmonellosis, France, 2008–2013. Foodborne Pathog Dis. 2015;12:664–9. http://dx.doi.org/10.1089/fpd.2015.1964
11. Spiegelhalter DJ, Abrams KR, Myles JP. Bayesian approaches to clinical trials and health-care evaluation. Chichester (UK): Wiley; 2004.
12. R Development Core Team. R: a language and environment for statistical computing. Vienna: R Foundation for Statistical Computing; 2016.
13. Tam CC, O'Brien SJ, Tompkins DS, Bolton FJ, Berry L, Dodds J, et al.; IID2 Study Executive Committee. Changes in causes of acute gastroenteritis in the United Kingdom over 15 years: microbiologic findings from 2 prospective, population-based studies of infectious intestinal disease. Clin Infect Dis. 2012; 54:1275–86. http://dx.doi.org/10.1093/cid/cis028
14. Ahmed SM, Hall AJ, Robinson AE, Verhoef L, Premkumar P, Parashar UD, et al. Global prevalence of norovirus in cases of gastroenteritis: a systematic review and meta-analysis. Lancet Infect Dis. 2014;14:725–30. http://dx.doi.org/10.1016/S1473-3099(14)70767-4
15. Scallan E, Hoekstra RM, Angulo FJ, Tauxe RV, Widdowson MA, Roy SL, et al. Foodborne illness acquired in the United States—major pathogens. Emerg Infect Dis. 2011;17:7–15. http://dx.doi.org/10.3201/eid1701.P11101
16. Verhoef L, Hewitt J, Barclay L, Ahmed SM, Lake R, Hall AJ, et al. Norovirus genotype profiles associated with foodborne transmission, 1999–2012. Emerg Infect Dis. 2015;21:592–9. http://dx.doi.org/10.3201/eid2104.141073
17. Petrignani M, Verhoef L, Vennema H, van Hunen R, Baas D, van Steenbergen JE, et al. Underdiagnosis of foodborne hepatitis A, the Netherlands, 2008–2010. Emerg Infect Dis. 2014;20:596–602. http://dx.doi.org/10.3201/eid2004.130753

18. Thomas MK, Murray R, Flockhart L, Pintar K, Fazil A, Nesbitt A, et al. Estimates of foodborne illness–related hospitalizations and deaths in Canada for 30 specified pathogens and unspecified agents. Foodborne Pathog Dis. 2015;12:820–7. http://dx.doi.org/10.1089/fpd.2015.1966

19. Kirk M, Ford L, Glass K, Hall G. Foodborne illness, Australia, circa 2000 and circa 2010. Emerg Infect Dis. 2014;20:1857–64. http://dx.doi.org/10.3201/eid2011.131315

20. Lake RJ, Cressey PJ, Campbell DM, Oakley E. Risk ranking for foodborne microbial hazards in New Zealand: burden of disease estimates. Risk Anal. 2010;30:743–52. http://dx.doi.org/10.1111/j.1539-6924.2009.01269.x

21. Guillois Y, Abravanel F, Miura T, Pavio N, Vaillant V, Lhomme S, et al. high proportion of asymptomatic infections in an outbreak of hepatitis E associated with a spit-roasted piglet, France, 2013. Clin Infect Dis. 2016;62:351–7. http://dx.doi.org/10.1093/cid/civ862

22. Renou C, Roque-Afonso AM, Pavio N. Foodborne transmission of hepatitis E virus from raw pork liver sausage, France. Emerg Infect Dis. 2014;20:1945–7. http://dx.doi.org/10.3201/eid2011.140791

23. Nogareda F, Le Strat Y, Villena I, De Valk H, Goulet V. Incidence and prevalence of *Toxoplasma gondii* infection in women in France, 1980–2020: model-based estimation. Epidemiol Infect. 2014;142:1661–70. http://dx.doi.org/10.1017/S0950268813002756

24. Lopman BA, Hall AJ, Curns AT, Parashar UD. Increasing rates of gastroenteritis hospital discharges in US adults and the contribution of norovirus, 1996–2007. Clin Infect Dis. 2011;52:466–74. http://dx.doi.org/10.1093/cid/ciq163

25. Morton VK, Thomas MK, McEwen SA. Estimated hospitalizations attributed to norovirus and rotavirus infection in Canada, 2006–2010. Epidemiol Infect. 2015;143:3528–37. http://dx.doi.org/10.1017/S0950268815000734

26. Havelaar AH, Haagsma JA, Mangen MJ, Kemmeren JM, Verhoef LP, Vijgen SM, et al. Disease burden of foodborne pathogens in the Netherlands, 2009. Int J Food Microbiol. 2012; 156:231–8. http://dx.doi.org/10.1016/j.ijfoodmicro.2012.03.029

27. Glass K, Ford L, Kirk MD. Drivers of uncertainty in estimates of foodborne gastroenteritis incidence. Foodborne Pathog Dis. 2014;11:938–44. http://dx.doi.org/10.1089/fpd.2014.1816

28. Hald T, Aspinall W, Devleesschauwer B, Cooke R, Corrigan T, Havelaar AH, et al. World Health Organization estimates of the relative contributions of food to the burden of disease due to selected foodborne hazards: a structured expert elicitation. PLoS One. 2016;11:e0145839. http://dx.doi.org/10.1371/journal.pone.0145839

29. Batz MB, Hoffmann S, Morris JG Jr. Ranking the disease burden of 14 pathogens in food sources in the United States using attribution data from outbreak investigations and expert elicitation. J Food Prot. 2012;75:1278–91. http://dx.doi.org/10.4315/0362-028X.JFP-11-418

30. Butler AJ, Thomas MK, Pintar KD. Expert elicitation as a means to attribute 28 enteric pathogens to foodborne, waterborne, animal contact, and person-to-person transmission routes in Canada. Foodborne Pathog Dis. 2015;12:335–44. http://dx.doi.org/10.1089/fpd.2014.1856

31. Havelaar AH, Galindo AV, Kurowicka D, Cooke RM. Attribution of foodborne pathogens using structured expert elicitation. Foodborne Pathog Dis. 2008;5:649–59. http://dx.doi.org/10.1089/fpd.2008.0115

32. Vally H, Glass K, Ford L, Hall G, Kirk MD, Shadbolt C, et al. Proportion of illness acquired by foodborne transmission for nine enteric pathogens in Australia: an expert elicitation. Foodborne Pathog Dis. 2014;11:727–33. http://dx.doi.org/10.1089/fpd.2014.1746

33. Butler AJ, Thomas MK, Pintar KD. Systematic review of expert elicitation methods as a tool for source attribution of enteric illness. Foodborne Pathog Dis. 2015;12:367–82. http://dx.doi.org/10.1089/fpd.2014.1844

Address for correspondence: Dieter Van Cauteren, Department of Infectious Diseases, Santé Publique France, French National Public Health Agency, F-94415, 12 rue du Val d'Osne, Saint-Maurice, France; email: vancauteren.dieter@hotmail.com

Epidemiology of *Salmonella enterica* Serotype Dublin Infections among Humans, United States, 1968–2013

R. Reid Harvey,[1] Cindy R. Friedman, Stacy M. Crim, Michael Judd, Kelly A. Barrett,
Beth Tolar, Jason P. Folster, Patricia M. Griffin, Allison C. Brown

Salmonella enterica serotype Dublin is a cattle-adapted bacterium that typically causes bloodstream infections in humans. To summarize demographic, clinical, and antimicrobial drug resistance characteristics of human infections with this organism in the United States, we analyzed data for 1968–2013 from 5 US surveillance systems. During this period, the incidence rate for infection with *Salmonella* Dublin increased more than that for infection with other *Salmonella*. Data from 1 system (FoodNet) showed that a higher percentage of persons with *Salmonella* Dublin infection

were hospitalized and died during 2005–2013 (78% hospitalized, 4.2% died) than during 1996-2004 (68% hospitalized, 2.7% died). Susceptibility data showed that a higher percentage of isolates were resistant to ≥7 classes of antimicrobial drugs during 2005–2013 (50.8%) than during 1996–2004 (2.4%).

*S*almonella Dublin is a zoonotic *Salmonella enterica* serotype that in recent years has increased in infection incidence, antimicrobial drug resistance, and illness clinical severity. The Centers for Disease Control and Prevention (CDC) estimates that each year in the United States, *Salmonella enterica* causes 1.2 million infections, 24,000 hospitalizations, and 450 deaths (*1*). Although >2,500 serotypes of *Salmonella* exist (*2*), only ≈50 serotypes are regularly isolated from humans. Illnesses caused by nontyphoidal *Salmonella* are often self-limiting and require no antimicrobial drug therapy, but for patients with invasive infections, treatment is critical. Antimicrobial drug–resistant strains of *Salmonella* are associated with more severe illness and are more likely to result in bloodstream infection, hospitalization, and death than are illnesses caused by drug-susceptible strains (*3,4*). According to surveillance data from the National Antimicrobial Resistance Monitoring System (NARMS), the proportion of resistant isolates is higher among *S. enterica* serotype Dublin than among other serotypes (*5*).

Unlike most nontyphoidal *Salmonella* serotypes, which affect a broad spectrum of unrelated host species, *Salmonella* Dublin is a cattle-adapted serotype (*6*). The most comprehensive analysis of cases of *Salmonella* Dublin infection was published in 1982 and demonstrated that this serotype causes rare but severe disease in humans (i.e., bloodstream infection) that often requires antimicrobial drug therapy (*7*). Using available data across various CDC surveillance systems, we analyzed the epidemiology of human infections with *Salmonella* Dublin in the United States, including antimicrobial drug resistance, and compared it with that of other *Salmonella* serotypes.

Methods

Data Sources

Laboratory-based Enteric Disease Surveillance, 1968–2013
Begun in 1968, the CDC Laboratory-based Enteric Disease Surveillance system (LEDS) collects serotype and demographic data for every *Salmonella* isolate obtained from a human and submitted to US state and territorial public health laboratories. We used LEDS data to estimate national incidence rates (no. cases/100,000 population, using US census population estimates) of reported *Salmonella* Dublin and other nontyphoidal *Salmonella*

serotypes. We excluded all typhoidal serotypes: Typhi, Paratyphi A, Paratyphi B (L[+] tartrate-negative), and Paratyphi C. We defined other nontyphoidal *Salmonella* as serotypes other than *Salmonella* Dublin (hereafter called other *Salmonella*). We also used LEDS data to evaluate differences in proportions of patients by race, ethnicity, and home state, infected with *Salmonella* Dublin and other *Salmonella* serotypes.

Foodborne Diseases Active Surveillance Network, 1996–2013
Since 1996, the Foodborne Diseases Active Surveillance Network (FoodNet) has conducted active, population-based surveillance for culture-confirmed cases of infection caused by 9 pathogens, including *Salmonella*, transmitted commonly through food in the United States. FoodNet is a collaboration of CDC, 10 state health departments, the US Department of Agriculture Food Safety and Inspection Service (USDA FSIS), and the US Food and Drug Administration (FDA). The FoodNet surveillance area includes 15% of the US population. For each reported case, FoodNet sites collect data on demographic characteristics, hospitalization, and outcome. Since 2004, FoodNet has also collected data on international travel (defined as travel abroad in the 7 days before illness began) and whether the case was associated with an outbreak. We used FoodNet data to compare demographics, clinical outcomes, and travel history among patients infected with *Salmonella* Dublin and those infected with other *Salmonella* serotypes.

National Molecular Subtyping Network for Foodborne Disease Surveillance, 1996–2013
Begun in 1996, the National Molecular Subtyping Network for Foodborne Disease Surveillance (PulseNet) is a national network of state and local public health laboratories and food regulatory agencies in the United States. Laboratorians upload pulsed-field gel electrophoresis patterns to PulseNet national databases. Comparison of these patterns enables identification of matches and possible outbreaks. The PulseNet database contains isolate data from human, food, environmental, and animal sources. We used PulseNet data to identify common nonhuman sources of *Salmonella* Dublin isolates.

Foodborne Disease Outbreak Surveillance System, 1973–2013
Since 1973, the Foodborne Disease Outbreak Surveillance System (FDOSS) has collected reports of enteric disease outbreaks transmitted by food in the United States. State and local public health agencies submit to CDC reports that include information about outbreak characteristics, food vehicles, and pathogens that caused each outbreak. We searched FDOSS data to describe the vehicles implicated in outbreaks of *Salmonella* Dublin infections.

NARMS, 1996–2013

Begun in 1996, NARMS is a collaboration among CDC, FDA, USDA, and state and local health departments. CDC asks public health laboratories that participate in LEDS to submit every 20th *Salmonella* isolate received from clinical laboratories to NARMS for the purpose of tracking changes in the antimicrobial susceptibility of certain enteric bacteria isolated from ill persons, retail meats, and food animals. We included NARMS data to compare antimicrobial resistance profiles (resistance to clinically important agents and the number of resistant classes) of *Salmonella* Dublin isolates from humans with those from other *Salmonella* serotypes. Susceptibility testing was conducted as previously described (*8*). In brief, isolates were tested for antimicrobial susceptibility by using broth microdilution (Sensititer; Trek Diagnostics, Cleveland, OH, USA) to determine the MIC for 14 antimicrobial agents (amikacin, gentamicin, streptomycin, ampicillin, amoxicillin/clavulanic acid, ceftiofur, ceftriaxone, cefoxitin, sulfamethoxazole/sulfisoxazole, trimethoprim/sulfamethoxazole, chloramphenicol, ciprofloxacin, nalidixic acid, and tetracycline). These agents were categorized into 8 classes, as defined by Clinical and Laboratory Standards Institute guidelines. When available, Clinical and Laboratory Standards Institute interpretive criteria were used to define resistance (*5*). A subset of isolates that showed resistance to ceftiofur or ceftriaxone were also tested for ceftazidime susceptibility. A multidrug-resistant (MDR) isolate was defined as one resistant to ≥3 classes of drug. We also examined specific resistance patterns, which included isolates that were resistant to at least ampicillin, chloramphenicol, streptomycin, sulfonamide (sulfamethoxazole/sulfisoxazole), and tetracycline (ACSSuT) and isolates that were also resistant to amoxicillin/clavulanic acid and ceftriaxone (ACSSuTAuCx). We compared antimicrobial resistance patterns of *Salmonella* Dublin between the 2 periods 1996–2004 and 2005–2013.

Statistical Analyses

We used the Pearson χ^2 test for statistical comparisons. We considered differences significant if the p value was <0.05. Statistical analyses were conducted by using SAS version 9.3 (SAS Institute, Cary, NC, USA).

Results

Incidence

During 1968–2013, states reported 3,903 cases of *Salmonella* Dublin infections to LEDS. These cases accounted for <0.25% of *Salmonella* infections reported. The incidence rate (no. *Salmonella* Dublin infections/100,000 persons) has been steadily rising since 1968 (0.0055 infections) with the exception of a distinct increase and subsequent decrease in incidence occurring throughout the 1980s, peaking in 1985 at 0.081 infections (Figure 1). The incidence rate for *Salmonella* Dublin infection was 7.6 times higher in 2013 (0.042 infections) than in 1968. In contrast, the incidence rate of other *Salmonella* infections has remained relatively stable since 1968 (9.5 infections compared with 11.2 infections in 2013). More than half (51%; 1,989/3,903) of all *Salmonella* Dublin infections were among California residents, including 74% (484/656) of infections during the peak in incidence from 1982 to 1985 (Figure 2). According to LEDS data, most *Salmonella* Dublin infections are reported from California; during 2005–2013, the 271 *Salmonella* Dublin infections reported from California accounted for 29% of the 943 cases reported to LEDS.

Demographics

Demographics differed markedly among those infected with *Salmonella* Dublin and those with other *Salmonella*. According to FoodNet data, 38% of *Salmonella* Dublin infections occurred in persons ≥65 years of age, compared
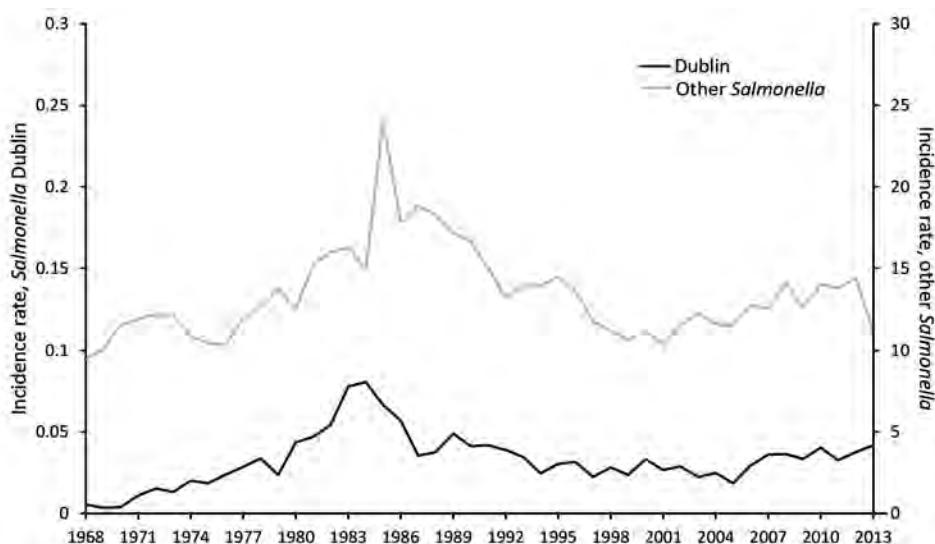
Figure 1. Incidence rates (no. cases/100,000 persons) for human infection with *Salmonella enterica* serotype Dublin and other nontyphoidal *Salmonella,* United States, 1968–2013. Data from the Centers for Disease Control and Prevention Laboratory-based Enteric Disease Surveillance system.

Figure 2. Incidence rates (no. cases/100,000 persons) for *Salmonella enterica* serotype Dublin infection in California and the rest of the United States, 1968–2013. Data from the Centers for Disease Control and Prevention Laboratory-based Enteric Disease Surveillance system.

with 11% of other *Salmonella* infections (p<0.01) (Table 1). The median age of *Salmonella* Dublin patients was 55 years; the median age of patients with other *Salmonella* infections was 23 years (p<0.01). A total of 7% of *Salmonella* Dublin infections and 28% of other *Salmonella* infections occurred in children <5 years of age (p<0.01); 60% of *Salmonella* Dublin and 48% of other *Salmonella* infections occurred in men (p<0.01). We found no significant difference in history of international travel between patients with *Salmonella* Dublin (5%; 6/101) and other *Salmonella* infections (9%; 4,297/46,764) (p = 0.15).

Clinical Outcomes and Severity of Disease

According to FoodNet data, *Salmonella* Dublin was more commonly isolated from blood (61%) than were other *Salmonella* (5%) (p<0.01) (Table 1). Hospitalization was reported for 75% of patients with *Salmonella* Dublin infection and 27% of patients with other *Salmonella* infections (p<0.01) (Table 1). Hospitalization lasted a median of 6

days for patients with *Salmonella* Dublin infection and 3 days for patients with other *Salmonella* infections (p<0.01). *Salmonella* infection resulted in death for 4% of patients with *Salmonella* Dublin infection and 0.5% of patients with other *Salmonella* infections (p<0.01).

The proportion of *Salmonella* Dublin isolates from blood remained relatively constant during 1996–2004 (60%) and 2005–2013 (61%) (Figure 3). Hospitalization among *Salmonella* Dublin patients increased from 68% during 1996–2004 to 78% during 2005–2013 (p<0.05). The mortality rate increased from 2.7% during 1996–2004 to 4.2% during 2005–2013 (p = 0.57).

Sources

Food and Animals

According to the PulseNet database, 478 *Salmonella* Dublin isolates were obtained from food during 1999–2013. Source data for 475 foodborne isolates indicated that 473

Table 1. Demographics, international travel, clinical outcomes, and isolate source for *Salmonella enterica* serotype Dublin and other *Salmonella*, United States, 1996–2013*

Patient characteristics	*Salmonella* Dublin, no. (%), n = 228	Other *Salmonella*, no. (%), n = 97,814	p value
Demographics			
Age group, y†			
<1	2/228 (0.9)	11,075/97,562 (11.4)	<0.01
1–4	13/228 (5.7)	16,481/97,562 (16.9)	<0.01
5–17	8/228 (3.5)	15,628/97,562 (16.0)	<0.01
18–64	119/228 (52.2)	43,819/97,562 (44.9)	<0.05
≥65	86/228 (37.7)	10,559/97,562 (10.8)	<0.01
Sex			
M	137/228 (60.1)	46,909/97,486 (48.1)	<0.01
F			
International travel	6/101 (5.0)	4,297/46,764 (8.6)	0.15
Clinical outcome			
Died	8/216 (3.7)	431/86,977 (0.5)	<0.01
Hospitalized‡	167/223 (74.9)	24,187/88,748 (37.3)	<0.01
Isolate source			
Blood	137/226 (60.7)	5,054/97,142 (5.2)	<0.01
Feces	49/226 (21.7)	8,6257/97,142 (88.8)	<0.01
Other	40/226 (17.7)	5,831/97,142 (6.0)	<0.01

*Data from the Foodborne Diseases Active Surveillance Network.
†Median ages: *Salmonella* Dublin 55 (range <1–97) y; other *Salmonella* 23 (range <1–110) y; p<0.01.
‡Median hospital stays: *Salmonella* Dublin, 6 d (range 1–76 d); other *Salmonella*, 3 d (range 0–374 d); p<0.01.
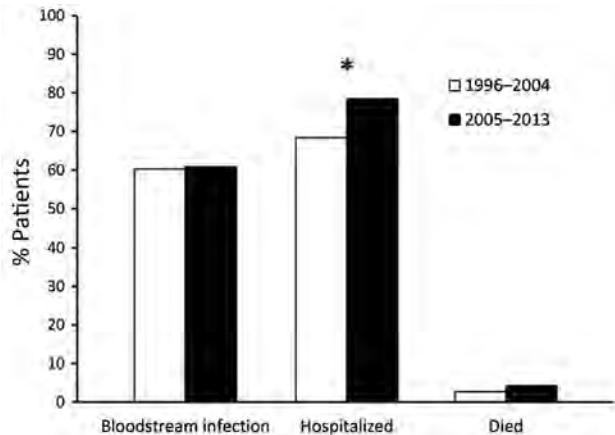
Figure 3. Percentage of patients with adverse clinical outcomes after infection with *Salmonella enterica* serotype Dublin, United States, 1996–2004 and 2005–2013. *p<0.05 (significant difference).

(99%) were from beef, 1 was from cooked pork, and 1 was from chili pepper. During this same period, another 376 *Salmonella* Dublin isolates were obtained from animals. Of the 331 of these isolates with source data available, 328 (99%) were from cattle and 3 were from a pig, a dog, and a horse.

Outbreaks
During 1973–2013, a total of 9 *Salmonella* Dublin outbreaks were reported to FDOSS. These outbreaks occurred in California (5 outbreaks), Washington (2), Arkansas (1), and Wisconsin (1). Of the 9 outbreaks, 6 (67%) occurred before 1982. For each of 3 outbreaks, the foodborne vehicle was identified (raw beef, raw milk, and Mexican-style cheese).

Sporadic Illnesses
We used LEDS data to determine the proportion of all *Salmonella* infections reported during 2007–2012. *Salmonella* Dublin infection was more common in states where the sale of raw milk is legal (328 cases/100,000 persons) (*9*) than in states where such sale is illegal (108 cases/100,000 persons) (p<0.01).

Antimicrobial Resistance
During 1996–2013, a total of 102 clinical isolates of *Salmonella* Dublin were tested by NARMS (Table 2). Of these 102 isolates, 42 (41%) were pansusceptible; of the 33,415 isolates from other *Salmonella*, 26,552 (79%) were pansusceptible (p<0.01). Ceftriaxone resistance increased from detection in 0 of 5 isolates in 1996 to detection in 11 (92%) of 12 isolates in 2013 and was higher among *Salmonella* Dublin isolates (31%; 32/102) than among other *Salmonella* isolates (3%; 947/33,415) (p<0.01). Of the 31 ceftriaxone-resistant isolates that were also tested for ceftazidime resistance, 28 (90%) were resistant.

Multidrug resistance was found for 56 (55%) of *Salmonella* Dublin isolates compared with 4,013 (12%) of other *Salmonella* isolates (p<0.01) (Table 2). Among MDR *Salmonella* Dublin isolates, 84% were resistant to ≥5 classes of antimicrobial drugs and 57% were resistant to ≥7 classes; among MDR isolates of other *Salmonella*, 59% (p<0.01) were resistant to ≥5 classes and 15% (p<0.01) were resistant to ≥7 classes. ACSSuT resistance was found in 41% of *Salmonella* Dublin isolates, compared with 7% of other *Salmonella* isolates (p<0.01).

ACSSuTAuCx resistance was found for 28% of *Salmonella* Dublin isolates and 2% of other *Salmonella* isolates (p<0.01). Resistance to nalidixic acid was found for 6% of *Salmonella* Dublin isolates and 2% of other *Salmonella* isolates (p<0.01). Among nalidixic acid–resistant isolates, 67% of *Salmonella* Dublin isolates and 6% of other *Salmonella* isolates were also resistant to ceftriaxone (p<0.01). The proportion of *Salmonella* Dublin isolates resistant to antimicrobial drugs increased markedly from 1996–2004 to 2005–2013, from 29% to 79% for resistance to ≥1 classes (p<0.01) and from 2% to 51% for resistance to ≥7 antimicrobial classes (p<0.01) (Figure 4). Among resistant isolates, the median number of classes to which isolates were resistant increased from 4.5 to 7.0 (p<0.01). Resistance to ceftriaxone increased from 3% during 1996–2004 to 52% during 2005-2013 (p<0.01), and resistance to nalidixic acid increased from 0 to 10% during these same periods (p<0.05).

Discussion
Decades of CDC surveillance data analyzed in this study illustrate that *Salmonella* Dublin more often causes bloodstream infections, hospitalizations (with longer hospital stays), and deaths than other *Salmonella* serotypes. Our findings support previous descriptions of *Salmonella* Dublin as a cattle-adapted serotype (*10*).

In the past decade, more than half of *Salmonella* Dublin infections have been resistant to ≥7 antimicrobial drug classes, and clinical outcomes have been more severe. The proportion of *Salmonella* Dublin isolates that were resistant was ≈2.7 times greater during 2005–2013 than during 1996–2004; isolates from the later period were also resistant to more antimicrobial drug classes. Multidrug resistance probably has direct clinical implications because bloodstream infections that require antimicrobial therapy tend to develop in patients with *Salmonella* Dublin infections (*3*). Most *Salmonella* Dublin isolates were resistant to third-generation cephalosporins (including ceftriaxone), which are often the treatment of choice for children with bloodstream infections because of the contraindication for fluoroquinolone use in children.

Clinical severity of *Salmonella* Dublin infections, as measured by the proportion of hospitalizations and deaths,

Table 2. Antimicrobial drug resistance in *Salmonella enterica* serotype Dublin and other *Salmonella*, United States, 1996–2013*

Resistance pattern	*Salmonella* Dublin, no. (%), n = 102	Other *Salmonella*, no. (%), n = 33,415
Pansusceptible	42 (41)	26,552 (79)
Resistant to >1 class	60 (59)	6,863 (21)
Resistant to >3 classes	56 (55)	4,013 (12)
Resistant to >5 classes	47 (46)	2,374 (7)
Resistant to >7 classes	32 (31)	601 (2)
Resistant to at least ACSSuT†	42 (41)	2,156 (6)
Resistant to at least ACSSuTAuCx‡	29 (28)	581 (2)
Resistant to ceftriaxone	32 (31)	947 (3)
Resistant to nalidixic acid	6 (6)	643 (2)
Resistant to nalidixic acid and ceftriaxone	4 (4)	39 (0.1)

*Data from the National Antimicrobial Resistance Monitoring System. p<0.01 for all.
†Resistant to ampicillin, chloramphenicol, streptomycin, sulfamethoxazole/sulfisoxazole,and tetracycline.
‡Resistant to ACSSuT, amoxicillin–clavulanic acid, and ceftriaxone.

also increased between 1996–2004 and 2005–2013. Our study did not directly measure the association between antimicrobial resistance and clinical severity of *Salmonella* Dublin infection by linking isolate data to outcome data. Nevertheless, by comparing both measures over the 2 periods, we showed that, for *Salmonella* Dublin infections, antimicrobial drug resistance and clinical severity increased in parallel. In addition to the older age of patients and concurrent conditions often associated with *Salmonella* Dublin infections (*7,11*), we hypothesize that the multidrug resistance profile has led to the higher rates of treatment failure, prolonged hospitalizations, and higher mortality rates observed in our study.

Virulence factors may also contribute, particularly those factors located on resistance plasmids that are coselected for when antimicrobial drugs are used in cattle. *Salmonella* Dublin has been described as having a serotype-specific virulence-associated plasmid that is associated with invasive infection and remains stable through multiple generations of nonselective bacterial passage (*12*). Additional analyses, with use of whole-genome sequencing, particularly methods like those developed by Pacific Biosciences (Menlo Park, CA, USA) to use long-sequence reads and facilitate plasmid analysis, would enable investigation into the respective contributions of virulence factors and resistance mechanisms.

The recently observed increase in human infections with *Salmonella* Dublin resistant to ceftriaxone and nalidixic acid probably resulted, in part, from the agricultural use of comparable antimicrobial drugs in animals. Over the past 15 years, ceftriaxone resistance among *Salmonella* Dublin isolates from FSIS-PR/HACCP (Pathogen Reduction/Hazard Analysis and Critical Control Point) samples from cattle increased from 0 to 86% (*13*). Davis et al. determined that among *Salmonella* Dublin isolates from cattle, resistance to the third-generation cephalosporin ceftazidime increased over a 5-year period; they suggested that antimicrobial resistance in *Salmonella* Dublin is probably driven by antimicrobial drug use in cattle without influence of antimicrobial drug use in humans (*14*). Berge et al. also observed increasing

resistance to third-generation cephalosporins and fluoroquinolones in calves in California during 1998–2002 (*15*). These findings demonstrate that antimicrobial stewardship and judicious use programs are essential for maintaining the efficacy of drugs used in human and veterinary medicine.

Our data indicate that the incidence of *Salmonella* Dublin infections has increased while the incidence of other *Salmonella* infections has remained mostly stable (Figure 1). The peak in overall *Salmonella* infections that occurred in the mid-1980s was driven by a nationwide outbreak of *Salmonella* Typhimurium (*16*). The simultaneous spike in *Salmonella* Dublin resulted largely from consumption of raw milk (*7,17*), particularly from a large California dairy (*18*). The dairy producer promoted its raw milk as having health benefits (*19*), and many persons with compromised immune systems (e.g., young, elderly, or HIV-positive) became ill (*20*). As a result of a public health investigation (*17*), production and sales were halted, and FDA banned the interstate sale of raw milk in 1987 (*21*). A sharp decline in *Salmonella* Dublin infections soon followed.

Although additional data on food histories and the role of the environment will help elucidate the sources of human infections, the risk for *Salmonella* Dublin infection among humans is probably still caused, in part, by consumption of raw milk and beef. Raw dairy products have been linked to numerous *Salmonella* Dublin illnesses in the United States (*17,22*) and abroad (*23,24*). Incidence of *Salmonella* Dublin infections was 3 times higher in states that allow the sale of raw milk or permit cow shares than in states where raw milk sales are illegal. US surveillance data from PulseNet, the USDA Agricultural Marketing Service (*25*), and FDOSS also indicate that *Salmonella* Dublin has been isolated from ground beef and boneless beef products and has been associated with outbreak-associated illnesses from beef products. *Salmonella* Dublin has also been found in beef cattle and calves (*26,27*).

In our study, the higher proportion of *Salmonella* Dublin infections among men than women may be partially attributable to consumption patterns. Although the 2006–2007 FoodNet Population Survey found no differences by sex for
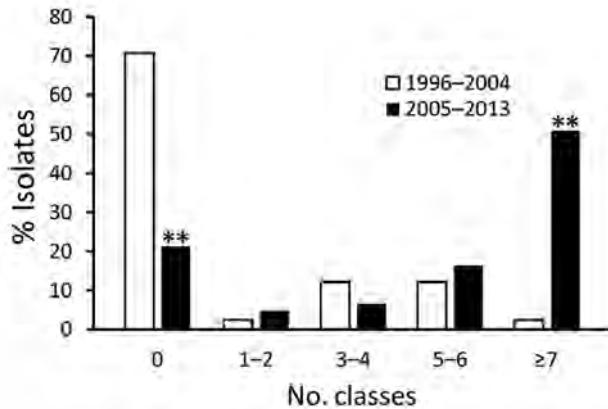
Figure 4. Number of Clinical Laboratory Standards Institute classes of antimicrobial drugs to which *Salmonella enterica* serotype Dublin isolates were resistant, 1996–2004 (n = 41) and 2005–2013 (n = 61). **p<0.01 (significant difference).

consumption of raw milk or cheese items (*28*), numerous studies have found that men consume more beef and more undercooked beef than women (*28,29*). Occupational exposure to cattle may also contribute to the increased frequency of infection among men.

Most *Salmonella* Dublin infections continue to be reported from California (Figure 2), but illnesses have occurred nationwide. They are probably associated with an ongoing outbreak of *Salmonella* Dublin infections among US dairy and beef cattle. A 2014 dairy study conducted by the USDA National Animal Health Monitoring System found antibodies directed against *Salmonella* Dublin lipopolysaccharide O-antigens in 8% of bulk tank milk samples (*30*). Of operations in participating western states (California, Colorado, Idaho, Texas, and Washington), 52% were positive, compared with 2.8% of operations in eastern states (Kentucky, Michigan, Minnesota, Missouri, New York, Ohio, Pennsylvania, Vermont, Virginia, Wisconsin). In 2013, the Animal Health Diagnostic Center at Cornell University (Ithaca, NY, USA) issued an animal health advisory, warning cattle owners about an increase in MDR *Salmonella* Dublin infections among cattle in the northeastern United States, treatment difficulties associated with these infections, the potential for long-term environmental contamination, and the dangers (including death) that these infections pose to animals and humans (*31*).

Changes in the geographic distribution of *Salmonella* Dublin infections in cattle probably explain the similar geographic spread among humans. Historically, *Salmonella* Dublin in cattle was associated with the western United States and was not discovered in cattle east of the Rocky Mountains until 1968 (*32*). *Salmonella* Dublin continued to spread by transport of animals and their products and can now be found in cattle populations throughout the contiguous United States (*26*).

In Denmark, in response to the specific threat to human and animal health posed by *Salmonella* Dublin infections, in 2006, the Danish government passed legislation intended to eradicate this serotype. Their policy actions included heightened surveillance for cattle and abattoirs, voluntary interventions to reduce environmental contamination and disease spread within infected herds, economic sanctions for producers who do not control *Salmonella* Dublin in their herds, and closing of infected herds to live-animal trade (*33,34*). In the United States, precedent for the successful eradication of other host-adapted *Salmonella* serotypes in production animals has been set by use of vaccines and improved management practices. An example is the USDA National Poultry Improvement Plan, which has successfully eradicated *Salmonella* Gallinarum and Pullorum from domestic commercial poultry (*35,36*). Efforts are under way to decrease the burden of *Salmonella* Dublin among cattle. An oral modified-live *Salmonella* Dublin vaccine has been evaluated for use in calves; however, this vaccine has not been effective for reducing the incidence of disease, and research into finding an effective vaccine continues (*37*).

Interventions developed for the Denmark cattle and US poultry industries may not be completely applicable to the US cattle industry because of regulatory and production differences. For example, in Denmark, to control *Salmonella* Dublin infections, trade restrictions are applied to farms with affected herds, and in the United States, biosecurity procedures for poultry producers generally enable tighter environmental control than do those for cattle producers. However, judicious use of antimicrobial drugs in cattle, coupled with improved specific husbandry and management practices on the farm, could decrease antimicrobial-resistant *Salmonella* Dublin infection in cattle. In 2012, FDA prohibited certain extralabel uses of cephalosporins in chickens, turkeys, cattle, and swine (*38*). This new prohibition has the potential to slow the spread of cephalosporin resistance among food animals and is a valuable step toward protecting the effectiveness of current antimicrobial drugs. Nevertheless, other extralabel uses of cephalosporin drugs are still permitted.

Salmonella Dublin is a cattle-adapted *Salmonella* serotype that causes severe and antimicrobial drug–resistant infections in humans and cattle, and its incidence is on the rise. Reducing *Salmonella* Dublin carriage by cattle could benefit animal and human health. Unlike most other *Salmonella* infections in food animals, *Salmonella* Dublin can cause high mortality rates, particularly among calves, and heavy economic burdens for producers (*39*). It is well established that use of antimicrobial agents is a major driving force for the global surge in antimicrobial resistance. Food animal management practices, including veterinary use of antimicrobial drugs, may be contributing to the increasing

resistance in *Salmonella* Dublin and to *Salmonella* Dublin–associated illness and death among humans (*15*). Therefore, careful evaluation of management practices and judicious use of antimicrobial drugs in cattle is critical for the control of antimicrobial drug–resistant *Salmonella* Dublin infections in cattle and humans. The 2016 FDA Veterinary Feed Directive aims to eliminate the use for food production purposes (i.e., growth promotion and feed efficiency) of antimicrobial drugs that are considered medically important in humans and seeks to bring all remaining therapeutic use of antimicrobial agents in feed and water under the oversight of licensed veterinarians (*40*). Agricultural and public health authorities will need to engage in ongoing, meaningful collaborations to reduce inappropriate antimicrobial use in food-producing animals to protect human and animal health.

Dr. Harvey completed this work as an Epidemic Intelligence Service Officer with the Division of Foodborne, Waterborne, and Environmental Diseases, National Center for Emerging and Zoonotic Infectious Diseases, CDC. He is currently an epidemiologist with the CDC National Institute for Occupational Safety and Health in Morgantown, WV. His research interest is work-related lung disease in manufacturing industries.
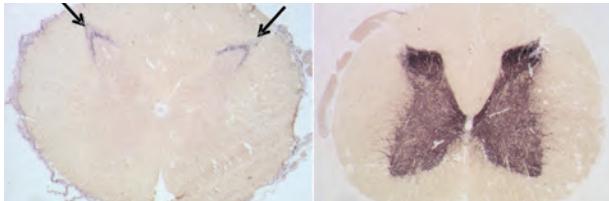
References

1. Scallan E, Hoekstra RM, Angulo FJ, Tauxe RV, Widdowson MA, Roy SL, et al. Foodborne illness acquired in the United States—major pathogens. Emerg Infect Dis. 2011;17:7–15. http://dx.doi.org/10.3201/eid1701.P11101
2. Su LH, Chiu CH. *Salmonella*: clinical importance and evolution of nomenclature. Chang Gung Med J. 2007;30:210–9.
3. Solghan SM, Dumas NB, Root TP, Quinlan TM, Armstrong LR, Spina NL, et al. Multidrug-resistant nontyphoidal *Salmonella* in New York state's Foodborne Diseases Active Surveillance Network counties. Foodborne Pathog Dis. 2010;7:167–73. http://dx.doi.org/10.1089/fpd.2009.0329
4. Mølbak K. Human health consequences of antimicrobial drug-resistant *Salmonella* and other foodborne pathogens. Clin Infect Dis. 2005;41:1613–20. http://dx.doi.org/10.1086/497599
5. Centers for Disease Control and Prevention. National Antimicrobial Resistance Monitoring System for Enteric Bacteria (NARMS): human isolates final report, 2013. Atlanta: The Centers; 2015.
6. Wray C, Sojka WJ. Reviews of the progress of dairy science: bovine salmonellosis. J Dairy Res. 1977;44:383–425. http://dx.doi.org/10.1017/S0022029900020355
7. Taylor DN, Bied JM, Munro JS, Feldman RA. *Salmonella* Dublin infections in the United States, 1979–1980. J Infect Dis. 1982;146:322–7. http://dx.doi.org/10.1093/infdis/146.3.322
8. Folster JP, Pecic G, Singh A, Duval B, Rickert R, Ayers S, et al. Characterization of extended-spectrum cephalosporin-resistant *Salmonella enterica* serovar Heidelberg isolated from food animals, retail meat, and humans in the United States 2009. Foodborne Pathog Dis. 2012;9:638–45. http://dx.doi.org/10.1089/fpd.2012.1130
9. Mungai EA, Behravesh CB, Gould LH. Increased outbreaks associated with nonpasteurized milk, United States, 2007–2012. Emerg Infect Dis. 2015;21:119–22. http://dx.doi.org/10.3201/eid2101.140447
10. Blaser MJ, Feldman RA. Bacteremia: reports to the Centers for Disease Control, 1968–1979. J Infect Dis. 1981;143:743–6. http://dx.doi.org/10.1093/infdis/143.5.743

11. Fang FC, Fierer J. Human infection with *Salmonella* Dublin. Medicine (Baltimore). 1991;70:198–207. http://dx.doi.org/10.1097/00005792-199105000-00004
12. Olsen JE, Baggesen DL, Nielsen BB, Larsen HE. The prevalence of plasmids in Danish bovine and human isolates of *Salmonella* Dublin. APMIS. 1990;98:735–40. http://dx.doi.org/10.1111/j.1699-0463.1990.tb04994.x
13. Food and Drug Administration. The 2012–2013 integrated NARMS report. Silver Spring (MD): The Administration; 2015.
14. Davis MA, Hancock DD, Besser TE, Daniels JB, Baker KN, Call DR. Antimicrobial resistance in *Salmonella enterica* serovar *Salmonella* Dublin isolates from beef and dairy sources. Vet Microbiol. 2007;119:221–30. http://dx.doi.org/10.1016/j.vetmic.2006.08.028
15. Berge AC, Thornburg E, Adaska JM, Moeller RB, Blanchard PC. Antimicrobial resistance in *Salmonella enterica* subspecies *enterica* serovar *Salmonella* Dublin from dairy source calves in the central San Joaquin Valley, California (1998–2002). J Vet Diagn Invest. 2008;20:497–500. http://dx.doi.org/10.1177/104063870802000414
16. Ryan CA, Nickels MK, Hargrett-Bean NT, Potter ME, Endo T, Mayer L, et al. Massive outbreak of antimicrobial-resistant salmonellosis traced to pasteurized milk. JAMA. 1987;258:3269–74. http://dx.doi.org/10.1001/jama.1987.03400220069039
17. Centers for Disease Control. *Salmonella Dublin* and raw milk consumption—California. MMWR Morb Mortal Wkly Rep. 1984;33:196–8.
18. Richwald GA, Greenland S, Johnson BJ, Friedland JM, Goldstein EJ, Plichta DT. Assessment of the excess risk of *Salmonella* Dublin infection associated with the use of certified raw milk. Public Health Rep. 1988;103:489–93.
19. Consumers Union of U.S., Inc. v. Alta-Dena Certified Dairy. 4 Cal App 4th 963: Court of Appeals of California, First District, Division Two; 1992.
20. Stevens A. Safety of raw milk at issue in lawsuit filed against dairy. Los Angeles Times. December 5, 1988.
21. Food and Drug Administration. Mandatory pasteurization for all milk and milk products in final package form intended for direct human consumption. 21CFR124061. Rockville (MD): The Administration; 1987.
22. Werner SB, Humphrey GL, Kamei I. Association between raw milk and human *Salmonella dublin* infection. BMJ. 1979;2:238–41. http://dx.doi.org/10.1136/bmj.2.6184.238
23. Ung A, Vignaud ML, Morand A, Donguy MP, Van Cauteren D, Lucas E, et al. Nationwide *Salmonella* Dublin outbreak associated with raw-milk cheese consumption, France 2015–2016: results from a case-case study. International Symposium *Salmonella* and Salmonellosis; June 6–8, 2016; Saint-Malo, France.
24. Vignaud ML, Marault M, Chaing E, Bachellerie P, Le Hello S, Michel Valérie, et al. MLVA for the subtyping of *Salmonella enterica* subsp. *enterica* serotype Dublin: report of France raw milk cheese outbreak in 2012. International Symposium *Salmonella* and Salmonellosis. June 6–8, 2016; Saint-Malo, France.
25. Doerscher DR, Lutz TL, Whisenant SJ, Smith KR, Morris CA, Schroeder CM. Microbiological testing results of boneless and ground beef purchased for the national school lunch program, 2011 to 2014. J Food Prot. 2015;78:1656–63. http://dx.doi.org/10.4315/0362-028X.JFP-15-101
26. McDonough PL, Fogelman D, Shin SJ, Brunner MA, Lein DH. *Salmonella enterica* serotype *Salmonella* Dublin infection: an emerging infectious disease for the northeastern United States. J Clin Microbiol. 1999;37:2418–27.
27. McGuirk SM, Peek, S. Salmonellosis in cattle: a review. American Association of Bovine Practitioners 36th Annual Conference. Sep 15–17, 2003; Columbus, Ohio [cited 2016 Nov 20]. http://www.vetmed.wisc.edu/dms/fapm/fapmtools/7health/Salmorev.pdf

28. Shiferaw B, Verrill L, Booth H, Zansky SM, Norton DM, Crim S, et al. Sex-based differences in food consumption: Foodborne Diseases Active Surveillance Network (FoodNet) population survey, 2006–2007. Clin Infect Dis. 2012;54(Suppl 5):S453–7. http://dx.doi.org/10.1093/cid/cis247

29. Daniel CR, Cross AJ, Koebnick C, Sinha R. Trends in meat consumption in the USA. Public Health Nutr. 2011;14:575–83. http://dx.doi.org/10.1017/S1368980010002077

30. Lombard JE, Thompson BS, Virkler PD, Wagner B, Kristensen C, Fossler C, et al. *Salmonella* Dublin antibodies in bulk-tank milk on U.S. dairy operations. Joint Annual Meeting of the American Society of Animal Science and the American Dairy Science Association. Jul 12–16, 2015; Orlando, Florida.

31. Cornell University. Animal health advisory: multi-drug resistant *Salmonella Dublin* in cattle. Ithaca (NY): The University; 2013.

32. Blackburn BO, Sutch K, Harrington R Jr. The changing distribution of *Salmonella dublin* in the United States. Proc Annu Meet U S Anim Health Assoc. 1980;84:445–51.

33. Nielsen LR. National strategies of *Salmonella* control in cattle and beef in Denmark. 10th International Symposium on Veterinary Epidemiology and Economics. Nov 17–21, 2003; Vina del Mar, Chile; 2003.

34. Nielsen LR, Nielsen SS. A structured approach to control of *Salmonella* Dublin in 10 Danish dairy herds based on risk scoring and test-and-manage procedures. Food Research International. 2011;45:1158–65.

35. US Department of Agriculture, Animal and Plant Health Inspection Service. National poultry improvement plan [cited 2016 Feb 29]. http://www.poultryimprovement.org

36. Hitchner SB. History of biological control of poultry diseases in the USA. Avian Dis. 2004;48:1–8. http://dx.doi.org/10.1637/6100

37. Habing GG, Neuder LM, Raphael W, Piper-Youngs H, Kaneene JB. Efficacy of oral administration of a modified-live *Salmonella* Dublin vaccine in calves. J Am Vet Med Assoc. 2011;238:1184–90. http://dx.doi.org/10.2460/javma.238.9.1184

38. Food and Drug Administration. New animal drugs; cephalosporin drugs; extralabel animal drug use; order of prohibition. Federal Register; 2012. 77 FR 735. p. 735–45. Codified at 21 C.F.R. Sect 530.

39. Peters AR. An estimation of the economic impact of an outbreak of *Salmonella dublin* in a calf rearing unit. Vet Rec. 1985;117:667–8. http://dx.doi.org/10.1136/vr.117.25-26.667

40. Food and Drug Administration. Fact sheet: veterinary feed directive final rule and next steps [cited 2017 Jun 16]. https://www.fda.gov/animalveterinary/developmentapprovalprocess/ucm449019.htm

Address for correspondence: Allison C. Brown, Centers for Disease Control and Prevention, 1600 Clifton Rd NE, Mailstop C16, Atlanta, GA 30329-4027; email: iyk6@cdc.gov

May 2013: **Zoonoses**

EMERGING INFECTIOUS DISEASES

https://wwwnc.cdc.gov/eid/articles/issue/19/5/table-of-contents

Prevalence of *Yersinia enterocolitica* Bioserotype 3/O:3 among Children with Diarrhea, China, 2010–2015

Ran Duan,[1] Junrong Liang,[1] Jing Zhang,[1] Yuhuang Chen,[1] Jing Wang, Jing Tong, Bangcheng Guo, Wanfu Hu, Mingliu Wang, Jiayong Zhao, Chang Liu, Huijing Hao, Xin Wang, Huaiqi Jing

Yersinia enterocolitica is thought to not significantly contribute to diarrheal disease in China, but evidence substantiating this claim is limited. We determined the prevalence of *Y. enterocolitica* infection and strain types present among children ≤5 years of age with diarrhea in China. The overall prevalence of pathogenic isolates was 0.59%. Prevalence of pathogenic bioserotype 3/O:3 varied geographically. In this population, the presence of fecal leukocytes was a characteristic of *Y. enterocolitica* infection and should be used as an indication for microbiological diagnostic testing, rather than for the diagnosis of bacillary dysentery. In contrast with *Y. enterocolitica* isolates from adults, which were primarily biotype 1A, isolates from children were primarily bioserotype 3/O:3. Most pathogenic isolates from children shared pulsed-field gel electrophoresis patterns with isolates from pigs and dogs, suggesting a possible link between isolates from animals and infections in children. Our findings underscore the need for improved diagnostics for this underestimated pathogen.

Yersinia enterocolitica is an emerging infectious pathogen that has caused wide public health concern since the 1980s. After campylobacteriosis and salmonellosis, yersiniosis ranks third most common among the notifiable bacterial zoonoses in the European Union (*1,2*). The incidence of human yersiniosis was 1.92 cases/100,000 population in 2013 in Europe (*3*); in the United States, incidence decreased from 1.0 cases/100,000 population in 1996 to 0.3 cases/100,000 population in 2009 (*4*). Gastroenteritis and enteritis are among the most common clinical signs. Autoimmune complications such as reactive arthritis sometimes occur (*2,5*). Deadly hemorrhagic septicemic yersiniosis occurs in immune-compromised patients. Strains of *Y. enterocolitica* biotype 1A (1 of the 6 biotypes) lack the pYV plasmid and the major chromosomal determinants of virulence and, thus, have been regarded as avirulent (*2*). However, this avirulent biotype has also been implicated in foodborne and nosocomial outbreaks and has reportedly produced disease symptoms indistinguishable from those produced by the known pathogenic biotypes (*6–8*).

In most countries in Europe, the bioserotype 4/O:3 accounts for ≈80% of human infections; 4/O:3 is also dominant in North America, where 3/O:3 infection is rarely reported (*9*). Conversely, 3/O:3 is the most prevalent bioserotype in China (*10–15*). Studies have shown that the prevalence of pathogenic strains among pigs in China is higher than that in countries of Europe (*15,16*). However, except for 2 outbreaks reported in the 1980s (*10*), we have little data concerning human infections in China. Because yersiniosis is not notifiable through the national surveillance systems in China, most hospitals do not routinely tested for *Y. enterocolitica*. In China, infectious diarrhea is primarily diagnosed on the basis of clinical examination rather than microbiological diagnostic testing (except for rotavirus, norovirus, and a few types of bacteria in some large hospitals). For example, shigellosis is often diagnosed in persons with signs such as tenesmus after leukocytes are found in their fecal samples. These diagnostic criteria render *Shigella*, *Salmonella*, enteroinvasive *Escherichia coli*, *Campylobacter*, and *Y. enterocolitca* infections indistinguishable.

According to surveys around the world, most *Yersinia* infections have occurred in infants and young children (*17,18*). In the United States, ≈100,000 episodes

Author affiliations: State Key Laboratory of Infectious Disease Prevention and Control, National Institute for Communicable Disease Control and Prevention, Chinese Center for Disease Control and Prevention, Beijing, China (R. Duan, J. Liang, J. Zhang, Y. Chen, C. Liu, H. Hao, X. Wang, H. Jing); Dongcheng Centre for Disease Control and Prevention, Beijing (J. Wang); Xuzhou Municipal Centre for Disease Control and Prevention, Xuzhou, China (J. Tong); Ningxia Hui Autonomous Region Center for Disease Control and Prevention, Yinchuan, China (B. Guo); Anhui Provincial Center for Disease Control and Prevention, Hefei, China (W. Hu); Guangxi Zhuang Autonomous Region Center for Disease Control and Prevention, Nanning, China (M. Wang); Henan Provincial Centre for Disease Control and Prevention, Zhengzhou, China (J. Zhao)

[1]These authors contributed equally to this article.

of foodborne illness caused by *Y. enterocolitica* occur annually, and risk for disease is higher among infants (*4,19*). In Germany, the average annual incidence of *Y. enterocolitica* infection among children <5 years of age was ≈12-fold higher than the average incidence among persons ≥5 years of age (*3,20*). Thus, in 10 regions of China, we performed microbiological diagnostic tests for children ≤5 years of age with diarrhea to determine the prevalence of *Y. enterocolitica* infection in this population and the need for improved diagnosis of yersiniosis. We also investigated possible links between strains from animals and humans.

Methods

Population Design and Collection of Case Information and Samples
During 2010–2015, we invited all patients with diarrhea from 17 hospitals to participate in this study. Diarrhea was defined according to the Global Enteric Multicenter Study: ≥3 loose stools within the previous 24 h (*21*). The study participants provided informed consent, fecal samples, and completed questionnaires. We followed the same protocol for all cases and excluded cases if either sample or questionnaire was lost.

Sampling from Children
We recruited children ≤5 years of age with diarrhea at sentinel pediatric hospitals in different parts of China: Henan in central China; Beijing and Tianjin in northern China; Jiangsu, Shandong, and Anhui in eastern China; Guangxi in southern China; Sichuan and Yunnan in southwestern China; and Ningxia in northwestern China. Within each region, we gave primary hospitals (such as community hospitals in cities and village clinics in the countryside) the opportunity to become sentinel sites for this study. The staff of sentinel hospitals were capable of collecting case information and specimens and taking into account patients' environment, folk customs, and eating habits during treatment. The same procedures were performed at each site to avoid bias in sampling procedures and in storing and handling samples. In some village clinics, fecal microscopy could not be conducted.

To compare the *Y. enterocolitica* prevalence between children and adults, we collected samples from 2 sites in central Beijing. We recruited adults from a general hospital and children from a pediatric hospital 5 km away that was also 1 of the sentinel hospitals for this study.

Questionnaire
The questionnaire included questions about demographics (name, sex, birth date, address, and contact information) and clinical features (date of onset, date of visiting doctor,

diarrhea frequency, body temperature, vomiting, fecal characteristics, and results of routine fecal sample inspection). Fecal samples were routinely examined for the presence of leukocytes and erythrocytes. Doctors wrote the primary diagnosis on the patient's questionnaire.

Sample Collection
Fresh fecal samples were collected from patients after enrollment in the study. Fecal samples were stored in peptone sorbitol bile broth (Fluka, Everett, WA, USA) at 4°C.

Y. enterocolitica Isolation and Identification
During the study, we conducted 2 technical trainings for sentinel hospital staff on *Y. enterocolitica* isolation and identification. *Y. enterocolitica* was isolated from samples by following the procedures described previously (*15*). To ensure laboratory capacity, we sent for assessment samples to the sentinel hospital staff who were blinded to sample identity. Hospital staff enriched the strains in peptone sorbitol bile broth at 4°C for 21 d and then amplified 2 *Y. enterocolitica* genes: *foxA* (conserved) and *ail* (pathogenic) (*22*). Samples positive for either or both of these genes were inoculated onto Yersinia Selective Agar (Schiemann's CIN [Cefsulodin, Irgasan, Novobiocin] agar; Oxoid, Basingstoke, UK). To obtain pure cultures, staff then inoculated the presumptive *Y. enterocolitica* colonies having a typical bull's-eye appearance on CIN agar onto brain–heart infusion agar plates and incubated them at 25°C for 24 h (*10*). Hospital staff performed the biochemical test Analytical Profile Index (API) 20E (bioMérieux, Marcy l'Etoile, France) and bioserotype identification methods reviewed by Wang et al. with all isolates (*13*). The Wauters' biotype method was used (*23*).

Identification of Pathogenic Strains and Cluster Analysis
We amplified virulence genes (*ail*, *ystA*, *ystB*, *virF*, and *yadA*) from the chromosomes and plasmids for all *Y. enterocolitica* isolates. We used the PCR method, including primer sequences and annealing temperatures, described by Liang et al. (*15*).

For the analysis of identified pathogenic isolates, we used the pulsed-field gel electrophoresis (PFGE) method described by Wang et al., with the following modifications: the DNA samples were digested with 25 U *Not*I and electrophoresed with pulse times from 2 to 20 s over 18 h at 200 V (*13*). For data analysis, we imported the images of gels into the PFGE database of *Y. enterocolitica* strains from China and performed a cluster analysis for the serotypes O:3 and O:9. The clustering of band patterns was performed by using BioNumerics software version 5.1 (http://www.applied-maths.com/bionumerics) and the Pearson algorithm. We visually inspected all patterns after computer analysis. For patterns that were indistinguishable by computer and visual inspection, we assigned a pattern designation.

Results

Characteristics of Pathogenic *Y. enterocolitica* Infection among Children

Prevalence and Demographics

We recruited a total of 7,304 patients ≤5 years of age with diarrhea from 10 regions of China. Fecal samples and answered questionnaires were collected for each patient, but 18 were excluded because either sample or questionnaire was lost. In total, we found 43 patients with pathogenic *Y. enterocolitica* infection. The average prevalence of *Y. enterocolitica* disease in all 10 regions was 0.59% (43/7,304); prevalence was highest in Anhui Province (2.29%, 3/131). *Y. enterocolitica* prevalence among young children with diarrhea was generally classified into 3 levels: 0.01%–0.50% (Shandong, Ningxia, and Henan); 0.51%–1.00% (Beijing, Guangxi, Tianjin, and Jiangsu); and 1.01%–2.29% (Anhui, Yunnan, and Sichuan) (Figure 1). Through year-round collection, we found that cases of pathogenic *Y. enterocolitica* infection occurred during January–November. The prevalence calculated for southern China (0.80%) was slightly higher than that for northern China (0.53%), when the northern and southern regions were defined by the Huaihe River, the natural border. Cases occurred more often in boys than in girls (1.63:1) (Figure 2). We found the largest proportion of *Y. enterocolitca* infections among children >0.5–2 years of age; among children in this age group, more cases also occurred in boys than in girls (1.45:1).

Fecal Characteristics

Fecal samples from children ≤5 years of age infected with pathogenic *Y. enterocolitica* had the following characteristics: mucous (37%), watery (30%), pasty (22%), and loose (4%) (Figure 3, panel A). Fecal microscopy was performed with fecal samples from all children; leukocytes were detected in samples from 85% (23/27) of children ≤5 years of age with diarrhea. A higher proportion of the fecal samples from those in the >0.5–2 years age group had leukocyte counts ≥15 cells/high-power field (HPF). Fecal leukocyte counts were >30 cells/HPF only among patients in this age group, and in 2 cases the concentration reached as high as 45 cells/HPF and 84 cells/HPF.

Bioserotypes of Isolates from Patients with Acute Diarrhea and Prolonged Shedding

The predominant cause of acute *Yersinia* infection among children ≤5 years of age was bioserotype 3/O:3 (Table); 41 of 43 patients were infected with this bioserotype. The other 2 patients were infected with 4/O:3 or 2/O:9, both found in Beijing. Except for one 3/O:3 infection, all isolates harbored the *Yersinia* virulence plasmid and virulence genes *ail*, *ystA*, *virF*, and *yadA*. In addition to the acute diarrhea cases, 3 cases from different regions involved prolonged *Y. enterocolitica* 3/O:3 shedding that had progressed from acute diarrhea. These patients were 1–1.5 years of age. Once pathogen shedding stopped, the diarrhea ceased as well. The period of shedding could be as long as ≈3 months.

Difference in *Y. enterocolitica* Prevalence between Children and Adults

A total of 2,127 children and 1,904 adults with diarrhea were enrolled at the Beijing sites. Pathogenic *Y. enterocolitica* infection accounted for 0.61% (13/2,127) of the children and 0.11% (2/1,904) of the adults tested. One child and 1 adult had 2/O:9 *Y. enterocolitica* infections; the other 13 patients had 3/O:3 infections. Leukocytes were detected in the fecal samples of all 13 children and 1 of the 2 adults.
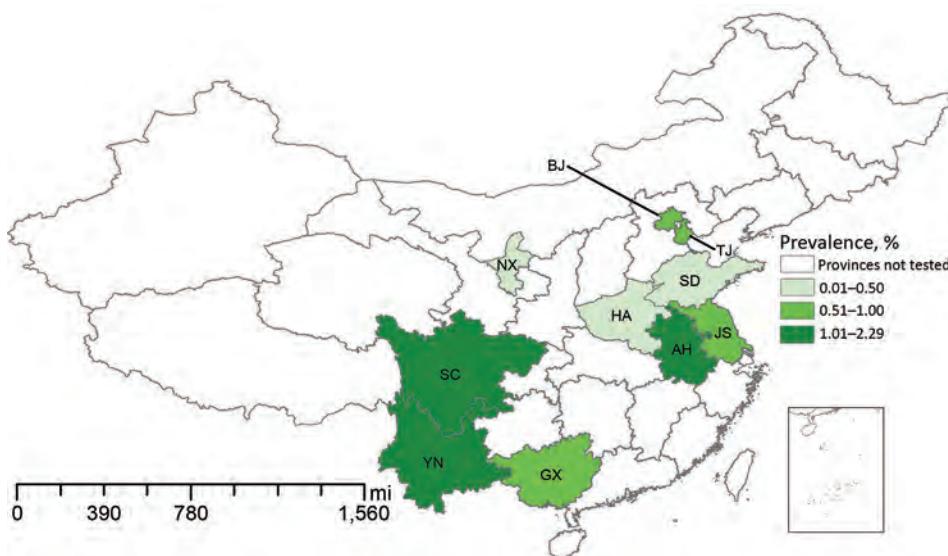
Figure 1. Prevalence of pathogenic *Yersinia enterocolitica* infection among children ≤5 years of age with diarrhea, by region, China, 2010–2015. Inset shows the islands of China in the South China Sea. AH, Anhui; BJ, Beijing; GX, Guangxi; HA, Henan; JS, Jiangsu; NX, Ningxia; SC, Sichuan; SD, Shandong; TJ, Tianjin; YN, Yunnan.

The overall prevalence of *Y. enterocolitica* biotype 1A was 0.28% among children (6/2,127) and 1.52% among adults (29/1,904) (Figure 4). Among the 35 patients with biotype 1A infections, we found leukocytes in the fecal samples of 33% (2/6) of children and 31% (9/29) of adults. Regardless of whether the samples had leukocytes or not, all isolates (6/6) from children and most isolates (20/29) from adults carried the *ystB* gene.

PFGE Analysis of Pathogenic *Y. enterocolitica* Isolates from Children and Animals

PFGE patterns for most of the pathogenic isolates from children (36/43, 84%), including the one 2/O:9 isolate, were indistinguishable from those of isolates from pigs and dogs (data not shown). The rest of the isolates (7/43), including the one 4/O:3 isolate, did not share a pattern with any bacteria isolates from these animals. Isolates from children, pigs, and dogs displayed many patterns, and some patterns appeared in bacteria isolated from multiple hosts in >1 region. We found the predominant patterns K6GN11C30021 and K6GN11C30012 of the 3/O:3 bioserotype (shared by isolates from children, pigs, and dogs) in 67% (24/36) of isolates from children. Among the 10 regions, we found 83% (30/36) of the isolates had patterns indistinguishable from isolates from local pigs and dogs (online Technical Appendix Figure 1, https://wwwnc.cdc.gov/EID/article/23/9/16-0827-Techapp1.pdf). The rest of the isolates (6/36) shared patterns with those from pigs from other regions (online Technical Appendix Figure 2).

Discussion

Y. enterocolitica is a zoonotic pathogen widely distributed throughout China. However, yersiniosis, predominantly a diarrheal illness, is not notifiable through the national surveillance systems of China. Our large-scale investigation of *Y. enterocolitica* infection among children ≤5 years of age with diarrhea in China found *Y. enterocolitica* bioserotype 3/O:3 is a major pathogen (prevalence 0.56%; 41/7,304). According to reports in various years from Finland, Canada, Chile, Holland,
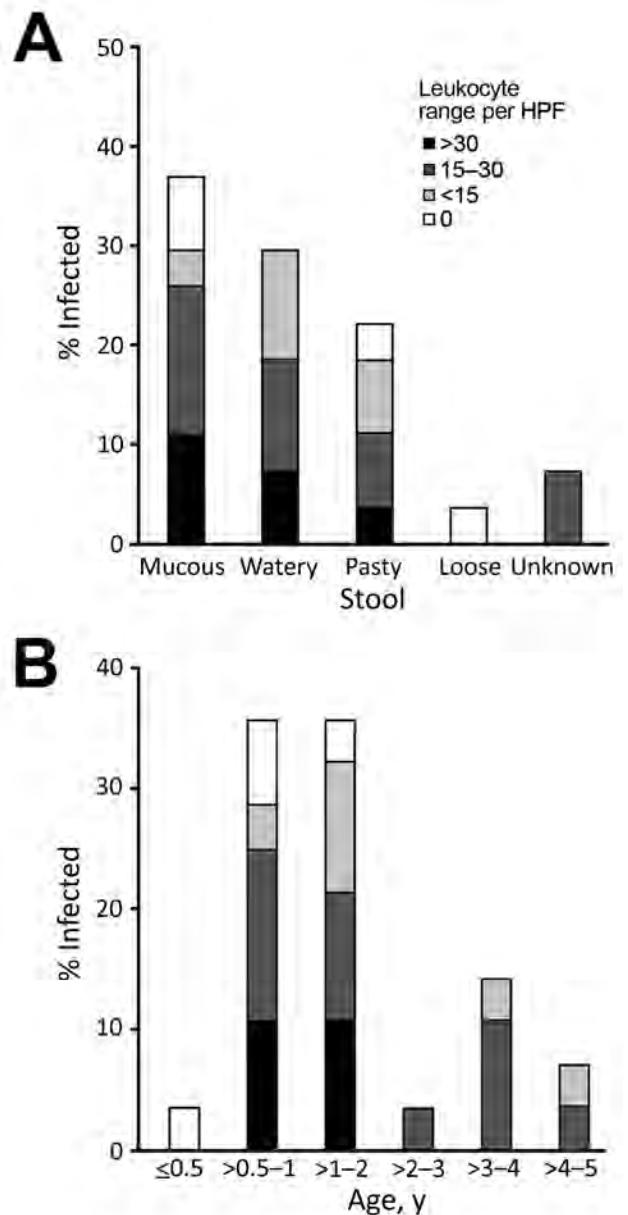
Figure 3. Fecal leukocyte ranges among children ≤5 years of age infected with pathogenic *Yersinia enterocolitica*, by fecal characteristics (A) and age (B), China, 2010–2015. HPF, high-power field.

Figure 2. Percentage infected with pathogenic *Yersinia enterocolitica*, by age and sex, of total infected with *Y. enterocolitica*, China, 2010–2015.

Table. Bioserotype and virulence genes of pathogenic *Yersinia enterocolitica* isolates from children ≤5 years of age with diarrhea, China, 2010–2015

Bioserotype	No. cases	*ail*	*ystA*	*ystB*	*yadA*	*virF*
3/O:3	40	+	+	−	+	+
	1	+	+	−	−	−
4/O:3	1	+	+	−	+	+
2/O:9	1	+	+	−	+	+

Italy, New Zealand, and the United States, the prevalence of *Y. enterocolitica* among patients with diarrhea was ≈0.6%–2.9% (*24–28*).

Most hospitals in China do not routinely test for *Y. enterocolitica*; diagnosis of diarrhea is mainly based on signs, symptoms, and fecal microscopy results. We found that a predominant characteristic of feces from young children with *Y. enterocolitica* infection was the presence of leukocytes (Figure 4), which were detectable despite the consistency of the fecal samples (Figure 3, panel A). However, the presence of fecal leukocytes is often regarded as a diagnostic feature of bacillary dysentery, a term that is used interchangeably with shigellosis, and consequently diagnosed as such, leading to confusion over which pathogen is the causative agent (*Shigella*, *Salmonella*, enteroinvasive *Escherichia coli*, *Campylobacter*, or *Yersinia*) (*29*). A decade (2004–2013) of surveillance in Beijing indicates that bacillary dysentery consistently ranked as the infectious disease of the highest incidence, except for a second place ranking in 2013, in which bacillary dysentery was 3–6-fold the national average incidence (*29*). The primary reason for the overdiagnosis of shigellosis has been the lack of microbiological diagnostic testing. In this study, according to the primary diagnoses listed on the questionnaires, quite a few cases among children were regarded as shigellosis. Conversely, diarrhea cases without fecal leukocytes tended not to be diagnosed as infectious diarrhea, which delayed administration of the correct and best treatments.

A limitation of our study was that fecal microscopy could not be conducted in some village clinics. Whether these children without fecal microscopy results were overlooked requires further investigation.

In countries where clinical signs guide diagnosis, a case of diarrhea with persistent abdominal pain and fever would prompt culture for *Y. enterocolitica* and cold enrichment (*30*). Using microbiological diagnostic techniques, we found that the prevalence of pathogenic *Y. enterocolitica* among children ≤5 years of age with diarrhea (0.61%) surpassed that of *Shigella* species in some regions (0.14%; data not shown).

Reports from some countries have shown the prevalence of pathogenic *Y. enterocolitica* infection among children to be higher and the prevalence of nonpathogenic strains to be lower than that among adults (*31*), which is consistent with our study. In Beijing, the prevalence

of pathogenic *Y. enterocolitica* among children ≤5 years of age with diarrhea was ≈6-fold higher than that among adults with diarrhea, and the prevalence of infection with biotype 1A was the reverse (≈6-fold higher among adults than among children ≤5 years of age with diarrhea). Besides other possible explanations, such as incidental infection or acquired immunity, misuse of antimicrobial drugs by adults might play a substantial role in limiting infection with pathogenic strains among adults in China; isolation of pathogenic strains from adult patients is generally difficult. However, a typical family in China would not readily administer antimicrobial drugs to young children. In this study, primary hospitals given the opportunity to be sentinel sites for *Y. enterocolitica* isolation were instructed to avoid giving patients antimicrobial drugs before enrollment as much as possible.

Biotype 1A is a *Y. enterocolitica* strain widely distributed throughout the natural environment that serves as a source of infection and food contamination (*32*). The diets of adults are not as restricted as that of children, which potentially explains why a higher percentage of adults have diarrhea attributable to biotype 1A. Biotype 1A isolates have generally been regarded as avirulent, but some isolates harboring genes such as *ystB*, which encodes a heat-stable enterotoxin, have been implicated in foodborne and nosocomial outbreaks (*6–8*). In this study, *ystB* was present in most biotype 1A isolates found from adults, suggesting possible pathogenicity of these isolates as well.

This study had another limitation. The diagnostics protocol included a cold enrichment step, which made identifying nonpathogenic strains and inapparent infections more likely and diagnosis more time-consuming (*33*). Consequently, early treatment decisions could not be guided by our diagnostic test results. However, cold enrichment did improve overall recovery of *Y. enterocolitica*, especially when the bacteria density of the fecal
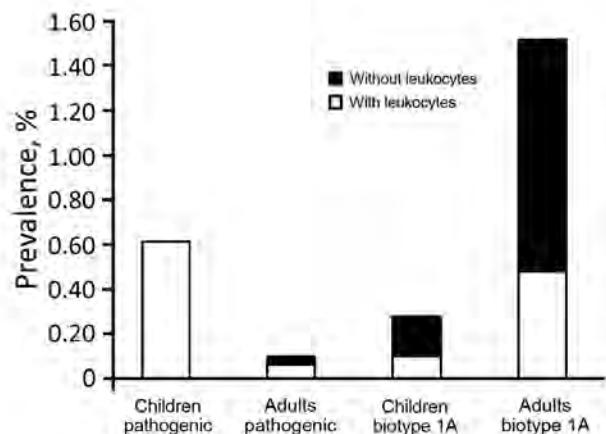
Figure 4. Prevalence of pathogenic and biotype 1A *Yersinia enterocolitica* infection among children ≤5 years of age and adults with diarrhea, by leukocyte positivity, Beijing, China, 2010–2015.

sample was low, such as during the convalescent phase or long-term shedding. Diarrhea is often considered to be mild and self-limiting in patients with *Y. enterocolitica* infection (*5*), but we found 3 cases of long-term bacterial shedding of *Y. enterocolitica* 3/O:3 among children. Low acquired immunity among children might be a possible explanation, and a timely and accurate diagnosis is greatly needed to prevent these types of cases from occurring. Although cold enrichment has its limitations, we included it in the protocol to more accurately and completely diagnose *Y. enterocolitica* infection in the study population. This method has been used in multiple surveillance studies around the world (*12,13,34–36*).

Generally, only a subset of bioserotypes are pathogenic, mainly 1B/O:8; 4/O:3; 2/O:5,27; 2/O:9; and 3/O:3 (mostly found in China). In recent decades in most countries and regions, the pathogenic bioserotypes of highest prevalence and incidence shifted from strain 1B/O:8 to 4/O:3. In China, the shift was from 2/O:9 to 3/O:3; as of July 2017, the 1B/O:8 strain has not been detected yet in China. Strain 4/O:3, having limited PFGE pattern diversity and high similarity with reference strains abroad (data not shown), has rarely been isolated in China. Only a single 4/O:3 isolate was found in this study, even though this strain is the predominant bioserotype found in other parts of the world. Whether this strain was acquired domestically or from travelers to China is not known. According to our previous research (*37*), the susceptibilities of strains 3/O:3 and 4/O:3 to O:3-specific phage are similar; thus, O:3-specific phage susceptibility cannot explain the rarity of 4/O:3 in China, but susceptibility to 4/O:3-specific phage might.

When comparing pathogenic isolates from different sources, isolates from children shared PFGE patterns with isolates from local pigs and dogs, suggesting a link between isolates from animals and human infection. Pigs have been shown to be a source of *Y. enterocolitica* infection (*20,38–41*). In correlation studies in Belgium and Norway, human infections have been associated with ingestion of raw or undercooked pork (*38,39*). In Germany, the state with the highest consumption of meat showed the highest incidence of yersiniosis (*20*). The prevalence of pathogenic *Y. enterocolitica* was even higher in China than in Europe, potentially because the population of China is a big consumer of pork (*15*). However, persons in China seldom eat undercooked pork; a more likely route of transmission is cross-contamination (*12*). Lee et al. described cases in which *Yersinia* seemed to have been transferred from raw tripe to infants on the unwashed hands of caregivers (*42*). Whether transmission is aided by transportation of pork products between regions needs further investigation. Pigs from multiple regions are slaughtered in Beijing, the location where we found the highest number of isolates from children with PFGE patterns indistinguishable from isolates from pigs. Researchers in Japan reported isolation of *Y. enterocolitica* of different bioserotypes from imported meat products (i.e., pork, beef, and chicken) from Europe, the United States, and other regions of Asia (*43*). PFGE patterns of some isolates from children in our study were not indistinguishable from those from animals, perhaps because our surveillance of isolates from animals is not complete.

The results of this nationwide investigation in China emphasize that *Y. enterocolitica* bioserotype 3/O:3 is a prominent pathogen of children ≤5 years of age with diarrhea and that microbiological diagnostic testing should be considered for patients who have leukocytes in their feces. Children might acquire infection from contaminated food, and to establish an epidemiologic link between the illness and the consumption of or contact with pork, a case–control study comparing exposures of ill and healthy children is needed. Geographic or seasonal differences in prevalence should also be examined in the future. Our team will continue its surveillance of *Y. enterocolitica* infection among children with diarrhea. We suggest that hospitals routinely test for *Y. enterocolitica* and report laboratory-confirmed cases to public health authorities.

Dr. Duan is a research assistant at the National Institute for Communicable Disease Control and Prevention, Chinese Center for Disease Control and Prevention. Her primary research interests relate to the pathology of pathogenic *Yersinia*.

References

1. Trček J, Fuchs TM, Trülzsch K. Analysis of *Yersinia enterocolitica* invasin expression *in vitro* and in *vivo* using a novel *luxCDABE* reporter system. Microbiology. 2010;156:2734–45. http://dx.doi.org/10.1099/mic.0.038240-0
2. Bottone EJ. *Yersinia enterocolitica*: the charisma continues. Clin Microbiol Rev. 1997;10:257–76.
3. European Food Safety Authority; European Centre for Disease Prevention and Control. The European Union summary report on trends and sources of zoonoses, zoonotic agents and food-borne outbreaks in 2013. EFSA J. 2015;13:3991. http://dx.doi.org/10.2903/j.efsa.2015.3991
4. Ong KL, Gould LH, Chen DL, Jones TF, Scheftel J, Webb TH, et al. Changing epidemiology of *Yersinia enterocolitica* infections: markedly decreased rates in young black children, Foodborne Diseases Active Surveillance Network (FoodNet), 1996–2009. Clin Infect Dis. 2012;54(Suppl 5):S385–90. http://dx.doi.org/10.1093/cid/cis053

5. Cover TL, Aber RC. *Yersinia enterocolitica*. N Engl J Med. 1989;321:16–24. http://dx.doi.org/10.1056/NEJM198907063210104

6. Singh I, Virdi JS. Production of *Yersinia* stable toxin (YST) and distribution of *yst* genes in biotype 1A strains of *Yersinia enterocolitica*. J Med Microbiol. 2004;53:1065–8. http://dx.doi.org/10.1099/jmm.0.45527-0

7. Burnens AP, Frey A, Nicolet J. Association between clinical presentation, biogroups and virulence attributes of *Yersinia enterocolitica* strains in human diarrhoeal disease. Epidemiol Infect. 1996;116:27–34. http://dx.doi.org/10.1017/S0950268800058921

8. Bhagat N, Virdi JS. The enigma of *Yersinia enterocolitica* biovar 1A. Crit Rev Microbiol. 2011;37:25–39. http://dx.doi.org/10.3109/1040841X.2010.506429

9. Valentin-Weigand P, Heesemann J, Dersch P. Unique virulence properties of *Yersinia enterocolitica* O:3—an emerging zoonotic pathogen using pigs as preferred reservoir host. Int J Med Microbiol. 2014;304:824–34. http://dx.doi.org/10.1016/j.ijmm.2014.07.008

10. Wang X, Qiu H, Jin D, Cui Z, Kan B, Xiao Y, et al. O:8 serotype *Yersinia enterocolitica* strains in China. Int J Food Microbiol. 2008;125:259–66. http://dx.doi.org/10.1016/j.ijfoodmicro.2008.04.016

11. Fukushima H, Hao Q, Wu K, Hu X, Chen J, Guo Z, et al. *Yersinia enterocolitica* O9 as a possible barrier against *Y. pestis* in natural plague foci in Ningxia, China. Curr Microbiol. 2001;42:1–7. http://dx.doi.org/10.1007/s002840010168

12. Wang X, Cui Z, Jin D, Tang L, Xia S, Wang H, et al. Distribution of pathogenic *Yersinia enterocolitica* in China. Eur J Clin Microbiol Infect Dis. 2009;28:1237–44. http://dx.doi.org/10.1007/s10096-009-0773-x

13. Wang X, Cui Z, Wang H, Tang L, Yang J, Gu L, et al. Pathogenic strains of *Yersinia enterocolitica* isolated from domestic dogs (*Canis familiaris*) belonging to farmers are of the same subtype as pathogenic *Y. enterocolitica* strains isolated from humans and may be a source of human infection in Jiangsu Province, China. J Clin Microbiol. 2010;48:1604–10. http://dx.doi.org/10.1128/JCM.01789-09

14. Fukushima H, Shimizu S, Inatsu Y. *Yersinia enterocolitica* and *Yersinia pseudotuberculosis* detection in foods. J Pathogens. 2011;2011:735308. http://dx.doi.org/10.4061/2011/735308

15. Liang J, Wang X, Xiao Y, Cui Z, Xia S, Hao Q, et al. Prevalence of *Yersinia enterocolitica* in pigs slaughtered in Chinese abattoirs. Appl Environ Microbiol. 2012;78:2949–56. http://dx.doi.org/10.1128/AEM.07893-11

16. Funk JA, Troutt HF, Davis SA, Fossler CP. In vitro susceptibility of *Yersinia enterocolitica* isolated from the oral cavity of swine. J Food Prot. 2000;63:395–9. http://dx.doi.org/10.4315/0362-028X-63.3.395

17. Jones TF, Buckingham SC, Bopp CA, Ribot E, Schaffner W. From pig to pacifier: chitterling-associated yersiniosis outbreak among black infants. Emerg Infect Dis. 2003;9:1007–9. http://dx.doi.org/10.3201/eid0908.030103

18. Chakraborty A, Komatsu K, Roberts M, Collins J, Beggs J, Turabelidze G, et al. The descriptive epidemiology of yersiniosis: a multistate study, 2005–2011. Public Health Rep. 2015;130:269–77. http://dx.doi.org/10.1177/003335491513000314

19. Scallan E, Hoekstra RM, Angulo FJ, Tauxe RV, Widdowson M-A, Roy SL, et al. Foodborne illness acquired in the United States—major pathogens. Emerg Infect Dis. 2011;17:7–15. http://dx.doi.org/10.3201/eid1701.P11101

20. Rosner BM, Stark K, Werber D. Epidemiology of reported *Yersinia enterocolitica* infections in Germany, 2001–2008. BMC Public Health. 2010;10:337. http://dx.doi.org/10.1186/1471-2458-10-337

21. Kotloff KL, Nataro JP, Blackwelder WC, Nasrin D, Farag TH, Panchalingam S, et al. Burden and aetiology of diarrhoeal disease in infants and young children in developing countries (the Global Enteric Multicenter Study, GEMS): a prospective, case-control study. Lancet. 2013;382:209–22. http://dx.doi.org/10.1016/S0140-6736(13)60844-2

22. Huang Y, Wang X, Cui Z, Yang Y, Xiao Y, Tang L, et al. Possible use of *ail* and *foxA* polymorphisms for detecting pathogenic *Yersinia enterocolitica*. BMC Microbiol. 2010;10:211. http://dx.doi.org/10.1186/1471-2180-10-211

23. Wauters G. Contribution à l'étude de *Yersinia enterocolitica*. Belgium: Vander Louvain; 1970.

24. Morris JG Jr, Prado V, Ferreccio C, Robins-Browne RM, Bordun AM, Cayazzo M, et al. *Yersinia enterocolitica* isolated from two cohorts of young children in Santiago, Chile: incidence of and lack of correlation between illness and proposed virulence factors. J Clin Microbiol. 1991;29:2784–8.

25. Fenwick SG, McCarthy MD. *Yersinia enterocolitica* is a common cause of gastroenteritis in Auckland. N Z Med J. 1995;108:269–71.

26. Stolk-Engelaar VM, Hoogkamp-Korstanje JA. Clinical presentation and diagnosis of gastrointestinal infections by *Yersinia enterocolitica* in 261 Dutch patients. Scand J Infect Dis. 1996;28:571–5. http://dx.doi.org/10.3109/00365549609037963

27. Zaidi AK, Macone A, Goldmann AD. Impact of simple screening criteria on utilization of low-yield bacterial stool cultures in a children's hospital. Pediatrics. 1999;103:1189–92. http://dx.doi.org/10.1542/peds.103.6.1189

28. Fredriksson-Ahomaa M. *Yersinia enterocolitica* and *Yersinia pseudotuberculosis*. In: Simjee S, editor. Foodborne diseases. Totowa (New Jersey): Humana Press; 2007. p. 79–113.

29. Wang X, Wang J, Sun H, Xia S, Duan R, Liang J, et al. Etiology of childhood infectious diarrhea in a developed region of China: compared to childhood diarrhea in a developing region and adult diarrhea in a developed region. PLoS One. 2015;10:e0142136. http://dx.doi.org/10.1371/journal.pone.0142136

30. Guerrant RL, Van Gilder T, Steiner TS, Thielman NM, Slutsker L, Tauxe RV, et al.; Infectious Diseases Society of America. Practice guidelines for the management of infectious diarrhea. Clin Infect Dis. 2001;32:331–51. http://dx.doi.org/ 10.1086/318514

31. Huovinen E, Sihvonen LM, Virtanen MJ, Haukka K, Siitonen A, Kuusi M. Symptoms and sources of *Yersinia enterocolitica*-infection: a case-control study. BMC Infect Dis. 2010;10:122. http://dx.doi.org/10.1186/1471-2334-10-122

32. Stephan R, Joutsen S, Hofer E, Säde E, Björkroth J, Ziegler D, et al. Characteristics of *Yersinia enterocolitica* biotype 1A strains isolated from patients and asymptomatic carriers. Eur J Clin Microbiol Infect Dis. 2013;32:869–75. http://dx.doi.org/10.1007/s10096-013-1820-1

33. Schmitz AMTR. *Yersinia enterocolitica* infections. Epidemiology and control. In: Brachman PS, Abrutyn E, editors. Bacterial infections of humans. New York: Springer; 2009. p. 939–57.

34. Mingrone MG, Fantasia M, Figura N, Guglielmetti P. Characteristics of *Yersinia enterocolitica* isolated from children with diarrhea in Italy. J Clin Microbiol. 1987;25:1301–4.

35. Galanakis E, Perdikogianni C, Maraki S, Giannoussi E, Kalmanti M, Tselentis Y. Childhood *Yersinia enterocolitica* infection in Crete. Eur J Clin Microbiol Infect Dis. 2006;25:65–6. http://dx.doi.org/10.1007/s10096-005-0058-y

36. El Qouqa IA, El Jarou MA, Samaha AS, Al Afifi AS, Al Jarousha AM. *Yersinia enterocolitica* infection among children aged less than 12 years: a case–control study. Int J Infect Dis. 2011;15:e48–53. http://dx.doi.org/10.1016/j.ijid.2010.09.010

37. Liang J, Li X, Zha T, Chen Y, Hao H, Liu C, et al. DTDP-rhamnosyl transferase RfbF, is a newfound receptor-related regulatory protein for phage phiYe-F10 specific for *Yersinia enterocolitica* serotype O:3. Sci Rep. 2016;6:22905. http://dx.doi.org/10.1038/srep22905

38. Tauxe RV, Wauters G, Goossens V, Van Noyen R, Vandepitte J, Martin SM, et al. *Yersinia enterocolitica* infections and pork: the missing link. Lancet. 1987;329:1129–32. http://dx.doi.org/10.1016/S0140-6736(87)91683-7

39. Ostroff SM, Kapperud G, Hutwagner LC, Nesbakken T, Bean NH, Lassen J, et al. Sources of sporadic *Yersinia enterocolitica* infections in Norway: a prospective case-control study. Epidemiol Infect. 1994;112:133–41. http://dx.doi.org/ 10.1017/S0950268800057496

40. Korte T, Fredriksson-Ahomaa M, Niskanen T, Korkeala H. Low prevalence of *yadA*-positive *Yersinia enterocolitica* in sows. Foodborne Pathog Dis. 2004;1:45–52. http://dx.doi.org/10.1089/153531404772914455

41. Fredriksson-Ahomaa M, Stolle A, Stephan R. Prevalence of pathogenic *Yersinia enterocolitica* in pigs slaughtered at a Swiss abattoir. Int J Food Microbiol. 2007;119:207–12. http://dx.doi.org/10.1016/j.ijfoodmicro.2007.07.050

42. Lee LA, Gerber AR, Lonsway DR, Smith JD, Carter GP, Puhr ND, et al. *Yersinia enterocolitica* O:3 infections in infants and children, associated with the household preparation of chitterlings. N Engl J Med. 1990;322:984–7. http://dx.doi.org/10.1056/NEJM199004053221407

43. Fukushima H, Hoshina K, Itogawa H, Gomyoda M. Introduction into Japan of pathogenic *Yersinia* through imported pork, beef and fowl. Int J Food Microbiol. 1997;35:205–12. http://dx.doi.org/10.1016/S0168-1605(96)01223-8

Address for correspondence: Xin Wang and Huaiqi Jing, National Institute for Communicable Disease Control and Prevention, China CDC, No. 155 Changbai Rd, Changping, Beiing, 102206, China; email: wangxin@icdc.cn, jinghuaiqi@icdc.cn

July 2016: **Zoonoses**

- Turtle-Associated Salmonellosis, United States, 2006–2014
- Pregnancy, Labor, and Delivery after Ebola Virus Disease and Implications for Infection Control in Obstetric Services, United States, 2015
- Response to Middle East Respiratory Syndrome Coronavirus, Abu Dhabi, United Arab Emirates, 2013–2014
- Current Guidelines, Common Clinical Pitfalls, and Future Directions for Laboratory Diagnosis of Lyme Disease, United
- *Tropheryma whipplei* as a Cause of Epidemic Fever, Senegal, 2010–2012

- Two Linked Enteroinvasive *Escherichia coli* Outbreaks, Nottingham, United Kingdom, June 2014
- Porcine Bocavirus Infection Associated with Encephalomyelitis in a Pig, Germany
- African Swine Fever Epidemic, Poland, 2014–2015
- Hepatitis E Virus in Dromedaries, North and East Africa, United Arab Emirates and Pakistan, 1983–2015
- Heatwave-Associated Vibriosis, Sweden and Finland, 2014
- A Literature Review of Zika Virus

- Vesicular Disease in 9-Week-Old Pigs Experimentally Infected with Senecavirus A

- High Incidence of Chikungunya Virus and Frequency of Viremic Blood Donations during Epidemic, Puerto Rico, USA, 2014
- Senecavirus A in Pigs, United States, 2015
- Outbreak of *Vibrio parahaemolyticus* Sequence Type 120, Peru, 2009
- Clinical Manifestations of Senecavirus A Infection in Neonatal Pigs, Brazil, 2015

- Infection with Possible Novel Parapoxvirus in Horse, Finland, 2013
- Travel-Associated Rabies in Pets and Residual Rabies Risk, Western Europe
- Naturally Circulating Hepatitis A Virus in Olive Baboons, Uganda
- Highly Pathogenic Avian Influenza Viruses and Generation of Novel Reassortants, United States, 2014–2015
- Detection and Genomic Characterization of Senecavirus A, Ohio, USA, 2015
- Red Fox as a Sentinel for *Blastomyces dermatitidis*, Ontario, Canada

EMERGING INFECTIOUS DISEASES

Visit our website to listen:
https://wwwnc.cdc.gov/eid/articles/issue/22/7/table-of-contents
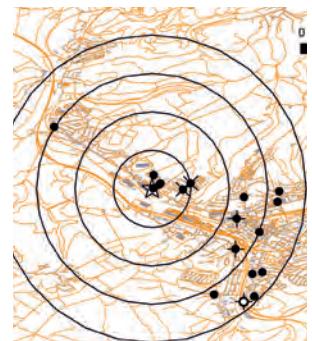
Risk for Low Pathogenicity Avian Influenza Virus on Poultry Farms, the Netherlands, 2007–2013

Ruth Bouwstra,[1,2] Jose L. Gonzales,[2] Sjaak de Wit, Julia Stahl, Ron A.M. Fouchier, Armin R.W. Elbers[2]

Using annual serologic surveillance data from all poultry farms in the Netherlands during 2007–2013, we quantified the risk for the introduction of low pathogenicity avian influenza virus (LPAIV) in different types of poultry production farms and putative spatial-environmental risk factors: distance from poultry farms to clay soil, waterways, and wild waterfowl areas. Outdoor-layer, turkey (meat and breeder), and duck (meat and breeder) farms had a significantly higher risk for LPAIV introduction than did indoor-layer farms. Except for outdoor-layer, all poultry types (i.e., broilers, chicken breeders, ducks, and turkeys) are kept indoors. For all production types, LPAIV risk decreased significantly with increasing distance to medium-sized waterways and with increasing distance to areas with defined wild waterfowl, but only for outdoor-layer and turkey farms. Future research should focus not only on production types but also on distance to waterways and wild bird areas. In addition, settlement of new poultry farms in high-risk areas should be discouraged.

Avian influenza is a disease of birds caused by influenza A viruses. Wild birds, particularly migratory water birds, form a natural reservoir of avian influenza viruses. Influenza viruses carry 2 glycoproteins on their surface, hemagglutinin (HA) and neuraminidase (NA), and on the basis of these glycoproteins are divided into subtypes. Eighteen distinct subtypes of HA (H1–H18) and 11 NA subtypes (N1–N11) have been described. Influenza A(H17N10) and A(H18N11), however, were recently detected in bats but not in birds. Virtually all remaining combinations of HA 1–16 and NA 1–9 subtypes have been isolated from wild birds (1). Wild birds pose a special risk for introducing avian influenza viruses of all subtypes to poultry kept in free-range or outdoor facilities (2).

Avian influenza virus infections in wild birds usually are asymptomatic. Infection of poultry ranges from no disease to severe disease and up to 100% mortality (3). A virus that causes no or mild disease in chickens is considered a low pathogenicity avian influenza virus (LPAIV); a virus that causes high rates of death in chickens is considered a highly pathogenic avian influenza virus (HPAIV) (4). HPAIV outbreaks in poultry cause huge direct and indirect economic losses (5). Furthermore, on several occasions during the last decade, bird-to-human transmissions of H5, H6, H7, H9, and H10 virus subtypes have occurred, emphasizing the threat to public health worldwide (6). Every HPAIV described has belonged to H5 and H7 subtypes and, until the spread of the Asian HPAIV subtype H5N1 to other parts of the world by wild birds since 2005 (7), mainly emerged after LPAIV of these subtypes were introduced in poultry, particularly in chickens and turkeys (8). Therefore, LPAIV of the H5 and H7 subtypes is notifiable to the World Organisation for Animal Health; consequently, member states of the European Union have implemented surveillance programs (9).

In the Netherlands, passive and active surveillance programs are in place. In the active serologic surveillance program, all poultry farms are tested 1–4 times a year. Frequency of sampling differs among poultry types (indoor- and outdoor-layer chickens, chicken breeders, broilers, ducks, and turkeys) and housing systems based on the supposed differences in the risk for LPAIV introduction. Except for outdoor-layers, all poultry types are kept indoors.

In a previous study (10), a significantly higher risk for LPAIV introduction was observed on poultry farms in Europe housing Anseriformes (duck, geese, and game birds) than on farms housing Galliformes (chicken breeders, broilers, layer chickens, and turkeys), and no significant differences were observed among Galliformes. In addition, Gonzales et al. (11) reported a significantly higher risk for LPAIV introduction on outdoor-layer, turkey, duck-breeder, and meat-duck farms than on indoor-layer farms in the Netherlands using surveillance data for 2007–2010. These studies (10,11) did not find differences in the risk for introduction among farms keeping chickens indoors, particularly between

Author affiliations: Wageningen Bioveterinary Research, Lelystad, the Netherlands (R. Bouwstra, J.L. Gonzales, A.R.W. Elbers); GD Animal Health, Deventer, the Netherlands (S. de Wit); Sovon Dutch Center for Field Ornithology, Nijmegen, the Netherlands (J. Stahl); Erasmus Medical Center, Rotterdam, the Netherlands (R.A.M. Fouchier)

[1]Current affiliation: GD Animal Health, Deventer, the Netherlands.
[2]These authors contributed equally to this article.

layers and broilers, possibly because of the limited data on positive introductions (or zero introductions) into broiler farms (11), which compromised the power of the comparisons. Our objective was to update the risk analysis of introduction of LPAIV infection using an extended surveillance period (2007–2013) and add spatial-environmental factors to the analysis that might explain part of the variation in LPAIV introductions on poultry farms in the Netherlands.

Materials and Methods

Data

We analyzed all data from the Netherlands' surveillance program collected during January 2007–December 2013. In the Netherlands, 3 types of surveillance programs are used to detect avian influenza virus infections on commercial poultry farms: passive surveillance, early warning, and serologic monitoring.

Passive surveillance for the early detection of notifiable avian influenza is based on clinical signs (12), an anamnesis of exponentially increasing death in the affected flock, or both. This surveillance is effective for acute infection causing severe disease (mainly HPAIV infection) but less so for LPAIV infection, which often causes mild or no disease. Samples (blood, tissue, and/or tracheal and cloacal swabs) of diseased/dead birds are tested by ELISA, PCR, and virus isolation.

Early warning includes signals such as aberrations in production parameters (decreased egg production, increased death rates, decreased feed and/or water intake). It excludes avian influenza as the cause of clinical problems in poultry flocks in situations in which birds show clinical signs that can be caused by other avian pathogens. Tracheal and cloacal swabs are tested for avian influenza by PCR (exclusion diagnostics).

The serologic monitoring program is active surveillance to detect all avian influenza virus incursions, even those that remain subclinical. This program is much more intense than required by the European Union: all poultry farms, except outdoor-layer farms and turkey farms, are tested at least once a year. Thirty samples per farm are screened by ELISA, and positive samples are confirmed by hemagglutination-inhibition test. Outdoor-layer farms are tested 4 times per year, and turkey farms are tested each production cycle. Meat-turkey farms have an average production cycle of ≈4 months; for broilers and meat ducks, this cycle is 5–6 weeks. All sampling is done just before slaughter, except the 3 extra samplings in outdoor-layer farms.

Farms were identified by their unique farm number and categorized on the basis of poultry production type (PT): duck breeders, meat ducks (meat production), turkey breeders, meat turkey, broilers, broiler breeders, indoor-layers, outdoor-layers, and layer breeders.

We selected putative spatial-environmental risk factors for LPAIV introduction related to farm location for incorporation in the risk model. These risk factors were distance to clay soil, distance to waterways, and distance to defined wild waterfowl areas.

We analyzed the farms' distance to clay soil (Geodesk database [GDB3]; Wageningen University, Wageningen, the Netherlands). Clay soil is a sediment of large rivers and is, in epidemiologic terms, a proxy for the presence of large water quantities, which is a proxy for an attractive environment for wild waterfowl. Wild waterfowl is presumed to be the most important reservoir for LPAIV. Presence of clay soil close to poultry farms was a risk factor for LPAIV introduction on outdoor-layer farms (13).

We also assessed distance from farms to waterways. Three sizes of waterways (width in meters) were included in the model: small (0.5–3 m wide), medium (3–6 m wide), and large (≥6 m wide). Presence of waterways is a proxy for an attractive environment for wild waterfowl; spatial data of waterways was available from the Dutch Land Registry (http://www.kadaster.nl/web/artikel/producten/TOP10NL.htm).

Distance to defined wild waterfowl areas is a direct proxy for a possible avian influenza virus reservoir. Wild waterfowl areas were defined as follows: areas with on average ≥5 wild water birds counted per hectare (based on systematic regular bird census schemes by Sovon [Nijmegen, the Netherlands], which coordinates the monitoring of wild bird populations in the Netherlands). Birds of the families *Anatidae*, *Laridae*, and *Rallidae* were included; these birds are known avian influenza virus carriers (14,15) (online Technical Appendix, https://wwwnc.cdc.gov/EID/article/23/9/17-0276-Techapp1.pdf).

Positive Farms

Positive farms were defined as follows: farms with ≥1 seropositive animal to any avian influenza strain in both the screening ELISA (IDEXX FLockCheck AI MultiScreen, IDEXX Europe B.V., Hoofddorp, the Netherlands) and the confirmatory hemagglutination-inhibition test; or farms with ≥3 positive results (of 30 serum samples) in the screening ELISA. Furthermore, we included in the analysis only primary cases (excluding secondary spread detected by epidemiologic tracing).

Period at Risk

Positive Farms

For every year, we estimated the period at risk (in months) as the sum of the period from January 1 and the last negative sampling plus half of the period between the last negative sampling and the positive sampling. In case of no negative sampling in the year the farm became positive, the last negative sampling of the year before was included. In that

instance, the time at risk was estimated as half of the period from the last negative sampling to the first positive sampling. Broilers, meat turkeys, and meat ducks were sampled 1 week before the end of their production. Therefore, the period at risk for these PTs was set at a fixed period.

Negative Farms

For every year, we estimated the period at risk (in months) as the period from January 1 through last negative sampling. This sampling was done for all PTs except broiler, meat-turkey, and meat-duck farms. For the latter, the period at risk was the same as for the corresponding positive farms.

Statistical Analysis

We analyzed data using the statistical software R version 3.1.3 (https://www.r-project.org/). The relative risk (RR) of introduction of LPAIV per type of poultry farm (PT), during the study period (2007–2013) was quantified using multivariate statistical models (known as generalized linear models or generalized linear mixed models [GLMMs]) (online Technical Appendix). We used indoor-layer chicken farms as the reference category. In terms of disease causation, if the RR is <1, the factor is considered a sparing factor, whereas if the RR is >1, the factor is considered a putative causal factor (16). In addition, we studied the effect of the spatial-environmental variables (distance to clay soil, waterways, and wild waterfowl areas) on the risk for LPAIV introduction. Statistical investigation started with a univariate analysis; distance of clay soil to the location of poultry farms was significantly associated with risk for LPAIV introduction only for layer (indoor and outdoor) farms. The different categories of waterways were significantly associated with risk for LPAIV introduction, but medium-sized waterways showed by far the strongest association. Thus, in the multivariate analysis, distance to clay soil and small- and large-sized waterways fell out of the model in the selection process; distance to medium-sized waterways and distance to wild waterfowl areas were strongly associated with risk for LPAIV introduction

and stayed in the model when tested together in the multivariate analysis.

Results

During 2007–2013, we surveyed 19,274 farms and detected 295 LPAIV introductions (Table 1). The Netherlands has a small population of turkey and duck breeder farms, and these small populations, in particular turkey breeders (only 1 farm in 2013 and a maximum of 5 in 2007), made it difficult to evaluate potential interactions (e.g., between PT and distance variables) when modeling the risk for introduction. Therefore, we first made an overall quantification of the RR for each PT and included the year of surveillance as a random effect in a GLMM. Broiler, broiler-breeder, and layer-breeder farms were at significantly lower risk for LPAIV introduction (p<0.05) than were indoor-layer farms (e.g., broiler farms had on average a 5 times [1/0.2] lower risk for LPAIV introduction than did indoor-layer farms) (Table 2). By contrast, the risk was significantly higher for outdoor-layer, duck, duck-breeder, meat-turkey, and turkey-breeder farms (p<0.05) (e.g., outdoor-layer farms had on average a 6.3 times higher risk for LPAIV introductions than indoor-layer farms). The effect of distance from medium-sized waterways to farm location was comparable for the different PTs, and we included this variable in the GLMM (Table 2). The risk for LPAIV introduction decreased with increasing distance from poultry farms to medium-sized waterways; RR was highest within the closest 500 m (Figure 1). To evaluate potential statistical interactions, we combined meat-turkey and turkey-breeder farms (which had similar RR estimates in our first analysis [Table 2]), and we evaluated the effect of the location variables and potential interactions. A generalized linear model fit better than a GLMM. We identified significant interactions between 1) year of surveillance and indoor- and outdoor-layer farms and 2) distance to wild waterfowl areas and outdoor-layer farms or meat turkey farms. The analysis showed a yearly decrease in the RR for indoor-layer farms (Table 3), in contrast to an increased risk for

Table 1. LPAIV surveillance data collated from poultry farms, the Netherlands, 2007–2013*

Type of farm	No. farms positive	Total no. farms	Median time at risk, mo	Median distance to wild water bird areas, m	Median distance to medium-sized waterway, m†	Probability of introduction‡	RR§
Indoor-layer	60	5,600	7.3	4,227	769	0.001	1
Outdoor-layer	143	2,549	6.3	3,996	670	0.009	6.0
Layer-breeder	14	2,174	9.5	4,157	738	0.001	0.5
Broiler	2	5,409	1.2	3,292	576	0.000	0.2
Broiler-breeder	14	2,718	8.5	4,002	824	0.001	0.4
Meat-turkey	30	469	3.7	3,208	1,042	0.017	11.7
Turkey-breeder	2	18	5.7	2,035	659	0.019	13.1
Meat-duck	16	267	1.2	3,477	1,180	0.050	33.9
Duck-breeder	14	70	5.8	4,107	767	0.034	23.4

*LPAIV, low pathogenicity avian influenza virus; RR, relative risk.
†Distance to clay soil and distance to small- and large-sized waterways also included in the multivariate analysis (data not shown). They did not have a significant effect on the risk for LPAIV introduction. Waterway sizes were defined as follows: small, 0.5–3 m wide; medium, 3–6 m wide; large, >6 m wide.
‡Unadjusted probabilities of LPAIV introduction per farm months at risk.
§These are the unadjusted RR estimates obtained by dividing the unadjusted probabilities of LPAIV introduction of each type of poultry farm by that of indoor-layer farms.

Table 2. Relative risks for introduction of low pathogenicity avian influenza virus infection in different types of poultry farms, the Netherlands, 2007–2013

Type of poultry farm	Relative risk (95% CI)	p value
Indoor-layer	1.0 (reference)	
Outdoor-layer	6.3 (4.7–8.6)	<0.00001
Layer-breeder	0.5 (0.3–0.8)	0.008
Broiler	0.2 (0.1–0.8)	0.02
Broiler-breeder	0.4 (0.2–0.8)	0.004
Meat-turkey	12.0 (7.8–18.8)	<0.00001
Turkey-breeder	11.3 (2.8–46.2)	0.0008
Meat-duck	39.5 (22.6–69.1)	<0.00001
Duck-breeder	25.5 (14.2–45.9)	<0.00001
Natural logarithm*	0.8 (0.7–0.9)	0.00005
*Of distance to medium-sized waterways in meters, i.e., 3–6 m wide.		

outdoor-layer farms for 2012 and 2013 (Figure 2). The risk for LPAIV introduction in outdoor-layer and meat turkey farms decreased with increasing distance to areas with wild waterfowl (Figures 2, 3). No significant risk was found for distance to clay soil.

Discussion

Our study shows that outdoor-layer, duck (breeder and meat), and turkey (breeder and meat) farms have a significantly higher RR for LPAIV introduction than do indoor-layer farms. The higher risk in outdoor-layer farms probably reflects their higher exposure to LPAIV from a contaminated environment. The presence of avian influenza in wild water birds and the frequency of direct or indirect contact between reservoir birds and poultry are risk components that enable transmission from wild birds to poultry. However, in addition to the higher introduction rate on outdoor-layer farms (this study) and the genetic relationship of wild

Figure 1. Risk for introduction of low pathogenicity avian influenza virus into duck-breeder, meat-duck, meat-turkey, and outdoor-layer farms, the Netherlands, 2007–2013. For the estimation of the relative risk as a function of distance to medium-sized waterways (3–6 m wide), distance to wild waterfowl areas was kept constant.

bird strains and avian influenza outbreak viruses (*17*), no scientific data have been available that could support this assumption, although physical environmental factors, such as surface water availability and proximity to lakes and wetlands, have been suggested as drivers of HPAIV H5N1 outbreaks in poultry and wild birds (*18*,*19*).

We described a significant spatial-environmental relationship: the closer to waterways—a proxy for an attractive environment for wild waterfowl—and wild waterfowl areas a farm is located, in particular outdoor-layer farms, the higher the risk for LPAIV introduction. Although waterfowl and shorebirds are known to form the major natural reservoir and source of all known influenza A viruses (*14*,*20*,*21*), there is little direct evidence for transmission of avian influenza virus from (wild) birds to poultry. Two lines of evidence suggest that wild birds can be the source of avian influenza infection in poultry: 1) temporal associations between avian influenza virus isolated from wild birds and from outbreaks in poultry flocks and 2) genetic similarity between avian influenza virus strains isolated from wild birds and from poultry. Phylogenetic studies support the presumed transmission route from wild birds to poultry. For example, an LPAIV H7N7 caused the HPAI H7N7 epidemic in the Netherlands that started at a free-range farm (*22*). This virus is believed to be a reassortant of an H7N3 virus and an H10N7 virus isolated from mallards in 2000 during survey studies of migratory wild birds in the Netherlands (*23*). Furthermore, recent genetic analyses of HPAIV H5N8 strains from the Netherlands, and of other strains from countries in Europe, South Korea, and Japan, suggested that the strains from Europe probably arrived through migratory wild birds from Asia, most likely through overlapping flyways and common breeding sites in Siberia (*24*,*25*).

In the Netherlands, turkeys are raised indoors, and despite the small number of turkey farms, we observed a higher RR for introduction of LPAIV infection to breeder and meat-turkey farms. This higher risk might be associated partly with the apparent higher susceptibility of turkeys than chickens to LPAIV infection (*26*).

As reported by Gonzales et al. (*10*), we found that duck-breeder farms have the highest RR for LPAIV introduction. This risk could be related to their higher susceptibility to infection with LPAIV of wild water bird origin (ducks, geese, and swans) than chickens (*27*) and
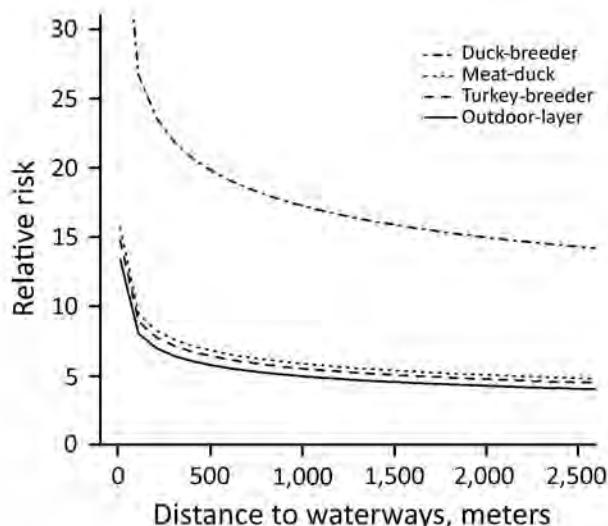
Table 3. Yearly relative risk for introduction of low pathogenicity avian influenza virus in indoor-layer farms, the Netherlands

Year	Relative risk (95% CI)
2007	1 (reference)
2008	0.65 (0.48–1.04)
2009	0.63 (0.28–0.84)
2010	0.41 (0.28–0.68)
2011	0.56 (0.44–0.70)
2012	0.5 (0.30–0.83)
2013	0.15 (0.04–0.27)
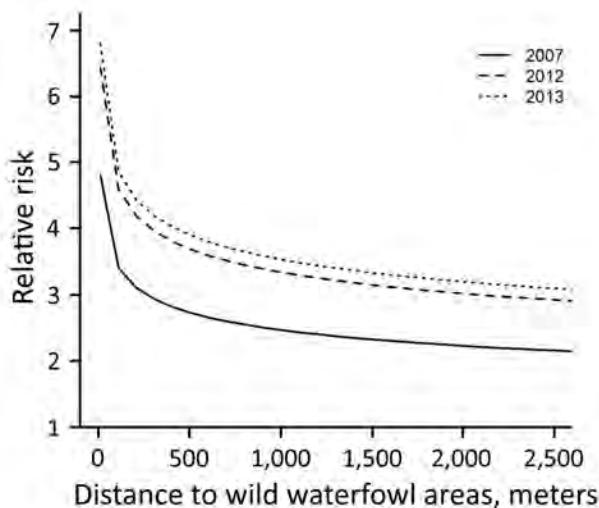
Figure 2. Risk for introduction of low pathogenicity avian influenza virus into outdoor-layer farms, the Netherlands, 2007–2013. Relative risk is shown for 2007 (reference for between-year comparison), 2012 (p = 0.08), and 2013 (p = 0.005). For the estimation of the relative risk as a function of distance to wild waterfowl areas, distance to medium-sized waterways (3–6 m wide) was kept constant.

their long production cycle (time of exposure). We also observed a significantly higher risk for LPAIV introduction into meat-duck farms than into indoor-layer farms. This finding is somewhat surprising because meat ducks are kept indoors and have a short production cycle (6.5 weeks), in contrast with broilers, which also are kept indoors, have a short production cycle (6 weeks), and had a very low risk for LPAIV introduction. The higher susceptibility of ducks than chickens to LPAIV (27) could be a reason to explain this contrast. In addition, poor biosecurity compliance might play a role. For instance, floor bedding for ducks is stored outside (often not protected by a cover) and transported inside the duck house several times during the growing period. Bedding material for broilers is mostly stored inside the poultry house and is placed only once during the production cycle or not replaced. Poor biosecurity compliance has been reported repeatedly in poultry production (28–30). Meat ducks and broilers are tested before slaughter, and considering that the time to build up a serologic prevalence after an LPAIV infection that can be detected by random sampling could take ≈2–3 weeks (31), LPAIV introductions that occur shortly before slaughter could be missed. Therefore, the RRs could be underestimated for both meat ducks and broilers. Nevertheless, by looking at the large number of broiler flocks tested along these years, the fact that only 2 LPAIV introductions were detected, and the fact that surveillance was able to detect a relatively high number of LPAIV introductions in meat ducks (also short production cycle),

we conclude that the risk for LPAIV introduction in broilers is low under housing conditions in the Netherlands.

In addition, the RR for layer-breeder farms was 5 times lower for LPAIV introduction than it was for indoor-layer farms (2011–2013). These findings might be related to the high biosecurity levels on these PTs.

Our finding that the RR for LPAIV introduction on outdoor-layer farms increased over time (a significantly higher RR in 2013 than in 2007, 2008, 2009, and 2011) can be explained by an increase of the number of introductions on outdoor-layer farms, especially in 2012 and 2013. An increase in the number of outdoor-layer farms and a decrease in the number of indoor-layer farms (for which RR decreased over time), particularly in 2012 and 2013, might partly explain these changes in risk. Further research is needed to gain insight into the factors that might affect introduction rates and differences over time. A plausible explanation might be increased direct or indirect contact between outdoor ranging poultry and infectious wild bird populations, but this explanation remains speculative because field data on the type and frequency of contact between wild birds and poultry in outdoor-layer farms is still missing. Climate and land use changes during the past decades have affected winter and breeding bird community composition (32); effects on herbivorous birds (such as many waterfowl species) through phenology-induced changes of plant forage quality and availability are most pronounced (33,34).

As recent experience shows, wild birds can introduce HPAIV directly into poultry (24,25), and HPAIV can
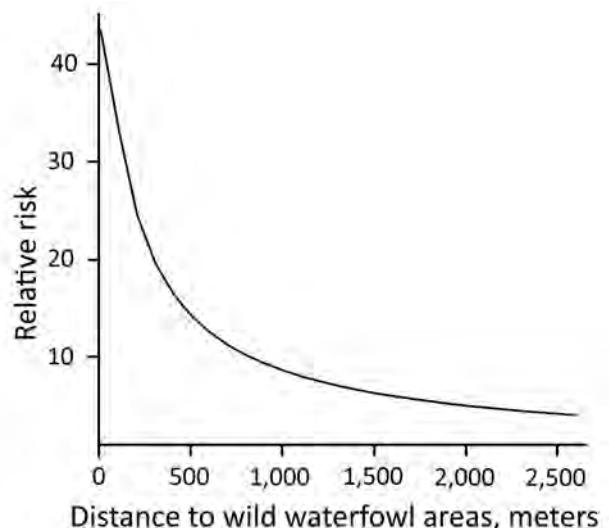
Figure 3. Relative risk for introduction of low pathogenicity avian influenza virus into meat-turkey farms, the Netherlands, 2007–2013. No difference in risk was observed between surveillance years. For the estimation of the relative risk as a function of distance to wild waterfowl areas, distance to medium-sized waterways (3–6 m wide) was kept constant.

emerge after an LPAIV H5/H7 introduction in poultry after varying lengths of time (*8*). If a notifiable LPAIV subtype infects a farm and later spreads to other farms before detection, the risk increases for mutation to HPAIV (*35*). Therefore, the sooner an introduction is detected, the sooner restrictive measures can be applied to contain the infection, ideally even to the index farm. Early detection and removal of infected poultry will help lower viral replication rounds.

Surveillance programs are important tools to prevent new HPAIV outbreaks. In the Netherlands the avian influenza surveillance program is much more intense than required by the European Union (*9*). Frequent sampling of high-risk poultry farms may help reduce the risk for transmission between farms (*31,36*). Based on expected risk factors for introduction, outdoor-layer farms (more contact with wild birds) and meat-turkey farms (higher susceptibility) are tested more frequently than other poultry farms. The results of our study indicate that duck farms also should be tested more frequently; passive surveillance will not easily detect LPAIV introductions in ducks because LPAIV will not cause observable clinical signs in them. Furthermore, it is clear that we should target surveillance not only toward PT, but also on location (e.g., within 500 m of waterways, wild bird areas, or both). In addition, there could be a discouraging strategy for settlement of new poultry farms in high-risk areas.

Dr. Bouwstra was a project leader of avian influenza and Newcastle disease at Wageningen Bioveterinary Research, Lelystad, the Netherlands, at the time of the study and currently is head of the poultry health department, GD Animal Health, Deventer. Her research interests are notifiable animal diseases and One Health.

References

1. Webster RG, Bean WJ, Gorman OT, Chambers TM, Kawaoka Y. Evolution and ecology of influenza A viruses. Microbiol Rev. 1992; 56:152–79. PMID: 1579108
2. Koch G, Elbers ARW. Outdoor ranging of poultry: a major risk factor for the introduction and development of high-pathogenicity avian influenza. NJAS—Wageningen Journal of Life Sciences . 2006;54:179–94. https://doi.org/10.1016/S1573-5214(06)80021-7
3. Swayne DE, Halvorson DA. Influenza. In: Saif YM, Barnes HJ, Glisson JR, Fadly AM, McDougald LR, Swayne DE, editors. Diseases of poultry. 11th ed. Ames (IA): Iowa State University Press; 2003. p. 135–60.
4. World Organization for Animal Health. Avian influenza (infection with avian influenza viruses). In: OIE manual of diagnostic tests and vaccines for terrestrial animals [cited 2017 Feb 13]. http://www.oie.int/fileadmin/Home/eng/Health_standards/tahm/2.03.04_AI.pdf
5. Elbers A, Knutsson R. Agroterrorism targeting livestock: a review with a focus on early detection systems. Biosecur Bioterror. 2013;11(Suppl 1):S25–35. http://dx.doi.org/10.1089/bsp.2012.0068
6. Capua I, Munoz O. Emergence of influenza viruses with zoonotic potential: open issues which need to be addressed. A review. Vet Microbiol. 2013;165:7–12. http://dx.doi.org/10.1016/j.vetmic.2013.01.044
7. Gilbert M, Xiao X, Domenech J, Lubroth J, Martin V, Slingenbergh J. Anatidae migration in the western Palearctic and spread of highly pathogenic avian influenza H5NI virus. Emerg Infect Dis. 2006;12:1650–6. http://dx.doi.org/10.3201/eid1211.060223
8. Alexander DJ. Should we change the definition of avian influenza for eradication purposes? Avian Dis. 2003;47(Suppl):976–81. http://dx.doi.org/10.1637/0005-2086-47.s3.976
9. European Commission. Commission decision 2007/268/EC of 13 April 2007 on the implementation of surveillance programmes for avian influenza in poultry and wild birds to be carried out in the Member States and amending decision 2004/450/EC. Official Journal of the European Union. 2007;115:2003.
10. Gonzales JL, Elbers ARW, Bouma A, Koch G, de Wit JJ, Stegeman JA. Low-pathogenic notifiable avian influenza serosurveillance and the risk of infection in poultry—a critical review of the European Union active surveillance programme (2005–2007). Influenza Other Respir Viruses. 2010;4:91–9. http://dx.doi.org/10.1111/j.1750-2659.2009.00126.x PMID: 20167049
11. Gonzales JL, Stegeman JA, Koch G, de Wit JJ, Elbers ARW. Rate of introduction of a low pathogenic avian influenza virus infection in different poultry production sectors in the Netherlands. Influenza Other Respir Viruses. 2013;7:6–10. http://dx.doi.org/10.1111/j.1750-2659.2012.00348.x PMID: 22376126
12. Elbers ARW, Koch G, Bouma A. Performance of clinical signs in poultry for the detection of outbreaks during the avian influenza A (H7N7) epidemic in the Netherlands in 2003. Avian Pathol. 2005;34:181–7. http://dx.doi.org/10.1080/03079450500096497
13. Van der Goot J, Verhagen J, Gonzales J, Backer J, Bongers J, Boender GJ, et al. Laag pathogene aviaire influenza virus infecties op pluimveebedrijven in Nederland. CVI rapport 12/CVI0036 [cited 2016 Oct 14]. https://www.wageningenur.nl/upload_mm/9/3/3/c49eea5e-dc40-4163-9ed8-3222e17c7c8a_LPAIoppluimveebedrijveninNL.pdf
14. Fouchier RAM, Olsen B, Bestebroer TM, Herfst S, van der Kemp L, Rimmelzwaan GF, et al. Influenza A virus surveillance in wild birds in northern Europe in 1999 and 2000. Avian Dis. 2003;47 (Suppl):857–60. http://dx.doi.org/10.1637/0005-2086-47.s3.857
15. Olsen B, Munster VJ, Wallensten A, Waldenström J, Osterhaus ADME, Fouchier RAM. Global patterns of influenza a virus in wild birds. Science. 2006;312:384–8. http://dx.doi.org/10.1126/science.1122438
16. Martin SW, Meek AH, Willeberg P. Disease causation. In: Veterinary epidemiology, principles and methods. Ames (IA): Iowa State University Press; 1987. p. 121–48.
17. Munster VJ, Veen J, Olsen B, Vogel R, Osterhaus AD, Fouchier RA. Towards improved influenza A virus surveillance in migrating birds. Vaccine. 2006;24:6729–33. http://dx.doi.org/10.1016/j.vaccine.2006.05.060 PMID: 16806601
18. Si Y, de Boer WF, Gong P. Different environmental drivers of highly pathogenic avian influenza H5N1 outbreaks in poultry and wild birds. PLoS One. 2013;8:e53362. http://dx.doi.org/10.1371/journal.pone.0053362
19. Gilbert M, Pfeiffer DU. Risk factor modelling of the spatio-temporal patterns of highly pathogenic avian influenza (HPAIV) H5N1: a review. Spat Spatio-Temporal Epidemiol. 2012;3:173–83. http://dx.doi.org/10.1016/j.sste.2012.01.002
20. Stallknecht DE. Ecology and epidemiology of avian influenza viruses in wild bird populations: waterfowl, shorebirds, pelicans,

cormorants, etc. In: Swayne DE, Slemons RD, editors. Proceedings of the 4th International Symposium on Avian Influenza; 1997 May 28–31; Athens Georgia. Jacksonville (FL): American Association of Avian Pathologists; 1998. p. 61–7.

21. Fouchier RAM, Osterhaus ADME, Brown IH. Animal influenza virus surveillance. Vaccine. 2003;21:1754–7. http://dx.doi.org/10.1016/S0264-410X(03)00067-7

22. Elbers ARW, Fabri TH, de Vries TS, de Wit JJ, Pijpers A, Koch G. The highly pathogenic avian influenza A (H7N7) virus epidemic in the Netherlands in 2003—lessons learned from the first five outbreaks. Avian Dis. 2004;48:691–705. http://dx.doi.org/10.1637/7149

23. Fouchier RA, Schneeberger PM, Rozendaal FW, Broekman JM, Kemink SA, Munster V, et al. Avian influenza A virus (H7N7) associated with human conjunctivitis and a fatal case of acute respiratory distress syndrome. Proc Natl Acad Sci U S A. 2004;101:1356–61. http://dx.doi.org/10.1073/pnas.0308352100

24. Bouwstra R, Heutink R, Bossers A, Harders F, Koch G, Elbers A. Full-genome sequence of influenza A(H5N8) virus in poultry linked to sequences of strains from Asia, the Netherlands, 2014. Emerg Infect Dis. 2015;21:872–4. http://dx.doi.org/10.3201/eid2105.141839

25. Bouwstra RJ, Koch G, Heutink R, Harders F, van der Spek AN, Elbers ARW, et al. Full genome sequence of HPAI H5N8 outbreak strains provide evidence for four separate introductions and one between-poultry farm transmission in the Netherlands, 2014. Euro Surveill. 2015;20:21174. http://dx.doi.org/10.2807/1560-7917.ES2015.20.26.21174

26. Tumpey TM, Kapczynski DR, Swayne DE. Comparative susceptibility of chickens and turkeys to avian influenza A H7N2 virus infection and protective efficacy of a commercial avian influenza H7N2 virus vaccine. Avian Dis. 2004;48:167–76. http://dx.doi.org/10.1637/7103

27. Mundt E, Gay L, Jones L, Saavedra G, Tompkins SM, Tripp RA. Replication and pathogenesis associated with H5N1, H5N2, and H5N3 low-pathogenic avian influenza virus infection in chickens and ducks. Arch Virol. 2009;154:1241–8. http://dx.doi.org/10.1007/s00705-009-0437-2

28. Hernández-Jover M, Schemann K, Toribio JA. A cross-sectional study on biosecurity practices and communication networks of poultry exhibition in Australia. Prev Vet Med. 2013;110:497–509. http://dx.doi.org/10.1016/j.prevetmed.2012.12.012

29. Ssematimba A, Hagenaars TJ, de Wit JJ, Ruiterkamp F, Fabri TH, Stegeman JA, et al. Avian influenza transmission risks: analysis of biosecurity measures and contact structure in Dutch poultry farming. Prev Vet Med. 2013;109:106–15. http://dx.doi.org/10.1016/j.prevetmed.2012.09.001

30. Van Steenwinkel S, Ribbens S, Ducheyne E, Goossens E, Dewulf J. Assessing biosecurity practices, movements and densities of poultry sites across Belgium, resulting in different farm risk-groups for infectious disease introduction and spread. Prev Vet Med. 2011;98:259–70. http://dx.doi.org/10.1016/j.prevetmed.2010.12.004

31. Gonzales JL, Boender G-J, Elbers ARW, Stegeman JA, de Koeijer AA. Risk based surveillance for early detection of low pathogenic avian influenza outbreaks in layer chickens. Prev Vet Med. 2014;117:251–9. http://dx.doi.org/10.1016/j.prevetmed.2014.08.015

32. Kampichler C, van Turnhout CAM, Devictor V, van der Jeugd HP. Large-scale changes in community composition: determining land use and climate change signals. PLoS One. 2012;7:e35272. http://dx.doi.org/10.1371/journal.pone.0035272

33. Van der Jeugd HP, Eichhorn G, Litvin KE, Stahl J, Larsson K, van der Graaf AJ, et al. Keeping up with early springs: rapid range expansion in an avian herbivore incurs a mismatch between reproductive timing and food supply. Global Change Biology. 2009;15:1057–71. http://dx.doi.org/10.1111/j.1365-2486.2008.01804.x

34. Van Eerden MR, Drent RH, Stahl J, Bakker JP. Connecting seas: western Palaearctic continental flyway for water birds in the perspective of changing land use and climate. Global Change Biology. 2005;11:894–908. http://dx.doi.org/10.1111/j.1365-2486.2005.00940.x

35. Alexander DJ. An overview of the epidemiology of avian influenza. Vaccine. 2007;25:5637–44. http://dx.doi.org/10.1016/j.vaccine.2006.10.051

36. Comin A, Stegeman A, Marangon S, Klinkenberg D. Evaluating surveillance strategies for the early detection of low pathogenicity avian influenza infections. PLoS One. 2012;7:e35956. http://dx.doi.org/10.1371/journal.pone.0035956

Address for correspondence: Armin R.W. Elbers, Wageningen Bioveterinary Research, PO Box 65, 8200 AB, Lelystad, the Netherlands; email: armin.elbers@wur.nl

Patterns of Human Plague in Uganda, 2008–2016

Joseph D. Forrester, Titus Apangu, Kevin Griffith, Sarah Acayo, Brook Yockey,
John Kaggwa, Kiersten J. Kugeler, Martin Schriefer, Christopher Sexton, C. Ben Beard,
Gordian Candini, Janet Abaru, Bosco Candia, Jimmy Felix Okoth, Harriet Apio, Lawrence Nolex,
Geoffrey Ezama, Robert Okello, Linda Atiku, Joseph Mpanga, Paul S. Mead

Plague is a highly virulent fleaborne zoonosis that occurs throughout many parts of the world; most suspected human cases are reported from resource-poor settings in sub-Saharan Africa. During 2008–2016, a combination of active surveillance and laboratory testing in the plague-endemic West Nile region of Uganda yielded 255 suspected human plague cases; approximately one third were laboratory confirmed by bacterial culture or serology. Although the mortality rate was 7% among suspected cases, it was 26% among persons with laboratory-confirmed plague. Reports of an unusual number of dead rats in a patient's village around the time of illness onset was significantly associated with laboratory confirmation of plague. This descriptive summary of human plague in Uganda highlights the episodic nature of the disease, as well as the potential that, even in endemic areas, illnesses of other etiologies might be being mistaken for plague.

Plague is a virulent zoonosis caused by the gram-negative bacillus *Yersinia pestis* (*1,2*). The organism cycles naturally among rodents and their fleas in areas with conducive ecology across the Americas, Asia, and Africa (*3*). Most human plague cases occur after the bite of an infected flea and manifest clinically as bubonic plague, with rapid onset of fever and painful regional lymphadenopathy (*4*). Infection with the bacteria can sometimes result in a generalized septic illness lacking obvious lymphadenopathy. Pneumonic plague occurs after dissemination of the bacteria from other parts of the body to the lungs or through direct inhalation of infectious droplets into the lungs. Unlike bubonic plague, pneumonic plague can be transmitted from person to person. Outbreaks of pneumonic plague with high human mortality rates can occur in resource-poor settings (*5–7*). The mortality rate for untreated infections ranges from ≈65% for bubonic plague to ≈100% for pneumonic plague (*8,9*). Early treatment with effective antimicrobial drugs greatly reduces the risk for death (*4,8*).

Currently, sub-Saharan Africa accounts for >95% of reported human plague cases worldwide (*10*). The West Nile region in northwestern Uganda encompasses the current plague focus of that country. This densely populated, remote area near the borders of the Democratic Republic of the Congo and South Sudan predominantly has a subsistence agriculture economy. Much of the region lies at 1,000–2,000 m above sea level and experiences 2 main periods of rainfall, with the heaviest precipitation occurring from late August through November (*11*). Living conditions that include close contact with rodents, a burdened healthcare infrastructure, and unreliable stocks of antimicrobial drugs, combined with infected persons delaying seeking healthcare, all contribute to plague illness and death. An understanding of the demographics, geographic distribution, and outcomes of infection is needed to guide prevention programs. Thus, we summarize the epidemiology of human plague in the West Nile region of Uganda during 2008–2016.

Methods

Data on human plague cases were collected as part of an ongoing collaboration between the Uganda Virus Research Institute (UVRI), the Ugandan Ministry of Health, and the US Centers for Disease Control and Prevention (CDC) to enhance education, clinical detection, laboratory diagnostic capacity, treatment, and control of plague in the West Nile region (*12*). During 2008–2016, active surveillance for human plague cases occurred in 10 clinics and 2 hospitals in the Arua and Zombo Districts of the West Nile region. In addition, active community engagement with village health workers and traditional healers was undertaken to identify cases occurring in villages among persons not seeking medical care. Clinic and hospital staff received annual training on the epidemiology and clinical management of plague.

CDC-trained UVRI laboratory staff located in the town of Arua (in the Arua District) performed microbiological testing on clinical specimens, including blood cultures and bubo aspirates or sputum when available. Isolation of *Y. pestis* from clinical samples was performed on sheep blood agar, and bacterial isolates were confirmed to be *Y. pestis*

by bacteriophage lysis (*13*). An acute serum sample was collected as soon as possible from patients upon their arrival at the clinic, and a convalescent serum sample was collected on days 14–28 after illness onset. Verification of *Y. pestis* cultures and all serologic testing was performed at CDC's Division of Vector-Borne Diseases, National Center for Emerging and Zoonotic Infectious Diseases, in Fort Collins, Colorado, USA.

For purposes of this summary, we defined a confirmed plague case as clinically compatible acute illness with isolation of *Y. pestis* from a clinical specimen or with ≥1 positive antibody titer against the F1 antigen of *Y. pestis*, a suspected case as clinically compatible acute illness without laboratory confirmation, and a probable case as a suspected case that was epidemiologically linked to a confirmed case or a suspected case with additional nonconfirmatory laboratory evidence of plague infection. Clinical signs suggestive of plague included sudden onset of fever with painful regional lymphadenopathy (bubonic), hematemesis or hematochezia (septicemic), or cough or chest pain with hemoptysis (pneumonic). Lack of laboratory confirmation could have occurred because specimens were unavailable for testing or because specimens were negative by all available presumptive and confirmatory tests. We defined adults as persons ≥18 years of age. We included patients who visited facilities where active surveillance was not being performed in this study; however, we excluded patients who sought healthcare in the region but were residents of another country (i.e., nearby Democratic Republic of the Congo) because of the inability to perform follow-up. The standard treatment for suspected plague in Uganda is doxycycline or chloramphenicol; during the period covered by this surveillance summary, a concurrent treatment trial evaluating the efficacy of oral ciprofloxacin against the national standard was also being conducted (*14*).

Upon notification from health facilities or community members regarding a suspected plague case, UVRI plague program staff immediately notified local public health officials and traveled to the reporting health facility to obtain additional information on the patient. In addition, staff visited the village and patient's home to obtain more details regarding exposure and to ascertain similar illnesses in the community. Additional persons suspected to have plague were identified and referred to the nearest health facility for assessment and care. If pneumonic plague was suspected, contact tracing and prophylaxis of exposed persons was initiated with active monitoring for at least 1 week to ensure that no additional illnesses developed. In all instances, program staff worked with village health volunteers to remind village members of the signs and symptoms of plague and the importance of prompt medical care.

Information collected for each patient was age, sex, place of residence, clinical form of plague, date of illness onset, outcome, and whether an unusual number of dead rats (a rat die-off) had been noted in the village preceding illness. We performed data management and analyses in Microsoft Excel (Microsoft, Redmond, WA, USA) and Epi Info version 7.1.1.14 (CDC, Atlanta, Georgia, USA) and used Fisher exact or χ^2 tests for comparisons, as appropriate.

Results

A total of 255 human plague cases were reported in the West Nile region of Uganda during 2008–2016. Overall, 140 (55%) cases were classified as suspected, 37 (15%) as probable, and 78 (31%) as confirmed, including 53 confirmed by culture only, 8 by serology only, and 17 by both culture and serology. Bacterial culture was attempted for 246 (96%) cases, and convalescent serum was available for 109 (43%) cases. Among those with negative culture results and available convalescent serum samples, 79 (89%) also had negative serologic testing results.

Although yearly case counts varied widely (Figure 1), approximately three fourths of all cases, regardless of case status, occurred during October–January. Cases were identified in 130 villages in 38 parishes and 2 counties (Vurra County in Arua District and Okoro County in Zombo District; Figure 2); a total of 51 villages had ≥1 confirmed or probable plague case. Most confirmed cases (49/77; 64%) were not isolated incidents but occurred with epidemiologic linkage to ≥1 additional confirmed case.

Overall median age of patients was 11 (range 1–70) years; 51% were women or girls. Among confirmed and probable cases, the sex distribution was equal among those <10 years of age, skewed toward the male sex among 10–14-year-olds, and strongly skewed toward the female sex among those ≥15 years of age (Figure 3). Most patients (217/255; 85%) had symptoms of bubonic plague, and the remainder were evenly split between patients with symptoms of septicemic (n = 20) or pneumonic plague (n = 18). Approximately one third of all cases, whether they were bubonic, septicemic, or pneumonic plague, were laboratory confirmed (Table).
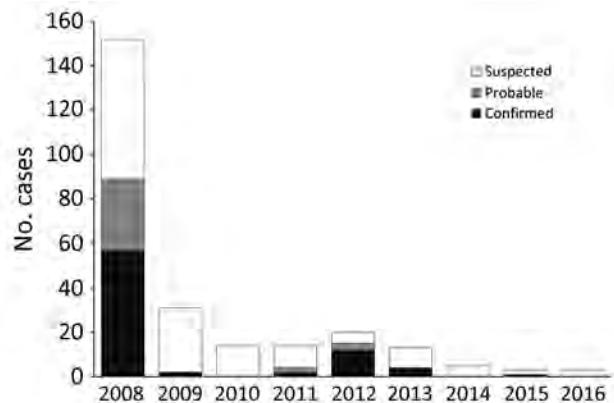
Figure 1. Suspected, probable, and confirmed human plague cases, by year, West Nile region, Uganda, 2008–2016.
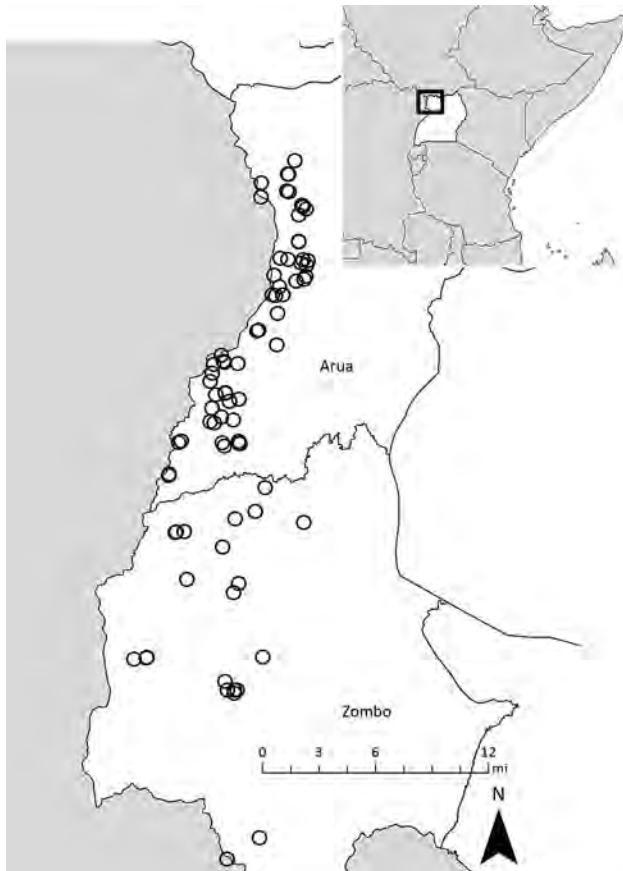
Figure 2. Residence locations of confirmed and probable human plague cases, by district, West Nile region, Uganda, 2008–2016. Inset shows location of Uganda in Africa.

Among the 253 cases with outcomes reported, 37 (15%) were fatal (Table). Nine (7%) of 138 patients with suspected plague died, compared with 8 (22%) of 37 patients with probable plague and 20 (26%) of 78 patients with confirmed plague (p<0.001). As expected, the mortality rate was higher among patients with signs and symptoms of pneumonic plague; 8 (44%) of 18 patients with a pneumonic plague died compared with 27 (13%) of 215 patients with a bubonic plague and 2 (10%) of 20 patients with a septicemic plague (Table). The overall mortality rate did not differ significantly between children and adults: 22 (13%) deaths occurred among persons <18 years of age and 15 (19%) among persons ≥18 years of age. The case-fatality rate did not differ by sex: 18 (16%) men and boys and 19 (15%) women and girls died. Among the 19 patients who did not seek care from a clinic or hospital, 17 (89%) were eventually classified as having confirmed or probable cases, and 15 (79%) died. Among the persons who sought care from a health clinic, the time between reported illness onset and notification of public health authorities was a median of 1 day (range 0–8 days).

Information on rat die-offs was available for all but 3 cases. Rat die-offs were noted around the time of illness onset in the villages of 98 (87%) of 113 patients with confirmed or probable plague, compared with only 65 (47%) of 139 patients whose infection remained unconfirmed after laboratory testing (odds ratio 7.4, 95% CI 3.9–14.1). The positive predictive value of rat die-offs for laboratory confirmation was 60%; the negative predictive value was 83%.

Discussion

Historical reports link the appearance of plague in Uganda to the construction of the Uganda railway during 1896–1901, a period when plague was spreading throughout many parts of the world (9). Plague is believed to have been present for several decades in the more southern part of the West Nile region (Okoro County, Zombo District), appearing in Vurra County of Arua District only in the late 1990s (15). During 2008–2016, laboratory-confirmed human plague occurred in >50 villages throughout the region. These villages were located throughout the westernmost part of the West Nile region, above the Rift Valley escarpment, where the elevation is generally >1,300 m, rainfall is high, and average temperature is relatively low compared with the neighboring lowlands (11,16–18). As is the case in other plague-endemic areas, human cases were highly episodic; 89 confirmed and probable cases were reported in 2008, only 4–15 in 2011–2013, and just 0–2 in the remaining years of the reporting period. Along with temporal clustering, confirmed cases tended to cluster spatially, with most occurring in association with other confirmed cases. Because all suspected cases were actively investigated, this clustering is unlikely to be explained by ascertainment bias. The demographic features, clinical forms, and seasonality of infection among these cases were similar to other reports from the region (15,19).

With a case-fatality rate of 15% overall and 26% among confirmed cases, plague mortality in the West Nile region is similar to the case-fatality rate in the United States but distinctly higher than that reported for Africa as a whole
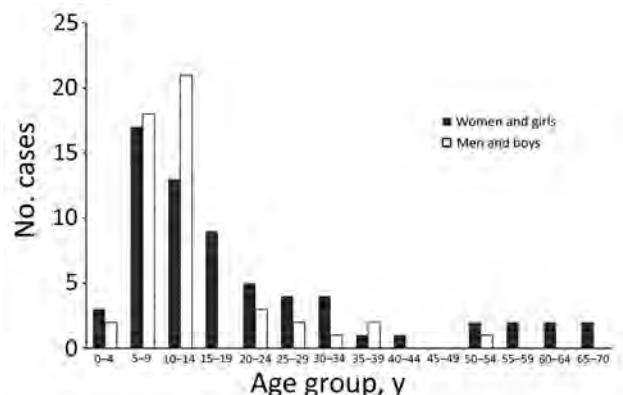
Figure 3. Confirmed and probable human plague cases, by sex and 5-year age group, West Nile region, Uganda, 2008–2016.

Table. Case status, clinical form, and mortality rate among human plague cases, West Nile region, Uganda, 2008–2016*

Clinical form	Case status, no. patients (mortality rate, %)			
	Confirmed	Probable	Suspected	Total
Bubonic	66 (26)	26 (8)	123 (7)	215 (13)
Pneumonic	6 (50)	5 (80)	7 (14)	18 (44)
Septicemic	6 (0)	6 (33)	8 (0)	20 (10)
Total	78 (26)	37 (22)	138 (7)	253 (15)
*Outcome was known for 253 of 255 total cases. The 2 suspected bubonic cases with unknown outcomes were excluded.				

(*8,10,20*). Although the clinical features of plague can be distinctive, they are not pathognomonic. In our series, many suspected cases failed to be confirmed despite laboratory testing. Although negative results might have resulted from prior self-treatment with antimicrobial drugs in some cases, it is likely that a proportion of suspected cases were, in fact, not plague. Convalescent serum samples were available for roughly half of all culture-negative cases, and among those, nearly 90% lacked immunologic reactivity to *Y. pestis*. If many suspected cases were not plague, this fact would simultaneously explain the lower mortality rate for clinically defined cases and underscore the need for diagnostic testing when plague is suspected. Even in an outbreak setting, clinically similar illnesses might be misattributed to plague (*21*).

In the West Nile region, plague occurs most commonly among children and women, a trend that has been attributed to children and women sleeping more often on the ground and in the structures where food is stored (*15,20*). It is unclear, however, why boys 10–14 years of age were more affected than girls of the same age in this setting; perhaps behavioral practices common among boys approaching maturity put them in greater contact with rodents and their fleas. The male preponderance in this age group could also be simply a reflection of small number bias, given the lack of confirmed or probable cases among men and boys in the next older age group.

Molecular analyses of *Y. pestis* cultures have revealed that human illnesses in this region are caused by 2 distinct subtypes: 1 occurring predominantly in the Arua District and the other in the Zombo District (*22*). This finding, supported by multiple subtyping methods, suggests that separate enzootic cycles of *Y. pestis* occur in these respective areas, possibly with different ecologic drivers, although no substantive differences in pathogenicity or other epidemiologic features exist among illnesses in the 2 districts.

Plague is less common than many other infectious diseases, yet it retains public health importance as a disease with epidemic potential. Although potentially fatal, plague is readily treatable if appropriate therapy is initiated early. Multifaceted educational engagement efforts are needed in endemic areas to reduce *Y. pestis* disease severity and death. Although rat die-offs or rat falls have been noted throughout history to precede human outbreaks (*9*), quantitative data to support these events as predictors of human plague have been lacking. We found a strong association between recognition of a rat die-off by villagers around dates of illness onset and illnesses being confirmed as plague. Engagement of communities in plague-endemic areas to encourage the prompt notification of local authorities when a rat die-off occurs could reduce the likelihood of subsequent human infection if followed by timely application of flea control products in nearby homes. Local educational efforts through schools and the engagement of village health teams and traditional healers to recognize the signs of plague and refer villagers with suspected plague to health clinics during early illness should be sustainable interventions that could prevent larger-scale human outbreaks and reduce plague mortality rates.

Although robust laboratory capacity was available in the region during the period we summarize, logistical challenges, such as impassable roads during the rainy season, can limit timely laboratory testing for plague in rural Africa. Sensitive and specific point-of-care diagnostic assays could improve plague diagnosis and help guide appropriate treatment in resource-limited settings.

Dr. Forrester was an Epidemic Intelligence Service officer with the Division of Vector-Borne Diseases, National Center for Emerging and Zoonotic Infectious Diseases, Centers for Disease Control and Prevention, Fort Collins, Colorado, USA, from 2013–2015. He is currently a chief resident in general surgery at Stanford University with an interest in public health, surgical infections, and trauma surgery.

References

1. Prentice MB, Rahalison L. Plague. Lancet. 2007;369:1196–207. http://dx.doi.org/10.1016/S0140-6736(07)60566-2
2. Perry RD, Fetherston JD. Yersinia pestis—etiologic agent of plague. Clin Microbiol Rev. 1997;10:35–66.
3. Gage KL, Kosoy MY. Natural history of plague: perspectives from more than a century of research. Annu Rev Entomol. 2005;50:505–28. http://dx.doi.org/10.1146/annurev.ento.50.071803.130337
4. Mead PS. Yersinia species (including plague). In: Bennett JE, Dolin R, Blaser MJ, editors. Principles and practice of infectious diseases. 8th ed. Philadelphia: Elsevier; 2015. p. 2607–18.
5. Begier EM, Asiki G, Anywaine Z, Yockey B, Schriefer ME, Aleti P, et al. Pneumonic plague cluster, Uganda, 2004. Emerg Infect Dis. 2006;12:460–7. http://dx.doi.org/10.3201/eid1203.051051
6. Bertherat E, Thullier P, Shako JC, England K, Koné ML, Arntzen L, et al. Lessons learned about pneumonic plague diagnosis from

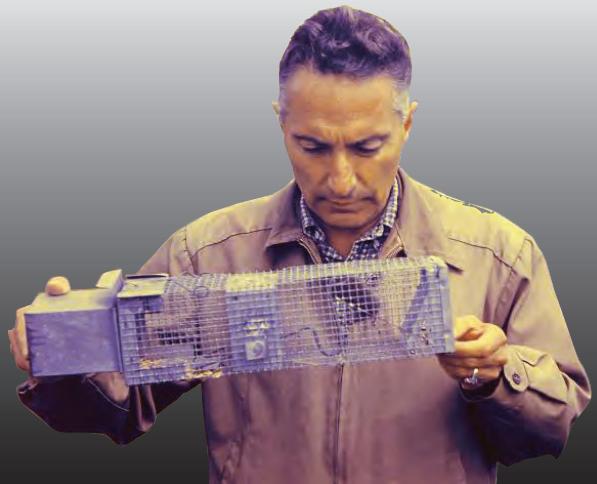two outbreaks, Democratic Republic of the Congo. Emerg Infect Dis. 2011;17:778–84. http://dx.doi.org/10.3201/eid1705.100029

7. Richard V, Riehm JM, Herindrainy P, Soanandrasana R, Ratsitoharina M, Rakotomanana F, et al. Pneumonic plague outbreak, northern Madagascar, 2011. Emerg Infect Dis. 2015;21:8–15. http://dx.doi.org/10.3201/eid2101.131828

8. Kugeler KJ, Staples JE, Hinckley AF, Gage KL, Mead PS. Epidemiology of human plague in the United States, 1900–2012. Emerg Infect Dis. 2015;21:16–22. http://dx.doi.org/10.3201/eid2101.140564

9. Pollitzer R. Plague. Geneva: World Health Organization; 1954.

10. Bertherat E. Plague around the world, 2010–2015. Wkly Epidemiol Rec. 2016;91:89–93.

11. Winters AM, Staples JE, Ogen-Odoi A, Mead PS, Griffith K, Owor N, et al. Spatial risk models for human plague in the West Nile region of Uganda. Am J Trop Med Hyg. 2009;80:1014–22.

12. Centers for Disease Control and Prevention. Bubonic and pneumonic plague—Uganda, 2006. MMWR Morb Mortal Wkly Rep. 2009;58:778–81.

13. Poland J, Dennis D. Diagnosis and clinical manifestations. Plague manual: epidemiology, distribution, surveillance, and control. Geneva: World Health Organization; 1999.

14. Apangu T, Griffith K, Abaru J, Candini G, Apio H, Okoth F, et al. Successful treatment of human plague with oral ciprofloxacin. Emerg Infect Dis. 2017;23:553–5. http://dx.doi.org/10.3201/eid2303.161212

15. Orochi Orach S. Plague outbreaks: the gender and age perspective in Okoro County, Nebbi District, Uganda. Nebbe (Uganda): Uganda Agency for Accelerated Regional Development; 2003.

16. Eisen RJ, MacMillan K, Atiku LA, Mpanga JT, Zielinski-Gutierrez E, Graham CB, et al. Identification of risk factors for plague in the West Nile region of Uganda. Am J Trop Med Hyg. 2014;90:1047–58. http://dx.doi.org/10.4269/ajtmh.14-0035

17. MacMillan K, Enscore RE, Ogen-Odoi A, Borchert JN, Babi N, Amatre G, et al. Landscape and residential variables associated with plague-endemic villages in the West Nile region of Uganda. Am J Trop Med Hyg. 2011;84:435–42. http://dx.doi.org/10.4269/ajtmh.2011.10-0571

18. Moore SM, Monaghan A, Griffith KS, Apangu T, Mead PS, Eisen RJ. Improvement of disease prediction and modeling through the use of meteorological ensembles: human plague in Uganda. PLoS One. 2012;7:e44431. http://dx.doi.org/10.1371/journal.pone.0044431

19. Kilonzo BS. Plague epidemiology and control in eastern and southern Africa during the period 1978 to 1997. Cent Afr J Med. 1999;45:70–6.

20. Davis S, Makundi RH, Machang'u RS, Leirs H. Demographic and spatio-temporal variation in human plague at a persistent focus in Tanzania. Acta Trop. 2006;100:133–41. http://dx.doi.org/10.1016/j.actatropica.2006.10.006

21. Bertherat E, Mueller MJ, Shako JC, Picardeau M. Discovery of a leptospirosis cluster amidst a pneumonic plague outbreak in a miners' camp in the Democratic Republic of the Congo. Int J Environ Res Public Health. 2014;11:1824–33. http://dx.doi.org/10.3390/ijerph110201824

22. Respicio-Kingry LB, Yockey BM, Acayo S, Kaggwa J, Apangu T, Kugeler KJ, et al. Two distinct Yersinia pestis populations causing plague among humans in the West Nile region of Uganda. PLoS Negl Trop Dis. 2016;10:e0004360. http://dx.doi.org/10.1371/journal.pntd.0004360

Address for correspondence: Paul S. Mead, Centers for Disease Control and Prevention, 3156 Rampart Rd, Fort Collins, CO 80521, USA; email: pfm0@cdc.gov

Protective Effect of Val$_{129}$-PrP against Bovine Spongiform Encephalopathy but not Variant Creutzfeldt-Jakob Disease

Natalia Fernández-Borges,[1] Juan Carlos Espinosa,[1] Alba Marín-Moreno, Patricia Aguilar-Calvo, Emmanuel A. Asante, Tetsuyuki Kitamoto, Shirou Mohri, Olivier Andréoletti, Juan María Torres

Bovine spongiform encephalopathy (BSE) is the only known zoonotic prion that causes variant Creutzfeldt-Jakob disease (vCJD) in humans. The major risk determinant for this disease is the polymorphic codon 129 of the human prion protein (Hu-PrP), where either methionine (Met$_{129}$) or valine (Val$_{129}$) can be encoded. To date, all clinical and neuropathologically confirmed vCJD cases have been Met$_{129}$ homozygous, with the exception of 1 recently reported Met/Val heterozygous case. Here, we found that transgenic mice homozygous for Val$_{129}$ Hu-PrP show severely restricted propagation of the BSE prion strain, but this constraint can be partially overcome by adaptation of the BSE agent to the Met$_{129}$ Hu-PrP. In addition, the transmission of vCJD to transgenic mice homozygous for Val$_{129}$ Hu-PrP resulted in a prion with distinct strain features. These observations may indicate increased risk for vCJD secondary transmission in Val$_{129}$ Hu-PrP–positive humans with the emergence of new strain features.

The presence of variant Creutzfeldt-Jakob disease (vCJD) is considered by strong epidemiologic, pathologic, and molecular evidence to be a likely consequence of human dietary exposure to the bovine spongiform encephalopathy (BSE) agent (1–3). Secondary vCJD infection has occurred through iatrogenic routes such as blood transfusion (4–7). The pathogenesis of these fatal transmissible spongiform encephalopathies (TSEs), called prion diseases, is associated with the accumulation of the abnormal isoform (PrP^{Sc}) of prion protein (PrP), which is converted from the normal cellular isoform (PrP^{C}) (8). This conversion process involves a posttranslational conformational change of PrP^{C} and PrP^{Sc} that can be distinguished biochemically from PrP^{C} by its partial resistance to proteolysis and detergent insolubility (9,10).

The neuropathological features of vCJD are characterized by the presence of abundant florid PrP plaques and the propagation of type 4 disease-related PrP^{Sc} in the brain (1,11). Differences in the level of glycosylation, as well as in the size of protease-digested PrP^{Sc}, are widely used as surrogates of prion strain typing; 2 main classifications are recognized in the prion field (1,12). According to 1 of these classifications (1,13), type 4 PrP^{Sc} is characterized by a fragment size and glycoform ratio similar to that seen in BSE and BSE transmitted to several other species, with a predominance of the diglycosylated PrP glycoform (1,13–15).

Polymorphism at codon 129 of the human PrP gene (*PRNP*), where methionine (Met) or valine (Val) can be encoded, strongly affects susceptibility to human prion diseases (16–20). vCJD has only been neuropathologically confirmed in persons homozygous for Met at residue 129 of human PrP (21), with 1 exception of heterozygosity (Met/Val) at this codon (22). In addition, asymptomatic peripheral involvement in vCJD infection has been reported in 2 Met/Val$_{129}$-positive persons (5,7). Retrospective studies of the prevalence of subclinical vCJD infection using appendectomy and tonsillectomy specimens in the United Kingdom described 6 appendixes that were positive for disease-associated prion protein in Val/Val$_{129}$ persons (23–25). All of these human studies, in addition to the extremely prolonged and variable incubation periods seen in prion transmission experiments when crossing a species barrier, suggest that persons encoding any of the 3 human PrP codon 129 genotypes may be susceptible to vCJD, including secondary vCJD transmitted through blood transfusion, blood products, tissue and organ transplantation, and other iatrogenic routes.

Because only 1 definite case of heterozygous Met/Val$_{129}$ vCJD and no homozygous Val$_{129}$ cases have been described, it is unknown whether the clinicopathologic

Author affiliations: Centro de Investigación en Sanidad Animal, Instituto Nacional de Investigación y Tecnología Agraria y Alimentaria (CISA-INIA); Valdeolmos, Madrid, Spain (N. Fernández-Borges, J.C. Espinosa, A. Marín-Moreno, P. Aguilar-Calvo, J.M. Torres); MRC Prion Unit, Department of Neurodegenerative Disease, University College London, Institute of Neurology, London, UK (E.A. Asante); Tohoku University Graduate School of Medicine, Sendai, Japan (T. Kitamoto, S. Mohri); UMR INRA ENVT 1225, Interactions Hôtes Agents Pathogènes, Ecole Nationale Vétérinaire de Toulouse, Toulouse, France (O. Andréoletti)

[1]These authors contributed equally to this article.

characteristics and biochemical properties of vCJD would appear in persons with these codon 129 genotypes. To gain insights into that question, vCJD/BSE transmission studies in which either humanized overexpressing or knock-in transgenic mice were used have been performed (2,26–30). However, some discrepancies in the transmission efficiency of vCJD to humanized knock-in transgenic mice can be found, depending on the origin of the mice and on the vCJD isolate (29,30). Previous studies in humanized overexpressing transgenic mice revealed that the 3 human PrP codon 129 genotypes can be infected with vCJD but show significant differences depending on the genotype. Moreover, mice with the Val/Val$_{129}$ genotype were more susceptible to vCJD infection than expected but lack the neuropathological characteristics observed with Met/Met$_{129}$ (2,26–28).

In this study, we evaluated the zoonotic potential of BSE and BSE adapted to different species by using transgenic mice overexpressing similar levels of human PrP^C carrying Met/Met, Met/Val, or Val/Val at position 129 of human PrP. Furthermore, we used these models to re-evaluate the potential for human-to-human spread of vCJD, as well as the differential susceptibility and characteristics of the transmitted disease across the different *PRNP* codon 129 genotypes in humans.

Materials and Methods

Ethics Statement
We carried out animal experiments in strict accordance with the recommendations in the guidelines of the Code for Methods and Welfare Considerations in Behavioral Research with Animals (Directive 86/609EC and 2010/63/EU), and all efforts were made to minimize suffering. Experiments were approved by the Committee on the Ethics of Animal Experiments of the Instituto Nacional de Investigación y Tecnología Agraria y Alimentaria (Madrid, Spain; permit nos. CEEA2012/024 and CEEA2009/004).

TSE Isolates
We used 11 isolates from different sources in this study (Table 1 [31–39]). For mouse inoculation, we prepared all isolates from brain tissues as 10% weight/volume (wt/vol) homogenates in 5% glucose. We performed second passages by inoculating transgenic mice with 10% (wt/vol) homogenates in 5% glucose of brains selected from passage 1.

Mouse Transmission Studies
We inoculated all isolates in 3 different transgenic mouse models: 1) HuPrP-Tg340-Met$_{129}$ (TgMet$_{129}$) mouse line expressing human Met$_{129}$-PrP^C variant (31); 2) HuPrP-Tg361-Val$_{129}$ (TgVal$_{129}$) mouse line expressing human Val$_{129}$-PrP^C variant (40); and 3) HuPrP-Tg351-Met/Val$_{129}$ (TgMet/Val$_{129}$) transgenic mouse line obtained by mating TgMet$_{129}$ and TgVal$_{129}$ mice (40). All of these transgenic lines show similar brain expression levels of PrP^C (around 4-fold the level of expression in the human brain) on a mouse PrP null background. We performed additional inoculations in HuPrP-Tg362-Val$_{129}$, a transgenic mouse line expressing 8-fold the level of PrP^C expression in human brain (TgVal$_{129}$ [8×]) (41). We performed subsequent bioassays for the detection of low-level propagation of infectious BSE and BSE-derived prions in BoPrP-Tg110 mice, which are highly susceptible to vCJD prions (42,43), probably caused by the trace-back phenomenon (30).

We anesthetized individually identified mice, 6–7 weeks of age, with isoflurane and inoculated them with a 2-mg equivalent of brain homogenate in the right parietal lobe by using a 25-gauge disposable hypodermic needle. We observed mice daily and assessed neurologic status 2 times per week. When progression of a TSE disease was evident or at the established experimental endpoint (700 days postinoculation [dpi]), we euthanized the animal for ethical reasons and performed necropsy, excising the brain. We then fixed part of the brain by immersion

Table 1. Description of prion isolates used in analysis of BSE and CJD*

Isolate	Sample codification	Description (reference)	Supplier†
Hu-sCJD MM1	BC 1011	sCJD PrP-Met$_{129}$ type 1 human natural case	BHUFA
Hu-sCJD VV2	BC 1452	sCJD PrP-Val$_{129}$ type 2 human natural case	BHUFA
Hu-TSE negative		TSE free human brain	NIBSC
Ca-BSE$_0$	Fr (139)	BSE naturally infected cow (31,32)	INRA
Ca-BSE$_2$	UK (PG1199/00)	BSE naturally infected cow (33,34)	VLA
Ca-BSE$_0$/TgPo	Ca-BSE$_0$/Tg001	BSE transmitted experimentally to porcine transgenic mice (32)	CISA
Ca-BSE$_0$/Sh(ARQ)	Fr (ARQ0)	Pool of brains from terminally ill ARQ/ARQ sheep inoculated with Ca-BSE (31,32)	INRA
Ca-BSE/Go	gBSE-P12	Pool of brains from 3 terminally ill wild type goats inoculated with a mixture of 4 cattle-BSE field cases (35–37)	Roslin
Go-BSE	Fr (CH636)	Goat BSE case (38)	AFSSA
Hu-vCJD$_1$	UK (NHBY/0014)	vCJD PrP-Met$_{129}$ human infected case (39)	NIBSC
Hu-vCJD$_2$	BC 1458	vCJD PrP-Met$_{129}$ human infected case	BHUFA

*BSE, bovine spongiform encephalopathy; Ca, cattle; CJD, Creutzfeldt-Jakob disease; Go, goat; Hu, human; Met$_{129}$, methionine; PrP, prion protein; sCJD, sporadic CJD; TSE, transmissible spongiform encephalopathy; Val$_{129}$, valine; vCJD, variant CJD.
†AFSSA, Agence Française de Sécurité Sanitaire des Aliments National TSE Reference Laboratory, Lyon, France; BHUFA, Biobanco Hospital Universitario Fundación Alcorcón, Madrid, Spain; CISA, Centro de Investigación en Sanidad Animal, Madrid, Spain; INRA, French National Institute for Agricultural Research, Nouzilly, France; NIBSC, National Institute for Biologic Standards and Control Creutzfeld-Jakob Disease Resource Centre, South Mimms, Potters Bar, United Kingdom; Roslin, The Roslin Institute and Royal (Dick) School of Veterinary Studies, University of Edinburgh, Easter Bush, Midlothian, United Kingdom; VLA, Veterinary Laboratory Agency, New Haw. Addlestone, Surrey, United Kingdom.

in neutral-buffered 10% formalin (4% 2-formaldehyde) and used the tissue for quantifying spongiform degeneration by histopathology. We froze the remaining tissue at –20°C and used it to determine the presence of disease-associated proteinase K (PK)–resistant PrP (PrP^{res}) by Western blot.

In all cases, we calculated mouse survival time and disease attack rate for each isolate. We expressed survival times as mean ±SD of the dpi for all mice positive for PrP^{res}. We defined the attack rate as the proportion of all inoculated mice whose samples tested positive for PrP^{res}. We used brain homogenates from PrP^{res}-positive mice, where available, for further passaging. When all mice were scored negative for PrP^{res} on primary passage, we used PrP^{res}-negative brain homogenates for second passage.

Western Blot

We homogenized frozen brain tissues (175 ± 20 mg) in 5% glucose in distilled water in grinding tubes (Bio-Rad, Hercules, CA, USA) adjusted to 10% (wt/vol) by using a TeSeE Precess 48TM homogenizer (Bio-Rad), according to the manufacturer's instructions. We determined presence of PrP^{res} in transgenic mouse brains by Western blot, using the reagents of the ELISA commercial test TeSeE (Bio-Rad). Based on a previously described protocol (31), we treated 10–100 µL of 10% wt/vol brain homogenates with proteinase K; the resulting samples were loaded in 12% Bis-Tris Gel (Criterion XT; Bio-Rad). We transferred proteins electrophoretically onto PVDF membranes (Millipore, Billerica, MA, USA), which were blocked overnight with 2% BSA blocking buffer (Sigma-Aldrich, St. Louis, MO, USA). For immunoblotting, we incubated with Sha 31 (44) monoclonal antibody (mAb) at a concentration of 1 µg/mL to identify the 145-WEDRYYRE-152 epitope of the human PrP^C sequence. To detect immunocomplexes, we incubated the membranes for 1 h with horseradish peroxidase conjugated anti-mouse IgG (GE Healthcare Amersham Biosciences, Little Chalfont, UK). Immunoblots were developed with enhanced chemiluminiscence ECL Select (GE Healthcare Amersham Biosciences). Images were captured using the ChemiDoc WRS+ System (Bio-Rad) and processed using Image Lab 5.2.1 software (Bio-Rad).

Histopathological Analysis

We performed procedures for the histopathological analysis of mouse brains as previously described (45). We immediately fixed mouse brain samples in neutral-buffered 10% formalin (4% 2-formaldehyde) during necropsy and embedded the tissues in paraffin later. After deparaffinization, we stained 2 µm–thick tissue slices with hematoxylin and eosin and established lesion profiles by using published standard methods (46). We conducted paraffin-embedded tissue (PET) blots as previously described (47).

Results

BSE Resistance in TgVal$_{129}$ Mice

To evaluate the relative susceptibility of the 3 human *PRNP* codon 129 genotypes to BSE, we performed serial transmission studies in 3 transgenic mouse lines expressing human PrP. These mouse lines were homozygous for Met (TgMet$_{129}$) or Val (TgVal$_{129}$) at codon 129 of human PrP or were their F1 cross (TgMet/Val$_{129}$). These mouse models expressed similar human PrP levels, ≈4-fold more than that seen in uninfected human brain tissue (40). We observed no clinical signs of prion disease or PrP^{res} accumulation in control mice inoculated with TSE-free control brain homogenate. The 3 human transgenic mouse models were readily infected when inoculated with sporadic CJD (sCJD) (Table 2). The 2 sCJD cases used as inocula in this study were classified as Met$_{129}$ type 1 (Hu-sCJD MM1) and Val$_{129}$ type 2 (Hu-sCJD VV2) (12) on the basis of the patient's *PRNP* genotype at codon 129 and the PrP^{res} Western blot profiles of these samples.

We inoculated the 3 mouse models intracerebrally with a panel of BSE isolates from different species (cattle, pig, sheep, and goat; Table 2). As previously described in TgMet$_{129}$ mice (31), we found a higher transmission efficiency adjudged by comparatively higher attack rates for BSE isolates previously passaged in other species than for cattle BSE, suggesting a strong transmission barrier to cattle BSE in these mice.

At completion of the first and second passages, none of the TgVal$_{129}$ mice challenged with the different BSE isolates developed clinical disease, and no PrP^{res} accumulation was found in their brains (Table 2). Because of intercurrent illnesses, the group of TgVal$_{129}$ mice challenged with Ca-BSE$_2$ was considerably reduced in size; however, the absence of transmission to TgVal$_{129}$ mice challenged with a second BSE inocula, Ca-BSE$_0$, reinforces this negative result. In addition, results of subsequent passage of brain homogenates from these mice to BoPrP-Tg110 mice were negative, ruling out the presence of subclinical infection, with the exception of TgVal$_{129}$ mice inoculated with Go-BSE. For this isolate, 3 of 6 BoPrP-Tg110 mouse brains showed detectable PrP^{res} and had a long incubation time of 427 ± 38 dpi, suggesting very low infectivity (online Technical Appendix Table 1, https://wwwnc.cdc.gov/eid/article/23/9/16-1948-Techapp.pdf).

To confirm that the lack of susceptibility of TgVal$_{129}$ mice to cattle BSE and to BSE previously adapted in different species was not caused by inadequate PrP substrate, we used the TgVal$_{129}$ (8×) mouse line (41). However, even under these high human PrP expression level conditions, none of the inoculated TgVal$_{129}$ (8×) mice showed any evidence of infection after challenge with the different BSE isolates (online Technical Appendix Table 2). This result indicates that even an increase in the TgVal$_{129}$ PrP expression level is not enough to allow transmission of BSE prions, irrespective of the species in which BSE has been previously passaged.

Table 2. Transmission of cattle, porcine, sheep, and goat BSE isolates to mice in transgenic mouse lines TgMet$_{129}$, TgMet/Val$_{129}$, and TgVal$_{129}$*

| | Mean survival time, d ±SD (no. PrP^{res}-positive/inoculated animals) [reference]†‡ | | | | | |
| | TgMet$_{129}$ | | TgMet/Val$_{129}$ | | TgVal$_{129}$ | |
Isolates	First passage	Second passage	First passage	Second passage	First passage	Second passage
Hu-sCJD MM1	219 ±17 (6/6) [40]	239 ±8 (6/6) [40]	243 ±14 (6/6) [40]	260 ±13 (6/6) [40]	327 ±19 (6/6) [40]	286 ±16 (6/6) [40]
Hu-sCJD VV2	618 ±81 (6/6) [40]	509 ±41 (6/6) [40]	588 ±74 (6/6) [40]	594 ±86 (6/6) [40]	168 ±12 (6/6) [40]	169 ±12 (6/6) [40]
Hu-TSE negative	>700‡ (0/6)	>700‡ (0/6)	>700‡ (0/6)	>700‡ (0/6)	>700‡ (0/6)	>700‡ (0/6)
Ca-BSE$_0$	739 (1/6) (31)	633 ±32 (6/6)	>700‡ (0/6)	>700‡ (0/6)	>700‡ (0/6)	>700‡ (0/6)
Ca-BSE$_2$	491 ±60 (0/9) [31]	572 ±37 (3/4) [31]	>700‡ (0/5)	ND	>700‡ (0/3)§	>700‡ (0/3§
Ca-BSE/TgPo	653 ±45 (3/5)	ND	ND	ND	>700‡ (0/6)	ND
Ca-BSE/Sh(ARQ)	615 ±84 (4/6) [31]	564 ±39 (5/5) [31]	>700b (0/6)	>700‡ (0/6)	>700‡ (0/6)	>700‡ (0/6)
Ca-BSE/Go	>700‡ (5/5)	>700‡ (5/5)	476 (1/10)	ND	>700‡ (0/5)¶	ND
Go-BSE	683 ± 36 (6/6)	675 ± 36 (5/5)	>700‡ (0/6)	ND	>700‡ (0/6)	ND

*BSE, bovine spongiform encephalopathy; Ca, cattle; CJD, Creutzfeldt-Jakob disease; Go, goat; Hu, human; Met$_{129}$, methionine; ND, not done; PrP^{res}, proteinase K–resistant PrP; sCJD, sporadic CJD; Val$_{129}$, valine; vCJD, variant CJD.
†Survival time is indicated for all mice that scored positive for PrP^{res}
‡Animals without clinical signs were euthanized at 700 dpi.
§Three additional animals were culled before the end of the experiment because of intercurrent illnesses; all were negative for brain PrP^{res} by using Western blot.
¶Positive subclinical infection tested in Bo-Tg110 mice.

In a similar manner to that seen in the TgVal$_{129}$ mice, we observed no clinical disease and no disease-associated PK-resistant PrP accumulation on first or second passage of the different BSE isolates in TgMet/Val$_{129}$ mice. However, we did observe an exception in 1 TgMet/Val$_{129}$ mouse inoculated with Go-BSE without clinical signs but with a positive score for brain PrP^{res} that died at 476 dpi (Table 2). These findings support the interpretation that human-PrP Val$_{129}$ polymorphism severely restricts propagation of the BSE prion strain independently of the species in which it had previously been adapted.

BSE Adaptation to the Human PrP Sequence

In parallel to the transmission experiments with the different BSE isolates, we also inoculated the 3 humanized transgenic mouse models with human brain material from 2 different cases of vCJD PrP-Met$_{129}$ (Hu-vCJD$_1$ and Hu-vCJD$_2$).

On first passage, 100% of the TgMet$_{129}$ mice developed clinical disease in response to all inocula in the panel (Table 3). However, only the inoculum Hu-vCJD$_2$ previously passaged in TgMet/Val$_{129}$ mice caused clinical disease in the same heterozygous genotype upon serial passages; the rest of the inocula caused only subclinical infections in this genotype (Table 3).

The PrP^{res} molecular profile (Figure 1, panel A, lanes 2, 3, and 5; Figure 1, panel B) and the PrP^{res} distribution patterns on paraffin-embedded tissue (PET) blots in the mouse brains (Figure 2, panels A, B, C) were similar in both the TgMet$_{129}$ and TgMet/Val$_{129}$ mice, with or without clinical disease. However, we consistently observed a lower PrP^{res} accumulation in TgMet/Val$_{129}$ mice compared with TgMet homozygous animals, particularly in the hippocampus area, probably caused by a slower conversion rate of PrP^{Sc} in these animals with a half dose of PrP-Met$_{129}$.

Table 3. Intracerebral inoculation of transgenic mice that express human PrP with vCJD and with vCJD previously adapted in TgMet$_{129}$ or TgMet/Val$_{129}$ mice*

| | Mean survival time, d ±SD (no. PrP^{res}-positive/inoculated animals) [reference]† | | |
Isolates	TgMet$_{129}$	TgMet/Val$_{129}$	TgVal$_{129}$
Hu-vCJD$_1$	626 ±29 (6/6) [31]	>700‡ (3/3)§	>700‡ (0/5)
Hu-vCJD$_1$→TgMet$_{129}$	650 ±60 (4/4)	>700‡ (5/5)	>700‡ (5/5)
Hu-vCJD$_2$	545 ±146 (5/5)	>700‡ (5/5)	>700‡ (0/6)#
Hu-vCJD$_2$→TgMet$_{129}$	564 ±39 (4/4)	>700‡ (5/5)	>700‡ (2/2)¶
Hu-vCJD$_2$→TgMet/Val$_{129}$	601 ±32 (5/5)	651 ±17 (7/7)	>700‡ (7/7)
Ca-BSE$_2$→TgMet$_{129}$	614 ±87 (6/6)	>700‡ (4/4)	>700‡ (3/4)
Ca-BSE/Sh(ARQ)→TgMet$_{129}$	534 ±55 (5/6)	>700‡ (5/6)	>700‡ (5/6)
Ca-BSE/Go→TgMet$_{129}$	609 ±67 (5/5)	>700‡ (4/4)	>700‡ (6/6)

*BSE, bovine spongiform encephalopathy; Ca, cattle; CJD, Creutzfeldt-Jakob disease; Go, goat; Hu, human; Met$_{129}$, methionine; PrP, prion protein; PrP^{res}, proteinase K–resistant PrP; sCJD, sporadic CJD; Val$_{129}$, valine; vCJD, variant CJD.
†Survival time is indicated for all mice scored positive for PrP^{res}.
‡Animals were euthanized without clinical signs at 700 dpi.
§Three additional animals had to be culled before the end of the experiment because of intercurrent illnesses; all were negative for brain PrP^{res} on WB.
¶Four additional animals had to be culled before the end of the experiment because of intercurrent illnesses; all were negative for PrP^{res} expression on Western blot.
#Positive subclinical infection tested in Bo-Tg110 mice.

In sharp contrast, none of the TgVal$_{129}$ mice challenged with the 2 vCJD primary inocula, Hu-vCJD$_1$ and Hu-vCJD$_2$, developed clinical disease and no PrP^{res} accumulation was found in their brains after Western blot (WB) analysis (Table 3). However, subsequent passage of brain homogenates from TgVal$_{129}$ mice inoculated with Hu-vCJD$_2$ (that remained apparently uninfected) to BoPrP-Tg110 mice showed evidence of subclinical infection. These subpassages led to a mean incubation time of 371 ± 5 dpi and to propagation of PrP^{res} that was detectable by WB in 100% of animals (online Technical Appendix Table 1), showing a biochemical pattern indistinguishable from that of cattle BSE infection in this mouse model.

These results suggest that the adaptation of the BSE agent to human PrP sequence could favor its transmission to the polymorphic human PrP Val$_{129}$ genotype. In this context, we passaged all isolates in TgMet$_{129}$ mice before subsequent inoculation in TgVal$_{129}$ mice. Although we did not observe clinical prion disease, the inoculated TgVal$_{129}$ mice had an infection rate remarkably close to 100%, as assessed by the presence of brain PrP^{res} at the end of the experiment (Table 3). We obtained similar results with the Hu-vCJD$_2$ isolate after 1 passage in TgMet/Val$_{129}$ mice and subsequent inoculation into TgVal$_{129}$ mice (Table 3). These observations support the hypothesis that adaptation of BSE agent to the human-PrP Met$_{129}$ amino-acid sequence promotes its transmission to human PrP Val$_{129}$–expressing hosts.

vCJD Prions in TgVal$_{129}$ Mice

Challenge of TgMet$_{129}$ or TgMet/Val$_{129}$ mice with vCJD prions resulted in faithful propagation of a typical PrP^{vCJD} (also named type 4), characterized by low size fragments (19-kDa fragment for the aglycosyl band) and prominent diglycosylated species on WB (Figure 1, panel A, lanes 2,
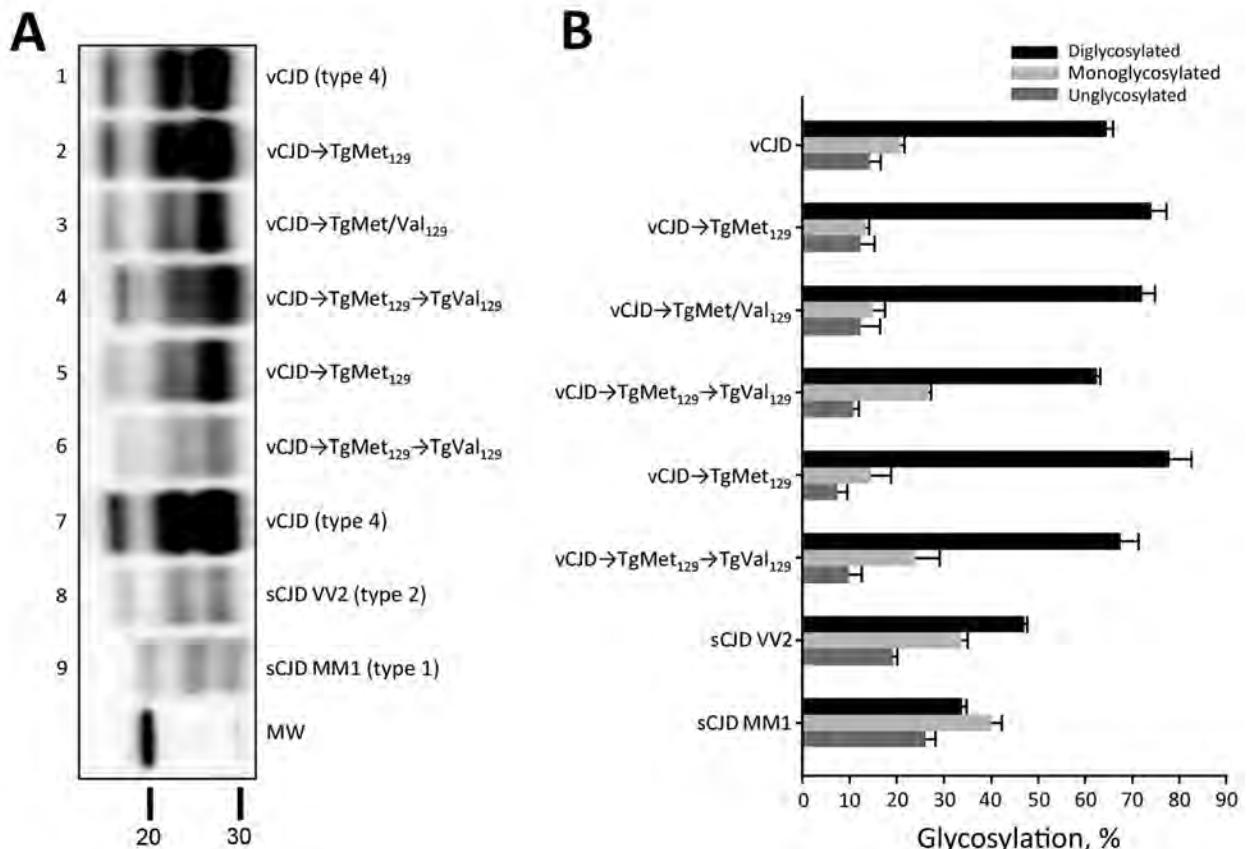
Figure 1. Biochemical features of the protease-resistant prion protein (PrP^{res}) detected in the brain of TgMet$_{129}$, TgMet/Val$_{129}$, and TgVal$_{129}$ mice inoculated with vCJD. A) PrP^{res} detected in TgMet$_{129}$ (lanes 2 and 5), TgMet/Val$_{129}$ (lane 3), and TgVal$_{129}$ (lanes 4 and 6) mice inoculated with vCJD brain homogenate or TgMet$_{129}$-passaged vCJD prions. Similar quantities of PrP^{res} were loaded for adequate comparison and immunoblots were detected with Sha31 monoclonal antibody (mAb). The original vCJD isolate (Hu-vCJD$_2$) used for mouse inoculations was also included in the blot (lanes 1 and 7). sCJD VV2 and MM1 isolates were included for biochemical comparative purposes (lanes 8 and 9, respectively). Molecular weight (MW) in kDa is shown. B) Glycoform analysis of PrP^{res} from TgMet$_{129}$, TgMet/Val$_{129}$, and TgVal$_{129}$ mice inoculated with vCJD brain homogenate or TgMet$_{129}$-passaged vCJD prions. PrP^{res} was detected by Western blot testing using the Sha31 mAb, as for panel A. The data shown are the means of ≥4 measurements in ≥2 different Western blots using the Image Lab (Bio-Rad, Hercules, CA, USA) program after capture with ChemiDoc XRS+ (Bio-Rad) under nonsaturating conditions. Error bars indicate SD. CJD, Creutzfeldt-Jakob disease; sCJD, sporadic CJD; vCJD, variant CJD.
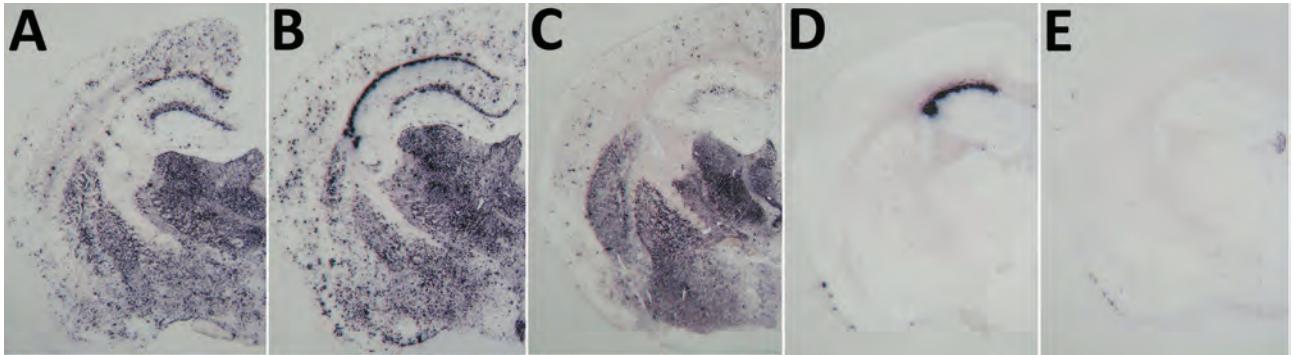
Figure 2. Protease-resistant prion protein distribution pattern in brains of prion protein humanized transgenic mice inoculated with variant Creutzfeldt-Jakob disease (vCJD) on second passage. A, B) TgMet$_{129}$ mice inoculated with vCJD. C) TgMet/Val$_{129}$ mice inoculated with vCJD. D, E) TgVal$_{129}$ mice inoculated with vCJD propagated in TgMet$_{129}$ mice. Original magnification ×20 for all panels.

3). These biochemical properties were accompanied by the key neuropathological hallmark of vCJD, the presence of abundant florid PrP plaques determined by immunohistochemical analysis of the brain (*31*) (data not shown).

In contrast, TgMet$_{129}$-passaged vCJD-inoculated TgVal$_{129}$ mice propagated a PrP^{Sc} with a WB signature that shared the same predominance of the diglycosylated glycoform seen in type 4 PrP^{Sc} but was distinguished by PK digestion products of greater molecular mass (Figure 1, panel A, lanes 4, 6), which closely resemble those seen in human type 2 PrP^{Sc} (Figure 1, panel A, lane 8). This differential biochemical pattern is associated with the presence of amyloid plaques restricted to the corpus callosum without a florid morphology. Moreover, we saw no specific vacuolar changes in the brains of these animals. PET blot analysis of these brains confirmed PrP^{Sc} deposition in corpus callosum and head of caudate nucleus in the brain of vCJD-inoculated TgVal$_{129}$ mice (Figure 2, panels D, E). However, PrP^{Sc} deposition was quite limited in comparison with those observed in vCJD-inoculated TgMet$_{129}$ (Figure 2, panels A, B) and TgMet/Val$_{129}$ mice (Figure 2, panel C).

These results resemble those previously described in a different TgVal$_{129}$ mouse line in which neuropathological and molecular features similar to those observed in our TgVal$_{129}$ were characterized (*2,27,28*). To prove the same PrP^{res} molecular profile identity between this previously characterized PrP^{Sc} (called type 5 PrP^{Sc}, vCJD→129VV Tg152c) and our vCJD-TgVal$_{129}$ PrP^{Sc}, we performed a biochemical characterization by WB and found no molecular profile differences in PrP^{res} from the various mouse lines (Figure 3, lanes 6 and 7). These particular molecular mass and glycoform profile characteristics seem to be a hallmark of vCJD transmission to human-PrP Val$_{129}$, since these features were also found in a different human-PrP Val$_{129}$ transgenic mouse line challenged with vCJD (vCJD→ Ki-Hu129V/V) (*26*) (Figure 3, lane 8). These results, suggesting vCJD prion infection can result in the generation of distinct molecular and neuropathological phenotypes

dependent on human-PrP polymorphic residue 129, are in accordance with those reported previously (*2,28,46*).

Discussion

We report a detailed comparison of the transmission properties of BSE and vCJD prions among humanized transgenic mice with different *PRNP* codon 129 genotypes. Because a high expression level of PrP in transgenic mice directly influences prion disease susceptibility and incubation time, these transgenic mice have an advantage over knock-in mice for evaluating these features in the different human PrP genotypes. In addition, the 3 mouse models used in our study have equivalent PrP expression levels, making them suitable for studying comparative susceptibilities across the different *PRNP* codon 129 genotypes.

In previous reports, we demonstrated that Met$_{129}$ homozygous individuals might be susceptible to a sheep or goat BSE agent to a higher degree than to cattle BSE and that these agents might transmit with molecular and neuropathological properties indistinguishable from those of vCJD (*31*). In this study, we wanted to extend these results to the other human *PRNP* genotypes: Met/Val$_{129}$ and Val/Val$_{129}$. We gained a different perspective when several BSE isolates adapted to different species inoculated in TgVal$_{129}$ mice showed an apparent lack of transmission. In addition, almost all inoculated TgMet/Val$_{129}$ mice did not transmit BSE; this finding supports the interpretation by Wadsworth et al. that human PrP Val$_{129}$ severely restricts propagation of the BSE prion strain (*27*).

An unexpected result of this study was the finding that 1 BSE isolate from a goat (Ca-BSE/Go) was clinically transmitted to 1 of 10 TgMet/Val$_{129}$ mice and subclinically transmitted to TgVal$_{129}$ mice. This particular isolate is characterized by a high infectious titer (*35*) that could explain the potential for this inoculum to overcome the restriction on BSE prions to propagate in TgVal$_{129}$ mice.

Although cattle BSE did not transmit to TgMet/Val$_{129}$ mice directly, adaptation of the BSE agent to human PrP

Met$_{129}$ sequence and subsequent inoculation of the resultant vCJD prions to TgMet/Val$_{129}$ mice produced a 100% attack rate. However, we did not detect clinical prion disease, supporting a slower rate of vCJD conversion compared with that among TgMet$_{129}$ mice. This slow but potential conversion rate in TgMet/Val$_{129}$ mice correlates well with the single vCJD case of a human carrying the PrP Met/Val$_{129}$ genotype (22) and with the description of subclinical secondary transmissions through human vCJD–infected tissues (4–7,47).

TgVal$_{129}$ mice challenged with Hu-vCJD$_2$ did not produce detectable brain PrP^{res} and clinical signs, in spite of the overexpression of HuPrP-Val$_{129}$ and the use of the more efficient intracerebral route of infection. However, subclinical infection in these TgVal$_{129}$ mice was demonstrated in BoPrP-Tg110 mice. These data suggest that PrP Val$_{129}$ could sustain a very slow and limited vCJD conversion rate that is consistent with the detection of PrP^{res} in tonsils and appendixes of asymptomatic PrP Val$_{129}$ persons (23–25). Previous studies of other transgenic mice expressing PrP Val$_{129}$ have also shown a low transmission efficiency of vCJD (2,27,30).

The fluctuating subclinical transmissibility of both vCJD inocula in TgVal$_{129}$ mice (negative for Hu-vCJD$_1$ and positive for Hu-vCJD$_2$) might be caused by differences in prion titer between inocula. This assessment was strengthened after the transmission of both vCJDs to TgMet$_{129}$ mice, in which a shorter incubation period was observed in animals inoculated with Hu-vCJD$_2$. A certain variability in subclinical transmissibility and incubation time between different vCJD isolates is not uncommon, as has been previously reported (2,27,30), suggesting that a Val$_{129}$ transmission barrier can only be overcome with highly infectious vCJD isolates.

The dramatic changes in the susceptibility of TgVal$_{129}$ mice (Table 3) challenged with vCJD isolates first passaged in TgMet$_{129}$ mice suggest an apparent increase in titer of both vCJD prion isolates; however, adaptation of the inocula to the new host mouse cannot be disregarded as being partly responsible for this increased susceptibility. We observed a 100% infection rate, but without clinical signs of prion disease. We observed similar transmission features when we passaged vCJD in TgMet/Val$_{129}$ mice. In addition, the apparent PrPVal$_{129}$ restricted propagation of cattle BSE and BSE from other species was completely abolished after its adaptation to human PrPMet$_{129}$.

Although PrP overexpression and the inoculation route can affect transmission efficiency, our results and those previously reported in both overexpressing and knock-in transgenic mice (2,27,30) suggest that the Val$_{129}$ PrP variant could sustain a very slow and limited vCJD conversion rate, and is unable to completely prevent vCJD transmission. Biochemical and neuropathological

features of vCJD transmission to TgVal$_{129}$ mice showed substantial differences compared to TgMet$_{129}$ or TgMet/Val$_{129}$ mice. Similar to previous reports (2,27,28,48), a type 5 PrP^{Sc} associated with very weak and diffuse PrP plaques without a florid morphology was the hallmark among these mice. In addition, our demonstration of previously unreported type 5 PrP^{Sc} in brain samples of vCJD-challenged knock-in Ki-Hu129V/V mice (30) establishes that the evolution of type 5 PrP^{Sc} associated with the transmission of vCJD prions to the Val$_{129}$ genotype is not
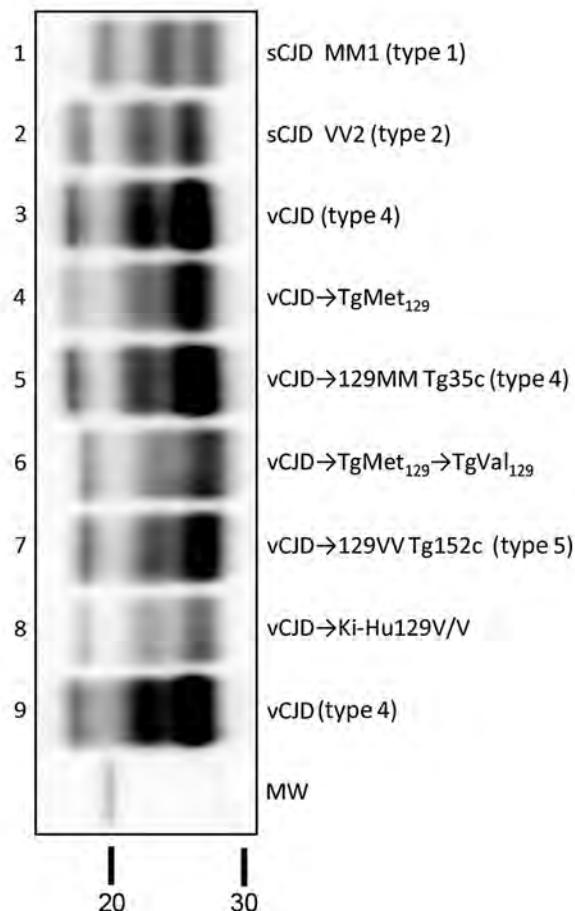
Figure 3. Biochemical comparison of brain protease-resistant prion protein (PrP^{res}) detected in transgenic mice expressing prion protein Met$_{129}$ and Val$_{129}$ mice and inoculated with vCJD brain homogenate. Similar quantities of PrP^{res} were loaded for adequate comparison, and immunoblots were detected by using Sha31 monoclonal antibody. Lanes 4 and 6 show passages from this study; lane 5 shows sample codification I-10629 and lane 7 sample codification I-11724 from the MRC Prion Unit in the United Kingdom (27); lane 8 shows sample codification #139-A5603 from Tohoku University Graduate School of Medicine, Sendai, Japan (30). The original vCJD isolate (Hu-vCJD$_2$) used for mouse inoculations in this study was also included on the blot (lanes 3 and 9); sCJD MM1 (lane 1) and VV2 (lane 2) isolates were included for biochemical comparative purposes. Molecular weight (MW) in kDa is shown. CJD, Creutzfeldt-Jakob disease; sCJD, sporadic CJD; vCJD, variant CJD.

an artifact of PrP overexpression. This finding further reinforces the specific biochemical features of vCJD when transmitted to the human-PrP Val$_{129}$ sequence.

Extrapolation of results from prion transmission studies based on transgenic mice has to be done with caution, especially when human susceptibility to prions is analyzed. However, our results clearly indicate that PrPVal$_{129}$ individuals are highly resistant to transmission of cattle BSE or BSE passaged in other species. Also, PrPVal$_{129}$ individuals might be susceptible to infection with human-passaged BSE (vCJD) prions, and the propagated agents might transmit with molecular and neuropathological properties distinguishable from those of type 4 PrP^{res}. Although the resultant type 5 PrP^{Sc} shares the same fragment sizes as those of type 2 PrP^{Sc}, the 2 PrP^{Sc} types can be distinguished by the predominance of the diglycosylated glycoform associated with type 5 PrP^{Sc}. Overall, our results indicate that human Val$_{129}$-PrP polymorphic variant is a strong molecular protector against BSE zoonotic transmission but fails to prevent human-to-human vCJD transmission. Because potential late-onset vCJD cases could appear in the population (*49,50*) these findings underline the need for continued investigation of all forms of human prion disease.

Acknowledgments

Dr. Fernández-Borges is a research scientist in the Prion Group at Centro de Investigación en Sanidad Animal–Instituto Nacional de Investigación y Tecnología Agraria y Alimentaria, Madrid, Spain. Her research interests include prion strain characterization and evolution and the pathogenesis of prion diseases and their effects on human and animal health.

References

1. Collinge J, Sidle KC, Meads J, Ironside J, Hill AF. Molecular analysis of prion strain variation and the aetiology of 'new variant' CJD. Nature. 1996;383:685–90. http://dx.doi.org/10.1038/383685a0
2. Hill AF, Desbruslais M, Joiner S, Sidle KC, Gowland I, Collinge J, et al. The same prion strain causes vCJD and BSE. Nature. 1997;389:448–50, 526. http://dx.doi.org/10.1038/38925
3. Bruce ME, Will RG, Ironside JW, McConnell I, Drummond D, Suttie A, et al. Transmissions to mice indicate that 'new variant' CJD is caused by the BSE agent. Nature. 1997; 389:498–501. http://dx.doi.org/10.1038/39057
4. Llewelyn CA, Hewitt PE, Knight RS, Amar K, Cousens S, Mackenzie J, et al. Possible transmission of variant Creutzfeldt-Jakob disease by blood transfusion. Lancet. 2004;363:417–21. http://dx.doi.org/10.1016/S0140-6736(04)15486-X
5. Peden AH, Head MW, Ritchie DL, Bell JE, Ironside JW. Preclinical vCJD after blood transfusion in a PRNP codon 129 heterozygous patient. Lancet. 2004;364:527–9. http://dx.doi.org/10.1016/S0140-6736(04)16811-6
6. Wroe SJ, Pal S, Siddique D, Hyare H, Macfarlane R, Joiner S, et al. Clinical presentation and pre-mortem diagnosis of variant Creutzfeldt-Jakob disease associated with blood transfusion: a case report. Lancet. 2006;368:2061–7. http://dx.doi.org/10.1016/S0140-6736(06)69835-8
7. Peden A, McCardle L, Head MW, Love S, Ward HJ, Cousens SN, et al. Variant CJD infection in the spleen of a neurologically asymptomatic UK adult patient with haemophilia. Haemophilia. 2010;16:296–304. http://dx.doi.org/10.1111/j.1365-2516.2009.02181
8. Prusiner SB, Scott MR, DeArmond SJ, Cohen FE. Prion protein biology. Cell. 1998;93:337–48. http://dx.doi.org/10.1016/S0092-8674(00)81163-0
9. Prusiner SB. Prions. Proc Natl Acad Sci U S A. 1998;95:13363–83. http://dx.doi.org/10.1073/pnas.95.23.13363
10. Collinge J. Prion diseases ofhumans and animals: their causes and molecular basis. Annu Rev Neurosci. 2001;24:519–50. http://dx.doi.org/10.1146/annurev.neuro.24.1.519
11. Will RG, Ironside JW, Zeidler M, Estibeiro K, Cousens SN, Smith PG, et al. A new variant of Creutzfeldt-Jakob disease in the UK. Lancet. 1996;347:921–5. http://dx.doi.org/10.1016/S0140-6736(96)91412-9
12. Parchi P, Castellani R, Capellari S, Ghetti B, Young K, Chen SG, et al. Molecular basis of phenotypic variability in sporadic Creutzfeldt-Jakob disease. Ann Neurol. 1996;39:767–78. http://dx.doi.org/10.1002/ana.410390613
13. Hill AF, Joiner S, Wadsworth JD, Sidle KC, Bell JE, Budka H, et al. Molecular classification of sporadic Creutzfeldt-Jakob disease. Brain. 2003;126:1333–46. http://dx.doi.org/10.1093/brain/awg125
14. Torres JM, Espinosa JC, Aguilar-Calvo P, Herva ME, Relaño-Ginés A, Villa-Diaz A, et al. Elements modulating the prion species barrier and its passage consequences. PLoS One. 2014;9:e89722. http://dx.doi.org/10.1371/journal.pone.0089722
15. Wadsworth JD, Collinge J. Update on human prion disease. Biochim Biophys Acta. 2007;1772:598–609. http://dx.doi.org/10.1016/j.bbadis.2007.02.010
16. Palmer MS, Dryden AJ, Hughes JT, Collinge J. Homozygous prion protein genotype predisposes to sporadic Creutzfeldt-Jakob disease. Nature. 1991;352:340–2. http://dx.doi.org/10.1038/352340a0
17. Collinge J, Palmer MS, Dryden AJ. Genetic predisposition to iatrogenic Creutzfeldt-Jakob disease. Lancet. 1991;337:1441–2. http://dx.doi.org/10.1016/0140-6736(91)93128-V
18. Mead S, Stumpf MP, Whitfield J, Beck JA, Poulter M, Campbell T, et al. Balancing selection at the prion protein gene consistent with prehistoric kurulike epidemics. Science. 2003;300:640–3. http://dx.doi.org/10.1126/science.1083320
19. Baker HE, Poulter M, Crow TJ, Frith CD, Lofthouse R, Ridley RM, et al. Aminoacid polymorphism in human prion protein and age at death in inherited prion disease. Lancet. 1991;337:1286. http://dx.doi.org/10.1016/0140-6736(91)92953-Y
20. Poulter M, Baker HF, Frith CD, Leach M, Lofthouse R, Ridley RM, et al. Inherited prion disease with 144 base pair gene insertion. 1. Genealogical and molecular studies. Brain. 1992;115:675–85. http://dx.doi.org/10.1093/brain/115.3.675
21. Will RG, Zeidler M, Stewart GE, Macleod MA, Ironside JW, Cousens SN, et al. Diagnosis of new variant Creutzfeldt-Jakob

disease. Ann Neurol. 2000;47:575–82. http://dx.doi.org/10.1002/1531-8249(200005)47:5<575::AID-ANA4>3.0.CO,2-W

22. Bishop MT, Diack AB, Ritchie DL, Ironside JW, Will RG, Manson JC. Prion infectivity in the spleen of a PRNP heterozygous individual with subclinical variant Creutzfeldt-Jakob disease. Brain. 2013;136:1139–45. http://dx.doi.org/10.1093/brain/awt032

23. Hilton DA, Ghani AC, Conyers L, Edwards P, McCardle L, Ritchie D, et al. Prevalence of lymphoreticular prion protein accumulation in UK tissue samples. J Pathol. 2004;203:733–9. http://dx.doi.org/10.1002/path.1580

24. Ironside JW, Bishop MT, Connolly K, Hegazy D, Lowrie S, Le Grice M, et al. Variant Creutzfeldt-Jakob disease: prion protein genotype analysis of positive appendix tissue samples from a retrospective prevalence study. BMJ. 2006;332:1186–8. http://dx.doi.org/10.1136/bmj.38804.511644.55

25. Gill ON, Spencer Y, Richard-Loendt A, Kelly C, Dabaghian R, Boyes L, et al. Prevalent abnormal prion protein in human appendixes after bovine spongiform encephalopathy epizootic: large scale survey. BMJ. 2013;347:f5675. http://dx.doi.org/10.1136/bmj.f5675

26. Asante EA, Linehan JM, Desbruslais M, Joiner S, Gowland I, Wood AL, et al. BSE prions propagate as either variant CJD-like or sporadic CJD-like prion strains in transgenic mice expressing human prion protein. EMBO J. 2002;21:6358–66. http://dx.doi.org/10.1093/emboj/cdf653

27. Wadsworth JD, Asante EA, Desbruslais M, Linehan JM, Joiner S, Gowland I, et al. Human prion protein with valine 129 prevents expression of variant CJD phenotype. Science. 2004;306:1793–6. http://dx.doi.org/10.1126/science.1103932

28. Asante EA, Linehan JM, Gowland I, Joiner S, Fox K, Cooper S, et al. Dissociation of pathological and molecular phenotype of variant Creutzfeldt-Jakob disease in transgenic human prion protein 129 heterozygous mice. Proc Natl Acad Sci U S A. 2006;103:10759–64. http://dx.doi.org/10.1073/pnas.0604292103

29. Bishop MT, Hart P, Aitchison L, Baybutt HN, Plinston C, Thomson V, et al. Predicting susceptibility and incubation time of human-to-human transmission of vCJD. Lancet Neurol. 2006;5:393–8. http://dx.doi.org/10.1016/S1474-4422(06)70413-6

30. Takeuchi A, Kobayashi A, Ironside JW, Mohri S, Kitamoto T. Characterization of variant Creutzfeldt-Jakob disease prions in prion protein-humanized mice carrying distinct codon 129 genotypes. J Biol Chem. 2013;288:21659–66. http://dx.doi.org/10.1074/jbc.M113.470328

31. Padilla D, Béringue V, Espinosa JC, Andreoletti O, Jaumain E, Reine F, et al. Sheep and goat BSE propagate more efficiently than cattle BSE in human PrP transgenic mice. PLoS Pathog. 2011;7:e1001319. PubMed http://dx.doi.org/10.1371/journal.ppat.1001319

32. Espinosa JC, Herva ME, Andréoletti O, Padilla D, Lacroux C, Cassard H, et al. Transgenic mice expressing porcine prion protein resistant to classical scrapie but susceptible to sheep bovine spongiform encephalopathy and atypical scrapie. Emerg Infect Dis. 2009;15:1214–21. http://dx.doi.org/10.3201/eid1508.081218

33. Castilla J, Gutiérrez Adán A, Brun A, Pintado B, Ramírez MA, Parra B, et al. Early detection of PrPres in BSE-infected bovine PrP transgenic mice. Arch Virol. 2003;148:677–91. http://dx.doi.org/10.1007/s00705-002-0958-4

34. Castilla J, Gutiérrez-Adán A, Brun A, Pintado B, Doyle D, Ramírez MA, et al. Subclinical bovine spongiform encephalopathy infection in transgenic mice expressing porcine prion protein. J Neurosci. 2004;24:5063–9. http://dx.doi.org/10.1523/JNEUROSCI.5400-03.2004

35. Aguilar-Calvo P, Fast C, Tauscher K, Espinosa JC, Groschup MH, Nadeem M, et al. Effect of Q211 and K222 PRNP polymorphic variants in the susceptibility of goats to oral infection with goat bovine spongiform encephalopathy. J Infect Dis. 2015;212:664–72. http://dx.doi.org/10.1093/infdis/jiv112

36. Foster JD, Hope J, Fraser H. Transmission of bovine spongiform encephalopathy to sheep and goats. Vet Rec. 1993;133:339–41. http://dx.doi.org/10.1136/vr.133.14.339

37. Goldmann W, Martin T, Foster J, Hughes S, Smith G, Hughes K, et al. Novel polymorphisms in the caprine PrP gene: a codon 142 mutation associated with scrapie incubation period. J Gen Virol. 1996;77:2885–91. http://dx.doi.org/10.1099/0022-1317-77-11-2885

38. Eloit M, Adjou K, Coulpier M, Fontaine JJ, Hamel R, Lilin T, et al. BSE agent signatures in a goat. Vet Rec. 2005;156:523–4. http://dx.doi.org/10.1136/vr.156.16.523-b

39. Cooper JK, Ladhani K, Minor PD. Reference materials for the evaluation of pre-mortem variant Creutzfeldt-Jakob disease diagnostic assays. Vox Sang. 2007;92:302–10.

40. Cassard H, Torres JM, Lacroux C, Douet JY, Benestad SL, Lantier F, et al. Evidence for zoonotic potential of ovine scrapie prions. Nat Commun. 2014;5:5821. http://dx.doi.org/10.1038/ncomms6821

41. Notari S, Xiao X, Espinosa JC, Cohen Y, Qing L, Aguilar-Calvo P, et al. Transmission characteristics of variably protease-sensitive prionopathy. Emerg Infect Dis. 2014;20:2006–14. http://dx.doi.org/10.3201/eid2012.140548

42. Feraudet C, Morel N, Simon S, Volland H, Frobert Y, Creminon C, et al. Screening of 145 anti-PrP monoclonal antibodies for their capacity to inhibit PrPSc replication in infected cells. J Biol Chem. 2005;280:11247–58.

43. Andréoletti O, Berthon P, Levavasseur E, Marc D, Lantier F, Monks E, et al. Phenotyping of protein-prion (PrPsc)-accumulating cells in lymphoid and neural tissues of naturally scrapie-affected sheep by double-labeling immunohistochemistry. J Histochem Cytochem. 2002;50:1357–70. http://dx.doi.org/10.1177/002215540205001009

44. Fraser H, Dickinson AG. The sequential development of the brain lesion of scrapie in three strains of mice. J Comp Pathol. 1968;78:301–11. http://dx.doi.org/10.1016/0021-9975(68)90006-6

45. Andréoletti O, Simon S, Lacroux C, Morel N, Tabouret G, Chabert A, et al. PrPSc accumulation in myocytes from sheep incubating natural scrapie. Nat Med. 2004;10:591–3. http://dx.doi.org/10.1038/nm1055

46. Wadsworth JD, Powell C, Beck JA, Joiner S, Linehan JM, Brandner S, et al. Molecular diagnosis of human prion disease. Methods Mol Biol. 2008;459:197–227. http://dx.doi.org/10.1007/978-1-59745-234-2_14

47. Vidal E, Fernández-Borges N, Pintado B, Ordóñez M, Márquez M, Fondevila D, et al. Bovine spongiform encephalopathy induces misfolding of alleged prion-resistant species cellular prion protein without altering its pathobiological features. J Neurosci. 2013;33:7778–86. http://dx.doi.org/10.1523/JNEUROSCI.0244-13.2013

48. de Marco MF, Linehan J, Gill ON, Clewley JP, Brandner S. Large-scale immunohistochemical examination for lymphoreticular prion protein in tonsil specimens collected in Britain. J Pathol. 2010; 222:380–7. http://dx.doi.org/10.1002/path.2767

49. Collinge J. Medicine. Prion strain mutation and selection. Science. 2010;328:1111–2. http://dx.doi.org/10.1126/science.1190815

50. Douet JY, Zafar S, Perret-Liaudet A, Lacroux C, Lugan S, Aron N, et al. Detection of infectivity in blood of persons with variant and sporadic Creutzfeldt-Jakob disease. Emerg Infect Dis. 2014;20:114–7. http://dx.doi.org/10.3201/eid2001.130353

Address for correspondence: Juan Maria Torres Trillo, Centro de Investigación en Sanidad Animal (CISA-INIA). 28130 Valdeolmos, Madrid, Spain; email: jmtorres@inia.es

Norovirus in Bottled Water Associated with Gastroenteritis Outbreak, Spain, 2016

Albert Blanco,[1] Susana Guix,[1] Noemí Fuster,
Cristina Fuentes, Rosa Bartolomé, Thais Cornejo,
Rosa Maria Pintó, Albert Bosch

In April 2016, an outbreak of gastrointestinal illness (4,136 cases) occurred in Catalonia, Spain. We detected high levels of norovirus genogroups I and II in office water coolers associated with the outbreak. Infectious viral titer estimates were 33–49 genome copies/L for genogroup I and 327–660 genome copies/L for genogroup II.

During April 11–25, 2016, a total of 4,136 cases of gastroenteritis were reported by the Public Health Agency of Catalonia (ASPCAT; Figure, panel A). A case-patient was defined as an exposed person who had vomiting or diarrhea (3 or more loose stools within 24 hours) and ≥ 2 of the following: nausea, abdominal pain, or fever ($\geq 37.8°C$). Six patients required hospitalization.

The epidemiologic investigation conducted by the ASPCAT pointed toward an association of the outbreak with drinking bottled spring water from office water coolers; the water had been bottled at a source in Andorra (M. Jané-Checa and A. Martínez-Mateo, Public Health Agency of Catalonia, pers. comm., 2016 Sep 1). Compared with other modes of transmission such as food or person to person, norovirus outbreaks associated with drinking water are rare in developed countries (1). On April 15, 2016, as a precautionary measure, the company producing the bottled water recalled >6,150 containers of water of suspected quality that had already been distributed to 925 companies. The water complied with all requirements of the European Commission directive on the exploitation and marketing of natural mineral waters (2), but these requirements do not include any virologic determination.

The Spanish Authority for Consumption, Food Safety, and Nutrition reported the outbreak at the national (http://www.aecosan.msssi.gob.es/AECOSAN/web/seguridad_alimentaria/ampliacion/gastroenteritis_agua_envasada.htm) and European (Rapid Alert System for Food and Feed, RASFF, expedient 2017/0469, https://webgate. ec.europa.eu/rasff-window/portal/?event = notificationDetail&NOTIF_REFERENCE = 2016.0469) levels. The numbers of cases reported by the ASPCAT peaked on April 18 and 21 (Figure, panel B), and the ASPCAT declared the outbreak over on April 25.

The Study

As part of the epidemiologic investigation of this outbreak, we took samples from four 19-L water coolers in 2 offices in the Barcelona metropolitan area, from which affected persons had drunk. We collected samples 1 and 2 on April 15 from 2 water coolers in 1 office, from which 36 cases had been reported. A private company provided samples 3 and 4, from 2 water coolers in a different office with an unknown number of cases, on April 20. We tested all samples immediately upon receipt at our laboratory. We used positively charged glass wool and polyethylene glycol precipitation for virus concentration. Sample volumes ranged from 2.0 L to 7.8 L; we reduced each sample to a final volume of 7 mL, as described previously (3). We extracted total RNA from 0.5 mL of the concentrates with the NucliSens miniMAG magnetic system (BioMérieux, Marcy-l'Étoile, France) and eluted the samples in 100 µL of elution buffer, following the manufacturer's specifications. We performed a standardized 1-step real-time TaqMan reverse transcription PCR (RT-qPCR; Ultrasense, Invitrogen Life Technologies, Barcelona, Spain), in which we used 5 µL of extracted RNA to determine the number of genome copies per liter of human norovirus genogroup I (GI) and genogroup II (GII) (4–7). We monitored virus/nucleic acid extraction and enzyme efficiencies as previously described; we used double-stranded DNA plasmids containing the target sequences as standards (8).

We detected high RNA levels for norovirus GI and GII, around 10^3 and 10^4 genome copies/L, in 2 of the 4 water cooler samples concentrated by glass wool filtration and polyethylene glycol precipitation (Table). Because molecular methods are unable to discern between infectious and noninfectious particles, we predicted the infectivity of norovirus in the concentrated samples by treating the samples with the nucleic acid intercalating dye PMA propidium monoazide; (50 µmol/L) and Triton X surfactant (0.5%) before RT-qPCR; this enabled us to distinguish between virions with intact and altered capsids (9). Following this approach, estimated infectious levels in the 2 positive

Author affiliations: University of Barcelona, Barcelona, Spain (A. Blanco, S. Guix, N. Fuster, C. Fuentes, R.M. Pintó, A. Bosch); Hospital Universitari Vall d'Hebron, Barcelona (R. Bartolomé, T. Cornejo)

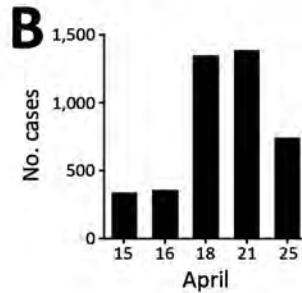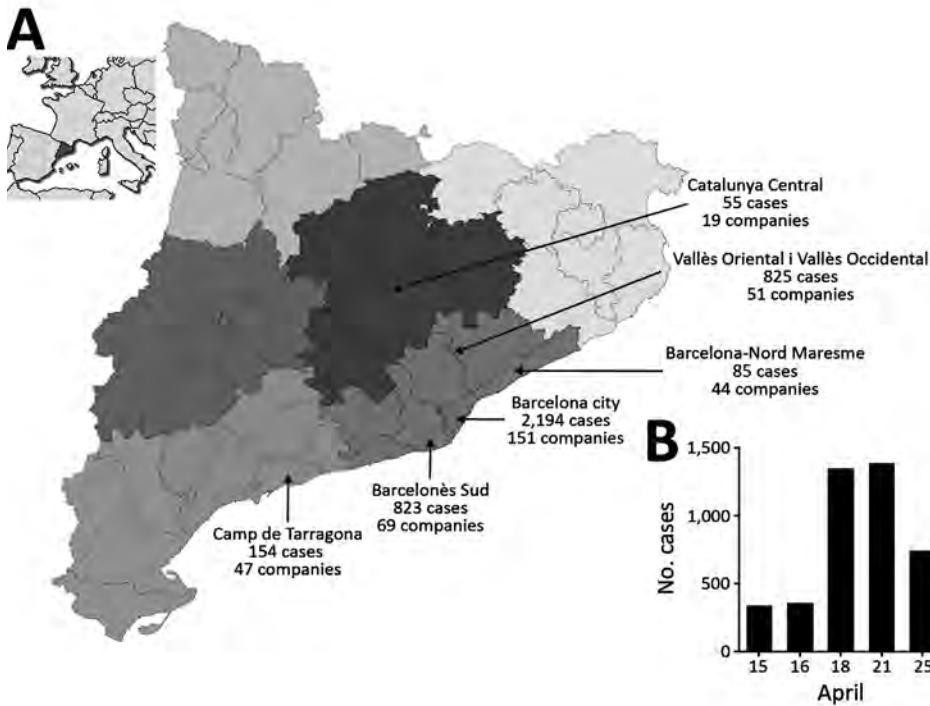[1]These authors contributed equally to this article.

Figure. Waterborne norovirus outbreak in Catalonia, Spain, April 15–25, 2016 (n = 4,136 cases). A) Geographic distribution of the number of cases and affected companies in the Catalonian Health regions. Inset shows location of region in Spain. Map outlines obtained from https://commons.wikimedia.org/wiki/File:Catalonia_location_map.svg. B) Time distribution of reported cases. Cases are displayed according to the dates of the press release from the Public Health Agency of Catalonia (http://premsa.gencat.cat/pres_fsvp/AppJava/notapremsavw/292423/ca/salut-publica-dona-tancat-brot-gastroenteritis-transmes-consum-daigua-envasada.do). Although the onset of the outbreak was on April 11, the first report of the number of cases was on April 15, and the outbreak was declared over on April 25 with a total of 4,136 reported cases, including both primary and secondary cases.

samples were 49 and 327 genome copies/L for norovirus GI and 33 and 660 genome copies/L for norovirus GII (Table).

Given the large number of persons involved in the outbreak and the reported 50% human infectious dose for norovirus of 18–1,300 particles (*10,11*), the high genome copy values in the water samples were not unexpected. In addition, the proportion of intact (infectious) virions in the water samples, estimated through PMA/Triton treatment before RT-qPCR assays, represented 0.3%–5.6% of the total number of physical particles, which was enough to cause gastrointestinal illness (*10,11*).

We assayed the presence of enteroviruses, astroviruses, sapoviruses, rotaviruses, adenoviruses, and hepatitis A virus in the 4 water samples by using commercial RT-qPCR kits (Viasure, Certest Biotec SL, Zaragoza, Spain), with negative results. We attempted genotyping of noroviruses in samples 1 and 2 using a semi-nested RT-PCR protocol with specific primers for GI and GII. We performed the first PCR with primers COG1F and G1SKR for GI and COG2F and G2SKR for GII (*6,12*). For the second PCR, we used primers G1SKF and G1SKR for GI and G2SKF and G2SKR for GII (*12*). We assigned genotypes based on clustering with reference strains from the sequence database of the European network NoroNet and norovirus genotyping tool (*13*). We detected a single sequence corresponding to genotype GII.4/Sydney/2012 (GenBank accession no. KX816644) in samples 1 and 2. Additionally, MiSeq next-generation sequence analysis (Illumina, San Diego, CA) of the amplified product confirmed the sole presence of genotype GII.4/Sydney/2012 (data not shown).

Although some fecal samples from persons who worked at the office from which water samples 1 and 2 were obtained contained genotypes GI.2 (n = 10) and GII.17 (n = 11) but not GII.4/Sydney/2012, we isolated genotypes GII.4/Sydney/2012 (n = 1), GI.2 (n = 1), GII.17 (n = 1), and GII.2 (n = 1) from fecal samples from persons from a different office who exhibited the same gastrointestinal symptoms after drinking water supplied by the same company (data not shown). We hypothesize that the spring water was contaminated by all 4 strains (GI.2, GII.2, GII.4, and GII.17) but levels of viral contamination for each genotype were not homogeneous in all bottled coolers. We may have detected only the GII.4 genotype in water samples 1 and 2 because of a higher concentration of this specific genotype or because of bias caused by the sampling, concentration, and molecular detection procedures. Finally, several reasons could explain why we did not find any GII.4/Sydney/2012 or GII.2 genotypes among the fecal samples from persons from the office that provided samples 1 and 2, including the existence of immune status among the exposed persons or differences in the proportion of infectious/physical particles between the different types.

Conclusions

We describe quantitative detection of norovirus in bottled water. Previously, several brands of mineral water were reported to contain norovirus, but the findings were later

Table. Human norovirus genome copies per liter in analyzed water cooler samples concentrated by glass wool filtration and polyethylene glycol precipitation, metropolitan area of Barcelona, Spain, April 15–20, 2016*

Sample	RT-qPCR		PMA/T	
	GI	GII	GI	GII
1	1.1×10^3	5.8×10^3	49	327
2	1.0×10^4	2.6×10^4	33	660
3	ND	ND	NT	NT
4	ND	ND	NT	NT

*G, genogroup; ND, not detected; NT, not tested; PMA/T, treatment with the nucleic acid intercalating dye propidium monoazide (PMA, 50 µmol/L) and Triton X surfactant (0.5%) before RT-qPCR; RT-qPCR, real-time TaqMan reverse transcription PCR.

attributed to laboratory contamination with control reagents (*14,15*). One limitation of our study is the low number of water samples analyzed. Four days after the onset of the outbreak, the company recalled all batches of water and water coolers of suspected quality, which hampered the collection of a larger number of samples for analysis.

The cause of the water contamination remains to be elucidated. However, the high number of affected persons from 381 offices that received water coolers, and the many different genotypes found in some patients' fecal specimens, point toward sewage pollution of the spring aquifer. Aquifer pollution was acknowledged by the Andorra Ministry of Health and Welfare, and further use of the spring was banned.

This large outbreak suggests that the management of microbial risks of commercially produced mineral waters, universally based solely on bacterial parameters, could benefit from additional analysis for relevant viral pathogens such as norovirus. However, the substantial costs incurred in developing, enhancing, and managing virus surveillance systems call for a balanced approach to keep both the cost and the time required for the analyses within feasibility limits.

Mr. Blanco is a PhD student at the Department of Genetics, Microbiology, and Statistics of the University of Barcelona in Barcelona, Spain. His research interests include molecular diagnostics and epidemiology of enteric viruses in clinical and environmental samples. Dr. Guix is an associate professor in the Department of Genetics, Microbiology and Statistics of the University of Barcelona, and is a member of the scientific committee of the Spanish Authority for Consumption, Food Safety, and Nutrition. Her research interests include epidemiology and food safety studies on viruses causing gastrointestinal diseases and hepatitis.

References

1. Bitler EJ, Matthews JE, Dickey BW, Eisenberg JN, Leon JS. Norovirus outbreaks: a systematic review of commonly implicated transmission routes and vehicles. Epidemiol Infect. 2013;141:1563–71. http://dx.doi.org/10.1017/S095026881300006X
2. European Union. Directive 2009/54/EC of the European Parliament and of the Council of 18 June 2009 on the exploitation and marketing of natural mineral waters. Recast. 2662009: L 164. Luxembourg; 2009.
3. Pérez-Sautu U, Sano D, Guix S, Kasimir G, Pintó RM, Bosch A. Human norovirus occurrence and diversity in the Llobregat river catchment, Spain. Environ Microbiol. 2012;14:494–502. http://dx.doi.org/10.1111/j.1462-2920.2011.02642.x
4. da Silva AK, Le Saux JC, Parnaudeau S, Pommepuy M, Elimelech M, Le Guyader FS. Evaluation of removal of noroviruses during wastewater treatment, using real-time reverse transcription-PCR: different behaviors of genogroups I and II. Appl Environ Microbiol. 2007;73:7891–7. http://dx.doi.org/10.1128/AEM.01428-07
5. Svraka S, Duizer E, Vennema H, de Bruin E, van der Veer B, Dorresteijn B, et al. Etiological role of viruses in outbreaks of acute gastroenteritis in The Netherlands from 1994 through 2005. J Clin Microbiol. 2007;45:1389–94. http://dx.doi.org/10.1128/JCM.02305-06
6. Kageyama T, Kojima S, Shinohara M, Uchida K, Fukushi S, Hoshino FB, et al. Broadly reactive and highly sensitive assay for Norwalk-like viruses based on real-time quantitative reverse transcription-PCR. J Clin Microbiol. 2003;41:1548–57. http://dx.doi.org/10.1128/JCM.41.4.1548-1557.2003
7. Loisy F, Atmar RL, Guillon P, Le Cann P, Pommepuy M, Le Guyader FS. Real-time RT-PCR for norovirus screening in shellfish. J Virol Methods. 2005;123:1–7. http://dx.doi.org/10.1016/j.jviromet.2004.08.023
8. International Organization for Standardization (ISO). ISO/TS 15216–1:2013. ISO/TS 15216. Microbiology of food and animal feed–Horizontal method for determination of hepatitis A virus and norovirus in food using real-time RT-PCR. Geneva: The Organization; 2013.
9. Fuster N, Pintó RM, Fuentes C, Beguiristain N, Bosch A, Guix S. Propidium monoazide RTqPCR assays for the assessment of hepatitis A inactivation and for a better estimation of the health risk of contaminated waters. Water Res. 2016;101:226–32. http://dx.doi.org/10.1016/j.watres.2016.05.086
10. Teunis PFM, Moe CL, Liu P, Miller SE, Lindesmith L, Baric RS, et al. Norwalk virus: how infectious is it? J Med Virol. 2008;80:1468–76. http://dx.doi.org/10.1002/jmv.21237
11. Atmar RL, Opekun AR, Gilger MA, Estes MK, Crawford SE, Neill FH, et al. Determination of the 50% human infectious dose for Norwalk virus. J Infect Dis. 2014;209:1016–22. http://dx.doi.org/10.1093/infdis/jit620

12. Kojima S, Kageyama T, Fukushi S, Hoshino FB, Shinohara M, Uchida K, et al. Genogroup-specific PCR primers for detection of Norwalk-like viruses. J Virol Methods. 2002;100:107–14. http://dx.doi.org/10.1016/S0166-0934(01)00404-9

13. Kroneman A, Vennema H, Deforche K, v d Avoort H, Peñaranda S, Oberste MS, et al. An automated genotyping tool for enteroviruses and noroviruses. J Clin Virol. 2011;51:121–5. http://dx.doi.org/10.1016/j.jcv.2011.03.006

14. Beuret C, Kohler D, Lüthi T. Norwalk-like virus sequences detected by reverse transcription-polymerase chain reaction in mineral waters imported into or bottled in Switzerland.

J Food Prot. 2000;63:1576–82. http://dx.doi.org/10.4315/0362-028X-63.11.1576

15. Sanchez G, Joosten H, Meyer R, Beuret C. Presence of norovirus sequences in bottled waters is questionable. Appl Environ Microbiol. 2005;71:2203–5, author reply 2203–5. http://dx.doi.org/10.1128/AEM.71.4.2203-2205.2005

Address for correspondence: Albert Bosch, Department of Genetics, Microbiology and Statistics, School of Biology, Diagonal 645, 08028, Barcelona, Spain; email: abosch@ub.edu
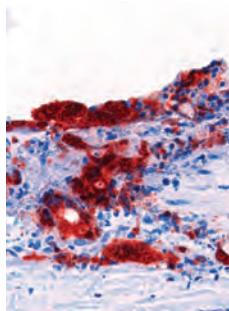
Group A Rotavirus Associated with Encephalitis in Red Fox

Chiara Busi, Vito Martella, Alice Papetti,
Cristiano Sabelli, Davide Lelli, G. Loris Alborali,
Lucia Gibelli, Daniela Gelmetti, Antonio Lavazza,
Paolo Cordioli,[1] M. Beatrice Boniotti

In 2011, a group A rotavirus was isolated from the brain of a fox with encephalitis and neurologic signs, detected by rabies surveillance in Italy. Intracerebral inoculation of fox brain homogenates into mice was fatal. Genome sequencing revealed a heterologous rotavirus of avian origin, which could provide a model for investigating rotavirus neurovirulence.

Group A rotaviruses are a major cause of diarrhea in humans and animals. Although group A rotaviruses infect particular species preferentially (homologous infection), they less frequently affect other species of mammals (heterologous infection), naturally and experimentally (*1*). In addition, there is evidence, albeit rare, that transmission of group A rotaviruses may occur between species of mammals and birds under natural and experimental conditions (*2–4*).

Group A rotaviruses have limited tissue tropism; infection is primarily restricted to cells of the small intestine. However, heterologous infection of mice with the rhesus group A rotavirus strain MMU 18006 was associated with extramucosal spread and hepatitis, but infections with bovine group A rotavirus WC3 and the homologous murine group A rotavirus EDIM were not (*5*), suggesting that some group A rotavirus strains may have unique or unexpected biological properties. In humans, group A rotavirus infection has been associated with acute encephalitis, although this association is based only on observational findings (*6–9*).

We detected a group A rotavirus strain in the brain of a fox with neurologic disorders. To determine the derivation of the virus, we further examined its genomic and biological features.

The Study

In 2011, as part of Italy's national surveillance program for rabies in wildlife, an adult red fox (*Vulpes vulpes*) with

Author affiliations: Istituto Zooprofilattico Sperimentale della Lombardia e dell'Emilia Romagna "Bruno Ubertini," Brescia, Italy (C. Busi, A. Papetti, C. Sabelli, D. Lelli, G.L. Alborali, L. Gibelli, D. Gelmetti, A. Lavazza, P. Cordioli, M.B. Boniotti); Università degli Studi di Bari, Bari, Italy (V. Martella)

neurologic signs was captured. Because its general condition worsened, the animal was euthanized and screened for a panel of neuropathogens (online Technical Appendix, https://wwwnc.cdc.gov/EID/article/23/9/17-0158-Techapp1.pdf). Test results indicated that the animal was negative for rabies, canine distemper, Aujeszky's disease, leishmaniasis, and flavivirus infection (online Technical Appendix). Following the standard diagnostic procedures for rabies, we inoculated brain homogenate from the fox intracerebrally into suckling and weanling mice. The suckling mice died after 3–4 days and the weanling mice after 5 days. However, immunofluorescence testing of the brains of all mice, using rabies-specific hyperimmune serum, produced negative results (data not shown).

Use of negative-staining electron microscopy revealed rotavirus-like virions in the fox and mouse brains (Figure 1, panels A, B). Histologically, several alterations/lesions, suggestive of acute inflammation, were observed in the cerebral cortex of the fox. Histologic analysis of gray matter revealed nonsuppurative encephalitis characterized by multifocal perivascular cuffing of lymphocytes, macrophages, and a few plasma cells as well as presence of multifocal small glial nodules. Perivascular accumulations varied from 1-cell thickness to thin cell accumulations (Figure 1, panel C). Neutrophils were observed within the lumen of some blood vessels and scattered in the gray matter. Neuronal necrosis and satellitosis were also present. By immunohistochemistry performed with a polyclonal serum raised against group A rotavirus, rotavirus antigen was detected in the cytoplasm of neurons, in dendrites, and in glial cells within inflamed areas of the brain (Figure 1, panel D).

An isolate, hereafter called fox-288356, was made from homogenates of the fox brain and from the brains of inoculated suckling and weanling mice, by using confluent monolayers of Marc-145 cells with and without trypsin. Cytopathic effect was characterized by foci of rounded cells, which tended to aggregate linearly on the surface of the monolayer and were clearly visible after 2 days (Figure 1, panel E). Electron microscopic observation identified rotavirus-like particles in the cell cryolysates (data not shown). The electropherotype of the cultured virus revealed a segmented genome characterized by a 5-1-3-2 profile with co-migration of segments 10 and 11 (online Technical Appendix Figure 1).

[1]Deceased.
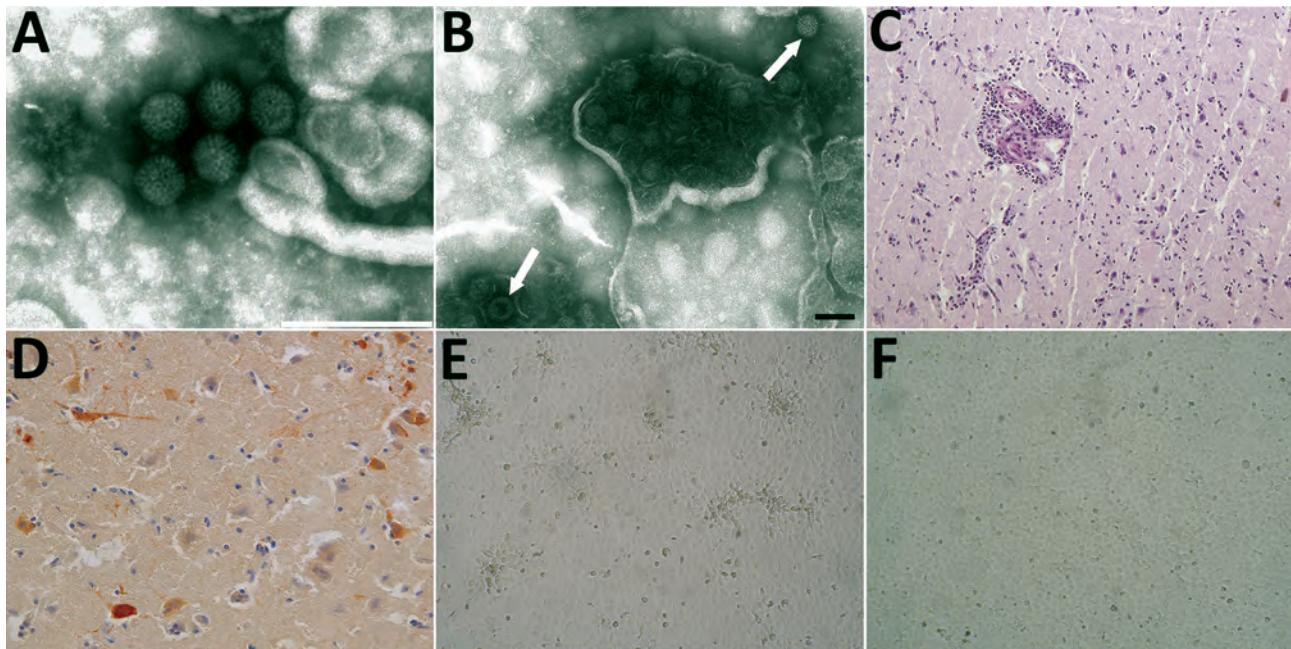
Figure 1. Images of brain of fox with group A rotavirus infection and brains of suckling and weanling mice inoculated with fox brain homogenates. A, B) Negative-staining electron microscopy. Presence of virions morphologically related to family *Reoviridae* from fox (A) and mouse (B) brain (arrows). Scale bar in panel A indicates 200 nm; in panel B, 100 nm. C, D) Histologic and immunohistochemical appearance of the cerebral cortex of the fox. C) Perivascular cuffing of inflammatory cells in the brain stained by hematoxylin and eosin (original magnification ×10). D) Viral antigen in the cytoplasm of neurons (immunohistochemistry, original magnification ×20). E) Foci with rounding cells of the confluent monolayers of Marc-145 cells infected with the brain homogenate from mouse at 2 days after inoculation (original magnification ×40). F) Mock cells (original magnification ×40).

The genome of fox-288356 was 18,849 nt and showed high sequence homology to avian strain PO-13, isolated from a pigeon (*2,4*). Homology was apparent in most genome segments (89%–94% nt and 91%–98% aa), except for the ninth segment, coding for viral protein (VP) 7 (86% nt and 88% aa), and the tenth segment, coding for nonstructural protein (NSP) 4 (79% nt and 83% aa) (Table 1). After phylogenetic analysis of the concatenated genome (Figure 2) and individual genome segments (online Technical Appendix Figure 3), fox-288356 grouped with avian group A rotaviruses. The genomic constellation of fox-288356 was G18P[17]-R4-C4-M4-A4-I4-T4-N4-E19-H4 (Table 2).

Several amino acid mutations were present in the major antigenic regions (A, B, and C) of VP7 (online Technical Appendix Figure 4) and in key residues of VP4 (online Technical Appendix Figure 5). VP4 contained only 1 of the 3 arginine residues required for trypsin-mediated cleavage into the VP8* and VP5* subunits (*10*). This finding seems consistent with the ability of fox-288356 to grow in cell cultures in the absence of trypsin, a feature that has been observed for some avian group A rotaviruses (*11*).

We classified the NSP4 of fox-288356 as a novel E genotype, E19, as indicated by the Rotavirus Classification Working Group. We also found differences between the

Table 1. Comparison of genome segment sizes and sequence similarities among group A rotaviruses isolated from fox and pigeon*

Segment number/encoded protein	Nucleotide/amino acid length (genotype)		% Nucleotide sequence identity	% Amino acid sequence identity
	Fox-288356†	PO-13‡		
1/VP1	3,305/1,089 (R4)	3,302/1,088 (R4)	93	98
2/VP2	2,738/897 (C4)	2,738/897 (C4)	91	97
3/VP3	2,583/829 (M4)	2,583/829 (M4)	91	94
4/VP4	2,349/770 (P[17])	2,349/770 (P[17])	92)	95
5/NSP1	1,871/576 (A4)	1,870/576 (A4)	86	91
6/VP6	1,348/397 (I4)	1,348/397 (I4)	94	98
7/NSP3	1,092/306 (T4)	1,092/306 (T4)	89	95
8/NSP2	1,043/315 (A4)	1,042/315 (N4)	93	95
9/VP7	1,065/329 (G18)	1,065/329 (G18)	86	88
10/NSP4	726/169 (E19)	727/169 (E4)	77	83
11/NSP5	729/218 (H4)	729/218 (H4)	93	90

*NSP, nonstructural protein; VP, viral protein.
†Rotavirus isolated from a red fox.
‡Rotavirus isolated from a pigeon.
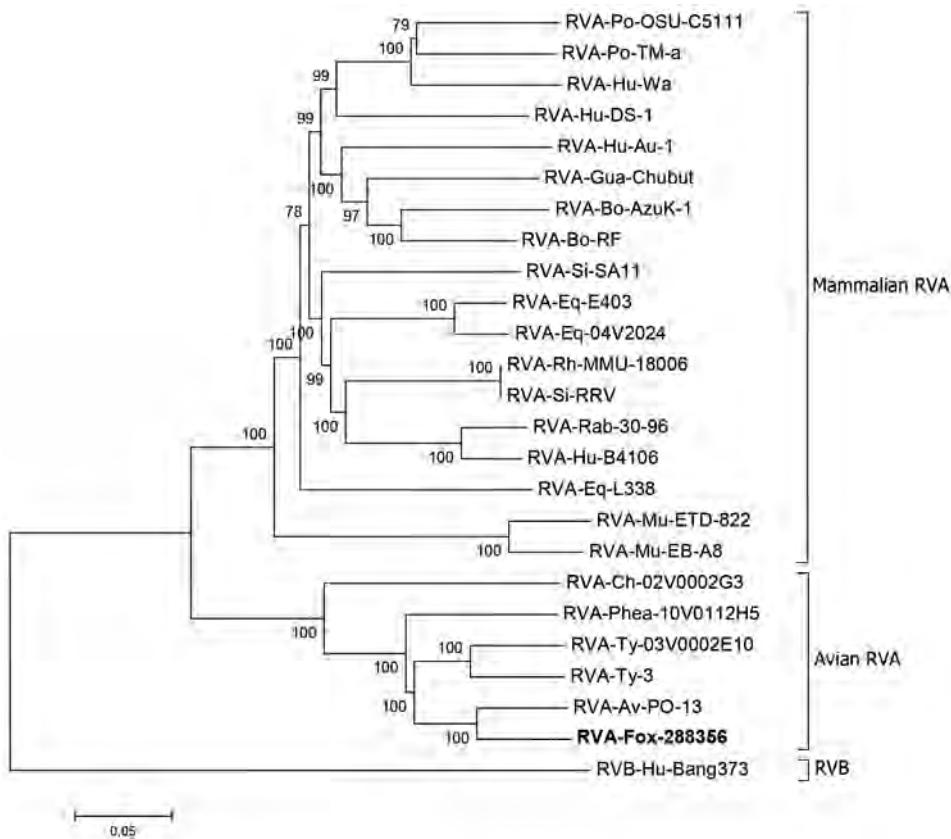
Figure 2. Phylogenetic analysis of RVA strain fox-288356. Analysis was performed on the basis of the concatenated nucleotide sequences of genomic segments. Fox-288356 is correlated with RVA PO-13 (from pigeon) and clustered with the avian RVA. Reference sequences are identified by strain name and GenBank accession number. Scale bar indicates nucleotide substitutions per site. RVA, group A rotavirus; RVB, group B rotavirus.

NSP4 of fox-288356 and other group A rotaviruses (online Technical Appendix Figure 6).

Conclusion

Although in humans group A rotaviruses are mainly associated with gastroenteritis, the literature indicates that group A rotaviruses may also be associated with acute encephalitis or encephalopathy (6–9). This correlation has been supposed for children in whom neurologic signs develop concomitantly or shortly after acute gastroenteritis caused by group A rotavirus (7,9) and after detection of group A rotavirus RNA in the cerebrospinal fluid of patients with neurologic signs (6,8). It remains unclear whether systemic spread of group A rotavirus and localization in the central nervous system is the result of host-related factors, whether it depends on intrinsic biological features of group A rotavirus strains, or whether it eventually results from a combination of both elements. Fox-288356 was probably responsible for the neurologic disease observed in the fox, as suggested by the results of our diagnostic investigations and by the inflammatory lesions in the brain of the animal.

Genomic characterization indicated that fox-288356 shared the same genetic backbone as avian strain PO-13 and avian-like bovine strain 993-83 (2). Under experimental conditions, oral inoculation of mice with pigeon group A rotavirus strain PO-13 infected and caused diarrhea in the mice, but inoculation with turkey group A rotavirus strain Tyr-1 did not (4). Also, the synthetic NSP4 toxic peptide of strain PO-13 elicited diarrhea in suckling mice (12). It is tempting to speculate that some avian group A rotaviruses (e.g., group A rotaviruses with the PO-13

Table 2. Genomic constellation of avian group A rotavirus strains*

Group A rotavirus strain	VP7	VP4	VP6	VP1	VP2	VP3	NSP1	NSP2	NSP3	NSP4	NSP5
Fox-wt/ITA/288356/2011/G18P[17]	G18	P[17]	I4	R4	C4	M4	A4	N4	T4	E19	H4
Pigeon-tc/JPN/PO-13/1983/G18P[17]	G18	P[17]	I4	R4	C4	M4	A4	N4	T4	E4	H4
Bovine-wt/GER/993_83/1983/G18P[17]	G18	P[17]	I4								
Turkey-tc/GER/03V0002E10/2003/G22P[35]	G22	P[35]	I4	R4	C4	M4	A16	N4	T4	E11	H4
Group A rotavirus/tTurkey-tc/IRL/Ty-3/1979/G7P[35]	G7	P[35]	I4	R4	C4	M4	A16	N4	T4	E11	H14
Group A rotavirus/Turkey-tc/IRL/Ty-1/1979/G17P[38]	G17	P[38]	I4	R4	C4	M4	A16	N4	T4	E4	H4
Pheasant-tc/GER/10V0112H5/2010/G23P[37]	G23	P[37]	I4	R4	C4	M4	A16	N10	T4	E4	H4
Chicken-tc/GER/02V0002G3/2002/G19P[30]	G19	P[30]	I11	R6	C6	M7	A16	N6	T8	E10	H8

*Gray shading indicates homology. NSP, nonstructural protein; VP, viral protein.

genome backbone) have the ability to cross the host-species barrier more easily than other avian group A rotaviruses (Table 1). Another bovine group A rotavirus strain, N2342, with a VP4 gene related to the avian strain PO-13, has been recently identified in Japan (*3*).

The virus isolated from the fox displayed a unique NSP4, which was proposed as a novel genotype, E19. NSP4 serves as an intracellular receptor for immature particles and interacts with viral capsid proteins during viral morphogenesis (*13*). NSP4 also acts as a viral enterotoxin (*13,14*), and the enterotoxic activity has been mapped to a region, the toxic peptide, spanning amino acids 114–135 of NSP4 (*14*). Changes in residues within the NSP4 toxic peptide have been associated with alterations in the toxigenic activity of NSP4 and in rotavirus virulence (*15*).

The detection of fox-288356 in the brain of a fox supports the accumulating clinical evidence for the association between group A rotaviruses and neurologic signs in human patients. Whether some group A rotavirus strains intrinsically possess the ability to spread to the central nervous system, thereby causing neurologic disease, remains to be explored.

References

1. Martella V, Bányai K, Matthijnssens J, Buonavoglia C, Ciarlet M. Zoonotic aspects of rotaviruses. Vet Microbiol. 2010;140:246–55. http://dx.doi.org/10.1016/j.vetmic.2009.08.028
2. Rohwedder A, Schütz KI, Minamoto N, Brüssow H. Sequence analysis of pigeon, turkey, and chicken rotavirus VP8* identifies rotavirus 993/83, isolated from calf feces, as a pigeon rotavirus. Virology. 1995;210:231–5. http://dx.doi.org/10.1006/viro.1995.1338
3. Mitake H, Ito N, Okadera K, Okada K, Nakagawa K, Tanaka T, et al. Detection of avian-like rotavirus A VP4 from a calf in Japan. J Vet Med Sci. 2015;77:221–4. http://dx.doi.org/10.1292/jvms.14-0379
4. Mori Y, Sugiyama M, Takayama M, Atoji Y, Masegi T, Minamoto N. Avian-to-mammal transmission of an avian rotavirus: analysis of its pathogenicity in a heterologous mouse model. Virology. 2001;288:63–70. http://dx.doi.org/10.1006/viro.2001.1051
5. Uhnoo I, Riepenhoff-Talty M, Dharakul T, Chegas P, Fisher JE, Greenberg HB, et al. Extramucosal spread and development of hepatitis in immunodeficient and normal mice infected with rhesus rotavirus. J Virol. 1990;64:361–8.
6. Dickey M, Jamison L, Michaud L, Care M, Bernstein DI, Staat MA. Rotavirus meningoencephalitis in a previously healthy child and a review of the literature. Pediatr Infect Dis J. 2009;28:318–21. http://dx.doi.org/10.1097/INF.0b013e31818ddbe9
7. Kobayashi S, Negishi Y, Ando N, Ito T, Nakano M, Togari H, et al. Two patients with acute rotavirus encephalitis associated with cerebellar signs and symptoms. Eur J Pediatr. 2010;169:1287–91. http://dx.doi.org/10.1007/s00431-010-1202-y
8. Arakawa C, Fujita Y, Imai Y, Ishii W, Kohira R, Fuchigami T, et al. Detection of group A rotavirus RNA and antigens in serum and cerebrospinal fluid from two children with clinically mild encephalopathy with a reversible splenial lesion. Jpn J Infect Dis. 2011;64:204–7.
9. Rath BA, Gentsch J, Seckinger J, Ward K, Deputy S. Rotavirus encephalitis with basal ganglia involvement in an 8-month-old infant. Clin Pediatr (Phila). 2013;52:260–4. http://dx.doi.org/10.1177/0009922811417301
10. Trask SD, Wetzel JD, Dermody TS, Patton JT. Mutations in the rotavirus spike protein VP4 reduce trypsin sensitivity but not viral spread. J Gen Virol. 2013;94:1296–300. 10.1099/vir.0.050674-0 http://dx.doi.org/10.1099/vir.0.050674-0
11. McNulty MS, Allan GM, Todd D, McFerran JB, McKillop ER, Collins DS, et al. Isolation of rotaviruses from turkeys and chickens: demonstration of distinct serotypes and RNA electropherotypes. Avian Pathol. 1980;9:363–75. http://dx.doi.org/10.1080/03079458008418420
12. Mori Y, Borgan MA, Ito N, Sugiyama M, Minamoto N. Diarrhea-inducing activity of avian rotavirus NSP4 glycoproteins, which differ greatly from mammalian rotavirus NSP4 glycoproteins in deduced amino acid sequence in suckling mice. J Virol. 2002;76:5829–34. http://dx.doi.org/10.1128/JVI.76.11.5829-5834.2002
13. Ramig RF. Pathogenesis of intestinal and systemic rotavirus infection. J Virol. 2004;78:10213–20. http://dx.doi.org/10.1128/JVI.78.19.10213-10220.2004
14. Lorrot M, Vasseur M. How do the rotavirus NSP4 and bacterial enterotoxins lead differently to diarrhea? Virol J. 2007;4:31. http://dx.doi.org/10.1186/1743-422X-4-31
15. Zhang M, Zeng CQ, Dong Y, Ball JM, Saif LJ, Morris AP, et al. Mutations in rotavirus nonstructural glycoprotein NSP4 are associated with altered virus virulence. J Virol. 1998;72:3666–72.

Address for correspondence: M. Beatrice Boniotti, Research and Development Laboratory, Istituto Zooprofilattico Sperimentale della Lombardia e Emilia Romagna, via Bianchi 9, 25124 Brescia (BS), Italy; email: mariabeatrice.boniotti@izsler.it

Imported Infections with
Mansonella perstans Nematodes, Italy

**Federico Gobbi, Anna Beltrame, Dora Buonfrate,
Silvia Staffolani, Monica Degani,
Maria Gobbo, Andrea Angheben,
Stefania Marocco, Zeno Bisoffi**

We report 74 patients in Italy infected with *Mansonella perstans* nematodes, a poorly described filarial parasite. *M. perstans* nematodes should be included in the differential diagnosis for patients with eosinophilia from disease-

Author affiliations: Sacro Cuore Hospital, Verona, Italy (F. Gobbi, A. Beltrame, D. Buonfrate, M. Degani, M. Gobbo, A. Angheben, S. Marocco, Z. Bisoffi); Azienda Ospedaliero Universitaria Umberto I-Lancisi-Salesi, Ancona, Italy (S. Staffolani)

endemic countries. Serologic analysis is useful for screening, and testing for microfilaremia in peripheral blood should be performed for parasite-positive patients.

Mansonella perstans is a filarial nematode present in 33 countries in sub-Saharan Africa; sporadic cases have been reported in Latin America, mostly in the Caribbean and along the Atlantic coast (*1*); ≈20% of inhabitants of disease-endemic countries are infected (*2*). Flies of the genus *Culicoides* transmit infective larvae to humans. Larvae transform into macrofilariae, which live in serous cavities of the human body, where they produce microfilariae, which are released into peripheral blood 9–12 months after infection.

Few studies/case series have reported signs and symptoms (e.g., subcutaneous edema, rash, abdominal pain,

eosinophilia) caused by infection with *M. perstans* nematodes because the parasite is widespread in remote areas and infected persons usually have other parasitic infections that could contribute to clinical manifestations (*1*). Diagnosis is based on detection of microfilariae in peripheral blood (*3*). An ELISA that uses antigens of *Acanthocheilonema vitae* nematodes is available but is not specific for *Mansonella* spp.

Optimal treatment is still debated. Many drugs have been used, including diethylcarbamazine, ivermectin, mebendazole, levamisole, albendazole, and thiabendazole (*1*). Doxycycline, which is active against the endosymbiont *Wolbachia* spp., showed good efficacy in a clinical trial (*4*), but comparisons of the efficacy of this drug with other treatments are lacking. Most case series identified in countries to which *M. perstans* nematodes are not endemic have not been reported. The purpose of this study was to analyze the clinical, epidemiologic, and laboratory characteristics of patients infected with *M. perstans* nematodes who were given a diagnosis at the Center for Tropical Diseases at Sacro Cuore Hospital in Negrar, Verona, Italy.

The Study

This retrospective study was approved by the Ethics Committee of Sacro Cuore Hospital in November 2016 (study protocol no. 56014). We reviewed medical records of patients admitted to Sacro Cuore Hospital during January 1, 1993–January 1, 2016. Inclusion criteria were available information about the most likely country of acquisition

Figure 1. Microfilaria in a patient infected with *Mansonella perstans* nematodes, Italy. Giemsa stain, 200 μm x 4 μm, original magnification x1,000.

of the infection and presence of *M. perstans* microfilaremia (Figure 1).

A total of 82 patients were considered for inclusion; 8 were excluded because information was incomplete. Thus, 74 patients, 23 immigrants and 51 expatriates, were included in the analysis. Immigrants were persons who were born in disease-endemic areas and then settled in Italy. Expatriates were persons from Italy residing in disease-endemic areas. Immigrants were younger than expatriates. Mean ages were 26.8 (range 5–51) years for immigrants and 55.6 (range 12–76) years for expatriates. Most (70.3%) patients were males.

We detected microfilaremia by using a leukoconcentration method with 13-mL samples of venous blood.
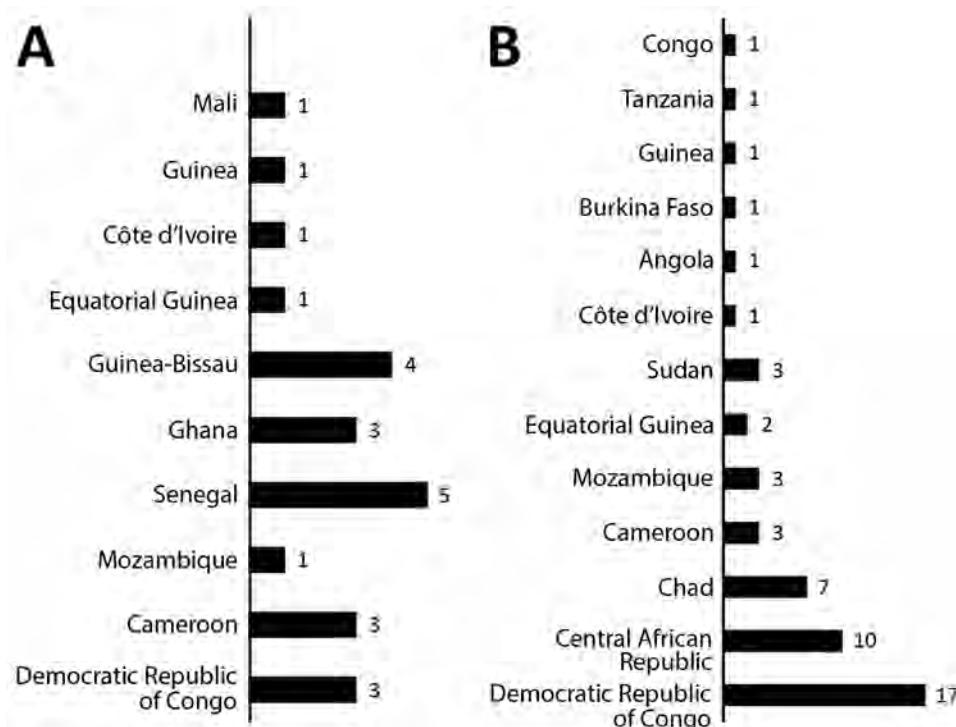
Figure 2. Countries of origin of patients infected with *Mansonella perstans* nematodes, Italy. A) Immigrants; B) expatriates. Immigrants were persons who were born in disease-endemic areas and then settled in Italy. Expatriates were persons from Italy residing in disease-endemic areas.

Table 1. Characteristics of 74 patients infected with *Mansonella perstans* nematodes, Italy*

Characteristic	Value
Age, y	48.9 (34.0–60.6)
Sex	
M	52 (70.3)
F	22 (29.7)
Viral co-infections	
HIV	4 (5.4)
HBV	3 (4.0)
HCV	3 (4.0)
HAV	1 (1.3)
Parasite diseases	
Plasmodium falciparum malaria	9 (12.1)
Giardiasis	2 (2.7)
Scabies	1 (1.3)
Other helminthiases	
Schistosomiasis	27 (36.4)
Strongyloidiasis	11 (14.9)
Hookworm infection	7 (9.4)
Loiasis	4 (5.4)
Trichuriasis	4 (5.4)
Onchocerciasis	2 (2.7)
Eosinophils/mm^3	820 (470–1,270)
Eosinophil count >1,000/μL	32/73 (43.8)
Microfilaria/mL	62 (14–255)
Signs/symptoms	66 (89.2)
Abdominal pain	17 (23.0)
Arthralgia	10 (13.5)
Headache	11 (15.0)
Itching	25 (33.8)
Myalgia	2 (3.0)
Edema	11 (14.9)
Skin eruption	9 (12.2)
IgE >100 IU/mL	60/72 (83.3)
Antifilarial ELISA	49/53 (92.4)

*Values are median (IQR), no. (%), or no. positive/no. tested (%). HAV, hepatitis A virus; HBV, hepatitis B virus; HCV, hepatitis C virus; IQR, interquartile range.

Microfilarial density was measured by examination of Giemsa-stained thick blood smears prepared from 100 μL of blood. We also performed retrospective ELISA for detection of filariasis (Bordier Affinity Products SA, Crissier, Switzerland) on available serum samples.

When necessary, we conducted other investigations to exclude other parasitic infections or other causes of eosinophilia. Other helminth infections were diagnosed by microscopic examination of multiple stool samples; agar stool culture (for hookworm and *Strongyloides stercoralis*); skin-snip (for *Onchocerca volvulus*); and serologic analysis (in-house immunofluorescence test for *S. stercoralis*; commercial immunofluorescence test until 2012, and an ELISA after 2012 for *Schistosoma* spp).

For each patient, information on clinical history, country of exposure, laboratory examinations, and treatment was obtained from medical records and entered into a study-specific database (Epi Info version 3.5.1; Centers for Disease Control and Prevention, Atlanta, GA, USA). Qualitative data were reported as frequencies and percentages, and quantitative data as medians and interquartile ranges.

We identified countries in which *M. perstans* infections were acquired (Figure 2), and clinical and laboratory characteristics of the 74 patients (Table 1) and characteristics of patients who were infected only with *M. perstans* nematodes (33/74, 44.6%) (Table 2). However, we could not exclude other possible co-infections on the basis of screening tests performed (e.g., 23/33 patients came from country to which *Loa loa*, another filarial nematode, was endemic, and amicrofilaremic infections cannot be ruled out).

Data for treatment were available for 60 (81.1%) of 74 patients. Most (34/60, 56.6%) patients were treated with levamisole (150 mg in 3 doses given every 48 h), followed by mebendazole (500 mg 3×/d for 15 d). After 2004, levamisole was no longer available, and patients were then treated with other drugs alone or in combination (doxycycline, mebendazole, ivermectin, diethylcarbamazine, albendazole, thiabendazole). Since 2009, first-line treatment has been mebendazole (500 mg 3×/d for 15 d), followed by doxycycline (100 mg 2×/d for 6 wks); this regimen was used for 11 (18.3%) of 60 patients. Clinical outcomes were available for only 5 of those patients, who showed complete clinical responses to the first-line treatment.

Conclusions

Our series of 74 patients is one focused on imported infections with *M. perstans* nematodes. Identification these infections is often complicated by co-infection with other infective agents. Bassene et al. analyzed patients infected only with *M. perstans* nematodes and concluded that these infections had little pathogenicity because infected persons were usually asymptomatic (*5*). Therefore, we considered as relevant identification of patients for whom other infections were excluded.

Our findings for this subgroup of patients are similar to those reported by Adolph et al. (*6*); however, we did not observe any major neurologic or psychological symptoms or extreme exhaustion. Among symptoms that we observed, transient swellings deserve particular attention. These swellings are similar to Calabar swellings caused by *L. loa* nematodes. When *L. loa* nematode infections are ruled out on the basis of an epidemiologic criterion (loiasis

Table 2. Characteristics of 33 patients infected only with *Mansonella perstans* nematodes, Italy*

Characteristic	Value
Eosinophils/mm^3	620 (415–1,210)
Microfilaria/mL	32 (9.5–112)
Signs/symptoms	30 (90.9)
Abdominal pain	8 (24.2)
Arthralgia	5 (15.1)
Headache	5 (15.1)
Itching	12 (36.3)
Edema	6 (18.2)
Skin eruption	3 (9.1)

*Values are median (IQR) or no. (%). IQR, interquartile range.

is present in a limited area of sub-Saharan Africa), *M. perstans* nematodes should be considered the probable cause of these swellings.

The proportion of patients with different grades of eosinophilia in our study is similar to that reported by Wiseman (*7*): ≈70% of those patients had >500 eosinophils/µL, and 45% had marked eosinophilia (>1,000 eosinophils/µL). Wiseman postulated that the proportion of symptomatic patients increased with increased eosinophil count (*7*). Conversely, increased eosinophil counts could be partially responsible for some symptoms, as reported by Fux et al. (*8*).

Of the 74 patients in our study, 68 (92.0%) had positive serologic results. One major strength of our study was that serologic analysis could be used to screen patients reporting compatible symptoms/signs and epidemiologic criteria. Thus, microscopic detection of microfilaremia, which requires more equipment and skills, could be used only for patients with positive serologic results.

Human infection with *M. perstans* nematodes raises questions about treatment (*1*) because of poor responses to standard antifilarial drugs and limited findings from controlled trials. In our case series, the first-line treatment changed over time on the basis of new evidence and availability of drugs. Therefore, we first administered mebendazole and levamisole on the basis of reports by Maertens and Wéry (*9*) and Wahlgren and Frolov (*10*). Subsequently, we administered mebendazole in combination with other drugs, as suggested by Bregani et al. (*11*). Since 2009, we have administered mebendazole plus doxycycline, according to the only available randomized clinical trial (*4*).

Our study had other limitations, which were caused mostly by the retrospective design. First, posttreatment follow-up was available for only a few patients because most resided only temporarily in Italy. Thus, we could not properly describe response to treatment. Second, most patients came to our center because of symptoms or an increased eosinophil count. Thus, the proportion of symptomatic patients is not representative of the general population with *M. perstans* nematode infections.

In summary, infection with *M. perstans* nematodes should be included in the differential diagnosis of patients with eosinophilia who have lived in disease-endemic countries. Serologic analysis (ELISA for filariae) can be used for screening, and detection of microfilaremia in peripheral blood should be performed for patients with positive serologic results.

Dr. Gobbi is a specialist in infectious diseases at the Center for Tropical Diseases, Sacro Cuore Hospital, Verona, Italy. His primary research interests are malaria, arbovirosis surveillance, and neglected tropical diseases.

References

1. Simonsen PE, Onapa AW, Asio SM. *Mansonella perstans* filariasis in Africa. Acta Trop. 2011;120(Suppl 1):S109–20. http://dx.doi.org/10.1016/j.actatropica.2010.01.014
2. Stoll NR. This wormy world. J Parasitol. 1947;33:1–18.
3. Asio SM, Simonsen PE, Onapa AW. Analysis of the 24-h microfilarial periodicity of *Mansonella perstans*. Parasitol Res. 2009;104:945–8. http://dx.doi.org/10.1007/s00436-008-1312-x
4. Coulibaly YI, Dembele B, Diallo AA, Lipner EM, Doumbia SS, Coulibaly SY, et al. A randomized trial of doxycycline for *Mansonella perstans* infection. N Engl J Med. 2009;361:1448–58. http://dx.doi.org/10.1056/NEJMoa0900863
5. Bassene H, Sambou M, Fenollar F, Clarke S, Djiba S, Mourembou G, et al. High prevalence of *Mansonella perstans* filariasis in rural Senegal. Am J Trop Med Hyg. 2015;93:601–6. http://dx.doi.org/10.4269/ajtmh.15-0051
6. Adolph PE, Kagan IG, McQuay RM. Diagnosis and treatment of *Acanthocheilonema perstans* filariasis. Am J Trop Med Hyg. 1962;11:76–88. http://dx.doi.org/10.4269/ajtmh.1962.11.76
7. Wiseman RA. *Acanthocheilonema perstans*, a cause of significant eosinophilia in the tropics: comments on its pathogenicity. Trans R Soc Trop Med Hyg. 1967;61:667–73. http://dx.doi.org/10.1016/0035-9203(67)90131-9
8. Fux CA, Chappuis B, Holzer B, Aebi C, Bordmann G, Marti H, et al. *Mansonella perstans* causing symptomatic hypereosinophilia in a missionary family. Travel Med Infect Dis. 2006;4:275–80. http://dx.doi.org/10.1016/j.tmaid.2005.07.001
9. Maertens K, Wéry M. Effect of mebendazole and levamisole on *Onchocerca volvulus* and *Dipetalonema perstans*. Trans R Soc Trop Med Hyg. 1975;69:359–60. http://dx.doi.org/10.1016/0035-9203(75)90134-0
10. Wahlgren M, Frolov I. Treatment of *Dipetalonema perstans* infections with mebendazole. Trans R Soc Trop Med Hyg. 1983;77:422–3. http://dx.doi.org/10.1016/0035-9203(83)90179-7
11. Bregani ER, Rovellini A, Mbaïdoum N, Magnini MG. Comparison of different anthelminthic drug regimens against *Mansonella perstans* filariasis. Trans R Soc Trop Med Hyg. 2006;100:458–63. http://dx.doi.org/10.1016/j.trstmh.2005.07.009

Address for correspondence: Federico Gobbi, Center for Tropical Diseases, Sacro Cuore Hospital, Via Sempreboni 5, 37024 Verona, Italy; email: federico.gobbi@sacrocuore.it

Genetic Diversity of Highly Pathogenic Avian Influenza A(H5N8/H5N5) Viruses in I taly, 2016–17

Alice Fusaro,[1] Isabella Monne,[1] Paolo Mulatti,
Bianca Zecchin, Lebana Bonfanti, Silvia Ormelli,
Adelaide Milani, Krizia Cecchettin,
Philippe Lemey, Ana Moreno,
Paola Massi, Tiziano Dorotea,
Stefano Marangon, Calogero Terregino

In winter 2016–17, highly pathogenic avian influenza A(H5N8) and A(H5N5) viruses of clade 2.3.4.4 were identified in wild and domestic birds in Italy. We report the occurrence of multiple introductions and describe the identification in Europe of 2 novel genotypes, generated through multiple reassortment events.

In spring 2016, highly pathogenic avian influenza (HPAI) outbreaks caused by the H5N8 subtype of clade 2.3.4.4 (group B) were reported in migratory wild birds in Qinghai Lake, China (*1*), and in the salt lake system of Uvs Nuur on the Russian Federation–Mongolia border (*2*). Since then, HPAI A(H5N8) viruses have been detected in several countries in Asia, Europe, and Africa. In Europe, the virus was detected for the first time in October 2016 in Hungary (*3*). Here, we describe the occurrence of multiple introductions of reassortant HPAI A(H5N8) and A(H5N5) viruses in Italy, in both wild and domestic birds.

The Study

During December 2016–January 2017, a Eurasian wigeon (*Anas penelope*) and a gadwall (*Anas strepera*) found dead at Grado Lagoon in northeastern Italy tested positive for HPAI A(H5N5). A second wigeon tested positive for HPAI A(H5N8). Since then, additional HPAI A(H5N8) cases were observed in a common shelduck (*Tadorna tadorna*) and in a mute swan (*Cygnus olor*) and in birds on 6 commercial turkey farms, 1 layer farm, and 3 backyard flocks

(Table 1; Figure 1). All of the cases in domestic poultry farms occurred in areas in close proximity to wetlands that are listed as important resting sites for migratory waterfowl. The onset of clinical signs in all the affected poultry species was generally associated with depression, reluctance to move, and a drop in feed consumption. The clinical condition often evolved into a more severe respiratory and nervous syndrome associated with an increased mortality rate (average mortality rate is 1.62% [95% CI 1.10%–2.14%]). Depopulation measures on the infected farms and 7 neighboring poultry premises considered at risk involved ≈510,000 birds.

The genomes of 10 positive samples collected from wild (n = 4) and domestic (n = 6) birds were fully sequenced (online Technical Appendix 1, https://wwwnc.cdc.gov/EID/article/23/9/17-0539-Techapp1.pdf). Phylogenetic analysis of the hemagglutinin (HA) gene showed that the HPAI A(H5N5) and A(H5N8) viruses clustered within the 2.3.4.4 clade, group B (Figure 1). However, the characterization of the complete genome (online Technical Appendix 1 Figures 1–8) revealed that these viruses belong to 4 distinct genotypes, which had very likely originated from multiple reassortment events.

Phylogenetic analyses indicated that the HPAI H5N5 viruses had been generated through intersubtype reassortment events between the H5N8 viruses from Asia (H5N8-Gs/Qinghai/2016-like) and the low pathogenicity avian influenza (LPAI) viruses of the Eurasian lineage (Figure 2). The A(H5N8) viruses from Asia were the source of the HA, polymerase acidic, matrix, and nonstructural protein genes. HPAI A(H5N5) viruses with similar HA and neuraminidase genes were identified in Croatia and Czech Republic in 2016–17. The time to the most recent common ancestor (tMRCA) estimated by pooling the information across all the gene segments in a hierarchical model (online Technical Appendix 1) suggested that a virus with this gene constellation emerged during October–December 2016 (Table 2; online Technical Appendix 1 Table 1).

Among the 8 HPAI A(H5N8) viruses in Italy investigated during this study, 5 were collected from wild and domestic birds in the Veneto region. In all the phylogenetic trees, these viruses clustered within the main European A(H5N8) group (A/wild duck/Poland/82A/

[1]These authors contributed equally to this article.

Table 1. Epidemiologic information for highly pathogenic avian influenza A(H5N5) and A(H5N8) viruses isolated from birds in Italy, 2016–17

Isolate	Type	Collection date	Region	Location	Site type	EpiFlu accession no.*
A/wigeon/Italy/16VIR9616-3/2016	H5N5	2016 Dec 29	Friuli Venezia Giulia	Grado (Gorizia)	Natural park	EPI888600-01, EPI954800-05
A/wigeon/Italy/17VIR57-3/2017	H5N8	2017 Jan 03	Friuli Venezia Giulia	Grado (Gorizia)	Natural park	EPI888085-92
A/gadwall/Italy/17VIR133-2/2017	H5N5	2017 Jan 10	Friuli Venezia Giulia	Grado (Gorizia)	Natural park	EPI954616-23
A/swan/Italy/17VIR537-2/2017	H5N8	2017 Jan 19	Friuli Venezia Giulia	Aquileia (Udine)	Natural park	EPI954552-59
A/turkey/Italy/17VIR538-1/2017	H5N8	2017 Jan 20	Veneto	Mira (Venice)	Fattening turkeys farm	EPI954560-67
A/turkey/Italy/17VIR576-11/2017	H5N8	2017 Jan 23	Veneto	Piove di Sacco (Padua)	Fattening turkeys farm	EPI954568-75
A/chicken/Italy/17VIR653-12/2017	H5N8	2017 Jan 25	Veneto	Porto Viro (Rovigo)	Laying hens farm	EPI954576-83
A/turkey/Italy/17VIR973-2/2017	H5N8	2017 Feb 01	Emilia Romagna	Sorbolo (Parma)	Fattening turkeys farm	EPI954584-91
A/turkey/Italy/17VIR1338-3/2017	H5N8	2017 Feb 14	Lombardy	Monzambano (Mantova)	Fattening turkeys farm	EPI954592-99
A/turkey/Italy/17VIR1452-22/2017	H5N8	2017 Feb 16	Veneto	Gazzo Veronese (Verona)	Fattening turkeys farm	EPI954600-07

*GISAID EpiFlu database (http://platform.gisaid.org).

2016-like) (Figure 2), previously described by Pohlmann et al. (*4*). The tMRCA for this group was May–June 2016 in the hierarchical gene segment model (Table 2; online Technical Appendix 1 Table 1). The first HPAI A(H5N8) virus detected in a turkey farm in the Veneto region displayed the gene composition of a virus isolated in October 2016 from a painted stork in an Indian zoo (*5*), which had not previously been reported in Europe (Figure 2). The tMRCA of this Indian–Italian group is July–October 2016, according to the hierarchical gene segment model (Table 2; online Technical Appendix 1 Table 1). The 2 outbreaks reported in 2 commercial turkey farms in the Emilia-Romagna and Lombardy regions were caused by HPAI A(H5N8) reassortant viruses containing the polymerase basic protein 2 and nucleoprotein genes of LPAI viruses of the Eurasian lineage and the remaining genes from the H5N8-Gs/Qinghai/2016-like genotype (Figure 2). Viruses with a similar gene pool were identified in Croatia and France. Estimation of the tMRCA by the hierarchical gene segment model indicated that this genotype might have emerged during June–August 2016 (Table 2; online Technical Appendix 1 Table 1).

Analyses of the phylogenetic topologies revealed that most of the sequences found in Italy were dispersed throughout the trees, indicating the occurrence of several independent introductions of the A(H5N8) virus into poultry farms from wild birds (online Technical Appendix 1 Figures 1–8). These results were confirmed by our median-joining network analyses for the HA gene (online Technical Appendix 1 Figure 9), which showed that the ancestral sequences of the samples from Italy represent viruses collected in other countries. In most cases ≥1 median

vector, representing the lost ancestral sequences, separated these viruses from the hypothetical progenitor. The only exception was for A/turkey/Italy/17VIR576-11/2017 and A/turkey/Italy/17VIR1452-22/2017, which proved to be almost identical for all the genes (similarity of 99.9%–100%), although they were collected 24 days apart in 2 turkey flocks located at a distance of ≈90 km from one another and no evident contacts were observed between them. However, because the 2 outbreaks had occurred in 2 farms operated by the same company, an exchange of virus cannot be ruled out.

Intravenous pathogenicity indexes obtained for 8 representative A(H5N8) and A(H5N5) isolates ranged from 2.85–3, comparable to an index of 2.93 for 2016 A(H5N8) viruses from Germany and 2.75–2.84 for 2016 A(H5N8) viruses from Russia (*2,4*). These data confirm that both of the A(H5N8) and A(H5N5) viruses from Italy, which shared the same HA cleavage site (PLREKRRKR), are highly pathogenic for poultry.

Conclusions

Since its emergence in China in 2013, the HPAI H5 of clade 2.3.4.4 has evolved in different genetic groups, namely A to D (*6*). Here, we describe the introductions of 4 different H5 viral genotypes of clade 2.3.4.4 group B in northern Italy. As previously observed for the 2014–15 A(H5N8) epidemic wave (*7*), our results confirm that these strains have a high propensity to reassort with co-circulating LPAI and HPAI viruses, causing the generation of several subtypes and genotypes with unique gene constellations. Unfortunately, the lack of sequences of the potential progenitors, exemplified by the
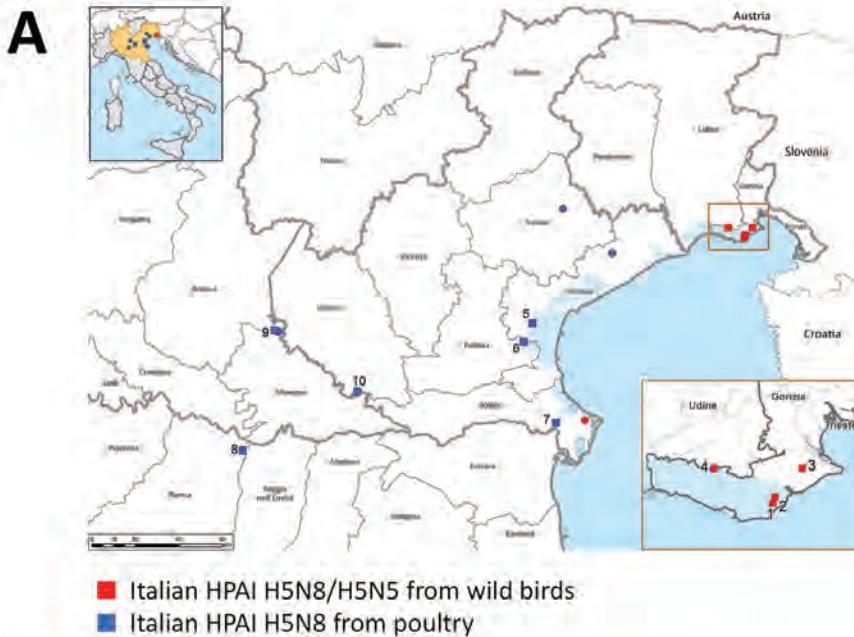
Figure 1. Highly pathogenic avian influenza A(H5N8) and A(H5N5) in birds, Italy, 2016–17). A) Geographic distribution of cases in wild (red) and domestic (blue) birds in northern Italy. Squares indicate the samples sequenced in this study; circles indicate positive samples for which no genetic information was available at the time of writing. B) Maximum-likelihood phylogenetic tree of the hemagglutinin gene of clade 2.3.4.4 viruses. Viruses analyzed in this study are indicated with red (wild birds) and blue (domestic birds) squares, numbered according to the collection date. Bootstrap supports >60% are indicated above the nodes. Scale bar indicates nucleotide substitutions per site.
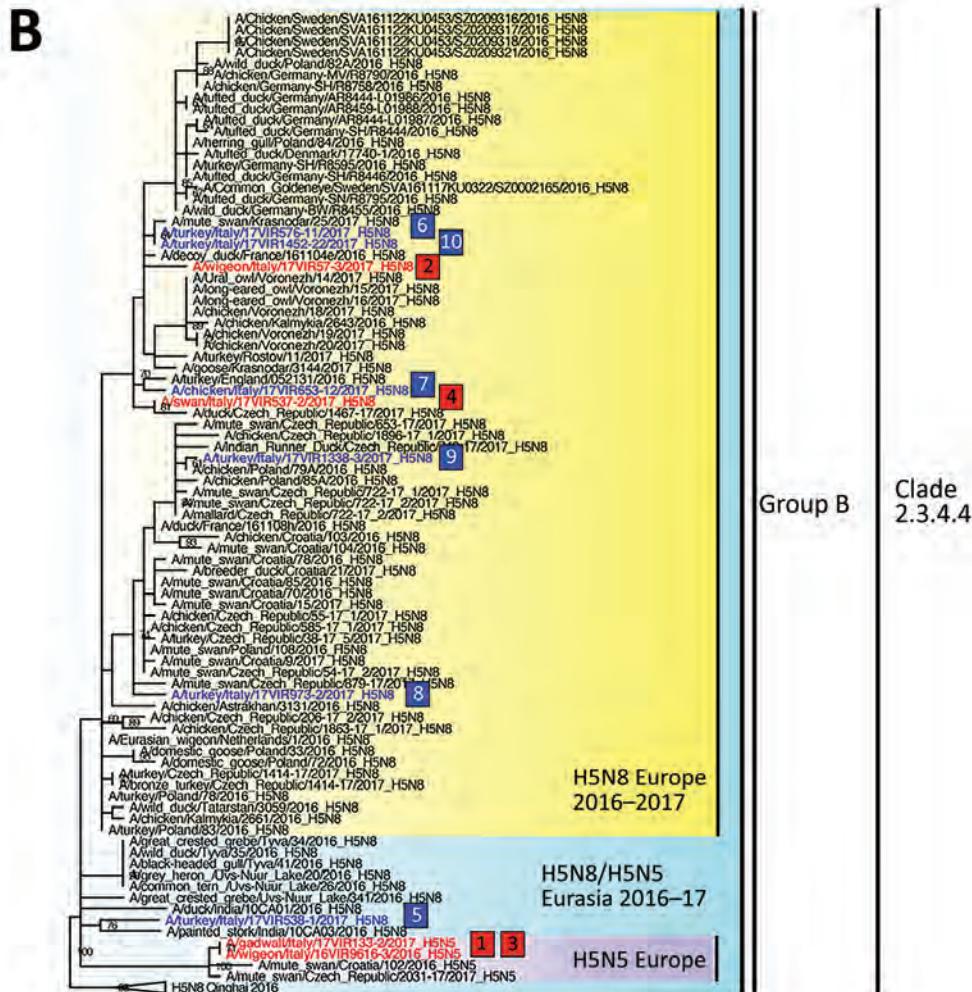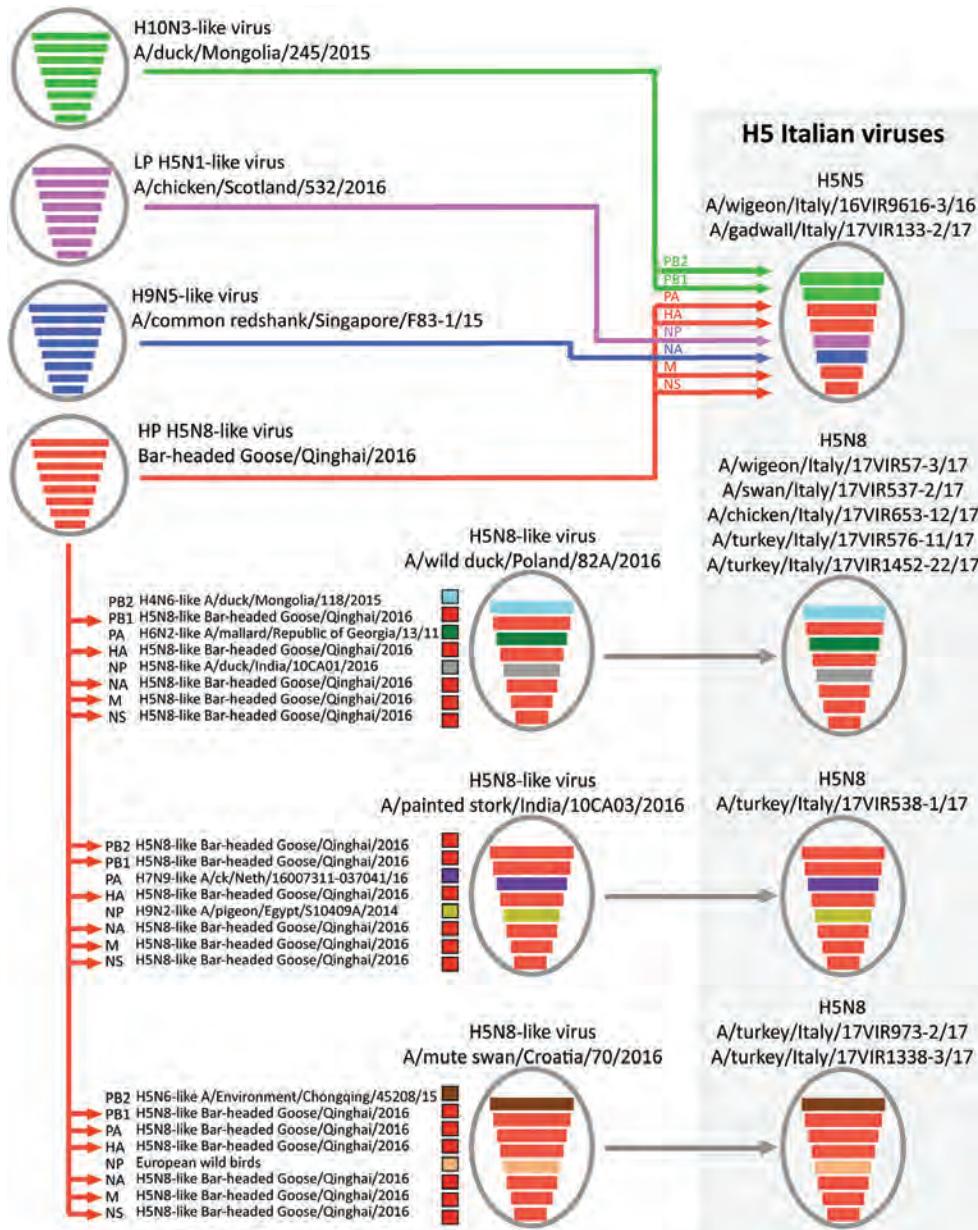
Figure 2. Probable genesis of highly pathogenic avian influenza A(H5N8) and A(H5N5) reassortant viruses identified in Italy, 2016–17 (gray box). Virus particles are represented by ovals containing horizontal bars that represent the 8 gene segments, colored according to their origin.

long branches observed in particular in the polymerase basic protein 2, polymerase acidic, and nucleoprotein phylogenies, makes it difficult to determine when and where these genotypes emerged. The genetic variability observed in the viruses identified in domestic birds, the similarity to viruses circulating in Europe and India, and the close proximity of the infected poultry farms to wetlands all suggest that wild birds did play a major role in the multiple and independent introductions of the virus into poultry holdings.

Table 2. tMRCA for the 4 avian influenza A(H5N5) and A(H5N8) virus genotypes identified in Italy, 2016–17*

Genotype	tMRCA	
	Mean	95% HPD
H5N5	November 2016	October–December 2016
H5N8 A/wild duck/Poland/82A/2016-like	May 2016	May–June 2016
H5N8 A/painted stork/India/10CA03/2016-like	August 2016	July–October 2016
H5N8 A/mute swan/Croatia/70/2016-like	July 2016	June–August 2016

*tMRCAs estimated for each gene segments are reported in online Technical Appendix 1 Table 1 (https://wwwnc.cdc.gov/EID/article/23/9/17-0539-Techapp1.pdf). HPD, highest posterior density; tMRCA, time to most recent common ancestor.

Our study highlights the importance of generating complete viral genome sequences in a timely fashion, which may help to monitor the viral spread and define appropriate disease control strategies. This, coupled with intensified wild bird surveillance on wetlands of ecologic importance for avian influenza viruses, can improve our understanding of the virus dissemination routes and support early detection of viruses highly pathogenic to poultry or believed to be of immediate concern to human health.

Dr. Fusaro is a biotechnologist working at the Istituto Zooprofilattico Sperimentale delle Venezie. Her primary research interests include molecular epidemiology, intra- and inter-host evolution, gene flow, and cross-species transmission of RNA viruses.

References

1. Li M, Liu H, Bi Y, Sun J, Wong G, Liu D, et al. Highly pathogenic avian influenza A(H5N8) virus in wild migratory birds, Qinghai Lake, China. Emerg Infect Dis. 2017;23:637–41. http://dx.doi.org/10.3201/eid2304.161866
2. Lee DH, Sharshov K, Swayne DE, Kurskaya O, Sobolev I, Kabilov M, et al. Novel reassortant clade 2.3.4.4 avian influenza A(H5N8) virus in wild aquatic birds, Russia, 2016. Emerg Infect Dis. 2017;23:359–60. http://dx.doi.org/10.3201/eid2302.161252
3. World Organisation for Animal Health. Updated on highly pathogenic avian influenza in animals (type H5 and H7), 2016 [cited 2017 Mar 10]. http://www.oie.int/animal-health-in-the-world/update-on-avian-influenza/2016
4. Pohlmann A, Starick E, Harder T, Grund C, Höper D, Globig A, et al. Outbreaks among wild birds and domestic poultry caused by reassorted influenza A(H5N8) clade 2.3.4.4 viruses, Germany, 2016. Emerg Infect Dis. 2017;23:633–6. http://dx.doi.org/10.3201/eid2304.161949
5. Nagarajan S, Kumar M, Murugkar HV, Tripathi S, Shukla S, Agarwal S, et al. Novel reassortant highly pathogenic avian influenza (H5N8) virus in zoos, India. Emerg Infect Dis. 2017;23:717–9. http://dx.doi.org/10.3201/eid2304.161886
6. Lee DH, Bahl J, Torchetti MK, Killian ML, Ip HS, DeLiberto TJ, et al. highly pathogenic avian influenza viruses and generation of novel reassortants, United States, 2014–2015. Emerg Infect Dis. 2016;22:1283–5. http://dx.doi.org/10.3201/eid2207.160048
7. Hall JS, Dusek RJ, Spackman E. Rapidly expanding range of highly pathogenic avian influenza viruses. Emerg Infect Dis. 2015;21:1251–2. http://dx.doi.org/10.3201/eid2107.150403

Address for correspondence: Alice Fusaro, Istituto Zooprofilattico Sperimentale delle Venezie, Research & Innovation Department, OIE and National Reference Laboratory for avian influenza & Newcastle disease, FAO Reference Centre for animal influenza and Newcastle disease, OIE Collaborating Centre for Diseases at the Human-Animal Interface, Viale dell'Università 10, 35020, Legnaro, Padua, Italy; email: afusaro@izsvenezie.it

Microcephaly Caused by Lymphocytic Choriomeningitis Virus

Maia Delaine, Anne-Sophie Weingertner,
Antoine Nougairede, Quentin Lepiller,
Samira Fafi-Kremer, Romain Favre, Rémi Charrel

We report congenital microencephaly caused by infection with lymphocytic choriomeningitis virus in the fetus of a 29-year-old pregnant women at 23 weeks' gestation. The diagnosis was made by ultrasonography and negative results for other agents and confirmed by a positive PCR result for lymphocytic choriomeningitis virus in an amniotic fluid sample.

Lymphocytic choriomeningitis virus (LCMV) is an arenavirus, discovered by Armstrong and Lillie in 1933 (1) that chronically infects small rodents. Humans can be infected by direct contact with rodents or their fomites, or by inhaling aerosolized particles (2). In immunocompetent adults, LCMV infection leads to an influenza-like illness or aseptic meningitis that usually resolves spontaneously; infection can also be asymptomatic (3).

When women are infected during pregnancy, the virus can be transmitted to the embryo or fetus transplacentally. Infection causes risk for miscarriage; in utero fetal death; fetopathy, including severe central nervous system or ocular malformations; and severe neurologic sequelae.

Little is known about the incidence and prevalence of LCMV. The association of Zika virus and microcephaly has been reviewed (4). Therefore, it is essential to emphasize that other viruses acquired during pregnancy can cause microcephaly and must be considered in differential diagnoses. We report a case of microcephaly caused by LCMV that was diagnosed prenatally.

The Study

The patient was a 29-year-old G1P0 pregnant woman hospitalized at 23 weeks' gestation after routine ultrasonography because of fetal ascites and minor ventriculomegaly. Her medical history was unremarkable. The woman and her husband were farmers. Written informed consent was obtained from the patient for participation in this study.

Author affiliations: Hôpitaux Universitaires de Strasbourg, Strasbourg, France (M. Delaine, A.-S. Weingertner, Q. Lepiller, S. Fafi-Kremer, R. Favre); Aix-Marseille University, Marseille, France (A. Nougairede, R. Charrel); Public Hospitals of Marseille, Marseille (A. Nougairede, R. Charrel)

Ultrasonography of the fetus showed symmetric ventriculomegaly and hyperechogenicity of the cerebral parenchyma (Figure). It also detected ascites, a minor pericardial effusion, and cardiomegaly with a hyperechogenic myocardium. The medium cerebral artery peak systolic velocity was 1.98 multiples of median, which indicated fetal anemia. Subsequent ultrasonography showed a rapid increase in ventriculomegaly, cortical atrophy, growth of ascites, and episodes of bradyarrhythmia.

An initial diagnosis of congenital infection with parvovirus B19 was rejected because maternal serologic results were negative for this virus. Serologic test results were also negative for cytomegalovirus, rubella virus, *Toxoplasma gondii*, and *Treponema pallidum*. The patient had been vaccinated against varicella virus.

We performed amniocentesis at 24 weeks' gestation: results showed a standard karyotype (46, XX). Results of PCR screening of amniotic fluid were negative for TORCH agents (**t**oxoplasmosis/*Toxoplasma gondii*, **o**ther infections, **r**ubella virus, **c**ytomegalovirus, **h**erpes simplex virus-2 or neonatal herpes simplex virus), as well as enterovirus, *Listeria monocytogenes*, *Mycoplasma* spp., and *Ureaplasma* spp. The biochemical profile of ascites indicated an infection. A fetal blood sample showed moderate anemia. Because of these negative results for virus infections, an ascitic fluid sample was tested by PCR for LCMV.

We extracted virus RNA from an ascite sample by using a Z1-XL Biorobot and a Virus Mini Kit (QIAGEN, Hilden, Germany). A 253-nt region in the small RNA segment was amplified by using sense primer CML-F0 (5′-ARCAARG-GIATYTGTAGYTGTGG-3′) and reverse primer CML-R3 (5′-CTYATGGAYTGCATCATYTTTGA-3′) in a QuantiTect SYBR Green Real-Time PCR Device (QIAGEN), a CFX96 thermal cycler (Bio-Rad Laboratories, Hercules, CA, USA), and the cycling protocol reported for flaviviruses (5).

To better characterize this strain, a 686-bp product was amplified by using primers for the virus polymerase gene (6) and directly sequenced. We used this sequence for alignment with homologous virus sequences in GenBank and performed phylogenetic analysis by using the maximum-likelihood method based on the Kimura 2-parameter model implemented in MEGA 6.06 software (7).

We tested 5 samples for virus small gene segment by using a specific Sybr Green Real Time PCR. Amniotic fluid was positive for LCMV. Fetal brain and placenta biopsy specimens and a serum sample from the mother were negative for LCMV. The matching sequence was
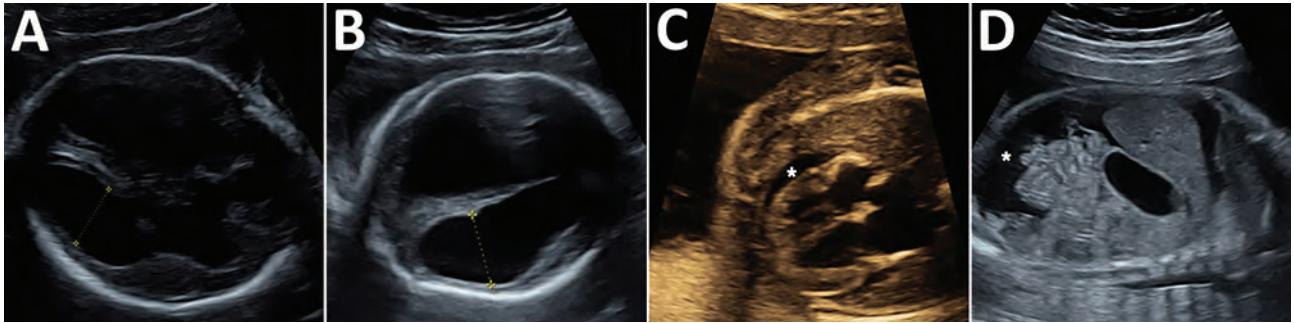
Figure. Ultrasonography of congenital microencephaly caused by infection with lymphocytic choriomeningitis virus diagnosed in the fetus of a 29-year-old pregnant women at 23 weeks' gestation. A) Fetal brain at 23 weeks' gestation showing symetric ventriculomegaly (14 mm). Yellow symbols indicate axis at which size of cerebral ventricle was measured. B) Fetal brain at 26 weeks' gestation showing symetric ventriculomegaly (20 mm) and thinning of the cortical mantle. Yellow symbols indicate axis at which size of cerebral ventricle was measured. C) Fetal heart at 24 weeks' gestation showing pericardial effusion (*) and cardiomyopathy with hyperechogenic muscle. D) Sagittal section of fetal abdomen at 26 weeks' gestation showing ascites (*).

compared with 42 other LCMV sequences by using BLAST (https://blast.ncbi.nlm.nih.gov/Blast.cgi). Genetic identities ranged from 77.2% to 90.8% at the nucleotide level.

For confirmation and better genetic characterization, we tested samples by using a reverse transcription PCR specific for virus large gene segment. Again, only amniotic fluid was positive. The 686-nt sequence matched 31 other sequences in GenBank (identity range 78.2%–88%). All specimens were inoculated onto Vero cells, but virus was not isolated.

The patient reported an influenza-like illness during the 16th week of pregnancy, which had resolved spontaneously in a few days. She also reported that there were mice on the farm.

On the basis of echographic findings, the couple decided to terminate the pregnancy at 28 weeks' gestation. A fetal blood sample showed increased anemia and thrombocythemia.

Fetopathologic examination showed hepatosplenomegaly, thymic hypertrophy, ascites, and pericardial and pleural effusion. Examination of the brain showed severe

microcephaly with polymicrogyria, a thin cortex, and diffuse periventricular calcifications. We also detected bilateral chorioretinitis. The placenta was unremarkable, and results of genetic analysis were within reference ranges.

Conclusions

The prevalence of LCMV appears to be low (LCMV IgG 0.3%) in France (8). Only 4 cases of LCMV infection have been described in France since 1978 (9–11). The laboratory of clinical microbiology at Public Hospitals of Marseille has received 83 samples for detection of LCMV during 2015–2016. The only other amniotic fluid specimen tested during this period was negative for LCMV by PCR. During 2005–2015, this laboratory has not reported a positive result for LCMV (R. Charrel, Aix-Marseille University, Marseille, France, 2017, pers. comm).

It is difficult to determine whether these findings were caused by low circulation of LCMV or lack of awareness of general practitioners and obstetricians. However, although Zika virus has been recently identified as a cause of microcephaly, physicians should consider other viruses

Table. Characteristics of neonates with congenital viral or bacterial infections, including a fetus with congenital microencephaly caused by infection with LCMV in a 29-year-old pregnant women at 23 weeks' gestation*

Virus infection or disease	VM	Intracranial hypertension	Calcification	Microcephaly	Retinopathy	Hearing impairment	HSM	Nonimmune anasarca	Fetal growth restriction
LCMV	+++	+	++++	+++	+++	?	?†	+	?‡
Toxoplasmosis	+	+	++	+	+++	+	++	+	+
Rubella virus	–	+	±	+	+	+++	+++	±	+
CMV	–	+	+	+++	+	+++	+++	+	+
HSV	–	+	+	+	+	–	+	+	+
Syphilis	±	+	–	–	+	+	+++	+	+
Parvovirus B19	–	–	–	–	–	–	+	++	+
Zika virus§	++	+	+	+++	+	?	?	+	++

*Data were obtained from Anderson et al. (2) and Barton and Mets (3). CMV, cytomegalovirus; HSM, hepatomegaly/splenomegaly; HSV, herpes simplex virus; LCMV, lymphocytic choriomeningitis virus; VM, ventriculomegaly. –, not observed; ±, possibly observed; +, rarely observed; ++, sometimes observed; +++, frequently observed; ++++, constantly observed; ?, not known.
†Diagnosed only by postmortem examination (8; this study).
‡Reported by Bonthius (14) in 6 of 20 neonates.
§Reported by Alvarado and Schwartz (4).

when dealing with signs compatible with congenital infection by Zika virus.

Since 1955, a total of 58 cases of congenital LCMV infections have been reported worldwide; all were diagnosed postnatally (*2,10,12,13*). An influenza-like illness was described in 50% of pregnant women, and exposure to rodents was reported by 33% (*2,10,12,13*). Chorioretinitis and chorioretinal scars were observed in 89%–100% of infected children, and hydrocephalus (mostly triventricular dilation) in 96% (*2,10,12,13*).

There are many prenatal ultrasonic signs of LCMV infection, involving mostly the central nervous system. Of these signs, ventriculomegaly is the most common. Bilateral cataracts are also observed. The estimated mortality rate for infants with prenatal LCMV infection is 30%–35% at the age of 21 months (*14,15*). Almost all survivors have neurologic sequelae (*14*), of which 67% are severe (*2,13,15*).

Differential diagnoses of congenital LCMV infection include testing for TORCH infections (Table). A definitive diagnosis relies on virus identification by serologic analysis or direct evidence, such as virus isolation or detection of LCMV RNA in fetal or maternal samples. For our patient, limited volumes of samples precluded additional serologic analysis; thus we performed testing by PCR. However, a positive PCR result and sequence confirmation are direct evidence for the presence of LCMV.

When ultrasonographic signs suggestive of infection are identified, complete ultrasonography can be performed to identify associated abnormalities and conventional congenital infections. If results of this initial assessment are negative, testing for LCMV is indicated for fetal samples and maternal serum samples. Medical termination of the pregnancy might need to be considered for some cases.

No vaccine or effective treatment is available for infection with LCMV. Ribavirin has been used for some cases of severe infection. However, this drug is contraindicated for pregnant women (*12*). For these women, only preventive measures are available.

LCMV infection is not included among occupation-related diseases in France, and there are few case reports of infection with this virus. Large-scale prospective studies are needed to determine the incidence of malformations associated with this virus. Lesions caused by LCMV might cover a broad spectrum, ranging from minor to severe and irreversible manifestations. Thus, LCMV infection should be considered a possible etiology requiring laboratory investigations for cases of evocative neurologic malformations or nonimmunologic anasarca not caused by a TORCH infection or genetic or chromosomal abnormalities.

Dr. Delaine is a gynecology and obstetrics intern at the University Hospital of Strasbourg, Strasbourg, France. Her research interests are obstetrics and fetal medicine.

References

1. Armstrong C, Lillie RD. Experimental lymphocytic choriomeningitis of monkeys and mice produced by a virus encountered in studies of the 1933 St. Louis encephalitis epidemic. Public Health Rep. 1934;49:1019–27. http://dx.doi.org/10.2307/4581290
2. Anderson JL, Levy PT, Leonard KB, Smyser CD, Tychsen L, Cole FS. Congenital lymphocytic choriomeningitis virus: when to consider the diagnosis. J Child Neurol. 2014;29:837–42. http://dx.doi.org/10.1177/0883073813486295
3. Barton LL, Mets MB, Congenital lymphocytic choriomeningitis virus infection: decade of rediscovery. Clin Infect Dis. 2001; 33:370–4. http://dx.doi.org/10.1086/321897
4. Alvarado MG, Schwartz DA. Zika virus infection in pregnancy, microcephaly, and maternal and fetal health: what we think, what we know, and what we think we know. Arch Pathol Lab Med. 2017;141:26–32. http://dx.doi.org/10.5858/arpa.2016-0382-RA
5. Moureau G, Temmam S, Gonzalez JP, Charrel RN, Grard G, de Lamballerie X. A real-time RT-PCR method for the universal detection and identification of flaviviruses. Vector Borne Zoonotic Dis. 2007;7:467–77. http://dx.doi.org/10.1089/vbz.2007.0206
6. Vieth S, Drosten C, Lenz O, Vincent M, Omilabu S, Hass M, et al. RT-PCR assay for detection of Lassa virus and related Old World arenaviruses targeting the L gene. Trans R Soc Trop Med Hyg. 2007;101:1253–64. http://dx.doi.org/10.1016/j.trstmh.2005.03.018
7. Tamura K, Stecher G, Peterson D, Filipski A, Kumar S. MEGA6: Molecular Evolutionary Genetics Analysis version 6.0. Mol Biol Evol. 2013;30:2725–9. http://dx.doi.org/10.1093/molbev/mst197
8. de Lamballerie X, Fulhorst CF, Charrel RN. Prevalence of antibodies to lymphocytic choriomeningitis virus in blood donors in southeastern France. Transfusion. 2007;47:172–3. http://dx.doi.org/10.1111/j.1537-2995.2007.01081.x
9. Chastel C, Bosshard S, Le Goff F, Quillien MC, Gilly R, Aymard M. Transplacental infection by lymphocytic choriomeningitis virus. Results of a retrospective serological study in France [in French]. Nouv Presse Med. 1978;7:1089–92.
10. Meritet JF, Krivine A, Lewin F, Poissonnier MH, Poizat R, Loget P, et al. A case of congenital lymphocytic choriomeningitis virus (LCMV) infection revealed by hydrops fetalis. Prenat Diagn. 2009; 29:626–7. http://dx.doi.org/10.1002/pd.2240
11. Brézin AP, Thulliez P, Cisneros B, Mets MB, Saron M-F. Lymphocytic choriomeningitis virus chorioretinitis mimicking ocular toxoplasmosis in two otherwise normal children. Am J Ophthalmol. 2000;130:245–7. http://dx.doi.org/10.1016/S0002-9394(00)00563-8
12. Jamieson DJ, Kourtis AP, Bell M, Rasmussen SA. Lymphocytic choriomeningitis virus: an emerging obstetric pathogen? Am J Obstet Gynecol. 2006;194:1532–6. http://dx.doi.org/10.1016/j.ajog.2005.11.040
13. El Feghaly RE, Hunstad DA. A newborn with hydrops, hydrocephalus, and ophthalmologic abnormalities. J Pediatric Infect Dis Soc. 2013;2:391–3. http://dx.doi.org/10.1093/jpids/pit047
14. Bonthius DJ. Lymphocytic choriomeningitis virus: an underrecognized cause of neurologic disease in the fetus, child, and adult. Semin Pediatr Neurol. 2012;19:89–95. http://dx.doi.org/10.1016/j.spen.2012.02.002
15. Wright R, Johnson D, Neumann M, Ksiazek TG, Rollin P, Keech RV, et al. Congenital lymphocytic choriomeningitis virus syndrome: a disease that mimics congenital toxoplasmosis or cytomegalovirus infection. Pediatrics. 1997;100:E9. http://dx.doi.org/10.1542/peds.100.1.e9

Address for correspondence: Maia Delaine, Centre Médico-Chirurgical Obstétrique, Hopitaux Universitaires de Strasbourg, 19 Rue Louis Pasteur, 67300 Schiltigheim, France; e-mail: maia.delaine@sfr.fr

Influenza A(H3N2) Virus in Agricultural Fairs and Transmission to Humans, Michigan and Ohio, USA, 2016

Andrew S. Bowman, Rasna R. Walia,
Jacqueline M. Nolting, Amy L. Vincent,
Mary Lea Killian, Michele M. Zentkovich,
Joshua N. Lorbach, Sarah E. Lauterbach,
Tavis K. Anderson, C. Todd Davis,
Natosha Zanders, Joyce Jones, Yunho Jang,
Brian Lynch, Marisela R. Rodriguez,
Lenee Blanton, Stephen E. Lindstrom,
David E. Wentworth, John Schiltz,
James J. Averill, Tony Forshey

In 2016, a total of 18 human infections with influenza A(H3N2) virus occurred after exposure to influenza-infected swine at 7 agricultural fairs. Sixteen of these cases were the result of infection by a reassorted virus with increasing prevalence among US swine containing a hemagglutinin gene from 2010–11 human seasonal H3N2 strains.

Influenza A virus infects many animal species. Zoonotic transmission allows for the introduction of novel influenza A virus strains to the human population, which has the potential to cause the next influenza pandemic. Swine exhibitions at agricultural fairs have emerged as a source for amplification of swine-lineage influenza A virus; these unique swine–human interfaces have generated most human infections with variant influenza A virus in the United States (*1*).

During July–August 2016, outbreaks of variant H3N2 virus (H3N2v) were reported in Ohio and Michigan, and 18 zoonotic influenza A virus infections were detected (*2*). All persons identified with H3N2v infections during these outbreaks reported swine exposure while attending ≥1 of 7 fairs in Ohio or Michigan. We examined the role of

exhibition swine in the transmission of this reassortant influenza A virus, which contained a hemagglutinin gene from 2010–11 human seasonal H3N2 strains.

The Study

Active influenza A virus surveillance among exhibition swine occurred during summer 2016 at 101 agricultural fairs across the midwestern United States; pigs were sampled at the end of exhibition irrespective of clinical signs of respiratory disease (*3*). Samples obtained using nasal swabs or nasal wipes were stored in viral transport medium at –80°C (*4,5*). Upon notification from the state animal health official, samples collected from pigs at fairs associated with H3N2v cases were screened for influenza A virus with real-time reverse transcription PCR, and positive samples were inoculated for virus isolation as previously described (*6*). The genomes of 1 or 2 isolates per fair were sequenced, and the nucleotide sequences were deposited into GenBank (*7*). Nucleotide sequences of the H3N2v viruses detected in humans were deposited in the GISAID database (online Technical Appendix, https://wwwnc.cdc.gov/EID/article/23/9/17-0847-Techapp.pdf).

We used MAFFT version 7.222 (*8*) to align sequences and manually corrected them in MEGA7 (*9*). We inferred maximum-likelihood trees by using IQ-TREE version 1.4.3 under a general time reversible plus gamma distribution plus invariant sites evolutionary model (*10*), and assessed branch support using an ultrafast bootstrap approximation with 1,000 replicates (*11*). We visualized and annotated trees using MEGA7.

We found that 7 fairs in Ohio (n = 4) and Michigan (n = 3) were associated with human H3N2v cases during July–August 2016. Of those, 6 (fairs A–F) were participating in the active influenza A virus swine surveillance program. We also included a diagnostic lab submission for a pig with respiratory disease at the seventh fair (fair G) in this study.

We sampled 161 pigs across the 7 fairs, and isolated H3N2 virus from ≥1 pig at each fair. Virus isolation data from fairs A–F (Table 1) indicated that the average prevalence of influenza A–infected swine in these fairs was 77.5% (individual fair range 60%–90%), indicating extensive influenza A virus amplification within the swine at each of these fairs. However, widespread influenza-like

Table 1. Influenza A virus rRT-PCR and virus isolation test results of samples from active surveillance among swine at agricultural fairs, Michigan and Ohio, USA, 2016*

Fair	ILI among swine reported	No. swine sampled	No. (%) positive rRT-PCR	Isolation
A	Yes	20	20 (100)	18 (90)
B	No	20	17 (85)	17 (85)
C	No	20	20 (100)	18 (90)
D	No	20	18 (90)	14 (70)
E	Yes	20	20 (100)	18 (90)
F	No	20	15 (75)	12 (60)

*Nasal swab or nasal wipe samples were collected from swine at the end of the fair. ILI, influenza-like illness; rRT-PCR, real-time reverse transcription PCR.

illness among swine was reported at only 2 of the fairs (fairs A and E), suggesting that subclinical influenza A infections in pigs remain a threat to public health (3).

A fair-by-fair comparison of the influenza A virus genomes sequenced from human H3N2v cases and isolates from swine provided strong molecular evidence of zoonotic influenza A virus transmission. The viruses recovered from swine were nearly identical to viruses identified in humans, and human virus gene segment sequences were nested within monophyletic swine virus clades. We identified 2 distinct H3 lineages in the pigs and humans across the implicated fairs (Figure 1). An influenza A virus from the well-established H3 cluster IV-A, found in the pigs at fair C, was responsible for 2 (11.1%) human cases. This cluster IV-A H3N2 genome belonged to the previously described H3 genotype 1 (Table 2) and was similar to the viruses responsible for the H3N2v infections detected in 2011–2013 (12). The influenza A virus detected in swine at the 6 fairs associated with the remaining 16 (88.9%) human H3N2v cases was a relatively new H3 lineage in swine. The HA gene of this virus descended from the human seasonal H3N2 virus circulating in 2010–11, which has since reassorted with enzootic swine influenza A viruses to produce novel viruses in the US swine herd (13). The other 7 gene segments in this human-like H3 reassortant virus were of the same lineages as those segments found in the cluster IV-A virus (Table 2).

Irrespective of the fair of origin, the genomic sequences of all 11 human-like H3N2 virus isolates from swine were ≥99.89% identical to each other, demonstrating clonal expansion of 1 virus across 2 states. This pattern of virus dissemination within the exhibition swine population was a hallmark of the 2012 fair season, when 306 H3N2v human cases were reported (6).

Influenza A virus was detected in pigs at each fair at least 1 day before each H3N2v virus infection was detected in humans (Figure 2). The observed lag time between the collection of human and swine samples is probably a function of the timing for active surveillance in swine (i.e., swine are sampled at the end of the fair), whereas specimens were collected from humans when they showed

symptoms of influenza-like illness (Figure 2). Retrospective investigations of infections in the swine from these fairs would not have been possible if the pig sampling relied on protocols triggered by the detection of H3N2v virus cases in humans because fairs typically run for 1 week and infected swine would have been dispersed before sampling could have occurred.

Conclusions

Variant influenza infections in humans continue to occur through contact with exhibition swine; often, the cases are in swine exhibitors with close and prolonged swine exposure. The concurrent detection of genetically identical influenza A viruses from exhibition swine across 2 states illustrates the rapidity with which this virus, and potentially other pathogens, can move within the highly mobile exhibition swine population. In addition to the zoonotic risks of influenza A virus, this pattern serves as a warning of possible dissemination of other emerging or high-consequence diseases in swine. Management practices common in the exhibition swine industry (i.e., frequent exhibition and relaxed biosecurity) facilitate the rapid dissemination of influenza virus across a large geographic landscape (14). Collaboration between animal and public health officials facilitated this investigation. Methods to control intraspecies and interspecies influenza virus transmission during swine shows have been outlined by the National Association of State Public Health Veterinarians (http://nasphv.org/Documents/Influenza_Transmission_at_Swine_Exhibitions_2016.pdf).

The recovery of human-like H3 influenza A viruses from exhibition swine supports previous studies demonstrating that the US commercial swine herd can serve as an influenza A reservoir for the much smaller exhibition swine population, which is more accessible to humans. Within the US commercial herd, the proportion of H3 isolates containing human-like H3 nearly doubled to 46% in spring and summer 2016 (data not shown). Whereas human-like H3s have been circulating, reassorting, and becoming more prevalent in the commercial swine population since 2012, introduction and expansion of the human-like H3 reassortant influenza A viruses in exhibition swine facilitated documented zoonoses from this genotype. The path traversed by this human-like H3, from initial introduction from humans to swine until the zoonotic transmission events of 2016, demonstrates how novel viruses can be generated and maintained in animal populations and, subsequently, can infect humans through specific ecologic niches like swine exhibitions or live-animal markets (15). Therefore, continued surveillance in swine populations is imperative for detecting novel influenza A viruses that threaten swine and human health.
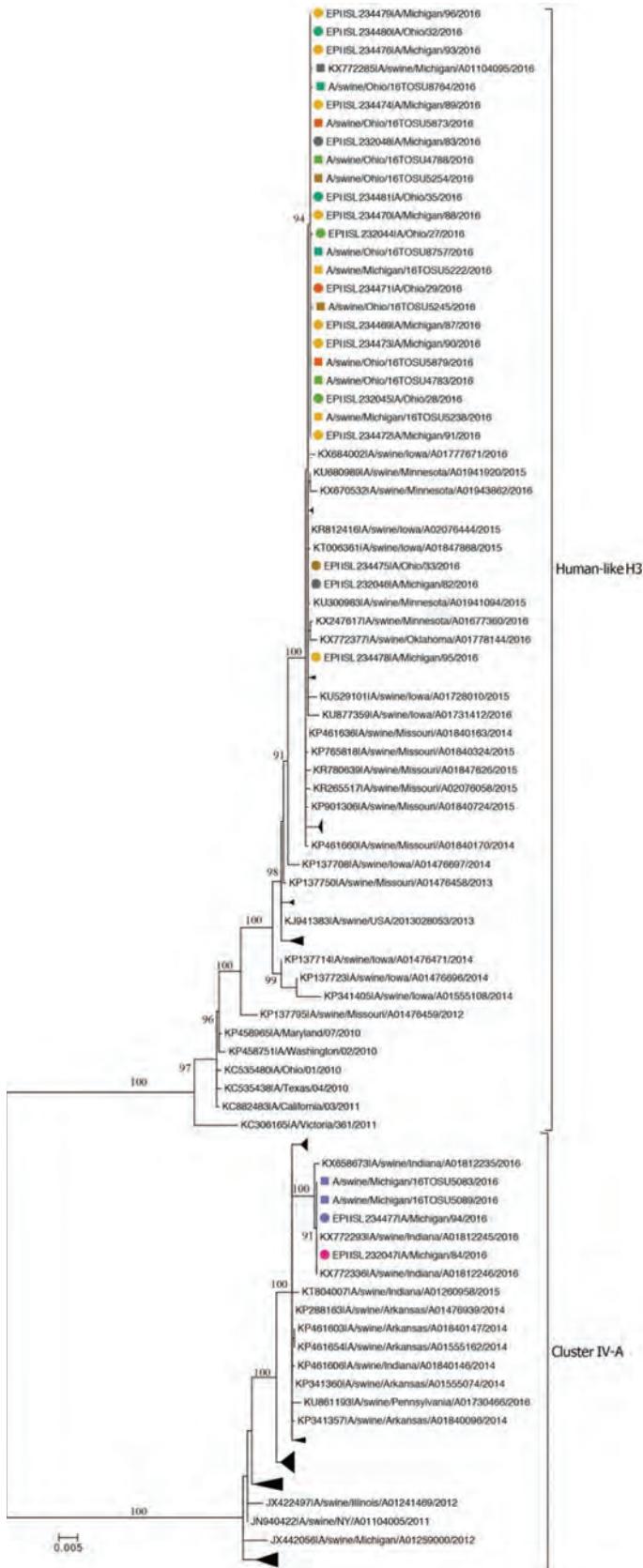
Figure 1. Phylogenetic relationships inferred for subtype H3 hemagglutinin genes of 2 distinct lineages (indicated on the right of the tree) from influenza A viruses isolated from swine and humans at agricultural fairs in Ohio and Michigan, USA, 2016. Isolates recovered are shown as squares for swine and circles for humans; colors indicate the fair attended. Scale bar indicates nucleotide substitutions per site; collapsed clades within each lineage are monophyletic clades of swine H3 HA genes.

Table 2. H3N2 genotypes identified in influenza A viruses detected in exhibition swine at agricultural fairs associated with 16 human variant H3N2 cases, Michigan and Ohio, USA, 2016*

Genotype	PB2	PB1	PA	HA	NP	NA	M	NS
H3 genotype 1, n = 2	trig	trig	trig	Swine cluster IV-A	trig	2002	pdm	trig
Human-like H3, n = 11	trig	trig	trig	Human-like H3	trig	2002	pdm	Trig

*Genomic constellations of 13 influenza A virus isolates from swine are organized by the 8 gene segments of the influenza A virus genome with HA categorized as derived from the 2010–11 human seasonal H3N2 virus (human-like H3) or the established swine lineage H3N2 (cluster IV-A). The 6 internal gene segments (PB2, PB1, PA, NP, M, NS) are classified as originating from either the 1998 triple-reassortant internal gene (trig) or influenza A(H1N1)pdm09 (pdm). All NA genes were descendants of the 2002 N2 lineage common among North American swine (12). HA, hemagglutinin; M, matrix; NA, neuraminidase; NP, nucleoprotein; NS, nonstructural protein; PA, polymerase acidic; PB, polymerase basic.

Figure 2. Timeline of detection of human and swine influenza A virus isolates at agricultural fairs in 2016. Isolates recovered are shown as squares for swine and circles for humans; colors indicate the fair attended. One person was exposed to pigs at 3 fairs (C, E, and H). Fair H is an eighth location not described in this study.

agreement between the US Department of Energy and USDA under contract number DE-AC05-06OR23100.

The findings and conclusions in this report are those of the authors and do not necessarily represent the views of USDA Animal and Plant Health Inspection Service, USDA-ARS, the Centers for Disease Control and Prevention, or the Agency for Toxic Substances and Disease Registry. USDA is an equal opportunity provider and employer.

Dr. Bowman is an assistant professor at The Ohio State University, where he leads a team researching the ecology and epidemiology of influenza A virus in swine and avian populations. He and his team are working to control influenza A virus in swine populations and reduce influenza A virus transmission across the swine–human interface.

References

1. Jhung MA, Epperson S, Biggerstaff M, Allen D, Balish A, Barnes N, et al. Outbreak of variant influenza A(H3N2) virus in the United States. Clin Infect Dis. 2013;57:1703–12. http://dx.doi.org/10.1093/cid/cit649
2. Schicker RS, Rossow J, Eckel S, Fisher N, Bidol S, Tatham L, et al. Outbreak of influenza A(H3N2) Variant virus infections among persons attending agricultural fairs housing infected swine—Michigan and Ohio, July–August 2016. MMWR Morb Mortal Wkly Rep. 2016;65:1157–60. http://dx.doi.org/10.15585/mmwr.mm6542a1
3. Bowman AS, Nolting JM, Nelson SW, Slemons RD. Subclinical influenza virus A infections in pigs exhibited at agricultural fairs, Ohio, USA, 2009–2011. Emerg Infect Dis. 2012;18:1945–50. http://dx.doi.org/10.3201/eid1812.121116
4. Nolting JM, Szablewski CM, Edwards JL, Nelson SW, Bowman AS. Nasal wipes for influenza A virus detection and isolation from swine. J Vis Exp. 2015;(106):e53313.
5. Edwards JL, Nelson SW, Workman JD, Slemons RD, Szablewski CM, Nolting JM, et al. Utility of snout wipe samples for influenza A virus surveillance in exhibition swine populations. Influenza Other Respi Viruses. 2014;8:574–9. http://dx.doi.org/10.1111/irv.12270
6. Bowman AS, Nelson SW, Page SL, Nolting JM, Killian ML, Sreevatsan S, et al. Swine-to-human transmission of influenza A(H3N2) virus at agricultural fairs, Ohio, USA, 2012. Emerg Infect Dis. 2014;20:1472–80. http://dx.doi.org/10.3201/eid2009.131082
7. Bowman AS, Sreevatsan S, Killian ML, Page SL, Nelson SW, Nolting JM, et al. Molecular evidence for interspecies transmission of H3N2pM/H3N2v influenza A viruses at an Ohio agricultural fair, July 2012. Emerg Microbes Infect. 2012;1:e33. http://dx.doi.org/10.1038/emi.2012.33
8. Katoh K, Standley DM. MAFFT multiple sequence alignment software version 7: improvements in performance and usability. Mol Biol Evol. 2013;30:772–80. http://dx.doi.org/10.1093/molbev/mst010
9. Kumar S, Stecher G, Tamura K. MEGA7: Molecular Evolutionary Genetics Analysis version 7.0 for bigger datasets. Mol Biol Evol. 2016;33:1870–4. http://dx.doi.org/10.1093/molbev/msw054
10. Nguyen LT, Schmidt HA, von Haeseler A, Minh BQ. IQ-TREE: a fast and effective stochastic algorithm for estimating maximum-likelihood phylogenies. Mol Biol Evol. 2015;32:268–74. http://dx.doi.org/10.1093/molbev/msu300
11. Minh BQ, Nguyen MA, von Haeseler A. Ultrafast approximation for phylogenetic bootstrap. Mol Biol Evol. 2013;30:1188–95. http://dx.doi.org/10.1093/molbev/mst024
12. Kitikoon P, Nelson MI, Killian ML, Anderson TK, Koster L, Culhane MR, et al. Genotype patterns of contemporary reassorted H3N2 virus in US swine. J Gen Virol. 2013;94:1236–41. http://dx.doi.org/10.1099/vir.0.051839-0
13. Rajão DS, Gauger PC, Anderson TK, Lewis NS, Abente EJ, Killian ML, et al. Novel reassortant human-like H3N2 and H3N1 influenza A viruses detected in pigs are virulent and antigenically distinct from swine viruses endemic to the United States. J Virol. 2015;89:11213–22. http://dx.doi.org/10.1128/JVI.01675-15
14. Nelson MI, Stucker KM, Schobel SA, Trovão NS, Das SR, Dugan VG, et al. Introduction, evolution, and dissemination of influenza A viruses in exhibition swine in the United States during 2009 to 2013. J Virol. 2016;90:10963–71. http://dx.doi.org/10.1128/JVI.01457-16
15. Choi MJ, Torremorell M, Bender JB, Smith K, Boxrud D, Ertl JR, et al. Live animal markets in Minnesota: a potential source for emergence of novel influenza A Viruses and interspecies transmission. Clin Infect Dis. 2015;61:1355–62. http://dx.doi.org/10.1093/cid/civ618

Address for correspondence: Andrew S. Bowman, The Ohio State University, Department of Veterinary Preventive Medicine, 1920 Coffey Rd, Columbus, OH 4310, USA; email: bowman.214@osu.edu

Serologic Evidence for Influenza C and D Virus among Ruminants and Camelids, Africa, 1991–2015

Elias Salem, Elizabeth A.J. Cook,
Hicham Ait Lbacha, Justine Oliva, Félix Awoume,
Gilbert L. Aplogan, Emmanuel Couacy Hymann,
Dishon Muloi, Sharon L. Deem, Said Alali,
Zaid Zouagui, Eric M. Fèvre, Gilles Meyer,
Mariette F. Ducatez

Influenza D virus has been identified in America, Europe, and Asia. We detected influenza D virus antibodies in cattle and small ruminants from North (Morocco) and West (Togo and Benin) Africa. Dromedary camels in Kenya harbored influenza C or D virus antibodies, indicating a potential new host for these viruses.

Influenza D virus (IDV) was recently discovered in the United States in a pig with influenza-like symptoms (1). So far, IDV or IDV antibodies have been detected in the United States, Mexico, France, Italy, China, and Japan, in healthy or sick cattle and pigs that had respiratory signs (1–6) (Figure 1). The pathogenesis and transmission of this virus are not fully understood, but recent experimental infection of calves showed that IDV can cause moderate respiratory disease (7) and that the virus is related to the bovine respiratory disease complex (2), which is a disease with very large economic costs and public health impact. The ability of IDV to replicate in ferrets, the animal model of choice for studying influenza virus in humans (1), and in guinea pigs (8) indicates that IDV might have a wider

Author affiliations: Interactions Hôtes Agents Pathogènes, Université de Toulouse, INRA, ENVT, Toulouse, France (E. Salem, J. Oliva, G. Meyer, M.F. Ducatez); International Livestock Research Institute, Nairobi, Kenya (E.A.J. Cook, D. Muloi, E.M. Fèvre); Institut Agronomique et Vétérinaire Hassan II, Rabat, Morocco (H.A. Lbacha, S. Alali, Z. Zouagui); Laboratoire Vétérinaire de Lomé, Lomé, Togo (F. Awoume); Laboratoire de Diagnostic Vétérinaire et de Sérosurveillance, Parakou, Benin (G.L. Aplogan); LANADA Central Laboratory for Animal Diseases, Bingerville, Côte d'Ivoire (E.C. Hymann); University of Edinburgh Centre for Immunity, Infection, and Evolution, Edinburgh, Scotland, UK (D. Muloi); St. Louis Zoo Institute for Conservation Medicine, St. Louis, Missouri, USA (S.L. Deem); University of Liverpool Institute of Infection and Global Health, England, UK (E.M. Fèvre)

host range than currently expected and that humans may be susceptible to infection. In addition to swine and cattle, anti-IDV antibodies have been detected in goats and sheep (9). We conducted a study to assess the putative IDV circulation in Africa.

The Study

During 1991–2015, a total of 2,083 serum samples were collected from cattle, swine, small ruminants, and dromedary camels in Morocco (n = 200), Togo (n = 540), Côte d'Ivoire (n = 203), Benin (n = 308), and Kenya (n = 1,231) (Table 1). We screened these samples by hemagglutination inhibition (HI) and microneutralization (MN) assays as described in the World Health Organization Manual for the Laboratory Diagnosis and Virological Surveillance of Influenza (10) (online Technical Appendix, https://wwwnc.cdc.gov/EID/article/23/9/17-0342-Techapp1.pdf).

Our results show that IDV has been circulating in North and West Africa since at least 2012, as shown by the antibodies detected in cattle in Morocco (from 2012 to 2015), cattle in Benin and Togo (as of 2014), and small ruminants in Togo (as of 2013) (Table 1; Figure 1). HI titers were low in ruminants, ranging 10–80 in West Africa and 10–640 in Morocco; geometric mean titers ranged 13–42 (Figure 2; HI antigen was D/bovine/Nebraska/9-5/2012). More recently, serum samples were more likely to be positive for IDV antibodies, as shown by a higher seroprevalence over time in cattle samples from Morocco and Togo (23%, 41%, and 42% seroprevalence in Morocco in 2013, 2014, and 2015, respectively; 0 and 21% seroprevalence in Togo in 2009 and 2015, respectively). None of the samples from swine or cattle in Côte d'Ivoire or small ruminants in Benin were IDV antibody–positive (Table 1; Figure 1).

To confirm our results, we tested samples from the Moroccan cohort (n = 200 cattle samples; Table 1) by using MN and HI with D/bovine/France/5920/2014 as antigen. These assays were in substantial agreement with a Cohen kappa coefficient (κ) of 0.647 (95% CI 0.541–0.753); 68% of the MN-positive samples were also positive by HI (Table 2). The agreement between HI assays with D/bovine/Nebraska/9-5/2012 and D/bovine/France/5920/2014 showed even more substantial agreement ($\kappa = 0.796$, 95% CI 0.709–0.883). All samples from Benin and Togo that
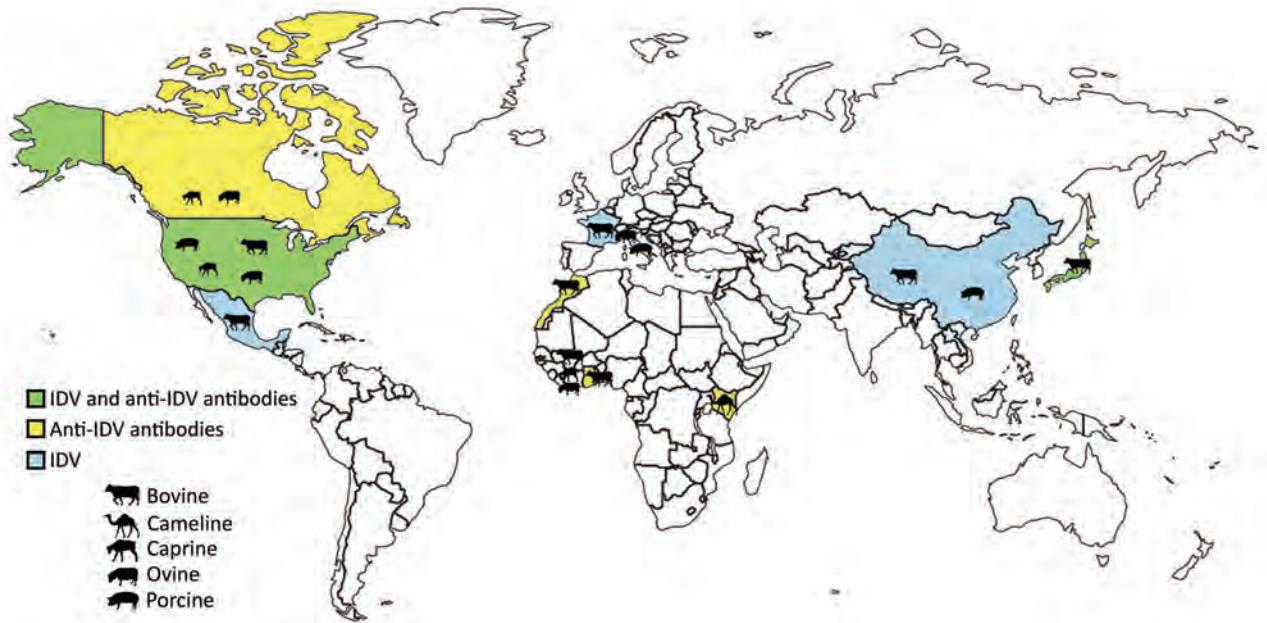
Figure 1. Locations where IDV or IDV antibodies had been detected as of April 2017. Species from which virus or antibodies were detected are indicated. IDV, influenza D virus.

were positive by HI using D/bovine/Nebraska/9-5/2012 were tested with D/bovine/France/5920/2014 and showed consistent positive results.

We then assessed IDV circulation in Kenya. None of the cattle serum samples were positive (Table 1). We first tested the 2015 camel samples from Kenya by using HI with both IDV antigens; testing with D/bovine/Nebraska/9-5/2012 showed 99% seroprevalence and with D/bovine/France/5920/2014 100% seroprevalence (Table 1; data not shown). HI titers were higher than those observed with ruminant samples from North and West Africa ($20 \leq$ HI titers ≤ 640, geometric mean titer = 150; Figure 2). When tested by using C/Victoria/1/11, the seroprevalence was 94% ($10 \leq$ HI titers ≤ 320, geometric mean titer = 38), suggesting ICV/IDV cross-reactivity. The samples were therefore adsorbed on 4 hemagglutination

Table 1. Influenza D virus seroprevalence among different animal species in 5 countries in Africa, 1991–2015*

Country	Species				
	Cattle	Swine	Sheep	Goats	Camels
Benin					
% Positive	1.9	ND	0	0	ND
No. samples	207 [1]	ND	67	34	ND
Years	2012, 2014	ND	2013–2014	2013–2014	ND
Togo					
% Positive	10.4	ND	2.2	1.4	ND
No. samples	201 [10]	ND	135 [2]	205 [0]	ND
Years	2009, 2015	ND	2013	2013	ND
Côte d'Ivoire					
% Positive	0	0	ND	ND	ND
No. samples	100	103	ND	ND	ND
Years	1991–2013	2013	ND	ND	ND
Morocco					
% Positive	35%	ND	ND	ND	ND
No. samples	200 [32]	ND	ND	ND	ND
Years	2012–2015	ND	ND	ND	ND
Kenya					
% Positive	0	ND	ND	ND	99†
No. samples	938	ND	ND	ND	293 [287]
Years	2010–2012	ND	ND	ND	2015

*A total of 2,083 serum samples were collected. Seroprevalence defined by HI titers ≥10 against D/bovine/Nebraska/9-5/2012. Numbers in brackets indicate animals with HI titers ≥40. HI, hemagglutination inhibition; ND, not done.
†No preadsorption on influenza C virus cross-reactivity likely.
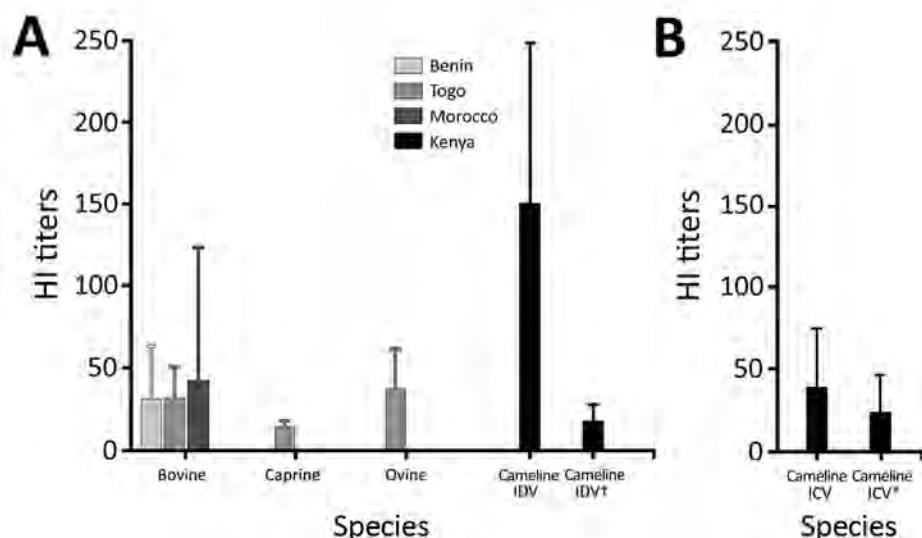
Figure 2. HI titers for ICV and IDV in serum samples from animals in Africa, by country. A) Titers against IDV by using D/bovine/Nebraska/9-5/2012 as antigen. B) Titers against ICV by using C/Victoria/1/2011 as antigen. Histograms represent mean HI titers per country and species as indicated on the *x*-axis. Error bars indicate SEM. *Post-IDV adsorption; †post-ICV adsorption. HI, hemagglutination inhibition; ICV, influenza C virus; IDV, influenza D virus.

units of C/Victoria/1/11 and hemadsorbed before being retested in HI with D/bovine/Nebraska/9-5/2012 and vice versa (all 293 samples were retested for IDV antibodies after preadsorption with ICV; 85 samples were preadsorbed on IDV and retested for ICV antibodies). Seroprevalences were 8.2% for IDV and 10.6% for ICV. All but 1 of the samples that were positive for IDV antibodies without ICV preadsorption lost $>2 \log_2$ (>4-fold decrease in titer) in HI titer once adsorbed on ICV, suggesting these samples had anti-ICV rather than anti-IDV antibodies. The picture was less clear for the reverse experiment: 11% of the IDV preadsorbed samples lost $>2 \log_2$ in titer (false ICV antibodies positive); 9% stayed within the 4-fold range (true positives); and the initial ICV antibody titer of the remaining 80% was too low (HI titers of 10 or 20) to determine a status post-IDV adsorption. Taken together, our serology results on camel samples show that almost all the animals had either anti-IDV or ICV antibodies, that there is cross-reactivity in camels between the 2 viruses, and that 9% of the tested samples had anti-ICV antibodies. Camels could therefore be a newly discovered host for ICV, and possibly for IDV. IDV/ICV cross-reactivity was ruled out for bovine samples after a cohort from France was preadsorbed the same way and retested in IDV HI without any change in HI titers (data not shown). Detection of antibodies against IDV in ruminants in Africa raises the question of the virus origin and transmission route. Although the virus has already been reported on 3 continents, the ruminant import/export from/to North and West Africa is limited (e.g., 21,000 cattle imported from Europe to Morocco, no exportations reported; no import or export of cattle reported to or from Togo or Benin; data for North and West Africa, 2013 [11]). Seroprevalences we calculated may also be underestimated because our HI assay was less sensitive than our MN assay (Table 2); numerous freezing and thawing cycles may have altered the samples; and our low titers in ruminants might have been caused by the circulation of a different IDV lineage in Africa or to the unique structure of camel antibodies, which are devoid of light chains and CH1 domain.

Although influenza A viruses are known to have non-human maintenance hosts, little is known on the host tropism of IDV and ICV. So far cattle, swine, sheep, goats, guinea pigs, and ferrets have been reported to be susceptible to IDV infection (1,6,8,9) and swine, dogs, and humans to ICV infections (12,13). Many aspects of camel health had not been studied before the emergence of Middle East respiratory syndrome coronavirus (14), but camels had been reported susceptible to influenza A(H1N1) on 1 occasion (15). Our data suggest that ICV and IDV have a wide host tropism and that further investigations on host tropism and on ICV and IDV circulation in camels are warranted.

Table 2. Comparison of HI and MN assay results for influenza D virus in 200 cattle serum samples from Morocco*

HI assay	MN assay		Total no.
	No. positive	No. negative	
No. positive	66	4	70
No. negative	31	99	130
Total no.	97	103	200
Comparison†	Sensitivity, 68% (95% CI 57.8%–77.2%)	Specificity, 96% (95% CI 90.4%–98.9%)	

*By using D/bovine/France/5920/2014 as antigen. Titers ≥10 were considered positive. HI, hemagglutination inhibition; MN, microneutralization.
†For HI as compared with MN.

Conclusions

Our results show that IDV is circulating in Africa. This virus has a wide host tropism because cattle, swine, small ruminants, and likely dromedary camels seem susceptible to IDV infection. In addition, we show that camels in Kenya are positive for ICV antibodies, suggesting that this virus also has a wider host range than previously thought. Further studies are warranted to clarify the cross-reactivity of the 2 viruses in serologic assays, to determine which IDV lineages circulate in Africa, and to assess whether ICV alone or both ICV and IDV may infect camels.

Mr. Salem is a PhD student at the Interactions Hôtes Agents Pathogènes in Toulouse. His research interests include bovine respiratory viruses and their interactions.

References

1. Hause BM, Ducatez M, Collin EA, Ran Z, Liu R, Sheng Z, et al. Isolation of a novel swine influenza virus from Oklahoma in 2011 which is distantly related to human influenza C viruses. PLoS Pathog. 2013;9:e1003176. http://dx.doi.org/10.1371/journal.ppat.1003176
2. Mitra N, Cernicchiaro N, Torres S, Li F, Hause BM. Metagenomic characterization of the virome associated with bovine respiratory disease in feedlot cattle identified novel viruses and suggests an etiologic role for influenza D virus. J Gen Virol. 2016;97:1771–84. http://dx.doi.org/10.1099/jgv.0.000492
3. Murakami S, Endoh M, Kobayashi T, Takenaka-Uema A, Chambers JK, Uchida K, et al. Influenza D virus infection in herd of cattle, Japan. Emerg Infect Dis. 2016;22:1517–9. http://dx.doi.org/10.3201/eid2208.160362
4. Ducatez MF, Pelletier C, Meyer G. Influenza D virus in cattle, France, 2011–2014. Emerg Infect Dis. 2015;21:368–71. http://dx.doi.org/10.3201/eid2102.141449
5. Jiang W-M, Wang S-C, Peng C, Yu J-M, Zhuang Q-Y, Hou G-Y, et al. Identification of a potential novel type of influenza virus in bovine in China. Virus Genes. 2014;49:493–6. http://dx.doi.org/10.1007/s11262-014-1107-3
6. Chiapponi C, Faccini S, De Mattia A, Baioni L, Barbieri I, Rosignoli C, et al. Detection of influenza D virus among swine and cattle, Italy. Emerg Infect Dis. 2016;22:352–4. http://dx.doi.org/10.3201/eid2202.151439
7. Ferguson L, Olivier AK, Genova S, Epperson WB, Smith DR, Schneider L, et al. Pathogenesis of influenza D virus in cattle. J Virol. 2016;90:5636–42. http://dx.doi.org/10.1128/JVI.03122-15
8. Sreenivasan C, Thomas M, Sheng Z, Hause BM, Collin EA, Knudsen DEB, et al. Replication and transmission of the novel bovine influenza D virus in a guinea pig model. J Virol. 2015;89:11990–2001. http://dx.doi.org/10.1128/JVI.01630-15
9. Quast M, Sreenivasan C, Sexton G, Nedland H, Singrey A, Fawcett L, et al. Serological evidence for the presence of influenza D virus in small ruminants. Vet Microbiol. 2015;180:281–5. http://dx.doi.org/10.1016/j.vetmic.2015.09.005
10. World Health Organization. Manual for the laboratory diagnosis and virological surveillance of influenza. Geneva: The Organization; 2011.
11. Food and Agriculture Organization of the United Nations. FAOSTAT [cited 2017 Mar 3]. http://www.fao.org/faostat/en/#data/TA
12. Kimura H, Abiko C, Peng G, Muraki Y, Sugawara K, Hongo S, et al. Interspecies transmission of influenza C virus between humans and pigs. Virus Res. 1997;48:71–9. http://dx.doi.org/10.1016/S0168-1702(96)01427-X
13. Ohwada K, Kitame F, Sugawara K, Nishimura H, Homma M, Nakamura K. Distribution of the antibody to influenza C virus in dogs and pigs in Yamagata Prefecture, Japan. Microbiol Immunol. 1987;31:1173–80. http://dx.doi.org/10.1111/j.1348-0421.1987.tb01351.x
14. Deem SL, Fèvre EM, Kinnaird M, Browne AS, Muloi D, Godeke GJ, et al. Serological evidence of MERS-CoV antibodies in dromedary camels (Camelus dromedaries) in Laikipia County, Kenya. PLoS One. 2015;10:e0140125. http://dx.doi.org/10.1371/journal.pone.0140125
15. Yamnikova SS, Mandler J, Bekh-Ochir ZH, Dachtzeren P, Ludwig S, Lvov DK, et al. A reassortant H1N1 influenza A virus caused fatal epizootics among camels in Mongolia. Virology. 1993;197:558–63. http://dx.doi.org/10.1006/viro.1993.1629

Address for correspondence: Mariette F. Ducatez, Interactions Hôtes Agents Pathogènes, Université de Toulouse, INRA, ENVT, 23 Chemin des Capelles, 31076 Toulouse, France; email: m.ducatez@envt.fr

Use of Blood Donor Screening to Monitor Prevalence of HIV and Hepatitis B and C Viruses, South Africa

Marion Vermeulen, Ronel Swanevelder,
Dhuly Chowdhury, Charlotte Ingram,[1]
Ravi Reddy, Evan M. Bloch, Brian S. Custer,
Edward L. Murphy, for the NHLBI Recipient
Epidemiology and Donor evaluation Study-III
(REDS-III) International Component

Among 397,640 first-time blood donors screened in South Africa during 2012–2015, HIV prevalence was 1.13%, hepatitis B virus prevalence 0.66%, and hepatitis C virus prevalence 0.03%. Findings of note were a high HIV prevalence in Mpumalanga Province and the near absence of hepatitis C virus nationwide.

South Africa has one of the largest HIV epidemics in the world. HIV prevalence is 18.8% among those 15–49 years of age, and estimated HIV incidence in sexually active persons is 1.21/100 person-years for men and 2.28/100 person-years for women (*1,2*). Chronic hepatitis B virus (HBV) infection is also common; among young adults, hepatitis B surface antigen (HBsAg) prevalence is ≈4%, and universal HBV vaccination of infants was introduced in 1995 (*3*). Other than in an outdated study that found PCR-positive hepatitis C virus (HCV) in 0.05% of blood donors (*4*), the prevalence of HCV infection in South Africa is poorly described but is probably lower than in other countries in Africa (*5*). Recent published data on the prevalence of HIV, HBV, and HCV among blood donors in South Africa are scant (*6,7*). We assessed prevalence of these viruses by demographic and geographic characteristics to inform donor-selection criteria and to aid public health surveillance.

The Study

We included all eligible first-time blood donors at South African National Blood Service (SANBS) facilities for January 2012–September 2015, covering all provinces except Western Cape Province. We excluded those deferred from donation because of risk behaviors or poor health.

We screened blood donations individually for HIV RNA, HCV RNA, and HBV DNA by using the Procleix Ultrio Plus assay (Grifols, Barcelona, Spain) and serologically for HIV antibodies, HCV antibodies, and HBsAg by using Abbott Prism ChLia (Abbott, Delkenheim, Germany). We further tested serologic repeat–reactive but nucleic acid testing (NAT)–negative donations by using supplemental assays: HIV Western blot (Bio-Rad, Hercules, CA, USA); HCV InnoLIA (Innogenetics, Ghant, Belgium); or HBsAg neutralization (Roche, Pleasanton, CA, USA).

We calculated prevalences and derived odds ratios (ORs) and 95% CIs for associations from multivariable logistic regression by using SAS/STAT 9.4 (SAS Institute, Inc., Cary, NC, USA). Because of statistically significant interactions between sex and age and between sex and race (online Technical Appendix 1, https://wwwnc.cdc.gov/EID/article/23/9/16-1594-Techapp1.pdf), we built separate models for male and female donors.

During January 2012–September 2015, a total of 3,075,422 blood donations were made at SANBS facilities from repeat donors; 397,640 (13%) donations were from first-time donors, who were predominantly young and equally distributed by sex (Table). Approximately half of donors were black, one third white, and the remainder of Asian; South African Colored (SAC) (an admixed group made up of 5 source populations [African Khoisan, African Bantu, European, South Asian, and East Asian]); or unknown race/ethnicity.

A total of 4,481 (1.13%) first-time donors were classified as HIV positive. Prevalence was highest (1.3%–1.9%) among persons 20–49 years of age, higher among female (1.4%) than male (0.8%) donors, and higher among those of black race/ethnicity (2.0%) than other races/ethnicities (Table). In logistic regression models (online Technical Appendix 2, https://wwwnc.cdc.gov/EID/article/23/9/16-1594-Techapp2.xlsx), HIV infection was more strongly associated with older age among male donors than among female donors and more strongly with black and unknown race/ethnicity among female donors than among male

Author affiliations: South African National Blood Service, Johannesburg, South Africa (M. Vermeulen, R. Swanevelder, C. Ingram, R. Reddy); RTI International, Rockville, Maryland, USA (D. Chowdhury); Johns Hopkins University School of Medicine, Baltimore, Maryland, USA (E.M. Bloch); Blood Systems Research Institute, San Francisco, California, USA (B.S. Custer, E.L. Murphy); University of California, San Francisco (E.L. Murphy)

[1]Current affiliation: South African Bone Marrow Registry, Cape Town, South Africa.

Table. Prevalence of HIV, HBV, and HCV, by demographic characteristics, among persons making blood donations through the South African National Blood Service, January 2012–September 2015*

Characteristic	No. first-time donors	No. (%)		
		HIV-positive	HBV-positive	HCV-positive
Overall	397,640	4,481 (1.13)	2,638 (0.66)	125 (0.03)
Age group, y				
<20	185,983	1,139 (0.61)	382 (0.21)	6 (0.00)
20–29	103,373	1,702 (1.65)	999 (0.97)	39 (0.04)
30–39	55,420	1,038 (1.87)	721 (1.30)	17 (0.03)
40–49	33,330	440 (1.32)	366 (1.10)	21 (0.06)
50–59	16,518	146 (0.88)	151 (0.91)	31 (0.19)
>60	3,016	16 (0.53)	19 (0.63)	11 (0.36)
Sex				
M	177,729	1,396 (0.79)	1,635 (0.92)	77 (0.04)
F	219,903	3,085 (1.40)	1,003 (0.46)	48 (0.02)
Race/ethnicity†				
Black	211,722	4,204 (1.99)	2,355 (1.11)	62 (0.03)
White	122,894	74 (0.06)	80 (0.07)	43 (0.03)
Asian	28,428	28 (0.10)	41 (0.14)	11 (0.04)
SAC	20,246	98 (0.48)	99 (0.49)	5 (0.02)
Unknown	14,350	77 (0.54)	63 (0.44)	4 (0.03)
Province				
Eastern Cape	37,055	365 (0.99)	315 (0.85)	4 (0.01)
Free State	20,759	241 (1.16)	68 (0.33)	3 (0.01)
Gauteng	175,623	1,774 (1.01)	967 (0.55)	77 (0.04)
KwaZulu-Natal	80,111	918 (1.15)	728 (0.91)	14 (0.02)
Limpopo	15,661	159 (1.02)	113 (0.72)	7 (0.04)
Mpumalanga	35,720	779 (2.18)	305 (0.85)	8 (0.02)
Northwest	19,205	124 (0.65)	65 (0.34)	7 (0.04)
Northern Cape	10,333	74 (0.72)	57 (0.55)	3 (0.03)

*3,173 donors had missing information on province. HBC, hepatitis B virus; HCV, hepatitis C virus; SAC, South African Colored.
†The Department of Home Affairs in South Africa classifies the South Africa population into 4 race groups: African, Indian, White, and Coloured. The SAC population is an admixed group made up of 5 source populations (African Khoisan, African Bantu, European, South Asian, and East Asian) dating back to slavery and the early settlers.

donors (online Technical Appendix 1). We observed a significant association between HIV and HBV infection in both sexes and a stronger association between HIV and HCV infection in female donors only. Compared with Gauteng Provence, HIV infection was associated with donation in Mpumalanga, KwaZulu-Natal, and Free State provinces for both sexes and with Eastern Cape Province for female donors and Northern Cape Province for male donors (Figure).

The 1.13% HIV prevalence among first-time blood donors in South Africa is much higher than that for high-income countries but lower than for many countries in sub-Saharan Africa, where HIV prevalence ranges from 3% to 5% (8). HIV prevalence among donors was substantially lower than that among the general adult population of South Africa (estimated at 18.8%), but similar demographic associations were observed (1,2). Geographic distributions of HIV infection were also generally similar to national data, although we found higher adjusted odds for HIV infection in Mpumalanga Province compared with KwaZulu-Natal Province (1). Incorporation of blood donor prevalence and incidence data might help to refine statistical models of the HIV epidemic, which have not performed well in some subgroups (2,9). In addition, blood bank testing for HIV includes men and older persons, who are not well-represented in current surveillance strategies (10).

A total of 2,638 (0.66%) first-time donors were classified as HBV-positive. HBV prevalence was 0.9%–1.3% among those 20–49 years of age, and only 0.2% among those <20 years of age (Table). HBV prevalence was 0.9% among male donors versus 0.5% among female donors, 1.1% among blacks, 0.5% among persons of SAC race/ethnicity, and 0.1% among whites. In the logistic regression models (online Technical Appendix 2), HBV infection was more strongly associated with older age among men than among women and had a geographic distribution slightly different from that of HIV.

The HBV prevalence of 0.66% was substantially less than the median of 4.35% for all countries in Africa; however, lack of confirmatory testing might inflate the proportion for all of Africa (11). In our study, a 5-fold lower prevalence among donors <20 years of age compared with those 20–29 years of age is consistent with the implementation of HBV vaccination of infants in South Africa in 1995 and could be used to estimate vaccination coverage (3). Male donors appear to be at higher risk for chronic HBV infection, as reported in the United States (12).

Only 125 (0.03%) donors were confirmed positive for HCV infection. HCV prevalence was highest (0.4%) among those ≥60 years of age (0.04% among men, 0.02% among women) (Table). We observed little difference in HCV prevalence by race/ethnicity. In logistic regression models, HCV
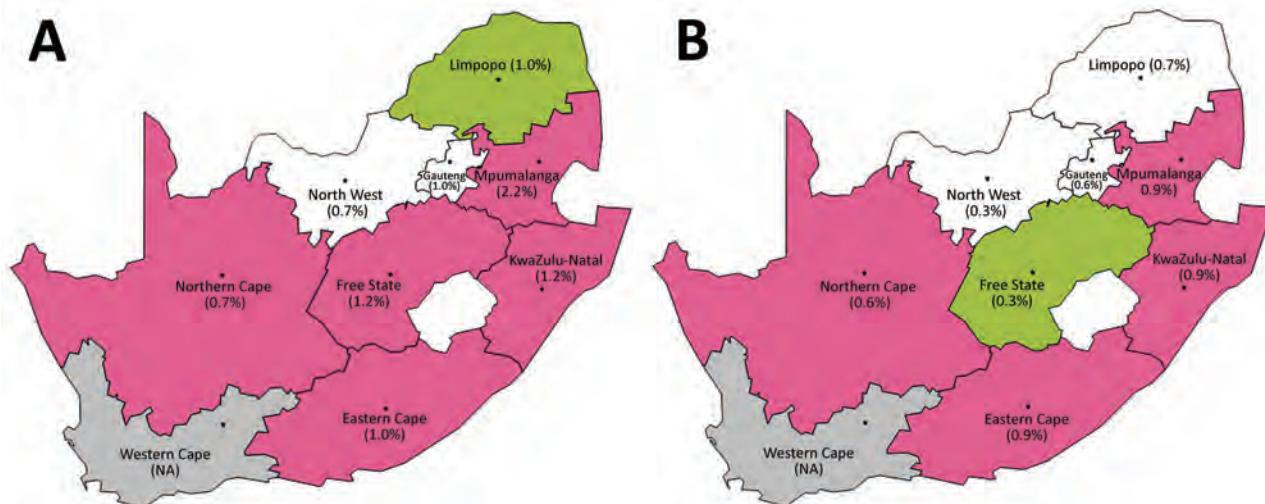
Figure. Overall prevalence of HIV (A) and hepatitis B virus (B) in South Africa, by province, among persons making blood donations through the South African National Blood Service, January 2012–September 2015. Pink indicates a significantly higher odds ratio and green indicates a lower odds ratio compared with Gauteng Province (Johannesburg region) and adjusting for other factors. Unadjusted prevalences are shown in parentheses. NA, not applicable.

infection was associated with older age and with HIV co-infection among women only (online Technical Appendix 2). Among men only, HCV was inversely associated with blood donation in Eastern Cape and KwaZulu-Natal Provinces.

Contrary to some reports, which included small studies and those lacking confirmatory testing (13), HCV infection appears to be rare among South Africa blood donors and, by extrapolation, its general population. The 0.03% blood donor prevalence we found is consistent with an older study (4) and much lower than the median of 0.86% for other countries in Africa (11). Reasons for this low prevalence are unclear but likely relate to the relative absence of injection drug use or other parenteral risk factors for HCV transmission. Further study of why South Africa has lower HCV prevalence than many countries in the world is warranted. One clue might be the predominance of infection among older and male persons, suggesting a possible birth cohort effect related to historical parenteral exposures (14).

Conclusions

Our study attests to the success of blood donor selection and screening: HIV prevalence was ≈18-fold lower and HBV prevalence 5-fold lower than that of the general population of South Africa. This difference is attributable to selection of low-risk and healthy donors and underrepresentation of blacks among blood donors. These biases need to be accounted for in extrapolating directly to the general population, but comparisons between donor subgroups or periods might still mirror population data. Prevalent infections in donors are detected by serologic testing, and blood products are discarded accordingly. To

mitigate the risk posed by seronegative window period infections, SANBS performs routine individual donation NAT. This parallel serology and NAT testing has generated substantial data on HIV and HBV incidence, further contributing to public health surveillance (6).

Ms. Vermeulen is Director of Operations Testing for the South African National Blood Service and oversees infectious disease testing of ≈800,000 blood donations annually. She has research interests in the evaluation and implementation of nucleic acid testing for viral infections in blood donors and its use in the estimation of HIV incidence.

References

1. Zuma K, Shisana O, Rehle TM, Simbayi LC, Jooste S, Zungu N, et al. New insights into HIV epidemic in South Africa: key findings from the National HIV Prevalence, Incidence and Behaviour Survey, 2012. Afr J AIDS Res. 2016;15:67–75. http://dx.doi.org/10.2989/16085906.2016.1153491
2. Eaton JW, Bacaër N, Bershteyn A, Cambiano V, Cori A, Dorrington RE, et al. Assessment of epidemic projections using recent HIV survey data in South Africa: a validation analysis of ten mathematical models of HIV epidemiology in the antiretroviral therapy era. Lancet Glob Health. 2015;3:e598–608. http://dx.doi.org/10.1016/S2214-109X(15)00080-7
3. Amponsah-Dacosta E, Lebelo RL, Rakgole JN, Burnett RJ, Selabe SG, Mphahlele MJ. Evidence for a change in the epidemiology of hepatitis B virus infection after nearly two decades of universal hepatitis B vaccination in South Africa. J Med Virol. 2014;86:918–24. http://dx.doi.org/10.1002/jmv.23910

4. Tucker TJ, Voigt M, Bird A, Robson S, Gibbs B, Kannemeyer J, et al. Hepatitis C virus infection rate in volunteer blood donors from the Western Cape—comparison of screening tests and PCR. S Afr Med J. 1997;87:603–5.

5. Rao VB, Johari N, du Cros P, Messina J, Ford N, Cooke GS. Hepatitis C seroprevalence and HIV co-infection in sub-Saharan Africa: a systematic review and meta-analysis. Lancet Infect Dis. 2015;15:819–24. http://dx.doi.org/10.1016/S1473-3099(15)00006-7

6. Bruhn R, Lelie N, Custer B, Busch M, Kleinman S; International NAT Study Group. Prevalence of human immunodeficiency virus RNA and antibody in first-time, lapsed, and repeat blood donations across five international regions and relative efficacy of alternative screening scenarios. Transfusion. 2013;53:2399–412. http://dx.doi.org/10.1111/trf.12299

7. Vermeulen M, Lelie N, Sykes W, Crookes R, Swanevelder J, Gaggia L, et al. Impact of individual-donation nucleic acid testing on risk of human immunodeficiency virus, hepatitis B virus, and hepatitis C virus transmission by blood transfusion in South Africa. Transfusion. 2009;49:1115–25. http://dx.doi.org/10.1111/j.1537-2995.2009.02110.x

8. Bloch EM, Vermeulen M, Murphy E. Blood transfusion safety in Africa: a literature review of infectious disease and organizational challenges. Transfus Med Rev. 2012;26:164–80. http://dx.doi.org/10.1016/j.tmrv.2011.07.006

9. Rehle T, Johnson L, Hallett T, Mahy M, Kim A, Odido H, et al. A comparison of South African national HIV incidence estimates: a critical appraisal of different methods. PLoS One.

10. Johnson LF, Rehle TM, Jooste S, Bekker LG. Rates of HIV testing and diagnosis in South Africa: successes and challenges. AIDS. 2015;29:1401–9. http://dx.doi.org/10.1097/QAD.0000000000000721

11. Apata IW, Averhoff F, Pitman J, Bjork A, Yu J, Amin NA, et al. Progress toward prevention of transfusion-transmitted hepatitis B and hepatitis C infection—sub-Saharan Africa, 2000–2011. MMWR Morb Mortal Wkly Rep. 2014;63:613–9.

12. Custer B, Kessler D, Vahidnia F, Leparc G, Krysztof DE, Shaz B, et al.; NHLBI Retrovirus Epidemiology Donor Study-II (REDS-II). Risk factors for retrovirus and hepatitis virus infections in accepted blood donors. Transfusion. 2015;55:1098–107. http://dx.doi.org/10.1111/trf.12951

13. Gower E, Estes C, Blach S, Razavi-Shearer K, Razavi H. Global epidemiology and genotype distribution of the hepatitis C virus infection. J Hepatol. 2014;61(Suppl):S45–57. http://dx.doi.org/10.1016/j.jhep.2014.07.027

14. Mohd Hanafiah K, Groeger J, Flaxman AD, Wiersma ST. Global epidemiology of hepatitis C virus infection: new estimates of age-specific antibody to HCV seroprevalence. Hepatology. 2013;57:1333–42. http://dx.doi.org/10.1002/hep.26141

Address for correspondence: Edward L. Murphy, University of California–San Francisco, Laboratory Medicine, 270 Masonic Ave, San Francisco, CA 94118, USA; email: murphy@ucsf.edu

@CDC_EIDjournal

Follow the EID journal on Twitter and get the most current information from Emerging Infectious Diseases.

Emergence of Plasmid-Mediated Fosfomycin-Resistance Genes among *Escherichia coli* Isolates, France

Yahia Benzerara, Salah Gallah,
Baptiste Hommeril, Nathalie Genel,
Dominique Decré, Martin Rottman,
Guillaume Arlet

FosA, a glutathione *S*-transferase that inactivates fosfomycin, has been reported as the cause of enzymatic resistance to fosfomycin. We show that multiple lineages of FosA-producing extended spectrum β-lactamase *Escherichia coli* have circulated in France since 2012, potentially reducing the efficacy of fosfomycin in treating infections with antimicrobial drug–resistant gram-negative bacilli.

Fosfomycin is a broad-spectrum bactericidal antibiotic commonly used in Europe as a first-line oral agent for uncomplicated urinary tract infection (*1*). In France, it is the only first-line antimicrobial drug recommended for treatment of cystitis (97% susceptibility) and is used in 20%–30% of such treatments (*2*). However, it is receiving renewed worldwide attention as one of the most active agents for sparing carbapenems in extended spectrum β-lactamase (ESBL)–producing isolates and for treatment of carbapeneme-resistant *Enterobacteriaceae* (CRE) in combination with colistin (*3*). In France, intravenous fosfomycin (3–4 g 4×/d) is used in combination with other drugs for the treatment of multidrug-resistant infections.

The evaluation of fosfomycin susceptibility in clinical strains is widely performed, but the molecular bases are rarely documented. Fosfomycin inhibits the initial step in peptidoglycan synthesis by irreversibly blocking MurA in both gram-positive and -negative bacteria. It is imported through the inner membrane through the glycerol-3-phosphate (G3P) transporter GlpT and the glucose-6-phosphate (G6P) transporter UhpT. Decreased expression or

Author affiliations: Assistance Publique des Hôpitaux de Paris Hôpitaux Universitaires Est Parisiens Paris, France (Y. Benzerara, S. Gallah, B. Hommeril, D. Decré, G. Arlet); Université Pierre et Marie Curie, Sorbonne Université, Paris (N. Genel, D. Decré, G. Arlet); Assistance Publique des Hôpitaux de Paris Hôpitaux Universitaires Paris Ile de France Ouest, Hôpital Raymond Poincaré, Garches, France (M. Rottman); Université de Versailles Saint-Quentin-en-Yvelines, St-Quentin en Yvelines, France (M. Rottman)

mutations in *glpT* or *uhpT* genes are the most frequent events leading to lowered susceptibility, whereas modification of the fosfomycin target MurA seems to be rare in clinical isolates (*4*). Another mechanism is the production of FosA, a glutathione *S*-transferase that inactivates fosfomycin by addition of a glutathione residue. This mechanism is particularly relevant because it is disseminative and frequently associated with ESBL-producing *Escherichia coli*. Since 2006, researchers in several countries in East Asia have described plasmid-mediated *fosA3* and, less frequently, *fosA5* (formerly *fosKp96*), which is mostly associated with CTX-M and co-harbored on a conjugative plasmid. Some studies have focused on human clinical strains in China (*5*), South Korea (*6*), or Japan (*7*), and others have addressed veterinary strains isolated throughout China from pets (*8*), livestock (*9*), or animal fodder (*10*). In 2016, Portugal reported the first imported case of a travel-related infection in Europe with an *E. coli* strain co-expressing *fosA3* and CTX-M-15 (*11*). The possible dissemination of this gene is worrisome because *fosA3* is generally surrounded by the IS*26* insertion sequence on a composite transposon borne by the IncFII conjugative plasmid, which is known to be a dissemination vector of resistance genes worldwide. Here we report the prevalence and mechanisms of fosfomycin resistance among clinical human *E. coli* strains isolated in Paris, France.

The Study

We investigated the occurrence and molecular features of all fosfomycin-resistant *E. coli* isolated from hospitalized patients during a 12-month period (August 2014–July 2015). We performed bacterial identification by using VITEK 2 (BioMérieux, Marcy l'Etoile, France) and tested antibiotic susceptibility by using the disk diffusion method in accordance with 2016 Comité de l'Antibiogramme de la Société Française de Microbiologie/European Committee on Antimicrobial Susceptibility Testing guidelines (http://www.sfm-microbiologie.org/UserFiles/files/casfm/CASFM2016_V1_0_FEVRIER.pdf). We screened for fosfomycin resistance by using a 200-µg disk with a diameter cutoff of ≤13 mm. We determined MIC by using the Etest method with Muller-Hinton agar containing 25 mg/L G6P.

Among 1,354 *E. coli* isolates tested, 12 (0.9%) showed confirmed resistance (MIC >128 mg/L). We explored the

Table 1. Oligonucleotide primers used in our study for detection of plasmid-mediated fosfomycin-resistance genes*

Target gene	Primer	Sequence, 5′ → 3′	Temp, C°	Amplicon size, bp	Reference
fosA	Fwd	ATCTGTGGGTCTGCCTGTCGT	50	271	(5)
	Rev	ATGCCCGCATAGGGCTTCT			
fosA3	Fwd	CCTGGCATTTTATCAGCAGT	55	221	(5)
	Rev	CGGTTATCTTTCCATACCTCAG			
fosA4	Fwd	CTGGCGTTTTATCAGCGGTT	60	230	This study
	Rev	CTTCGCTGCGGTTGTCTTT			
fosA5	Fwd	TATTAGCGAAGCCGATTTTGCT	55	177	(5)
	Rev	CCCCTTATACGGCTGCTCG			
fosC2	Fwd	TGGAGGCTACTTGGATTTG	50	209	(8)
	Rev	AGGCTACCGCTATGGATTT			
*Fwd, forward; Rev, reverse.					

mechanism of fosfomycin resistance by growing these isolates for 48 hours at 35°C in M9 minimal medium agar supplemented with either G3P or G6P at 0.2% as the sole carbon source. Lack of growth showed impaired fosfomycin transport (*12*). Of the 12 isolates, 7 were double auxotrophic mutants with G6P and G3P (mean MIC 384 mg/L), 3 were auxotrophic only for G3P (mean MIC 597 mg/L), and 2 were capable of using both substrates and exhibited high-level resistance (MIC >1,024 mg/L). Paradoxically, single and double auxotroph strains had lower mean MICs

Figure. Inhibition of FosA-mediated fosfomycin resistance by phosphonoformiate. A modified Kirby-Bauer disk diffusion susceptibility assay was performed. In brief, a Mueller-Hinton agar plate was streaked with a 0.5 McFarland suspension of the isolate assayed. Three disks were placed on the agar: a 200-µg fosfomycin disk (upper left), a 100-µg phosphonoformiate disk (lower center), and a disk with both 200-µg fosfomycin and 100-µg phosphonoformiate (upper right). The diameter of the growth inhibition zone around each disk was measured after 18–24 h incubation at 35°C (+2°C). FosA-mediated fosfomycin resistance is inhibited by phosphonoformiate and is demonstrated by an increase in the diameter of the growth inhibition zone by >4 mm.

than the 2 nonauxotroph strains. Because transport deficit could not account for the observed phenotype, we screened by PCR and sequenced genes coding enzymatic glutathione S-transferase variants *fosA*, *fosA2*, *fosA3*, *fosA4*, *fosA5*, and *fosC2* (Table 1). In parallel, we screened inhibition of glutathione *S*-transferase activity by using FosA inhibitor phosphonoformiate (Figure) as described by Nakamura et al. (*12*). Results of these 2 tests were in agreement, with each detecting an ESBL-producing strain with enzymatic activity encoded by the *fosA3* gene (MIC ≥1,024 mg/L). Neither strain had been previously reported in France.

We determined the prevalence of enzymatic resistance to fosfomycin in ESBL-producing strains isolated since 2012 by using the same 2 tests. Surprisingly, among 23 strains resistant to fosfomycin with no epidemiologic link, 7 additional FosA3-producing and 1 FosA5-producing strains were detected, each with MIC ≥1,024 mg/L. Overall 83% of fosfomycin-resistant ESBL-producing *E. coli* with MIC ≥1,024 mg/L were FosA-positive. Auxotrophic tests showed that in addition of FosA production, fosfomycin transport was impaired in 6 strains. Chronologically, 2 strains were isolated in 2012, three in 2013, three in 2014, and two in 2015, meaning that FosA3-producing strains were present in France 6 years after the first isolation in Japan. The FosA5-producing strain was isolated from a clinical sample in France simultaneously with the original description of the strain in China (*13*). The sequencing of *fosA5* showed 99% identity (with 96% coverage) with pHKU1, earlier described as an *fosKP96*-carrying IncN plasmid in *Klebsiella pneumoniae* (*5*).

Our sequencing of CTX-M genes showed that FosA3-producing strains were associated with CTX-M-15 (n = 5), CTX-M-55 (n = 3), and CTX-M-2 (n = 1), whereas the 1 FosA5-producing strain expressed CTX-M-14. We also conducted multilocus sequence typing and plasmid incompatibility group typing (*14*) (Table 2). These results show unambiguously that 8 strains of *E. coli* of different sequence types hosted 5 plasmid types that could be distinguished by their CTX-M variant and plasmid-incompatibility group types.

Nine out of 10 isolates yielded transconjugants in *E. coli* C600 (*E. coli* K12 derivative) or transformants in TOP10 (DH10B derivative) *E. coli*. All 9 of these isolates

Table 2. Characteristics of clinical fosfomycin-resistant *Escherichia coli* isolates considered in our study*

No. isolates	Year isolated	Origin	CTX-M variant	*fosA* type	Sequence type	Plasmid-carrying *fosA* type
9	2012	Urine	CTX-M-55	A3	ST-559 (ST-10 complex)	FII, I1
12	2012	Urine	CTX-M-55	A3	ST-559 (ST-10 complex)	FII, I1
36	2013	Blood	CTX-M-55	A3	ST-1 (new)	FII
19	2013	Urine	CTX-M-15	A3	ST-2 (new)	FII
34	2013	Urine	CTX-M-2	A3	ST-2015	Nontypeable
24	2013	Urine	CTX-M-15	A3	ST-4508	FII
35	2014	Urine	CTX-M-15	A3	ST-69	FII
39	2014	Joint fluid	CTX-M-15	A3	ST-69	FII
42	2015	Urine	CTX-M-14	A3	ST-457	colE nontypeable
20	2015	Feces	CTX-M-15	A5	ST-3 (new)	N

*All genetic determinants were different except for isolates 9 and 12 (ST-559) and isolates 35 and 39 (ST-69). The yearly number of extended spectrum β-lactamase–producing *E. coli* screened was 1,044 in 2012, 1,142 in 2013, 1,251 in 2014, and 1,381 in 2015. ST, sequence type.

expressed high-level resistance to fosfomycin (MIC >1,024 mg/L), confirming that the observed resistance of the parent strain was indeed attributable to the *fosA* gene.

Conclusions

Although the prevalence of plasmid-mediated *fosA3* genes in human clinical *E. coli* isolates has remained low in France since 2012, these genes are observed across numerous clones, sequence types, and molecular determinants and are always associated with ESBL CTX-M enzymes, suggesting multiple propagation events. Our results are consistent with FosA3-producing clinical strains previously isolated in Asia, which also co-express CTX-M enzymes. However, the CTX-M variant distribution between the strain in France and the strain in Asia is different, with CTX-M-15 having high prevalence in our collection. Medical records examination did not show a history of international travel in our patient population, and such a variety of fosfomycin-resistant *E. coli* lineages probably were not imported or transmitted. The broad use of oral fosfomycin has provided the opportunity to select for FosA producers. With the spread of CTX-M urinary tract infections in the community, the use of fosfomycin is likely to select for CTX-M–FosA co-producers and could lead to an increase of treatment failures with ESBL-producing organisms. Conversely, treatment of ESBL producers with fosfomycin should only be undertaken after testing for susceptibility because these ESBL-producers can be linked to the same genetic determinant. Moreover, the indiscriminate use of the oral formulation in the community is jeopardizing the usefulness of this antimicrobial agent. While the world is bracing for an epidemic of infectious diseases bearing plasmid-mediated colistin resistance (*15*), a vast and ubiquitous reservoir for conjugative transmissible resistance to fosfomycin exists and can preclude its efficacy against extremely drug-resistant bacteria if the guidelines for the indiscriminate use of fosfomycin–trometamol are not urgently revised to safeguard this potent and well-tolerated agent. Because antimicrobial treatment of cystitis typically is motivated by concern for patient's comfort, withholding treatment

or the promotion of pivmecillinam as a first-line antimicrobial drug should seriously be considered.

Mr. Benzerara is an engineer and leads translational research, including emerging mechanisms of antimicrobial resistance, at the Hôpitaux Universitaires Est Parisiens Paris, France.

References

1. Société de Pathologie Infectieuse de Langue Française. Diagnostic et antibiothérapie des infections urinaires bactériennes communautaires de l'adulte [cited 2017 Jun 21]. http://www.infectiologie.com/UserFiles/File/spilf/recos/infections-urinaires-spilf.pdf
2. Agence Nationale de Sécurité du Médicaments. Etude d'utilisation de la nitrofurantoïne en France—période mars 2012–février 2015 [cited 2017 Jun 21]. http://ansm.sante.fr/var/ansm_site/storage/original/application/d807c8e39321445201911cf314263f07.pdf
3. Kaye KS, Gales AC, Dubourg G. Old antibiotics for multidrug-resistant pathogens: from in vitro activity to clinical outcomes. Int J Antimicrob Agents. 2017;49:542–8. http://dx.doi.org/10.1016/j.ijantimicag.2016.11.020
4. Castañeda-García A, Blázquez J, Rodríguez-Rojas A. Molecular mechanisms and clinical impact of acquired and intrinsic fosfomycin resistance. Antibiotics (Basel). 2013;2:217–36. http://dx.doi.org/10.3390/antibiotics2020217
5. Ho PL, Chan J, Lo WU, Lai EL, Cheung YY, Lau TC, et al. Prevalence and molecular epidemiology of plasmid-mediated fosfomycin resistance genes among blood and urinary *Escherichia coli* isolates. J Med Microbiol. 2013;62:1707–13. http://dx.doi.org/10.1099/jmm.0.062653-0
6. Lee SY, Park YJ, Yu JK, Jung S, Kim Y, Jeong SH, et al. Prevalence of acquired fosfomycin resistance among extended-spectrum β-lactamase-producing *Escherichia coli* and *Klebsiella pneumoniae* clinical isolates in Korea and IS*26*-composite transposon surrounding *fosA3*. J Antimicrob Chemother. 2012;67:2843–7. http://dx.doi.org/10.1093/jac/dks319
7. Wachino J, Yamane K, Suzuki S, Kimura K, Arakawa Y. Prevalence of fosfomycin resistance among CTX-M-producing *Escherichia coli* clinical isolates in Japan and identification of novel plasmid-mediated fosfomycin-modifying enzymes. Antimicrob Agents Chemother. 2010;54:3061–4. http://dx.doi.org/10.1128/AAC.01834-09
8. Hou J, Huang X, Deng Y, He L, Yang T, Zeng Z, et al. Dissemination of the fosfomycin resistance gene *fosA3* with CTX-M β-lactamase genes and *rmtB* carried on IncFII plasmids

among *Escherichia coli* isolates from pets in China. Antimicrob Agents Chemother. 2012;56:2135–8. http://dx.doi.org/10.1128/AAC.05104-11

9. Chan J, Lo WU, Chow KH, Lai EL, Law PY, Ho PL. Clonal diversity of *Escherichia coli* isolates carrying plasmid-mediated fosfomycin resistance gene *fosA3* from livestock and other animals. Antimicrob Agents Chemother. 2014;58:5638–9. http://dx.doi.org/10.1128/AAC.02700-14

10. Hou J, Yang X, Zeng Z, Lv L, Yang T, Lin D, et al. Detection of the plasmid-encoded fosfomycin resistance gene *fosA3* in *Escherichia coli* of food-animal origin. J Antimicrob Chemother. 2013;68:766–70. http://dx.doi.org/10.1093/jac/dks465

11. Mendes AC, Rodrigues C, Pires J, Amorim J, Ramos MH, Novais Â, et al. Importation of fosfomycin resistance *fosA3* gene to Europe. Emerg Infect Dis. 2016;22:346–8. http://dx.doi.org/10.3201/eid2202.151301

12. Nakamura G, Wachino J, Sato N, Kimura K, Yamada K, Jin W, et al. Practical agar-based disk potentiation test for detection of fosfomycin-nonsusceptible *Escherichia coli* clinical isolates

13. Ma Y, Xu X, Guo Q, Wang P, Wang W, Wang M. Characterization of *fosA5*, a new plasmid-mediated fosfomycin resistance gene in *Escherichia coli*. Lett Appl Microbiol. 2015;60:259–64. http://dx.doi.org/10.1111/lam.12366

14. Compain F, Poisson A, Le Hello S, Branger C, Weill FX, Arlet G, et al. Targeting relaxase genes for classification of the predominant plasmids in *Enterobacteriaceae*. Int J Med Microbiol. 2014;304:236–42. http://dx.doi.org/10.1016/j.ijmm.2013.09.009

15. Al-Tawfiq JA, Laxminarayan R, Mendelson M. How should we respond to the emergence of plasmid-mediated colistin resistance in humans and animals? Int J Infect Dis. 2017;54:77–84. http://dx.doi.org/10.1016/j.ijid.2016.11.415

producing glutathione *S*-transferases. J Clin Microbiol. 2014;52:3175–9. http://dx.doi.org/10.1128/JCM.01094-14

Address for correspondence: Guillaume Arlet, Hôpital Tenon – Bacteriology, 4 Rue de la Chine, Paris 75020 France; email: guillaume.arlet@tnn.aphp.fr
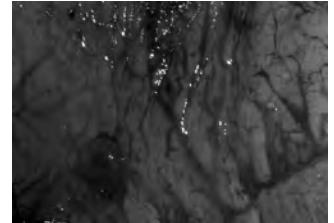
December 2011: **Zoonoses**

EMERGING INFECTIOUS DISEASES

https://wwwnc.cdc.gov/eid/articles/issue/17/12/table-of-contents

Determination of Ferret Enteric Coronavirus Genome in Laboratory Ferrets

Tian-Cheng Li, Sayaka Yoshizaki, Michiyo Kataoka, Yen Hai Doan, Yasushi Ami, Yuriko Suzaki, Tomofumi Nakamura, Naokazu Takeda, Takaji Wakita

Ferret enteric coronavirus (FRECV) RNA was detected in laboratory ferrets. Analysis of the complete genome sequence of 2 strains, FRCoV4370 and FRCoV063, revealed that FRECV shared 49.9%–68.9% nucleotide sequence identity with known coronaviruses. These results suggest that FRECV might be classified as a new species in the genus *Alphacoronavirus.*

Ferret coronavirus (FRCoV), a novel animal coronavirus (CoV), was identified in ferrets (*Mustela putorius furo*) in 2006 (*1*). However, only partial sequences of FRCoV have been analyzed, including portions of open reading frame (ORF) 1b and the full-length spike protein (S), nonstructural protein 3c (3c), envelope protein (E), membrane protein (M), nucleocapsid protein (N), and accessory genes (3x and 7b), and only in 3 strains: 1 ferret systemic coronavirus (FRSCV), FRSCV MSU-1 strain (GenBank accession no. GU338456); and 2 ferret enteric coronaviruses (FRECVs), FRECV MSU-2 strain (GenBank accession no. GU338457) and FRECV No22 strain (GenBank accession no. LC029419) (*2,3*). Genetic analyses based on these partial sequences showed that FRCoV is closer to mink coronavirus (MCoV) than to other CoVs and appears to be a member of the genus *Alphacoronavirus* in the subfamily *Coronovirinae*, which also contains the genera *Betacoronavirus* and *Gammacoronavirus* (*4*). To further understand the constellation of FRCoVs, we analyzed the complete genome.

The Study

In our previous study, we detected ferret hepatitis E virus (HEV) in fecal samples from laboratory ferrets and confirmed that 40 (63.5%) of the 63 ferrets were infected with ferret HEV (*5*). For the observation of the ferret HEV

Author affiliations: National Institute of Infectious Diseases, Tokyo, Japan (T.-C. Li, S. Yoshizaki, M. Kataoka, Y.H. Doan, Y. Ami, Y. Suzaki, T. Wakita); Research Foundation for Microbial Diseases of Osaka University, Kagawa, Japan (T. Nakamura); Osaka University, Osaka, Japan (N. Takeda)

particles by electron microscopy, we used a 10% suspension prepared from the fecal specimen from 1 of the ferrets (no. F4370), concentrated by ultracentrifugation and purified by sucrose gradient ultracentrifugation. However, instead of finding ferret HEV particles, we observed many coronavirus-like particles in fractions 4, 5, and 6, with densities of 1.230 g/cm^3, 1.214 g/cm^3, and 1.198 g/cm^3 (data not shown). These particles ranged from 60 nm to 120 nm in diameter; most of them had a spike structure, suggesting that the ferrets were infected with a CoV-like virus.

To precisely examine these CoV-like particles, we diluted 63 fecal specimens with 10-mmol/L PBS for preparation of the 10% suspension. We extracted the RNA by using a MagNA Pure LC Total Nucleic Acid isolation kit (Roche Applied Science, Mannheim, Germany) according to the manufacturer's recommendations. We performed an FRSCV-specific reverse transcription PCR (RT-PCR) with the primer set G1F (5′-CTGGTGTTTGTGCAACATC-TAC-3′) and G1R (5′-TCTATTTGCACAAAATCAGA-CA-3′) and an FRECV-specific RT-PCR with the primer set G2F (5′-GGCATTTGTTTTGATAACGTTG-3′) and G2R (5′-CTATTAATTCGCACGAAATCTGC-3′) (*2*).

RT-PCR results revealed that, of the 63 ferret fecal specimens, 22 (34.9%) were positive for FRSCV RNA, 53 (84.1%) were positive for FRECV RNA, and 15 (23.8%) were positive for both FRSCV and FRECV RNA. The specimen from ferret F4370 was positive only for FRECV RNA. These results indicated that the ferrets were infected extensively with FRCoV. However, we observed no signs such as weight loss or diarrhea in the ferrets.

We extracted RNA from a pool of fractions 4, 5, and 6 from the F4370 fecal sample suspension and analyzed the complete genome sequence of FRCoV by using a next-generation sequence analysis (*6*). FRCoV4370 (GenBank accession no. LC119077) has a genome size, gene order, genomic organization, and structure similar to those of known alphacoronaviruses. The complete genome of FRCoV4370 contains 28,525 nt and a poly (A) tail. Except for the 5′-terminus 261 nt and 3′-terminus 247 nt untranslated regions, FRCoV4370 encodes 9 proteins: ORF1a, ORF1a/1b, S, 3c, E, M, N, 3x, and 7b (Table). Although the ORF7a protein was found in the MCoVs WD1127 (GenBank accession no. HM245925) and WD1133 (accession no. HM245926), we did not find it in FRCoV4370.

The complete genome of FRCoV4370 shared 49.9%–68.9% nucleotide identity with other known CoVs.

Table. Nucleotide positions of proteins of FrCoVs from analysis of complete virus genome and number of amino acids compared with MCoVs*

Proteins	Nucleotide position		No. amino acids						
	FRCoV4370	FRCoV063	FRCoV4370	FRCoV063	MSU-2	MSU-1	No22	WD1127	WD1133
ORF1a	262–12228	262–12231	3,988	3,989	NA	NA	NA	4,018	4,006
ORF1a/b	262–20222	262–20225	6,653	6,554	NA	NA	NA	6,682	6,670
Spike	20215–24564	20218–24567	1,449	1,449	1,449	1,457	1,435	1,438	1,429
ORF3c	24585–25328	24585–25328	247	247	247	83	247	247	69
E	25297–25545	25297–25545	82	82	82	82	82	82	82
M	25560–26351	25560–26363	263	267	263	263	265	268	268
N	26368–27492	26380–27504	374	374	374	374	374	376	376
ORF7a			NI	NI	NI	NI	NI	98	98
ORF3x	27501–27725	27514–27738	74	74	74	14	74	73	73
ORF7b	27664–28278	27677–28291	204	204	204	204	202	204	204

*E, envelope protein; FrCOV, ferret coronavirus; M, membrane protein; MCoV, mink coronavirus; N, nucleocapsid protein; NI, protein not identified; NA, sequence not available; ORF, open reading frame.

Phylogenetic trees based on the complete genome demonstrated that FRCoV4370 is closer to MCoVs than to other CoVs, although it clearly separated into a distinct cluster (Figure, panel A). We observed similar phylogenetic clustering when we compared ≈8,300 nt sequences of the 3′-termini of CoVs. FRCoV4370 forms a new cluster with FRSCV MSU-1, FRECV MSU-2, and No22, being separated from the cluster formed by MCoVs (Figure, panel B). In addition, BLAST analysis (http://blast.ncbi.nlm.nih.gov/Blast.cgi) using the nucleotide sequences described previously revealed that FRCoV4370 shared 94% identity with FRECV MSU-2, which is higher than that of FRSCV MSU-1 (89%), indicating that FRCoV4370 belongs to the FRECVs.

As is the case for other CoVs, 2 long ORFs were predicted in the FRCoV4370 genome: ORF1a contains 11,967 nt, from nt 262 to 12228, encoding 3,988 aa; ORF1b encodes 7,830 nt, from nt 12393 to 20222. The coronaviruses have a pseudoknot tertiary structure that allows a ribosomal shift of the reading frame between ORF1a and ORF1b (7–9). We also found the slippery sequence for the ribosomal shift (UUUAAAC) in the FRCoV4370 genome at nt positions 12192–12198. The ribosomal shift may have resulted in generation of the ORF1a/b protein encoding 19,962 nt and the deduced 6,653 aa.

We identified 4 structural proteins in FRCoV4370: S, E, M, and N. The S protein is the largest, consisting of 1,449 aa, which shared 92.5% aa identity with FRECV MSU-2, 81.4% with FRSCV MSU-1, and 84.5% with FRECV No22. The BLAST analysis of the S protein showed that it had low aa identities (43%–66%) with other CoVs.
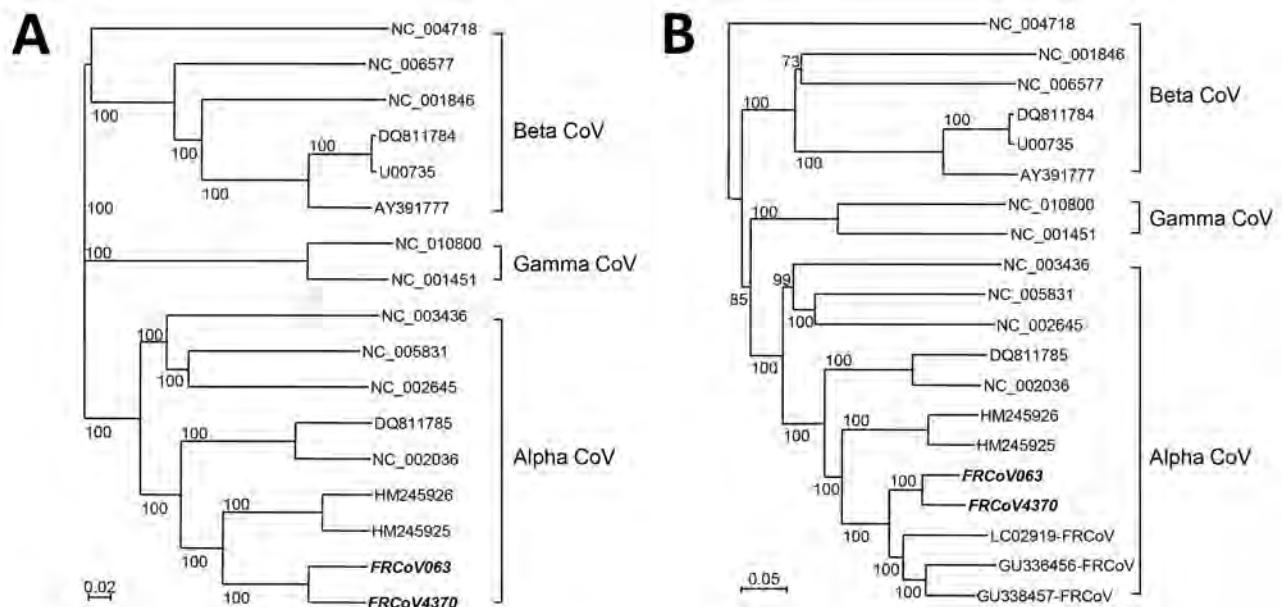
Figure. Phylogenetic relationships between ferret coronaviruses (FrCoVs, shown in bold italics) and other known coronaviruses (CoVs). A) Complete genome; B) partial 3′-terminus genome. The nucleic acid sequence alignment was performed using ClustalX version 1.81 (http://www.clustal.org). The genetic distance was calculated by Kimura's 2-parameter method. Phylogenetic trees with 1,000 bootstrap replicates were generated by the neighbor-joining method (Njplot 2.3, http://njplot.sharewarejunction.com/). Comparison CoVs identified by GenBank accession number. Scale bars indicate substitutions per site.

Because the S protein is a major inducer of virus-neutralizing antibodies, the antigenicity and serotype of FRCoVs might be different from those of other CoVs.

The E protein, the smallest structural protein, encodes 82 aa (which is the same number encoded by other known FRCoVs) and shared 94.8% aa identity with FRECV MSU-2, 85.6% with FRSCV MSU-1, and 86.7% with FRECV No22. The 263-aa M protein shared 81.6% aa identity with FRECV MSU-2. The low aa identity between the FRECV strains suggests that the membrane gene is highly variable. The N protein of FRCoV4370 contains 374 aa, making it the shortest among the alphacoronaviruses. The N protein shared 96.3% aa identity with FRECV MSU-2, 93.4% with FRSCV MSU-1, and 80.2% with FRECV No22.

ORF3c was identified in FRCoV4370, as observed in MCoVs. This protein is an accessory triple-spanning membrane protein and is analogous to SARS-CoV 3a protein (*10*). The predicted ORF3c protein contains 247 aa and shared 96.8% aa identity with FRECV MSU-2 and 77.6% with FRECV No22. The 2 other nonstructural proteins, 3x and 7b, are located downstream of the N protein and encode 74 aa and 204 aa, respectively.

We also detected FRECV RNA in the fecal specimens of 9 ferrets from another farm in the United States and analyzed the complete genome of 1 strain, FRCoV063 (LC215971). The genome of FRCoV063 shared 94.0% nucleotide identity with FRCoV4370 and had a similar structure (Table; Figure), suggesting that ferret coronavirus infection is common in ferrets, and genetically similar FRCoV strains circulate at the ferret farms.

Conclusions

Since the initial identification of FRCoV in ferrets in 2006, many sequences of FRSCV and FRECV strains have been analyzed (*1–3,11–15*). However, the complete genome sequences have not been determined and added to the public databases. In this study, we successfully analyzed the complete genome of 2 strains of FRECV, FRCoV4370 and FRCoV063, and found that they shared 94.0% nucleotide identity with each other but 49.9%–68.9% nucleotide identities with other known CoVs, suggesting that the ferret coronaviruses might be classified as a new species in the genus *Alphacoronavirus*. This new knowledge of the complete genome sequence of FRECV will contribute to investigations of the diversity of animal CoVs and will help establish new taxonomic units.

Dr. Li is a senior researcher at the National Institute of Infectious Diseases in Tokyo, Japan. His research focuses on epidemiology, the expression of viral proteins, and advances in the diagnosis of and vaccines for hepatitis E virus.

References

1. Wise AG, Kiupel M, Maes RK. Molecular characterization of a novel coronavirus associated with epizootic catarrhal enteritis (ECE) in ferrets. Virology. 2006;349:164–74. http://dx.doi.org/10.1016/j.virol.2006.01.031
2. Wise AG, Kiupel M, Garner MM, Clark AK, Maes RK. Comparative sequence analysis of the distal one-third of the genomes of a systemic and an enteric ferret coronavirus. Virus Res. 2010;149:42–50. http://dx.doi.org/10.1016/j.virusres.2009.12.011
3. Terada Y, Minami S, Noguchi K, Mahmoud HY, Shimoda H, Mochizuki M, et al. Genetic characterization of coronaviruses from domestic ferrets, Japan. Emerg Infect Dis. 2014;20:284–7. http://dx.doi.org/10.3201/eid2002.130543
4. Vlasova AN, Halpin R, Wang S, Ghedin E, Spiro DJ, Saif LJ. Molecular characterization of a new species in the genus *Alphacoronavirus* associated with mink epizootic catarrhal gastroenteritis. J Gen Virol. 2011;92:1369–79. http://dx.doi.org/10.1099/vir.0.025353-0
5. Li TC, Yang T, Ami Y, Suzaki Y, Shirakura M, Kishida N, et al. Complete genome of hepatitis E virus from laboratory ferrets. Emerg Infect Dis. 2014;20:709–12. http://dx.doi.org/10.3201/eid2004.131815
6. Li TC, Yang T, Yoshizaki S, Ami Y, Suzaki Y, Ishii K, et al. Construction and characterization of an infectious cDNA clone of rat hepatitis E virus. J Gen Virol. 2015;96:1320–7. http://dx.doi.org/10.1099/vir.0.000072
7. Brierley I, Boursnell ME, Binns MM, Bilimoria B, Blok VC, Brown TD, et al. An efficient ribosomal frame-shifting signal in the polymerase-encoding region of the coronavirus IBV. EMBO J. 1987;6:3779–85.
8. Brierley I, Digard P, Inglis SC. Characterization of an efficient coronavirus ribosomal frameshifting signal: requirement for an RNA pseudoknot. Cell. 1989;57:537–47. http://dx.doi.org/10.1016/0092-8674(89)90124-4
9. Thiel V, Ivanov KA, Putics A, Hertzig T, Schelle B, Bayer S, et al. Mechanisms and enzymes involved in SARS coronavirus genome expression. J Gen Virol. 2003;84:2305–15. http://dx.doi.org/10.1099/vir.0.19424-0
10. Oostra M, de Haan CA, de Groot RJ, Rottier PJ. Glycosylation of the severe acute respiratory syndrome coronavirus triple-spanning membrane proteins 3a and M. J Virol. 2006;80:2326–36. http://dx.doi.org/10.1128/JVI.80.5.2326-2336.2006
11. Dominguez E, Novellas R, Moya A, Espada Y, Martorell J. Abdominal radiographic and ultrasonographic findings in ferrets (*Mustela putorius furo*) with systemic coronavirus infection. Vet Rec. 2011;169:231. http://dx.doi.org/10.1136/vr.d4705
12. Garner MM, Ramsell K, Morera N, Juan-Sallés C, Jiménez J, Ardiaca M, et al. Clinicopathologic features of a systemic coronavirus-associated disease resembling feline infectious peritonitis in the domestic ferret (*Mustela putorius*). Vet Pathol. 2008;45:236–46. http://dx.doi.org/10.1354/vp.45-2-236
13. Lescano J, Quevedo M, Gonzales-Viera O, Luna L, Keel MK, Gregori F. First case of systemic coronavirus infection in a domestic ferret (*Mustela putorius furo*) in Peru. Transbound Emerg Dis. 2015;62:581–5. http://dx.doi.org/10.1111/tbed.12407
14. Murray J, Kiupel M, Maes RK. Ferret coronavirus-associated diseases. Vet Clin North Am Exot Anim Pract. 2010;13:543–60. http://dx.doi.org/10.1016/j.cvex.2010.05.010
15. Provacia LB, Smits SL, Martina BE, Raj VS, Doel PV, Amerongen GV, et al. Enteric coronavirus in ferrets, the Netherlands. Emerg Infect Dis. 2011;17:1570–1.

Address for correspondence: Tian-Cheng Li, Department of Virology II, National Institute of Infectious Diseases, 4-7-1 Gakuen, Musashi-murayama, Tokyo 208-0011, Japan; email: litc@nih.go.jp

Myocarditis Caused by Human Parechovirus in Adult

Khai Lin Kong, Jillian S.Y. Lau, Su Mei Goh, Heather L. Wilson, Mike Catton, Tony M. Korman

The infectious etiology of myocarditis often remains unidentified. We report a case of myocarditis associated with human parechovirus (HPeV) infection in an adult. HPeV is an emerging pathogen that can cause serious illness, including myocarditis, in adults. Testing for HPeV should be considered in differential diagnosis of myocarditis.

Infections with human parechovirus (HPeV) are rarely reported in adults. We report a case of myocarditis associated with HPeV infection in an adult.

The Study

During the summer of 2015, a 26-year-old man in Victoria, Australia, was admitted to Casey Hospital (Berwick, VIC, Australia) because of 4 days of fever, rigors, headache, dry cough, sore throat, myalgia, and a history of erythematous macular rash on arms bilaterally that had resolved by the time of admission. The patient smoked cigarettes and reported use of methamphetamines, but no other medical history was reported. He lived in a rural area but had no close contact with animals. He lived with 3 young children, including an 8-week-old infant who had recently had otitis externa.

At admission, he was febrile (temperature 38.2°C) and had sinus tachycardia ($\leq$130 beats/min). Results of a physical examination were otherwise unremarkable. Peripheral blood lymphocyte count was 0.70×10^9 cells/L (reference range $1–4 \times 10^9$ cells/L), C-reactive protein level 111 mg/L (reference value <5 mg/L), erythrocyte sedimentation rate 94 mm/h (reference value <10 mm/h), serum bilirubin level 49 µmol/L (reference value <20 µmol/L), and albumin level 24 g/L (reference range 35–45 g/L).

Microscopic analysis of cerebrospinal fluid (CSF) showed 2×10^6 polymorphonuclear cells/L, 2×10^6 lymphocytes/L, a total protein level of 0.5 g/L (reference range 0.1–0.3 g/L), and glucose and lactate levels within reference ranges. Blood and CSF cultures showed no bacterial growth. Because of a low leukocyte count, molecular studies for viruses (including enterovirus) were not performed for the CSF sample.

Fever and tachycardia persisted for 5 days and chest discomfort and dyspnea developed. A transthoracic echocardiogram showed a mildly dilated left ventricle with an ejection fraction of 15%. There were no valvular vegetations. Peak creatine kinase level was 713 U/L (reference value <230 U/L), and troponin level was 15.28 µg/L (reference value <0.080 µg/L).

The patient was given intravenous benzylpenicillin and oral doxycycline as empirical therapy for possible bacterial infection; Q fever and leptospirosis were considered possible diagnoses. Fever and chest discomfort improved, and he was discharged 7 days after admission. Two weeks later, the patient was well and had minimal dyspnea.

Throat swab specimens were obtained on day 6 of illness, and rectal swab specimens were obtained on day 8 of illness. Specimens were tested for enterovirus and HPeV RNA by reverse transcription PCR (RT-PCR) and primers specific for the highly conserved 5′ untranslated region (1) (details for HPeV primers and probes are available on request). HPeV was detected in the throat swab specimen, but not the rectal swab specimen.

We attempted molecular typing of HPeV by using the method of Papadakis et al. (1) and primers AN353, AN355, AN357, AN358, and AN369 described by Nix et al. (2). However, typing was not successful because of low copy numbers, probably caused by specimens being collected late in the illness.

Multiple investigations showed no other infectious causes of myocarditis. Serologic results were negative for previous or recent infections with hepatitis A, B, and C viruses and HIV, as well as *Leptospira* spp., *Coxiella burnetii*, rickettsia, *Treponema pallidum*, and *Toxoplasma* spp. Serologic analysis showed evidence of previous infections with cytomegalovirus and Epstein-Barr virus. However, a convalescent-phase serum sample was not available for additional serologic testing.

A multiplex PCR (Respiratory Pathogens B; AusDiagnostics, Beaconsfield, NSW, Australia) was performed for a nasopharyngeal swab specimen. Results were negative for influenza A virus; A(H1N1)pdm09 virus; influenza B virus; respiratory syncytial virus; rhinoviruses/enterovirus; human parainfluenza virus 1, 2, and 3; adenovirus (groups B, C, E, some A, D); human metapneumovirus; *Bordetella*

Author affiliations: Monash University, Clayton, Victoria, Australia (K.L. Kong, J.S.Y. Lau, S.M. Goh, T.M. Korman); Monash Health, Clayton (K.L. Kong, J. Lau, S.M. Goh, T.M. Korman); Peter Doherty Institute for Infection and Immunity, Melbourne, Victoria, Australia (H.L. Wilson, M. Catton)

pertussis and *B. parapertussis*; *Legionella pneumophila* and *L. longbeachae*; *Mycoplasma pneumoniae*; and *Chlamydia/Chlamydophila* spp. (including *C. psittaci*, *C. pneumoniae*, and *C. trachomatis*).

Conclusions

HPeVs were previously classified as a subgenus of echoviruses (*3*). Echovirus subtypes 22 and 23 were renamed HPeV type 1 and 2; sixteen different types of HPeV thus far have been identified. Serosurveillance studies showed that by 2 years of age, ≤90% of children are infected with ≥1 type of HPeV (*3*). Infections with human parechoviruses show various clinical manifestations, notably sepsis-like disease and encephalitis in infants. A recent large outbreak of HPeV type 3 infections in infants was reported in Australia (*4*).

HPeV infections in adults are rarely reported. Mizuta et al. reported 22 adults with myalgia, muscular weakness, sore throat, orchiodynia, and increased levels of creatine phosphokinase; 14 had HPeV type 3 infections confirmed by virus isolation, positive RT-PCR results for throat swab or stool specimens, or serologic analysis (*5*). HPeV was also reported to be associated with flaccid paralysis and diarrheal illness in adults (*6,7*).

The rarity of HPeV infection in adults could be related to immunity conferred by previous exposure during childhood to HPeV. Few seroprevalence data are available for HPeV infections in adults. However, as part of an investigation of infant deaths associated with HPeV type 3 in Wisconsin, USA, limited serologic testing of 59 adults demonstrated that infections were not common, suggesting that either HPeV3 was a new pathogen being introduced to this community, or that there was waning immunity, which made antibody titers difficult to detect in adults (*8*).

The lack of documented reports of HPeV infection in adults could also be caused by lack of widespread testing for adults. HPeV RNA is not detected by routine enterovirus PCRs and requires additional HPeV testing. The Victorian

Infectious Diseases Reference Laboratory (Melbourne, VIC, Australia) routinely tests specimens for enterovirus and HPeV when a request is made, regardless of the age of the patients. During January 2015–May 2016, this laboratory tested 3,525 specimens for HPeV, of which 1,425 (40%) were obtained from adults. HPeV was detected by RT-PCR in 5 (0.35%) of 1,425 specimens: 2 in throat swab specimens, 2 in blood, and 1 in CSF. In comparison, 286 (13.6%) of 2,100 specimens from persons <18 years of age were positive for HPeV; most (271, 94.8%) were from children <1 year of age. This finding suggests that, although increased testing for HPeV could increase the detection rate of HPeV infection in adults, it is an uncommon infection in the adult population. This finding is consistent with results of a study from a reference laboratory in Scotland that tested 3,739 CSF samples from persons of all ages and found that although enteroviruses were common in adults, HPeV infections were found exclusively in young infants (*9*).

Enteroviruses are recognized as a major cause of acute myocarditis and are associated with ≤14% of cases (*10*). Myocarditis associated with HPeV infections is rarely reported (Table). This disease has been reported in 3 children <2 years of age and 1 adolescent. Two of the patients were immunosuppressed, 1 of whom died. A study of 109 patients infected with echovirus 22 (now HPeV subtype 1) in Sweden included a case of myocarditis in a child; virus was isolated from a stool sample and a major increase in antibody titer was observed (*11*).

There is no proven effective therapy for HPeV infection. Intravenous immunoglobulin (IVIG) was used for 2 patients (Table). IVIG has been used for treatment of enterovirus infections, particularly in immunocompromised patients (*15*), but the efficacy of IVIG might be limited for treatment of HPeV infection because of low seroprevalence in adults (*8*).

In summary, we report a case of myocarditis associated with HPeV infection in an adult. A large proportion of cases of myocarditis has no identified infectious cause.

Table. Characteristics of 5 patients with myocarditis caused by infection with human parechovirus*

Patient (reference)	Age/sex	Underlying disease	Clinical features	Sample in which virus was detected	Subtype	Echocardiographic finding	Therapy	Outcome
1 (*11*)	NA/M	NA	NA	Stool, blood	1†	NA	NA	NA
2 (*13*)	14 mo/M	Congenital AGG	Myocarditis	Myocardium, pericardial fluid	1†	NA	None	Died
3 (*14*)	6 wk/M	None	Myocarditis	Stool	1†	NA	None	Survived
4 (*12*)	16 y/F	SLE, rituximab-induced HGG	Myocarditis, encephalitis	Myocardium, CSF, stool	3	Biventricular dysfunction, LVEF 13%	IVIG	Survived, prolonged neurologic recovery
5 (this study)	26 y/M	None	Myocarditis	Throat swab specimen	Unknown	Dilated left ventricle, LVEF 15%	None	Survived, Well at 6-mo follow up

*AGG, agammaglobulinemia; CSF, cerebrospinal fluid; HGG, hypogammaglobulinemia; IVIG, intravenous immunoglobulin; LVEF, left ventricular ejection fraction; NA, not available; SLE, systemic lupus erythematosus.
†Previously known as echovirus subtype 22.

Thus, testing of throat swab, stool, and blood specimens for HPeV should be considered for adults with myocarditis. HPeV is an emerging pathogen that can cause major illness, including myocarditis, in adults.

Dr. Kong is an infectious diseases fellow at Monash Health, Melbourne, Victoria, Australia. His primary research interest is emerging virus infections.

References

1. Papadakis G, Tsortos A, Kordas A, Tiniakou I, Morou E, Vontas J, et al. Acoustic detection of DNA conformation in genetic assays combined with PCR. Sci Rep. 2013;3:2033. http://dx.doi.org/10.1038/srep02033
2. Nix WA, Maher K, Pallansch MA, Oberste MS. Parechovirus typing in clinical specimens by nested or semi-nested PCR coupled with sequencing. J Clin Virol. 2010;48:202–7. http://dx.doi.org/10.1016/j.jcv.2010.04.007
3. de Crom SCM, Rossen JWA, van Furth AM, Obihara CC. Enterovirus and parechovirus infection in children: a brief overview. Eur J Pediatr. 2016;175:1023–9. http://dx.doi.org/10.1007/s00431-016-2725-7
4. Khatami A, McMullan BJ, Webber M, Stewart P, Francis S, Timmers KJ, et al. Sepsis-like disease in infants due to human parechovirus type 3 during an outbreak in Australia. Clin Infect Dis. 2015;60:228–36. http://dx.doi.org/10.1093/cid/ciu784
5. Mizuta K, Kuroda M, Kurimura M, Yahata Y, Sekizuka T, Aoki Y, et al. Epidemic myalgia in adults associated with human parechovirus type 3 infection, Yamagata, Japan, 2008. Emerg Infect Dis. 2012;18:1787–93. http://dx.doi.org/10.3201/eid1811.111570
6. Saikruang W, Khamrin P, Suantai B, Okitsu S, Hayakawa S, Ushijima H, et al. Detection of diarrheal viruses circulating in adult patients in Thailand. Arch Virol. 2014;159:3371–5. http://dx.doi.org/10.1007/s00705-014-2191-3
7. Figueroa JP, Ashley D, King D, Hull B. An outbreak of acute flaccid paralysis in Jamaica associated with echovirus type 22. J Med Virol. 1989;29:315–9. http://dx.doi.org/10.1002/jmv.1890290418
8. Sedmak G, Nix WA, Jentzen J, Haupt TE, Davis JP, Bhattacharyya S, et al. Infant deaths associated with human parechovirus infection in Wisconsin. Clin Infect Dis. 2010;50:357–61. http://dx.doi.org/10.1086/649863
9. Harvala H, McLeish N, Kondracka J, McIntyre CL, McWilliam Leitch EC, Templeton K, et al. Comparison of human parechovirus and enterovirus detection frequencies in cerebrospinal fluid samples collected over a 5-year period in Edinburgh: HPeV type 3 identified as the most common picornavirus type. J Med Virol. 2011;83:889–96. http://dx.doi.org/10.1002/jmv.22023
10. Knowlton KU, Narexkina A, Savoia MC, Oxman MN. Myocarditis and pericarditis. In: Bennett JE, Dolin R, Blaser MJ, editors. Mandell, Douglas, and Bennett's principles and practice of infectious diseases. 8th ed. Amsterdam: Elsevier; 2015. p. 1066–79.
11. Ehrnst A, Eriksson M. Epidemiological features of type 22 echovirus infection. Scand J Infect Dis. 1993;25:275–81. http://dx.doi.org/10.3109/00365549309008499
12. Mardekian SK, Fortuna D, Nix A, Bhatti T, Wiley CA, Flanders A, et al. Severe human parechovirus type 3 myocarditis and encephalitis in an adolescent with hypogammaglobulinemia. Int J Infect Dis. 2015;36:6–8. http://dx.doi.org/10.1016/j.ijid.2015.05.008
13. Maller HM, Powars DF, Horowitz RE, Portnoy B. Fatal myocarditis associated with ECHO virus, type 22, infection in a child with apparent immunological deficiency. J Pediatr. 1967;71:204–10. http://dx.doi.org/10.1016/S0022-3476(67)80073-8
14. Russell SJ, Bell EJ. Echoviruses and carditis. Lancet. 1970;1:784–5. http://dx.doi.org/10.1016/S0140-6736(70)91021-4
15. Dendle C, Gilbertson M, Korman TM, Golder V, Morand E, Opat S. Disseminated enteroviral infection associated with obinutuzumab. Emerg Infect Dis. 2015;21:1661–3. http://dx.doi.org/10.3201/eid2109.150104

Address for correspondence: Khai Lin Kong, Department of Infectious Diseases, Monash Health, 246 Clayton Rd, Clayton VIC 3168, Australia: email: kong.khailin@gmail.com

The Public Health Image Library (PHIL)
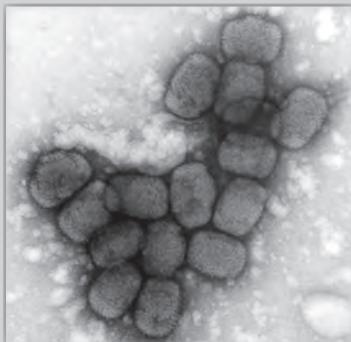
The Public Health Image Library (PHIL), Centers for Disease Control and Prevention, contains thousands of public health-related images, including high-resolution (print quality) photographs, illustrations, and videos.

PHIL collections illustrate current events and articles, supply visual content for health promotion brochures, document the effects of disease, and enhance instructional media.

PHIL images, accessible to PC and Macintosh users, are in the public domain and available without charge.

Visit PHIL at http://phil.cdc.gov/phil

Cost of Nosocomial Outbreak Caused by NDM-1–Containing *Klebsiella pneumoniae* in the Netherlands, October 2015–January 2016

**Madelief Mollers, Suzanne P. Lutgens,
Annelot F. Schoffelen, Peter M. Schneeberger,
Anita W.M. Suijkerbuijk**

During October–December 2015, 29 patients in a hospital in the Netherlands acquired nosocomial infection with a multidrug-resistant, New Delhi-metallo-β-lactamase–positive *Klebsiella pneumoniae* strain. Extensive infection control measures were needed to stop this outbreak. The estimated economic impact of the outbreak was $804,263; highest costs were associated with hospital bed closures.

In 2008, New Delhi-metallo-β-lactamase (NDM), an enzyme that confers bacteria with resistance to a range of antimicrobial drugs, was detected for the first time in a patient from Sweden during a trip to India (*1*). Subsequently, NDM-producing isolates rapidly spread and have been found dispersed throughout the world. However, in western and northern Europe, identification of patients with NDM-producing *Enterobacteriaceae* is uncommon (*2*). Infections with multidrug-resistant, gram-negative bacteria are a concern worldwide, given restricted treatment options and excess costs of care (*3,4*).

During October 1–December 30, 2015, an outbreak of *Klebsiella pneumoniae* containing an NDM-1 plasmid affected 29 patients residing in Jeroen Bosch Hospital ('s-Hertogenbosch, the Netherlands), a 683-bed tertiary teaching hospital. This hospital outbreak started in a surgical ward. On November 23, 2015, NDM-producing extended-spectrum β-lactamase (ESBL)–positive *K. pneumoniae* bacteria were cultured and isolated from surgical drain fluid. At the time of identification, the patient was already discharged. Shortly thereafter, screening cultures of long-term admitted surgical patients revealed 2 additional patients with NDM-producing *K. pneumoniae*. Contact tracing and weekly screening rounds of all in-hospital patients were performed, identifying additional NDM carriers. Weekly screening rounds revealed 7 wards with uncontrolled NDM transmission (i.e., $\geq$2 NDM carriers). On the basis of an epidemiologic curve of the NDM carriers detected, all patients admitted to 1 of these wards beginning October 1 were defined as at risk of carrying NDM. Because the policy that was chosen was search and destroy (detect patients as quickly as possible and isolate them to protect the others), all patients residing in high-risk wards were tested.

Six months after the start of the outbreak, 2,964 patients had been flagged as at-risk patients; >95% of these patients had been screened, and a total of 29 NDM carriers were identified. No risk factors, such as recent travel abroad or a common source of transmission, were identified among the cases of this outbreak. In 2016, weekly screening rounds were continued in wards with at-risk populations to confirm the outbreak was successfully controlled.

Apart from the physical burden to patients and hospitals caused by multidrug-resistant microorganisms, nosocomial outbreaks also entail an economic burden. Estimates of the cost of outbreaks of multidrug-resistant bacteria in healthcare institutions are scarce. Insight on outbreak costs can help to justify the necessary investments in infection prevention and control measures, facilitating the decision-making process on prevention and control policy. In this study, we assessed the total costs of this outbreak on the basis of interviews and data from the affected hospital.

The Study

The outbreak occurred in a hospital with 683 registered beds, including a separate rehabilitation center. We assessed outbreak-related costs by using an activity-based costing model and performed interviews with staff working in the hospital to gather additional information about outbreak control activities performed and costs (online Technical Appendix, https://wwwnc.cdc.gov/EID/article/23/9/16-1710-Techapp1.pdf). We calculated hospital costs from October 1, 2015, the beginning of the outbreak, through January 31, 2016, one month after the end of the outbreak, when the greater part of costs had been made. We divided outbreak costs into diagnostics costs, ward-related costs, and other outbreak-related control measure costs. All costs are expressed as 2015 US dollars and Euros. Euros were

Author affiliations: European Centre for Disease Prevention and Control, Stockholm, Sweden (M. Mollers); National Institute for Public Health and the Environment, Bilthoven, the Netherlands (M. Mollers, A.F. Schoffelen, A.W.M. Suijkerbuijk); Jeroen Bosch Hospital, 's-Hertogenbosch, the Netherlands (S.P. Lutgens, P.M. Schneeberger)

converted to US dollars by using the data on the purchasing power parity of the Organization for Economic Co-operation and Development (https://data.oecd.org/conversion/purchasing-power-parities-ppp.htm): €1 = US $1.23.

The laboratory of the hospital performed diagnostic tests (bacteria cultures and PCR tests) and antimicrobial drug susceptibility testing for patients. All PCR tests were performed in batches. Items that were included in the determination of the costs of diagnostics were testing materials, procedures, and laboratory personnel. Personnel time of the microbiologists was valued by multiplying the time spent on laboratory and outbreak management activities, as quoted during the interviews, by unit costs per hour, taken from Dutch guidelines for economic evaluations (*5*).

We retrieved loss of revenues caused by closed beds after the outbreak from the hospital database and list prices online (*5*) and adjusted this number for the occupancy rate of the hospital, which was 85% on average. The extra expenses for personal protective equipment (disposable aprons, gloves, and masks) and cleaning the wards affected by the outbreak were gathered by the department of technical and facility services.

We also included costs associated with the additional time spent by healthcare workers on patient isolation. Following Wassenberg et al., we assumed 30 min/d for nurses and 10 min/d for physicians as the time required for adhering to control measures (*6*). The infection prevention expert provided the number of staff meetings in which outbreak interventions were discussed and the number of employees participating in these meetings. Both the executive manager and the communication manager provided data on the amount of time associated with outbreak

response activities. Finally, other costs included costs for sending test kits to persons who had been hospitalized in the outbreak period.

We estimated total outbreak costs at $804,263 or €653,801 (Table), corresponding to a cost of $27,700 per patient. The loss of revenues due to of closure of beds contributed the most to the total costs. Other cost drivers were diagnostic tests and personnel time spent by laboratory employees and infection prevention experts.

Conclusions

The NDM-1 outbreak at Jeroen Bosch Hospital in the Netherlands in 2015 was associated with substantial costs incurred by the hospital, estimated at $804,263 or €653,801, which was 12% of the total budget allocated that year for medical microbiology and infection prevention, and $27,700 per patient. Blocked beds had the highest effect on the total costs, followed by staff time targeted at infection prevention activities.

A few studies have evaluated outbreak costs in hospitals; however, none of these were targeted at NDM outbreaks. Compared with other studies on the costs of hospital outbreaks with other pathogens, such as *Acinetobacter baumanni* (*7,8*), norovirus (*9*), ESBL-producing *K. pneumoniae* (*9*), and *Enterococcus faecium* (*9*), our estimates are higher. One major factor explaining this difference was the testing of a relatively high number of patients; the closure of beds was the main cost driver in all applicable studies.

Despite being substantial, the cost we calculated for the outbreak is an underestimate. At least 9 NDM-1–positive patients and 28 other patients were discharged

Table. Total outbreak costs stratified by type of cost, Jeroen Bosch hospital, the Netherlands, Oct 2015–Jan 2016*

Type of cost	Explanation	Total cost, US $	Total cost, €
Diagnostics			
Other laboratory personnel	Estimated 2,517 h†	93,789	76,251
Microbiological tests	Material costs to perform cultures in batches	60,070	48,837
Microbiologists	Estimated 376 h†	46,017	37,412
Molecular diagnostics	Material costs to perform PCRs in batches	24,523	19,937
Subtotal diagnostics		224,399	182,437
Ward-related costs			
No. blocked beds	582 beds, occupancy rate 0.85 at $550/d or €447/d (*5*)	272,085	221,131
Personal protective equipment	Expenditures for extra disposable aprons, gloves, and masks	55,121	44,814
Cleaning wards	Purchase of 2 fogging devices and personnel time for extra cleaning	46,881	38,115
Subtotal ward-related costs		374,087	304,060
Other outbreak control costs			
Infection prevention experts	Estimated 2,336 h for internal advice and guidance†	105,356	85,655
Patients in isolation	280 patients, averaged at 5.2 d of hospitalization, at $31.40/d or €25.53/d (*6*)	45,718	37,172
Staff meetings	23 staff meetings with on average 21 participants × 0.75 h × $1,525/h†	26,306	21,390
Communication	320 h for internal and patient-related communication spent by several communication employees†	17,696	14,387
Costs for mailings		10,701	8,700
Subtotal outbreak control costs		205,777	167,304
Total costs		804,263	653,801

*Resource use related to this outbreak was provided by the hospital.
†Labor costs/h were determined by using the Dutch manual for economic evaluations (*5*).

to a long-term care facility, resulting in additional infection control measures and costs that were not taken into account for this report. In addition, a medical doctor, infection prevention expert, and infectious diseases nurse of the Municipal Health Service spent 95 h, 65 h, and 30 h, respectively, on the outbreak, accounting for $9,551 additional costs. Furthermore, phylogenetic molecular methods were performed at the National Institute of Public Health to confirm the outbreak. Finally, we only calculated the outbreak costs through January 31, 2016, but additional costs probably were incurred after this date.

As shown in this study, the expansion of multidrug-resistant, gram-negative bacteria is of great concern; these bacteria both threaten patient safety and increase healthcare costs. The intensive outbreak control measures of the hospital were costly and inconvenient for patients and staff. In countries where NDM-1–positive *K. pneumoniae* is not endemic, early detection of colonized patients and adequate infection prevention control strategies will be key factors in minimizing the spread of multidrug-resistant bacteria.

Dr. Mollers is a policy advisor for the Department of Preparedness and Response at the Centre for Infectious Diseases of the Dutch National Institute for Public Health and the Environment. She is also part of the European Programme for Intervention Epidemiology Training fellowship program. She is interested in the public health response to and epidemiology of communicable diseases.

References

1. Yong D, Toleman MA, Giske CG, Cho HS, Sundman K, Lee K, et al. Characterization of a new metallo-beta-lactamase gene, bla_{NDM-1}, and a novel erythromycin esterase gene carried on a unique genetic structure in *Klebsiella pneumoniae* sequence type 14 from India. Antimicrob Agents Chemother. 2009;53:5046–54. http://dx.doi.org/10.1128/AAC.00774-09
2. Glasner C, Albiger B, Buist G, Tambić Andrasević A, Canton R, Carmeli Y, et al.; European Survey on Carbapenemase-Producing Enterobacteriaceae (EuSCAPE) Working Group. Carbapenemase-producing *Enterobacteriaceae* in Europe: a survey among national experts from 39 countries, February 2013. Euro Surveill. 2013; 18:20525. http://dx.doi.org/10.2807/1560-7917.ES2013.18.28.20525
3. Giske CG, Monnet DL, Cars O, Carmeli Y; ReAct-Action on Antibiotic Resistance. Clinical and economic impact of common multidrug-resistant gram-negative bacilli. Antimicrob Agents Chemother. 2008;52:813–21. http://dx.doi.org/10.1128/AAC.01169-07
4. Levy SB, Marshall B. Antibacterial resistance worldwide: causes, challenges and responses. Nat Med. 2004;10(Suppl):S122–9. http://dx.doi.org/10.1038/nm1145
5. Zorginstituut Nederland. Guidance for carrying out economic evaluations in healthcare [in Dutch]. Amsterdam: Zorginstituut Nederland; 2015.
6. Wassenberg MW, Kluytmans JA, Box AT, Bosboom RW, Buiting AG, van Elzakker EP, et al. Rapid screening of methicillin-resistant *Staphylococcus aureus* using PCR and chromogenic agar: a prospective study to evaluate costs and effects. Clin Microbiol Infect. 2010;16:1754–61. http://dx.doi.org/10.1111/j.1469-0691.2010.03210.x
7. Ayraud-Thévenot S, Huart C, Mimoz O, Taouqi M, Laland C, Bousseau A, et al. Control of multi-drug-resistant *Acinetobacter baumannii* outbreaks in an intensive care unit: feasibility and economic impact of rapid unit closure. J Hosp Infect. 2012;82:290–2. http://dx.doi.org/10.1016/j.jhin.2012.08.016
8. Jiang Y, Resch S, Liu X, Rogers SO Jr, Askari R, Klompas M, et al. The cost of responding to an *Acinetobacter* outbreak in critically ill surgical patients. Surg Infect (Larchmt). 2016; 17:58–64. http://dx.doi.org/10.1089/sur.2015.036
9. Dik JW, Dinkelacker AG, Vemer P, Lo-Ten-Foe JR, Lokate M, Sinha B, et al. Cost-analysis of seven nosocomial outbreaks in an academic hospital. PLoS One. 2016;11:e0149226. http://dx.doi.org/10.1371/journal.pone.0149226

Address for correspondence: Anita W.M. Suijkerbuijk, Antonie van Leeuwenhoeklaan 9, 3720 BA, Bilthoven, the Netherlands; email: anita.suijkerbuijk@rivm.nl

Evaluation of 5 Commercially Available Zika Virus Immunoassays

David Safronetz, Angela Sloan, Derek R. Stein,
Emelissa Mendoza, Nicole Barairo,
Charlene Ranadheera, Leanne Scharikow,
Kimberly Holloway, Alyssia Robinson,
Maya Traykova-Andonova, Kai Makowski,
Kristina Dimitrova, Elizabeth Giles,
Joanne Hiebert, Rhonda Mogk,
Sharla Beddome, Michael Drebot

Because of the global spread of Zika virus, accurate and high-throughput diagnostic immunoassays are needed. We compared the sensitivity and specificity of 5 commercially available Zika virus serologic assays to the recommended protocol of Zika virus IgM-capture ELISA and plaque-reduction neutralization tests. Most commercial immunoassays showed low sensitivity, which can be increased.

Zika virus is a mosquito-borne member of the family *Flaviviridae*, genus *Flavivirus*, that was originally discovered in 1947 in Uganda (*1*). For several decades, Zika virus seemed to be geographically restricted to equatorial Africa with a few documented incursions into Asia (*2,3*). Although several studies demonstrated serologic evidence of human exposures to Zika virus across Africa, it was believed that this virus was not a major public health threat. However, in 2007, the epidemic potential of Zika virus became apparent when it was identified as the causative agent of an outbreak in Yap State, Federated States of Micronesia, which consisted of 49 confirmed cases, 59 probable infections, and dozens more suspected cases (*4,5*). Since 2007, several epidemics have occurred across the Pacific Ocean Region, including an outbreak in 2013–14 with thousands of confirmed cases in French Polynesia (*6*).

In 2015, the first cases of Zika virus infection were confirmed in Brazil, which indicated the beginning of the largest outbreak recorded with autochthonous vectorborne transmission documented in >65 countries across the Americas (*2,3,7*). Although it is still widely believed that most Zika virus infections in humans are asymptomatic or mild with self-limiting clinical manifestations, it is now documented that Zika virus infections can lead to major complications and long-term sequelae, including congenital birth defects, neurologic disorders, and prolonged risk for sexual transmission of this virus (*3,8*).

Before 2007, only 14 laboratory-confirmed cases of Zika virus infection had been documented worldwide. Thus, it is not surprising that diagnostics for Zika virus were conducted only in specialized arbovirus reference laboratories (*2*). During the outbreak on Yap Island, samples were sent to the Arbovirus Diagnostic Laboratory, Centers for Disease Control and Prevention (Fort Collins, CO, USA), where molecular and serologic assays were quickly developed for confirmatory testing (*5*). Many of these in-house methods developed in 2007, including real-time molecular assays, an IgM-capture ELISA (MAC-ELISA), and a plaque reduction neutralization test (PRNT), have been used during the current outbreak. However, the magnitude of the outbreak, combined with the in-house production of key reagents involved in diagnostics of Zika virus infection, has taxed the few reference laboratories capable of producing, standardizing, and distributing such materials. Therefore, application and evaluation of sensitive and specific diagnostic assays, particularly those that can be used in frontline laboratories, has become a top public health priority.

Several laboratories and commercial vendors have developed and evaluated molecular assays for rapid identification of Zika virus RNA, and, in some instances, other clinically relevant arboviruses, such as dengue virus (DENV) and chikungunya virus, in acute-phase clinical specimens (*9*). However, high-throughput commercially produced immunoassays have proven to be more challenging because of strong serologic cross-reactivity of closely related flaviviruses, such as DENV. We compared the sensitivity and specificity of 5 commercially available Zika virus serologic assays to the recommended protocols of Zika virus MAC-ELISA and PRNT.

The Study

Samples were submitted to the National Microbiology Laboratory of the Public Health Agency of Canada (Winnipeg, Manitoba, Canada) for arbovirus diagnostic testing. All samples were obtained from Canadian travelers who visited areas with known Zika virus transmission and consulted their physicians after symptoms consistent with Zika virus infection developed upon return.

We obtained deidentified samples from 75 patients. Thirty samples were from patients with serologically confirmed Zika virus infections; 10 from patients with

Author affiliation: Public Health Agency of Canada, Winnipeg, Manitoba, Canada

confirmed Zika virus infections identified by 2-target real-time reverse transcription PCR (RT-PCR); 10 from patients with suspected Zika virus infections, which were subsequently identified as DENV infections; and 25 acute-phase samples from flavivirus-negative persons tested by Zika virus RT-PCR and MAC-ELISA. Primary Zika virus diagnostic testing for all samples was conducted by using an in-house CDC-based MAC-ELISA and subsequent confirmation of Zika virus infection by cross-PRNTs for Zika virus and DENV, or molecular assays as described (5).

We evaluated 5 Zika virus immunoassays in this study. We tested a conventional IgM ELISA (EI 2668-9601 M; Euroimmun AG, Luebeck, Germany) and 3 MAC-ELISAs: Zika Virus Detect (InBios International Inc., Seattle, WA, USA); Ab213327 (Abcam, Cambridge, UK); and NovaLisa ZVM0790 (Novatec Inc., Baltimore, MD, USA). On the

basis of preliminary testing, we also tested the Euroimmun IgM ELISA in parallel with the Euroimmun conventional Zika virus IgG ELISA (EI 2668-9601 G). Both Euroimmun assays use recombinant Zika virus nonstructural protein 1 as the antigen; the InBios Zika Virus Detect uses a recombinant Zika virus envelope glycoprotein as the positive antigen, an unspecified cross-reactive control, and reference cell antigens; and the Novatec and Abcam ELISAs use an unspecified Zika virus antigen.

Most tests evaluated provided algorithms that resulted in positive, negative, or equivocal results. However, the In-Bios kits account for antigenics in associated with secondary flavivirus infections and reports results as Zika virus positive, possible Zika virus positive, or presumptive other flavivirus positive or negative on the basis of calculations of optical density ratios obtained from a sample with the 3

Table 1. Results of in-house and commercially available Zika virus immunoassays*

Sample collection dpo	In-house Zika virus diagnostic results				Commercial Zika virus serologic assays results				
	RT-PCR	MAC-ELISA	PRNT titer	DENV PRNT titer	Euroimmun IgM	Euroimmun IgG	Novatec IgM	Abcam IgM	InBios IgM
12	ND	Pos	>40	Neg	Pos	Pos	Pos	Pos	Pos
9	ND	Pos	>40	Neg	**Neg**	**Neg**	**Neg**	**Neg**	Pos
4	ND	Pos	>40	Neg	**Neg**	**Neg**	**Neg**	Pos	Pos
27	ND	Pos	>40	Neg	Pos	Pos	Pos	Pos	Pos
39	ND	Pos	>40	Neg	**Neg**	Pos	Pos	Pos	Pos
11	ND	Pos	>40	Neg	Pos	Pos	Pos	Pos	Pos
109	ND	Pos	1,280	20	**Neg**	Pos	**Neg**	**Neg**	Pos
49	ND	Pos	>40	Neg	**Neg**	Pos	Pos	Pos	Pos
Unknown	ND	Pos	>40	Neg	**Neg**	**Neg**	**Neg**	**Neg**	Pos
4	ND	Pos	>40	Neg	Pos	**Neg**	Pos	Pos	Pos
7	ND	Pos	>40	Neg	**Neg**	Pos	**Neg**	**Neg**	Pos
46	ND	Pos	>40	Neg	**Neg**	Pos	Pos	Pos	Pos
Unknown	ND	Pos	>40	Neg	**Neg**	Pos	**Neg**	**Neg**	Pos
Unknown	ND	Pos	>40	Neg	**Neg**	Pos	_Eq_	Pos	Pos
118	ND	Pos	>40	Neg	**Neg**	Pos	**Neg**	**Neg**	Pos
57	ND	Pos	>40	Neg	Pos	**Neg**	Pos	Pos	Pos
66	ND	Pos	>40	Neg	**Neg**	Pos	**Neg**	_Eq_	Pos
43	ND	Pos	40	Neg	**Neg**	Pos	_Eq_	Pos	Pos
2	ND	Pos	>40	Neg	**Neg**	**Neg**	Pos	**Neg**	Pos
41	ND	Pos	>40	Neg	Pos	Pos	**Neg**	**Neg**	Pos
5	ND	Pos	>40	Neg	**Neg**	**Neg**	**Neg**	**Neg**	Pos
38	ND	Pos	>40	Neg	**Neg**	Pos	**Neg**	**Neg**	_PZ_
4	ND	Pos	>80	Neg	Pos	**Neg**	**Neg**	Pos	Pos
6	ND	Pos	>80	Neg	Pos	Pos	**Neg**	**Neg**	Pos
2	ND	Pos	>80	Neg	Neg	Pos	**Neg**	_Eq_	Pos
12	ND	Pos	40	Neg	Pos	**Neg**	Pos	Pos	Pos
Unknown	ND	Pos	>80	Neg	Pos	**Neg**	Pos	Pos	Pos
28	ND	Pos	>80	Neg	Pos	Pos	**Neg**	**Neg**	Pos
75	ND	Pos	>80	20	**Neg**	Pos	**Neg**	**Neg**	Pos
68	ND	Pos	>40	Neg	**Neg**	Pos	**Neg**	**Neg**	Pos
9	ND	**Pos**	Neg	>40	Neg	Neg	Neg	Neg	_PZ_
7	ND	**Pos**	Neg	>40	Neg	Neg	Neg	Neg	_PZ_
31	ND	**Pos**	Neg	>40	Neg	Neg	Neg	Neg	_PZ_
6	ND	**Pos**	Neg	>40	**Pos**	**Pos**	Neg	Neg	Pos
20	ND	**Pos**	Neg	>40	Neg	Neg	**Pos**	**Pos**	_PZ_
36	ND	**Pos**	Neg	>80	Neg	Neg	Neg	Neg	OF
Unknown	ND	**Pos**	320	>5,120	Neg	Neg	Neg	Neg	Pos
Unknown	ND	**Pos**	Neg	40	Neg	Neg	**Pos**	Neg	Neg
3	ND	**Pos**	Neg	>80	Neg	Neg	_Eq_	Neg	Pos
Unknown	ND	**Pos**	Neg	>640	Neg	Neg	Neg	Neg	Pos

***Bold** indicates false-positive/false-negative results. Underlining indicates inconclusive results that required further testing. DENV, dengue virus; dpo, days postsymptom onset; Eq, equivalent; MAC-ELISA, IgM-capture ELISA; ND, not done; Neg, negative; OF, other flavivirus; Pos, positive; PRNT, plaque reduction neutralization test; PZ, possible Zika virus; RT-PCR, reverse transcription PCR.

Table 3. Detection of IgM in RT-PCR–positive serum samples by using in-house and commercial Zika virus serologic assays*

Sample collection, dpo	In-house Zika virus diagnostic results			DENV PRNT	Commercial Zika virus serologic assays results				
	RT-PCR	MAC-ELISA	PRNT		Euroimmun IgM	Euroimmun IgG	Novatec IgM	Abcam IgM	InBios IgM
0	Pos	Neg	ND	ND	Neg	Neg	Neg	Neg	Neg
2	Pos	Neg	ND	ND	Neg	Neg	Eq	Neg	Pos
5	Pos	Neg	ND	ND	Neg	Neg	Neg	Neg	Neg
7	Pos	Pos	ND	ND	Pos	Pos	Pos	Pos	Pos
3	Pos	Neg	ND	ND	Neg	Neg	Neg	Neg	Neg
2	Pos	Neg	ND	ND	Neg	Neg	Neg	Neg	Pos
2	Pos	Pos	ND	ND	Neg	Neg	Pos	Neg	Pos
3	Pos	Neg	ND	ND	Neg	Neg	Neg	Neg	Pos
3	Pos	Neg	ND	ND	Neg	Neg	Pos	Neg	PZ
2	Pos	Neg	ND	ND	Neg	Neg	Neg	Neg	Neg

*DENV, dengue virus; dpo, days postsymptom onset; Eq, equivalent; MAC-ELISA, IgM-capture ELISA; ND, not done; Neg, negative; Pos, positive; PRNT, plaque reduction neutralization test; PZ, possible Zika virus; RT-PCR, reverse transcription PCR.

different antigens. Two independent laboratory technicians blindly evaluated the 5 assays by using the panel outlined, according to the manufacturer's instructions. Comparisons and performance calculations were conducted by the Quality Control Office of the National Microbiology Laboratory.

The assays generally showed reproducible results during independent evaluations, although specificity and sensitivity of each varied (Table 1). The Euroimmun IgM and IgG ELISAs and the Abcam IgM ELISA showed a specificity of 100% for negative specimens with similar results (≥90%) for confirmed DENV-positive samples (Table 2, https://wwwnc.cdc.gov/EID/article/23/9/16-2043-T2.htm). The NovaTec ELISA showed a specificity of 66% for negative specimens and 70% for DENV-positive specimens. Although the InBios Zika Detect ELISA showed similar specificity results for flavivirus-seronegative specimens, it showed decreased specificity for DENV-positive samples. This assay incorrectly identified 40% of these samples as Zika virus IgM positive and 40% as possible Zika virus positive.

Although specificity is a key factor, for a front-line diagnostic test, sensitivity is a major factor in determining its usefulness. With appropriate diagnostic testing in place, including use of Zika virus conformational cross-PRNTs, false-positive results caused by specificity issues can usually be overcome. However, poor sensitivity will lead to false-negative results that might not be followed up by testing of additional sample collections. When compared with the in-house diagnostics (MAC-ELISA with PRNT confirmation), the IgM assays of Euroimmun, Abcam, and Novatec demonstrated sensitivities of 37%, 57%, and 65%, respectively. When we combined results of the Euroimmun IgM and IgG ELISAs, sensitivity increased to 82%. The InBios Zika Virus Detect IgM assay correctly identified all confirmed Zika IgM-positive samples identified by the recommended diagnostic assays, resulting in a sensitivity of 100%. The InBios ELISA also detected IgM in 50% of samples that were positive for Zika virus by RT-PCR, whereas the other assays did not detect IgM in most of these samples (Table 3).

Conclusions

The low sensitivity of most immunoassays evaluated could be improved by testing a repeat sample collected a few weeks after the initial specimen, although this sampling is not always practical, particularly if resources are limited. When performed in combination, the Euroimmun Zika Virus IgM and IgG ELISAs provide improved sensitivity. However, interpretation of recent versus past infections could be problematic, particularly when IgM results are negative and IgG results are positive. On the basis of our findings, the InBios Zika Virus Detect MAC-ELISA provides diagnostic results comparable to the CDC-based in-house MAC-ELISA for specimens collected from patients with primary flavivirus exposures (i.e., no detectable background immunity to DENV). A needed follow-up to our study will be further evaluation of IgM detection by commercial ELISAs involving cases of secondary flavivirus exposures or previous immunization to related viruses, such as yellow fever virus.

Dr. Safronetz is a research scientist in the Zoonotic Diseases and Special Pathogens Section, National Microbiology Laboratory, Public Health Agency of Canada, Winnipeg, Manitoba, Canada. His research interests include the ecology, epidemiology, and pathogenicity of emerging virus pathogens.

References

1. Dick GW, Kitchen SF, Haddow AJ. Zika virus. I. Isolations and serological specificity. Trans R Soc Trop Med Hyg. 1952;46:509–20. http://dx.doi.org/10.1016/0035-9203(52)90042-4
2. Wikan N, Smith DR. Zika virus: history of a newly emerging arbovirus. Lancet Infect Dis. 2016;16:e119–26. http://dx.doi.org/10.1016/S1473-3099(16)30010-X
3. Weaver SC, Costa F, Garcia-Blanco MA, Ko AI, Ribeiro GS, Saade G, et al. Zika virus: history, emergence, biology, and prospects for control. Antiviral Res. 2016;130:69–80. http://dx.doi.org/10.1016/j.antiviral.2016.03.010
4. Duffy MR, Chen TH, Hancock WT, Powers AM, Kool JL, Lanciotti RS, et al. Zika virus outbreak on Yap Island, Federated States of Micronesia. N Engl J Med. 2009;360:2536–43. http://dx.doi.org/10.1056/NEJMoa0805715

5. Lanciotti RS, Kosoy OL, Laven JJ, Velez JO, Lambert AJ, Johnson AJ, et al. Genetic and serologic properties of Zika virus associated with an epidemic, Yap State, Micronesia, 2007. Emerg Infect Dis. 2008;14:1232–9. http://dx.doi.org/10.3201/eid1408.080287

6. Cao-Lormeau VM, Roche C, Teissier A, Robin E, Berry AL, Mallet HP, et al. Zika virus, French Polynesia, South Pacific, 2013. Emerg Infect Dis. 2014;20:1085–6. http://dx.doi.org/10.3201/eid2011.141380

7. Campos GS, Bandeira AC, Sardi SI. Zika virus outbreak, Bahia, Brazil. Emerg Infect Dis. 2015;21:1885–6. http://dx.doi.org/10.3201/eid2110.150847

8. Grossi-Soyster EN, LaBeaud AD. Clinical aspects of Zika virus. Curr Opin Pediatr. 2017;29:102–6. http://dx.doi.org/10.1097/MOP.0000000000000449

9. Landry ML, St George K. Laboratory diagnosis of Zika virus infection. Arch Pathol Lab Med. 2017;141:60–7. http://dx.doi.org/10.5858/arpa.2016-0406-SA

Address for correspondence: David Safronetz, Zoonotic Diseases and Special Pathogens, National Microbiology Laboratory, Public Health Agency of Canada, Winnipeg, MB, R3E 3R2, Canada; email: david.safronetz@phac-aspc.gc.ca

October 2010: **Zoonoses**

EMERGING INFECTIOUS DISEASES
https://wwwnc.cdc.gov/eid/articles/issue/16/10/table-of-contents

Epidemiology of *Neisseria gonorrhoeae* Gyrase A Genotype, Los Angeles, California, USA

Ashima A. Bhatti, Lao-Tzu Allan-Blitz, Mariana Castrejon, Romney M. Humphries, Peera Hemarajata, Jeffrey D. Klausner

We investigated the epidemiology of the mutant gyrase A gene, a reliable predictor of ciprofloxacin resistance, in *Neisseria gonorrhoeae* infections at UCLA Health in Los Angeles, California, USA, during November 1, 2015–August 31, 2016. Among 110 patients with *N. gonorrhoeae* infections, 48 (44%) had the mutant gyrase A gene.

In 2013, the Centers for Disease Control and Prevention (Atlanta, GA, USA) declared that multidrug-resistant *Neisseria gonorrhoeae* infections were 1 of the top 3 urgent antimicrobial drug resistance threats (*1*). To combat this growing threat, we developed and implemented a real-time reverse transcription PCR at the University of California, Los Angeles (Los Angeles, CA, USA), to detect the codon 91 mutation in the gyrase A (*gyrA*) gene in *N. gonorrhoeae* remnant clinical specimens (*2*). Mutations in the *gyrA* gene of *N. gonorrhoeae*, specifically at codon 91, have been demonstrated to reliably predict resistance to ciprofloxacin (*3*).

Current clinical practice uses mostly nucleic acid amplification tests to detect *N. gonorrhoeae* and not culture-based methods (*4*). Although those tests yield better clinical outcomes, they do not provide useful antimicrobial drug susceptibility data. Therefore, factors associated with antimicrobial drug resistance in the general community are not routinely available (*4,5*).

The Study

We characterized the epidemiology of fluoroquinolone resistance at UCLA Health (Los Angeles, CA, USA) by using a rapid molecular *gyrA* gene assay that predicts ciprofloxacin susceptibility (*3,6*). UCLA Health is a large healthcare system in Los Angeles County composed of 2 hospitals, 2 emergency departments, and >150 primary care clinics serving ≈500,000 patient-visits each year. We reviewed electronic patient medical records for November 1, 2015–August 31, 2016, for all cases of *N. gonorrhoeae*

Author affiliations: University of California, Los Angeles, California, USA (A.A. Bhatti, L.-T. Allan-Blitz, M. Castrejon, R.M. Humphries, P. Hemarajata, J.D. Klausner); UCLA Health, Los Angeles (M. Castrejon, J.D. Klausner)

infection detected by using the Cobas 4800 CT/NG Assay (Roche Molecular Systems, Pleasanton, CA, USA).

We collected data on age, sex, sex of sex partners, race/ethnicity, HIV infection status, pregnancy, HIV preexposure prophylaxis use, *gyrA* gene results by anatomic site of infection, presence of other sexually transmitted infections, substance use, history of fluoroquinolone exposure in the past 2 years, and history of previous *N. gonorrhoeae* infection. Each positive *N. gonorrhoeae* result in a single patient was considered a unique infection. The date of *N. gonorrhoeae* specimen collection was considered the infection date.

Patients were considered to have no fluoroquinolone exposure only if they had medical records going back ≥2 years from infection date and no documentation of having been prescribed a fluoroquinolone during that time. Patients were considered to have no history of previous *N. gonorrhoeae* infection if they had medical records going back ≥2 years from current infection date and no documentation of having a positive *N. gonorrhoeae* test result at UCLA Health during those 2 years.

Descriptive statistics, prevalence ratios (PRs), and p values by χ^2 test or Fisher exact test are reported. We performed analysis by using STATA software version 14.2 (StataCorp LLC, College Station, TX, USA). UCLA determined that analysis of unidentified data was exempt from ethical review.

Among 141 patients for whom *N. gonorrhoeae* genotyping was attempted, 110 (78%) had a genotype identified; 31 (22%) had an indeterminate genotype. Of the 110 patients who had a genotype identified, 48 (44%) had a mutant genotype and 62 (56%) had a wild-type genotype. Twenty (18%) of the patients were women, 1 of whom was a transgender woman. The remaining 90 (82%) patients were men, and 58 (64%) were men who have sex with men (MSM). Forty (42%) patients who had documentation of HIV status were infected. Sixteen women had pregnancy tests performed; 6 (37%) of these women were pregnant. We obtained demographic characteristics and other factors for all patients (Table).

Among 35 patients with a *gyrA* mutant genotype who had medical records going back ≥2 years, 9 (26%) were exposed to fluoroquinolones during that time, compared with 6 (15%) of 41 patients with wild-type *gyrA* genotype with medical records going back ≥2 years (PR 1.4, 95% CI 0.85–2.3; p = 0.23). A recent study demonstrated that treatment might be a major driver of resistance (*7*), and a previous study demonstrated that a history of fluoroquinolone exposure is associated with an increased prevalence of

Table. Characteristics of 110 patients infected with *Neisseria gonorrhoeae* containing gyrase A mutant and wild-type genes, UCLA Health, Los Angeles, California, USA, November 1, 2015–August 31, 2016*

Characteristic	No. (%)	No. (%) with *gyrA* mutant gene	Prevalence ratio (95% CI)	p value†
No. patients	110	48 (44)		
Age, y, n = 110				
17–34	68 (62)	29 (43)	1	Referent
≥35	42 (38)	19 (45)	1.1 (0.69–1.6)	0.79
Sex and sexual orientation, n = 110				
Men who have sex with men	58 (53)	25 (43)	1	Ref
Men who have sex with women only	11 (10)	6 (55)	1.3 (0.68–2.3)	0.48
Men of unknown orientation	21 (19)	10 (48)	1.1 (0.65–1.9)	0.72
Women	20 (18)	7 (35)	0.81 (0.42–1.6)	0.52
Race/ethnicity, n = 110				
White	42 (38)	16 (38)	1	Referent
Hispanic	12 (11)	3 (25)	0.66 (0.23–1.9)	0.51‡
Black/African American	20 (18)	12 (60)	1.6 (0.93– 2.7)	0.11
Asian or Indian	5 (5)	2 (40)	1.1 (0.37–6.8)	1‡
Other or nonspecified	31 (28)	15 (48)	1.3 (0.75–2.2)	0.38
HIV infection status, n = 95				
Uninfected	55 (58)	24 (44)	1	Referent
Infected	40 (42)	18 (45)	1.03 (0.65–1.6)	0.89
Genotype by anatomic site, n = 125 samples				
Pharyngeal	19 (15)	5 (26)	1	Referent
Cervical/vaginal	7 (5.6)	3 (43)	1.6 (0.52–5.1)	0.64‡
Rectal	35 (28)	17 (49)	1.8 (0.81–4.2)	0.11
Urethral	64 (51)	27 (42)	1.6 (0.72–3.6)	0.21
History of *N. gonorrhoeae* infection, n = 77				
No	55 (71)	21 (38)	1	Referent
Yes	22 (29)	12 (55)	1.4 (0.86–2.4)	0.19
Other sexually transmitted infections, n = 110				
None	71 (65)	33 (46)	1	Referent
Chlamydia trachomatis	31 (28)	13 (42)	0.90 (0.56–1.5)	0.67
Treponema pallidum	6 (5)	1 (17)	0.36 (0.06–2.2)	0.22‡
Trichomonas vaginalis	2 (2)	1 (50)	1.1 (0.26–4.4)	1‡
Pregnant, n = 16				
No	10 (63)	3 (30)	1	Referent
Yes	6 (37)	2 (33)	1.1 (0.25–4.9)	1‡
Recent methamphetamine or heroin use, n = 66				
No	59 (89)	30 (51)	1	Referent
Yes	7 (11)	3 (43)	0.84 (0.35–2.1)	1‡
PrEP use, n = 73				
No	56 (77)	22 (39)	1	Referent
Yes	17 (23)	8 (47)	1.2 (0.66–2.2)	0.57
History of fluoroquinolone exposure, n = 76				
No	61 (80)	26 (43)	1	Referent
Yes	15 (20)	9 (60)	1.4 (0.85–2.3)	0.23
Past 3 mo	2 (3)	2 (100)	2.3 (1.8–3.1)	0.19‡
Past 4–12 mo	9 (12)	6 (67)	1.6 (0.91–2.7)	0.28‡
Past 13–24 mo	4 (5)	1 (25)	0.59 (0.10–3.3)	0.64‡

*n values indicate number of patients for which data were available or total number of samples collected. *gyrA*, gyrase A; PrEP, preexposure prophylaxis.
†By χ^2 test unless otherwise noted.
‡By 2-sided Fisher exact test.

fluoroquinolone resistance (*8*). The lack of statistical significance between previous fluoroquinolone exposure and presence of *N. gonorrhoeae* mutant *gyrA* genotype in our study might be caused by small sample size.

Patients ≥35 years of age were more likely to have medical records going back ≥2 years than persons 17–34 years of age (PR 1.6, 95% CI 1.2–2.0; p<0.001). Men were more likely than women to have medical records going back ≥2 years (PR 1.6, 95% CI 1.0–2.5; p = 0.048). MSM were more likely to have medical records going back ≥2 years than all other men (PR 1.4, 95% CI 1.06–1.9;

p = 0.019). These findings indicate the possibility of selection bias regarding medication exposure in our study.

During the 10-month study period, there were 171 site-specific *N. gonorrhoeae* infections. For these infections, none of the patients with infections at multiple anatomic sites showed discordant genotypes. One patient with repeat infections during the study showed a change in *gyrA* genotype from wild-type to mutant during the subsequent infection. There were no differences in distribution of genotype among anatomic sites (Figure, panel A; Table). Most infections were successfully genotyped regardless of anatomic
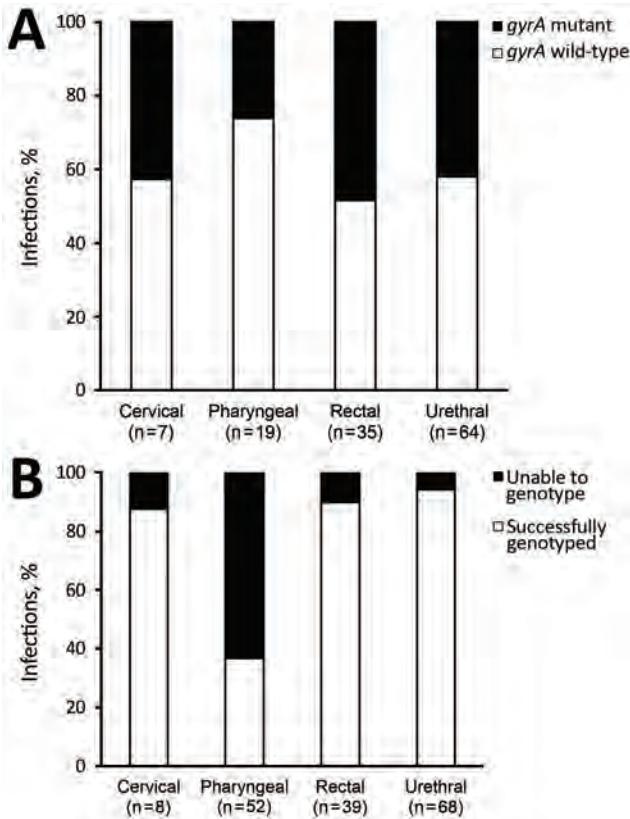
Figure. Proportion of *Neisseria gonorrhoeae* infections genotyped for gyrase A gene by anatomic site, UCLA Health, Los Angeles, California, USA, November 1, 2015–August 31, 2016. A) Gyrase A gene; B) gyrase A mutant and wild-type genes.

site, except for the pharyngeal site, which yielded genotypes for only 37% of infections (Figure, panel B).

Of the 42 infections that could not be genotyped, 32 were in 31 patients who had no other genotyped infections. These infections were excluded from our analyses. The remaining 10 infections were in patients who had a genotyped infection at another anatomic site: 9 of these patients were MSM and 1 was a woman. There was no major difference in distribution of sexual orientation, age, or genotype for indeterminate samples with identified genotypes for another simultaneous infection compared with those that did not have successful genotyping of another simultaneous infection.

Conclusions

Previous studies have reported a similar low sensitivity of the *N. gonorrhoeae* gyrA gene assay for pharyngeal specimens, but the cause remains uncertain (*6,9*). It was previously believed that PCR inhibitors were present in pharyngeal reservoirs, perhaps from commensal *Neisseria* spp.; however, this suggestion is no longer believed to be the case (*6,9*).

Our study had some limitations. First, patients who had medical records that go back <2 years might have received fluoroquinolones or had *N. gonorrhoeae* infections diagnosed at other institutions. If we were able to access that information, we would probably see a stronger association between mutant *gyrA* genotype and fluoroquinolone exposure and history of *N. gonorrhoeae* infection. Second, the UCLA Health system is a large, well-established institution in a large metropolitan area. Therefore, our results might not be representative of trends in *N. gonorrhoeae* resistance in other regions or healthcare systems.

In summary, we found a prevalence of 44% for the mutant *gyrA* genotype, which confers ciprofloxacin resistance, among patients infected with *N. gonorrhoeae*. Molecular methods to predict susceptibility testing offer a potential new way to monitor *N. gonorrhoeae* drug resistance in the United States. Replication of our work in other settings is urgently needed.

Ms. Bhatti is a registered nurse and master's degree candidate at UCLA Fielding School of Public Health, Los Angeles. Her research interests include sexually transmitted infections, especially in marginalized populations.

References

1. Barton J, Braxton J, Darlene D, de Voux A, Flagg E, Grier L, et al. Division of STD Prevention, Centers for Disease Control and Prevention. Sexually transmitted disease surveillance 2015. Atlanta. October 2016 [cited 2017 Jun 12]. https://www.cdc.gov/std/stats15/std-surveillance-2015-print.pdf
2. Allan-Blitz LT, Humphries RM, Hemarajata P, Bhatti A, Pandori MW, Siedner MJ, et al. Implementation of a rapid genotypic assay to promote targeted ciprofloxacin therapy of *Neisseria gonorrhoeae* in a large health system. Clin Infect Dis. 2016;64:1268–70. http://dx.doi.org/10.1093/cid/ciw864
3. Allan-Blitz LT, Wang X, Klausner JD. Wild-type gyrase A genotype of *Neisseria gonorrhoeae* predicts in vitro susceptibility to ciprofloxacin: a systematic review of the literature and meta-analysis. Sex Transm Dis. 2017;44:261–5. http://dx.doi.org/10.1097/OLQ.0000000000000591
4. Garrett TA, Davies-Cole J, Furness B. Laboratory capacity for antimicrobial susceptibility surveillance of *Neisseria gonorrhoeae*, District of Columbia, 2007–2012. Sex Transm Dis. 2015;42:413–6. http://dx.doi.org/10.1097/OLQ.0000000000000304
5. Hook EW III. Generalized testing for gonococcal antibiotic susceptibility or sentinel surveillance. Sex Transm Dis. 2015;42:417–8. http://dx.doi.org/10.1097/OLQ.0000000000000321
6. Hemarajata P, Yang S, Soge OO, Humphries RM, Klausner JD. Performance and verification of a real-time PCR assay targeting the *gyrA* gene for prediction of ciprofloxacin resistance in *Neisseria gonorrhoeae*. J Clin Microbiol. 2016;54:805–8. http://dx.doi.org/10.1128/JCM.03032-15

7. Fingerhuth SM, Bonhoeffer S, Low N, Althaus CL. Antibiotic-resistant *Neisseria gonorrhoeae* spread faster with more treatment, not more sexual partners. PLoS Pathog. 2016;12:e1005611. http://dx.doi.org/10.1371/journal.ppat.1005611

8. Klausner JD, Aplasca MR, Mesola VP, Bolan G, Whittington WL, Holmes KK. Correlates of gonococcal infection and of antimicrobial-resistant *Neisseria gonorrhoeae* among female sex workers, Republic of the Philippines, 1996–1997. J Infect Dis. 1999;179:729–33. http://dx.doi.org/10.1086/314625

9. Low N, Unemo M. Molecular tests for the detection of antimicrobial resistant *Neisseria gonorrhoeae*: when, where, and how to use? Curr Opin Infect Dis. 2016;29:45–51. http://dx.doi.org/10.1097/QCO.0000000000000230

Address for correspondence: Jeffrey D. Klausner, Department of Medicine, Division of Infectious Disease, University of California, Los Angeles, 10833 Le Conte Ave, Los Angeles, CA 90095, USA; email: jdklausner@mednet.ucla.edu

February 2010: Emerging Zoonoses

- Proximity of *Leishmania donovani*–positive goats is a risk factor for human infection
- Imported MRSA, Sweden
- Household Responses to Pandemic (H1N1) 2009–related School Closures, Australia
- Employment and Compliance with Pandemic Influenza Mitigation Recommendations
- Coronavirus Infections in Children
- Community-associated *Clostridium difficile* Infection, North Carolina
- Human Hendra Virus Encephalitis and Equine Outbreak, Australia, 2008
- Cost-effectiveness of Pharmaceutical-based Pandemic Mitigation Strategies
- Domestic Animals and Visceral Leishmaniasis, Nepal
- Influenza Vaccination Program for Children, Hawaii
- *Cryptococcus gattii*, British Columbia, Canada, 1999–2007
- *Tropheryma whipplei* in Patients with Pneumonia
- Increased Resistance in Tuberculosis Despite Treatment Adherence, South Africa
- Association Between *Mycobacterium tuberculosis* Strains and Phenotypes
- Cause of Epidemic among Native Americans, New England, 1616–1619
- Clonal Distribution of Invasive Pneumococci, Czech Republic, 1996–2003
- White-Nose Syndrome Fungus in Bat, France
- Nontuberculous Mycobacteria, Taiwan, 2000–2008
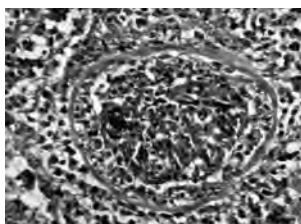
- Tularemia Outbreak, Germany
- *Bordetella pertussis* Clones Identified by Multilocus Variable-Number Tandem-Repeat Analysis
- *Plasmodium falciparum* Malaria, Southern Algeria, 2007
- Pandemic (H1N1) 2009 Outbreak on Pig Farm, Argentina
- Sin Nombre Virus Infections in Field Workers, Colorado
- Pandemic (H1N1) 2009 Cases, Buenos Aires, Argentina
- Mammalian Ancestry of Pandemic (H1N1) 2009 Virus
- Concurrent Silicosis and Mycosis at Death
- Coccidioidiomycosis among College Students, Arizona
- Novel Human Bocavirus in Children with Acute Respiratory Tract Infection
- Lymphocytic Choriomeningitis Virus Meningitis, New York, NY, 2009
- Severe Leptospirosis in Hospitalized Patients, Guadeloupe

- *Enterocytozoon bieneusi* Infection, Czech Republic
- Hendra Virus Outbreak with Novel Clinical Features, Australia, 2008
- Permanent Specimens of Hosts and Vectors in Public Health and Epidemiology
- Perinatal Pandemic (H1N1) 2009 Infection, Thailand
- Bronchial Casts and Pandemic (H1N1) 2009 Virus Infection
- Methicillin-Resistant *Staphylococcus aureus* ST398, Italy

EMERGING INFECTIOUS DISEASES

https://wwwnc.cdc.gov/eid/articles/issue/16/2/table-of-contents

Conveyance Contact Investigation for Imported Middle East Respiratory Syndrome Cases, United States, May 2014

Susan A. Lippold, Tina Objio, Laura Vonnahme, Faith Washburn, Nicole J. Cohen, Tai-Ho Chen, Paul J. Edelson, Reena Gulati, Christa Hale, Jennifer Harcourt, Lia Haynes, Amy Jewett, Robynne Jungerman, Katrin S. Kohl, Congrong Miao, Nicolette Pesik, Joanna J. Regan, Efrosini Roland, Chris Schembri, Eileen Schneider, Azaibi Tamin, Kathleen Tatti, Francisco Alvarado-Ramy

In 2014, the Centers for Disease Control and Prevention conducted conveyance contact investigations for 2 Middle East respiratory syndrome cases imported into the United States, comprising all passengers and crew on 4 international and domestic flights and 1 bus. Of 655 contacts, 78% were interviewed; 33% had serologic testing. No secondary cases were identified.

Two cases of imported Middle East respiratory syndrome (MERS) in the United States were confirmed in May 2014 in travelers from Saudi Arabia (*1*). Both persons were symptomatic at the time of travel. The Centers for Disease Control and Prevention (CDC) conducted large-scale (entire plane) contact investigations for the affected flights and for an interstate bus.

The Study

The investigation had 3 objectives: 1) notify travelers, 2) identify symptomatic contacts and facilitate prompt evaluation and isolation, and 3) determine the extent of onboard transmission. CDC approved the protocol as nonresearch.

We obtained passenger information and distributed it to state health departments as described (*2*). Foreign public health authorities were notified for US citizens abroad and foreign passport holders located outside the United States within the 14-day incubation period.

State health departments, CDC, or airline occupational health staff interviewed contacts using a standard questionnaire. Contacts interviewed within 14 days after exposure were advised to monitor themselves for fever

and respiratory symptoms and to report symptoms to their state or local health department. Symptomatic contacts were reinterviewed about coexisting conditions and other exposure risks. When clinically indicated, state health departments coordinated specimen collection for testing by real-time reverse transcription PCR (rRT-PCR) (Table 1).

With contacts' consent, serum specimens were collected at least 14 days after exposure. Serologic tests were a recombinant MERS coronavirus (MERS-CoV) nucleocapsid protein–based ELISA, followed by confirmatory testing for MERS-CoV–specific antibodies by immunofluorescence assay and microneutralization test on ELISA-positive serum specimens. Serologic assays were developed and performed at CDC, and microneutralization testing was done in a BioSafety Level 3 laboratory at CDC. Symptomatic contacts (contact definition category 1) were evaluated and tested at state health department laboratories using the CDC MERS-CoV rRT-PCR (*4*).

Index case-patient 1 was a 65-year-old resident of Saudi Arabia who developed myalgia, fatigue, and a low-grade fever around April 18. On April 24, he flew from Riyadh to London, UK (Boeing 747–400, flight time 6 h 50 min), then London to Chicago, IL, USA (Boeing 767–300, 8 h 45 min). He then traveled to Indiana by bus (1 h 10 min). On April 27, cough, shortness of breath, increasing fever, and rhinorrhea developed; he was hospitalized April 28. MERS was diagnosed May 1 by the Indiana State Department of Health and confirmed May 2 by CDC (*1*).

Index case-patient 2, unconnected to case-patient 1, was a 43-year-old resident of Saudi Arabia who traveled on 2 international and 2 domestic US flights on May 1. He felt ill on his Riyadh–London flight (Boeing 777–300ER, 6 h 30 min); fever, chills, and myalgia developed on a flight from London to Boston, MA, USA (Boeing 767–400, 7 h 40 min), and cough on the domestic flights: Boston–Atlanta, GA, USA (McDonnell Douglas D-90, 2 h 50 min), and Atlanta–Orlando, FL, USA (Boeing 757, 1 h 30 min). On May 9, he sought care at a Florida emergency department with fever, cough, chills, and myalgia. Bilateral crackles were noted on exam; chest radiograph was normal. On May 11, the Florida Department of Health diagnosed MERS, subsequently confirmed by CDC (*1*).

CDC investigated the 2 international flights inbound to the United States and 2 domestic flights. Nine additional

Table 1. CDC case and contact definitions during MERS contact investigations*

Status	Definition	Signs and symptoms
Index case	Laboratory-confirmed MERS-CoV infection in a person who traveled by commercial aircraft or bus while symptomatic. A traveler who tested positive for MERS-CoV was considered to have been contagious if symptomatic while on the conveyance.	Fever ($\geq$38°C [$\geq$100.4°F]) or feverishness;† or symptoms of acute respiratory illness (i.e., cough, shortness of breath, rhinorrhea, sore throat); or myalgia, malaise; or gastrointestinal symptoms (i.e., nausea, diarrhea, or vomiting).
Conveyance contact	A person who traveled on the same conveyance as the index case-patient and who had:	
Category 1	Compatible symptoms within 2–14 d after the flight or bus ride.	Fever ($\geq$38°C [100.4°F]) or feverishness; or symptoms of acute respiratory illness (i.e., cough, shortness of breath, rhinorrhea, sore throat); or myalgia, malaise; or gastrointestinal symptoms (i.e., nausea, diarrhea, or vomiting).
Category 2	Unrelated symptoms.	An illness before the flight or an illness with onset either <2 d or >14 d after the flight; or symptoms attributable to a chronic illness; or symptoms that were musculoskeletal, neurologic, or dermatologic in origin.
Category 3	No symptoms.	
Patient under investigation‡	Clinical features (severe or milder illness), including fever and respiratory symptoms, and epidemiologic risk factors, including travel, healthcare setting, and contact history.	
Incubation period for MERS-CoV infection	2–14 d after exposure.	

*CDC, Centers for Disease Control and Prevention; MERS, Middle East respiratory syndrome; MERS-CoV, MERS coronavirus.
†A subjective sense of fever.
‡From (*3*).

US contacts were provided for the Riyadh–London flight of case-patient 1 and none for case-patient 2. CDC identified a total of 655 contacts for both persons. For case-patient 1, these were 89 passengers (Figure 1) and 12 crew members. The bus company reported 10 potential contacts but was able to identify only the driver and 5 passengers who had paid by credit card. For case-patient 2, a total of 521 passengers and 23 crew members were identified for the flights investigated by CDC (Figure 2).

For case-patient 1, passenger-locating information was provided to 17 health departments (1–12/state) the day MERS was confirmed, 8 days after exposure; interviews were sought during and after the incubation period. CDC notified 1 country for 22 passengers. For case-patient 2, contact information provided to 35 health departments (1–80/state), 11–12 days after the flight; 1 interview was sought. CDC notified 15 countries for 77 passengers.

Of the total 655 contacts, 631 (96%) were notified, of whom 512 (81%) were interviewed an average of 2.8 days after MERS confirmation. Of these, 435 (85%) reported no symptoms, 42 (8%) MERS-compatible symptoms, and 35 (7%) unrelated symptoms (Table 2, https://wwwnc.cdc.gov/EID/article/23/9/17-0365-T2.htm).

Of 42 contacts with MERS-compatible symptoms, 7 reported acute respiratory illness with fever/feverishness, 32 acute respiratory illness without fever, 4 myalgia, 4 gastrointestinal symptoms, and 2 malaise. For 12 (29%), rRT-PCR was performed; MERS-CoV RNA was not detected.

One contact who tested negative had been in the Middle East during the 14 days before the flight but reported no exposures of concern.

Blood was drawn for serum testing a mean of 33 days after exposure (median 21 days, range 9–90 days) from 218 (62%) aircraft passengers; 11 had unknown collection dates. Twelve (5%) specimens were collected within 14 days, 11 on day 12 or 13; the remainder were collected 14–90 days after the flight. Serologic test results were available for 11 (25%) passengers from both flights who sat within 2 rows of the case-patient and for 13 passengers who reported MERS-compatible symptoms. All serum tested negative for antibodies to MERS-CoV.

All flight crew were interviewed and reported no or unrelated symptoms. The bus driver and 4 of 5 passengers were interviewed and remained asymptomatic. No flight crew or bus contacts provided serum.

Conclusions

Close collaboration between state and local health departments, CDC, airline and bus industries, and federal partners was critical to rapidly complete these resource-intensive investigations. The 3 protocol objectives were met: achieving a high rate of timely notifications, identifying and evaluating symptomatic contacts, and using serology to detect transmission. The investigation detected no transmission on any of the conveyances. Concurrent household and healthcare facility contact investigations for these cases also did not identify MERS-CoV transmission (*5*).
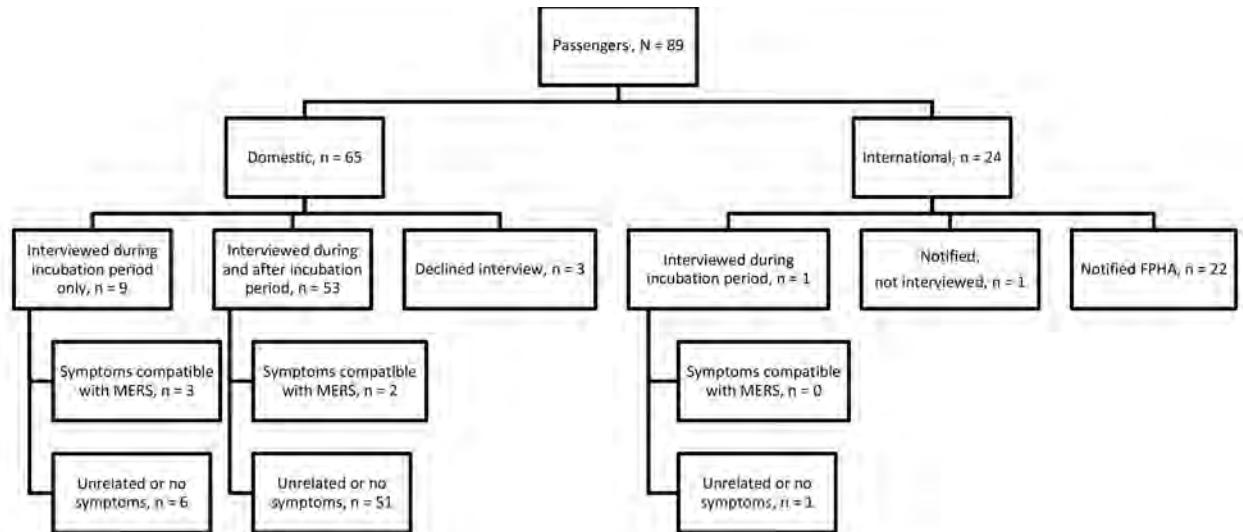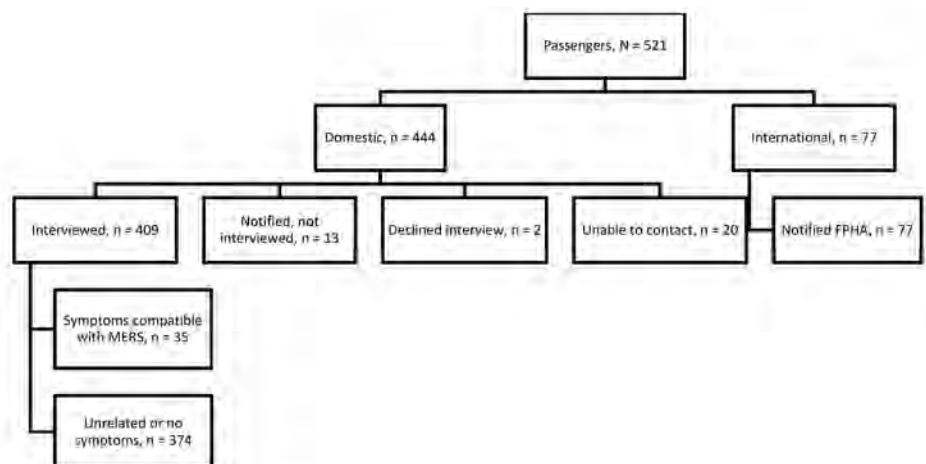
Figure 1. Flowchart of aircraft passengers exposed to index case-patient 1 in investigation of 2 imported US cases of Middle East respiratory syndrome, by location at time of notification, May 2014. Of all passengers, 78 (88%) were on the London–Chicago flight, 9 (10%) on the Riyadh–London flight, and 2 (2%) on the Riyadh–London and London–Chicago flights. Domestic passengers were assigned to state health departments for follow-up if contact information indicated they lived in that state; CDC assumed responsibility for interviewing passengers if they lacked contact information that would enable state health department assignment. One US citizen was interviewed by CDC while traveling abroad; 1 US citizen with dual citizenship on the Riyadh–London flight was notified by CDC but already had been interviewed by authorities in the country of residence. FPHA notifications were made for foreign passport holders and US citizens living or traveling abroad. The incubation period for MERS is 2–14 days after exposure. Symptoms compatible with MERS were fever ($\geq$38°C [$\geq$100.4°F]), feverishness, symptoms of acute respiratory illness (i.e., cough, shortness of breath, rhinorrhea, sore throat), myalgia, malaise or gastrointestinal symptoms 2–14 days after travel on the same conveyance as the index case-patient. CDC, Centers for Disease Control and Prevention; FPHA, foreign public health authority; MERS, Middle East respiratory syndrome; MERS-CoV, MERS coronavirus.

At least 8 other aircraft and 2 bus investigations have been reported, totaling >400 evaluated contacts (6–13). Index case-patient symptoms have varied; flight times ranged from 1.5 to 10 hours. Contact definitions ranged from 2 adjacent seats in all directions to the entire plane; most common was within 2 rows of the index case-patient. Several investigations included laboratory testing of symptomatic or asymptomatic contacts. No transmission on aircraft or buses has been documented.

Figure 2. Flowchart of aircraft passengers exposed to index case-patient 2 in investigation of 2 imported US cases of Middle East respiratory syndrome, by location at time of notification, May 2014. Of all passengers 188 (36%) were on the London–Boston flight, 158 (30%) on the Boston–Atlanta flight, and 175 (34%) on the Atlanta–Orlando flight. Domestic passengers were assigned to state health departments for follow-up if contact information indicated they lived in that state. CDC assumed responsibility for interviewing passengers if they lacked contact information that would enable state health department

assignment. A total of 337 contacts were interviewed late in the incubation period (days 11–14 after exposure) and were not contacted for a follow-up interview after the incubation period; remaining contacts were interviewed after the incubation period. FPHA were notified for foreign passport holders and US citizens living or traveling abroad. The incubation period for MERS is 2–14 days after exposure. Symptoms compatible with MERS were fever ($\geq$38°C [100.4°F]), feverishness, symptoms of acute respiratory illness (i.e., cough, shortness of breath, rhinorrhea, sore throat), myalgia, malaise, or gastrointestinal symptoms in persons who traveled on the same conveyance as the index case-patient. CDC, Centers for Disease Control and Prevention; FPHA, foreign public health authority; MERS, Middle East respiratory syndrome.

Table 2. Characteristics of passenger and crew contacts during 2 MERS conveyance contact investigations, May 2014*

Contact characteristic	Case-patient 1				Case-patient 2†					Total
	RUH–LHR,‡ LHR–ORD	Crew§	Bus¶	Total	LHR–BOS	BOS–ATL	ATL–MCO	Crew§	Total	
No. contacts	89	12	10	111	188	158	175	23	544	655
Level of contact, no. (%)										
Consented to interview#	63 (71)	12 (100)	5 (50)	80 (72)	134 (71)	136 (86)	139 (79)	23 (100)	432 (79)	512 (78)
Notified, not interviewed**	1†† (1)	NA	NA	1 (0.9)	2 (1)	9 (6)	2 (1)	NA	13 (2)	14 (2)
FPHA notified	22 (25)	NA	NA	22 (20)	46 (24)	3 (2)	28 (16)		77 (14)	99 (15)
Declined interview	3 (3)	NA	NA	4 (3.6)	2 (1)	NA	NA	NA	2 (0.4)	6 (0.9)
Unable to contact‡‡	NA	NA	NA	4 (3.6)	4 (2)	10 (6)	6 (3)	NA	20 (4)	24 (4)
Age**										
Mean, y	44.1	NA	55.5	44.8	47.8	41.1	35.9	NA	41	41.5
Median, y	47	NA	56.5	48	47	41	37	NA	42	43
Range (Q1–Q3), y	35–55	NA	40.5–70.5	32–56	36–55	31.5–50.5	21–49.5	NA	30–53	30–53
No. unknown	3	12	1	16	9	4	15	23	50	66
Sex, no. (%)**										
M	35 (56)	4 (33)	4 (80)	43 (54)	89 (66)	94 (69)	68 (49)	NA	251 (58)	294 (57)
F	28 (44)	5 (42)	1 (20)	34 (43)	43 (33)	41 (30)	71 (51)	1 (4)	156 (36)	190 (37)
Unknown	NA	3 (25)	NA	3 (4)	2 (1)	1 (0.7)	NA	22 (96)	25 (6)	28 (5)
Passengers who changed seats, no. (%)§§,¶¶	2 (3)	NA	NA	2 (3)	1 (0.7)	NA	NA	NA	1 (0.2)	3 (0.6)
Consent for serologic testing, no. (%)¶¶										
Yes	NA	NA	4 (80)	45 (56)	91 (68)	116 (85)	101 (73)	NA	308 (71)	353 (69)
No	NA	NA	NA	10 (13)	34 (25)	16 (12)	28 (20)	23 (100)	78 (18)	88 (17)
Unknown	12 (100)	12 (100)	1 (20)	25 (31)	9 (7)	4 (3)	10 (7)	NA	46 (11)	71 (14)

*FPHA, foreign public health authorities; LHR, London Heathrow Airport (London, UK); BOS, Boston Logan International Airport (Boston, MA, USA); ATL, Hartsfield-Jackson Atlanta International Airport (Atlanta, GA, USA); MCO, Orlando International Airport (Orlando, Florida, USA); NA, not applicable; ORD, Chicago O'Hare International Airport (Chicago, IL, USA); Q, quartile; RUH, King Khalid International Airport (Riyadh, Saudi Arabia).
†CDC was not contacted about any US citizens exposed to case-patient 2 on the Riyadh–London flight.
‡Includes 9 US citizens who were passengers on RUH–LHR flight only and 2 US citizens who were passengers on both RUH–LHR and LHR–ORD flights.
§Includes all cabin crew and pilots for all flights.
¶Includes bus driver.
#New denominator used for calculating all passenger demographic information.
**Defined as either a notification sent to FPHA for a contact who was not interviewed while in the United States, certified mail sent to a valid address, voicemail left for a working phone number, or email sent to a valid email address.
††One US citizen with dual citizenship on Riyadh–London flight was notified by CDC but had already been interviewed by authorities in country of residence.
‡‡Unable to locate or contact because of lack of or incorrect contact information.
§§Seat was reassigned if passenger sat in new seat for more than half of flight and could clearly articulate the new seat number or location.
¶¶Denominator includes only contacts who consented to interview.

Limitations of our investigation included incomplete follow-up, self-reported symptoms, and potential recall bias. Cases may have been missed because a small number of travelers were interviewed or had specimens collected only during the 14-day incubation period.

The results of this and other investigations suggest the risk for MERS-CoV transmission on conveyances is low. Recent publications concluded that aircraft contact tracing required extensive preparation, resources, and passenger compliance; was an inconvenience to passengers; had mixed outcomes (*14*); and caused psychological distress to contacts (*12*). Our investigation required substantial resources of airlines, a bus company, local and state health departments, federal agencies, and foreign public health

authorities. For future aircraft contact investigations for MERS, CDC will include only passengers seated within 2 rows of the index case-patient, although modifications may be made depending on circumstances. Comprehensive conveyance contact investigations with laboratory evaluation can guide future public health practice for emerging communicable diseases.

Acknowledgments

Maryland, Massachusetts, Michigan, Minnesota, Missouri, New Hampshire, New York, North Carolina, Ohio, Oklahoma, Oregon, Pennsylvania, Rhode Island, South Carolina, Tennessee, Texas, Utah, Vermont, Virginia, US Virgin Islands, Washington, and Wisconsin. We also thank our colleagues in CDC's Division of Viral Diseases, National Center for Immunization and Respiratory Diseases, and Division of State and Local Readiness and Division of Emergency Operations, Office of Public Health Preparedness and Response. We especially thank the many staff members who augmented our team at the Emergency Operations Center during this response and all of our CDC colleagues at CDC Quarantine Stations throughout the United States who worked tirelessly during this response.

Dr. Lippold is CDC's Occupational Health Clinic Medical Director. Her primary research interests include program evaluation, health equity, and healthcare quality.

References

1. Bialek SR, Allen D, Alvarado-Ramy F, Arthur R, Balajee A, Bell D, et al. First confirmed cases of Middle East respiratory syndrome coronavirus (MERS-CoV) infection in the United States, updated information on the epidemiology of MERS-CoV infection, and guidance for the public, clinicians, and public health authorities—May 2014. MMWR Morb Mortal Wkly Rep. 2014/63;63:431–6.
2. Regan JJ, Jungerman MR, Lippold SA, Washburn F, Roland E, Objio T, et al. Tracing airline travelers for a public health investigation: Middle East respiratory syndrome coronavirus (MERS-CoV) infection in the United States, 2014. Public Health Rep. 2016;131:552–9. http://dx.doi.org/10.1177/0033354916662213
3. Centers for Disease Control and Prevention. Middle East respiratory syndrome (MERS). Interim patient under investigation (PUI) guidance and case definitions [cited 2017 May 9]. https://www.cdc.gov/coronavirus/mers/case-def.html
4. Centers for Disease Control and Prevention. CDC laboratory testing for Middle East respiratory syndrome coronavirus (MERS-CoV) [cited 2017 May 8]. http://www.cdc.gov/coronavirus/mers/lab/lab-testing.html
5. Breakwell L, Pringle K, Chea N, Allen D, Allen S, Richards S, et al. Lack of transmission among close contacts of patient with case of Middle East respiratory syndrome imported into the United States, 2014. Emerg Infect Dis. 2015;21:1128–34. http://dx.doi.org/10.3201/eid2107.150054
6. Tsiodras S, Baka A, Mentis A, Iliopoulos D, Dedoukou X, Papamavrou G, et al. A case of imported Middle East respiratory syndrome coronavirus infection and public health response, Greece, April 2014. Euro Surveill. 2014;19:20782. http://dx.doi.org/10.2807/1560-7917.ES2014.19.16.20782
7. Puzelli S, Azzi A, Santini MG, Di Martino A, Facchini M, Castrucci MR, et al. Investigation of an imported case of Middle East respiratory syndrome coronavirus (MERS-CoV) infection in Florence, Italy, May to June 2013. Euro Surveill. 2013;18:20564. http://dx.doi.org/10.2807/1560-7917.ES2013.18.34.20564
8. Premila Devi J, Noraini W, Norhayati R, Chee Kheong C, Badrul AS, Zainah S, et al. Laboratory-confirmed case of Middle East respiratory syndrome coronavirus (MERS-CoV) infection in Malaysia: preparedness and response, April 2014. Euro Surveill. 2014;19:20797. http://dx.doi.org/10.2807/1560-7917.ES2014.19.18.20797
9. Wu J, Yi L, Zou L, Zhong H, Liang L, Song T, et al. Imported case of MERS-CoV infection identified in China, May 2015: detection and lesson learned. Euro Surveill. 2015;20:21158. http://dx.doi.org/10.2807/1560-7917.ES2015.20.24.21158
10. Racelis S, de los Reyes VC, Sucaldito MN, Deveraturda I, Roca JB, Tayag E. Contact tracing the first Middle East respiratory syndrome case in the Philippines, February 2015. Western Pac Surveill Response J. 2015;6:3–7. http://dx.doi.org/10.5365/wpsar.2015.6.2.012
11. Mollers M, Jonges M, Pas SD, van der Eijk AA, Dirksen K, Jansen C, et al.; MERS-CoV Outbreak Investigation Team of the Netherlands. Follow-up of contacts of Middle East respiratory syndrome coronavirus–infected returning travelers, the Netherlands, 2014. Emerg Infect Dis. 2015;21:1667–9. http://dx.doi.org/10.3201/eid2109.150560
12. Parry-Ford F, Boddington N, Pebody R, Phin N; Incident Management Team. Public health response to two incidents of confirmed MERS-CoV cases travelling on flights through London Heathrow Airport in 2014—lessons learnt. Euro Surveill. 2015;20:21114. http://dx.doi.org/10.2807/1560-7917.ES2015.20.18.21114
13. Kang M, Song T, Zhong J, Wang J, Li J, Wu J, et al. Contact tracing for imported case of Middle East respiratory syndrome, China, 2015. Emerg Infect Dis. 2016;22:1644–6. PMID: 27532887
14. Huizer YL, Swaan CM, Leitmeyer KC, Timen A. Usefulness and applicability of infectious disease control measures in air travel: a review. Travel Med Infect Dis. 2015;13:19–30. http://dx.doi.org/10.1016/j.tmaid.2014.11.008

Address for correspondence: Susan A. Lippold, Centers for Disease Control and Prevention, 1600 Clifton Rd NE, Mailstop A29, Atlanta, GA 30329-4027, USA; email: stl5@cdc.gov

Possible Role of Fish as Transport Hosts for *Dracunculus* spp. Larvae

**Christopher A. Cleveland, Mark L. Eberhard,
Alec T. Thompson, Stephen J. Smith,
Hubert Zirimwabagabo,
Robert Bringolf, Michael J. Yabsley**

To inform *Dracunculus medinensis* (Guinea worm) eradication efforts, we evaluated the role of fish as transport hosts for *Dracunculus* worms. Ferrets fed fish that had ingested infected copepods became infected, highlighting the importance of recommendations to cook fish, bury entrails, and prevent dogs from consuming raw fish and entrails.

The campaign to eradicate *Dracunculus medinensis* infection (Guinea worm disease) has helped 17 of 21 countries interrupt transmission (*1*). Endemic transmission of Guinea worm disease typically occurred via contamination of drinking water sources, resulting in community disease outbreaks. The absence of outbreaks of Guinea worm disease in Chad, coupled with increasing infections among domestic dogs in the transmission cycle (*2–6*), led to the hypothesis that transmission was occurring by different means.

Previous work on *Dracunculus* and related spirurids indicates that paratenic hosts might be used to facilitate transmission (*7,8*). Recently, an experimental study showed *D. medinensis* worms could use tadpoles as paratenic hosts, and a naturally infected frog was detected in Chad (*9,10*). Few data exist on the potential role of fish as paratenic hosts; however, fish are suspected on the basis of epidemiologic data in Chad (*2*). Previous experimental attempts to infect Nile tilapia (*Oreochromis niloticus*) and fathead minnows (*Pimephales promelas*) with *D. medinensis* worms were not successful (*9*). However, in trials with *D. insignis* worms, 2 of 7 fish species exposed to high numbers of larvae became infected with low numbers of larvae (*11*). Collectively, these data suggest that fish are generally resistant to infection, need to ingest very high numbers of larvae to establish infection, or have variable species susceptibility.

Alternatively, it is possible that fish might ingest infected copepods and, if consumed by a host within short enough intervals, act as transport hosts. Our objective was to evaluate this potential role by allowing fish to ingest *Dracunculus* worm–infected copepods and then feed them to domestic ferrets to evaluate whether transmission could occur.

The Study

In April 2016, we used first-stage larvae (L1) from gravid *D. insignis* worms from raccoons (*Procyon lotor*) in Georgia (USA) to infect colony-reared cyclopoid copepods (*7*). At 21 days postinfection, *D. insignis* larvae were examined to determine if they had developed to the infective third stage (i.e., trifid tail). If ≥25% of copepods were infected, they were used for transmission trials. Gravid *D. medinensis* worms were recovered from naturally infected dogs in Chad, and L1s were used to infect cyclopoid copepods collected from N'Djamena.

We then exposed groups of 5 Nile tilapia, fathead minnows, or mosquitofish (*Gambusia affinis*) to groups of 50 copepods (Table). We exposed fish to copepods for 3 hours in the first day of the *D. insignis* trial; on subsequent days, we exposed fish for 2 hours. All copepods provided to fish were consumed during exposures. Individual fish were removed, euthanized by exposure to neutral buffered tricaine methane sulfonate (MS-222) followed by pithing, and dissected. We observed digested copepods and free larvae in the intestine.

We fed the euthanized fish to laboratory-raised ferrets. If fish were not immediately ingested, we mixed the fish carcasses with cat food. Ferrets were fed fish in small batches. For *D. insignis* worms, we conducted exposures using copepods infected with larvae originating from 2 female worms at 2 different times (i.e., 5 fish per day for 3 days in April 2016 and another 5 fish per day for 3 days in July 2016, resulting in exposure to ≈300 copepods) (Table). Because there was only 1 *D. medinensis* worm, fewer *D. medinensis* worm–infected copepods were available. We exposed only 1 species of fish (mosquitofish). A ferret was given 5 fish per day for 6 days for a total of ≈300 copepods. (Table).

We maintained exposed ferrets for 77–134 days, then anesthetized and humanely euthanized them using 30 mg/kg ketamine followed by sodium pentobarbital. We necropsied the ferrets and examined the recovered *Dracunculus* worms to determine sex and whether females were mated or gravid. All animal procedures were reviewed and

Author affiliations: University of Georgia, Athens, Georgia, USA (C.A. Cleveland, S.J. Smith, R. Bringolf, M.J. Yabsley); Centers for Disease Control and Prevention, Atlanta, Georgia (M.L. Eberhard); University of Oklahoma, Norman, Oklahoma, USA (A.T. Thompson); The Carter Center, Atlanta (H. Zirimwabagabo)

Table. Results of ferret exposure trials with 3 different fish species exposed to copepods infected with *Dracunculus medinensis* or *D. insignis* worms

Fish species	*Dracunculus* sp.	No. fish consumed/no. offered*	Total no. copepods†	Days until euthanasia of ferret‡	*Dracunculus* infection status of ferret	No. worms recovered and sex§
Mosquitofish (*Gambusia affinis*)	*D. insignis*	28/30	300	91 and 134	–	0
	D. medinensis	30/30	300	77	+	1M/11F
Tilapia (*Oreochromis niloticus*)	*D. insignis*	27/30	300	91 and 134	+	6F¶
Fathead minnow (*Pimephales promelas*)	*D. insignis*	30/30	300	91 and 118	+	1M

*In groups of 5 fish/day for 6 days.
†≥25% of copepods infected.
‡The *D. insignis* worm–exposed ferrets have 2 entries for days until euthanasia because these animals were exposed to fish at 2 different time points with copepods infected with larvae from 2 different worms.
§All worms were recovered from the subcutaneous tissues of the limbs.
¶Of these 6 female worms, 5 were gravid, indicating a male worm either was missed or had died before necropsy.

approved by the University of Georgia's Institutional Animal Care and Use Committee (no. A2014 11–010).

Of the 3 ferrets we fed fish that had ingested *D. insignis* worm–infected copepods, 2 were infected (Table). One ferret was infected with 6 *D. insignis* females (5 gravid), the other with 1 male worm (Table). The 1 ferret fed fish exposed to *D. medinensis* worm–infected copepods became infected with 12 worms; female worms were mated but not gravid because of their young age (Table).

Conclusions

The infection of ferrets with *Dracunculus* spp. worms after consuming fish that had eaten infected copepods demonstrates a novel transmission route. The unprecedented increase in the number of *D. medinensis* worm infections in dogs in Chad suggests the potential role of aquatic paratenic hosts (*2,12*). Classically, paratenic hosts become infected and facilitate transmission by bridging a trophic level, maintaining long-term infections, or concentrating larger worm burdens in their tissues (*3*). We suggest that fish can serve the role of transport hosts because fish did not have disseminated *Dracunculus* worm infection develop in our initial trials (C.A. Cleveland, unpub. data). Because most cases of Guinea worm disease occur in areas known for intense artisanal fishing and residents' dependence on fish protein, it is likely that fish and other aquatic animals play a role in transmission.

In 2014, preventive measures such as cooking fish thoroughly, burying fish entrails, and preventing dogs from consuming fish entrails were implemented in Chad. By May 2015, interventions were implemented in >50% of at-risk communities (*1*). Although limited, surveys for natural infections in fish from Chad's Chari River have not detected *D. medinensis* larvae (*2*; C.A. Cleveland, unpub. data). However, our findings suggest that the proposed intervention strategies involving fish are relevant and should continue. It is unclear what happens in Chad to small fish caught by fishermen; the fish might be consumed whole without cooking or, more likely, are discarded where dogs could consume them. During previous surveys of fish for *D. medinensis* worms, large numbers of copepods were observed in their gastrointestinal tracts, supporting their potential role as transport hosts (C.A. Cleveland, unpub. data). Despite the interventions implemented in Chad, sporadic dog and human infections are still reported, suggesting a need for continued educational campaigns.

The recent report of a natural amphibian paratenic host, combined with the results of our study, indicates that the transmission of *D. medinensis* worms is not as simple as once believed (*10*). Despite the highly successful eradication campaign, 4 countries (South Sudan, Mali, Ethiopia, and Chad) still report endemic *D. medinensis* worm transmission. All 4 countries now report infections in dogs, so novel intervention and eradication strategies are needed.

Although our study showed that fish can transmit *Dracunculus* larvae to ferrets, many questions remain. For example, it is likely that different fish species feed on copepods at different rates and have different gastrointestinal tract transit times. This might also explain why individual exposure of mosquitofish to *D. medinensis* or *D. insignis* worms led to infection in only the *D. medinensis*–exposed ferrets; the *D. insignis*–exposed fish were fed to ferrets an hour later than *D. medinensis*–exposed fish. It is possible that mosquitofish transit material through the gastrointestinal tract faster than the other species. Alternatively, the ferrets may not have become infected simply because, as previous work has shown, not all ferrets exposed to *Dracunculus* worms become infected (*12*). Additional data are especially needed for those fish species that might be caught and ingested by humans or dogs in Guinea worm–endemic countries. Furthermore, 2 fish species retained *D. insignis* larvae in their tissues for 7–11 days, demonstrating the need for further experimental and field work on the role of fish as paratenic hosts for *Dracunculus* spp. worms (*6*).

Acknowledgments

Mr. Cleveland is a PhD student in the Warnell School of Forestry and Natural Resources and the Southeastern Cooperative Wildlife Disease Study at the University of Georgia. He has broad interests in parasite life cycles and transmission dynamics, wildlife management, and the ecology of infectious diseases.

References

1. Hopkins DR, Ruiz-Tiben E, Eberhard ML, Roy SL. Progress toward global eradication of dracunculiasis, January 2014–June 2015. MMWR Morb Mortal Wkly Rep. 2015;64:1161–5. http://dx.doi.org/10.15585/mmwr.mm6441a1
2. Eberhard ML, Ruiz-Tiben E, Hopkins DR, Farrell C, Toe F, Weiss A, et al. The peculiar epidemiology of dracunculiasis in Chad. Am J Trop Med Hyg. 2014;90:61–70. http://dx.doi.org/10.4269/ajtmh.13-0554
3. Callaway E; The Lancet Infectious Diseases. Guinea worm disease nears eradication. Lancet Infect Dis. 2016;16:131. http://dx.doi.org/10.1016/S1473-3099(16)00020-7
4. Galán-Puchades MT. Dogs and Guinea worm eradication. Lancet Infect Dis. 2016;16:770. http://dx.doi.org/10.1016/S1473-3099(16)30080-9
5. Eberhard ML, Ruiz-Tiben E, Hopkins DR. Dogs and Guinea worm eradication. Lancet Infect Dis. 2016;16:1225–6. http://dx.doi.org/10.1016/S1473-3099(16)30380-2
6. Anderson RC. Nematode parasites of vertebrates: their development and transmission. New York: Cabi Publishing; 2000.
7. Eberhard ML, Brandt FH. The role of tadpoles and frogs as paratenic hosts in the life cycle of *Dracunculus insignis* (Nematoda: Dracunculoidea). J Parasitol. 1995;81:792–3. http://dx.doi.org/10.2307/3283979
8. Eberhard ML, Yabsley MJ, Zirimwabagabo H, Bishop H, Cleveland CA, Maerz JC, et al. Possible role of fish and frogs as paratenic hosts of *Dracunculus medinensis*, Chad. Emerg Infect Dis. 2016;22:1428–30. http://dx.doi.org/10.3201/eid2208.160043
9. Eberhard ML, Cleveland CA, Zirimwabagabo H, Yabsley MJ, Ouakou PT, Ruiz-Tiben E. Guinea worm (*Dracunculus medinensis*) infection in a wild-caught frog, Chad. Emerg Infect Dis. 2016;22:1961–2. http://dx.doi.org/10.3201/eid2211.161332
10. Crichton VFJ, Beverley-Burton M. Observations on the seasonal prevalence, pathology and transmission of *Dracunculus insignis* (Nematoda: Dracunculoidea) in the raccoon (*Procyon lotor* (L.) in Ontario. J Wildl Dis. 1977;13:273–80. http://dx.doi.org/10.7589/0090-3558-13.3.273
11. Eberhard ML, Ruiz-Tiben E, Wallace SV. *Dracunculus insignis*: experimental infection in the ferret, *Mustela putorius furo*. J Helminthol. 1988;62:265–70. http://dx.doi.org/10.1017/S0022149X00011640
12. Hopkins DR, Ruiz-Tiben E, Eberhard ML, Roy SL, Weiss AJ. Progress toward global eradication of Dracunculiasis—January 2015–June 2016. MMWR Morb Mortal Wkly Rep. 2016;65:1112–6. http://dx.doi.org/10.15585/mmwr.mm6540a5

Address for correspondence: Christopher A. Cleveland, University of Georgia, Warnell School of Forestry and Natural Resources, 180 E Green St, Athens, GA 30602, USA; email: ccleve@uga.edu

Similarities of Variant Creutzfeldt-Jakob Disease Strain in Mother and Son in Spain to UK Reference Case

Abigail B. Diack, Aileen Boyle, Diane Ritchie, Chris Plinston, Dorothy Kisielewski, Jesús de Pedro-Cuesta, Alberto Rábano, Robert G. Will,[1] Jean C. Manson[1]

We investigated transmission characteristics of variant Creutzfeldt-Jakob disease in a mother and son from Spain. Despite differences in patient age and disease manifestations, we found the same strain properties in these patients as in UK vCJD cases. A single strain of agent appears to be responsible for all vCJD cases to date.

In 2008 in Spain, 2 cases of variant Creutzfeldt-Jakob disease (vCJD) in first-degree relatives were identified. After the death of a 41-year-old man (patient 1) from vCJD, his 64-year-old mother (patient 2) began showing symptoms of anxiety and depression and, 2 months later, a gait disorder and progressive dementia. Although the clinical duration was relatively short and the early symptoms uncommon in comparison to vCJD cases in the United Kingdom, the overall clinical phenotype and posterior thalamic hyperintensities as seen in an MRI brain scan led to a diagnosis of suspected vCJD. Neuropathological examination confirmed the diagnosis of vCJD. Both patients were 129MM homozygous, had never received a blood transfusion or tissue graft, and had lived in the same town within the Castilla-León region of Spain (Table 1) (1). The region is a farming area at high risk for bovine spongiform encephalopathy (BSE); 3 of the 5 cases of vCJD reported in Spain came from this region (1). The patients had similar eating habits, which included ingestion of bovine brain. We conducted a study to determine whether these 2 vCJD cases were caused by the BSE agent, whether the agent strain was similar to previously characterized human vCJD cases, and whether the age of the patients would influence the strain characteristics.

The Study

We challenged cohorts of mice (RIII, C57BL/6J, and VM) with frozen central nervous system tissue from the

Author affiliations: The Roslin Institute, Easter Bush, Scotland, UK (A.B. Diack, A. Boyle, C. Plinston, D. Kisielewski, J.C. Manson); University of Edinburgh, Edinburgh, Scotland, UK (D. Ritchie, R.G. Will); Carlos III Institute of Health, Madrid, Spain (J. de Pedro-Cuesta, A. Rábano)

2 patients from Spain and 1 patient originating from the United Kingdom (Table 1) (2). The Lothian NHS Board Research Ethics Committee provided ethical consent for the use of the UK material for research; the vCJD tissue samples from Spain were provided by NEIKER-Tecnalia (Derio, Spain). We conducted inoculation, clinical scoring, and neuropathological and biochemical analysis of the mice as previously described (3–5). Animal studies were conducted according to the regulations of the UK Home Office Animals (Scientific Procedures) Act 1986.

All 3 vCJD brain isolates transmitted successfully, with the appearance of clinical and pathological signs associated with spongiform encephalopathy transmission (Table 2). Inocula from patients 1 and 2 showed the same temporal order of clinical endpoint in each mouse line when compared with inocula from the UK case (Figure 1). We observed a wide range of incubation periods for each mouse line both within and between inocula (Table 2), which is not unusual in primary transmissions.

We generated vacuolation profiles for each mouse line/inocula combination. In RIII and C57BL/6J mice, we observed moderate to mild vacuolation in the medulla and hypothalamus; C57BL/6J mice also exhibited mild vacuolation in the cerebellar peduncle (Figure 2, panels A, B). VM mice showed mild to moderate vacuolation in the medulla, thalamus, and septum, but typically not in the hypothalamus (Figure 2, panel C). Although the distribution of vacuolation was similar between isolates in the different mouse lines, the intensity of vacuolation distribution varied. This difference was most evident in the VM mice, in which the transmission from patient 2 appeared to have a lower intensity of vacuolation than that of patient 1 and the UK patient.

We observed a widespread accumulation of abnormal prion protein (PrP) throughout the brains of inoculated mice, with greatest accumulations apparent in the medulla, hypothalamus, and thalamic areas. We observed variability in the intensity of PrP accumulation between mice both within and between groups. Fine punctate/punctate deposits were the most common form of PrP accumulation in the mice; however, subtle differences were apparent in the hippocampus. In RIII and C57BL/6J, we observed a characteristic PrP deposition in the CA2 region of the hippocampus, whereas VM exhibited PrP deposition in

---

[1]These senior authors contributed equally to this article.

Table 1. Demographic and clinical features of 2 case-patients from Spain with variant CJD and reference cases from the United Kingdom*

Characteristic	Patient 1	Patient 2	UK cases, n = 150
Patient sex	M	F	
Case-patient age at illness onset, y	41	64	29 (mean)
Case-patient age at death, y	41	64	30 (mean)
Disease duration, mo	9	7	14 (mean)
Early visual symptoms	+	–	6%
Early unsteadiness	–	+	11%
No typical appearance of sporadic CJD on EEG	+	+	100%
Bilateral symmetric pulvinar high signal on MRI scan of brain	Yes	Yes	93%
Positive tonsil biopsy result	ND	ND	19%
History of travel to or residence in United Kingdom	No	No	100%
Codon 129MM	Yes	Yes	100%†
Type 2B PrP	Yes	Yes	100%†

*CJD, Creutzfeldt-Jakob disease; EEG, electroencephalogram; MRI, magnetic resonance imaging; PrP, prion protein; ND, not done; –, negative; +, positive.
†Of those tested.

the molecular dentate gyrus with occasional small plaques present in the corpus callosum (online Technical Appendix Figure 1, https://wwwnc.cdc.gov/EID/article/23/9/17-0159-Techapp1.pdf).

Biochemical analysis of inocula confirmed the presence of protease-resistant prion protein (PrP^{res}) in each of the 3 isolates. We identified a similar PrP^{res} type in isolates from the Spain patients that resembled that of the UK patient and the vCJD diagnostic standard, with a banding pattern dominated by the diglycosylated fragment of the protein and an unglycosylated fragment of ≈19 kDa (online Technical Appendix Figure 2). PrP^{res} was readily detected in the brain of RIII and VM mice challenged with all 3 isolates. We identified a similar glycosylation pattern in both mouse lines; a dominant diglycosylated fragment of ≈30 kDa and an unglycosylated fragment of ≈20k Da. We found no apparent differences between the different mouse line/inocula combinations (online Technical Appendix Figure 3).

Conclusions

This transmission study of central nervous system tissue from 2 first-degree relatives with vCJD confirms that the same infectious transmissible spongiform encephalopathy (TSE) agent was responsible for both cases. Comparisons of incubation period, TSE neuropathology, and PrP^{res} biochemistry indicate that this strain is consistent with that of a UK case of vCJD and with historical vCJD transmission data (6). The epidemiologic investigation of the 2 related patients indicated that they had shared a common residence and dietary habits, including cattle brain consumption, for >30 years. This finding suggests a common source of infection linked to the consumption of high-risk material in a known BSE area, and these transmission studies support the hypothesis that consumption of BSE-contaminated food products is a major risk factor for vCJD (7).

A feature of the UK vCJD epidemic was the relatively young age of the patients at onset. During 1995–2014, only 6 of 177 cases of vCJD identified in the United Kingdom were in persons ≥55 years of age at the onset of symptoms. Clinical phenotypes in these 6 patients were less consistent than those observed in younger patients (8). The evidence suggests that age is not a barrier to either infection or developing the disease; diagnosis of vCJD may become more important as exposed populations become older. Our study demonstrates that older persons harbor the vCJD agent in the central nervous system in a similar manner to younger

Table 2. Results of inoculation of brain tissue homogenates from 2 patients from Spain with vCJD and a reference patient from the United Kingdom into a panel of wild-type mice*

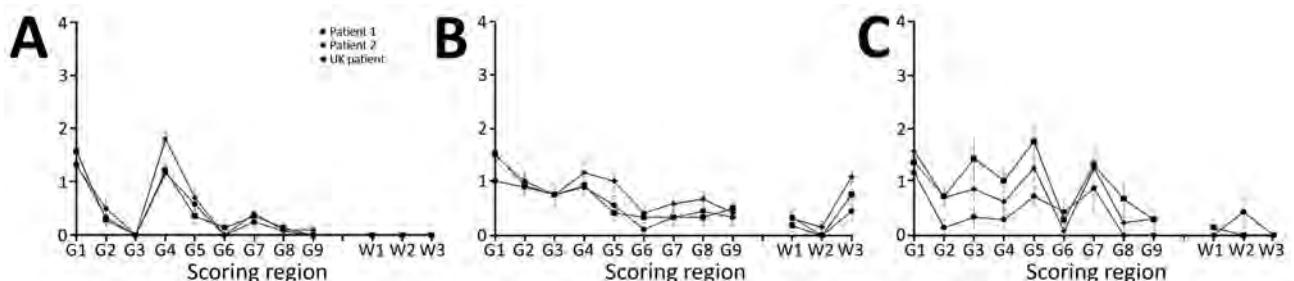|	No. mice positive/no. total		
Brain inoculum source and mouse line	Clinical signs of prion disease	Vacuolar pathology	Incubation period, d, ± SEM (range)
UK reference case			
RIII	10/15	10/15	395.3 ± 17.9 (295–489)
C57BL/6	13/17	15/17	523.7 ± 19.7 (372–637)
VM	13/16	14/16	472.2 ± 16.1 387–552
Patient 1			
RIII	14/17	15/17	417 ± 14.2 (336–516)
C57BL/6	12/18	12/18	588.4 ± 25.1 (405–706)
VM	7/18	11/18	**472.2 ± 16.1 (387–552)**
Patient 2			
RIII	12/16	13/16	427.5 ± 18.4 (323–547)
C57BL/6	9/18	11/18	**604.9 ± 12.4 (567–692)**
VM	4/16	7/16	524 ± 16.8 (501–573)

***Bold** indicates significant difference (p<0.05) when compared to the mouse line challenged with UK vCJD. vCJD, variant Creutzfeldt-Jakob disease.
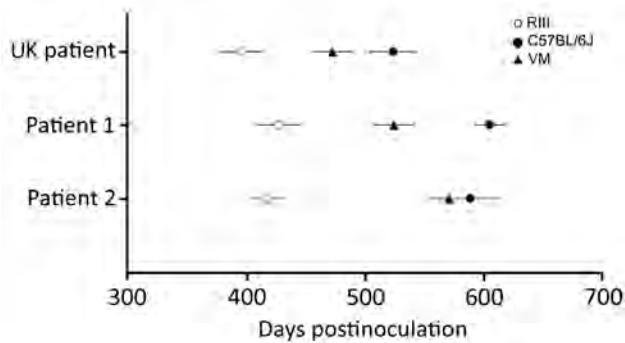
Figure 1. Comparison of vCJD incubation periods in wild-type mice from inoculation of brain tissue homogenates from 2 patients from Spain (son, patient 1; mother, patient 2) with vCJD and a reference patient from the United Kingdom. Results show similar incubation period ranking. Incubation periods were calculated in mice showing clinical and pathologic signs of transmissible spongiform encephalopathy disease. There was a single positive case in VM mice from patient 2. Data show mean incubation period ± SEM. vCJD, variant Creutzfeldt-Jakob disease.

persons. Small differences in incubation periods and the intensity of TSE vacuolation are apparent, which may be indicative of variation in the titer of the isolates. It is unknown when the 2 patients from Spain were infected, but if they were exposed at the same time, the 23-year difference in age at time of exposure may have influenced pathogenesis and the ability of the agent to replicate. A delay in neuroinvasion or slower rates of replication in the brain could explain why clinical symptoms are more variable in older patients.

Although our study demonstrates that clinical presentation and infective titer may differ between patients, the overall strain characteristics remain similar. Thus, the vCJD strain can be identified using our strain typing panel regardless of these variable factors.

This study highlights the need for awareness of vCJD in older age groups, particularly in patients with clinical manifestations of atypical dementias. These findings add additional supporting evidence to the hypothesis that a single strain of TSE agent is responsible for vCJD cases, regardless of geographic origin or age at infection, and indirectly support the hypothesis of a dietary origin for primary cases of vCJD.

Dr. Diack is a Career Track Fellow at the Roslin Institute, University of Edinburgh. Her research interests focus on prion diseases, in particular strain characterization and modeling of human diseases.

References

1. Riverol M, Palma J-A, Alañá M, Guerrero-Márquez C, Luquin MR, Rábano A. Variant Creutzfeldt–Jakob disease occurring in mother and son. J Neurol Neurosurg Psychiatry. 2012;83:235–6. http://dx.doi.org/10.1136/jnnp.2010.232074
2. Heath CA. Clinical aspect of variant CJD in the UK 1995–2005. University of Aberdeen; 2008.
3. Diack AB, Ritchie D, Bishop M, Pinion V, Brandel JP, Haik S, et al. Constant transmission properties of variant Creutzfeldt-Jakob disease in 5 countries. Emerg Infect Dis. 2012;18:1574–9. http://dx.doi.org/10.3201/eid1810.120792

Figure 2. Vacuolation profile of vCJD in wild-type mice from inoculation of brain tissue homogenates from 2 patients from Spain (son, patient 1; mother, patient 2) with vCJD and a reference patient from the United Kingdom. A) RIII mice; B) C57BL/6J mice; C) VM mice. Profiles show similarities in vacuolar pathology intensity and distribution in wild-type mouse brains. Data show mean ± SEM of clinical and pathologic positive mice, with the exception of VM mice arising from the Spain patients, which also include pathologic positive only mice (n≥6 per group). G1–G9, gray matter scoring regions: G1, medulla; G2, cerebellum; G3, superior colliculus; G4, hypothalamus; G5, thalamus; G6, hippocampus; G7, septum; G8, retrosplenial and adjacent motor cortex; G9, cingulate and adjacent motor cortex. W1–W3, white matter scoring regions: W1, cerebellar white matter; W2, mesencephalic tegmentum; W3, pyramidal tract. vCJD, variant Creutzfeldt-Jakob disease.

4. Dickinson AG, Meikle VMH, Fraser H. Identification of a gene which controls the incubation period of some strains of scrapie agent in mice. J Comp Pathol. 1968;78:293–9. http://dx.doi.org/10.1016/0021-9975(68)90005-4

5. Fraser H, Dickinson AG. The sequential development of the brain lesion of scrapie in three strains of mice. J Comp Pathol. 1968;78:301–11. http://dx.doi.org/10.1016/0021-9975(68)90006-6

6. Ritchie DL, Boyle A, McConnell I, Head MW, Ironside JW, Bruce ME. Transmissions of variant Creutzfeldt-Jakob disease from brain and lymphoreticular tissue show uniform and conserved bovine spongiform encephalopathy-related phenotypic properties on primary and secondary passage in wild-type mice. J Gen Virol. 2009;90:3075–82. http://dx.doi.org/10.1099/vir.0.013227-0

7. Ward HJ, Everington D, Cousens SN, Smith-Bathgate B, Leitch M, Cooper S, et al. Risk factors for variant Creutzfeldt-Jakob disease: a case-control study. Ann Neurol. 2006;59:111–20. http://dx.doi.org/10.1002/ana.20708

8. el Tawil S, Mackay G, Davidson L, Summers D, Knight R, Will R. Variant Creutzfeldt-Jakob disease in older patients. J Neurol Neurosurg Psychiatry. 2015;86:1279–80. http://dx.doi.org/10.1136/jnnp-2014-309397

Address for correspondence: Abigail B. Diack, The Roslin Institute, Easter Bush, Scotland, UK; email: abigail.diack@roslin.ed.ac.uk

December 2010: **Zoonoses**

- Surveillance of Wild Birds for Avian Influenza Virus

- Cyprinid Herpesvirus 3

- Reassortant Group A Rotavirus from Straw-colored Fruit Bat

- Hantavirus Pulmonary Syndrome in Argentina, 1995–2008

- Bluetongue Virus Serotype 8

- Epizootic Wave, France, 2007–2008

- Eastern Equine Encephalitis Virus in Mosquitoes and Their Role as Bridge Vectors

- *Bartonella* spp. in Bats, Kenya

- Alkhurma Hemorrhagic Fever in Humans, Najran, Saudi Arabia

- Environmental Sampling for Avian Influenza Virus A (H5N1) in Live-Bird Markets, Indonesia

- Surveillance and Analysis of Avian Influenza Viruses, Australia

- Freshwater Aquaculture Nurseries and Infection of Fish with Zoonotic Trematodes, Vietnam

- Pandemic (H1N1) 2009 Infection in Patients with Hematologic Malignancy

- Yellow Fever Virus in *Haemagogus leucocelaenus* and *Aedes serratus* Mosquitoes, Southern Brazil, 2008

- Reemergence of Rabies in Chhukha District, Bhutan, 2008

- Mortality Risk Factors for Pandemic Influenza on New Zealand Troop Ship, 1918

- Oseltamivir-Resistant Pandemic (H1N1) 2009 Virus, South Korea

- Emergence of African Swine Fever Virus, Northwestern Iran

- *Mycobacterium tuberculosis* Infection of Domesticated Asian Elephants, Thailand

- Hantaviruses and Hantavirus Pulmonary Syndrome, Maranhão, Brazil

- Wild Chimpanzees Infected with 5 *Plasmodium* Species

- Online Flutracking Survey of Influenza-like Illness during Pandemic (H1N1) 2009, Australia

- *Bartonella henselae* in Skin Biopsy Specimens of Patients with Cat-Scratch Disease

- *Brucella ceti* Infection in Harbor Porpoise

- Bundibugyo Ebola Virus Infection, Uganda

- *Leishmania tropica* Infection in Golden Jackals and Red Foxes, Israel

- Co-detection of Pandemic (H1N1) 2009 Virus and Other Respiratory Pathogens

- Alkhurma Hemorrhagic Fever in Travelers Returning from Egypt
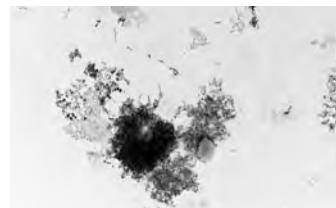
- Multispacer Typing of *Bartonella henselae* Isolates from Humans and Cats, Japan

- Ocular Thelaziosis in Dogs, France

EMERGING INFECTIOUS DISEASES

https://wwwnc.cdc.gov/eid/articles/issue/16/12/table-of-contents

Carbapenemase-Producing *Enterobacteriaceae* and Nonfermentative Bacteria, the Philippines, 2013–2016

John Mark Velasco, Maria Theresa Valderama, Trent Peacock,[1] Nirdnoy Warawadee, Kathyleen Nogrado, Fatima Claire Navarro, Domingo Chua, Jr., Srijan Apichai, Ruekit Sirigade, Louis R. Macareo, Brett Swierczewski

Author affiliations: US Army Medical Directorate–Armed Forces Research Institute of Medical Sciences, Bangkok, Thailand (J.M. Velasco, M.T. Valderama, T. Peacock, N. Warawadee, K. Nogrado, S. Apichai, R. Sirigade, L.R. Macareo, B. Swierczewski); V. Luna Medical Center, Quezon City, the Philippines (F.C. Navarro, D. Chua, Jr.)

During 2013–2016, we isolated bla_{NDM}- and bla_{VIM}-harboring *Enterobacteriaceae* and nonfermentative bacteria from patients in the Philippines. Of 130 carbapenem-resistant isolates tested, 45 were Carba NP–positive; 43 harbored bla_{NDM}, and 2 harbored bla_{VIM}. Multidrug-resistant microbial pathogen surveillance and antimicrobial drug stewardship are needed to prevent further spread of New Delhi metallo-β-lactamase variants.

Carbapenemase-producing *Enterobacteriaceae* can efficiently hydrolyze carbapenems and most β-lactam drugs. Since the identification of New Delhi metallo-β-lactamase-1 (NDM-1) in 2008 (*1*), there has been great concern regarding the spread of the Ambler class B metallo-β-lactamases (MBLs). Confirmed infections with MBL-positive bacteria are rarely identified in the Philippines, but bla_{IMP}-harboring *Enterobacteriaceae* were reported in 2014 (*2*), an *Escherichia coli* (sequence type [ST] 131) isolate harboring bla_{NDM-1} was reported in 2014 (*3*), and 2 *Klebsiella pneumoniae* (ST626 and ST903) isolates harboring bla_{NDM-1} and bla_{NDM-7} genes were reported in 2016 (*4*).

We performed isolate identification and antimicrobial drug susceptibility testing by using the MicroScan Walk-Away 40 plus System (Beckman Coulter, Brea, CA, USA) on 1,516 gram-positive and gram-negative isolates from patients admitted to various wards in the V. Luna Medical Center, a tertiary-care military hospital in Manila, the Philippines, during August 2013–April 2016. To better

assess the distribution of carbapenem resistance and the underlying molecular mechanisms of resistance, we selected gram-negative isolates with imipenem or meropenem (or both) MICs of ≥ 8 μg/mL. We used microbroth dilution susceptibility testing (*5*) to select and verify 130 gram-negative nonrepeat isolates (i.e., each isolate was tested once) and then tested the isolates for carbapenemase production by using the Carba NP test as previously described (*6*). We tested all isolates with a Carba NP–positive result for bla_{NDM} and bla_{KPC} by using a multiplex real-time PCR assay as previously described (*7*,*8*); isolates with PCR-negative results were further tested, using the Xpert Carba-R PCR test with the GeneXpert IV System (both from Cepheid, Sunnyvale, CA, USA), for the presence of bla_{NDM}, bla_{KPC}, bla_{VIM}, bla_{IMP-1}, and bla_{OXA-48}.

Of the 130 bacterial isolates tested, 45 (35%) had positive Carba NP test results and 43 (33%) harbored bla_{NDM}; 25 (58%) of the bla_{NDM}-carrying isolates were identified as *K. pneumoniae* (online Technical Appendix Table, https://wwwnc.cdc.gov/EID/article/23/9/16-1237-Techapp1.pdf). None of the isolates was positive for bla_{KPC}. Two *Pseudomonas aeruginosa* isolates that had positive Carba NP test results were negative for bla_{NDM} and bla_{KPC} but positive for bla_{VIM}. During the collection period, we also tested 8 environmental samples collected from the hospital's neonatal intensive care unit and obstetrics and gynecology wards; 3 (38%) of the 8 isolates were positive for bla_{NDM} and identified as *K. pneumoniae* (online Technical Appendix Table).

We report the identification of bla_{NDM}-positive bacterial isolates in several genera of *Enterobacteriaceae* and nonfermentative bacteria in the Philippines. This finding is particularly significant because NDM-like enzymes have a broad range of activity against most β-lactam antimicrobial drugs and are often associated with serious clinical infections (*9*). A higher risk for plasmid-mediated transfer of NDM-1 exists through conjugation between different gram-negative bacterial strains (*10*), and NDM-1 can spread rapidly via nosocomial transmission or community-acquired infection. Furthermore, although limited in number, the environmental samples in this study were also positive for bla_{NDM}, which suggests the possibility of nosocomial transmission and local circulation.

We conducted multiplex real-time PCR testing only for bla_{NDM}, bla_{KPC}, bla_{VIM}, bla_{IMP-1}, and bla_{OXA-48} and did not investigate clonality; thus, further investigation into other carbapenemase genes should be conducted. In addition, further experiments should be performed to characterize the plasmids carrying the carbapenemase genes. Strengthening of multidrug-resistant microbial pathogen surveillance and antimicrobial drug stewardship is urgently needed to better characterize drug-resistance patterns and improve early detection and containment strategies in developing countries.

Acknowledgments

References

1. Yong D, Toleman MA, Giske CG, Cho HS, Sundman K, Lee K, et al. Characterization of a new metallo-β-lactamase gene, bla_{NDM-1}, and a novel erythromycin esterase gene carried on a unique genetic structure in *Klebsiella pneumoniae* sequence type 14 from India. Antimicrob Agents Chemother. 2009;53:5046–54. http://dx.doi.org/10.1128/AAC.00774-09
2. Peirano G, Lascols C, Hackel M, Hoban DJ, Pitout JD. Molecular epidemiology of *Enterobacteriaceae* that produce VIMs and IMPs from the SMART surveillance program. Diagn Microbiol Infect Dis. 2014;78:277–81. http://dx.doi.org/10.1016/j.diagmicrobio.2013.11.024
3. Peirano G, Bradford PA, Kazmierczak KM, Badal RE, Hackel M, Hoban DJ, et al. Global incidence of carbapenemase-producing *Escherichia coli* ST131. Emerg Infect Dis. 2014;20:1928–31. http://dx.doi.org/10.3201/eid2011.141388
4. Chou A, Roa M, Evangelista MA, Sulit AK, Lagamayo E, Torres BC, et al. Emergence of *Klebsiella pneumoniae* ST273 carrying bla_{NDM-7} and ST656 carrying bla_{NDM-1} in Manila, Philippines. Microb Drug Resist. 2016;22:585–8. http://dx.doi.org/10.1089/mdr.2015.0205
5. Clinical and Laboratory Standards Institute. Performance standards for antimicrobial susceptibility testing: twenty-fifth informational supplement (M100–S25). Wayne (PA): The Institute, 2015.
6. Nordmann P, Poirel L, Dortet L. Rapid detection of carbapenemase-producing *Enterobacteriaceae*. Emerg Infect Dis. 2012;18:1503–7. http://dx.doi.org/10.3201/eid1809.120355
7. Milillo M, Kwak YI, Snesrud E, Waterman PE, Lesho E, McGann P. Rapid and simultaneous detection of bla_{KPC} and bla_{NDM} by use of multiplex real-time PCR. J Clin Microbiol. 2013;51:1247–9. http://dx.doi.org/10.1128/JCM.03316-12
8. Milillo M, Kwak YI, Snesrud E, Waterman PE, Lesho E, McGann P. Correction for Milillo et al., Rapid and simultaneous detection of blaKPC and blaNDM by use of multiplex real-time PCR. J Clin Microbiol. 2015;53:1460. http://dx.doi.org/10.1128/JCM.00373-15
9. Schwaber MJ, Klarfeld-Lidji S, Navon-Venezia S, Schwartz D, Leavitt A, Carmeli Y. Predictors of carbapenem-resistant *Klebsiella pneumoniae* acquisition among hospitalized adults and effect of acquisition on mortality. Antimicrob Agents Chemother. 2008;52:1028–33. http://dx.doi.org/10.1128/AAC.01020-07
10. Kulkova N, Babalova M, Sokolova J, Krcmery V. First report of New Delhi metallo-β-lactamase-1–producing strains in Slovakia. Microb Drug Resist. 2015;21:117–20. http://dx.doi.org/10.1089/mdr.2013.0162

Chronic Wasting Disease Prion Strain Emergence and Host Range Expansion

Allen Herbst,[1] Camilo Duque Velásquez,[1] Elizabeth Triscott, Judd M. Aiken, Debbie McKenzie

Author affiliation: University of Alberta, Edmonton, Alberta, Canada

Human and mouse prion proteins share a structural motif that regulates resistance to common chronic wasting disease (CWD) prion strains. Successful transmission of an emergent strain of CWD prion, H95⁺, into mice resulted in infection. Thus, emergent CWD prion strains may have higher zoonotic potential than common strains.

Chronic wasting disease (CWD) is a contagious prion disease of cervids that is spreading globally. CWD is enzootic in multiple cervid species, including deer and elk; the major foci of disease are Colorado/Wyoming (USA), Wisconsin/Illinois (USA), and Alberta/Saskatchewan (Canada). CWD is also present in captive cervids in South Korea and wild reindeer and moose in Norway (https://www.nwhc.usgs.gov/images/cwd/cwd_map.jpg). CWD results from the conformational transformation of the host-encoded cellular prion protein (PrP^C) into protease-resistant, detergent-insoluble, β-sheet rich, amyloidogenic conformers, termed prions (PrP^{CWD}). Within their conformation, prion strains encipher the information that directs the templated misfolding and aggregation of PrP^C molecules into additional prions (*1*).

Although the sequence homology of PrP among mammals is high, the ability of particular prion strains to cause disease in different species is determined by the conformational compatibility between a given strain and the host PrP^C (*2*). We

[1]These authors contributed equally to this article.

previously identified 2 strains of CWD prion in white-tailed deer (*3*), Wisc-1 and H95+; these strains exhibit distinct biological properties in deer and transgenic cervidized mice. To ascertain the host range of different strains from cervids, we inoculated CWD prions isolated from experimentally infected deer with different *PRNP* genotypes (Q95G96 [wild type (wt)], S96/wt, H95/wt, and H95/S96) and from elk (CWD2 strain) into hamsters and mice. All isolates have been successfully transmitted into transgenic mice expressing wt cervid PrP and contain high titers of CWD prions (*3*).

Mice inoculated with H95+ CWD prions succumbed to clinical disease at 575 ± 47 or 692 ± 9 days, depending on the H95+ isolate (Table). Mice inoculated with Wisc-1 or elk CWD or uninfected deer homogenates were euthanized at day 708 after infection with no signs of prion disease. Clinical signs of H95+ CWD in C57Bl/6 mice included ataxia, lethargy, tail rigidity, and dermatitis. Protease-resistant PrP^CWD was present in all mice infected with H95+ prions and was not detected in mice infected with Wisc-1 or CWD2 (online Technical Appendix, https://wwwnc.cdc. gov/EID/article/23/9/16-1474-Techapp1.pdf).

In contrast to mice, hamsters succumbed to clinical disease when inoculated with Wisc-1 CWD prions but were less susceptible to H95+ CWD prions (Table). Clinical signs of CWD in hamsters began with lethargy and, upon arousal, retrocollis; as the disease progressed, lethargy declined with increased dystonic movement including ataxia and tremors. Hyperesthesia was not observed. Subclinical disease (no clinical signs but PrP-res positive by Western blot) was observed in a subset of hamsters (online Technical Appendix).

Successful interspecies prion transmission at the molecular level depends on the compatibility of the invading prion conformers and structural determinants imposed by host PrP^C. One structural motif is the loop region between β sheet 2 and α helix 2 of PRP^C at aa 170–174 (online Technical Appendix). Host species containing PrP^C molecules with a flexible β2-α2 loop (mice and humans) are hypothesized to be incompatible with prions derived from species containing a rigid loop (deer and elk) (*4*,*5*). Previous attempts to transmit CWD to mice have failed (*6*,*7*). Our data show that prions from a prototypic rigid-loop species (deer) can transmit to a flexible-loop species (mice). The transmission is strain dependent. H95+ overrides the conformational restriction imposed by the mouse PrP flexible loop that Wisc-1 and CWD2 cannot overcome, suggesting that the invading prion strain is a dominant contributor to the species/transmission barrier. How the N terminal amino acid polymorphism (Q95H) affects the conformation of PrP, altering the deer-to-mouse transmission barrier, is unknown. Further structural studies may clarify the effect of N terminal residues on β2-α2 loop rigidity.

Transmission of H95+ CWD prions to mice further confirms the value of specifying strain when defining species barriers. Experimental transmission of CWD prion into macaques and transgenic mice expressing human PrP suggests a considerable transmission barrier to CWD prions (although squirrel monkeys are susceptible), and human prion protein is converted inefficiently in vitro (*8*,*9*). Successful infection of a flexible-loop species (mice) with H95+ CWD raises concerns for the potential pathogenicity of H95+ prions to other flexible-loop species. Transmission studies with Wisc-1 and H95+ in transgenic humanized and bovinized mice are ongoing.

The increasing prevalence of CWD indicates selection for cervids with resistance alleles, such as S96 and H95. Genetic resistance to a given prion strain selects for the emergence of novel prion strains with altered properties such as H95+ and Nor98 (*3*,*10*). The iterative transmission of CWD prions to cervids with protective alleles of PrP^C and the consequent emergence of new CWD prion strains highlights the dynamics of the CWD panzootic and the value of characterizing the host range of emergent CWD prion strains.

Table. Results of CWD prion inoculation into rodents*

Recipient and CWD inocula	No.	PrP-res+		Incubation period, d
		Clinical	Subclinical	
Mice				
wt/wt	6	0	0	NA
S96/wt	6	0	0	NA
H95/wt	7	5	2	669, 671, 706, 706, 706
H95/S96	7	7	0	306, 593, 593, 593, 593, 673, 675
Elk	4	0	0	NA
Control	4	0	0	NA
Hamsters				
wt/wt	8	3	5	652, 653, 653
S96/wt	8	1	4	634
H95/wt	8	1	6	652
H95/S96	8	0	1	NA
Elk	8	2	2	673, 719
Control	8	0	0	NA

*Mice infected with CWD prions were observed for up to 708 d; hamsters infected with white-tailed deer and elk CWD prions were observed for 659 and 726 d, respectively. Control mice and hamsters were inoculated with brain homogenates from CWD-negative wt/wt deer. CWD, chronic wasting disease; NA, not applicable; PrP-res+, positive for proteinase-K–resistant prion protein; wt, wild type.

Acknowledgments

References

1. Bessen RA, Marsh RF. Identification of two biologically distinct strains of transmissible mink encephalopathy in hamsters. J Gen Virol. 1992;73:329–34. http://dx.doi.org/10.1099/0022-1317-73-2-329
2. Capobianco R, Casalone C, Suardi S, Mangieri M, Miccolo C, Limido L, et al. Conversion of the BASE prion strain into the BSE strain: the origin of BSE? PLoS Pathog. 2007;3:e31. http://dx.doi.org/10.1371/journal.ppat.0030031
3. Duque Velásquez C, Kim C, Herbst A, Daude N, Garza MC, Wille H, et al. Deer prion proteins modulate the emergence and adaptation of chronic wasting disease strains. J Virol. 2015; 89:12362–73. http://dx.doi.org/10.1128/JVI.02010-15
4. Gossert AD, Bonjour S, Lysek DA, Fiorito F, Wüthrich K. Prion protein NMR structures of elk and of mouse/elk hybrids. Proc Natl Acad Sci U S A. 2005;102:646–50. http://dx.doi.org/10.1073/pnas.0409008102
5. Sigurdson CJ, Nilsson KP, Hornemann S, Heikenwalder M, Manco G, Schwarz P, et al. De novo generation of a transmissible spongiform encephalopathy by mouse transgenesis. Proc Natl Acad Sci U S A. 2009;106:304–9. http://dx.doi.org/10.1073/pnas.0810680105
6. Raymond GJ, Raymond LD, Meade-White KD, Hughson AG, Favara C, Gardner D, et al. Transmission and adaptation of chronic wasting disease to hamsters and transgenic mice: evidence for strains. J Virol. 2007;81:4305–14. http://dx.doi.org/10.1128/JVI.02474-06
7. Kurt TD, Bett C, Fernández-Borges N, Joshi-Barr S, Hornemann S, Rülicke T, et al. Prion transmission prevented by modifying the β2-α2 loop structure of host PrP^C. J Neurosci. 2014;34:1022–7. http://dx.doi.org/10.1523/JNEUROSCI.4636-13.2014
8. Race B, Meade-White KD, Phillips K, Striebel J, Race R, Chesebro B. Chronic wasting disease agents in nonhuman primates. Emerg Infect Dis. 2014;20:833–7. http://dx.doi.org/10.3201/eid2005.130778
9. Barria MA, Telling GC, Gambetti P, Mastrianni JA, Soto C. Generation of a new form of human PrP(Sc) in vitro by interspecies transmission from cervid prions. J Biol Chem. 2011;286:7490–5. http://dx.doi.org/10.1074/jbc.M110.198465
10. Le Dur A, Béringue V, Andréoletti O, Reine F, Laï TL, Baron T, et al. A newly identified type of scrapie agent can naturally infect sheep with resistant PrP genotypes. Proc Natl Acad Sci U S A. 2005;102:16031–6. http://dx.doi.org/10.1073/pnas.0502296102

Address for correspondence: Debbie McKenzie, University of Alberta, 120 Brain and Aging Research Building, Edmonton, AB T6G 2R3, Canada; email: debbie.mckenzie@ualberta.ca

Rabies Virus Transmission in Solid Organ Transplantation, China, 2015–2016

Shuilian Chen,[1] Heng Zhang,[1] Meiling Luo, Jingfang Chen, Dong Yao, Faming Chen,[2] Ruchun Liu,[2] Tianmu Chen[2]

Author affiliation: Changsha Center for Disease Control and Prevention, Changsha, Hunan, China

We report rabies virus transmission among solid organ transplantation recipients in Changsha, China, in 2016. Two recipients were confirmed to have rabies and died. Our findings suggest that more attention should be paid to the possibility of rabies virus transmission through organ transplantation for clinical and public health reasons.

In 2016, Zhou et al. reported a case of rabies virus transmission in China that was probably a result of organ transplantation (1). We report on rabies transmission that occurred among solid organ transplant recipients in Changsha, China, during December 2015–January 2016.

In November 2015, the donor, a previously healthy boy, showed development of fever, insomnia, and agitation. On day 6 of infection, these symptoms progressed, and he was sent to a healthcare center. At this time, he experienced weariness, no desire to drink water, poor appetite, and panic. One day later, he began vomiting, and was admitted to a local hospital (hospital A), where he exhibited anemophobia, convulsions, limb rigidity, and hypersalivation. The patient was moved to hospital B (days 7–14) in Changsha. At admission, some examination findings indicated a possibility of viral encephalitis (online Technical Appendix, Table 1, https://wwwnc.cdc.gov/EID/article/23/9/16-1704-Techapp1.pdf). Subhypothermia hibernation therapy and assisted ventilation were administered within 72 hours of admission, and the patient's vital signs became stable. On day 10, hyponatremia was observed, and on day 11, the patient again became febrile and tachycardic, with hypertensive abdominal distention and alimentary tract hemorrhage. On day 13, viral encephalitis was diagnosed, and rabies was suspected. However, rabies virus antibody tests performed on serum samples by using ELISA yielded negative results.

On day 14, the patient was transferred to hospital C, where he became comatose and was declared brain dead. Permission was granted for organ donation, because no specific pathogen had been detected and China's organ

transplant policy allows for organ donations in cases of viral encephalitides without laboratory-confirmed pathogens. Rabies virus–specific binding antibodies were also not detected in the serum samples. The donor had possibly been exposed to rabies but had not been vaccinated against rabies (online Technical Appendix). The patient's kidneys and liver were removed for transplantation in hospital D in Changsha on the following day.

Kidney and liver transplantations were performed on December 10, 2015. Two female recipients in hospital D received the kidneys, and an 8-month-old girl in hospital E in Shanghai, China, received the liver. No other organs were collected or transplanted from this donor. The surgeries were all uneventful, and the recipients were discharged after transplantation. However, all 3 recipients were eventually readmitted to the hospital with complex symptoms (Figure).

On the 40th day after transplantation, the left kidney recipient (29 years of age) revisited hospital D, reporting worsening right lower quadrant abdominal pain and vomiting. In the next 3 days, she successively had anemophobia, shortness of breath, chest tightness, anxiety, insomnia, and hypersalivation. During hospitalization, her blood pressure was as high as 248/148 mm Hg. On her 7th day in the hospital, she became comatose and then died.

On the 43rd day after transplantation, the right kidney recipient (age 47 years) developed aches in her lower limbs, insomnia, and a decreased appetite. She was readmitted to hospital D the next day. On the 3rd day after admission, she exhibited hydrophobia, anemophobia, photesthesia, and fatigue. She showed agitation, dyspnea, and hypersalivation on the 4th day; she became comatose and died 1 day later.

The liver recipient was readmitted with pneumonia on the 34th day after transplantation and died of asphyxia and
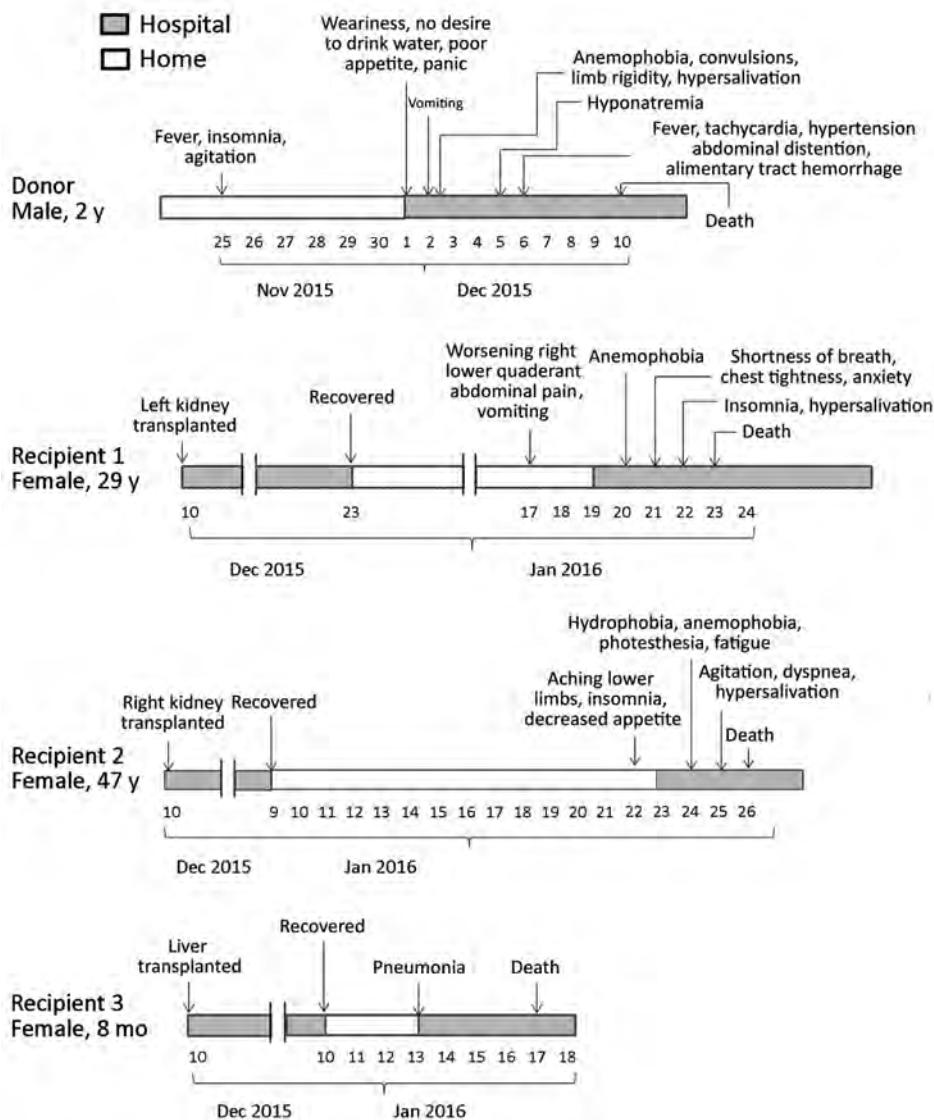
Figure. Clinical course of a donor and 3 recipients in a rabies outbreak associated with solid organ transplantation, Changsha, China, 2015–2016.

multiple organ failure within 5 days. This patient did not show any signs or symptoms of rabies or encephalitis.

None of the recipients had been exposed to potentially rabid animals or had been vaccinated previously for rabies (online Technical Appendix). Both kidney recipients tested positive for rabies virus (online Technical Appendix Table 2). The genome sequences of the rabies virus isolates from the right kidney recipient (isolate no. CCS1501H) were ≈11 kb nucleotides in length and belonged to the China I lineage. No testing for rabies was done on the donor or on the liver recipient.

In the past 10 years, rabies transmission by solid organ transplantation has been described occasionally worldwide (2–4). Hence, rabies transmission through organ transplantation is a clinical and public health concern. To prevent future cases such as this, we recommend that patients with unexplained encephalitis or mental status changes should not be used as organ donors even if tests for some infectious causes of encephalitis are negative. In addition, if rabies is suspected in the donor after organs have been transplanted, the recipients should also not be used as organ donors. An antibody test is not the ideal choice for the diagnosis of rabies virus and by itself cannot reliably exclude rabies from the differential diagnosis. For this reason, a combination of multiple techniques, preferably direct fluorescent antibody test and reverse transcription PCR, should be used before organ transplantation, especially when the donor is suspected of having rabies or a potential exposure to rabies. In addition, if a patient has meningoencephalitis of unknown cause, a specific epidemiologic and laboratory evaluation should be performed to conclusively rule out rabies as a cause of illness before organ donation.

Dr. Shuilian Chen is a medical doctor in the Changsha Center for Disease Control and Prevention in Changsha, China. Her main field of research is emerging infectious disease control and prevention.

References

1. Zhou H, Zhu W, Zeng J, He J, Liu K, Li Y, et al. Probable rabies virus transmission through organ transplantation, China, 2015. Emerg Infect Dis. 2016;22:1348–52. http://dx.doi.org/10.3201/eid2208.151993
2. Srinivasan A, Burton EC, Kuehnert MJ, Rupprecht C, Sutker WL, Ksiazek TG, et al.; Rabies in Transplant Recipients Investigation Team. Transmission of rabies virus from an organ donor to four transplant recipients. N Engl J Med. 2005;352:1103–11. http://dx.doi.org/10.1056/NEJMoa043018
3. Bronnert J, Wilde H, Tepsumethanon V, Lumlertdacha B, Hemachudha T. Organ transplantations and rabies transmission. J Travel Med. 2007;14:177–80. http://dx.doi.org/10.1111/j.1708-8305.2006.00095.x
4. Vora NM, Basavaraju SV, Feldman KA, Paddock CD, Orciari L, Gitterman S, et al.; Transplant-Associated Rabies Virus Transmission Investigation Team. Raccoon rabies virus variant transmission through solid organ transplantation. JAMA. 2013;310:398–407. http://dx.doi.org/10.1001/jama.2013.7986

Identification of Clade E Avipoxvirus, Mozambique, 2016

Lourenço P. Mapaco, Zeiss Lacerda, Iolanda V.A. Monjane, Esayas Gelaye, Afonso H. Sussuro, Gerrit J. Viljoen, William G. Dundon, Sara J. Achá

Author affiliations: Agrarian Research Institute of Mozambique, Maputo, Mozambique (L.P. Mapaco, I.V.A. Monjane, A.H. Sussuro, S.J. Achá); Eduardo Mondlane University, Maputo (Z. Lacerda); National Veterinary Institute, Debre Zeit, Ethiopia (E. Gelaye); International Atomic Energy Agency, Vienna, Austria (G.J. Viljoen, W.G. Dundon)

Analysis of scab samples collected from poultry during outbreaks of fowlpox in Mozambique in 2016 revealed the presence of clade E avipoxviruses. Infected poultry were from flocks that had been vaccinated against fowlpox virus. These findings require urgent reevaluation of the vaccine formula and control strategies in this country.

Avipoxviruses are large, enveloped DNA viruses that belong to the genus *Avipoxvirus* in the *Chordopoxvirinae* subfamily of the family *Poxviridae*. These viruses cause disease in a large number of bird species and are generally named after the species from which the virus was first isolated and characterized (1). Fowlpox virus (FPV) has caused substantial economic losses in domestic poultry resulting from reduced egg production and growth, blindness, and death, with a death ratio that can reach as high as 50%.

Phylogenetic analyses of the *Avipoxvirus* genus are usually conducted with the segments of the genes encoding the 4b core-like protein (P4b) and the DNA polymerase, which are both highly conserved among poxviruses (2,3). Using these loci, researchers have seen that most strains cluster into 3 major clades, namely A, B, and C, with clade A being subdivided further into subclades A1–A7 and clade B into subclades B1–B3 (3–5). Two additional clades

(i.e., D and E), each with just a single isolate, have also been proposed (*5,6*).

Little is known about avipoxviruses in Africa. Avipoxviruses isolated from chickens, turkeys, and pigeons in 2011 in northern Egypt belonged to either subclade A1 or A2 (*7*). In 2013, thirteen avipoxviruses from different bird species from different regions of South Africa grouped into either subclade A2 or A3 (*8*). Sequences generated from isolates from naturally infected chickens in Tanzania were also found to belong to clade A1 (*9*). Therefore, all avipoxviruses previously identified in Africa belonged to clade A.

Fowlpox is endemic in Mozambique and commonly reported. The effect of the disease is more severe in backyard production systems affecting mostly young chickens and turkeys. An official control program for FPV in Mozambique does not exist, and because the country does not have a poultry production system that meets the national demand, birds are often imported from neighboring countries, such as South Africa, Swaziland, and Zimbabwe.

During August 2015–November 2016, scab samples from 16 separate FPV outbreaks were collected by the Agrarian Research Institute of Mozambique from 4 locations: Gaza Province, Maputo Province, Maputo City, and Tete Province. The outbreaks primarily affected backyard chickens and commercial laying hens, although a flock of broiler chickens and a flock of turkeys were also investigated. The clinical signs reported and postmortem examination findings included reduction of appetite; listlessness; nodules or scabs of different sizes on less-feathered body areas (e.g., wattles, comb, eye lids, ear lobes, limbs, and interdigit spaces); and pronounced ulcerations on the interdigit space. Different color tones and irregular wrinkled shells were also observed on eggs.

The 16 scab samples were positive for FPV P4b gene following PCR amplification with specific primers (online Technical Appendix, https://wwwnc.cdc.gov/EID/article/23/9/16-1981-Techapp1.pdf); the amplicons were purified and sequenced. A phylogenetic analysis of the P4b gene sequences revealed that most of the samples collected contained virus that clustered in subclade A1 (Figure, panel A). However, the 2 samples that did not cluster in subclade A1 (FPV-MOZ-608/2016 and FPV-MOZ-980/2016) were of interest; these samples were obtained from 2 separate outbreaks in layer chickens 3 months apart (i.e., in Maputo City [25°55′55.5″S, 32°32′53.4″E] on July 7, 2016, and in Maputo Province [25°53′22.3″S, 32°27′16.6″E] on October 25, 2016). To characterize FPV-MOZ-608/2016 and FPV-MOZ-980/2016 further, we amplified and sequenced a segment of the DNA polymerase gene (online Technical
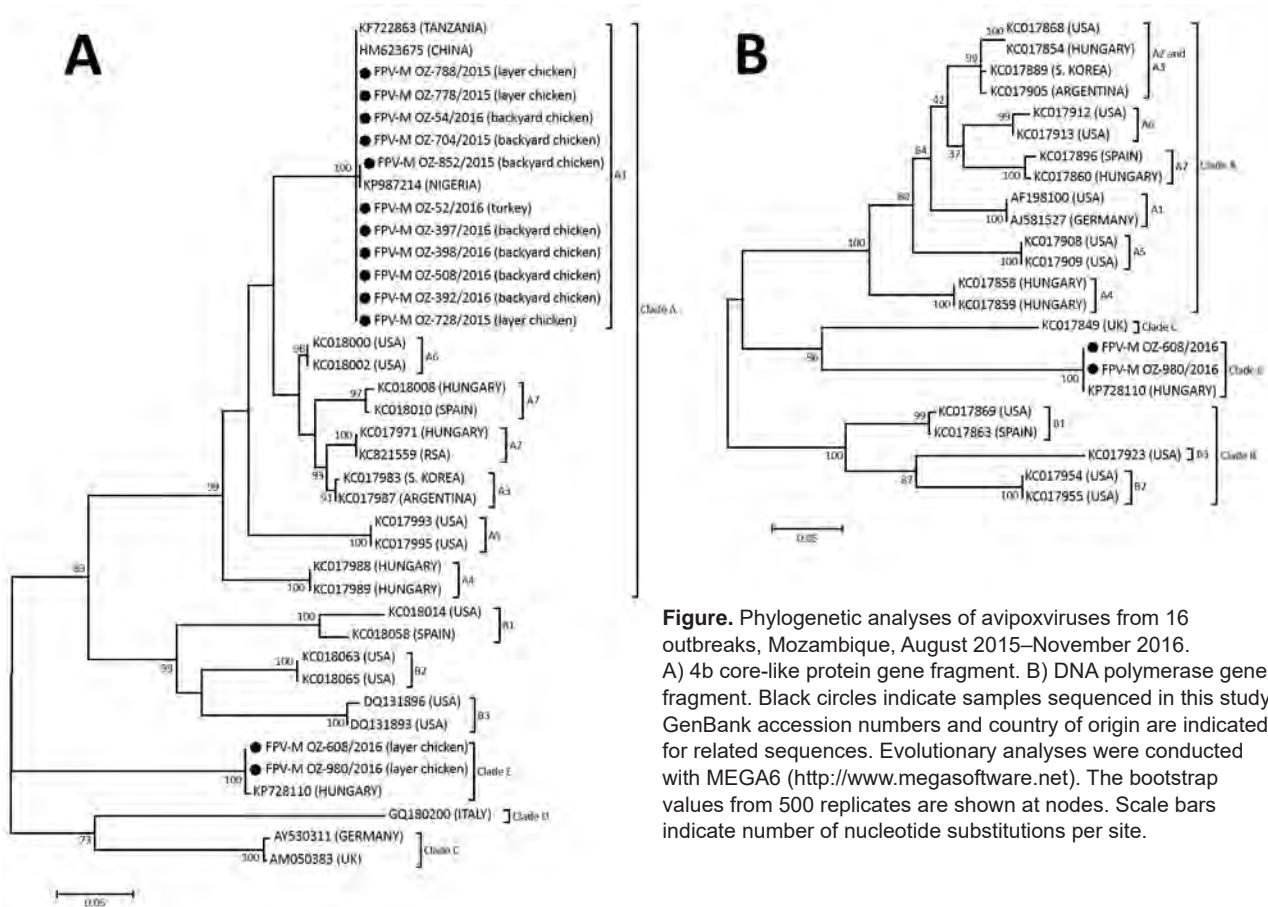
Figure. Phylogenetic analyses of avipoxviruses from 16 outbreaks, Mozambique, August 2015–November 2016. A) 4b core-like protein gene fragment. B) DNA polymerase gene fragment. Black circles indicate samples sequenced in this study. GenBank accession numbers and country of origin are indicated for related sequences. Evolutionary analyses were conducted with MEGA6 (http://www.megasoftware.net). The bootstrap values from 500 replicates are shown at nodes. Scale bars indicate number of nucleotide substitutions per site.

Appendix). The maximum-likelihood analysis using both P4b and DNA polymerase gene fragments showed that FPV-MOZ-608/2016 and FPV-MOZ-980/2016 clustered in clade E with the APV isolated in Hungary in 2011 (TKPV-HU1124/2011) (Figure, panels A and B) (6).

TKPV-HU1124/2011 was isolated from a flock of turkeys vaccinated with a commercial vaccine for FPV, and FPV-MOZ-608/2016 and FPV-MOZ-980/2016 were also obtained from vaccinated chickens. The laying pullets imported from South Africa had already been vaccinated for FPV on day 1 with the commercial fowlpox-vectored infectious laryngotracheitis vaccine and day 17 with the fowlpox-vectored infectious laryngotracheitis/avian encephalomyelitis vaccine. Our data suggest a possible failure of the vaccine to protect against clade E viruses, similar to what has been reported previously for TKPV-HU1124/2011 (6).

The identification of a clade E avipoxvirus in Mozambique requires further investigation to clarify how a virus that has only been reported once found its way to this country. Because the chickens in both infected flocks were purchased from the same pullet reseller who had (for both flocks) imported the birds from South Africa, it is likely that the source of infection was the same. However, the specific source has not been identified. FPVs are known to infect >230 species of wild birds, many of which are migratory (5); thus, introduction through migratory wild birds is a possibility.

Resolution of the full genome of these viruses might provide hints to their origin. The presence of fowlpox disease in birds vaccinated against FPV requires urgent re-evaluation of the vaccine formula and control strategies in Mozambique.

Dr. Mapaco is a researcher at the Central Veterinary Laboratory of the Agrarian Research Institute of Mozambique. His research interests are viral diseases of animals, including zoonoses.

References

1. Weli SC, Tryland M. Avipoxviruses: infection biology and their use as vaccine vectors. Virol J. 2011;8:49. http://dx.doi.org/10.1186/1743-422X-8-49
2. Binns MM, Boursnell ME, Tomley FM, Campbell J. Analysis of the fowlpoxvirus gene encoding the 4b core polypeptide and demonstration that it possesses efficient promoter sequences. Virology. 1989;170:288–91. http://dx.doi.org/10.1016/0042-6822(89)90380-2
3. Gyuranecz M, Foster JT, Dán Á, Ip HS, Egstad KF, Parker PG, et al. Worldwide phylogenetic relationship of avian poxviruses. J Virol. 2013;87:4938–51. http://dx.doi.org/10.1128/JVI.03183-12
4. Jarmin S, Manvell R, Gough RE, Laidlaw SM, Skinner MA. Avipoxvirus phylogenetics: identification of a PCR length polymorphism that discriminates between the two major clades.
5. Manarolla G, Pisoni G, Sironi G, Rampin T. Molecular biological characterization of avian poxvirus strains isolated from different avian species. Vet Microbiol. 2010;140:1–8. http://dx.doi.org/10.1016/j.vetmic.2009.07.004
6. Bányai K, Palya V, Dénes B, Glávits R, Ivanics É, Horváth B, et al. Unique genomic organization of a novel avipoxvirus detected in turkey (Meleagris gallopavo). Infect Genet Evol. 2015;35:221–9. http://dx.doi.org/10.1016/j.meegid.2015.08.001
7. Abdallah FM, Hassanin O. Detection and molecular characterization of avipoxviruses isolated from different avian species in Egypt. Virus Genes. 2013;46:63–70. http://dx.doi.org/10.1007/s11262-012-0821-y
8. Offerman K, Carulei O, Gous TA, Douglass N, Williamson AL. Phylogenetic and histological variation in avipoxviruses isolated in South Africa. J Gen Virol. 2013;94:2338–51. http://dx.doi.org/10.1099/vir.0.054049-0
9. Mzula A, Masola SN, Kasanga CJ, Wambura PN. Existence of variant strains fowlpox virus integrated with reticuloendotheliosis virus in its genome in field isolates in Tanzania. Trop Anim Health Prod. 2014;46:711–6. http://dx.doi.org/10.1007/s11250-014-0552-2

J Gen Virol. 2006;87:2191–201. http://dx.doi.org/10.1099/vir.0.81738-0

Address for correspondence: William G. Dundon, APHL Joint FAO/IAEA Division, International Atomic Energy Agency Laboratories, Seibersdorf A-2444, Austria; email: w.dundon@iaea.org

Indication of Cross-Species Transmission of Astrovirus Associated with Encephalitis in Sheep and Cattle

Céline L. Boujon, Michel C. Koch, Daniel Wüthrich, Simea Werder, Dennis Jakupovic, Rémy Bruggmann, Torsten Seuberlich

Author affiliation: University of Bern, Bern, Switzerland

We report the identification of a neurotropic astrovirus associated with encephalitis in a sheep. This virus is genetically almost identical to an astrovirus recently described in neurologically diseased cattle. The similarity indicates that astroviruses of the same genotype may cause encephalitis in different species.

Astroviruses are nonenveloped viruses with a single stranded, positive-sense RNA genome. They are best known to be associated with gastroenteritis, especially in humans. Recently, reports of these viruses in association

with encephalitis have increased dramatically, with reports of cases in humans (1), mink (2), and cattle (3–6).

The most common causes for viral encephalitis in sheep include maedi-visna virus, Borna disease virus, and rabies virus. In a high proportion of cases of nonsuppurative encephalitis cases (which is indicative of a viral infection) in sheep, however, the etiologic agent remains unknown (7). To investigate that matter, we subjected 3 ovine encephalitis samples from our archives to next-generation sequencing and a bioinformatics pipeline for virus discovery (online Technical Appendix, https://wwwnc.cdc.gov/EID/article/23/9/17-0168-Techapp1.pdf). In 1 animal (ID 41669), 1 of the contigs obtained had high similarity (>98%) to bovine astrovirus CH15 (BoAstV-CH15), a virus found recently in 2 cases of nonsuppurative encephalitis in cattle (5). The affected sheep was a 7-year-old Swiss white alpine ewe that was culled for reasons other than human consumption. No other information about the clinical history of the animal was available. Histological diagnosis consisted of severe nonsuppurative meningoencephalitis. Routine diagnostic tests for Borna, rabies, and maedi-visna viruses were all negative.

We used primers based on the BoAstV-CH15 genome sequence (GenBank accession no. KT956903) and the Sanger method to sequence the complete genome of the ovine strain (online Technical Appendix Figure 1), which we named ovine astrovirus CH16 (OvAstV-CH16). The sequence we obtained shared >98% identity with BoAstV-CH15 on the nucleotide and amino acid level (Genbank accession no. KY859988; online Technical Appendix Table 1). The virus reported here is genetically clearly distinct from intestinal OvAstV strains described previously (OvAstV-1 and OvAstV-2; online Technical Appendix Table 1).

A phylogenetic comparison confirmed the close relationship of OvAstV-CH16 with BoAstV-CH15 (5) and BoAstV-BH89/14, another astrovirus detected in association with encephalitis in a cow in Germany (6). Recently, 2 astroviruses were reported in association with encephalitis in sheep in Scotland (OvAstV UK/2013/ewe/lib01454 and UK/2014/lamb/lib01455) (8), and we included their genomic data in the study comparison. All these strains clustered in the same branch of the phylogenetic tree, with >95% amino acid sequence similarity in the viral capsid protein (online Technical Appendix Figure 2) and, therefore, should be considered 1 genotype species (9). When we compared all these viruses more closely on the amino acid level, we were not able to find any sequence variant that could be specifically associated with a tropism for sheep or cattle (online Technical Appendix Table 3).

We then analyzed brain samples of sheep with nonsuppurative encephalitis of unknown etiology (n = 47), which had been identified within the framework of active disease surveillance in Switzerland (7), by RT-PCR specific for BoAstV-CH15 (online Technical Appendix). None reacted positively, implying a low incidence of OvAstV-CH16 infection associated with encephalitis in the sheep population in Switzerland.

To confirm the presence of OvAstV-CH16 in situ, we used polyclonal antisera targeted at the putative capsid protein of BoAstV-CH15 and tested formalin-fixed, paraffin-embedded brain tissues of sheep 41669 by immunohistochemistry (online Technical Appendix). We observed positive staining of neurons, assessed as such on the basis of morphological criteria, in all brain regions examined (e.g., medulla oblongata, cerebellum, thalamus, hippocampus, cortex, caudate nucleus), in particular in some areas (Figure; online Technical Appendix Figure 3). This finding supports a plausible biological association of OvAstV-CH16 infection and encephalitis in the sheep under investigation and underlines again the close relationship between OvAstV-CH16 and BoAstV-CH15. The identification of similar astroviruses in sheep and cattle with comparable diseases, by different methods and in distinct geographic areas, further strengthens these findings. We consider it unlikely that the ovine cases reported in Scotland and Switzerland are epidemiologically related and speculate that the respective viruses were already geographically widely spread but were undetected until recently, which also seems to be the case for neurotropic astroviruses in cattle.

The importance of the link between astroviruses and encephalitis is increasingly being brought to light, but the factors determining their tropism and neuroinvasion are still unknown. Deeper epidemiologic, genetic, and molecular investigations will help to clarify these aspects of astrovirus pathology. Astroviruses were traditionally considered to be host specific, but in recent years, several reports challenged this assumption; for instance, when human astroviruses were found in fecal samples of primates (10). In such cases, however, effective infection of atypical hosts was never shown. In this study, we demonstrated the presence of the virus in situ, a finding that strengthens the likelihood of such an infectious event. The fact that a virus of the same genotype was described in cattle with similar pathologic findings also challenges this concept of host specificity and suggests that astroviruses can cross the species barrier and, therefore, represent a zoonotic threat as not only a gastroenteritic agent but also a potential cause of encephalitis.
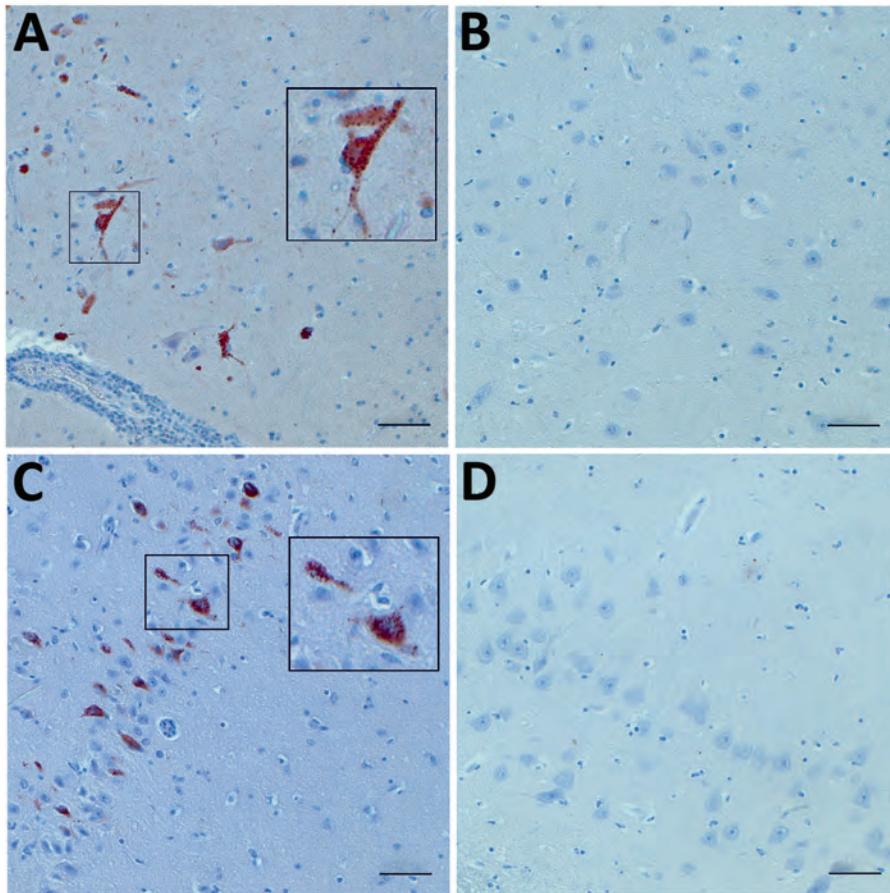
Figure. Immunohistochemistry (IHC) for ovine astrovirus CH16 in brain tissues (hippocampus) of a sheep (ID 41669) with encephalitis using 2 polyclonal antisera targeted at the putative capsid protein of bovine astrovirus CH15. A) IHC using antiserum against the conserved region of the capsid protein showing positive staining (box at left; box at right shows area at higher magnification); B) negative control. C) IHC using antiserum against the variable regions of the capsid protein n showing positive staining (box at left; box at right shows area at higher magnification); D) negative control. Scale bars indicate 50 μm.

Dr. Boujon is a veterinarian and PhD student at the Vetsuisse Faculty in Bern. Her primary research lies in the study of neurotropic astroviruses in cattle.

References

1. Vu DL, Cordey S, Brito F, Kaiser L. Novel human astroviruses: Novel human diseases? J Clin Virol. 2016;82:56–63. http://dx.doi.org/10.1016/j.jcv.2016.07.004
2. Blomström AL, Widén F, Hammer AS, Belák S, Berg M. Detection of a novel astrovirus in brain tissue of mink suffering from shaking mink syndrome by use of viral metagenomics. J Clin Microbiol. 2010;48:4392–6. http://dx.doi.org/10.1128/JCM.01040-10
3. Li L, Diab S, McGraw S, Barr B, Traslavina R, Higgins R, et al. Divergent astrovirus associated with neurologic disease in cattle. Emerg Infect Dis. 2013;19:1385–92. http://dx.doi.org/10.3201/eid1909.130682
4. Bouzalas IG, Wüthrich D, Walland J, Drögemüller C, Zurbriggen A, Vandevelde M, et al. Neurotropic astrovirus in cattle with nonsuppurative encephalitis in Europe. J Clin Microbiol. 2014;52:3318–24. http://dx.doi.org/10.1128/JCM.01195-14
5. Seuberlich T, Wüthrich D, Selimovic-Hamza S, Drögemüller C, Oevermann A, Bruggmann R, et al. Identification of a second encephalitis-associated astrovirus in cattle. Emerg Microbes Infect. 2016;5:e5. http://dx.doi.org/10.1038/emi.2016.5
6. Schlottau K, Schulze C, Bilk S, Hanke D, Höper D, Beer M, et al. Detection of a novel bovine astrovirus in a cow with encephalitis. Transbound Emerg Dis. 2016;63:253–9. http://dx.doi.org/10.1111/tbed.12493
7. Oevermann A, Botteron C, Seuberlich T, Nicolier A, Friess M, Doherr MG, et al. Neuropathological survey of fallen stock: active surveillance reveals high prevalence of encephalitic listeriosis in small ruminants. Vet Microbiol. 2008;130:320–9. http://dx.doi.org/10.1016/j.vetmic.2008.01.015
8. Pfaff F, Schlottau K, Scholes S, Courtenay A, Hoffmann B, Höper D, et al. A novel astrovirus associated with encephalitis and ganglionitis in domestic sheep. Transbound Emerg Dis. 2017;64:677–82. http://dx.doi.org/10.1111/tbed.12623
9. Bosch A, Pintó RM, Guix S. Human astroviruses. Clin Microbiol Rev. 2014;27:1048–74. http://dx.doi.org/10.1128/CMR.00013-14
10. Karlsson EA, Small CT, Freiden P, Feeroz MM, Matsen FA IV, San S, et al. Non-human primates harbor diverse mammalian and avian astroviruses including those associated with human infections. PLoS Pathog. 2015;11:e1005225. http://dx.doi.org/10.1371/journal.ppat.1005225

Address for correspondence: Torsten Seuberlich, NeuroCenter, Division of Neurological Sciences, Vetsuisse Faculty, University of Bern, Bremgartenstrasse 109 a, CH-3001 Bern, Switzerland; email: torsten.seuberlich@vetsuisse.unibe.ch

A New Bat-HKU2–like Coronavirus in Swine, China, 2017

Lang Gong,[1] Jie Li,[1] Qingfeng Zhou, Zhichao Xu, Li Chen, Yun Zhang, Chunyi Xue, Zhifen Wen, Yongchang Cao

Author affiliations: State Key Laboratory of Biocontrol, Life Sciences School, Sun Yat-sen University, Guangzhou, China (L. Gong, J. Li, Z. Xu, L. Chen, Y. Zhang, C. Xue, Z. Wen, Y. Cao); Guangdong Wen's Foodstuffs Group Co., Ltd., Yunfu, China (J. Li, Q. Zhou, L. Chen, Z. Wen)

We identified from suckling piglets with diarrhea in China a new bat-HKU2–like porcine coronavirus (porcine enteric alphacoronavirus). The GDS04 strain of this coronavirus shares high aa identities (>90%) with the reported bat-HKU2 strains in Coronaviridae-wide conserved domains, suggesting that the GDS04 strain belongs to the same species as HKU2.

Several pathogens are thought to be responsible for porcine diarrhea, including porcine epidemic diarrhea virus (PEDV) (1), transmissible gastroenteritis virus (2), porcine deltacoronavirus (3), porcine group A rotavirus (4), and emerging viruses like porcine kobuvirus (5). To add to the list, we have identified from suckling piglets with diarrhea in China a new bat-HKU2–like porcine coronavirus (porcine enteric alphacoronavirus [PEAV]).

Since December 2010, large-scale outbreaks of diarrhea in suckling piglets have been reported across China (1), and vaccination against PEDV has been relatively effective for diarrhea prevention. However, in February 2017, outbreaks of severe diarrhea occurred in swine herds vaccinated against PEDV in Guangdong, China. All ill pigs showed severe watery diarrhea, and their clinical onset occurred a few days later than those infected with PEDV. In initial tests with reverse transcription PCR using specific primers for PEDV, transmissible gastroenteritis virus, porcine group A rotavirus, or porcine deltacoronavirus, none of these viruses could be detected in all clinical samples. Furthermore, the recovered sows showed no seroneutralizing antibodies against PEDV.

To investigate the possible causative pathogen or pathogens causing this recent severe diarrhea in suckling piglets, we obtained excreta from 32 ill newborn piglets from 3 farms. We divided 5-day-old piglets into 4 groups of 5 each (3 groups according to the origin of the excreta, plus 1 control group). We inoculated each animal with 5 mL of excreta through the oral route. After 2 days, all inoculated animals exhibited similar clinical symptoms, including diarrhea and dehydration. We randomly selected 2 inoculated pigs in each group and performed necropsies on days 3 and 5 postinoculation, respectively. We filtrated homogenate of small intestine and intestinal contents, using the resultant supernatant for RNA extraction as described previously (2). We extracted total RNA by using a TRIzol reagent (Invitrogen Life Technologies, Grand Island, NY, USA) and eliminated ribosomal RNA with the Ribo-Zero rRNA Removal Kit (Illumina, San Diego, CA, USA) according to the manufacturer's instructions. After reverse transcription PCR with random primers, we performed 150-bp paired-end shotgun metatranscriptome sequencing on the cDNA libraries by using an Illumina HiSeq system.

After assembling and mapping sequencing reads, we obtained a complete genome sequence of the PEAV GDS04 strain, which we then deposited in GenBank (accession no. MF167434). The full length of the PEAV genome is 27,171 nt (excluding the poly-A tail); this size is similar to that of bat-like HKU2 strains of coronavirus (6). The full genome of PEAV GDS04 strain shares high nucleotide identities (≈95%) with the reported bat-HKU2 strains.

Our phylogenetic analysis based on the whole genome of GDS04 and representatives of 4 established coronavirus genera, including the human and bat-like coronaviruses, demonstrated that GDS04 clusters with bat-like coronaviruses (Figure). According to the phylogenetic tree, the position of GDS04 is between HKU2 and BtRf alphacoronavirus. The HKU2 strain was identified in Hong Kong and Guangdong Province, China, in 2007 (6), and the BtRf alphacoronavirus strain was detected in China in 2012 (http://www.ncbi.nlm.nih.gov/nuccore/NC_028824.1). Both viruses are bat-associated viruses. However, the 2 strains are distributed in relatively different branches (Figure). Based on a comprehensive comparative analysis of the genomes of various groups of coronaviruses, we classified GDS04 as an alphacoronavirus. Our sequence analysis revealed that GDS04 has 80% nt and 87% aa identity with the spike (S) protein of the HKU2 strain. Moreover, the S protein of the GDS04 genome is 6 bp longer than the S protein in the HKU2 strain, which has the smallest S protein among all coronaviruses. Nevertheless, the GDS04 strain shares 95.7% aa identity with HKU2 in nonstructural protein (nsp) 3 (adenosine diphosphate-ribose 1′-phosphatase), 96.4% in nsp5 (3C-like protease), 94.6% in nsp12 (RNA-dependent RNA polymerase), 99.8% in nsp13 (helicase), 99.2% in nsp14 (3′-to-5′ exonuclease), 99.4% in nsp15 (poly[U]-specific endoribonuclease), and 97.6% in nsp16 (2'-O-ribose methyltransferase). These nonstructural proteins are Coronaviridae-wide conserved domains in replicase polyprotein pp1ab. A threshold of >90% in aa sequence identity

---

[1]These authors contributed equally to this article.
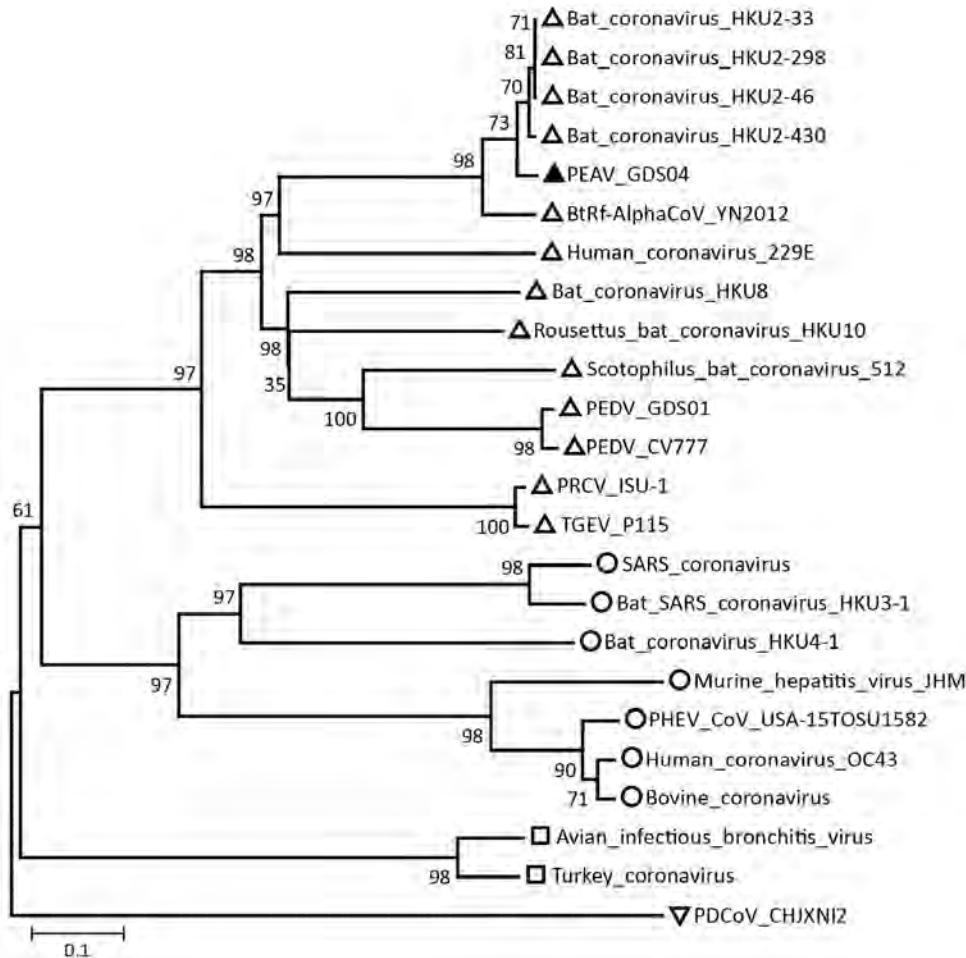
Figure. Phylogenetic tree based on the whole-genome sequences of PEAV, bat CoVs, and other representative CoVs, China, 2017. Analyses were conducted by using MEGA software version 6.0 (http://www.megasoftware.net) with the neighbor-joining algorithm. Bootstrap values were calculated with 1,000 replicates. The number on each branch indicates bootstrap values. Solid triangle indicates the GDS04 strain, open triangles alphacoronaviruses, circles betacoronaviruses, squares gammacoronavirus, inverted triangle deltacoronavirus. Scale bar indicates nucleotide substitutions per site. CoV, coronavirus; PDCoV, porcine deltacoronavirus; PEAV, porcine enteric alphacoronavirus; PEDV, porcine epidemic diarrhea virus; PHEV, porcine hemagglutinating encephalomyelitis virus; PRCV, porcine respiratory coronavirus; SARS, severe acute respiratory syndrome; TGEV, transmissible gastroenteritis virus.

suggests that 2 viruses are of the same species; our findings suggest that the GDS04 strain belongs to the same species as HKU2.

Furthermore, we designed specific primers of the n gene for the detection of the GDS04 strain. By using reverse-transcription PCR with these primers, we found that 97 out of 308 clinical intestinal or fecal samples were positive for GDS04. We collected all clinical samples from 25 farms in Guangdong Province during February–April 2017 and used 20 samples collected from healthy vaccinated piglets as negative controls.

In summary, we report preliminary data on our detection of a new coronavirus-like virus, PEAV. PEAV is thought to be responsible for the most recent diarrhea endemic in pig herds in southern China. Virus isolation and serologic testing are under way. The outbreak of the newly discovered virus arose among swine with severe diarrhea in swine breeding farms in southern China, suggesting the regional outbreaks of diarrhea could contribute to the emergence of new pandemic viruses. Extensive surveillance for GDS04 PEAV is required to define its epidemiology and evolution.

Mr. Gong is a PhD student in the life sciences school at Sun Yat-sen University. His primary research interests include the molecular epidemiology of novel coronaviruses and influenza vaccine. Dr. Li is a postdoctoral fellow in the life sciences school at Sun Yat-sen University. His research focuses on bioinformatics, genomics and molecular epidemiology of coronaviruses.

References

1. Sun RQ, Cai RJ, Chen YQ, Liang PS, Chen DK, Song CX. Outbreak of porcine epidemic diarrhea in suckling piglets, China. Emerg Infect Dis. 2012;18:161–3. http://dx.doi.org/10.3201/eid1801.111259
2. Pensaert MB, de Bouck P. A new coronavirus-like particle associated with diarrhea in swine. Arch Virol. 1978;58:243–7. http://dx.doi.org/10.1007/BF01317606

3. Dong N, Fang L, Zeng S, Sun Q, Chen H, Xiao S. Porcine deltacoronavirus in mainland China. Emerg Infect Dis. 2015;21:2254–5. http://dx.doi.org/10.3201/eid2112.150283

4. Theuns S, Vyt P, Desmarets LM, Roukaerts ID, Heylen E, Zeller M, et al. Presence and characterization of pig group A and C rotaviruses in feces of Belgian diarrheic suckling piglets. Virus Res. 2016;213:172–83. http://dx.doi.org/10.1016/j.virusres.2015.12.004

5. Reuter G, Boros A, Pankovics P. Kobuviruses—a comprehensive review. Rev Med Virol. 2011;21:32–41. http://dx.doi.org/10.1002/rmv.677

6. Lau SK, Woo PC, Li KS, Huang Y, Wang M, Lam CS, et al. Complete genome sequence of bat coronavirus HKU2 from Chinese horseshoe bats revealed a much smaller spike gene with a different evolutionary lineage from the rest of the genome. Virology. 2007;367:428–39. http://dx.doi.org/10.1016/j.virol.2007.06.009

Antimicrobial Drug–Resistant Shiga Toxin–Producing *Escherichia coli* Infections, Michigan, USA

Sanjana Mukherjee, Rebekah E. Mosci, Chase M. Anderson, Brian A. Snyder, James Collins, James T. Rudrik, Shannon D. Manning

Author affiliations: Michigan State University, East Lansing, Michigan, USA (S. Mukherjee, R.E. Mosci, C.M. Anderson, B.A. Snyder, S.D. Manning); Michigan Department of Health and Human Services, Lansing (J. Collins, J.T. Rudrik)

High frequencies of antimicrobial drug resistance were observed in O157 and non-O157 Shiga toxin–producing *E. coli* strains recovered from patients in Michigan during 2010–2014. Resistance was more common in non-O157 strains and independently associated with hospitalization, indicating that resistance could contribute to more severe disease outcomes.

Shiga toxin–producing *Escherichia coli* (STEC) contributes to 265,000 cases of foodborne illness annually in the United States (*1*). Most infections are caused by O157 strains; however, non-O157 STEC infections have increased (*2*). Antimicrobial drug resistance among STEC has been reported (*3–5*) but is probably underestimated. Given the importance of resistance in *E. coli* pathotypes, we sought to determine the prevalence of resistant STEC infections and assess the effects of resistance on disease.

We obtained 358 STEC isolates from the Michigan Department of Health and Human Services (MDHHS) Reference Laboratory (Lansing, MI, USA), collected during 2010–2014. Of these, 14 were outbreak associated. We examined 1 strain per outbreak using protocols approved by Michigan State University (MSU; Lansing, MI, USA; IRB #10-736SM) and MDHHS (842-PHALAB). Overall, 31 (8.8%) strains (23 non-O157, 8 O157) were resistant to antimicrobial drugs (Table). Resistance to ampicillin (7.4%) was most common, followed by trimethoprim/sulfamethoxazole (SXT) (4.0%) and ciprofloxacin (0.3%). Compared with national rates, resistance to ampicillin and SXT was higher, but not significantly different, for O157 isolates from Michigan (online Technical Appendix Figure 1, https://wwwnc.cdc.gov/EID/article/23/9/17-0523-Techapp1.pdf) (*6*). One strain was resistant to all drugs, and all resistant strains had high MICs (ampicillin, >64 μg/mL; ciprofloxacin, >32 μg/mL; SXT, in 1:19 ratio, >32/608 μg/mL). Notably, resistance was twice as common for non-O157 (11.1%) than for O157 (5.5%) strains. O111 strains (n = 7) had significantly higher resistance frequencies (24.1%) than other non-O157 serogroups (p = 0.03). We found variation by year and season; resistance frequencies were highest in 2012 (online Technical Appendix, Figure 2) and during winter/spring (online Technical Appendix Table 1), but neither trend was significant. We also observed a strong but nonsignificant association between resistance and hospitalization but no association for urban versus rural residence (*7*) or county after stratifying by prescription rates (*8*) in the univariate analyses.

We conducted a multivariate analysis using logistic regression, with hospitalization as the dependent variable; we included variables with significant (p≤0.05) and strong (p≤0.20) associations from the univariate analysis as independent variables. Forward selection indicated that hospitalized patients were more likely to have resistant infections (odds ratio [OR] 2.4, 95% CI 1.00–5.82) and less likely to have non-O157 infections (OR 0.4, 95% CI 0.21–0.61) (online Technical Appendix Table 2), suggesting that resistant infections or O157 infections may cause more severe clinical outcomes. Patients ≥18 years of age, women, and patients with bloody diarrhea were also more likely to be hospitalized.

Although we found no significant difference by *stx* profile, strains possessing *stx*1 only were more commonly resistant than strains with *stx*2 alone (p = 0.27 by Fisher exact test). All 23 (100%) resistant non-O157 STEC and 1

Table. Antimicrobial drug resistance in 353 clinical Shiga toxin–producing *Escherichia coli* isolates, by serotype, Michigan, USA, 2010–2014*

Serotype	No. isolates	No. (%) isolates			
		Any resistance	Ampicillin resistance	Ciprofloxacin resistance	SXT resistance
O157	146	8 (5.5)	7 (4.8)	0 (0)	5 (3.4)
Non-O157	207	23 (11.1)	19 (9.2)	1 (0.5)	9 (4.3)
O26	53	4 (7.6)	4 (7.6)	0 (0)	1 (1.9)
O45	50	6 (12.0)	5 (10.0)	0 (0)	2 (4.0)
O103	75	6 (8.0)	5 (6.7)	1 (1.3)	4 (5.3)
O111	29	7 (24.1)	5 (17.2)	0 (0)	2 (6.9)

*We tested 358 isolates by disk diffusion for resistance to ampicillin (10 µg in disk), SXT (25 µg in disk), and ciprofloxacin (5 µg in disk). MICs were determined by using Etest. Strains were classified as resistant or susceptible according to Clinical Laboratory Standards Institute guidelines; *E. coli* ATCC 25922 was used as a control. Five isolates had unknown serotypes and were excluded from analysis. Isolate numbers for individual antibiotics do not always add up to the total number of isolates with any resistance because some isolates were resistant to >1 drug. SXT, trimethoprim/sulfamethoxazole.

(12.5%) resistant O157 strain had *stx*1 only. Strains positive for *eae* were less likely to be resistant (n = 27; 8.4%) than *eae*-negative strains (n = 4; 23.5%); this nonsignificant difference (p = 0.07 by Fisher exact test) could be due to small sample sizes. All 8 resistant O157 strains and 18 (78.3%) of 23 resistant non-O157 strains had *eae*, demonstrating correlations between virulence genes and serogroups.

Overall, we detected a high frequency of resistance among non-O157 STEC (11.2%), similar to findings from Mexico (15%), although we evaluated fewer drugs (5). Resistance to ciprofloxacin was low despite its routine use for treating enteric infections, perhaps because resistance development in *E. coli* requires multiple mutations (9). Resistance frequencies in STEC were low relative to other *E. coli* pathotypes such as extraintestinal *E. coli*, which may be attributable to differences in the source of the infections (3).

The higher O157 resistance frequencies in Michigan than nationwide indicate that selection pressures vary by location and source. Although we observed no difference in resistance frequencies for counties with high versus low antimicrobial drug prescription rates (8), we have not investigated selection pressures from drug use in farm environments that may affect resistance emergence in Michigan. Approximately 12×10^6 kg of antimicrobial drugs are administered to food animals annually in the United States; roughly 61% of these are medically relevant. Higher resistance frequencies in winter/spring (12.2%) than summer/fall (7.5%) could be attributed to variation in prescription rates by season (10).

Because Michigan is not part of the Centers for Disease Control and Prevention Foodborne Diseases Active Surveillance Network and resistance in STEC has not been widely researched, data about the prevalence and impact of resistance are lacking. This study detected a high frequency of STEC resistance to antimicrobial drugs commonly used in human and veterinary medicine, particularly for non-O157 serotypes, which have increased in frequency (2). Monitoring resistance in STEC is essential because of the risk of transmitting resistant strains from food animals to humans and the high likelihood of horizontal transfer of resistance genes from STEC to other pathogens. Routine monitoring can uncover new treatment approaches and guide development of strategies for controlling emergence and spread of resistance in STEC and other *E. coli* pathotypes.

Miss Mukherjee is a PhD student in the Department of Microbiology and Molecular Genetics at MSU. She is studying antimicrobial drug resistance in STEC and nontyphoidal *Salmonella*. Her primary research interests are molecular epidemiology and medical microbiology.

References

1. Scallan E, Hoekstra RM, Angulo FJ, Tauxe RV, Widdowson MA, Roy SL, et al. Foodborne illness acquired in the United States—major pathogens. Emerg Infect Dis. 2011;17:7–15. http://dx.doi.org/10.3201/eid1701.P11101
2. Tseng M, Sha Q, Rudrik JT, Collins J, Henderson T, Funk JA, et al. Increasing incidence of non-O157 Shiga toxin-producing *Escherichia coli* (STEC) in Michigan and association with clinical illness. Epidemiol Infect. 2016;144:1394–405. http://dx.doi.org/10.1017/S0950268815002836
3. Schroeder CM, Meng J, Zhao S, DebRoy C, Torcolini J, Zhao C, et al. Antimicrobial resistance of *Escherichia coli* O26, O103, O111, O128, and O145 from animals and humans. Emerg Infect Dis. 2002;8:1409–14. http://dx.doi.org/10.3201/eid0812.0200770
4. Mora A, Blanco JE, Blanco M, Alonso MP, Dhabi G, Echeita A, et al. Antimicrobial resistance of Shiga toxin (verotoxin)–producing *Escherichia coli* O157:H7 and non-O157 strains isolated from humans, cattle, sheep and food in Spain. Res Microbiol. 2005;156:793–806. http://dx.doi.org/10.1016/j.resmic.2005.03.006
5. Amézquita-López BA, Quiñones B, Soto-Beltrán M, Lee BG, Yambao JC, Lugo-Melchor OY, et al. Antimicrobial resistance profiles of Shiga toxin-producing *Escherichia coli* O157 and

non-O157 recovered from domestic farm animals in rural communities in northwestern Mexico. Antimicrob Resist Infect Control. 2016;5:1–6. http://dx.doi.org/10.1186/s13756-015-0100-5

6. Centers for Disease Control and Prevention. NARMS now: human data 2016 [cited 2016 Oct 12]. http://wwwn.cdc.gov/narmsnow/

7. Ingram DD, Franco SJ. 2013 NCHS urban-rural classification scheme for counties. Vital Health Stat 2. 2014;(166):1–73.

8. Center for Healthcare Research and Transformation. Antibiotic prescribing and use. 2011 [cited 2016 Oct 12]. http://www.chrt.org/document/antibiotic-prescribing-and-use/

9. Jacoby GA. Mechanisms of resistance to quinolones. Clin Infect Dis. 2005;41(Suppl 2):S120–6. http://dx.doi.org/10.1086/428052

10. Suda KJ, Hicks LA, Roberts RM, Hunkler RJ, Taylor TH. Trends and seasonal variation in outpatient antibiotic prescription rates in the United States, 2006 to 2010. Antimicrob Agents Chemother. 2014;58:2763–6. http://dx.doi.org/10.1128/AAC.02239-13

White-Nose Syndrome Fungus in a 1918 Bat Specimen from France

Michael G. Campana, Naoko P. Kurata, Jeffrey T. Foster, Lauren E. Helgen, DeeAnn M. Reeder, Robert C. Fleischer, Kristofer M. Helgen

Author affiliations: Smithsonian Institution, Washington, DC, USA (M.G. Campana, N.P. Kurata, L.E. Helgen, R.C. Fleischer); University of New Hampshire, Durham, New Hampshire, USA (J.T. Foster); Bucknell University, Lewisburg, Pennsylvania, USA (D.M. Reeder); University of Adelaide, Adelaide, South Australia, Australia (K.M. Helgen)

White-nose syndrome, first diagnosed in North America in 2006, causes mass deaths among bats in North America. We found the causative fungus, *Pseudogymnoascus destructans*, in a 1918 sample collected in Europe, where bats have now adapted to the fungus. These results are consistent with a Eurasian origin of the pathogen.

We report the earliest known historical incidence of the fungus *Pseudogymnoascus* (formerly *Geomyces*) *destructans*, detected in a museum specimen of a bat (*Myotis bechsteinii*) collected in France in 1918. This fungal pathogen causes white-nose syndrome (WNS) in bats (*1*). Since its introduction into eastern North America around 2006, WNS has devastated bat populations across the continent (*2*). *P. destructans* has also been found across the Eurasian landmass (*3*,*4*) without documented mass bat deaths. Epidemiologic evidence among bats and fungal genetics indicate that the fungus has been recently introduced into North American bat populations (*5*–*7*).

To clarify the epidemiologic history of WNS and to investigate physical evidence of its presence in specific locations in the past, we screened 138 19th- and 20th-century bat specimens (housed at the National Museum of Natural History [USNM], Washington, DC) from North America (n = 41), Europe (n = 83), and East Asia (n = 14) for *P. destructans* DNA (online Technical Appendix, https://wwwnc.cdc.gov/EID/article/23/9/17-0875-Techapp1.pdf). We sampled dry museum skins and intact bodies stored in 70% ethanol; some were originally fixed in formalin. We swabbed bat rostra and wings to collect potentially preserved *P. destructans* biomolecules and stored swabs in 100% ethanol until DNA extraction.

We extracted DNA in a dedicated ancient DNA laboratory at the National Zoological Park (Washington, DC) by using stringent protocols to prevent false positive results from modern DNA contamination (*8*). Before extraction, we removed swabs from the ethanol and let them air dry. We then let swabs digest overnight at 55°C in 600 μL extraction buffer (1× Tris-EDTA buffer, pH 8.0, 0.019 mmol/L EDTA, 0.01 mmol/L NaCl, 1% SDS, 10 mg/mL DTT, and 1 mg/mL proteinase K) (*8*). Later extractions omitted DTT. We extracted digested samples twice in 600 μL phenol and once in 600 μL chloroform. We removed and concentrated the aqueous phase by using Amicon Ultra-4 30 kDA molecular weight cutoff columns (Millipore Sigma, Merck, Billerica, MA, USA) to a final volume of ≈250 μL. We included 1 extraction blank for every 10–11 historical samples.

We screened extracts for *P. destructans* by using a previously described species-specific quantitative PCR targeting 103 bp (including primers) of the intergenic spacer region (*9*). Each extract was amplified in 2–8 replicate PCRs. Multiple, no-template controls (*2*,*3*) were included in each PCR setup. Positive products from experiments in which quantifiable contamination (>0.1 genome equivalents/μL sample) was observed in ≥1 negative control were discarded; these experiments were repeated with fresh reagents.

One sample (USNM 231170) tested positive in 2 of 3 PCRs. We performed a second independent extraction on this sample. The replicate extraction tested positive in 4 of 5 PCRs. Two of the USNM 231170–positive PCR products were confirmed by using Sanger sequencing and comparison to publicly available *P. destructans* sequences in GenBank. These sequences were 100% identical to *P. destructans* sequences from North America (GenBank accession nos. JX270192.1

and JX415267.1). In addition, 2 samples (USNM 15513 and 154222) yielded positive products in a single PCR each, but we were unable to replicate these results. No usable sequence was obtained from the USNM 15513 amplicon; the USNM 154222 sequence differed from the North American sequence by a single thymine deletion. DNA sequences were deposited in GenBank (accession nos. MF370925–6).

The 1 confirmed case of *P. destructans* infection among the museum samples we studied (USNM 231170, male, skin and skull) was in a Bechstein's bat (*Myotis bechsteinii*) collected on May 9, 1918, at Forêt de Russy, Centre-Val de Loire, France. This sequence is unlikely to represent *P. destructans* from a recently collected infected bat from North America because recently collected specimens have been purposefully stored with care in a separate room within the USNM mammal department, away from the historical bat collection. Furthermore, none of the historical samples of bats collected in North America, which are more likely to be cross-contaminated with potentially infected specimens compared with European specimens, tested positive for *P. destructans.*

We provide evidence of the presence of *P. destructans* ≈100 years ago in Europe. In addition, we found no evidence of *P. destructans* in bats collected in eastern North America during 1861–1971. Although false negatives are highly likely because of the age, preparation, and storage of these specimens, these results are consistent with a Eurasian origin of the current WNS epidemic and strong association of the fungus with Eurasian bats of the genus *Myotis* (*3,6,10*). Bats across Eurasia have adapted to *P. destructans* over more than a century, but the fungus was initially detected in North America during the early 21st century, and the bats on this continent have no immunity. This result extends the documented temporal occurrence of *P. destructans* as a bat-associated fungus to the early 20th century and highlights the value of archived museum specimens for epidemiologic study of emerging fungal diseases, including WNS.

Acknowledgments

Dr. Campana is a computational genomics scientist at the Smithsonian Institution Conservation Biology Institute's Centers for Conservation Genomics. His research interests include analysis of animal and pathogen population genomics by using a combination of ancient DNA and computational genomics.

References

1. Lorch JM, Meteyer CU, Behr MJ, Boyles JG, Cryan PM, Hicks AC, et al. Experimental infection of bats with *Geomyces destructans* causes white-nose syndrome. Nature. 2011;480:376–8. http://dx.doi.org/10.1038/nature10590
2. Frick W, Puechmaille SJ, Hoyt JR, Nickel BA, Langwig KE, Foster JT, et al. Disease alters macroecological patterns of North American bats. Glob Ecol Biogeogr. 2015;24:741–9. http://dx.doi.org/10.1111/geb.12290
3. Puechmaille SJ, Wibbelt G, Korn V, Fuller H, Forget F, Mühldorfer K, et al. Pan-European distribution of white-nose syndrome fungus (*Geomyces destructans*) not associated with mass mortality. PLoS One. 2011;6:e19167. http://dx.doi.org/10.1371/journal.pone.0019167
4. Hoyt JR, Sun K, Parise KL, Lu G, Langwig KE, Jiang T, et al. Widespread bat white-nose syndrome fungus, northeastern China. Emerg Infect Dis. 2016;22:140–2. http://dx.doi.org/10.3201/eid2201.151314
5. Warnecke L, Turner JM, Bollinger TK, Lorch JM, Misra V, Cryan PM, et al. Inoculation of bats with European *Geomyces destructans* supports the novel pathogen hypothesis for the origin of white-nose syndrome. Proc Natl Acad Sci U S A. 2012;109:6999–7003. http://dx.doi.org/10.1073/pnas.1200374109
6. Leopardi S, Blake D, Puechmaille SJ. White-nose syndrome fungus introduced from Europe to North America. Curr Biol. 2015;25:R217–9. http://dx.doi.org/10.1016/j.cub.2015.01.047
7. Zukal J, Bandouchova H, Brichta J, Cmokova A, Jaron KS, Kolarik M, et al. White-nose syndrome without borders: *Pseudogymnoascus destructans* infection tolerated in Europe and Palearctic Asia but not in North America. Sci Rep. 2016;6:19829. Erratum in: Sci Rep. 2016;6:26049. http://dx.doi.org/10.1038/srep19829
8. Fleischer RC, Olson SL, James HF, Cooper AC. Identification of the extinct Hawaiian eagle (*Haliaeetus*) by mtDNA sequence analysis. Auk. 2000;117:1051–6. http://dx.doi.org/10.1642/0004-8038(2000)117[1051:IOTEHE]2.0.CO;2
9. Muller LK, Lorch JM, Lindner DL, O'Connor M, Gargas A, Blehert DS. Bat white-nose syndrome: a real-time TaqMan polymerase chain reaction test targeting the intergenic spacer region of *Geomyces destructans.* Mycologia. 2013;105:253–9. http://dx.doi.org/10.3852/12-242
10. Wibbelt G, Kurth A, Hellmann D, Weishaar M, Barlow A, Veith M, et al. White-nose syndrome fungus (*Geomyces destructans*) in bats, Europe. Emerg Infect Dis. 2010; 16:1237–43. http://dx.doi.org/10.3201/eid1608.100002

Address for correspondence: Kristofer M. Helgen, University of Adelaide, Adelaide, Australia; e-mail kristofer.helgen@adelaide.edu.au

Peter Paul Rubens (1577–1640), *Hippopotamus and Crocodile Hunt* **(ca. 1615–1616)** (detail)**.** Oil on canvas 97.6 in × 126.4 in/248 cm × 321 cm. Alte Pinakothek, Kunstareal, Munich, Germany; digital image from Art Resource, New York, New York, USA.

Hidden Dangers from the Hunt

Byron Breedlove and Nkuchia M. M'ikanatha

In 1577, Peter Paul Rubens was born in Siegen, Germany, to Belgian parents from Antwerp. He lived there until he was 10 years old, when his father died and his mother moved the family back to Antwerp. By age 13, Rubens knew he wanted to be an artist. In 1600, he traveled to Italy where he studied firsthand Renaissance and classical works by masters such as Michelangelo, Bassano, Titian, and Veronese and established his reputation as an artist. He furthered his studies during trips to Spain before returning to Antwerp in 1609.

Those influences, and his penchant for creating large-scale works, are evident in *Hippopotamus and Crocodile Hunt*, this month's cover art, one of four paintings that Maximilian I, Elector of Bavaria, commissioned Rubens to create for display in the Schleissheim Palace, a summer residence for nobility. This work, as well as its companions that depicted lion, wolf, and boar hunts, was plundered from the palace during the Napoleonic Wars. Although this

Author affiliations: Centers for Disease Control and Prevention, Atlanta, Georgia, USA (B. Breedlove); Pennsylvania Department of Health, Harrisburg, Pennsylvania, USA (N.M. M'ikanatha)

painting was recovered, the others are believed to have been destroyed.

In characteristic Baroque style that evokes emotion and passion, Rubens depicts a vicious, imaginary hunt. A well-armed, finely dressed trio of hunters astride their Arabian horses have caught their prey from behind. The mounted hunters, each wearing a turban and brandishing finely crafted weapons, clearly relish the battle, their spears poised to finish their prey. Three vicious hunting dogs are eager participants in the skirmish against the enraged hippopotamus and thrashing crocodile.

Rubens' hunters and horses are fixated on the hippopotamus, which raises one eye toward the viewer as it flares its tusks and tramples the crocodile. The crocodile, menacing jaws agape, may not have been the intended prey, but stirred from its torpor on the river bank, it has become an accidental combatant. The terrified expression of the surviving footman, trapped on the ground, offers another perspective on the unfolding scrum. His companion has already fallen in the fray, and a snake that has emerged from the muck crawls over the dead footman's arm.

In this scene, the artist depicts man's struggle not just with these exotic beasts but with nature as a whole. The website Peter Paul Rubens: Paintings and Biography notes "It is a painting of opposites between smooth and scaly, dark and light, the high and low, beauty and barbaric."

Daniel Margocsy states that Rubens' painting is the best early-modern European picture of a hippopotamus. Until 1800, it "remained the only realistic image of this fearsome animal to be produced north of the Mediterranean." Rubens likely saw a pair of stuffed hippopotami while he was traveling in Italy, and Margocsy states that the artist relied on "his knowledge of comparative anatomy to recreate the musculature of the animal. He also obscured much of the hippo's body, hiding little-known details in the background, and put the well-preserved mouth in the foreground."

Rubens' riveting work illustrates the dangers inherent in hunting fearsome wildlife. Both the hippopotamus and crocodile are inherently dangerous prey; through their bulk and bite, either could easily inflict casualties on the hunters and their own animals. Yet those dangers pale in comparison with the potential threats posed by the emergence and resurgence of invisible pathogens transmitted from animals to humans.

Wildlife have historically been a significant source of infectious disease pathogens, and a plethora of known pathogenic agents can be transmitted directly or indirectly from animals to humans via a variety of routes. Assuming Rubens' hunters bested their quarry, then other exposures to pathogenic agents, including bacteria, viruses, parasites, and fungi that cause zoonotic diseases, could occur when the animals are field-dressed for their meat, bones, ivory, and hides; consumed during a celebratory banquet; or shared with others. Besides Rubens' hippopotamus and crocodile, other sources of pathogen exposure include rodents; mosquitoes and other insects; and birds that dwell on the riverbank, in the water, or among the vegetation.

As our understanding of the process of cross-species transmission of pathogens continues to unfold, the enhanced interface between humans and animals through hunting, commerce, animal husbandry, and domestication of exotic pets increases the likelihood of zoonotic infections. Because so many infectious diseases in humans are acquired from animals, initiatives such as One Health that encourage collaboration among multiple disciplines are useful for achieving the best health for people, animals, and the environment.

Bibliography

1. Centers for Disease Control and Prevention. One Health [cited 2017 Jul 23]. https://www.cdc.gov/onehealth/index.html
2. Encyclopedia of World Biography. Peter Paul Rubens biography [cited 2017 Jul 21]. http://www.notablebiographies.com/Ro-Sc/Rubens-Peter-Paul.html
3. Freedberg D. Peter Paul Rubens: Oil paintings and oil sketches. New York: Gagosian Gallery Exhibition Catalogue; 1995 [cited 2017 Jul 26]. http://www.columbia.edu/cu/arthistory/faculty/Freedberg/Rubens-book.pdf
4. Pike BL, Saylors KE, Fair JN, Lebreton M, Tamoufe U, Djoko CF, et al. The origin and prevention of pandemics. Clin Infect Dis. 2010;50:1636–40. http://dx.doi.org/10.1086/652860
5. Kruse H, Kirkemo AM, Handeland K. Wildlife as source of zoonotic infections. Emerg Infect Dis. 2004;10:2067–72. http://dx.doi.org/10.3201/eid1012.040707
6. Liedtke W. Peter Paul Rubens (1577–1640) and Anthony van Dyck (1599–1641): Paintings [cited 2017 Jul 18] http://www.metmuseum.org/toah/hd/rvd_p/hd_rvd_p.htm
7. Margocsy D. How one 17th-century artist produced a good painting of an animal he'd never seen [cited 2017 Jul 17]. http://www.slate.com/blogs/the_vault/2014/11/12/history_of_animals_in_art_rubens_hippo_painting_and_accuracy.html
8. The National Gallery. Peter Paul Rubens [cited 2017 July 18]. https://www.nationalgallery.org.uk/artists/peter-paul-rubens
9. Peter Paul Rubens. Paintings and biography: The Hippopotamus and Crocodile Hunt, 1615 by Rubens [cited 2017 Jul 16]. http://www.peterpaulrubens.net/the-hippopotamus-and-crocodile-hunt.jsp

EMERGING INFECTIOUS DISEASES®

Upcoming Issue

- Fatal Rocky Mountain Spotted Fever along the US–Mexico border, 2013–2016

- Enteric Infections Circulating during Hajj Seasons, 2011–2013

- Economic Assessment of Waterborne Outbreak of Cryptosporidiosis

- Disease Burden of *Clostridium difficile* Infections in Adults, Hong Kong, China, 2006–2014

- Investigation of Outbreaks of *Salmonella enterica* Serovar Typhimurium and Its Monophasic Variants Using Whole-Genome Sequencing, Denmark

- Molecular Tracing to Find Source of Protracted Invasive Listeriosis Outbreak, Southern Germany, 2012–2016

- Off-Label Use of Bedaquiline in Children and Adolescents with Multidrug-Resistant Tuberculosis

- Bedaquiline and Delamanid Combination Treatment of 5 Patients with Pulmonary Extensively Drug-Resistant Tuberculosis

- Mild Illness and Absence of Hemolytic Uremic Syndrome during Shiga Toxin–Producing *Escherichia coli* O157 Outbreak Associated with Agricultural Show, Australia, 2013

- Enterovirus D68–Associated Acute Flaccid Myelitis in Immunocompromised Woman, Italy

- Hantavirus Pulmonary Syndrome Caused by Maripa Virus in French Guiana, 2008–2016

- Usutu Virus RNA in Mosquitoes, Israel, 2014–2015

- Macrolide-Resistant *Mycoplasma pneumoniae* Infection, Japan, 2008–2015

- Monitoring Avian Influenza Viruses from Chicken Carcasses Sold at Markets, China, 2016

- Berlin Squirrelpox Virus, a New Poxvirus in Red Squirrels, Berlin, Germany

- Bedaquiline and Linezolid for Extensively Drug-Resistant Tuberculosis in Pregnant Woman

- Dengue Virus Exported from Côte d'Ivoire to Japan, June 2017

- Six-Month Response to Delamanid Treatment in MDR TB Patients

Complete list of articles in the October issue at http://www.cdc.gov/eid/upcoming.htm

Upcoming Infectious Disease Activities

October 1–3, 2017
Emerging and Re-emerging Viruses Symposia
Arlington, VA, USA
http://cell-symposia.com/emerging-viruses-2017/

October 3–7, 2017
ID Week
San Diego, CA, USA
http://www.idweek.org/

November 5–9, 2017
ASTMH
American Society for Tropical Medicine and Hygiene
66th Annual Meeting
The Baltimore Convention Center
Baltimore, MD, USA
http://www.astmh.org/

December 5–8, 2017
6th National Congress of Tropical Medicine and
International Symposium on HIV/AIDS Infection
9th National Congress of Microbiology and Parasitology
80th Anniversary of the Institute of Tropical Medicine Pedro Kourí
Havana, Cuba
http://microbiologia2017.sld.cu/index.php/microbiologia/2017

February 1–3, 2018
8th Advances in Aspergillosis
Lisbon, Portugal
www.AAA2018.org

March 1–4, 2018
18th International Congress on Infectious Diseases (ICID)
Buenos Aires, Argentina
http://www.isid.org/icid/

To submit an announcement, send an email message to EIDEditor (eideditor@cdc.gov). In 50–150 words, describe timely events of interest to our readers. Include the date of the event, the location, the sponsoring organization(s), and a web site that readers may visit or a telephone number or email address that readers may contact for more information.

Announcements may be posted on the journal Web page only, depending on the event date.

Earning CME Credit

To obtain credit, you should first read the journal article. After reading the article, you should be able to answer the following, related, multiple-choice questions. To complete the questions (with a minimum 75% passing score) and earn continuing medical education (CME) credit, please go to http://www.medscape.org/journal/eid. Credit cannot be obtained for tests completed on paper, although you may use the worksheet below to keep a record of your answers.

You must be a registered user on http://www.medscape.org. If you are not registered on http://www.medscape.org, please click on the "Register" link on the right hand side of the website.

Only one answer is correct for each question. Once you successfully answer all post-test questions, you will be able to view and/or print your certificate. For questions regarding this activity, contact the accredited provider, CME@medscape.net. For technical assistance, contact CME@medscape.net. American Medical Association's Physician's Recognition Award (AMA PRA) credits are accepted in the US as evidence of participation in CME activities. For further information on this award, please go to https://www.ama-assn.org. The AMA has determined that physicians not licensed in the US who participate in this CME activity are eligible for AMA PRA Category 1 Credits™. Through agreements that the AMA has made with agencies in some countries, AMA PRA credit may be acceptable as evidence of participation in CME activities. If you are not licensed in the US, please complete the questions online, print the AMA PRA CME credit certificate, and present it to your national medical association for review.

Article Title
Epidemiology of *Salmonella enterica* Serotype Dublin Infections among Humans, United States, 1968–2013

CME Questions

1. You are advising a large health maintenance organization about anticipated needs regarding *Salmonella* serotype Dublin human bloodstream infections. On the basis of the analysis of US national surveillance data by Harvey and colleagues, which one of the following statements about incidence and demographics of *Salmonella* serotype Dublin human bloodstream infections is correct?

A. Incidence rate of *Salmonella* Dublin has overall been stable since 1968, except for a decrease and subsequent increase in incidence occurring throughout the 1980s
B. More than half of all *Salmonella* Dublin infections occurred in Oklahoma residents
C. 38% of *Salmonella* Dublin infections occurred in persons ≥65 years vs 11% of those with other *Salmonella* infections
D. History of international travel was significantly more common in *Salmonella* Dublin patients than in other *Salmonella* patients

2. According to the analysis of US national surveillance data by Harvey and colleagues, which one of the following statements about clinical severity of *Salmonella* serotype Dublin human bloodstream infections is correct?

A. Mortality rate decreased from 1996–2004 to 2005–2013
B. During 1996 to 2004, 58% of patients were hospitalized compared with 38% in 2005 to 2013

C. Reasons underlying the severity of *Salmonella* Dublin serotype infections are unknown
D. *Salmonella* Dublin has a serotype-specific virulence-associated plasmid that is associated with invasive infection and is stable through multiple generations of nonselective bacterial passage

3. On the basis of the analysis of US national surveillance data by Harvey and colleagues, which one of the following statements about antimicrobial resistance of *Salmonella* serotype Dublin human bloodstream infections is correct?

A. Resistance to 7 or more antimicrobial classes was present in 2.4% of isolates collected during 1996 to 2004 and in 8.8% of isolates collected during 2005 to 2013
B. Resistance to 3 or more antimicrobial classes was present in 21% of *Salmonella* Dublin isolates collected during 1996 to 2013 and in 12% of other *Salmonella* isolates
C. Less than 10% of *Salmonella* Dublin isolates were resistant to third-generation cephalosporins
D. Increases in human *Salmonella* Dublin infections with ceftriaxone and nalidixic acid resistance are likely caused in part by use of similar antimicrobials in animal agriculture

Earning CME Credit

To obtain credit, you should first read the journal article. After reading the article, you should be able to answer the following, related, multiple-choice questions. To complete the questions (with a minimum 75% passing score) and earn continuing medical education (CME) credit, please go to http://www.medscape.org/journal/eid. Credit cannot be obtained for tests completed on paper, although you may use the worksheet below to keep a record of your answers.

You must be a registered user on http://www.medscape.org. If you are not registered on http://www.medscape.org, please click on the "Register" link on the right hand side of the website.

Only one answer is correct for each question. Once you successfully answer all post-test questions, you will be able to view and/or print your certificate. For questions regarding this activity, contact the accredited provider, CME@medscape.net. For technical assistance, contact CME@medscape.net. American Medical Association's Physician's Recognition Award (AMA PRA) credits are accepted in the US as evidence of participation in CME activities. For further information on this award, please go to https://www.ama-assn.org. The AMA has determined that physicians not licensed in the US who participate in this CME activity are eligible for AMA PRA Category 1 Credits™. Through agreements that the AMA has made with agencies in some countries, AMA PRA credit may be acceptable as evidence of participation in CME activities. If you are not licensed in the US, please complete the questions online, print the AMA PRA CME credit certificate, and present it to your national medical association for review.

Article Title
Imported Infections with *Mansonella perstans* Nematodes, Italy

CME Questions

1. You are seeing a 30-year-old man who recently emigrated from sub-Saharan Africa. His sister, who emigrated from their home country years ago, brings him in "to get checked out for any illnesses or parasites." You consider whether the patient might have infection with *Mansonella perstans*. Which one of the following statements regarding the life cycle of *M. perstans* is most accurate?

A. It is transmitted to humans via mosquitoes
B. Macrofilariae live in serous body cavities
C. Macrofilariae are the final infection stage of *M. perstans*
D. Microfilariae are released into the bloodstream approximately 1 month after the initial infection

2. Which one of the following countries was associated with the highest number of infections with *M. perstans* in the current study?

A. Tanzania
B. Democratic Republic of the Congo
C. Mozambique
D. Sudan

3. You perform a review of systems for infection. Which one of the following symptoms was most common among individuals with *M. perstans* in the current study?

A. Itching
B. Edema
C. Arthralgia
D. Abdominal pain

4. The patient's symptoms and serologic testing suggest infection with *M. perstans*. According to the results of the current study, what has been first-line treatment for *M. perstans* since 2009?

A. Levamisole, followed by mebendazole
B. Mebendazole alone
C. Albendazole, followed by ivermectin
D. Mebendazole, followed by doxycycline
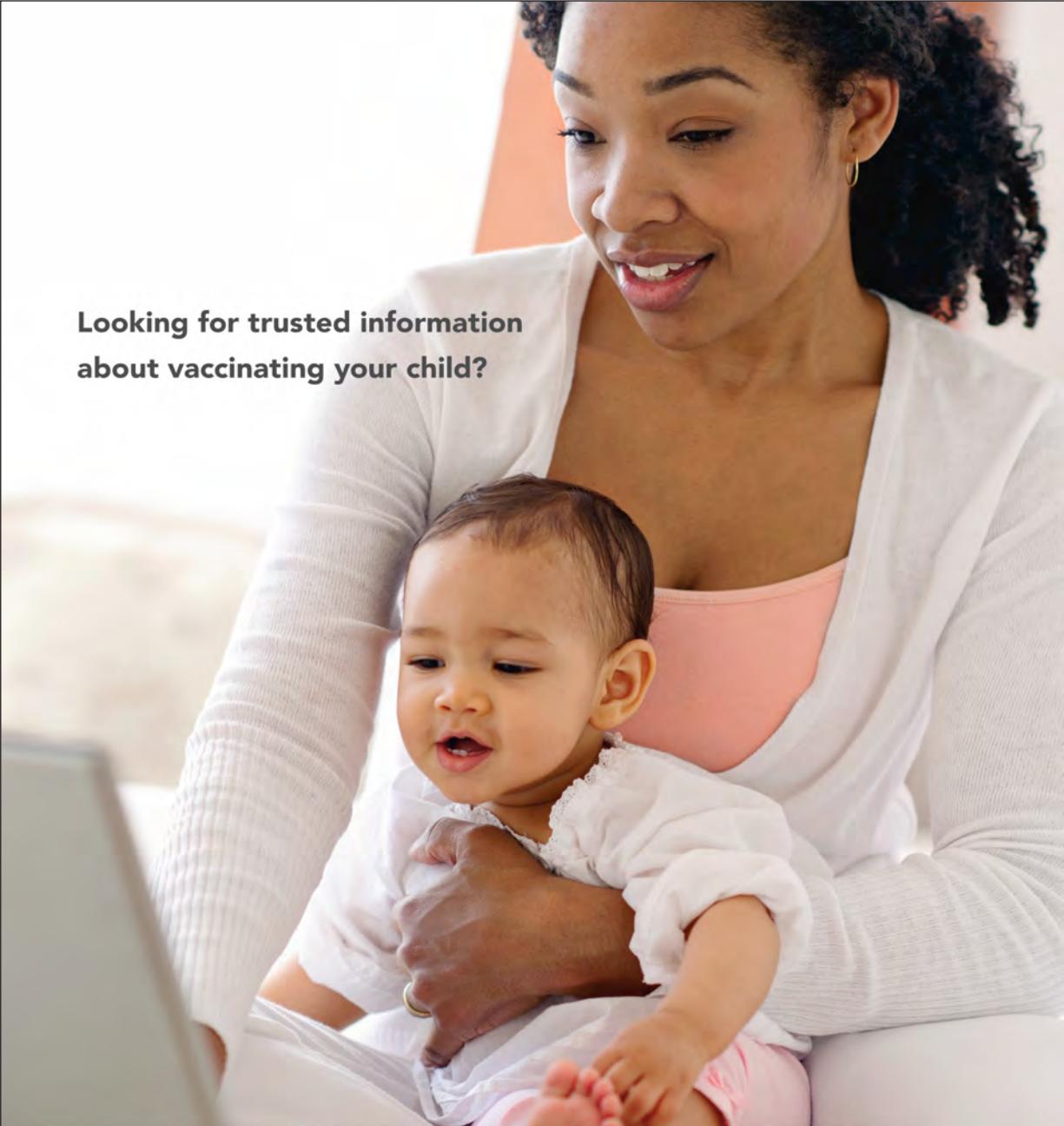
Looking for trusted information about vaccinating your child?

Visit www.cdc.gov/vaccines/parents. Learn about the vaccines your baby needs from a reliable source. The CDC's website explains the 14 diseases vaccines prevent, CDC's recommended schedule, possible side effects, how to comfort your baby during vaccine visits and more. Talk to your child's doctor, and visit our website to get the facts about vaccines.

U.S. Department of Health and Human Services
Centers for Disease Control and Prevention

Immunization. Power to Protect.

⚬DPDx
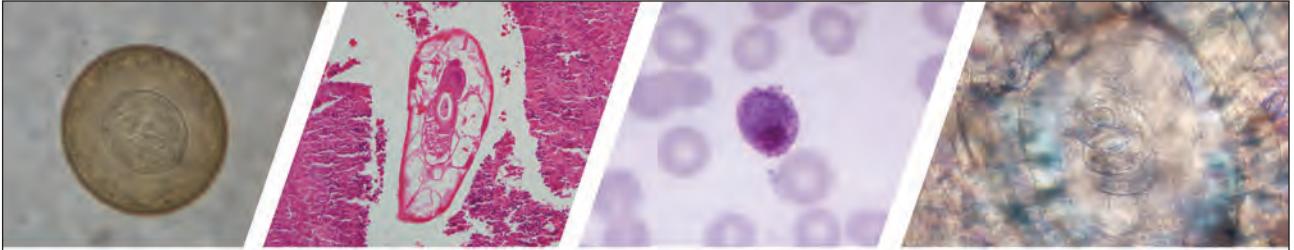
Diagnostic Assistance and Training in Laboratory Identification of Parasites

A free service of CDC available to laboratorians, pathologists, and other health professionals in the United States and abroad

Diagnosis from photographs of worms, histological sections, fecal, blood, and other specimen types

Expert diagnostic review

Formal diagnostic laboratory report

Submission of samples via secure file share

Visit the DPDx website for information on laboratory diagnosis, geographic distribution, clinical features, parasite life cycles, and training via Monthly Case Studies of parasitic diseases.

www.cdc.gov/dpdx
dpdx@cdc.gov

CS272346-DE

**U.S. Department of
Health and Human Services**
Centers for Disease
Control and Prevention

EID *SPOTLIGHT*

These spotlights highlight the latest articles and information on emerging infectious disease topics in our global community.

Antimicrobial Resistance

Food Safety

Ebola

HIV/AIDS

Lyme Disease

Influenza

MERS

Pneumonia

Rabies

Tuberculosis

Ticks

Zika

EMERGING INFECTIOUS DISEASES®

http://wwwnc.cdc.gov/eid/page/spotlight-topics

Emerging Infectious Diseases is a peer-reviewed journal established expressly to promote the recognition of new and reemerging infectious diseases around the world and improve the understanding of factors involved in disease emergence, prevention, and elimination.

The journal is intended for professionals in infectious diseases and related sciences. We welcome contributions from infectious disease specialists in academia, industry, clinical practice, and public health, as well as from specialists in economics, social sciences, and other disciplines. Manuscripts in all categories should explain the contents in public health terms. For information on manuscript categories and suitability of proposed articles, see below and visit http://wwwnc.cdc.gov/eid/pages/author-resource-center.htm.

Summary of Authors' Instructions

Author's Instructions. For a complete list of EID's manuscript guidelines, see the author resource page: http://wwwnc.cdc.gov/eid/page/author-resource-center.

Manuscript Submission. To submit a manuscript, access Manuscript Central from the Emerging Infectious Diseases web page (www.cdc.gov/eid). Include a cover letter indicating the proposed category of the article (e.g., Research, Dispatch), verifying the word and reference counts, and confirming that the final manuscript has been seen and approved by all authors. Complete provided Authors Checklist.

Manuscript Preparation. For word processing, use MS Word. Set the document to show continuous line numbers. List the following information in this order: title page, article summary line, keywords, abstract, text, acknowledgments, biographical sketch, references, tables, and figure legends. Appendix materials and figures should be in separate files.

Title Page. Give complete information about each author (i.e., full name, graduate degree(s), affiliation, and the name of the institution in which the work was done). Clearly identify the corresponding author and provide that author's mailing address (include phone number, fax number, and email address). Include separate word counts for abstract and text.

Keywords. Use terms as listed in the National Library of Medicine Medical Subject Headings index (www.ncbi.nlm.nih.gov/mesh).

Text. Double-space everything, including the title page, abstract, references, tables, and figure legends. Indent paragraphs; leave no extra space between paragraphs. After a period, leave only one space before beginning the next sentence. Use 12-point Times New Roman font and format with ragged right margins (left align). Italicize (rather than underline) scientific names when needed.

Biographical Sketch. Include a short biographical sketch of the first author—both authors if only two. Include affiliations and the author's primary research interests.

References. Follow Uniform Requirements (www.icmje.org/index.html). Do not use endnotes for references. Place reference numbers in parentheses, not superscripts. Number citations in order of appearance (including in text, figures, and tables). Cite personal communications, unpublished data, and manuscripts in preparation or submitted for publication in parentheses in text. Consult List of Journals Indexed in Index Medicus for accepted journal abbreviations; if a journal is not listed, spell out the journal title. List the first six authors followed by "et al." Do not cite references in the abstract.

Tables. Provide tables within the manuscript file, not as separate files. Use the MS Word table tool, no columns, tabs, spaces, or other programs. Footnote any use of boldface. Tables should be no wider than 17 cm. Condense or divide larger tables. Extensive tables may be made available online only.

Figures. Submit editable figures as separate files (e.g., Microsoft Excel, PowerPoint). Photographs should be submitted as high-resolution (600 dpi) .tif or .jpeg files. Do not embed figures in the manuscript file. Use Arial 10 pt. or 12 pt. font for lettering so that figures, symbols, lettering, and numbering can remain legible when reduced to print size. Place figure keys within the figure. Figure legends should be placed at the end of the manuscript file.

Videos. Submit as AVI, MOV, MPG, MPEG, or WMV. Videos should not exceed 5 minutes and should include an audio description and complete captioning. If audio is not available, provide a description of the action in the video as a separate Word file. Published or copyrighted material (e.g., music) is discouraged and must be accompanied by written release. If video is part of a manuscript, files must be uploaded with manuscript submission. When uploading, choose "Video" file. Include a brief video legend in the manuscript file.

Types of Articles

Perspectives. Articles should not exceed 3,500 words and 50 references. Use of subheadings in the main body of the text is recommended. Photographs and illustrations are encouraged. Provide a short abstract (150 words), 1-sentence summary, and biographical sketch. Articles should provide insightful analysis and commentary about new and reemerging infectious diseases and related issues. Perspectives may address factors known to influence the emergence of diseases, including microbial adaptation and change, human demographics and behavior, technology and industry, economic development and land use, international travel and commerce, and the breakdown of public health measures.

Synopses. Articles should not exceed 3,500 words in the main body of the text or include more than 50 references. Use of subheadings in the main body of the text is recommended. Photographs and illustrations are encouraged. Provide a short abstract (not to exceed 150 words), a 1-line summary of the conclusions, and a brief biographical sketch of first author or of both authors if only 2 authors. This section comprises case series papers and concise reviews of infectious diseases or closely related topics. Preference is given to reviews of new and emerging diseases; however, timely updates of other diseases or topics are also welcome. If detailed methods are included, a separate section on experimental procedures should immediately follow the body of the text.

Research. Articles should not exceed 3,500 words and 50 references. Use of subheadings in the main body of the text is recommended. Photographs and illustrations are encouraged. Provide a short abstract (150 words), 1-sentence summary, and biographical sketch. Report laboratory and epidemiologic results within a public health perspective. Explain the value of the research in public health terms and place the findings in a larger perspective (i.e., "Here is what we found, and here is what the findings mean").

Policy and Historical Reviews. Articles should not exceed 3,500 words and 50 references. Use of subheadings in the main body of the text is recommended. Photographs and illustrations are encouraged. Provide a short abstract (150 words), 1-sentence summary, and biographical sketch. Articles in this section include public health policy or historical reports that are based on research and analysis of emerging disease issues.

Dispatches. Articles should be no more than 1,200 words and need not be divided into sections. If subheadings are used, they should be general, e.g., "The Study" and "Conclusions." Provide a brief abstract (50 words); references (not to exceed 15); figures or illustrations (not to exceed 2); tables (not to exceed 2); and biographical sketch. Dispatches are updates on infectious disease trends and research that include descriptions of new methods for detecting, characterizing, or subtyping new or reemerging pathogens. Developments in antimicrobial drugs, vaccines, or infectious disease prevention or elimination programs are appropriate. Case reports are also welcome.

Another Dimension. Thoughtful essays, short stories, or poems on philosophical issues related to science, medical practice, and human health. Topics may include science and the human condition, the unanticipated side of epidemic investigations, or how people perceive and cope with infection and illness. This section is intended to evoke compassion for human suffering and to expand the science reader's literary scope. Manuscripts are selected for publication as much for their content (the experiences they describe) as for their literary merit. Include biographical sketch.

Research Letters Reporting Cases, Outbreaks, or Original Research. EID publishes letters that report cases, outbreaks, or original research as Research Letters. Authors should provide a short abstract (50-word maximum), references (not to exceed 10), and a short biographical sketch. These letters should not exceed 800 words in the main body of the text and may include either 1 figure or 1 table. Do not divide Research Letters into sections.

Letters Commenting on Articles. Letters commenting on articles should contain a maximum of 300 words and 5 references; they are more likely to be published if submitted within 4 weeks of the original article's publication.

Commentaries. Thoughtful discussions (500–1,000 words) of current topics. Commentaries may contain references (not to exceed 15) but no abstract, figures, or tables. Include biographical sketch.

Books, Other Media. Reviews (250–500 words) of new books or other media on emerging disease issues are welcome. Title, author(s), publisher, number of pages, and other pertinent details should be included.

Conference Summaries. Summaries of emerging infectious disease conference activities (500–1,000 words) are published online only. They should be submitted no later than 6 months after the conference and focus on content rather than process. Provide illustrations, references, and links to full reports of conference activities.

Online Reports. Reports on consensus group meetings, workshops, and other activities in which suggestions for diagnostic, treatment, or reporting methods related to infectious disease topics are formulated may be published online only. These should not exceed 3,500 words and should be authored by the group. We do not publish official guidelines or policy recommendations.

Photo Quiz. The photo quiz (1,200 words) highlights a person who made notable contributions to public health and medicine. Provide a photo of the subject, a brief clue to the person's identity, and five possible answers, followed by an essay describing the person's life and his or her significance to public health, science, and infectious disease.

Etymologia. Etymologia (100 words, 5 references). We welcome thoroughly researched derivations of emerging disease terms. Historical and other context could be included.

Announcements. We welcome brief announcements of timely events of interest to our readers. Announcements may be posted online only, depending on the event date. Email to eideditor@cdc.gov.

In This Issue